



Seismic risk analysis of masonry buildings in aggregate

Dissertation

submitted to and approved by the

Department of Architecture, Civil Engineering and Environmental Sciences
University of Braunschweig – Institute of Technology

and the

Department of Civil and Environmental Engineering
University of Florence

in candidacy for the degree of a

Doktor-Ingenieur (Dr.-Ing.) /

**Dottore di Ricerca in Processes, Materials and Constructions in Civil and
Environmental Engineering and for the Protection of the Historic-
Monumental Heritage^{*)}**

by

Sonia Boschi

born 26.10.1985

from Poppi, Italy

Submitted on	16.03.2015
Oral examination on	11.05.2015
Professorial advisors	Prof. Andrea Vignoli Prof. Martin Empelmann

2016

^{*)} Either the German or the Italian form of the title may be used.

ABSTRACT

The Italian territory is currently defined a total seismic area. The historical city centres in Italy, as well as in other European countries, consist mainly of load-masonry buildings in aggregate, composed by a group of structural units (ss.uu.), not necessarily homogeneous, interacting each other by links more or less effective.

The vulnerability assessment on existing masonry buildings is a key aspect for the seismic risk mitigation: most of the existing structures belonging to the cultural heritage are not designed against seismic actions. After the Italian recent seismic events (Abruzzo 2009, Emilia Romagna 2012), historical city centres have showed several structural damages with implications of both social and economic resources.

The seismic risk is a function of three main aspects, the seismic hazard of the territory, the structural vulnerability, that is the propensity of a structure to suffer damage when a seismic event occurs, and the exposure. Seismic vulnerability of a masonry aggregate is due to both the intrinsic characteristics of the masonry that constitute the structural units (masonry type, stones quality, etc,...) and to the particular configuration of the aggregate (geometry, plan and height shape, number of structural units, etc..).

There are different approaches for the evaluation of structural vulnerability: empirical/expeditious methods referring to a territorial scale analysis, analytical/numerical that interest the study of single buildings with refined numerical models and a combination of the previous two ones, the hybrid methods. A seismic risk analysis addressed to earthquake emergency management requires vulnerability and damage evaluation performed at territorial scale (empirical methods), to highlight in an urban density mesh area the most vulnerable aggregates in order to focus on them Administration resources, for deep mechanical analysis and the definition of strengthening interventions.

In the first part of this work, after an overview of the state of art of the structural vulnerability assessment methods, the results of the application of an empirical approach will be illustrated. The method is the Vulnerability Index Method, with the filling out of the "Aggregate Form" or "5 Parameters Form", implemented by the University of Aveiro, 2012. The 74 masonry aggregates of Castelnuovo, a hamlet in the L'Aquila's valley (center of Italy), have been exploited as case study, since all information about geometrical, structural parameters and loads were widely known about them. The village of Castelnuovo was hit by the earthquake of L'Aquila of 2009 (mainshock in 06/04/2009): most of aggregates have showed several damages on structural elements. The vulnerability analysis results allowed to build damage scenarios on buildings of Castelnuovo, varying macroseismic intensity of possible earthquakes. In particular, damage scenario were defined for the macroseismic intensity recorded in Castelnuovo after the earthquake of 2009. The application of this method helped to obtain information about the seismic behaviour of the masonry structures and, in particular, to determine the factors that mostly influenced their behaviour against horizontal actions. It also allowed a continuous comparison between the results of the aforementioned damage scenarios found through vulnerability assessment and those actually presented after the earthquake. Analysing the distribution of the obtained Vulnerability Indexes and basing on the results of the predicted damage scenario, a new Vulnerability Aggregate Form has been introduced. The integration of the original Aggregate Form implied the insertion of an additional parameter, "P6-Current state" of the building. The P6 vulnerability classes were defined in analogy with what already expressed in vulnerability Form commonly used in literature (i.e. GNDT II Level Form (Benedetti and Petrini, 1984)) and its importance factor (parameter weight) in order to bridge the existing gap between the estimated and real damage scenarios assessed for the Castelnuovo aggregates.

Afterwards the attention has been paid on the mechanical models (vulnerability analytical methods) that can be used for a detailed analysis of masonry aggregates, considering both the local and the global behaviour that a masonry structure can show if excited by a seismic action. Based on the results of mechanical analyses done, and looking at the real type of damage mechanisms individuated in Castelnuovo aggregates (characterised by disorganised stone masonries and lack of connections among vertical and horizontal structural elements), local out-of-plane mechanisms have been chosen as analysis type to study these structures with the final goal to estimate their minimum seismic capacity. The local kinematic methodologies have been applied to each structural units principally in main façades. This procedure has allowed to understand which are the parameters that mostly influence the seismic out-of-plane behaviours of the masonry façades,

setting the basis for the definition of a new Vulnerability Form for Façades. This Façade Form, considering only simple and qualitative geometrical information of the structures, allows a first estimation of the capacity for out-of-plane mechanism, expressed in terms of $a_{g,c}$ (peak ground acceleration of capacity), and the relative Safety Index considering the seismic hazard of the site in which the aggregate is collocated.

ZUSAMMENFASSUNG

Das italienische Territorium wird zur Zeit als durch und durch seismisches Gebiet bezeichnet. Die historischen Stadtzentren in Italien wie auch in anderen europäischen Ländern bestehen hauptsächlich aus zusammenhängenden Gebäuden aus tragendem Mauerwerk, die durch eine Anzahl nicht unbedingt homogener Baueinheiten zusammengefügt wurden und die sich gegenseitig durch mehr oder weniger wirkungsvolle Verbindungen beeinflussen.

Die Einschätzung der Verletzlichkeit vorhandener Gebäude aus Mauerwerk ist ein Schlüsselaspekt zur Milderung des seismischen Risikos. Die meisten der existierenden Bauwerke, die zum kulturellen Erbe gehören, wurden nicht gegen seismische Bewegungen geplant. Nach den letzten seismischen Ereignissen in Italien (Abruzzo 2009, Emilia Romana 2012) erlitten die historischen Stadtzentren verschiedene bauliche Schäden mit sowohl sozialen als auch wirtschaftlichen Folgen.

Das seismische Risiko setzt sich aus drei Hauptbestandteilen zusammen: das seismische Risiko des Gebietes, die bauliche Verwundbarkeit, das heißt, die Neigung eines Gebäudes, bei einem seismischen Ereignis Schaden zu nehmen und die Lage. Die seismische Verletzlichkeit eines verbundenen Mauerwerks hängt sowohl mit seinen inneren Besonderheiten (Typ des Mauerwerks, Steinqualität usw.) als auch mit der besonderen Gestaltung des Gebäudekomplexes (Geometrie, Planung, Höhe, Anzahl der Gebäude usw.) zusammen.

Es gibt verschiedene Herangehensweisen zur Auswertung der Verletzlichkeit von Gebäuden: empirische/zeitsparende Methoden, die sich auf territoriale Tabellenanalysen beziehen, analytische/numerische, die einzelne Gebäude mit exakten Zahlenmodellen studieren und eine Kombination der beiden, die Mischmethoden. Eine Analyse des seismischen Risikos für ein Erdbeben – Notfall – Management erfordert die Auswertung von Verletzlichkeit und Schäden mit empirischen Methoden, um in einer dichten urbanen Bebauung die verletzlichsten Gebäudekomplexe hervorzuheben und auf diese die Hilfsmittel der Verwaltung zu konzentrieren, sowie eine grundlegende mechanische Analyse und die Festlegung von Maßnahmen zur Stabilisierung.

In dem ersten Teil dieser Arbeit werden nach einem Überblick über die Methoden zur Einschätzung der baulichen Verletzlichkeit die Ergebnisse der Anwendung einer empirischen Herangehensweise dargestellt. Die Methode ist die VULNERABILITY INDEX METHODE, bei der das AGGREGATE – Formular oder 5 PARAMETER – Formular, erstellt 2012 von der Universität in Aveiro, zur Anwendung kam. Die 74 Gebäudeeinheiten von Castelnuovo, einem Weiler im Tal von L'Aquila (Zentralitalien), wurden als Fallstudie ausgewertet, seitdem sind alle Informationen über geometrische und bauliche Parameter weithin bekannt.

Das Dorf Castelnuovo wurde durch das Erdbeben von L'Aquila 2009 (stärkster Erdstoß am 6.4.2009) betroffen. Die meisten Bauten zeigten schwere strukturelle Schäden. Die Ergebnisse der Verletzlichkeitsanalyse erlaubten, Schadensszenarien an Gebäuden von Castelnuovo darzustellen, indem man die makroseismische Stärke von möglichen Erdbeben variierte. Insbesondere wurde das Schadensszenario für die makroseismische Intensität definiert, die nach dem Erdbeben 2009 in Castelnuovo festgestellt wurde. Die Anwendung dieser Methode half, Informationen über das seismische Verhalten von Mauerstrukturen zu erhalten und insbesondere die Faktoren zu bestimmen, die das Verhalten bei horizontalen Bewegungen beeinflussten. Sie erlaubte auch einen ständigen Vergleich zwischen den Ergebnissen des oben erwähnten Schadensszenarios durch die Einschätzung der Verletzlichkeit und denen, die sich nach dem Erdbeben tatsächlich zeigten. Basierend auf Analysen der erhaltenen Verletzlichkeitsdaten und unter Einbeziehung der Ergebnisse vorausgegangener Schadensszenarien wurde ein neues Formular zur Verletzlichkeit von Baustrukturen erstellt.

Die Vereinheitlichung mit dem ursprünglichen Formular erforderte die Einfügung eines zusätzlichen Parameters (PC – CURRENT – STATE OF THE BUILDING). Die P 6 - Klassen der Verletzlichkeit wurden analog zu dem bereits allgemein verwendeten GNDT – LEVEL Formular (Benedetti und Petrini 1984) und analog zu seinem Bedeutungsfaktor (Parametergewicht) beim Überbrücken der existierenden Diskrepanz zwischen den geschätzten und tatsächlichen Schäden an den Gebäuden in Castelnuovo definiert.

Danach richtete sich die Aufmerksamkeit auf die mechanischen Modelle (analytische Methoden zur Verletzlichkeit), die für eine detaillierte Analyse von Gebäuden aus Mauerwerk benutzt werden können, wobei sowohl das örtliche als auch das gesamte Verhalten betrachtet wurde, die eine Mauerwerkstruktur zeigen kann, wenn sie von einer seismischen Bewegung erschüttert wird. Basierend auf den Ergebnissen der durchgeführten mechanischen Analysen und nach Betrachtung des tatsächlichen Typs der Schadensmechanismen, die in Castelnovo festgestellt wurden (charakterisiert durch in Unordnung geratene Steinmauern und das Fehlen von Verbindungen zwischen vertikalen und horizontalen Strukturelementen) wurden einzelne ungewöhnliche Mechanismen als Analysetyp ausgewählt mit dem Endziel, sie zu studieren und ihre minimale seismische Kapazität einzuschätzen. Die lokalen Methoden zur Bewegungsmessung wurden bei allen Bauten angewandt, vor allem in den Hauptfassaden. Dieses Vorgehen erlaubte zu verstehen, welche Parameter den meisten Einfluss auf die unvorhersehbaren Reaktionen von Mauerwerksfassaden ausüben, wodurch die Basis für die Erstellung eines neuen Verletzlichkeitsformulars für Fassaden geschaffen wurde. Diese Formular, das nur einfache und qualitative geometrische Informationen der Baustruktur berücksichtigt, erlaubt eine erste Einschätzung des tatsächlichen Umfangs von nicht vorhersehbaren Mechanismen, bezeichnet mit agc (Höchst mögliche Beschleunigung der Kapazität) und einen relativen Sicherheitsindex hinsichtlich des seismischen Risikos in dem Gebiet, in dem sich die Gebäude befinden.

SOMMARIO

Il territorio italiano è attualmente caratterizzato come interamente sismico. I centri storici in Italia, così come per le altre nazioni europee, sono caratterizzati da un consistente patrimonio edilizio costituito da edifici in muratura portante in aggregato, composti da gruppi di unità strutturali (ss.uu.) non necessariamente omogenee che interagiscono tra loro attraverso vincoli strutturali più o meno efficaci.

La valutazione della vulnerabilità strutturale di edifici esistenti in muratura risulta dunque un'attività scientifica attuale ed un aspetto chiave per la mitigazione del rischio sismico: molte delle strutture esistenti in muratura in aggregato appartengono all'edificato storico e, per questo, non sono state adeguatamente progettate per azioni sismiche. Inoltre, i recenti terremoti italiani maggiori (Abruzzo 2009, Emilia Romagna 2012) hanno provocato ingenti danni agli aggregati murari con implicazioni socio-economiche e culturali disastrose.

Il rischio sismico è definito classicamente come funzione di tre componenti, pericolosità del territorio, la vulnerabilità strutturale ed esposizione: la pericolosità sismica è la probabilità che si verifichi, in una data area circoscritta, entro un dato periodo di tempo, un terremoto con assegnate caratteristiche; la vulnerabilità è intesa come misura della propensione dell'organo strutturale a subire danni al verificarsi dell'evento sismico e l'esposizione rappresenta il valore dei beni sociali, economici e culturali che sono presenti nell'area soggetta all'evento.

La vulnerabilità sismica di edifici in aggregato è dovuta sia alle intrinseche vulnerabilità della muratura che costituisce le unità strutturali, (qualità della muratura e della malta, etc.), sia dalle particolari configurazioni dell'aggregato (geometria in pianta ed elevazione, numero di unità strutturali, differenze tipologico/strutturali delle u.s., etc.).

La valutazione di vulnerabilità sismica può essere svolta utilizzando differenti livelli di approfondimento a seconda del campione di studio considerato o della quantità delle informazioni e degli strumenti che si utilizzano per la valutazione della stessa. Una possibile categorizzazione suddivide i metodi in tre gruppi: i metodi empirici/speditivi riferiti ad una scala territoriale per campioni di studio elevati, i metodi analitici/meccanici che interessano la definizione di modelli numerici raffinati per lo studio di singoli edifici ed i metodi ibridi che rappresentano una combinazione dei due metodi sopra esposti. Una analisi di rischio sismico rivolta alla gestione delle emergenza sismica richiede dapprima una analisi di vulnerabilità e definizione di scenari di danno a scala territoriale, per evidenziare in aree ad alta densità di costruito gli edifici in aggregato maggiormente vulnerabili, e successivamente analisi dettagliate sugli edifici risultati più vulnerabili, in cui focalizzare le risorse economiche per l'esecuzione di interventi di consolidamento.

Nella prima parte di questo lavoro, a seguito di una panoramica riguardante lo stato dell'arte dei metodi di valutazione della vulnerabilità sismica strutturale, sono illustrati i risultati dell'applicazione di un metodo di vulnerabilità empirico: il metodo dell'indice di vulnerabilità, attraverso la compilazione della "Scheda Aggregato" o "Scheda a 5 Parametri" - Università di Aveiro, 2012. Le "Schede Aggregato" sono state applicate al caso studio degli aggregati in muratura di Castelnuovo, una frazione del comune di San Pio delle Camere, nel cratere aquilano (centro Italia), per cui erano note tutte le informazioni geometriche, costruttive e strutturali. Il paese di Castelnuovo è stato colpito dal terremoto de L'Aquila del 2009: la maggior parte di aggregati ha mostrato danni su elementi strutturali ingenti ed, in alcuni casi, collassi. I risultati dell'analisi di vulnerabilità hanno permesso di costruire scenari di danno sulle costruzioni di Castelnuovo, al variare delle intensità macrosismiche di possibili eventi sismici. In particolare, sono state effettuate delle stime del danno strutturale per l'effettiva intensità registrata a Castelnuovo a seguito della scossa del 2009. L'applicazione di questo metodo al caso studio di Castelnuovo ha permesso di ottenere informazioni sul comportamento sismico delle strutture in muratura ed, in particolare, determinare quali sono i fattori maggiormente influenti sulla vulnerabilità strutturale. Inoltre, ha permesso un continuo confronto tra i risultati degli scenari di danno predetti attraverso la valutazione della vulnerabilità e quelli realmente presentatisi a seguito dell'evento sismico. Analizzando la distribuzione degli indici di vulnerabilità ottenuti e con la ricerca dell'ottimizzazione della risposta tra la previsione dello scenario di danno atteso e quello effettivamente presente a Castelnuovo è stato possibile implementare una nuova "Scheda Aggregato". L'integrazione della scheda originale ha implicato l'inserimento di un parametro aggiuntivo, "P6-stato di conservazione" dell'aggregato, le cui classi di vulnerabilità

sono state definite in analogia con quanto già espresso in schede di vulnerabilità per edifici isolati comunemente usate nella letteratura e comunità scientifica (GNDT II Modulo di Livello (Benedetti e Petrini, 1984)).

Successivamente l'attenzione è stata rivolta ai modelli analitici (metodi di vulnerabilità analitici/numerici) che possono essere utilizzati per un'analisi dettagliata degli aggregati in muratura, considerandone sia il comportamento locale sia globale, comportamenti tipici che una struttura muraria può avere se eccitata da una azione sismica. Sulla base dei risultati numerici delle analisi meccaniche eseguite e sulla base dell'analisi dei meccanismi di danno individuati negli aggregati di Castelnuovo (caratterizzati da murature in pietra disorganizzata e mancanza di collegamenti tra elementi strutturali verticali ed orizzontali), sono stati scelti i meccanismi di collasso fuori piano come modelli e metodi di analisi per studiare questa tipologia di strutture con l'obiettivo finale di valutare la loro minima capacità sismica.

La valutazione della sicurezza è stata svolta attraverso una analisi cinematica lineare ad ogni facciata principale delle unità strutturali degli aggregati. Questa procedura ha consentito di capire quali parametri influenzano principalmente la risposta strutturale fuori piano delle strutture murarie, individuando le basi per la definizione di una "Scheda Facciata". Tale "Scheda Facciata", considerando solo semplici informazioni qualitative riguardanti la geometria ed i carichi delle strutture, permette una prima stima della capacità sismica per il meccanismo di ribaltamento semplice della parete fuori piano, espresso in termini di $a_{g,c}$ (accelerazione di picco di capacità) ed il relativo indice di sicurezza sismica, considerando la pericolosità sismica del sito in cui l'aggregato murario si colloca.

TABLE OF CONTENTS

LIST OF ABBREVIATIONS	IX
LIST OF FIGURES	XI
LIST OF TABLES	XVI
INTRODUCTION.....	1
CHAPTER 1. SEISMIC RISK ANALYSIS FOR BUILDINGS IN AGGREGATE	3
1.1 SEISMIC RISK FOR MASONRY AGGREGATES	3
1.1.1 SEISMIC HAZARD.....	6
CHAPTER 2. STRUCTURAL VULNERABILITY: REVIEW OF THE STATE OF ART	17
2.1 CLASSIFICATION OF VULNERABILITY ASSESSMENT METHODS - VAMs	17
2.2 EMPIRICAL METHODS	18
2.2.1 DAMAGE PROBABILITY MATRIX - DPM	18
2.2.2 VULNERABILITY INDEX METHODS	20
2.2.3 VULNERABILITY CURVES	33
2.3 ANALYTICAL METHODS	36
2.3.1 MECHANISMS METHODS	36
2.3.2 CAPACITY SPECTRUM BASED METHODS.....	37
2.4 HYBRID METHODS.....	38
2.5 VULNERABILITY METHODS USED IN THIS THESIS	38
CHAPTER 3. CASTELNUOVO DATABASE	39
3.1 METHODOLOGY	40
3.1.1 AGGREGATE FORM	41
3.1.2 S.U. FORM.....	41
3.2 HISTORICAL ASPECTS	41
3.3 ANALYSIS OF THE BUILT HERITAGE	43
3.3.1 VERTICAL ELEMENTS (MASONRY TYPES)	46
3.3.2 HORIZONTAL ELEMENTS (FLOOR TYPES)	48
3.3.3 BUILDING CELL TYPE	53
3.4 KNOWLEDGE LEVELS, CONFIDENCE FACTORS AND MECHANICAL CHARACTERISTICS.....	54
CHAPTER 4. THE L'AQUILA EARTHQUAKE	57
4.1 EARTHQUAKE CHARACTERISTICS	57
4.2 DAMAGE IN CASTELNUOVO BUILDING STOCK	60
CHAPTER 5. AGGREGATE FORM: APPLICATION OF THE 5 PARAMETERS FORM AND DEFINITION OF A NEW AGGREGATE FORM	65
5.1 RESULTS	65
5.1.1 VULNERABILITY INDEX	65
5.1.2 DAMAGE	73
5.2 CRITICAL ANALYSIS OF THE DATA COLLECTED	75
5.3 6 PARAMETERS FORM – AGGREGATE FORM	79
5.4 CONCLUSION.....	87

CHAPTER 6. STRUCTURAL UNITS FORMS: APPLICATION AND MAIN RESULTS.....	89
6.1 GNDT II LEVEL FORM (11 PARAMETERS) FOR SS.UU. AND AGGREGATES	89
6.2 “FORMISANO FORM” (15P) AND “AVEIRO FORM” (14P)	93
6.3 COMPARISON AMONG THE FORMS	94
6.4 DAMAGE	95
6.5 CRITICAL ANALYSIS OF THE RESULTS IN RELATION WITH THE LOCAL BEHAVIOUR OF AGGREGATES	102
6.5.1 EVALUATION OF THE DAMAGE LEVEL IN THE FAÇADES	104
CHAPTER 7. SEISMIC RESPONSE OF MASONRY BUILDINGS IN AGGREGATE	111
7.1 INTRODUCTION	111
7.2 OUT-OF-PLANE MECHANISMS.....	114
7.2.1 CALCULATION METHOD	115
7.2.2 DEFINITION OF THE SEISMIC CAPACITY OF OUT-OF-PLANE MECHANISM	136
7.2.3 PARAMETERS THAT INFLUENCE THE KINEMATIC ANALYSIS	142
7.3 IN PLANE MECHANISMS COLLAPSE AND GLOBAL BEHAVIOUR OF MASONRY AGGREGATES: SIGNS	151
7.3.1 TYPES OF IN-PLANE MECHANISMS IN MASONRY PANELS	151
7.3.2 IN-PLANE MECHANISM FOR AN IDEAL PANEL AND EXAMPLES IN CASTELNUOVO AGGREGATES.....	153
7.4 CHOICE OF THE METHODOLOGY TO EVALUATE SEISMIC CAPACITY ON AGGREGATES	157
7.5 RESULTS FOR THE CASE STUDY (189 MASONRY FAÇADES).....	158
7.5.1 GEOMETRICAL, STRUCTURAL AND LOADS CHARACTERISTICS	159
7.5.2 CAPACITY OF THE FAÇADES.....	161
CHAPTER 8. NEW VULNERABILITY FORM FOR FAÇADES IN HISTORICAL CITY CENTRES.....	165
8.1 INTRODUCTION	165
8.2 DEFINITION OF THE PARAMETERS IN THE NEW VULNERABILITY FORM FOR FAÇADES	166
8.3 SAMPLE OF STUDY FOR THE DETERMINATION OF THE FAÇADE FORM.....	172
8.4 DEFINITION OF THE NEW VULNERABILITY FORM FOR FAÇADES	174
8.5 ESTIMATION OF THE RISK INDEX	178
8.6 EXAMPLES OF THE METHOD TEST.....	179
CONCLUSION AND OUTLOOKS.....	185
REFERENCES.....	189
ANNEX 1 – CASTELNUOVO DATABASE: DEFINITION OF THE AGGREGATES AND MAIN CHARACTERISTICS	A1
ANNEX 2 – EXAMPLE OF MASONRY PANEL FORMS – IQM	A3
ANNEX 3 – INFLUENCE OF THE GEOMETRICAL AND STRUCTURAL PARAMETERS IN THE ANALYSIS RESULTS	A5

LIST OF ABBREVIATIONS

List of main abbreviations related to Chapters 1, 2, 5, 7 and 8. The other symbols and abbreviations not directly mentioned here are explained in the text.

a_g	= Seismic acceleration in A ground type and T1 topography category, $a_{g,D}$
$a_{g,Ci}$	= Seismic acceleration of capacity of the i-mechanism
AMU	= Analysis minimum units
α_0	= Horizontal loads multiplier of collapse
a_0^*	= Seismic acceleration of capacity for out-of-plane mechanism
a_s^*	= Secant acceleration (corresponding to the displacement d_s^* , out-of-plane non-linear analysis)
$C_{k,aG}$	= Coefficient that generates a seismic action able to produce on a certain building (T fixed) built on a certain soil (ground class “k”), the same effect as if it was built on Rock (ground class “A”), for stable topographic category (both in A ground and k-ground).
C_U	= Use coefficient
d_e	= Index of economic damage
d_s^*	= Secant displacement (out-of-plane non-linear analysis)
d_u^*	= Capacity displacement (last displacement) of the out-of-plane mechanisms
D_K	= Damage Grade related to EMS-98 Scale
DSL	= Damage limit state DLS (SLD in italian);
DPM	= Damage Probability Matrix
DPMs	= Damage Probability Matrixes
F_0	= Maximum amplification factor of the spectrum in acceleration
I	= Macroseismic Intensity
I_{EMS-98}	= Macroseismic Intensity of a seismic event for the EMS-98 scale
IMU	= Intervention minimum units
I_s	= Safety (or risk) Index
I_v	= Vulnerability Index
I_{V11}	= Vulnerability Index for GNDT II Level Form for ss.uu.
$I_{V11,A}$	= Vulnerability Index for GNDT II Level Form for aggregate
I_{VA}	= Vulnerability Index for Aggregate Form
$I_{VA,6}$	= Vulnerability Index for Aggregate Form with 6 parameters
I_{V15}	= Vulnerability Index for “Formisano Form” for ss.uu.
I_{V14}	= Vulnerability Index for “Aveiro Form” for ss.uu.
$I_{Vi,av}$	= Average value of Vulnerability Index
MLR	= Multi Linear Regression
M_L	= Local Magnitude
M_W	= Moment Magnitude
μ_D	= Mean Damage grade (in the thesis it is associated to an estimation result of the vulnerability assessment)
η	= Viscous damping coefficient (it is 1 for damping coefficient equal to 5%)
PGA	= Peak Ground Acceleration
P_i	= i-parameter of the Vulnerability Form
PO	= Push over
P_{VR}	= Probability of exceedance in the reference period
q	= Behaviour factor
REL	= Reliability (of the I_v)

$r_{x,y}$	= Sample correlation coefficient
r^2	= Coefficient of determination
S	= Ground factor ($S_T \cdot S_S$); S_T = topographic coefficient; S_S = soil coefficient.
SDOF	= Single Degree of Freedom
SLV	= Preservation of life Limit State
s.u.	= Structural Unit
ss.uu.	= Structural Units
T_C^*	= Upper limit of the period of the constant spectral acceleration range
T_B	= Period corresponding to the beginning of the constant acceleration range of the spectrum $T_B = T_C/3$;
T_D	= Period corresponding to the beginning of the constant displacement range: $T_D = 4.0 \cdot a_g/g + 1.6$
T_S	= Secant period (out-of-plane non-linear analysis)
T_R	= Return period of the seismic action
Θ	= Angle or rotation of the panel (out-of-plane non-linear analysis)
VAM	= Vulnerability Assessment Method
VAMs	= Vulnerability Assessment Methods
VIM	= Vulnerability Index Method
VIMs	= Vulnerability Index Methods
VF	= Vulnerability Form
VFs	= Vulnerability Forms
V_N	= Nominal life
V_R	= Reference period

LIST OF FIGURES

FIGURE 1: PALACE IN L'AQUILA AND CASTELNUOVO (AERIAL VIEW) AFTER THE EARTHQUAKE	3
FIGURE 2: EXAMPLES OF MASONRY AGGREGATES: IN THE CENTRE OF FIRENZE (A) AND IN CASTELNUOVO (AQ) (B).	4
FIGURE 3: AGGREGATE (IN BLUE) AND STRUCTURAL UNITS. IN RED SU6, IN GREEN AN EXAMPLE OF AMU, ANALYSIS MINIMUM UNITS.	4
FIGURE 4: AGGREGATE EVOLUTION: INDIVIDUATION OF THE INNER CORE AND THE SECONDARY CELLS (RIGHT PICTURE IN INDELICATO, 2010).	5
FIGURE 5: EVOLUTION PROCESS OF AGGREGATE (10-088).	5
FIGURE 6: INTERACTIVE MAP OF SEISMIC HAZARD FOR THE CITY OF ST. DELLE CAMERE (AQ) FOR A P_{VR} OF 10% IN 50 YEARS.	7
FIGURE 7: RESPONSE SPECTRA FOR CASTELNUOVO, $S_E(T)$, $S_{ED}(T)$ AND $S_D(T)$	11
FIGURE 8: VULNERABILITY TABLE AND DAMAGE LEVELS IN EMS-98.	14
FIGURE 9: GRAPHIC COMPARISON BETWEEN THE MSC AND MSK SCALE (MARGOTTINI ET AL., 1992).	15
FIGURE 10: CORRELATIONS BETWEEN INTENSITY AND A_{MAX} (GÓMEZ ET AL., 2007).	16
FIGURE 11: DIFFERENT CLASSIFICATIONS OF VULNERABILITY ASSESSMENT METHODS. IN RED THE METHODS USED IN THIS WORK.	18
FIGURE 12: VULNERABILITY ASSESSMENT METHODS FOR BUILDINGS (LANG, 2002).	18
FIGURE 13: DPM, SAN FERNANDO EARTHQUAKE 1971.	19
FIGURE 14: QUANTITIES IN EMS-98 SCALE AND DPM (VULNERABILITY CLASSES AND DAMAGE).	20
FIGURE 15: GNDT 11 PARAMETERS MASONRY FORM.	21
FIGURE 16: AGGREGATE 23-102, 26-415 AND 21-25 EXAMPLES OF DAMAGE IN TERMS OF OUT-OF-PLANE OVERTURNING.	22
FIGURE 17: EXAMPLE OF VERTICAL STRUCTURES, TYPE OF MASONRY AND DEFINITION OF THE CLASSES OF P2.	22
FIGURE 18: TYPE OF DEFORMABLE FLOORS.	23
FIGURE 19: NOT EFFECTIVE CONSTRAINTS AND OUT-OF-PLANE MECHANISM OF OVERTURNING OF WEDGE WALLS.	24
FIGURE 20: EXAMPLE OF TWO R.C. ROOFS IN CASTELNUOVO (AQ).	24
FIGURE 21: "FORMISANO" FORM (15P.): PARAMETERS, SCORES AND WEIGHTS.	26
FIGURE 22: POSSIBLE CONFIGURATIONS OF INTERNAL S.U. WITHIN AN AGGREGATE AND CLASSES FOR P11.	26
FIGURE 23: POSSIBLE PLAN CONFIGURATIONS AND CLASSES FOR PARAMETER 12.	26
FIGURE 24: CLASSES OF PARAMETER 13 AND POSSIBLE CONFIGURATION OF STAGGERED FLOORS AMONG SS.UU.	27
FIGURE 25: A) EXAMPLE OF DIFFERENT % BETWEEN TWO SS.UU. (AGGR. 13-158); B) DIFFERENT N° OF FLOORS.	27
FIGURE 26: "AVEIRO" FORM (14P.): PARAMETERS, SCORES AND WEIGHTS.	28
FIGURE 27: AGGREGATE FORM: PARAMETERS, SCORES AND WEIGHTS.	29
FIGURE 28: FAÇADE FORM: PARAMETERS AND WEIGHTS.	31
FIGURE 29: COMPARISON AMONG SS.UU. FORMS.	32
FIGURE 30: AVEIRO FORM (14P.), WEIGHTS AND SCORES AND INDIVIDUATION OF THE MORE INFLUENTIAL PARAMETERS.	33
FIGURE 31: AGGREGATE FORM (15P) WEIGHTS AND SCORES AND INDIVIDUATION OF THE MORE INFLUENTIAL PARAMETERS.	33
FIGURE 32: GROUND ACCELERATION – DAMAGE PROBABILISTIC LAW (GNDT, 1993).	34
FIGURE 33: VULNERABILITY CURVES, TRILINEAR APPROXIMATION FUNCTION (D,Y CURVES).	34
FIGURE 34: (A) CORRELATION BETWEEN VULNERABILITY AND DAMAGE (B) RELATION VULNERABILITY-DAMAGE AND ACCELERATION.	34
FIGURE 35: A) CORRELATIONS BETWEEN THE DAMAGE INDEX (D_e) AND THE MEAN DAMAGE GRADE (μ_D); B) MACROSEISMIC METHOD: COMPARISON WITH GNDT II LEVEL FORM FOR A AND B CLASSES OF EMS-98.	35
FIGURE 36: THE ELECTRONIC FORM FOR THE COLLECTION OF DATA FOR FAMIVE (D'AYALA & SPERANZA, 2002).	37
FIGURE 37: TERRITORIAL FRAMEWORK AND INDIVIDUATION OF THE L'AQUILA EARTHQUAKE EPICENTRE (HTTPS://MAPS.GOOGLE.IT/).	39
FIGURE 38: LIMIT OF THE PERIMETER. EXAMPLE OF AGGREGATE AND DIVISION IN STRUCTURAL UNITS.	40
FIGURE 39: (A) FIRST LAYOUT OF AGGREGATE FORM. (B) HISTORICAL SETTLEMENT OF CASTELNUOVO.	41
FIGURE 40: PAGES.1, 2, 3 AND 4 OF THE SS.UU. FORM OF 57-179 S.U.1.	42
FIGURE 41: CASTELLO, THE OLDEST ZONE OF CASTELNUOVO.	43
FIGURE 42: ANTE AND POST EARTHQUAKE AERIAL PHOTOS.	44
FIGURE 43: NUMBER OF FLOOR FOR STRUCTURAL UNITS.	44
FIGURE 44: DIFFERENT TYPE OF BUILDINGS: ISOLATED (YELLOW), ROW BUILDINGS (GREEN) AND COMPLEX BUILDINGS (BLUE).	45
FIGURE 45: MASONRY TYPES AND PANELS.	47
FIGURE 46: MASONRY PANELS ANALYSED.	47
FIGURE 47: STONE MASONRY, FRONT AND CROSS SECTIONS.	48

FIGURE 48: PREDOMINANT HORIZONTAL TYPE FOR GROUND FLOOR (A), FIRST FLOOR (B), SECOND FLOOR (C) AND ROOF (D).	49
FIGURE 49: PARTITION WALL'S DISTRIBUTION AT THE FIRST LEVEL OF 10-088 AGGREGATE.	49
FIGURE 50: ROOF TYPE 1.	50
FIGURE 51: STONE MASONRY BARREL VAULTS IN THE "CASTELLO" AGGREGATES.	51
FIGURE 52: BRICK MASONRY VAULT "IN FOLIO": (A) REPRESENTATION OF THE CONSTRUCTION PHASES ("G. CANGI – MANUALE DEL RECUPERO STRUTTURALE E ANTISISMICO). SOME EXAMPLES IN CASTELNUOVO BUILDINGS. LAST PICTURE IS A CEILING PT EXAMPLE.	52
FIGURE 53: EXTRACT OF LONGITUDINAL SECTION AND CROSS-SECTION OF S.U.8 OF AGGREGATE 10-088.	54
FIGURE 54: LONGITUDINAL SECTION FOR AGGREGATE 57-179, IN "CASTELLO" BUILDINGS.	54
FIGURE 55: SEISMIC SEQUENCE OF THE EARTHQUAKE OF L'AQUILA (SOURCE: HTTP://WWW.INGV.IT).	57
FIGURE 56: LOCATION OF THE ACCELEROMETRIC STATIONS LESS THAN 100 KM FAR FROM THE EPICENTRE (L'AQUILA).	58
FIGURE 57: ACCELEROGRAMS COMPONENTS OF AQV STATION (L'AQUILA EARTHQUAKE).	58
FIGURE 58: COMPARISON BETWEEN AQV RESPONSE SPECTRA AND THE DESIGN RESPONSE SPECTRA FOLLOWING ITALIAN ACTUAL CODE NTC, 2008. (TOP: HORIZONTAL COMPONENTS, BOTTOM VERTICAL COMPONENTS).	59
FIGURE 59: (FROM THE TOP). EXAMPLE OF CASTELNUOVO BUILDINGS FOR DIFFERENT LEVEL OF DAMAGE (D0-D1, D2, D3 AND D4).	61
FIGURE 60: EXAMPLE OF CASTELNUOVO BUILDINGS WITH D5 DAMAGE. FROM THE TOP, AGGREGATE 05, 44 AND 36.	61
FIGURE 61: HISTOGRAM AND MAPS OF THE DAMAGE FOR SS.UU.	63
FIGURE 62: HISTOGRAMS OF DAMAGE DISTRIBUTION FOR DIFFERENT SS.UU. POSITIONS.	63
FIGURE 63: HISTOGRAMS OF DAMAGE DISTRIBUTION FOR DIFFERENT SS.UU. POSITIONS FOR MASONRY AGGREGATES.	64
FIGURE 64: THREE AGGREGATES: EVOLUTION PROCESS AND DAMAGE LEVEL FOR EACH STRUCTURAL UNIT.	64
FIGURE 65: 5 PARAMETERS MASONRY "AGGREGATE FORM" FOR THE EVALUATION OF I_v .	65
FIGURE 66: AGGREGATE NOT TAKEN INTO ACCOUNT IN THE FILLING OUT OF THE "AGGREGATE FORM".	65
FIGURE 67: EXAMPLE OF FILLING OUT OF THE 5 PARAMETER FORM.	66
FIGURE 68: VULNERABILITY INDEXES MAPS FOR BUILDINGS.	67
FIGURE 69: DISTRIBUTION OF THE PARAMETERS' CLASSES FOR 72 MASONRY AGGREGATE.	68
FIGURE 70: STATISTICAL ANALYSIS AND DISTRIBUTION OF THE I_{vA} FOR THE 72 AGGREGATES.	70
FIGURE 71: (A) DISTRIBUTION OF I_{vA} IN TERMS OF NUMBER OF BUILDINGS AND % OF BUILDING; (B) DISTRIBUTION OF I_{vA} IN TERMS OF VOLUME OF BUILDINGS AND % OF BUILDING; (C) % OF BUILDINGS AND VOLUME (WITH LESS VALUES OF CLASSES); (D) NORMAL DISTRIBUTION.	70
FIGURE 72: A) AGGREGATE 66-583, ONE FLOOR, THREE SS.UU., REGULAR PLAN. B) INDIVIDUATION OF THE SAME CLASSES AND WEIGHTS.	71
FIGURE 73: AGGREGATES RANKING WITH INCREASING I_{vA} .	71
FIGURE 74: DISTRIBUTION OF THE PARAMETERS CLASSES FOR AGGREGATES AND ISOLATED BUILDINGS.	71
FIGURE 75: RESULTS FOR AGGREGATES AND ISOLATED BUILDINGS.	71
FIGURE 76: "CASTELLO", ANTE-POST EARTHQUAKE AERIAL PHOTOS.	72
FIGURE 77: RESULTS FOR AGGREGATES AND ISOLATED BUILDINGS WITHOUT "CASTELLO" (66 AGGREGATES).	72
FIGURE 78: (A) DAMAGE DISTRIBUTION FOR AGGREGATES, HISTOGRAM,; (B) AVERAGE DAMAGE GRADE WEIGHTED IN VOLUME.	73
FIGURE 79: REAL DAMAGE GRADE WITH THE INDIVIDUATION OF THE MAJOR VULNERABILITY ZONES.	73
FIGURE 80: VULNERABILITY CURVES FOR THE MOST AND LESS VULNERABLE AGGREGATES.	74
FIGURE 81: ESTIMATED MEAN DAMAGE GRADE WITHOUT AND WITH ZONE 2 AND 3; (B) INDIVIDUATION OF DAMAGE ZONES IN AERIAL PHOTO.	75
FIGURE 82: A) I_v DISTRIBUTION (5P-FORM) FOR AGGREGATES. B) DISTRIBUTION OF THE JUDGMENTS IN THE P1 ALONG THE VULNERABILITY RANKING.	76
FIGURE 83: DISTRIBUTION OF THE JUDGMENTS IN THE P2, P3, P4 AND P5 WITH THE VULNERABILITY RANKING.	76
FIGURE 84: MATRIX OF PLOT OF THE AGGREGATE FORM PARAMETERS WITH THE LEVEL OF DAMAGE.	77
FIGURE 85: A) (TOP). MATRIX OF CORRELATION: INDEXES OF CORRELATION FOR EACH COUPLE OF PARAMETERS, I_{vA} AND D_k , WITH THE REAL SCORES OF JUDGMENT. B) (BOTTOM) MATRIX OF CORRELATION WITH EQUIDISTANT SCORES AMONG JUDGMENTS.	78
FIGURE 86: A) D_k VS VULNERABILITY INDEX RANKING; B) AVERAGE D_k FOR THE 28 POSITIONS OF THE VULNERABILITY RANKING.	78
FIGURE 87: A) REAL DAMAGE VS VULNERABILITY INDEX; B) AVERAGE REAL DAMAGE FOR THE 28 POSITIONS OF THE VULNERABILITY INDEX.	79
FIGURE 88: (A) OCCUPATION STATUS; (B) PROPERTY.	80
FIGURE 89: (A) PARAMETERS 6 – CURRENT STATE FOR SS.UU.; (B) AGGREGATES.	81
FIGURE 90: MATRIX OF CORRELATION FOR 6P-FORM (REAL SCORE FOR JUDGMENTS).	82
FIGURE 91: AGGREGATE FORM (6P) WITH DIFFERENT PROPOSED SOLUTIONS.	83
FIGURE 92: 6 PARAMETERS FORM: TWO PROPOSALS.	84

FIGURE 93: DISTRIBUTION OF THE VULNERABILITY INDEX (6P FORM) FOR AGGREGATES. LEFT: PROPOSAL 1. RIGHT: PROPOSAL 2.	85
FIGURE 94: REAL DAMAGE VS VULNERABILITY INDEX RANKING. LEFT: PROPOSAL 1. RIGHT: PROPOSAL 2.	85
FIGURE 95: A) REAL DAMAGE VS VULNERABILITY INDEX. LEFT: PROPOSAL 1. RIGHT: PROPOSAL 2.	85
FIGURE 96: AVERAGE REAL DAMAGE FOR THE POSITIONS OF THE VULNERABILITY RANKING. LEFT: PROPOSAL 1. RIGHT: PROPOSAL 2.	86
FIGURE 97: AVERAGE REAL DAMAGE FOR THE POSITIONS OF THE VULNERABILITY INDEX. LEFT: PROPOSAL 1. RIGHT: PROPOSAL 2.	86
FIGURE 98: VULNERABILITY INDEX VS REAL DAMAGE. RANGE OF CONFIDENCE.	86
FIGURE 99: PROPOSAL 1. (A) % OF BUILDINGS AND VOLUME; (D) NORMAL DISTRIBUTION.	87
FIGURE 100: (A) AGGREGATE 54-246, POST EARTHQUAKE. (B) AGGREGATE 47-051 PHOTO ANTE EARTHQUAKE.	87
FIGURE 101: DISTRIBUTION OF $I_{VA,6}$ AND $\mu_{D,E6}$	87
FIGURE 102: AGGREGATE FORM PROPOSED.	88
FIGURE 103: EXAMPLE OF SS.UU. NOT CONSIDERED IN THE FORMS.	89
FIGURE 104: STATISTICAL ANALYSIS AND DISTRIBUTION OF THE I_{V11} FOR 124 SS.UU.	90
FIGURE 105: 09-160 S.U.1 (1A) AND IT REINFORCED CONCRETE SLAB (1B). 18-163 SS.UU. 2-3 (2A) WITH COLLAPSED FLEXIBLE FLOOR (2B).	90
FIGURE 106: A) DISTRIBUTION OF I_{V11} IN TERMS OF % OF BUILDINGS (SS.UU.) AND % OF VOLUME; B) VULNERABILITY INDEXES MAPS FOR SS.UU.	90
FIGURE 107: DISTRIBUTION OF THE PARAMETERS' CLASSES FOR 124 SS.UU.	91
FIGURE 108: STATISTICAL ANALYSIS AND DISTRIBUTION OF THE $I_{V11,A}$ FOR 26 AGGREGATES.	92
FIGURE 109: A) DISTRIBUTION OF I_{V11} IN TERMS OF % OF AGGREGATES AND % OF VOLUME; B) VULNERABILITY INDEXES MAPS FOR AGGREGATES.	92
FIGURE 110: DISTRIBUTION OF I_{V11} IN TERMS OF % N° OF BUILDING (SS.UU. & AGGREGATES) AND % OF VOLUME (SS.UU. & AGGREGATES).	93
FIGURE 111: DISTRIBUTION OF THE I_{V15} I_{V14} FOR 124 SS.UU.	94
FIGURE 112: DISTRIBUTION OF I_{V15} IN TERMS OF % N° OF BUILDING (SS.UU. & AGGREGATES) AND % OF VOLUME (SS.UU. & AGGREGATES).	94
FIGURE 113: VULNERABILITY INDEXES MAPS FOR SS.UU.	94
FIGURE 114: COMPARISON OF THE DISTRIBUTIONS OF THE I_V FOR % VOLUME OF SS.UU.	95
FIGURE 115: COMPARISON OF THE NORMAL DISTRIBUTIONS OF THE I_V FOR SS.UU.	95
FIGURE 116: HISTOGRAM OF THE DISTRIBUTION OF ESTIMATED μ_D (EMS-98) FOR SS.UU. WITH GNDT 11P AND SEISMIC DAMAGE MAPS.	96
FIGURE 117: HISTOGRAM OF THE DISTRIBUTION OF ESTIMATED μ_D (EMS-98) FOR AGGREGATES WITH GNDT 11P AND SEISMIC DAMAGE MAPS.	96
FIGURE 118: VULNERABILITY CURVES FOR THE MAX, MIN AND AVERAGE VALUE OF THE I_{V11} FOR: A) SS.UU.; B) AGGREGATES.	96
FIGURE 119: DISTRIBUTION HISTOGRAM OF ESTIMATED μ_D (EMS-98) FOR SS.UU. WITH FORMISANO FORM (15 P.) AND SEISMIC DAMAGE MAPS.	97
FIGURE 120: DISTRIBUTION HISTOGRAM OF ESTIMATED μ_D (EMS-98) FOR SS.UU. WITH AVEIRO FORM (15 P.) AND SEISMIC DAMAGE MAPS.	97
FIGURE 121: REAL D_K VS VULNERABILITY RANKING FOR AGGREGATES. IN RED GNDT FORM AND IN BLACK THE AGGREGATE FORM (6P).	98
FIGURE 122: FORM TOP. REAL D_K VS VULNERABILITY INDEXES FOR THE SS.UU.. IN RED GNDT FORM, YELLOW "FORMISANO" AND GREEN "AVEIRO" FORMS.	99
FIGURE 123: DISTRIBUTION OF THE REAL DAMAGE FOR SS.UU. AND ESTIMATED WITH DIFFERENT FORMS.	100
FIGURE 124: DISTRIBUTION OF THE REAL DAMAGE FOR AGGREGATES AND ESTIMATED WITH DIFFERENT FORMS.	101
FIGURE 125: ERRORS % AMONG THE ESTIMATED AND REAL DAMAGES.	101
FIGURE 126: DISTRIBUTION OF THE REAL AND ESTIMATED DAMAGE FOR DIFFERENT FORMS GROUPED FOR THE POSITION OF THE SS.UU.. (TOP, INTERNAL, HEADER AND CORNER POSITION).	102
FIGURE 127: GNDT FORM WITH INFLUENCE IN TERMS OF LOCAL AND GLOBAL BEHAVIOUR OF THE MASONRY STRUCTURES.	103
FIGURE 128: ADDITIONAL PARAMETER OF 15 AND 14 PARAMETERS FORMS: INFLUENCE IN TERMS OF LOCAL AND GLOBAL BEHAVIOUR.	103
FIGURE 129: CLASSIFICATION OF THE DAMAGE FOR OUT-OF-PLANE MECHANISMS OF OVERTURNING. FROM THE TOP: CLASS D, CLASS C, CLASS B.	104
FIGURE 130: DAMAGE INTENSITY IN TERMS OF OUT-OF-PLANE MECHANISMS FOR A REDUCED SAMPLE OF BUILDINGS IN CASTELNUOVO.	105
FIGURE 131: DISTRIBUTION OF CLASSES OF DAMAGES FOR OUT-OF-PLANE MECHANISMS.	106
FIGURE 132: (A) BUBBLE GRAPH FOR THE PARAMETER "DAMAGE LEVEL" AND ITSELF. (B) BUBBLE GRAPH FOR "DAMAGE LEVEL" AND P6 (GNDT).	108
FIGURE 133: (FROM THE TOP) BUBBLE GRAPH FOR THE PARAMETER "DAMAGE LEVEL" AND PARAMETERS 2-3-9-11 GNDT AND 11-14 FORMISANO.	109
FIGURE 134: BUBBLE GRAPH FOR THE PARAMETER "DAMAGE LEVEL" AND PARAMETER 8 GNDT.	109
FIGURE 135: ORIGIN OF OUT-OF-PLANE MECHANISM AND IN-PLANE MECHANISMS (PICTURES FROM TOULIATOS 1996 AND (STADATA, 2012)).	111
FIGURE 136: A) EXAMPLE OF IN-PLANE SHEAR COLLAPSE; B) EXAMPLE OF OVERTURNING OF THE MAIN FAÇADE.	112
FIGURE 137: A) LOCAL OUT-OF-PLANE MECHANISMS (WWW.RELUIS.IT); B) IN PLANE MECHANISMS DUE TO DIAGONAL CRACKING.	113
FIGURE 138: A_0 CALCULATION IN THE CASE OF OVERTURNING OF A MONOLITHIC WALL WITH 2 FLOORS: FORCES AND HINGE INDIVIDUATIONS.	116
FIGURE 139: SINGLE FLOOR STRUCTURE, WITH ONE SINGLE FORCE APPLIED (SELF-WEIGHT); TREND OF A_0 VERSUS THE PANEL'S SLENDERNESS.	117
FIGURE 140: (A) KINEMATIC ANALYSIS WITH FINITE ROTATION; (B) ANGLE θ SUCH AS THE COLLAPSE IS GUARANTEED.	118

FIGURE 141: EVOLUTION OF THE CAPACITY CURVE OF THE MECHANISM.	119
FIGURE 142: SCHEME OF THE EVOLUTION OF THE MECHANISMS BASED ON THE ITALIAN SEISMIC CODE (C.M. N.617, 2009) (NTC, 2008).	120
FIGURE 143: S.U. 9 OF 10-088 AGGREGATE.....	122
FIGURE 144: FRONT OF THE S.U. 9, TRANSVERSE SECTION AND IDENTIFICATION OF THE 3 LEVEL OF THE STRUCTURE.....	123
FIGURE 145: (A) TREND OF HORIZONTAL MULTIPLIER VS DISPLACEMENT OF THE CONTROL POINT; (B) CAPACITY CURVES.....	124
FIGURE 146: CAPACITY CURVE FOR EACH MECHANISM, INDIVIDUATION OF THE CAPACITY LAST DISPLACEMENTS AND DEMAND DISPLACEMENT.	125
FIGURE 147: AERIAL PHOTO OF AGGREGATE 18-163 AFTER EARTHQUAKE. RENDER OF AGGREGATE (FROM FABIO FERRARI, MASTER THESIS)	126
FIGURE 148: S.U. 1. FRONTAL AND LATERAL OVERTURNING (FROM FABIO FERRARI, MASTER THESIS).....	126
FIGURE 149: OVERTURNING OF SS.UU. 2 AND 3, 4, 5, 7, 8, 9 AND 10.	127
FIGURE 150: EFFECT ON SLABS OF THE OVERTURNING FAÇADE MECHANISMS. (A) CEILING VAULTS (B) FLOOR.	128
FIGURE 151: S.U. 1 OF 10-088 AGGREGATE. (A) SIMPLE 3-FLOOR OVERTURNING (B)OVERTURNING WITH CORNER IN THE THIRD FLOOR.	128
FIGURE 152: (A) VERTICALLY ALIGNMENT OF THE BARYCENTRE OF THE PANEL (G') AND THE HINGE CONFIGURATION (POINT A). (B) RECESSION OF THE HINGE CONFIGURATION DUE THE FINITE RESISTANCE OF THE MASONRY (ELASTIC AND PLASTIC SCHEME).	130
FIGURE 153: EXAMPLE OF FAÇADES WITH METALLIC TIE-RODS - PHOTOS (AGGREGATE 10-088 AND 13-158).	133
FIGURE 154: (A) TIE-ROD. IDENTIFICATION OF THE POSSIBLE COLLAPSES MECHANISMS. (B) FAÇADE WITH SQUARED BOLT PLATES (01-222).	133
FIGURE 155: MASONRY CROSSED VAULTS IN FIRENZE CITY CENTRES (TIRATOIO SQUARE) AND LOGGIA DEI LANZI IN SIGNORIA SQUARE.	134
FIGURE 156: A) CURVE D_k-A_0 ; B) CAPACITY CURVE FOR THE CASE OF COLLAPSE SLAB.	135
FIGURE 157: A) CURVE D_k-A_0 ; B) CAPACITY CURVE FOR THE CASE OF COLLAPSE OF A TIE-ROD.	136
FIGURE 158: RESTRAINS IN THE OUT-OF-PLANE MECHANISMS: PRESENCE OF EXTERNAL STAIRS OR OUTBUILDING (AGGREGATE 10-088).....	137
FIGURE 159: (A) RESEARCH OF THE A_{GC} WITH FIXED T_R (475 YEARS); (B) EXAMPLE OF SHAPE OF THE SPECTRA WITH T_R VARIABLE.	139
FIGURE 160: VARIABILITY OF THE PARAMETERS A_G [G] AND F_0 WITH THE RETURN PERIOD T_R (PICTURES FROM SPETTRI DI RISPOSTA V 1.0.3 - C.S.L.P. HTTP://WWW.CSLP.IT).	139
FIGURE 161: PERIOD OF ALL THE OUT-OF-PLANE MECHANISMS OF THE FAÇADES.	140
FIGURE 162: EXAMPLE OF THE VARIATION OF THE PARAMETER "THICKNESS" OF THE TOP FLOOR.	143
FIGURE 163: RESULTS OF THE LINEAR ANALYSES A_0 , A_c^* , A_{GC} AND I_{SL} FOR OVERTURNING MECHANISMS FOR DIFFERENT VALUES OF CF (1÷1.35)...	144
FIGURE 164: RESULTS OF THE NON-LINEAR ANALYSES ϕ_i , du^* AND I_{SNL} FOR OVERTURNING MECHANISMS FOR DIFFERENT VALUES OF CF (1÷1.35). LAST GRAPH REFERS TO THE RATIO BETWEEN THE RESULTS FOR THE LINEAR AND NON-LINEAR ANALYSES.	144
FIGURE 165: CAPACITY CURVES AND INDIVIDUATION OF THE T_s^* FOR DIFFERENT VALUE OF CF.	145
FIGURE 166: RESULTS OF THE LINEAR ANALYSES FOR OVERTURNING MECHANISMS FOR DIFFERENT VALUES OF SECOND FLOOR'S THICKNESS.....	145
FIGURE 167: RESULTS OF THE NON-LINEAR ANALYSES ϕ_i , du^* AND I_{SNL} FOR OVERTURNING MECHANISMS FOR DIFFERENT VALUES OF SECOND FLOOR'S THICKNESS. LAST GRAPH (D) REFERS TO THE RATIO BETWEEN THE RESULTS FOR THE LINEAR AND NON-LINEAR ANALYSES.	146
FIGURE 168: RESULTS OF THE LINEAR AND NON-LINEAR ANALYSES FOR DIFFERENT VALUES OF THICKNESS OF THE 1 ST AND 2 ND FLOORS (5-57 CM).	146
FIGURE 169: RESULTS OF THE LINEAR ANALYSES FOR DIFFERENT VALUES OF GROUND, 1 ST AND 2 ND FLOORS' THICKNESS.	147
FIGURE 170: RESULTS OF THE NON-LINEAR ANALYSES FOR DIFFERENT VALUES GROUND, 1 ST AND 2 ND FLOORS' THICKNESS.	147
FIGURE 171: IN PLANE MECHANISMS: (FROM THE LEFT) SHEAR FAILURE JOINTS BED SLIDING, DIAGONAL CRACKING AND ROCKING.	151
FIGURE 172: SHEAR-DISPLACEMENT LAW OF THE PANEL.	153
FIGURE 173: COLLAPSE'S DOMAINS OF THE PANELS (A) AGGREGATE 10-088, (B) 18-163, (C) 57-179 AND (D) 27-415.....	155
FIGURE 174:(A) DOMAINS OF THE IDEAL PANEL. (B) DOMAINS OF THE 10-088, 18-163 AND 57-179 AGGREGATE PANELS.	155
FIGURE 175: PANEL COLLAPSE.	155
FIGURE 176: GLOBAL MODEL OF AGGREGATE (EQUIVALENT FRAME MODEL, 3MURI) AND CAPACITY CURVES.	156
FIGURE 177: EXAMPLES OF LACK OF CONNECTIONS AMONG VERTICAL ORTHOGONAL WALLS AND HORIZONTAL AND VERTICAL ELEMENTS.	157
FIGURE 178: DAMAGE MECHANISMS ANALYSED IN THE POST-EARTHQUAKE CASTELNUOVO AGGREGATES.....	158
FIGURE 179: INDIVIDUATION OF THE MECHANISMS ANALYSED FOR THE FAÇADES (IN RED).....	158
FIGURE 180: DISTRIBUTION OF NUMBER OF FLOORS AND LENGTH.	159
FIGURE 181: DISTRIBUTION OF THICKNESS AND HEIGHT FOR THE SAMPLE OF DATA AND DIFFERENT FLOORS.....	160
FIGURE 182: DISTRIBUTION OF THE TOTAL HEIGHT AND HEIGHT FOR EACH FLOORS.	160
FIGURE 183: (A) DISTRIBUTION OF SLENDERNESS FOR DIFFERENT FLOORS; (B) H/L DISTRIBUTION.	160
FIGURE 184: (A) DISTRIBUTION OF THE NET AREA AVERAGE AND FOR EACH FLOOR; (B) DISTRIBUTION OF THE AXIAL LOAD FOR EACH FLOOR.....	161
FIGURE 185: (A) DISTRIBUTION OF THE BARYCENTRE IN HEIGHT FOR EACH FLOOR.	161
FIGURE 186: VAULTS, TIE-RODS AND QUALITATIVE INFORMATION (PARAMETERS OF THE VULNERABILITY FORM).	161

FIGURE 187: CAPACITY ACCELERATIONS OF THE STRUCTURES, A_{GC} , WITH THE TIE-RODS	162
FIGURE 188: LAST DISPLACEMENT (CAPACITY DISPLACEMENT) OF THE STRUCTURE WITH THE TIE-RODS EFFECTIVE	162
FIGURE 189: CAPACITY ACCELERATIONS OF THE STRUCTURES, A_{GC} , WITH AND WITHOUT THE INFLUENCE OF THE TIE-RODS.	163
FIGURE 190: LAST DISPLACEMENT (CAPACITY DISPLACEMENT) OF THE STRUCTURE WITH AND WITHOUT THE TIE-RODS.	163
FIGURE 191: LAST DISPLACEMENT (CAPACITY DISPLACEMENT) OF THE STRUCTURE FOR THE COLLAPSE OF SLABS (CS).	163
FIGURE 192: SAFETY INDEXES FOR THE 189 PANELS FOR THE 4 ANALYSES (RIGHT: ZOOM).....	163
FIGURE 193: DISTRIBUTION OF THE CLASSES OF THE P4 PARAMETER WITH THE TWO DEFINITION OF THE BARYCENTRE.....	170
FIGURE 194: EXAMPLE OF THE REAL BARYCENTRE POSITION OF THE REAL BARYCENTRE AND THE BARYCENTRE OF THE FULL AREA FAÇADE.	171
FIGURE 195: EXAMPLE OF DIFFERENT POSITION OF THE BARYCENTRE FOR DIFFERENT NUMBERS OF FLOORS.	172
FIGURE 196: MULTI-LINEAR REGRESSION FOR THE ESTIMATION OF THE A_{GC} WITH 5 PARAMETER AND WITH 4 PARAMETERS.	176
FIGURE 197: TREND OF REAL AND ESTIMATED CAPACITY FOR THE FAÇADES OF CASTELNUOVO, FOR THE TWO FAÇADES FORMS.	177
FIGURE 198: TREND OF REAL AND ESTIMATED CAPACITY (5-PARAMETERS) FOR THE FAÇADES AND CONTRIBUTION OF ALL PARAMETERS.....	177
FIGURE 199: REAL AND ESTIMATED INDEXES OF SAFETY FOR THE FAÇADES OF CASTELNUOVO, FOR THE TWO FAÇADES FORMS.	177
FIGURE 200: REAL AND ESTIMATED INDEXES OF SAFETY FOR THE FAÇADES OF CASTELNUOVO, FOR THE TWO FAÇADE FORMS: ZOOM.....	178
FIGURE 201: CASA VASARI MUSEUM, AERIAL PHOTO, PLAN, REAR AND FRONTAL FAÇADE WITH THE INDIVIDUATION OF THE STUDIED MECHANISMS..	179

LIST OF TABLES

TABLE 1: NOMINAL LIFE FOR DIFFERENT TYPE OF BUILDINGS.	7
TABLE 2: COEFFICIENT C_U	7
TABLE 3: PROBABILITY OF EXCEEDANCE (P_{VR}) IN THE REFERENCE PERIOD (V_R).	8
TABLE 4: GEOGRAPHIC COORDINATES.	8
TABLE 5: SPECTRAL FEATURES OF THE SEISMIC HAZARD FOR CASTELNUOVO FOR DIFFERENT LIMIT STATES.	8
TABLE 6: GROUND TYPES.	9
TABLE 7: EXPRESSIONS OF S_s AND C_C FOR DIFFERENT SOIL TYPE.	9
TABLE 8: TOPOGRAPHIC TYPES.	10
TABLE 9: SPECTRAL FEATURES OF THE SEISMIC HAZARD FOR CASTELNUOVO FOR DIFFERENT GROUND TYPE.	12
TABLE 10: COEFFICIENTS $C_{K,AG}$ FOR THE ELASTIC SPECTRUM IN TERM OF ACCELERATION.	12
TABLE 11: INTENSITY DEGREES FROM VI TO XII OF EMS-98 SCALE.	14
TABLE 12: CLASSES OF PARAMETER 15 AND POSSIBLE CONFIGURATIONS OF MISALIGNMENTS OF OPENINGS IN SS.UU..	28
TABLE 13: DESCRIPTION OF THE 5 PARAMETERS AND CLASSES OF THE VULNERABILITY FORM (FERREIRA ET AL., 2012).....	29
TABLE 14: MAXIMUM INFLUENCE OF EACH PARAMETER IN GNDT (11P) AND FORMISANO (15P) VULNERABILITY FORM.	32
TABLE 15: CORRELATION BETWEEN THE I_V AND THE V PARAMETERS FOR VULNERABILITY CLASSES (BERNARDINI, ET AL., 2007).	35
TABLE 16: AGGREGATION TYPE: STATISTICS AND HISTOGRAM.	45
TABLE 17: AGGREGATION TYPE AND STRUCTURAL POSITION FOR MASONRY AGGREGATES: STATISTICS AND HISTOGRAM.	45
TABLE 18: MECHANICAL CHARACTERISTICS OF STONE MASONRY.....	46
TABLE 19: PARTITION WALLS' TYPE AND LOADS.....	49
TABLE 20: ROOF SYSTEM 1: CHARACTERISTICS AND WEIGHTS.....	50
TABLE 21: ROOF 2 AND 3: LOADS IN kN/m^2	51
TABLE 22: FLOOR SYSTEM 1: CHARACTERISTICS AND WEIGHTS.....	52
TABLE 23: FLOOR TYPES 2 AND 3: LOADS IN kN/m^2	53
TABLE 24: FLOOR TYPES 4 AND 5: LOADS IN kN/m^2	53
TABLE 25: CONFIDENCE FACTORS (CF) AND KNOWLEDGE LEVEL.	55
TABLE 26: HOW GETTING THE KNOWLEDGE LEVELS.	55
TABLE 27: MECHANICAL DESIGN CHARACTERISTICS OF STONE MASONRY ($KL2 \rightarrow CF=1.2$).	56
TABLE 28: DISTRIBUTION % OF REAL DAMAGE LEVEL IN SS.UU. (IN TERMS OF SS.UU. AND VOLUME) AND FOR MASONRY AGGREGATE ONLY.....	62
TABLE 29: DISTRIBUTION % OF DAMAGE AND POSITION OF SS.UU (IN TERMS OF VOLUME).....	63
TABLE 30: DISTRIBUTION % OF DAMAGE AND POSITION OF SS.UU (IN TERMS OF VOLUME) FOR STONE MASONRY AGGREGATES.....	63
TABLE 31: INFORMATION QUALITY AND RELIABILITY OF THE PARAMETERS.	66
TABLE 32: DISTRIBUTION OF THE CLASS WITHIN THE 5 PARAMETERS FOR 72 AGGREGATE.	68
TABLE 33: CHARACTERISTICS OF THE BUILDING STOCK WITH REFERENCE TO THE AGGREGATE FORM.	69
TABLE 34: AGGREGATE FORM RESULTS FOR AGGREGATE 11-125 AND 66-583.	69
TABLE 35: DISTRIBUTION % OF ESTIMATED DAMAGE LEVEL.....	74
TABLE 36: DISTRIBUTION OF THE CLASS FOR THE 11P FOR 124 SS.UU.....	91
TABLE 37: SAMPLE CORRELATION COEFFICIENTS FOR GNDT (11P.) PARAMETERS AND CLASSES OF LOCAL MECHANISMS IN FAÇADES.....	106
TABLE 38: SAMPLE CORRELATION COEFFICIENTS FOR AVEIRO AND FORMISANO PARAMETERS AND LOCAL MECHANISMS CLASSES IN FAÇADES.	107
TABLE 39: DISTRIBUTION OF % IN DIAGONAL AND TRI-DIAGONAL, UPPER SUM AND LOWER SUM FOR THE MOST CORRELATED COEFFICIENTS.	108
TABLE 40: TYPE OF MECHANISMS AND EXAMPLES IN CASTELNUOVO FAÇADES (DRAWINGS FROM CIAVATTONE MASTER THESIS, UNIFI).	114
TABLE 41: AGGREGATE 10-088 AND 30-283 MAIN FAÇADES: REAL PHOTO AND OVERTURNING REPRESENTATIONS.....	122
TABLE 42: GEOMETRY AND LOADS DATA: INPUT FOR THE KINEMATIC LINEAR AND NON-LINEAR ANALYSIS.....	123
TABLE 43: RESULTS FOR THE LINEAR ANALYSES.	124
TABLE 44: RESULTS FOR THE NON-LINEAR ANALYSES.	125
TABLE 45: RESULTS FOR THE NON-LINEAR ANALYSES, IN THE CASE OF COLLAPSE OF FLOOR FOR MAXIMUM DISPLACEMENT OF 15 CM.	125
TABLE 46: DIFFERENCES AMONG THE SAFETY INDEXES.....	125
TABLE 47: GEOMETRY AND LOADS FOR PANELS (Z IS THE HEIGHT OF THE HINGE FROM THE FOUNDATION SOIL).	130
TABLE 48: STRENGTHS AND DISTANCE OF RETRACTION OF THE HINGE.	130

TABLE 49: RESULT FOR OUT-OF-PLANE MECHANISM WITH AND WITHOUT CONSIDERING THE HINGE RETRACTION.	131
TABLE 50: MECHANICAL CHARACTERISTICS OF DISORGANISED STONE MASONRY.	132
TABLE 51: TIE-ROD FORCE - CASE OF SQUARED PLATED.....	133
TABLE 52 TIE-ROD FORCE - CASE OF REAL BOLTED PLATED.....	133
TABLE 53: GEOMETRY AND LOADS FOR PANELS.	134
TABLE 54: RESULTS FOR LINEAR AND NON-LINER ANALYSIS FOR THE STANDARD CASE ($FC=1.35$).	143
TABLE 55: VARIATION OF THE RESULTS OF THE LINEAR AND NON-LINEAR ANALYSES FOR GEOMETRICAL AND LOADING PARAMETERS VARYING.	150
TABLE 56: PANEL GEOMETRY.....	153
TABLE 57: PANEL MASONRY CHARACTERISTICS.....	153
TABLE 58. ULTIMATE VALUES OF THE SHEAR FORCE.....	153
TABLE 59. GEOMETRICAL CHARACTERISTICS OF THE MASONRY IDEAL PANELS, LOADS AND VALUE OF THE ULTIMATE SHEAR.	154
TABLE 60. MASONRY WALLS INVESTIGATED.	154
TABLE 61: FAÇADE FORM: DEFINITION OF THE PARAMETERS AND THEIR CLASSES.....	166
TABLE 62: CLASSES OF P1 AND DISTRIBUTION OF THE CLASSES AMONG THE SAMPLE OF STUDY OF CASTELNUOVO FAÇADES.	168
TABLE 63: CLASSES OF P2 AND DISTRIBUTION OF THE CLASSES AMONG THE SAMPLE OF STUDY OF CASTELNUOVO FAÇADES.	168
TABLE 64: CLASSES OF P3 AND DISTRIBUTION OF THE CLASSES AMONG THE SAMPLE OF STUDY OF CASTELNUOVO FAÇADES.	169
TABLE 65: CLASSES OF P4 AND DISTRIBUTION OF THEIR JUDGMENTS AMONG THE SAMPLE OF STUDY OF CASTELNUOVO FAÇADES.....	170
TABLE 66: BARYCENTRE JUDGMENTS DISTRIBUTION AMONG THE SAMPLE OF STUDY OF CASTELNUOVO FAÇADES.	172
TABLE 67: COMBINATION OF MECHANISMS I_s AND LEVEL OF DAMAGE TAKEN INTO ACCOUNT FOR THE SAMPLE OF DATA.....	173
TABLE 68: PEAK GROUND ACCELERATIONS OF CAPACITY AND SAFETY INDEXES.	180
TABLE 69: SAFETY INDEXES CLASSES FOR CASA VASARI PANELS.	183

INTRODUCTION

The seismicity of the Italian territory is one of the highest both at European and at world level. Only considering the last fifty years, earthquakes caused about 4500 casualties and more than 110 billion Euros were spent for the reconstruction. Moreover, Italian earthquakes produced high damages on buildings, as well as foreign ones, but the latter characterised of related energy more than 10 times higher (Dolce, 2004). The reason of these wide differences is probably due to the high vulnerability of the Italian real estate characterised by historical and old buildings, which do not guarantee adequate seismic resistance. The vulnerability assessment for existing buildings, the knowledge of the propensity of a structure to suffer damage when an earthquake occurs, is a key aspect for the seismic risk mitigation (C.M. n.617, 2009).

Scientific Italian community have been moved in the seismic risk mitigation since the first years of 1900, through the seismic zoning and the introduction of seismic codes.

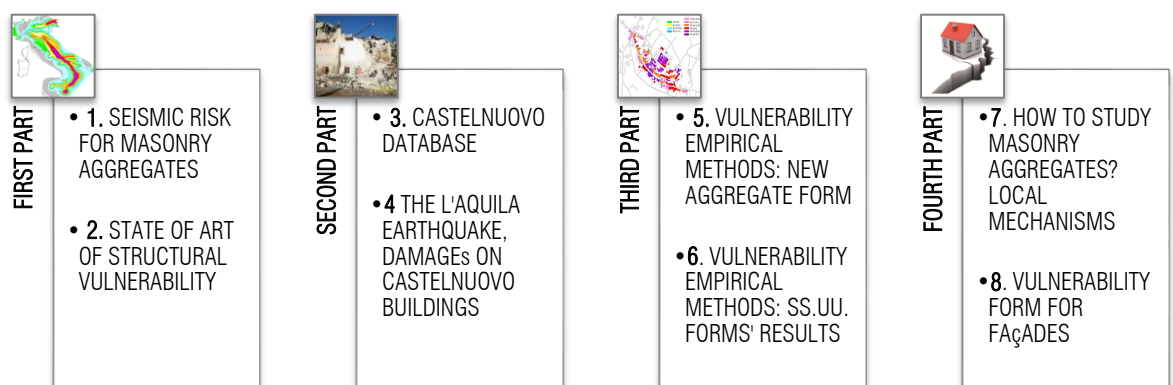
In particular, the earthquake that hit the Abruzzo region in 2009, and the damage that has affected most of the urban centers of the "L'Aquila valley", have dramatically highlighted the necessity to address strengthening and improvement interventions in buildings in aggregate, according to a specific methodology, proper for the peculiarity of these structures. Aggregates are often characterized by a wide structural variety because they are the result of a complex historical and temporal process of evolution. Structural units that compose them may differ on geometry, materials, methods of construction, status of conservation and Code used to design the structural project that make the structure even more susceptible to the seismic actions.

In the last years, attention has been paid in developing adequate prevention policy for the strengthening retrofitting of old buildings; considering the limited amount of the economic resources, the seismic risk assessment is of primary importance in order to set up a priority list of intervention.

In detail, Castelnuovo, a village in the L'Aquila valley (center of Italy, Abruzzo Region), was assumed as case study to develop seismic vulnerability analyses in this thesis. The choice of this village is due to the past experience that the DICEA (Department of Civil and Environmental Engineering)'s team has been performed there in consequence of the earthquake of 06/04/2009 that hit the hamlet. This occurrence, though it has to be remembered as a catastrophic event that destroyed the country, has allowed to understand how the masonry ancient aggregates could behave against seismic actions.

OUTLINE

The thesis is organized in 8 Chapters. The chapters can be grouped in four parts, following the scheme below.



The first part, corresponding to Chapter 1 and 2, focuses on the principal main aspects of the work and describes the motivations behind the selection of this research topic, the literature review and the presentation of some preliminary concepts. In particular, Chapter 1 shortly describes the main themes of the research and it explains a general overview of risk assessment focusing on the determination of the seismic hazard. Chapter 2 reviews existing structural vulnerability methods.

The second part, corresponding to Chapters 3 and 4, describes the case study, which is represented by the aggregates of the small historical city centre of Castelnuovo, to whom the vulnerability methods have been applied. In particular, Chapter 3 describes, after a brief paragraph of the historical aspects, the sample of data collected, which refers to 74 aggregates of Castelnuovo (San Pio delle Camere Municipality, AQ - Abruzzo Region), hit by the earthquake of 06/04/2009. The results obtained from the statistical analysis of the information collected during the surveys are reported. In the first part of Chapter 4 there is the description of the mainshock of the L'Aquila earthquake and its main characteristics. The second part shows the level of damage suffered by the aggregates of Castelnuovo with identification of crack patterns and type of damages.

The third part is composed by Chapter 5 and 6, in which there are the results of the application of the Vulnerability Empirical Methods to the case study of Castelnuovo. In particular, in Chapter 5, the results coming from the vulnerability assessment of Castelnuovo through an Aggregate Form are reported. Starting from the vulnerability results campaign, a damage scenario has been associated to each aggregate and compared with the real damage scenario observed after the 2009 earthquake on aggregates. Using the information achieved during the in situ surveys over the aggregates and by the critical analysis of the real damages, in the last part of the chapter an improvement of the Vulnerability Form is presented, with the association of a new parameter that evaluates the conservation state of the aggregates. In Chapter 6, the same procedure is presented at the scale of the structural units within the aggregate, considering different type of ss.uu. Form present in scientific literature. The results of the vulnerability analyses have been combined and crossed with the real damages that structural units have showed after the earthquake, in terms of both global and local mechanisms.

The fourth part is composed by Chapter 7 and 8. Chapter 7 provides the general rules to study masonry structures in aggregates through detailed analysis, both in a local and global way, as typical of the existing masonry structures. Afterwards, the choice of the methodology to evaluate the seismic capacity for a structural unit has been identified with the kinematic linear and non-linear analysis of out-of-plane mechanisms. That choice is due to different aspects, as the particular structural technologies in Castelnuovo database (very similar to the zones of centre of Italy as Tuscany, Abruzzo or Umbria Regions), the particular type of masonry of those zones (poor quality mortar and irregular stone with the identification of multi-leaf brickmasonry), the damages that has been critically analysed in aggregates and the results of different seismic analysis performed in case studies within the Castelnuovo database.

A Vulnerability Form for Façades able to evaluate the seismic capacity towards the out-of-plane mechanisms of overturning system is then defined in final Chapter 8, exploiting the overall detailed analyses done on the database of structural units of Castelnuovo aggregates.

CHAPTER 1. SEISMIC RISK ANALYSIS FOR BUILDINGS IN AGGREGATE

The chapter provides a general overview of the main features and concepts of the thesis. It describes the masonry aggregate buildings that are the most representative construction type in historical city centres and, within the seismic risk assessment, it provides an introduction of the vulnerability evaluation.

1.1 SEISMIC RISK FOR MASONRY AGGREGATES

The Italian territory, such as other European Countries, is currently defined as a totally seismic area. Historical city centres in Italy are generally made of masonry load-bearing buildings in aggregate. The evaluation of seismic risk of this kind of structures represents a current research issue, especially after last seismic main events like the earthquake of L'Aquila, (M_w 6.3, 06/04/2009 06, 01:32:UTC, Figure 1) or Emilia Romagna (M_w 5.9 29/05/2012, 07:00UTC and M_w 5.8 31/05/2012 14:58 UTC) (<http://www.ingv.it/it>). Those events dramatically highlight the high vulnerability of the masonry aggregates and, in parallel, the necessity of the definition of specific procedures to assess seismic risk on such particular buildings, in order to both reduce human and environmental risk and to mitigate destruction of cultural heritage building stock.



Figure 1: Palace in L'Aquila and Castelnovo (aerial view) after the earthquake.

For years, since the beginning of the 70s, seismic scientific research has developed a strong interest for the assessment of seismic risk in the historic city centres, in which the buildings, mainly assembled in aggregate, are made in load-masonry buildings. Furthermore, recent past seismic events originated many human losses, several damages on building stock of many historical city centres, and, as a consequence the destruction of cultural heritage. Indeed, many investigation campaigns of vulnerability in historical centres or in strategic and relevant public buildings have been promoted by Public Administrations. The goal was to get a ranking of most vulnerable buildings in order to define a prioritization scale of strengthening interventions in structures with greater vulnerability to focus on them primarily Administration resources. It is worth nothing that, for existing structures, the mitigation of the seismic risk, necessary passes through the reduction of the structural vulnerability of structures (Chiarandini, UniUD).

An *aggregate* is a group of structural units, not necessarily homogeneous, interacting with each other by more or less effective links. Generally, in historical centres, an aggregate can assume the shape of an urban block, spatially defined by streets in front and rear sides or defined by public spaces (Figure 2). Examples of aggregates are reported in Figure 2.

A *structural unit* (s.u.) is the portion of a building that possesses structural continuity from top to the bottom, characterized by a common manufacturing process or by vertical and horizontal homogeneous elements that contribute to the uniform distribution of vertical and horizontal loads (Borghini et al., 2011). The Italian actual code (NTC, 2008, par. 8.7.1) also expresses the definition of the structural units as a "...building which has structural continuity from the ground until the top for the gravity loads and it is normally delimited by open spaces, structural joints or buildings realized with different construction methods..."(Figure 3, in red).

Seismic vulnerability of masonry aggregates is due to both the intrinsic characteristics of the masonry that constitutes the buildings (class of buildings, quality of stones and mortar, etc...) and to the particular configurations and features of the

aggregates (geometry, plan shape, number of structural units within the aggregate, position of ss.uu., connections,...). The adjacent ss.uu. have generally different seismic behaviour and, therefore, they may produced unexpected effects in themselves.

Aggregates are often characterized by a wide structural variety because they are the result of a complex historical and temporal process of evolution (Figure 4, Figure 5) (Giuffrè & Carocci, 1999) (Carocci, 2001) (Indelicato, 2010). Structural units that compose them may differ on geometry, materials, methods of construction, status of conservation and Code used to design the structural project. The evolution process implies that in an aggregate only a few houses are constituted by close masonry cells. Only the perimeter walls carried out contemporarily have, for instance, a correct organization of the angular connections (Carocci, 2001)(Figure 4). Strictly linked to the latter aspects, the structural units can have different type of connections among their principal walls, issue that mostly influences their ways to respond and collapse against seismic actions (ReLUIS, 2010). If the main façades are not well linked to the orthogonal walls, they show major propensity to collapse in local way, overturning in the orthogonal direction to their development or creating vertical bending (§7.2). Staggered floors are frequent if the ss.uu. in the aggregate were not built in a same period, as well as when the aggregate lays on a slope (characterised by inclination of the ground). These two factors, in addition to the possibility of realisation in different materials for the contiguous structural units, with sometimes different numbers of floors, made the aggregate very susceptible to the seismic actions which can involve interaction between the ss.uu. and pounding phenomenon.

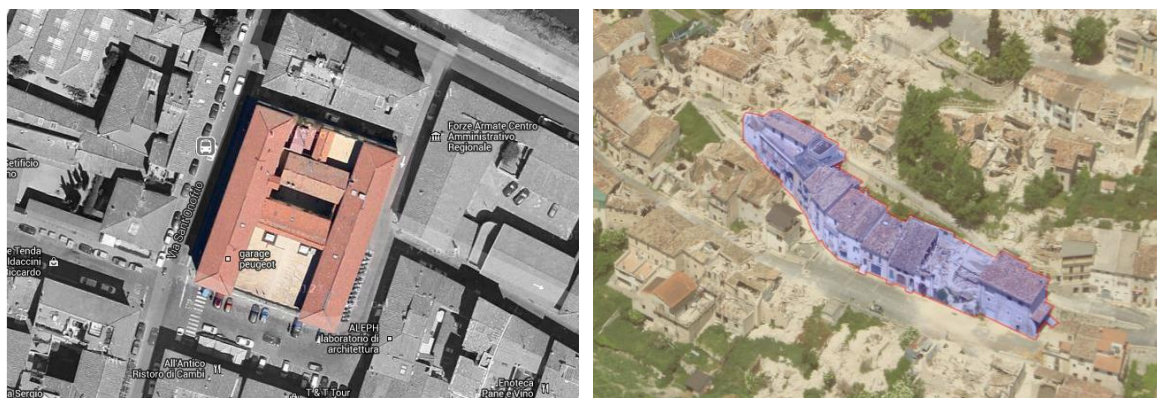


Figure 2: Examples of masonry aggregates: in the centre of Firenze (a) and in Castelnuovo (AQ) (b).

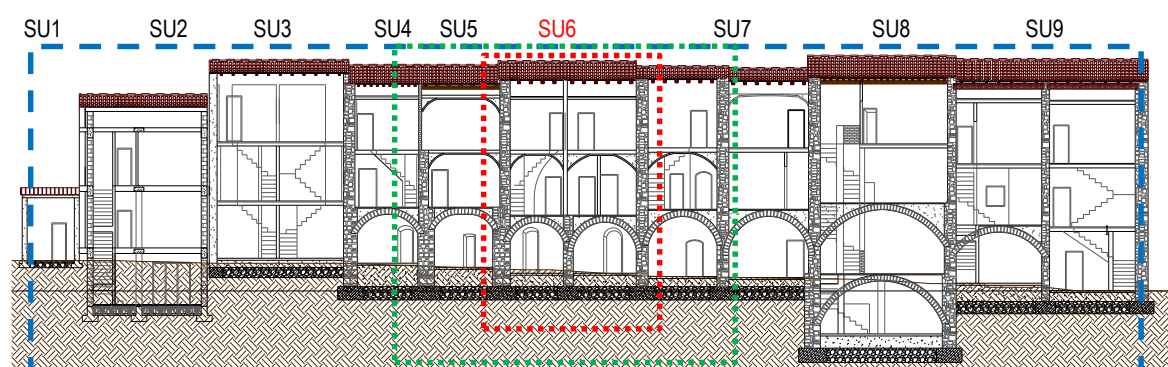


Figure 3: Aggregate (in blue) and structural units. In red SU6, in green an example of AMU, analysis minimum units.

On the base of the evaluation of the crack patterns of post-earthquake surveys, on the architectonic and environmental features, and keeping into account the historical evolution of the process of construction, within an aggregates, the *intervention minimum units* (IMU) can be individuated. They are indeed defined as "...the ss.uu. consisting of several buildings where the repair, restoration and seismic strengthening or reconstruction must be designed jointly, to be implemented through a single construction project..." (LR, 2012) (ReLUIS, 2010). It means that the ss.uu. part of the IMU are those with the same architectonical and structural characteristics able to show a unitary behaviour vs seismic actions.

Different meaning have the AMU, *analysis minimum units*. They are defined as “...the portions of the aggregate in respect of which it is possible (but also recommended) to evaluate all the effects of interaction between constituent units... (ReLUIS, 2010)”. The AMU is not known a priori and currently there is not a recognised and standardize criterion in the actual Code to identify them (in green in Figure 3). Anyway, the individuation of the AMU is necessary when a detailed analysis should be performed in a s.u.. It allows to take under control the possible interactions resulting from structural contiguity with the adjacent buildings, as required by the technical standards to design structural strengthening interventions.

A *façade* is in this thesis considered as the “principal main *structural* wall of the s.u.”. It is in front of the main street for internal structural units and both the lateral and frontal for the corner or header structural units (Figure 23). The *façades* are one of the elements of major vulnerability, since they can overturn in the public streets or spaces if excited by a seismic action in the direction orthogonal their development, if no restraints with the orthogonal walls or slabs are present in the aggregates.

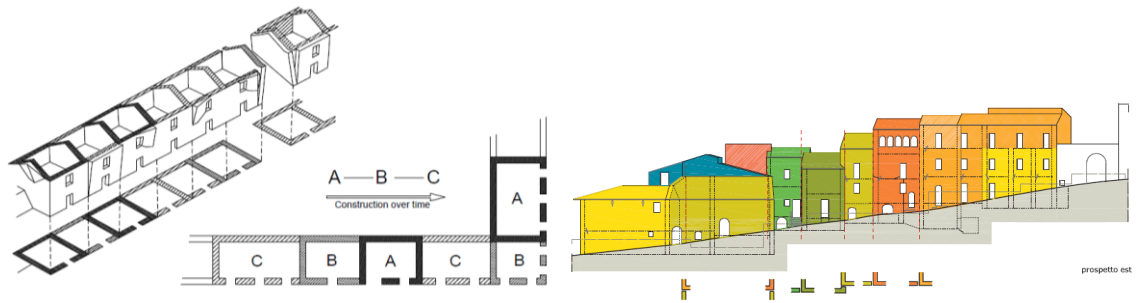


Figure 4: Aggregate evolution: individuation of the inner core and the secondary cells (right picture in Indelicato, 2010).

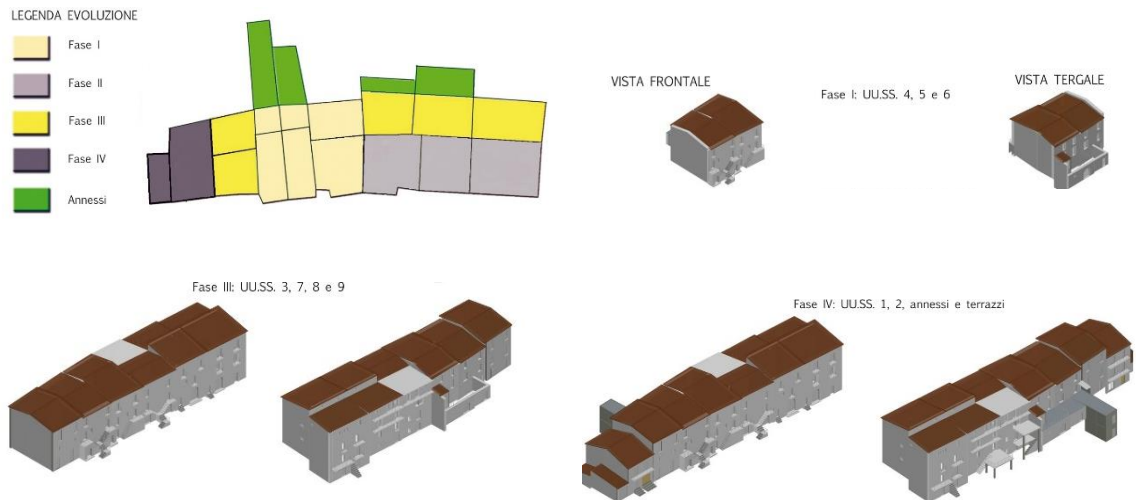


Figure 5: Evolution process of aggregate (10-088).

§

Risk is defined as the potential of negative consequences of hazardous events that may occur in a specific area in a period of time. In particular, seismic risk measures the potential of economic, social and environmental consequences of a seismic events (Giovinazzi, 2005, http://www.protezionecivile.gov.it/jcms/it/descrizione_sismico.wp). An in deep overview of the issues related to the seismic risk can be found in Dolce et al. (1994).

The seismic risk can be expressed as a mathematical relationship of convolution of three different aspect of a certain area, as reported in eq.(1):

$$(1) R_{ie}|T = |(H_i) \otimes (V_e) \otimes E|_T$$

R is the seismic risk, defined as the probability of exceedance of a certain level of loss in a certain period of time (T) of a certain exposed element (E) for a seismic event of fixed I intensity.

H is the seismic Hazard, is the probability that in a certain period of time (T) an earthquake of I intensity happens in reference territory.

Exposure (E) represents the measure of the objects' values exposed to the seismic risk. It takes into account the direct price of structural and non-structural elements, as well as indirect prices associated with the discontinuation of services and communications but also the social prices. The exposure mainly depends on location, accessibility, level and type of employment, function of the building and the presence of economic goods and historic/cultural services (www.protezionecivile.gov.it and Zuccaro, 2004).

Vulnerability V (of the exposed elements E) is defined as the measure of structures propensity to suffer damage when the earthquake of I intensity occurs. Vulnerability depends on the intrinsic structure characteristics and predispositions and it is not influenced by the external loads.

A study of vulnerability of structures has always the main goal to establish a set of tools able to provide a predict damage on buildings, doing in this way a *risk analysis* (D'Ayala & Novelli, 2010). If in CHAPTER 2 there is a global overview of all the *vulnerability* methods used in last years to assess structural vulnerability on masonry structures and aggregates, on the following, some definitions for the assessment of *hazard* are provided. For what concern the *exposure*, the thesis refers to masonry aggregates, typical buildings of the historical city centres, considering them in the structural point of view, (without any references to human or economic, artistic or cultural resources).

1.1.1 SEISMIC HAZARD

Seismic hazard of the territory expresses the probability that, in a given area and in a certain period of time, an earthquake of a given intensity occurs. Nowadays, in Italy the seismicity of a territory, in absence of more accurate geotechnical investigations, is defined by the structural Code, in terms of the peak ground acceleration ($PGA=a_{gc} \cdot S$, see paragraph 1.1.1.1) and response spectra the latter both in accelerations and displacements.

The description of the major issues linked to the seismic hazard for a territory, following the recommendations of the Code, and the description of the major macroseismic intensity scales to date used are provided in the following paragraph.

1.1.1.1 PEAK GROUND ACCELERATION AND RESPONSE SPECTRA

The most common physical parameters to describe the amplitude of the ground motion of a given earthquake are the peak ground acceleration (PGA) and the response spectrum in acceleration. The PGA for a given component of earthquake is the largest value of horizontal acceleration obtained from accelerogram of that component, in a specific territory.

The response spectrum describes the maximum response of a Single-Degree-Of-Freedom (SDOF) system to a particular input motion as a function of its natural period and damping ratio (usually 5.0%) (NTC, 2008). The SDOF's response may be expressed in terms of acceleration, velocity or displacement. The maximum values of each of these parameters depend only on the natural frequency and damping ratio of the SDOF system. The response spectrum in terms of acceleration for the natural period equal to zero assumes the value of PGA.

1.1.1.1.1 Definition of the response spectra

To provide seismic hazard of the Italian territory, Standard (NTC, 2008) (C.M. n.617, 2009) divided Italian territory in grids of 5x5 kilometres. For each point of the grid line, parameters of the seismic hazard were identified. The three base parameters of the seismic hazard are:

- the peak ground acceleration a_g (for A category of soil [rock] and T_1 topography category, see below), in g unit;
- the T_C^* , the upper limit of the period of the constant spectral acceleration range;
- the maximum amplification factor F_0 of the spectrum in acceleration.

The peak ground acceleration (a_g) and the ordinates of the elastic response spectrum in acceleration $S_e(T)$ are relative to a fixed probability of exceedance for a individuated state limit (P_{VR}) in a period of reference (V_R).

The National Institute of Geophysics and Volcanology makes available interactive maps of seismic hazard through which

obtain a distribution of the maximum PGA (a_g) for the common interests [<http://esse1-gis.mi.ingv.it/>]:

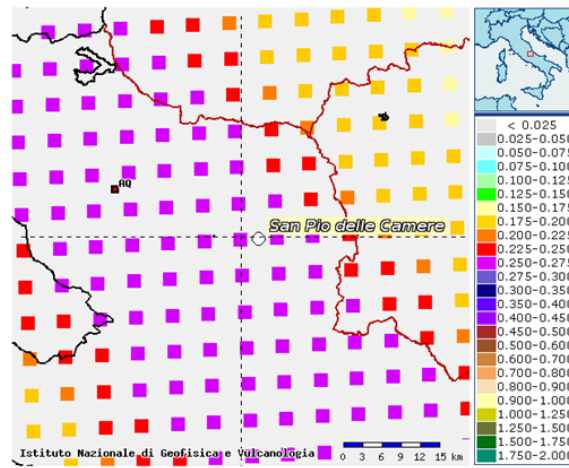


Figure 6: Interactive map of seismic hazard for the City of St. delle Camere (AQ) for a P_{VR} of 10% in 50 years.

Nominal life and reference period

For the determination of the seismic action, for each limit state, it is necessary to fix the period of reference V_R of the construction and determine the probability of exceedance in the reference period (P_{VR}). The period of reference, V_R , is individuated by the multiplication of the nominal life of the structure V_N and the use coefficient C_U (Table 2 and §2.4.1 of (NTC, 2008)):

$$(2) \quad V_R = V_N \cdot C_U$$

V_N is defined as the number of years in which the structure, with ordinary interventions, is used for the goal it was built for. Depending on the type of the structure a V_N is assigned in the table 2.4.I of NTC 2008 (Table 1).

Table 1: Nominal life for different type of buildings.

CONSTRUCTION TYPE		NOMINAL LIFE V_N [YEARS]
1	Provisional building – structure in construction phase	≤ 10
2	Ordinary building, bridges, infrastructural buildings, dams of small dimension	≥ 50
3	Big buildings of big dimensions or strategic relevance	≥ 100

In presence of seismic actions, with reference to the consequences of an interruption of the operativity or collapse, the constructions are divided into *use classes* (namely “importance class” in EC8):

- Class I: Buildings with only occasional presence of people, agricultural buildings;
- Class II: Buildings the use of which provides normal crowds, no content dangerous to the environment and without essential public and social functions...;
- Class III: Buildings the use of which provides significant crowding;
- Class IV: Buildings with public functions or strategic importance, also with reference to the management of civil protection in the event of disasters (buildings whose integrity is of vital importance for civil protection...).

For each *use class* the table 2.4.II NTC 08 (Table 2) provides the relevant coefficient of Use C_U .

Table 2: Coefficient C_U .

Use class	I	II	III	IV
Coefficient C_U	0.7	1.0	1.5	2.0

The definition of the seismic actions should be possible for all the reference period and all limit states considered in NTC 08. It is convenient to use, as a parameter characterizing the seismic hazard, the return period of the seismic action, T_R , expressed in years. Fixed V_R , the two parameters T_R and P_{VR} are expressible by the expression:

$$T_R = -\frac{V_R}{\ln(1-P_{VR})}$$

Limit state and probability of exceedance

At 3.2.1 of NTC 2008, there are the definitions of the different limit state for seismic verifications. Two are the limit states for *damage limitation* state:

- Operativity limit state, OLS (SLO, in italian);
- Damage limit state DLS (SLD in italian);

Two are the *ultimate* limit states:

- Preservation of life limit state (SLV);
- Collapse limit state CLS (SLC, in italian).

The probability of exceeding a given T_R , P_{VR} , is shown in Table 3.

Table 3: Probability of exceedance (P_{VR}) in the reference period (V_R).

LIMIT STATE		P_{VR} : PROBABILITY OF EXCEEDANCE IN THE REFERENCE PERIOD V_R
Damage limitation state	SLO	81%
	SLD	63%
Ultimate limit state	SLV	10%
	SLC	6%

Following the criteria exposed, nominal life and use class are individuated for the aggregates of Castelnovo.

Nominal Life: $V_N \geq 50$ years (costruction type n.2);

Use class II, use coefficient, C_U equal to 1.

Reference life is $V_R = V_N \cdot C_U$ equal to 50 years.

Castelnovo is characterised by the following geographic coordinates (WGS84):

Table 4: Geographic coordinates.

Latitude	42°17'41.98" N
Longitude	13°37'40.18" E

The return period of the seismic actions for each of the considered Limit State, and the features of the expected seismic hazard for the site of Castelnovo site are resumed in Table 5:

Table 5: Spectral features of the seismic hazard for Castelnovo for different limit states.

LIMIT STATE	T_R [years]	a_g [g]	F_0	T^*_c [s]
SLO	30	0.078	2.379	0.274
SLD	50	0.103	2.325	0.283
SLV	475	0.257	2.367	0.345
SLC	975	0.331	2.404	0.363

Response spectra

The elastic response spectrum in acceleration is defined by the following expressions:

- (3) $0 \leq T < T_B$ $S_e(T) = a_g \cdot S \cdot \eta \cdot F_0 \cdot \left[\frac{T}{T_B} + \frac{1}{\eta \cdot F_0} \left(1 - \frac{T}{T_B} \right) \right]$
- (4) $T_B \leq T < T_C$ $S_e(T) = a_g \cdot S \cdot \eta \cdot F_0$
- (5) $T_C \leq T < T_D$ $S_e(T) = a_g \cdot S \cdot \eta \cdot F_0 \cdot \left(\frac{T_C}{T} \right)$
- (6) $T_D \leq T$ $S_e(T) = a_g \cdot S \cdot \eta \cdot F_0 \cdot \left(\frac{T_C T_D}{T^2} \right)$

In which T and $S_e(T)$ are, respectively, the vibration period and the horizontal acceleration spectral coordinate.

S is the coefficient that takes into account the ground type and topographical condition, $S = S_S \times S_T$. S_S is identified in

Table 7 for different ground types and S_T is defined in Table 8.

η is a coefficient depending the viscous damping; it is 1 for damping coefficient equal to 5%;

F_0 maximum amplification factor of the spectrum in acceleration;
 T_C is the period corresponding to the beginning of the constant velocity range in the spectrum, $T_C = T_C^* C_C$. C_C is defined in Table 7.
 T_B is the period corresponding to the beginning of the constant acceleration range of the spectrum $T_B = T_C/3$;
 T_D is the period corresponding to the beginning of the constant displacement range: $T_D = 4.0 \cdot a_g/g + 1.6$.

Ground type

In the spectrum expressions the ground effect is taken into account with the coefficients S and C_C , considering different spectra for the dynamic amplification connected with the fundamental frequencies of soil-structures. In paragraph §3.2.2 NTC 2008 (and at European level at Table 3.1 of (EC8, 1998)) is shown how to characterize a soil. There are five categories (Table §3.2.II) from "A" to "E", describing the soil stratigraphic profiles and characteristics. The site will be classified according to the value of the average shear wave velocity, $v_{s,30}$, if available. Otherwise the value of N_{SPT} should be used (Standard Penetration Test)¹.

Table 6: Ground types.

GROUND TYPE	DESCRIPTION OF STRATIGRAPHIC PROFILE	PARAMETERS		
		$V_{s,30}$ (m/s)	N_{SPT} (blows/30cm)	C_U (kPa)
A	Rock or other rock-like geological formation, including at most 5 m of weaker material at the surface	>800	-	-
B	Deposits of very dense sand, gravel, or very stiff clay, at least several tens of m in thickness, characterised by a gradual increase of mechanical properties ..	360-800	>50	>250
C	Deep deposits of dense or medium dense sand, gravel or stiff clay with thickness from several tens to many hundreds of m	180-360	15-50	70-250
D	Deposits of loose-to-medium cohesionless soil (with or without some soft cohesive layers), or of predominantly soft-to-firm cohesive soil	<160	<15	<70
E	A soil profile consisting of a surface alluvium layer with v_s values of type C or D and thickness varying between about 5 m and 20 m..	-	-	-

Table 7: Expressions of S_S and C_C for different soil type.

GROUND TYPE	S_S	C_C
A	1.00	1.00
B	$1.00 \leq 1.40 - 0.40 \cdot F_0 \cdot \frac{a_g}{g} \leq 1.20$	$1.10 \cdot (T^* C_C)^{-0.20}$
C	$1.00 \leq 1.70 - 0.60 \cdot F_0 \cdot \frac{a_g}{g} \leq 1.50$	$1.25 \cdot (T^* C_C)^{-0.33}$
D	$0.90 \leq 2.40 - 1.50 \cdot F_0 \cdot \frac{a_g}{g} \leq 1.80$	$1.05 \cdot (T^* C_C)^{-0.50}$
E	$1.00 \leq 2.00 - 1.10 \cdot F_0 \cdot \frac{a_g}{g} \leq 1.60$	$1.15 \cdot (T^* C_C)^{-0.40}$

Topographical conditions

For surface configurations can be adopted the classification of Table 3.2.IV (NTC, 2008). Once the topographic category has been individuated, the table 3.2.VI (Table 8) provides the values of the coefficient S_T , which is necessary to derive the horizontal spectral acceleration. In the graphs in Figure 7, T_1 category is considered: "Flat country, slopes and isolated hills with average inclination $i \leq 15^\circ$ ".

¹ There are other two ground types S_1 and S_2 (not written in Table 7) for which special studies for the definition of the seismic action are required. For these types, and particularly for S_2 , the possibility of soil failure under the seismic action may be considered.

Table 8: Topographic types.

TOPOGRAPHIC TYPE	DESCRIPTION OF TOPGRAPHIC TYPE	TOPOGRAPHIC COEFFICIENT
T_1	Flat country, slopes and isolated hills with average inclination $i \leq 15$	1
T_2	Slope with average inclination $i > 15$	1.2
T_3	Elevation with crest width much smaller than the base and average inclination $15^\circ < i < 30^\circ$	1.2
T_4	Elevation with crest width much smaller than the base and average inclination $i > 30^\circ$	1.4

Design response spectrum

To take into account the ductility of the structure, the response spectra in terms of acceleration can be divided for q , defined as a structure coefficient. The definition provided in EC8 (1998) is:

The behaviour factor q is an approximation of the ratio of the seismic forces that the structure would experience if its response was completely elastic with 5% viscous damping, to the minimum seismic forces that may be used in design - with a conventional elastic analysis model - still ensuring a satisfactory response of the structure.

In CHAPTER 7 the evaluation of the seismic capacity is provided both with local analyses with the evaluation of local failures due to local mechanisms and through global analysis, with the definition of a global model of the aggregates. For the first case, in the linear analysis of the mechanisms, the behaviour factor q assumes fixed value equal to 2 (§7.2.1.6 and NTC, 2008) and this can be interpreted as a factor of geometric ductility rather than a factor of mechanical ductility. A masonry wall, as characterized by the absence of plastic dissipation, can be schematized with an elastic bilinear oscillator subjected to actions at the base. In dynamic conditions, when the rotation changes direction, a geometric dissipation is experienced by the masonry and that justifies the reduction peak ground acceleration by the factor $q=2$ (Damoni et al., 2013).

In second case, a non-linear static analysis will be performed (push over analysis) for which the demand spectrum in term of acceleration is considered assuming behaviour factor equal to 1, since the non-linearity of the structure is already taken into account by the type of analysis).

Displacement response spectrum

The elastic displacement response spectrum, $S_{De}(T)$, shall be obtained by direct transformation of the elastic acceleration response spectrum, $S_e(T)$, using the following expression:

$$(7) \quad S_e(T^*) = S_{De}(T^*) \cdot \omega^2 = S_{De}(T^*) \cdot (2\pi/T^*)^2$$

T^* is the period of the structure.

Figure 7a shows the elastic response spectra for the different ground types for Castelnuovo, and the plastic spectra for two different types of behaviour factor, $q=2$ and $q=3$. Figure 7b shows the (elastic) response spectra in terms of displacements, for different ground types.

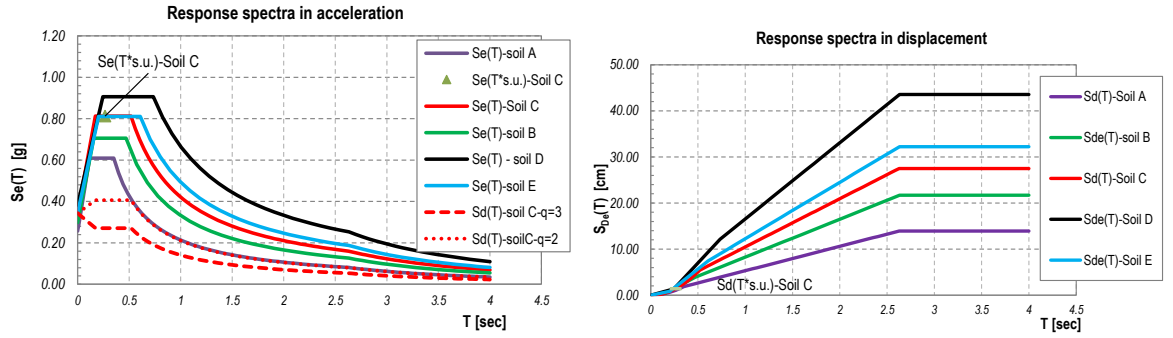


Figure 7: Response Spectra for Castelnovo, $S_e(T)$, $S_{ed}(T)$ and $S_d(T)$.

§

The definition of the seismic spectra in EC8 are similar, reported in the equations below.

$$\begin{aligned}
 0 \leq T < T_B & \quad S_e(T) = a_g \cdot S \cdot \eta \cdot \left[1 + \frac{T}{T_B} (\eta 2.5 - 1) \right] \\
 T_B \leq T < T_C & \quad S_e(T) = a_g \cdot S \cdot \eta \cdot 2.5 \\
 T_C \leq T < T_D & \quad S_e(T) = a_g \cdot S \cdot \eta \cdot 2.5 \cdot \left(\frac{T_C}{T} \right) \\
 T_D \leq T & \quad S_e(T) = a_g \cdot S \cdot \eta \cdot 2.5 \cdot \left(\frac{T_C T_D}{T^2} \right)
 \end{aligned}$$

The F_0 coefficient is equal to 2.5, fixed for all the spectra. In Italian Standard it is a function of the site of reference, and it changes with the geographical position, with reference to the (5x5) km network in which Italian territory is divided. The values of T_B , T_C and T_D periods and the value of S factor, defining the shape of the spectrum, depend on the ground type. EC8 provides these parameters differently depending on the size of the surface-wave magnitude M_s that is supposed to have generated the earthquake, with reference to two types of earthquakes (Type 1 and Type 2). The values of the periods and S are reported in Table 3.2 and Table 3.3 of EC8 (1998). The shape of the response spectra for EC8 is thus stable, and the ratio among the periods of different ground conditions are the same, for zone considered. Moreover, the S coefficient depends only on the ground type.

As reported in paragraph above, in Italian actual Code the shape of the spectra can change both with the type of soil and the seismic zone. S , equal to $S_T \cdot S_s$, the first changing with the coefficient of topographic, and the latter refers to the seismic zonation. The periods T_B , T_C and T_D are all changing with the seismic hazard, with the coefficients a_g , F_0 , T_C^* and C_C .

An observation regards the difference in the determination of the response spectra for different types of ground in a seismic homogeneous zone is reported in the following.

The calculations and safety verification with the analytical models (CHAPTER 7) refer to seismic demand in standard situation, in order to make general the results. That correspond to "A" ground category for Castelnovo (rock soil) and first category of topography (T_1). Therefore, in real situation, Castelnovo territory is classified as "C" category of soil and at the top of the hill with no negligible slope, the topographic condition is T_2 .

In order to take into account the analysis results when the seismic ground profile and the different periods of the structures change, a coefficient is introduced, the $C_{K,aG}$.

For what concern the period variation, it is possible to take into account the different periods linked to the out-of-plane mechanisms (Figure 161), which refers to the simplified calculation of the 1st vibration period expressed both in EC8 and in §7.3.3.2 of NTC 08.

With regard to the ground type, the ground classes defined by EC8 and NTC 2008 (Table 6) have been considered. The multiplier factor $C_{K,aG}$ is that one that generates a seismic action able to produce on a certain building (T fixed) built on a certain soil (ground class "k"), the same effect as if it was built on Rock (ground class "A"), for stable topographic category (both in A ground and k-ground).

With reference to the elastic response spectra equations, the coefficient $C_{K,aG}$ is defined:

$$C_{k,aG} = \begin{cases} \frac{S_k}{S_A} \frac{T_{B,A}}{T_{B,k}} \left[\frac{T_{B,k} + T(F_0 - 1)}{T_{B,A} + T(F_0 - 1)} \right] & \text{for } 0 \leq T < T_B \\ \frac{S_k}{S_A} & \text{for } T_B \leq T < T_C \\ \frac{S_k}{S_A} \frac{T_{C,k}}{T_{C,A}} & \text{for } T_C \leq T < T_D \\ \frac{S_k}{S_A} \frac{T_{C,k}}{T_{C,A}} \frac{T_{D,k}}{T_{D,A}} T_D & T \leq T_D \end{cases}$$

Making reference to elastic response spectra and to the values provided for the parameters of Table 9, $C_{k,aG}$ factors have been evaluated according to the previous equations for a building standard (cell type, for height enter 3÷12 m) for Castelnovo. The results for another location also can be extended, but in that case, in the expression of $C_{k,aG}$ appears also the parameters of the seismic hazard, that obviously changes from location to location (a_g , F_0 , T_C^*). The coefficients calculated are working only for the spectrum in acceleration, as it was considered for detailed analysis in linear analysis². In detail the $C_{k,aG}$ are useful for the calculation of the capacity for the formation of the hinge at different floors, for different types of ground profile. However, the capacity estimated for masonry façades in this thesis is related to the hinge configuration at the ground floor (§7.2.2). The demand acceleration is the peak ground acceleration (PGA) and $C_{k,aG}$ is equal to S factor. In correspondence of the $T=0$, the elastic acceleration spectrum is provided by the first equation of the formula which in correspondence of $T=0$ is equal to $a_g \cdot S$.

For The case study of Castelnovo, the T and the S parameters for the different types of ground are reported in next table:

Table 9: Spectral features of the seismic hazard for Castelnovo for different ground type.

CASTELNUOVO, $T_1 = S_T = 1$					
GROUND	S_S	C_C	T_B sec	T_C	T_D
A	1.00	1.00	0.12	0.35	2.36
B	1.16	1.36	0.16	0.47	2.63
C	1.33	1.49	0.17	0.52	2.63
D	1.48	2.13	0.25	0.74	2.63
E	1.33	1.76	0.20	0.61	2.63

Table 10: Coefficients $C_{k,aG}$ for the elastic spectrum in term of acceleration.

$C_{k,aG}$ CASTELNUOVO, $T_1 = S_T = 1$				
BUILDINGS	B	C	D	E
$T_{min}=0.13$ sec	0.97	1.07	1.01	0.98
$T_{min}=0.32$ sec	1.16	1.33	1.48	1.33

1.1.1.2 MACROSEISMIC INTENSITY SCALES

As known from the literature review, many seismic intensity scales have been defined over the years from the beginning of the twentieth century. The major distinction between the scales concerns the way to measure the intensity of a seismic event. It can detect through instrumental measurements or according to the type and amount of damages that it produces on the objects exposed to the earthquake (E). The Richter scale of 1935 is an example of a seismic scale of the first type in which the definition of the degrees is related to the magnitude of an earthquake, while an example of a second type is the Mercalli-Cancani-Sieberg.

The magnitude of an earthquake measures indirectly the amount of mechanical energy that is given off at the hypocentre, based on the records measured in the surface. Indeed, it has been observed that plotting in a logarithmic scale the ratio

² In the case of non-linear analysis the coefficient related to the elastic spectrum in terms of displacements should be considered.

between the seismographic waves and the distance from the epicentre to the record station for two different seismic events, it is possible to obtain two parallel curves, shifted by a certain amount according to the ordinate axis (Eq.(8)):

$$(8) \log(A_1 - A_2)_{\Delta=stable}$$

It has been chosen a design earthquake, such that it produces a soil drift of maximum amplitude of $1\mu\text{m}$ from a hypo central distance $\Delta=100\text{ km}$. Thus, a Local Magnitude can be defined as:

$$(9) M_L = \log \frac{A_1}{A_0}$$

Therefore, the logarithm of the maximum amplitude recorded by a seismograph during an earthquake, put in relation to the value of reference (A_0), proposes a logarithmic, called Richter Scale. The magnitude is a quantity characterizing the single earthquake in its entirety, regardless of location, contrary to what happens for the macroseismic scales.

The second-type intensity scales are related to the description of the earthquake effects, which may depend on local conditions (presence and type of construction, distance from the epicentre, etc.) and the characteristics of the earthquake. Although they are related to the subjectivity of the point of evaluation of the earthquake (an earthquake with fixed local magnitude can have different effects if it occurs in the desert or in a city), the macroseismic intensity scales are fundamental for the description of the intensity of historical earthquakes. They represent the only type of measure of earthquakes ante-instrumental records and it is a universal recognized parameter to provide, immediately after an earthquake event, an indicator of the overall earthquake damages (Giovinazzi, 2005).

Macroseismic scales have been known since the seventeenth century. The first modern macroseismic scale was that of De Rossi- Forel, 1873 with ten degrees. Such a proposal was then taken up by Mercalli, 1902 (ten degrees). This scale was further modified by Cancani Sieberg in 1904 and in 1912, in the version as amended is now known as the Mercalli - Sieberg Cancani, 1912 (MCS, I_{MCS}). It is composed of 12 levels, from the first "very light event", with almost no perception of the earthquake up to the twelfth "heavy catastrophic event", with the collapses of structural elements.

Richter in 1956 proposed a further improvement to Mercalli Scale by introducing four different classifications for masonry buildings depending on the seismic resistance (Modified Mercalli, 1956, MM). Similar to the MM there is the Sponheuer-Medvedev-Karnik, 1964 (MSK), which classifies all non-seismic designed buildings into three categories, classifying the percentage quantities and degrees of damage.

In 1988, the European Seismological Commission that bring the MSK scale in line with modern building types arriving to define a new scale, called the European Macroseismic Scale (EMS), published in Grünthal (Grünthal, 1998), (Musson et al., 2010), called in the following EMS-98.

The first macroseismic intensity scales did not take into account the variation of damage in different structural types. Currently, an earthquake develops different levels of damage on different types of buildings, depending on the type of structural organization, the conservation state, the type of materials. The MCS and MSK scales began to divide into classes of *vulnerability* the buildings, but at preliminary level. The significant difference between the MCS and MSK scale is that the first one takes into account the total damage without considering the presence of different kinds of structures, while the MSK scale presents five classes of damage for three classes of buildings (Margottini et al., 1992).

This concept has been implemented by EMS-98. In this scale, there is a vulnerability classification of structures for building of different materials: masonry, reinforced concrete, steel and timber, dependent on geometrical and structural parameters. Seven classes (from "A" to "F") at decreasing vulnerability are considered by the scale, being class "A" the one who represents the behaviour of the weakest buildings and "F" the one representative of the building with the highest level of Earthquake Resistant Design (ERD).

The Vulnerability Table (provided by the EMS-98 Scale (Figure 8)) is an attempt to categorise the strength of structures, taking both building type and specific structural factors into account, such as the state of disrepair, quality of construction, irregularity of building shape, level of earthquake resistant design (ERD), etc... (Grünthal, 1998).

For each building type, the Vulnerability Table gives a line showing the most likely vulnerability class(es) for it, and also the probable variation range (shown as a dashed line). The vulnerability classes to buildings are assigned according to the greater frequency of damage they showed after past seismic events. For masonry buildings the vulnerability class depends

markedly from the structural organization of the building ("box behaviour" (§7.1)) and the masonry's type and organisation.

In EMS-98 the damage is described in a systematic way for each material type, in the load bearing masonry structures or non-structural elements. The Scale provides details of the collapse types and explanatory images taken from recent earthquakes, both for reinforced concrete and load-masonry type structures. Damage level on buildings, D_K , is expressed according to 6 levels ("D0"÷"D5") ascending, where "D0" is the damage absence, Figure 8b, while the D5 means the collapse. The damage level is caused on buildings by the seismic event that has a certain macroseismic intensity. Table 11 shows the EMS-98 scale definition of intensity degrees from VI, when most vulnerable buildings start to suffer damage, up to the XII grade, that is the destructive damage level for different ERD structural system.

Type of Structure		Vulnerability Class					
		A	B	C	D	E	F
MASONRY	rubble stone, fieldstone	○					
	adobe (earth brick)	○					
	simple stone	○	○				
	massive stone	○	○	○			
	unreinforced, with manufactured stone units	○	○	○			
	unreinforced, with RC floors reinforced or confined	○	○	○	○		
STEEL REINFORCED CONCRETE (RC)	frame without earthquake-resistant design (ERD)	○	○				
	frame with moderate level of ERD	○	○	○			
	frame with high level of ERD	○	○	○	○		
	walls without ERD	○	○				
	walls with moderate level of ERD	○	○	○			
WOOD	steel structures		○	○			
	timber structures		○	○			

○ most likely vulnerability class; — probable range;
--- range of less probable, exceptional cases

Classification of damage to masonry buildings	
	Grade 1: Negligible to slight damage (no structural damage, slight non-structural damage) Hair-line cracks in very few walls. Fall of small pieces of plaster only. Fall of loose stones from upper parts of buildings in very few cases.
	Grade 2: Moderate damage (slight structural damage, moderate non-structural damage) Cracks in many walls. Fall of fairly large pieces of plaster. Partial collapse of chimneys.
	Grade 3: Substantial to heavy damage (moderate structural damage, heavy non-structural damage) Large and extensive cracks in most walls. Roof tiles detach. Chimneys fracture at the roof line; failure of individual non-structural elements (partitions, gable walls).
	Grade 4: Very heavy damage (heavy structural damage, very heavy non-structural damage) Serious failure of walls; partial structural failure of roofs and floors.
	Grade 5: Destruction (very heavy structural damage) Total or near total collapse.

Figure 8: Vulnerability Table and damage levels in EMS-98.

Table 11: Intensity degrees from VI to XII of EMS-98 scale.

VI	Slightly damaging	a) Felt by most indoors and by many outdoors. A few persons lose their balance. Many people are frightened and run outdoors. b) Small objects of ordinary stability may fall and furniture may be shifted. In few instances dishes and glassware may break. Farm animals (even outdoors) may be frightened. c) Damage of grade 1 is sustained by many buildings of vulnerability class A and B; a few of class A and B suffer damage of grade 2; a few of class C suffer damage of grade 1.
VII	Damaging	a) Most people are frightened and try to run outdoors. Many find it difficult to stand, especially on upper floors. b) Furniture is shifted and top-heavy furniture may be overturned. Objects fall from shelves in large numbers. Water splashes from containers, tanks and pools. c) Many buildings of vulnerability class A suffer damage of grade 3; a few of grade 4. Many buildings of vulnerability class B suffer damage of grade 2; a few of grade 3. A few buildings of vulnerability class C sustain damage of grade 2. A few buildings of vulnerability class D sustain damage of grade 1.
VIII	Heavily damaging	a) Many people find it difficult to stand, even outdoors. b) Furniture may be overturned. Objects like TV sets, typewriters etc. fall to the ground. Tombstones may occasionally be displaced, twisted or overturned. Waves may be seen on very soft ground. c) Many buildings of vulnerability class A suffer damage of grade 4; a few of grade 5. Many buildings of vulnerability class B suffer damage of grade 3; a few of grade 4. Many buildings of vulnerability class C suffer damage of grade 2; a few of grade 3. A few buildings of vulnerability class D sustain damage of grade 2.
IX	Destructive	a) General panic. People may be forcibly thrown to the ground. b) Many monuments and columns fall or are twisted. Waves are seen on soft ground. c) Many buildings of vulnerability class A sustain damage of grade 5. Many buildings of vulnerability class B suffer damage of grade 4; a few of grade 5. Many buildings of vulnerability class C suffer damage of grade 3; a few of grade 4. Many buildings of vulnerability class D suffer damage of grade 2; a few of grade 3. A few buildings of vulnerability class E sustain damage of grade 2.

X	Very destructive	c) Most buildings of vulnerability class A sustain damage of grade 5. Many buildings of vulnerability class B sustain damage of grade 5. Many buildings of vulnerability class C suffer damage of grade 4; a few of grade 5. Many buildings of vulnerability class D suffer damage of grade 3; a few of grade 4. Many buildings of vulnerability class E suffer damage of grade 2; a few of grade 3. A few buildings of vulnerability class F sustain damage of grade 2.
XI	Devastating	c) Most buildings of vulnerability class B sustain damage of grade 5. Most buildings of vulnerability class C suffer damage of grade 4; many of grade 5. Many buildings of vulnerability class D suffer damage of grade 4; a few of grade 5. Many buildings of vulnerability class E suffer damage of grade 3; a few of grade 4. Many buildings of vulnerability class F suffer damage of grade 2; a few of grade 3.
XII	Completely devastating	c) All buildings of vulnerability class A, B and practically all of vulnerability class C are destroyed. Most buildings of vulnerability class D, E and F are destroyed. The earthquake effects have reached the maximum conceivable effects.

Scientific studies carried out in past time show the difficulty to switch from a macroseismic scale to another one, because of the different concepts inside the definition of the degrees of each scale. An example of transformation from the MCS and MSK scales is represented in Figure 9 and Eq.(10), (Margottini et al.,1992). To have a complete idea, the non-prescriptive guidelines to change values from different scale to the EMS-98 are present in the work of Musson et al., (2010), not reported in a exhaustive way here.

$$(10) I_{EMS-98} = I_{MSK} = 0.74 + 0.814I_{MCS}$$

Mercali Sieberg (MCS)	Medvedev Sponheuer,Karnik (MSK)	Mercali Cancani,Sieberg (MCS)
II	I	I
III	II	II
IV	III	III
V	IV	IV
VI	V	V
VII	VI	VI
VIII	VII	VII
IX	VIII	VIII
X	IX	IX
XI	X	X
XII	XI	XI
	XII	XII

(A)

(B)

Figure 9: Graphic comparison between the MSC and MSK scale (Margottini et al., 1992).

1.1.1.3 CORRELATION PGA-EARTHQUAKE INTENSITY

Several studies have been made to correlate the macro seismic intensity of an earthquake and peak ground acceleration (a_g). These evaluations are based on records of past earthquakes coming from all over the world data: the results are some functions that offer the possibility of transforming qualitative, readily observed data (intensity) into parameters which are useful for engineering purposes (PGA or others quantitative measures of ground motions (Margottini et al., 1992)).

Below, some of these representations are reported for what concern the Italian situation (Gómez et al., 2007).

The first one comes from Guagenti and Petrini (Guagenti & Petrini, 1989) referring to the Italian data and that describes macroseismic intensity with the MCS intensity (in term of g):

$$\ln a_{max} = 0.602I - 7.073 \quad (1, \text{ in the figure})$$

Margottini (1992) provides two equations: one for general intensities and another for local ones (n.2 and n.3).

More recent studies (Faccioli e Cauzzi, 2006) refers to the equation n. 4 and n.5.

$$\log a_{max} = 0.687 + 0.179I \quad (a_{max} \text{ in terms of cm/s}^2) \quad (\text{Margottini, 1992, global} - n.2 \text{ in the figure})$$

$$\log a_{max} = 0.525 + 0.22I \quad (a_{max} \text{ in terms of cm/s}^2) \quad (\text{Margottini, 1992, local} - n.3 \text{ in the figure})$$

$$\log a_{max} = -1.33 + 0.20I \quad (a_{max} \text{ in terms of cm/s}^2) \quad (\text{Faccioli e Cauzzi, 2006, Regression} - n.4 \text{ in the figure})$$

$$I_{MCS} = 1.96 \log PGA + 6.54 \quad (a_{max} \text{ in terms of cm/s}^2) \quad (\text{Faccioli e Cauzzi, 2006, Mediterraneo} - n.5 \text{ in the figure})$$

There is wide difference in terms of a_g coming from the different correlations for a given macroseismic intensity level, as it possible to see in Figure 10.

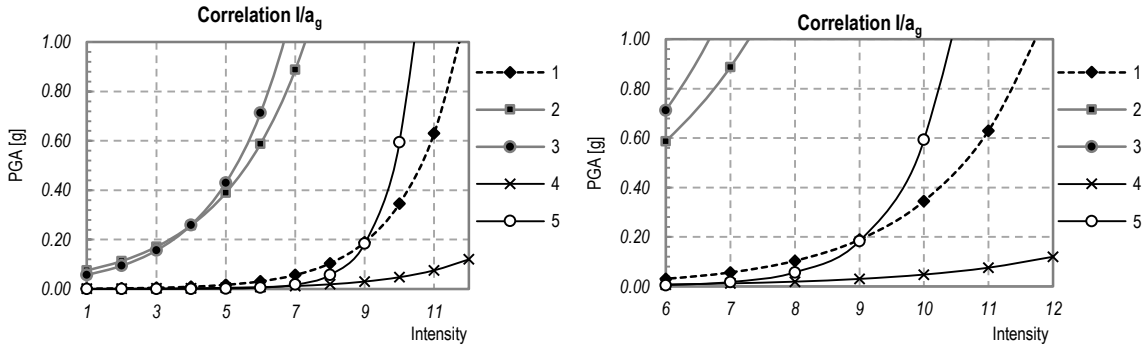


Figure 10: Correlations between Intensity and a_{max} (Gómez et al., 2007).

CHAPTER 2. STRUCTURAL VULNERABILITY: REVIEW OF THE STATE OF ART

The chapter provides an overview of the existing literature about the vulnerability assessment of masonry structures, with a focus on the masonry aggregates. In the initial part of the chapter, particular attention has been paid to the Vulnerability Index Methods. In the last part, the chosen vulnerability methods exploited in the thesis are reported.

2.1 CLASSIFICATION OF VULNERABILITY ASSESSMENT METHODS - VAMS

Many vulnerability assessment methods have been developed in the seismic research in last 30' years, using various working criteria. There are several attempts to provide significant classifications for the VAMs, because of the wide difference among factors involved in their assessment, such as the nature and the objective of the project, quality and availability of information, characteristics of the building stock inspected, scale of assessment, methodology criteria, etc...(Figure 11).

Therefore, the decision to carry on a certain vulnerability assessment method (VAM) is a complex issue and it is a consequence of the awareness of the type of available data and the "scale" of the project; the choice of one or few suitable methods should come out by the screening of different aforementioned criteria (D'Ayala & Novelli, 2010).

The first classification of the VAMs can be done by considering the "*level of detail*" of the elements studied. Indeed, it is possible to assess vulnerability through three different approaches, with increasing level of detail:

- *First level of approach.* The methods here grouped consider large amount of simple and qualitative parameters. They are suitable for a large-scale assessment, considering an entire historical city centre or more; the level of detail of the information they require is not sophisticated. The information can be achieved from the Municipalities (ISTAT data) or through in situ inspections.
- *Second level of approaches* is based on mechanical models and rely on a higher quality of information (geometrical and structural) regarding building stock;
- *The third level* involves the use of numerical modelling techniques that require a complete and rigorous survey of individual buildings and the whole knowledge of the disposition of masses and stiffness of the structural elements.

The second classification refers to the "*intended results*" of the methods: Corsanego (1990) proposed a division in three main groups. All VAMs goal is to establish a method able to provide tools to predict damage levels on buildings for plausible earthquake intensities. To achieve this purpose, the VAMs could employ one or more steps. The differentiation criterion depends on the number of steps involved in the definition of the risk evaluation. There are:

- *Direct techniques:* they use only one-step to estimate the damage caused to a structure by an earthquake, employing two types of methods; typological and mechanical. Example of typological methods: Damage Probability Matrixes (DPM, in par.2.2.1). Example of mechanical methods: Analysis of the mechanisms methods (Vulnus in (Bernardini, 1990) and FaMIVE in par. 2.3.1.1 (D'Ayala & Speranza, 2002)).
- *Indirect techniques:* they involve two steps to study seismic vulnerability. Initially defining a Vulnerability Index (Iv, see par. 2.2.2), afterwards an estimated damage level, using correlations supported by statistical studies of post-earthquake damage data available. The Vulnerability Form, widely used in Italia since 80 years, are an example of this method. The first VFs was developed in Italy in 80 years (GNDT, 1993);
- *Hybrid techniques,* which use both of the VAMs type described above. An example is the macroseismic method developed by Lagomarsino and Giovinazzi (2006). It combines the characteristics of typological and indirect methods using the vulnerability classes defined in the EMS-98 scale and a vulnerability index.

The third classification places the VAMs in different ways in function of their *quality "of the source of information and tools*

used” in the project: there are, indeed, *empirical*, *analytical-theoretical* and *hybrid* methods. In next paragraph, there is an explanation in detail of each method, considering the last classification.

In Figure 11 there is the intersection of the classification criteria of the VAM; highlighted in red, there are the VAMs used in this thesis, applied to the aggregates of the case study of Castelnuovo §3.3.

Depending on the level of detail of the analyses that have to be done in the VAM, to each VAM is associated a cost in terms of computation effort to sustain. The Figure 12 shows a classification of VAMs in terms of “expenditure”: the higher the level of detail (the lower the scale of the project), the higher the computation effort for the methods.

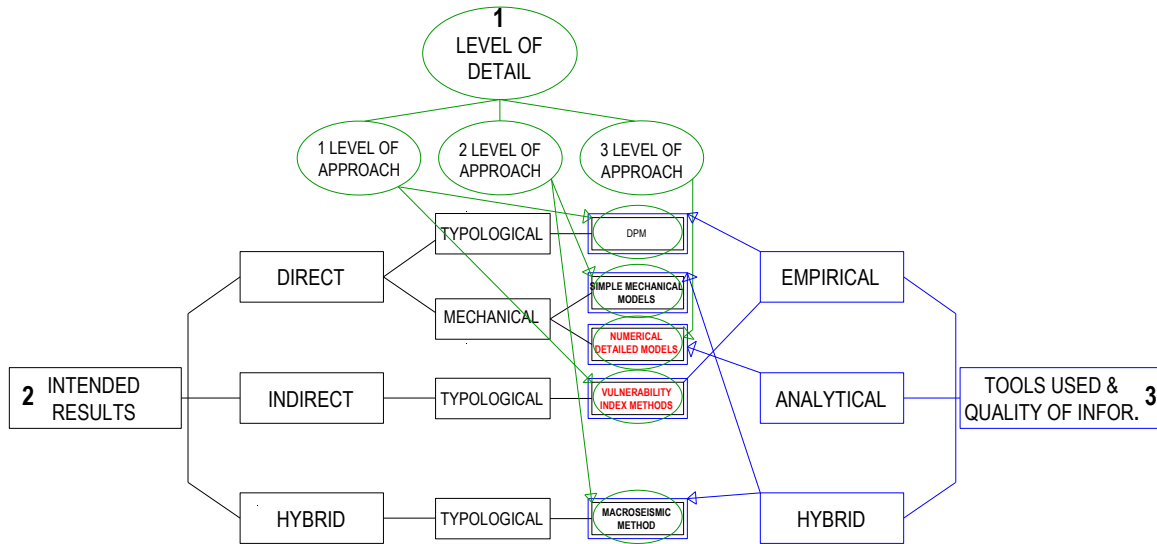


Figure 11: Different classifications of vulnerability assessment methods. In red the methods used in this work.

Expenditure	Increasing computation effort →				
Application	Building stock		Individual building		
methods	Observed vulnerability	Expert opinions	Simple analytical models	Score assignment	Detailed analysis procedures
	First level of approach		Second level of approach		Third level of approach

Figure 12: Vulnerability assessment methods for buildings (Lang, 2002).

2.2 EMPIRICAL METHODS

The empirical methods are those VAMs based on expert’s judgement opinions and/or the observations of the damage data caused on buildings after seismic events. These methods require the knowledge of some parameters in a qualitative way, usually gained with in situ observations. They are used for a large-scale assessment of vulnerability evaluation (first level of approach). The results they provide are qualitative and representative for a building class, with common structural characteristics.

2.2.1 DAMAGE PROBABILITY MATRIX - DPM

Damage Probability Matrix is an empirical VAM, developed at first by Whitman (Whitman, 1973), which provides the use of probabilistic matrices of damage (in a discrete way) for the prediction of buildings damage caused by seismic events. The DPM represents the probability of a certain damage state to be present for a level of macroseismic intensity in a

specific building stock. Whitman compiled DPMs for various structural typologies (over 1600 buildings) according to the damage they suffered after the 1971 San Fernando earthquake, California ($M_L = 6.6$ Richter Scale and XI Mercalli Scale). By the analysis of the results obtained, Whitman observed that three factors are important to classify buildings 1. Building materials; 2. Age of the building and 3. Floors number. Figure 13 is an extract of the Whitman report, in which some results of vulnerability assessment are shown.

On the base of the DPM developed by Withman, several studies have been done after recent past seismic events: Braga et al., (1982). Grimaz et al., (1997), Dolce et al. (2004) who collected information of vulnerability and damage data after the earthquake of 1990 for buildings sample in Potenza and Di Pasquale et al. (2005) about the seismic risk assessment at national level in Italy.

Giovinazzi (2004) and D'Ayala & Novelli (2010), in their analysis of the state of art about VAMs, pointed out that the major limitations of the DPM concern the definition of the discrete damage probability functions, the lack of information relative to damage scenario for the possible intensity degrees and the dependence on a specific seismic and architectonic context of their results. The previsions damage scenario in using the DPM would be working only for specific case of types of buildings.

Date Const.	Pre-1933				Post-1947					
No. Stories	5-7		8-13		5-7		8-13		14-18	19+
Type of Const.	Co	St	Co	St	Co	St	Co	St	St	St
Damage State										
0	16	18	16	6	21	24	27	44	43	21
1	16	9	12	13	26	28	33	31	43	54
2	26	46	28	53	16	38	32	6	0	25
3	21	27	14	16	26	5	8	16	14	0
4	11	0	21	0	11	5	0	3	0	0
5	0	0	7	9	0	0	0	0	0	0
6	10	0	2	3	0	0	0	0	0	0
7	0	0	0	0	0	0	0	0	0	0
MDR - %	4.4	1.1	2.7	2.5	1.1	.66	.43	.52	.43	.24
No. Bldgs.	19	11	43	32	19	21	37	32	14	24

Figure 13: DPM, San Fernando earthquake 1971.

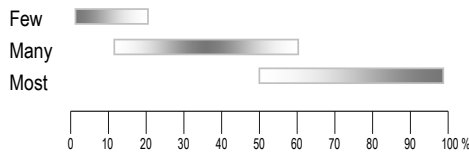
2.2.1.1 EMS-98 DAMAGE PROBABILITY MATRIXES

The EMS-98, the European modern macroseismic scale, contains the classification of the buildings' vulnerability classes and provides for them the definition of the damage levels for the degrees of intensity of an earthquake. For its contents, it may be considered an example of DMP. Indeed, if the aim of a macroseismic Scale is the measure of the earthquake severity from the observations of the damage suffered by the buildings, it can represent, if reversed, a vulnerability model able to supply, for a given intensity, the probable damage distribution on them (Giovinazzi, 2004).

In particular, EMS-98 encloses a clear definition of damage typologies correlated to each degree of intensity. Seven classes (from "A" to "F") at decreasing vulnerability are considered by the scale, being class "A" the more vulnerable one.

For each vulnerability class, the damage pattern described for intensity varying may be reported in terms of a Damage Probability Matrix (Figure 14). In other words, that matrix contains the probability to suffer a certain damage level for a given intensity, for the buildings belonging to a certain vulnerability class.

Giovinazzi (2004) and (Bernardini et al., 2007a and 2007b) observed that also in the of EMS-98 DPM Scale the definition of the discrete damage probability functions was incomplete, due to the vagueness characterisation of the damage level through the quantitative terms "Few", "Many", "Most", represented by the scale as three narrowly overlapping percentage ranges, as showed in Figure 14a and Figure 14b. These problems were overcome by the macroseismic method, expressed in next paragraph.



EMS-98 Damage Grade - Vulnerability classes					
Intensity	D1	D2	D3	D4	D5
V	Few A-B				
VI	Many A-B Few C	Few A-B			
VII		Many B Few C	Many A Few B	Few A	
VIII		Many C Few D	Many B Few C	Many A Few B	Few A
IX		Many D Few E	Many C Few D	Many B Few C	Many A Few B
X		Many E Few F	Many D Few E	Many C Few D	Most A Many B Few C
XI		Many F	Many E Few F	Most C Many D Few E	Most B Many C Few D
XII					All A-B, Nearly All C, Most D-E-F

Figure 14: Quantities in EMS-98 scale and DPM (vulnerability classes and damage).

2.2.1.2 MACROSEISMIC METHODS

In 2.2.1.1 the EMS-98's DPMs have been introduced. The DPMs were derived from the EMS-98 definitions of quantitative designations ("Few", "Many", "Most") of the degrees of damage for six classes of building type characterised by different vulnerability level, from "A" up to "F" (Grünthal, 1998)(Figure 14b).

With the macroseismic methods, Giovinazzi (2004) overcame the problems of the vagueness and incompleteness of the DPMs associated to the definition of the quantitative terms "Few", "Many", "Most" and their overlapping percentage ranges (Figure 14a). In that study, indeed, the uncertainty of the non-rigorous definitions damage in EMS-98 were solved by the use of probabilistic and fuzzy set theory, with which boundary limits for the correlation between the macroseismic intensity and damage grades were derived for each type of vulnerability class. In the methodology, the vulnerability of the structures is expressed with a conventional vulnerability index, V , assuming values from 0 to 1 that allows to cover all seismic behaviour of the construction types (exposed through the "A" ÷ "F" classes). The results of this procedure provide an analytical continuous expression to describe the vulnerability curves (Eq.(12)), that represents the relationship among the vulnerability of the structures, the intensity of the earthquake (I_{EMS-98}) and the damage grade that the structure can suffer, named μ_D . An observation referring the damage definition must be done: the mean damage grade is the determined in a set of buildings subjected to a certain earthquake of macroseismic intensity I fixed. By considering the histogram of the damage grades occurred to a set of buildings, the mean damage grade μ_D is defined as the weighted sum of the damage grade D_k occurred in the structural and non-structural elements and the probability of having that k-damage, p_k (Eq.(11)).

$$(11) \mu_D = \sum_{k=0}^5 p_k D_k \quad 0 < \mu_D < 5$$

In Eq.(12), Q is the ductility factor assumed equal to 2.3 in the study of Giovinazzi (2005) and I_{EMS-98} , refers at the level of macroseismic intensity of a seismic event defined in the EMS-98 Scale, already reported in Table 11.

$$(12) \mu_D = 2.5 + (1 + \tanh\left(\frac{I+6.25 \cdot V - 13.1}{Q}\right)) \quad 0 \leq \mu_D \leq 5$$

2.2.2 VULNERABILITY INDEX METHODS

The Vulnerability Index Methods (VIMs) are those methods that are able to define seismic vulnerability starting from the qualitative knowledge of the resistance system of the structure and of the non-structural elements. The methods consist in the calculation of a Vulnerability Index (I_v), through the filling out a Vulnerability Form. The Form contains, in the "parameters", the features that are important for the assessment of seismic vulnerability. A judgment should be defined for all the parameters ("A" best conditions, "B", "C" and "D" worst conditions), by the knowledge of the effective situation of the

construction. To each class is associated a score with increasing value from “A” up to “D”. The Form associates to each parameter a specific weight: the higher the weight, the higher is the impact factor of the parameter in the determination of the global I_v . Indeed, the I_v is the result of the weight sum of the scores multiplied for the weight associated to each parameter. A normalized I_v is calculated dividing it for the maximum value of Vulnerability Index that the Form could provide, as all the parameters were put in “D” class.

In the following paragraphs, there is a description of the different type of Vulnerability Forms existing in literature, specifying the field of reference of each one and if they refer to isolated buildings, to aggregates or structural units. Each Form's parameter is described and with the purpose of clearly explain the type and the information associated to the parameter, in some cases, direct references to the Casetlnuovo aggregates were reported. Each Forms provides an handbook in which each parameter is well explained, with some pictures and examples reported. For the first Form introduced, the GNDT II Level, the Toscana Region have implemented a very detailed handbook, the “Rilevamento della vulnerabilità sismica degli edifici in muratura. Manuale per la compilazione della Scheda GNDT/CNR di II livello” (AA.VV., 2003).

2.2.2.1 VULNERABILITY INDEX METHODS – GNDT II LEVEL FORM OR 11 PARAMETERS FORM

The method of the vulnerability index, calibrated on a large sample of data in recent years, was developed in the 80's by Benedetti e Petrini (1984) and GNDT (1993)³. This method consists in filling out in a *survey form* composed of 11 parameters, depending of the structure's characteristics and materials. To each parameter, a score is assigned choosing within “A” (optimal) and “D” (unfavourable) and middle classes (“B” and “C”). Each parameter has a weight coefficient related to its importance in the vulnerability aspects: it means that if a parameter has a higher weight coefficient, it represents a fundamental aspect in the vulnerability analysis against seismic actions. By the sum of the multiplication of the scores and weight coefficients, the vulnerability index I_v , usually normalized in a 0-100 range, is calculated. Figure 15 describes in detail each parameter of the Form, with the scores associated to each parameter and their weights. The Form was built and it is working for isolated structural units (see definition in 1.1).

GNDT II LEVEL FORM - 11 PARAMETERS - MASONRY BUILDINGS					
Parameters	scores				weight
	A	B	C	D	
1 - Type and organisation of resistant system	0	5	20	45	1.00
2 - Quality of resistant system	0	5	25	45	0.25
3 - Conventional strength	0	5	25	45	1.50
4 - Building position and type of foundation	0	5	25	45	0.75
5 - Horizontal elements (floors)	0	5	15	45	var.
6 - Planimetrical configuration	0	5	25	45	0.50
7 - Configuration in elevation	0	5	25	45	var.
8 - Maximum distance among the walls	0	5	25	45	0.25
9 - Coverage/roof	0	15	25	45	var.
10 - Non structural elements	0	5	25	45	0.25
11 - Actual state (conservation status)	0	5	25	45	1.00

Figure 15: GNDT 11 parameters masonry Form.

PARAMETER 1 - Type and organization of the resistant system

In this parameter the organization of the structure is evaluated; the most important aspect to analyse is the presence of connections between orthogonal walls, that are necessary to guarantee the so called “box behaviour” of the structures (Figure 16, Figure 135). To verify this situation it is necessary to perform edges' essays on the structure and detect the presence of links among the vertical and horizontal elements. It is also possible to evaluate how the structure has evolved over time and to know which principal walls were built.

PARAMETER 2 - Quality of the resistant system

The quality of the resistant system is a function mainly of the masonry quality, widely discussed in (Borri & De Maria, 2008)

³ At first, the method was developed for masonry structures and later, it had extended to the r.c. structures too.

and, for the particular case of the masonry type collocated in Tuscany Region in (Boschi, et al., 2015). It depends on:

- the type of material, quality of the blocks and mortar conservation state. It is worth noticed that a mortar of high mechanical characteristics may confer to a masonry a sufficient degree of monolithic state, if it is homogeneous distributed in the facing.
- the type of construction system in terms of the regularity of the stones and the mortar inside the masonry. The disposition, the homogeneity and the shape and size of the stones and mortar joints;
- the presence of the elements across the leaves of the masonry (diatones) within a masonry.

A description of vertical elements in Castelnuovo is reported in paragraph 3.3.1: most of elements refers to irregular type of masonry or concrete block masonry, that fall in “D” or “B” classes of P2, as reported in Figure 17.



Figure 16: Aggregate 23-102, 26-415 and 21-25 examples of damage in terms of out-of-plane overturning.

<p>CLASS: D</p> <p>IRREGULAR MASONRY IN NON SQUARED STONES OF MEDIUM OR HIGH POROSITY; NO STRINGCOURSES EXTENDED TO THE ENTIRE THICKNESS MASONRY, POOR QUALITY OF THE MORTAR, ALSO DUE TO THE POOR STATE OF CONSERVATION</p>	 
<p>CLASS: B</p> <p>BLOCK MASONRY SEMISOLID (HOLES BETWEEN 15% AND 45%) IN BRICK OR CONCRETE, WITH GOOD EQUIPMENT</p> <p>MASONRY FRAMED, PRESENCE OF VERTICAL AND HORIZONTAL ELEMENTS IN CONCRETE, CONFINEMENT OF THE WALLS.</p>	 

Figure 17: Example of vertical structures, type of masonry and definition of the classes of P2.

PARAMETER 3 - Conventional strength

This parameter allows the estimation of the horizontal conventional strength of the building. Under the hypothesis of global “box-behaviour”, the evaluation of the building’s resistance consists in the calculation of the minimum shear force resistant associated to the minor capacity direction and afterward in the calculation of the ratio enter it and the estimated building seismic mass. The results is an estimation of the horizontal minimum acceleration capacity (Eq.(13)). For the calculation, that follows the steps reported in the following, it is necessary to individuate for each plan:

N: number of floors (from the ground floor);

A_t: average covered area over the section that identify the verification plan;

A_x, A_y : total cross sections of resistance elements in the two orthogonal directions. The length of the resistant elements is measured between the inter-axis of the orthogonal walls. The area of the inclined elements (angle α) have to be multiplied by $\cos^2\alpha$.

A = A minimum value of A_x, A_y

B = maximum value of A_x, A_y

$A_0 = A / A_t$ and $\gamma = B/A$

The ratio, C , between the resistant shear plan and the estimated weight P is given by:

$$(13) \quad C = \frac{\alpha_0 \tau_k}{qN} \sqrt{1 + \frac{qN}{1.5\alpha_0 \tau_k (1+\gamma)}}$$

In which τ_k is the shear resistance (in absence of normal load) associated to the diagonal cracking and it can be estimated considering the actual Italian code, as reported in paragraph 3.4 (C.M. n.617, 2009). q is the average weight per unit of covered area. It is calculated as the sum of the weight of a floor and a masonry inter-storey. The q can be estimated as a function of the average specific weight of the masonry p_m , the average weight per unit area of the floor p_s and the average inter-storey height h :

$$(14) \quad q = \frac{(A+B)h}{A_t} p_m + p_s$$

The structural units analysed fall mainly in the category “D” (with only few cases in “C”) and the discriminant is mainly linked to the quality of the masonry (and the correspondence τ_k §Table 27).

PARAMETER 4 - Building position and type of foundations

This parameter takes into account the local morphology of the construction site and the type of foundations. In particular, it considers the ground's natural slope, the possible presence of different levels of foundation.

The buildings here studied fall mainly in classes “B” and “C”, depending on the slope of the areas where they are located.

PARAMETER 5 - Horizontal elements (floors)

In the evaluation of this parameter should be considered: the in-plane stiffness of the floors (in order to guarantee an uniform distribution of the horizontal forces among all the vertical elements), their degree of effective connections with the vertical walls and the presence of staggered floors. The parameter expresses the role of horizontal elements in respect to the “box behaviour” of the building (§7.3). Horizontal elements of Castelnuovo aggregates is mainly fall in “D” category (with only few cases in “C”), due their flexibility and their lack of effective connections with vertical elements.

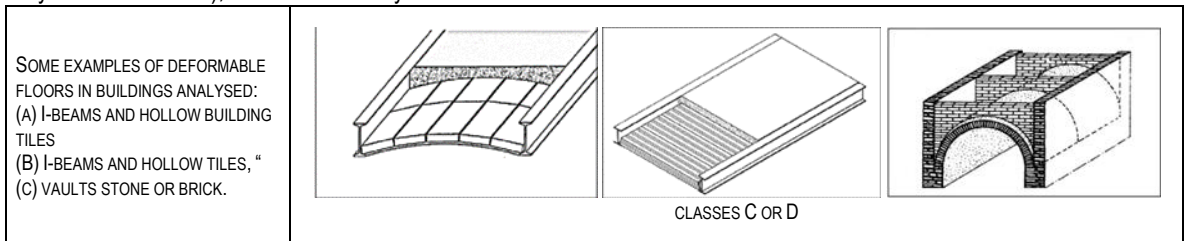


Figure 18: Type of deformable floors.

PARAMETER 6 - Planimetric configuration

The parameter studies the planimetric shape of the building. Two coefficients should be calculated to define the class of this parameter. In the case of rectangular buildings is significant the relationship $\beta_1 = a/l$ between the shorter and the longer side. In the case of plans that differ from the rectangular shape is necessary to take into account the measures of their deviations (coefficient $\beta_2 = b/l$).

PARAMETER 7 - Configuration in elevation

The parameter considers the presence of different stiffness at each level of the structure; it evaluates the presence of porticos or lodges at the ground level or the existence of towers or turrets. The difference of masses at each level should

be less than 10% between two consecutives floors. The ratio $\pm \Delta M/M$ can be replaced by the ratio $\pm \Delta A/A$ (the covered area of the plan and its variation in different floors), if the masonry type is the same at each level of the structure. Castelnuevo buildings fall mainly into the following classes: “A”, “B” and “C”.

PARAMETER 8 - Maximum distance among the walls

This parameter takes into account the presence of walls intersected by orthogonal walls, which constitute an effective constraint to the activation of the out-of-plane mechanisms (§7.2). The effectiveness of the orthogonal links depends on the texture of walls and on the presence of openings close to the edge. Indeed, these two factors determine the angle of detachment of the wedge in the diagonal mechanisms (Figure 19).

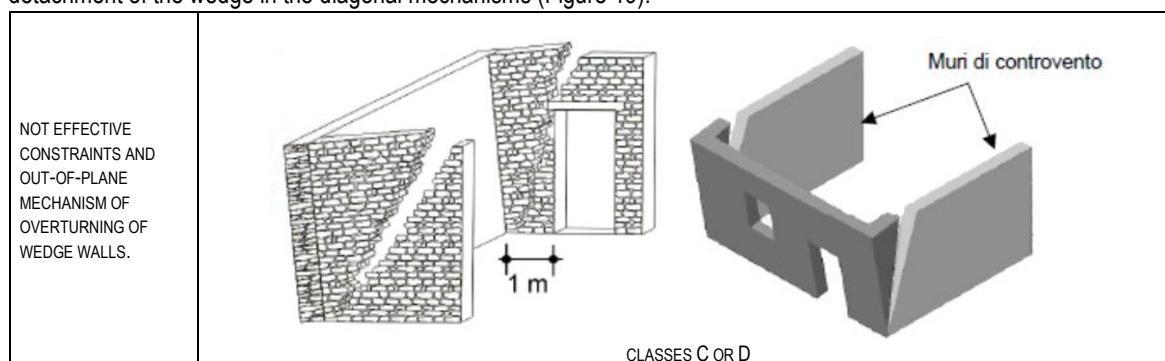


Figure 19: Not effective constraints and out-of-plane mechanism of overturning of wedge walls.

PARAMETER 9 - Coverage roof

This parameter assess the role of the coverage in the seismic response of the masonry building. The roof's issues that influence in a negative way the seismic behaviour should be evaluated, and they are relative to:

- the presence of unbalanced and elevated weight pushing force in the perimeters (thrusting roofs);
- the presence of not effective connections of the covering and the perimeter walls;
- the stiffness difference between the roof and the vertical masonry under-structure. The presence of concrete beams at the top of masonry walls can modify the global behaviour of the structure. In the past decades (80's-90's), the substitution of light roofs (i.e. wooden roofs), in favour to r.c. ones was common. The earthquakes occurred in the last 30 years have highlighted that this type of intervention changed substantially the dynamic behaviour of the structures. It adds a considerable mass on the top of the building with a higher stiffness: these two aspects caused the slipping of the roofs and the consequent collapse of the vertical masonry under-structure if not well strengthened (Figure 20).

The different type of roofs are described in 3.3.2.1 and fall in “B”, “C” and “D” classes.



Figure 20: Example of two r.c. roofs in Castelnuevo (AQ).

PARAMETER 10 – Non-structural elements

Here the presence of fixtures, appendages, ceilings, (etc..) are taken into account. Even if they are non-structural aspects, they may cause damages if excited from a seismic action.

For the case study of Castelnuevo, the principal element of vulnerability is the presence of non-structural ceilings, made

most of the time in masonry vaults, fragile, and not well linked to the vertical elements (Figure 52). Generally, the structural units fall in classes “C” and “D”, the most vulnerable.

PARAMETER 11 - State of conservation

The building's current conditions are taken here in consideration, distinguishing among the following classes:

A → good condition masonries, without crack patterns or damages;

B → capillary crack patterns of non-seismic origins;

C → wide large (2-3 mm) crack patterns or capillary crack patterns of seismic origins or state of conservation that denounces loss of masonries resistance;

D → out of plumb, heavy crack patterns, bad conservation state.

Observation

In the Vulnerability Form, there are three variable weights (Figure 15), depending on the structural characteristics. Tuscany Region assumed to calculate them considering criteria exposed in the Manual of the Form (AA.VV., 2003)

Once filled out the Form, the vulnerability index is obtained as weighted sum of the scores of each parameter:

$$(15) I_V = \sum_{i=1 \rightarrow 11} V_i \cdot P_i$$

where V_i is the score and P_i is the weight related to each parameter (Figure 15).

The vulnerability index belongs to [0, 382.5] range: it is 0 when all the parameters have “A” class and 382.5 when they are all in “D” class. It is normalized in the 0-100% range dividing the calculated I_V by the maximum values it can reach (382.5).

The GNDT II Level Form is suitable for isolated masonry buildings. Starting from that Form, Vulnerability Forms were created ad hoc for aggregate masonry structures in scientific recent study.

The first two methods (“Formisano Form” and “Aveiro Form”) refers to the vulnerability assessment of ss.uu. within the masonry aggregate, while the last one (“Aggregate Form”) refers to the study of vulnerability of an entire aggregate and it is composed by 5 parameters. There is also a Vulnerability Façade Form (“Aveiro Façades Form”).

For all the Forms, the calculation of the Vulnerability Index (I_V) follows what already written for the GNDT Form (§2.2.2).

Only the “new” parameters are described for each of the following Forms.

2.2.2.2 VULNERABILITY INDEX METHODS – FORMISANO FORM OR 15 PARAMETERS FORM

A review of the Benedetti and Petrini Form has been done by Formisano et al. (2009), with the definition of a new Vulnerability Form able to estimate the vulnerability of a structural unit within an aggregate, for which the seismic behaviour is conditioned by the presence of adjacent buildings. In the “Formisano Form”, 5 more parameters in addition to the GNDT II Level Form are included while the P3 (§2.2.2.1) is deleted. From past literature reviews (Giovinnazzi, 2005) Formisano (2009) individuated the new parameters that keep into account specific features of building in aggregates in:

- P11. presence of adjacent buildings with different height;
- P12. position of the building within the aggregate;
- P13. presence and number of staggered floors;
- P14. effect of structural or typological heterogeneity among adjacent structural units;
- P15. difference of the holes percentage of openings among adjacent façades.

As well as for the vulnerability GNDT Form, all these issues are differentiated into four classes (“A”÷“D”, with increasing level of vulnerability). Scores and weights to the “new” parameters were assigned according to the results of the application of static non-linear analyses to some case studies. The aggregates were schematized as equivalent frame models and 3MURI® software have been used (§7.3, Lagomarsino et al., 2013) to perform detailed analyses to estimate the global capacity of the structure. The results have been discussed in term global capacity, not taking into account the local single behaviour of the masonry (out-of-plane mechanisms). Some parameters influence in a positive way the capacity of the

structural units studied, to which negative scores related to the “positive” vulnerability classes (“A” or “B”) were assigned. In particular, for the P12 (Figure 21), all the classes produces negative weight*score. Considering the best condition for P12, its judgment influences (in *reducing* the vulnerability index) the 13% of the vulnerability index.

FORMISANO FORM -15 PARAMETERS - MASONRY BUILDINGS SS.UU.					
Parameters	scores				weight
	A	B	C	D	
1 - Vertical elements organization	0	5	20	45	1.00
2 - Type and quality of vertical elements	0	5	25	45	0.25
3 - Building position and type of foundation	0	5	25	45	0.75
4 - Plan distribution of structural elements	0	5	25	45	1.50
5 - Regularity in plan	0	5	15	45	0.50
6 - Regularity in elevation	0	5	25	45	1.00
7 - Floors	0	5	25	45	0.75
8 - Roof	0	15	25	45	0.75
9 - Details (non structural elements)	0	0	25	45	0.25
10 - Actual state (conservation status)	0	5	25	45	1.00
11 - Interaction in elevation - Presence of adjacent buildings with different heights	-20	0	15	45	1.00
12 - Interaction in plan - position of the building in the aggregate	-45	-25	-15	0	1.50
13 - Staggered floors	0	15	25	45	0.50
14 - Typological and structural differences	-15	-10	0	45	1.20
15 - Different percentage of opening areas among adjacent facades	-20	0	25	45	1.00

Figure 21: “Formisano” Form (15p.): parameters, scores and weights.

PARAMETER 11: Interaction in elevation

The interaction in elevation between two structural units generally influence in a negative way the seismic response. The optimal condition is when two ss.uu. have the same height, as they perform a confinement action. The plausible configurations of the interaction in elevation are reported in Figure 22. An example of “B” class is reported in Figure 25b.

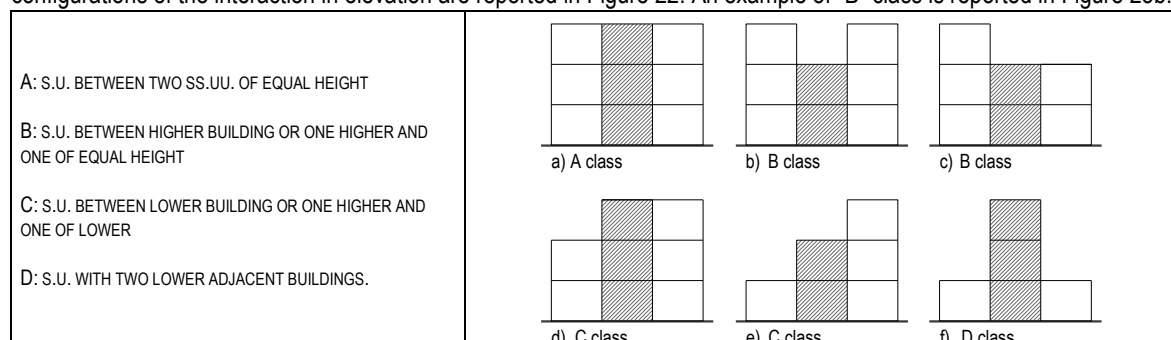


Figure 22: Possible configurations of internal s.u. within an aggregate and classes for P11.

PARAMETER 12: Interaction in plan, position of the building inside the aggregate.

The plan interaction with adjacent ss.uu. focuses on the possible position that ss.uu. can cover inside the aggregates. They can have *corner* (A) position, *external* or *header* (E) position or *internal* (I) one. Isolated aggregate (IS) refers aggregate with one single s.u..

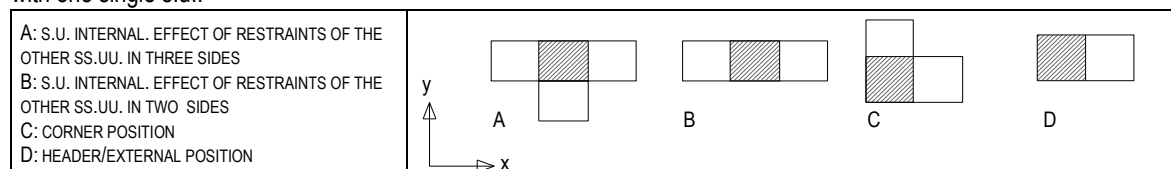


Figure 23: Possible plan configurations and classes for parameter 12.

PARAMETER 13: Staggered floors

The presence of staggered floors can cause local thrusting force (pounding) in the common walls among adjacent buildings. This parameter assesses the presence of horizontal misalignment of holes and staggered floors. The type of class depends on the ratio between the number of staggered floors and the total number of the floors that are considered

adjacent (Figure 24). The authors of the Form suggested to consider staggered floors when they have almost 50 cm of altitude of difference. The ground floor is excluded from this computation.

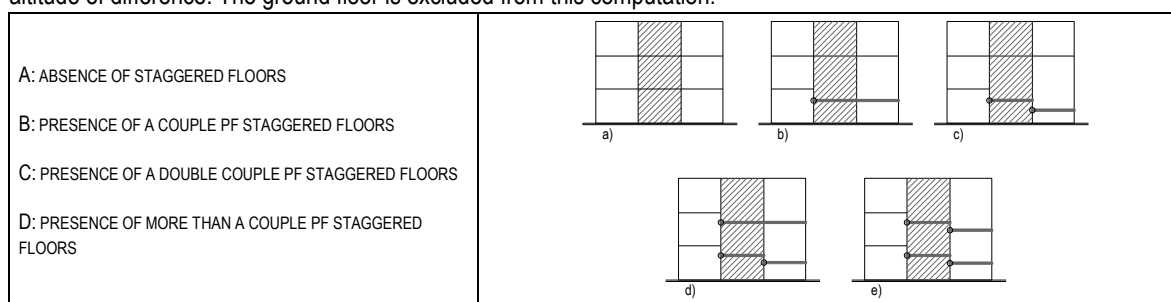


Figure 24: Classes of parameter 13 and possible configuration of staggered floors among ss.uu..

PARAMETER 14: Typological and structural differences

With this parameter, differences in terms of structural characteristics are assessed for adjacent structural units.

PARAMETER 15: Different percentage of opening areas among adjacent façades

The difference among open areas may influence the distribution of horizontal actions between the façades (the geometrical dimension of piers and spandrel change). The four vulnerability classes differentiate for the holes percentages among two adjacent structural units. In particular, when the % of difference for adjacent buildings is less than 5%, the class is "A", "B" when it is between 5% and 10%, "C" if it is between 10% and 20% and "D" when it is major than 20%.



Figure 25: a) Example of different % between two ss.uu. (aggr. 13-158): b) different n° of floors.

2.2.2.3 VULNERABILITY INDEX METHODS – AVEIRO FORM OR 14 PARAMETERS FORM

This vulnerability Form is developed by Vicente (2008) (University of Aveiro, Portugal) and it is composed ad hoc for masonry ss.uu. inside the aggregate. It is composed of 14 parameter that can be divided into 4 macro-classes. The starting point of the form is the GNDT II Level Form, in which 3 parameters were added (Figure 26). As well as the "Formisano Form", "Aveiro Form" aims to evaluate the effect of the specific issues of aggregates buildings in the definition of the structural vulnerability.

PARAMETER 5: Number of floors

The parameter evaluates the variation of mass and stiffness in the floors and the height configuration. Masonry structures tend to be more vulnerable with the growing of the number of floors, due to the irregularities in the structural frame (and lack of verticality of the walls), the second order effects etc .. The parameter does not evaluate the percentage of variation of mass and stiffness for the storeys; rather, it takes into account the stability collateral to the height of the structure. "A" class refers to one-floor building, "B" to two or three-floors ones, "C" to four-five-storeys and "D" for more than 5 storeys.

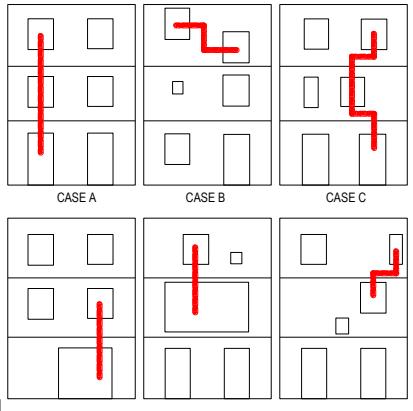
AVEIRO FORM - 14 PARAMETERS - MASONRY BUILDINGS SS.UU.					
Parameters	scores				weight
	A	B	C	D	
1. Structural building system					
P1 Type of resisting system	0	5	20	50	0.75
P2 Quality of the resisting system	0	5	20	50	1
P3 Conventional strength	0	5	20	50	1.5
P4 Maximum distance between walls	0	5	20	50	0.5
P5 Number of floors	0	5	20	50	1.5
P6 Location and soil conditions	0	5	20	50	0.75
2. Irregularities and interaction					
P7 Aggregate position and interaction	0	5	20	50	1.5
P8 Plan configuration	0	5	20	50	0.75
P9 Regularity in height	0	5	20	50	0.75
P10 Wall façade openings and alignments	0	5	20	50	0.5
3. Floor slabs and roofs					
P11 Horizontal diaphragms	0	5	20	50	1
P12 Roofing system	0	5	20	50	1
4. Conservation status and other elements					
P13 Fragilities and conservation state	0	5	20	50	1
P14 Non-structural elements	0	5	20	50	0.5

Figure 26: “Aveiro” Form (14p.): parameters, scores and weights.

PARAMETER 10: Wall façade openings and alignments

The seismic-resistance of masonry walls must have continuity from top to the bottom, up to the footing system, net of the openings. The higher holes misalignment, the lower the number of seismic-resistant piers for the transmission of horizontal and vertical loads with the consequence of greater vulnerability for the structures (Table 12).

Table 12: Classes of parameter 15 and possible configurations of misalignments of openings in ss.uu..

<p>A: OPENINGS WITH REGULAR SIZE AND ALIGNED IN HEIGHT</p> <p>B: REGULAR OR IRREGULAR OPENINGS HORIZONTALLY MISALIGNED MORE THAN $\frac{1}{2}$ OF THEIR HEIGHT.</p> <p>C: OPENINGS REGULAR OR IRREGULAR VERTICALLY MISALIGNED BY MORE THAN $\frac{1}{2}$ OF THEIR WIDTH.</p> <p>D: REGULAR OR IRREGULAR OPENINGS TOTALLY MISALIGNED HORIZONTALLY OR VERTICALLY; IS THE CASE OF LARGE OPENINGS PLACED IN ANY PLANE.</p>	 <p>The diagram shows four cases of wall openings and alignments. Case A shows a single vertical opening. Case B shows two openings horizontally misaligned. Case C shows two openings vertically misaligned. Case D shows a large opening at the bottom of the wall.</p>
--	---

2.2.2.4 VULNERABILITY INDEX METHODS – AGGREGATE FORM OR 5 PARAMETERS FORM

This Form (Ferreira et al., 2012) is conceptually different from the previous reported above; indeed, this Form is composed by 5 parameters, to assess a vulnerability index to an aggregate in its entirety. The parameters evaluated are almost qualitative, suitable for a preliminary screening of the buildings, in case of large-scale assessment, for which the sample of study refers to high number of buildings. The parameters are expressed in Figure 27 and Table 13 (significant pictures of Castelnuovo aggregates explaining these issues are reported in CHAPTER 5).

PARAMETER P1: Quality of the masonry fabric

This parameter assesses the type of masonry among the ss.uu. of the aggregate, defining sub-classes of masonry. The sub-classes are different in terms of element types, presence of connections and type of mortar. The sub classes are individuated in Table 13 (row 1).

AGGREGATE FORM - 5 PARAMETERS					
Parameters	scores				weight
	A	B	C	D	
1 - Quality of the masonry fabric	0	5	20	50	1.50
2 - Misalignment of openings	0	5	20	50	0.50
3 - Irregularities in height	0	5	20	50	0.75
4 - Plan geometry	0	5	20	50	0.75
5 - Location and soil quality	0	5	20	50	0.75

Figure 27: Aggregate Form: parameters, scores and weights.

PARAMETER P2: Misalignment of openings

This parameter assesses the horizontal misalignments of openings and staggered floors. The type of class depends on the ratio between the number of staggered floors and the total number of the adjacent floors. Formisano et al., 2009 suggested to consider staggered floors if there is at least 50 cm of altitude of difference. The ground floor level is not considered in the computation of this parameter, differences in altitude at that level influence the P5.

PARAMETER P3: Irregularities in height

This parameter assesses the difference in height among adjacent structural units. The criterion of classification concerns the deviation of the height of each ss.uu., from the average height of the aggregate. The type of class depends on the ratio between the sum of the number of floors missing enter two adjacent structural units and the total number of the ss.uu. inside the aggregate.

PARAMETER P4: Plan geometry

This parameter concerns the plan irregularity, using, as a decisional criterion, a relationship between the area, A, and the perimeter, P, of the plan shape of the aggregate. : $P_4=16A/P^2$.

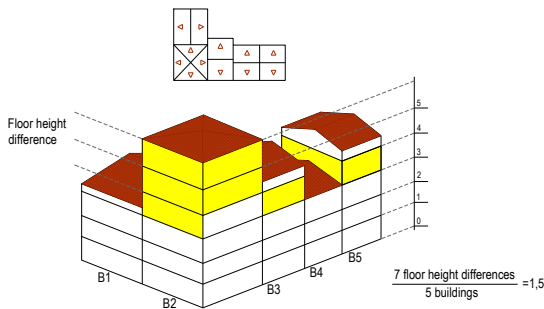
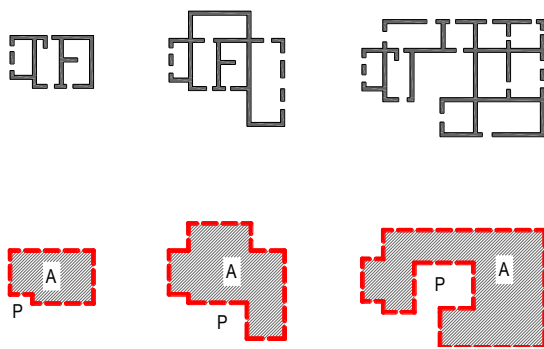
PARAMETER P5: Location and soil quality

This parameter assesses the quality of the ground foundation and the slope of the aggregate.

Vulnerability classes' classification and criteria of the "Aggregate Form" 5P are shown in next figure (Ferreira et al., 2012).

Table 13: Description of the 5 parameters and classes of the Vulnerability Form (Ferreira et al., 2012)

Vulnerability class definition for Parameter P1		Vulnerability class definition for Parameter P2	
A	More than 75% of buildings belong to subclass Sc1	A	Less than 25% of cases of horizontal misalignment of openings between adjacent buildings.
B	Less than 25% of buildings belong to subclass Sc3 and Sc4 and more than 25% of buildings belong to subclass Sc2, Sc3 and Sc4.	B	More than 25% and less than 50% of cases of horizontal misalignment of openings between adjacent buildings.
C	Less than 25% of buildings belong to subclass Sc4 and more than 25% of buildings belong to subclass Sc3 and Sc4	C	More than 50% and less than 75% of cases of horizontal misalignment of openings between adjacent buildings
D	More than 25% of buildings belong to subclass Sc4	D	More than 75% of cases of horizontal misalignment of openings between adjacent buildings.
Sc1	Brick masonry of good quality and fabric (solid bricks or hollow bricks with less than 45% of voids). Well-tailored stone masonry with homogeneous size units. Well mortared irregular stone masonry, well interlocked, presenting transversal elements in the connection between leafs.		
Sc2	Brick masonry (less than 45% of voids). Well-tailored stone masonry with little homogeneous units. Irregular stone masonry with transversal connection between leafs.		
Sc3	Brick masonry of poor quality with connection and bricklaying irregularities. Stone masonry with no tailored and heterogeneous units. Irregular stone masonry well mortared and well interlocked but with no transversal connection elements.		
Sc4	Poor quality brick masonry incorporating stone and brick fragments. Loose stone masonry. Rubble stone masonry, with no transversal connection and poorly mortared.		
Parameter 1 :vulnerability classes and sub classes of masonry		Parameter 2: vulnerability classes	

<div>  <div> $\frac{n^{\circ} \text{ of floor height differences}}{n^{\circ} \text{ of buildings}} = \alpha_{P3}$ <table> <tr><th colspan="2">Vulnerability class for Parameter P3</th></tr> <tr><td>A</td><td>$\alpha_{P3} < 0.2$</td></tr> <tr><td>B</td><td>$\alpha_{P3} < 0.5$</td></tr> <tr><td>C</td><td>$\alpha_{P3} < 0.8$</td></tr> <tr><td>D</td><td>$\alpha_{P3} \geq 0.8$</td></tr> </table> </div> </div>		Vulnerability class for Parameter P3		A	$\alpha_{P3} < 0.2$	B	$\alpha_{P3} < 0.5$	C	$\alpha_{P3} < 0.8$	D	$\alpha_{P3} \geq 0.8$
Vulnerability class for Parameter P3											
A	$\alpha_{P3} < 0.2$										
B	$\alpha_{P3} < 0.5$										
C	$\alpha_{P3} < 0.8$										
D	$\alpha_{P3} \geq 0.8$										
Parameter 3: schematisation of the floor difference in height and definition of vulnerability classes											
	<table> <tr><th colspan="2">Vulnerability class for Parameter P4</th></tr> <tr><td>A</td><td>$\frac{16A}{p^2} < 1$</td></tr> <tr><td>B</td><td>$0.75 \leq \frac{16A}{p^2} < 1$</td></tr> <tr><td>C</td><td>$0.5 \leq \frac{16A}{p^2} < 0.75$</td></tr> <tr><td>D</td><td>$\frac{16A}{p^2} < 0.5$</td></tr> </table>	Vulnerability class for Parameter P4		A	$\frac{16A}{p^2} < 1$	B	$0.75 \leq \frac{16A}{p^2} < 1$	C	$0.5 \leq \frac{16A}{p^2} < 0.75$	D	$\frac{16A}{p^2} < 0.5$
Vulnerability class for Parameter P4											
A	$\frac{16A}{p^2} < 1$										
B	$0.75 \leq \frac{16A}{p^2} < 1$										
C	$0.5 \leq \frac{16A}{p^2} < 0.75$										
D	$\frac{16A}{p^2} < 0.5$										
Parameter 4: schematisation of the plan geometry and definition of vulnerability classes											
<table> <tr><th colspan="2">Vulnerability class definition for Parameter P5</th></tr> <tr><td>A</td><td>Aggregate founded on rock or on a coherent soil with less than 10% slope. Located in areas with no special constraints and no gaps.</td></tr> <tr><td>B</td><td>Aggregate founded on rock or on a coherent soil with a slope between 10 and 30%. Landfill soils with gaps.</td></tr> <tr><td>C</td><td>Aggregate founded on rock or on a coherent soil with a slope between 30 and 50%. Landfill soils with probable impulses.</td></tr> <tr><td>D</td><td>Aggregate founded on rock or on a coherent soil with more than 50% slope or on heterogeneous soil with more than 50% slope. Located in ravine or cliff. Possible soil liquefaction, soil slip (landfill and alluvial layers), layered soil heterogeneity, soft and loose clay soil, landfills</td></tr> </table>	Vulnerability class definition for Parameter P5		A	Aggregate founded on rock or on a coherent soil with less than 10% slope. Located in areas with no special constraints and no gaps.	B	Aggregate founded on rock or on a coherent soil with a slope between 10 and 30%. Landfill soils with gaps.	C	Aggregate founded on rock or on a coherent soil with a slope between 30 and 50%. Landfill soils with probable impulses.	D	Aggregate founded on rock or on a coherent soil with more than 50% slope or on heterogeneous soil with more than 50% slope. Located in ravine or cliff. Possible soil liquefaction, soil slip (landfill and alluvial layers), layered soil heterogeneity, soft and loose clay soil, landfills	Parameter 5 (on the left cell): schematisation of the plan geometry and definition of vulnerability classes
Vulnerability class definition for Parameter P5											
A	Aggregate founded on rock or on a coherent soil with less than 10% slope. Located in areas with no special constraints and no gaps.										
B	Aggregate founded on rock or on a coherent soil with a slope between 10 and 30%. Landfill soils with gaps.										
C	Aggregate founded on rock or on a coherent soil with a slope between 30 and 50%. Landfill soils with probable impulses.										
D	Aggregate founded on rock or on a coherent soil with more than 50% slope or on heterogeneous soil with more than 50% slope. Located in ravine or cliff. Possible soil liquefaction, soil slip (landfill and alluvial layers), layered soil heterogeneity, soft and loose clay soil, landfills										

2.2.2.5 VULNERABILITY FORMS FOR FAÇADES

In historical city centres, the evolution process has a fundamental role within the buildings. A masonry aggregate is the result of a complex and time process of construction which gives a certain asset to the ss.uu. inside it. The ss.uu. have generally common walls and not very stable links between horizontal elements and the vertical ones. The absence of restraints among structural main elements and orthogonal walls generally does not allow the global participation of all resistant elements, with consequent structural independent behaviour of them. In particular, masonry façades are disconnected from the remaining part of the structure (orthogonal walls), and they have generally staggered floors increasing their propensity to show out-of-plane mechanisms. Indeed, the major parts of the damages observed after the recent earthquakes (Abruzzo 2009, Molise e Puglia, 2002) were related to the collapse local parts of aggregates out-of-their planes. Based on the work done by D'Ayala & Speranza (2002), Vincente (2008) implemented a Vulnerability Façade Form, describing the most vulnerable issues of the façades toward out-of-plane mechanisms. In analogy with the other Forms explained, this method consists in filling out in a survey form composed of 10 parameters (Figure 28), depending on the façade structure's characteristics and it allows the estimation of the vulnerability index, in a scale [0, 100].

FaçADES FORMS - MASONRY BUILDINGS SS.UU.					
Parameters	scores				weight
	A	B	C	D	
Holes geometry					
P1 Geometry of the façade	0	5	20	50	0.5
P2 Maximum height	0	5	20	50	0.5
P3 Opening area	0	5	20	50	0.5
P4 Misalignment of the openings	0	5	20	50	0.5
2. Materials and state of deterioration					
P5 Quality of materials	0	5	20	50	0.75
P6 State of conservation	0	5	20	50	0.75
3. Connection to other structural elements					
P7 Efficiency of connection between orthogonal walls	0	5	20	50	0.5
P8 Connection between horizontal diaphragm and roof	0	5	20	50	0.5
P9 Impuls of roof	0	5	20	50	0.5
4. Connection elements of facade					
P10 Non-structural elements	0	5	20	50	0.5

Figure 28: Façade Form: parameters and weights.

2.2.2.6 OBSERVATIONS AMONG THE VIM

The critical comparison of the different Forms has allowed to highlight the major differences and similarities among the VIMs (Figure 29). In particular, equal parameters have different values of scores in different procedure or even different weight in the calculation of the vulnerability index.

The GNDT 11P Form, originally implemented for isolated structures, is the base Form the other ones, in which some parameters are added, that refer to the major issues of the masonry construction of aggregate type.

In the 15P Form ("Formisano Form") the conventional strength (P3 in GNDT Form) is deleted. It is a big-importance parameter, not only because it assumes the highest weight (1.5) but also because it is the only "analytical" parameter in the calculation of I_v , not subjected by judgment of the person who fills out the Form. P11 ("interaction in elevation") and P14 ("typological and structural differences" between storeys or adjacent buildings) are parameters present only in the "Formisano Form".

The number of floor (P5) is considered in explicit way only in "Aveiro Form", not directly in the others.

The interaction in plan (that refers to the ss.uu. position) is present both in "Formisano" and "Aveiro Forms". The weight of the parameter is the same but the scores related to the judgments' classes are different and with opposite values.

For each Form, the percentage of importance of the parameters were calculated and reported on the following (Table 14). In the GNDT II Level Form, P3 ("conventional strength") is the most influent, with a percentage of importance of 18%; there are 5 parameters characterized by a percentage of importance of 12%. The less influence parameters are the P2 ("quality of the resistant system"), P8 ("maximum distance among walls") and P10 ("non structural elements") with a 3% of importance. It means that if one of the latter parameters change its relative value, the global value of I_v does not change significantly.

It is worth noting that two of the less important parameters, P8 and P10, deal principally about the out-of-plane behaviour of the structure (mechanisms of first mode, §7.2).

In the "Formisano Form", the P4, "Plan distribution of structural elements" reaches importance of 13%, which is, despite the absolute less value, the higher impact parameter in the Form. "New" parameters have negative scores for less vulnerability classes. This means that the P11, P12, P14 and P15 parameters influence in an opposite way the global vulnerability of the structure. For example, in P12 all the classes available produce negative weight*scores. Considering the best judgment for P2 ("A" class), its influence (in *reducing* the vulnerability index) is 13%, while if the judgment is in "D" class it has no influence.

MASONRY BUILDINGS - COMPARISON AMONG FORMS FOR SS.UU. WITHIN THE AGGREGATE					
FORMISANO FORM 15 P	GNDT 11P	AVEIRO FORM 14P	AVEIRO FORM 14P	GNDT 11P	FORMISANO FORM 15 P
1 - Vertical elements organization	1	P1	P1 Type of resisting system	1	1
2 - Type and quality of vertical elements	2	P2	P2 Quality of the resisting system	2	2
3 - Building position and type of foundation	4	P6	P3 Conventional strength	3	-
4 - Plan distribution of structural elements	8	P4	P4 Maximum distance between walls	8	4
5 - Regularity in plan	6	P8	P5 Number of floors	-	-
6 - Regularity in elevation	7	P9	P6 Location and soil conditions	4	3
7 - Floors	5	P11	P7 Aggregate position and interaction	-	12
8 - Roof	9	P12	P8 Plan configuration	6	5
9 - Details	10	P14	P9 Regularity in height	7	6
10 - Current state	11	P13	P10 Wall façade openings and alignments	-	15
11 - Interaction in elevation	-	-	P11 Horizontal diaphragms	5	7
12 - Interaction in plan - position...	-	P7	P12 Roofing system	9	8
13 - Staggered floors	-	-	P13 Fragilities and conservation state	11	10
14 - Typological and structural differences	-	-	P14 Non-structural elements	10	9
15 - Different % of opening adjacent facades	-	P10			

Figure 29: Comparison among ss.uu. Forms.

Table 14: Maximum influence of each parameter in GNDT (11p) and Formisano (15p) Vulnerability Form.

GNDT II LEVEL FORM - 11 PARAMETERS - MASONRY BUILDINGS							
Parameters	scores				weight	Weighted scores	% of influence
	A	B	C	D			
1 - Type and organisation of resistant system	0	5	20	45	1.00	45.00	12%
2 - Quality of resistant system	0	5	25	45	0.25	11.25	3%
3 - Conventional strength	0	5	25	45	1.5	67.50	18%
4 - Building position and type of foundation	0	5	25	45	0.75	33.75	9%
5 - Horizontal elements (floors)	0	5	15	45	1.00	45.00	12%
6 - Planimetrical configuration	0	5	25	45	0.50	22.50	6%
7 - Configuration in elevation	0	5	25	45	1.00	45.00	12%
8 - Maximum distance among the walls	0	5	25	45	0.25	11.25	3%
9 - Coverage/roof	0	15	25	45	1.00	45.00	12%
10 - Non structural elements	0	5	25	45	0.25	11.25	3%
11 - Actual state (conservation status)	0	5	25	45	1.00	45.00	12%

FORMISANO FORM -15 PARAMETERS - MASONRY BUILDINGS SS.UU.							
Parameters	scores				weight	Weighted scores	% of influence
	A	B	C	D			
1 - Vertical elements organization	0	5	20	45	1	45.00	9%
2 - Type and quality of vertical elements	0	5	25	45	0.25	11.25	2%
3 - Building position and type of foundation	0	5	25	45	0.75	33.75	7%
4 - Plan distribution of structural elements	0	5	25	45	1.5	67.50	13%
5 - Regularity in plan	0	5	15	45	0.5	22.50	4%
6 - Regularity in elevation	0	5	25	45	1	45.00	9%
7 - Floors	0	5	25	45	0.75	33.75	7%
8 - Roof	0	15	25	45	0.75	33.75	7%
9 - Details (non structural elements)	0	0	25	45	0.25	11.25	2%
10 - Actual state (conservation status)	0	5	25	45	1	45.00	9%
11 - Interaction in elevation - Presence of adjacent buildings...	-20	0	15	45	1	45.00	9%
12 - Interaction in plan - position of the building in the aggregate	-45	-25	-15	0	1.5	0.00	0%
13 - Staggered floors	0	15	25	45	0.5	22.50	4%
14 - Typological and structural differences	-15	-10	0	45	1.2	54.00	10%
15 - Different percentage of opening areas among adjacent facades	-20	0	25	45	1	45.00	9%

In the “Aveiro Form”, the scores are equal for all the classes (0, 5, 20 e 50), while the weight assumes different values. The parameter’s impact is then due to the parameters’ weight. P3 (“conventional strength”) and P8 (“plan configuration”), characterised by major weight, have the major importance, 12%. The parameters with lower importance level (4%) are “maximum distance between walls” (P4), “wall façade openings and alignments” (P10) and “non-structural elements” (P14) (Figure 30).

As well as for “Aveiro Form”, for the “Aggregate Form” (5P), having the parameters equal scores for the judgments, the importance of the parameter is due to the parameters’ weight. P1 assumes 35% of importance, while P2 the lower, 12%. The other parameters are collaborating for 18%, having equal values of their weights, 0.75.

AVEIRO FORM - 14 PARAMETERS - MASONRY BUILDINGS SS.UU.								
Parameters	scores				weight	Weighted scores	% of influence	
	A	B	C	D				
P1 Type of resisting system	0	5	20	50	0.75	37.50	6%	
P2 Quality of the resisting system	0	5	20	50	1	50.00	8%	
P3 Conventional strength	0	5	20	50	1.5	75.00	12%	
P4 Maximum distance between walls	0	5	20	50	0.5	25.00	4%	
P5 Number of floors	0	5	20	50	1.5	75.00	12%	
P6 Location and soil conditions	0	5	20	50	0.75	37.50	6%	
P7 Aggregate position and interaction	0	5	20	50	1.5	75.00	12%	
P8 Plan configuration	0	5	20	50	0.75	37.50	6%	
P9 Regularity in height	0	5	20	50	0.75	37.50	6%	
P10 Wall façade openings and alignments	0	5	20	50	0.5	25.00	4%	
P11 Horizontal diaphragms	0	5	20	50	1	50.00	8%	
P12 Roofing system	0	5	20	50	1	50.00	8%	
P13 Fragilities and conservation state	0	5	20	50	1	50.00	8%	
P14 Non-structural elements	0	5	20	50	0.5	25.00	4%	

Figure 30: Aveiro Form (14p.), weights and scores and individuation of the more influential parameters.

AGGREGATE FORM - 5 PARAMETERS								
Parameters	scores				weight	Weighted scores	% of influence	
	A	B	C	D				
1 - Quality of the masonry fabric	0	5	20	50	1.5	75.00	35%	
2 - Misalignment of openings	0	5	20	50	0.5	25.00	12%	
3 - Irregularities in height	0	5	20	50	0.75	37.50	18%	
4 - Plan geometry	0	5	20	50	0.75	37.50	18%	
5 - Location and soil quality	0	5	20	50	0.75	37.50	18%	

Figure 31: Aggregate Form (15P) weights and scores and individuation of the more influential parameters.

2.2.3 VULNERABILITY CURVES

As expressed at the beginning of the chapter, each VIM's goal is to provide information about the structure's propensity to suffer a certain level of damage due to seismic events of certain intensity.

But, which is the correlation among vulnerability, seismic intensity and the expected damage on structures?

A vulnerability curve is the result of the correlation enter vulnerability, the intensity of the seismic event (hazard) and the damage that could be appear in the structure (μ_D).

The first studies on vulnerability-damage correlations started in 1970-1980 years, with the analysis of Guagenti and Petrini, (Guagenti & Petrini, 1989), based on observations of past damage data found on masonry buildings hit by earthquakes. They defined the quantities y_i , the ground acceleration, and d , damage level as stochastic quantities. Ground accelerations, in particular, may vary between y_i , which corresponds to the starting point of the damage for the structure and the y_c , which refers to the collapse, while d varies in the [0-1] range. Benedetti and Petrini referred to a numerical index of damage (d_e), able to take into account, with the physical structural damage for masonry structures, the social, economic losses associated to post earthquake management (Meroni, Petrini, & Zonno) defined in the vulnerability GNDT I Level Form (GNDT, 1993) (Colonna et al., 1994).

In Figure 32, there quantities y_i and y_c are individuated, in which their aleatory behaviours are shown. Indeed, both the value of y_i and y_c may have different values, following a probabilistic density function. For a certain y_k values, it is possible to know the d_h -quantity, characterised by a certain probability density conditioned function $p\{d_h/y_k\}$ as expressed on a quality level in Figure 32.

The DPM (§2.2.1) are the *discretisation* of the probabilistic approach of this problem, in which for a certain level of vulnerability, a certain damage level can be found. In the deterministic way, the function y_k - d_h is expressed Figure 33 in which the equation for the tri-linear law is:

$$\begin{aligned}
 d &= 0 && \text{when } y_k < y_i \\
 d &= (y - y_i) / (y_c - y_i) && \text{when } y_i < y_k < y_c \\
 d &= 1 && \text{when } y_k > y_c
 \end{aligned}$$

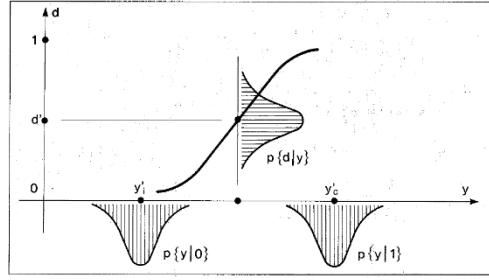


Figure 32: Ground acceleration – damage probabilistic law (GNDT, 1993).

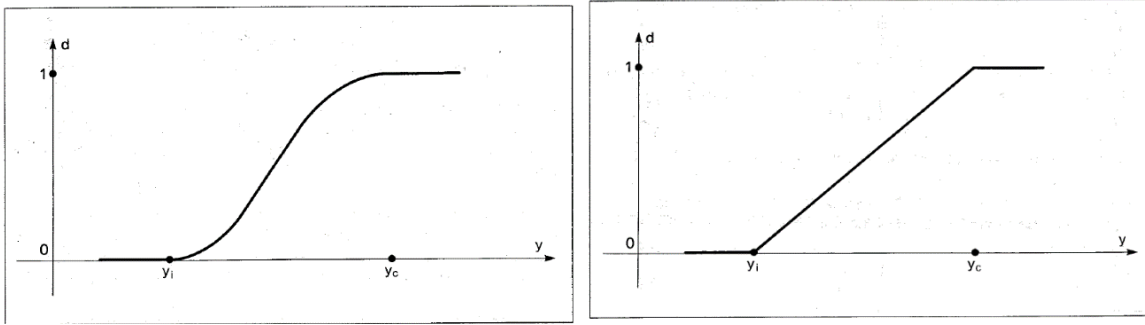


Figure 33: Vulnerability curves, trilinear approximation function (d,y curves).

Through the study of a consistent sample of buildings within city centres hit by seismic events, the vulnerability curves have been derived for masonry structures, with reference to ground accelerations related to MCS intensity scale. Figure 34a shows the correlation found for buildings divided in three systems depending on the seismic intensity recorded: Venzone (IX), Tarcento and San Daniele (VIII) and Barrea (VII). The proposed vulnerability curves are those on Figure 34b. Their equations are expressed by:

$$y_i = \alpha_i \cdot \exp(-\beta_i \cdot I_V) \quad y_c = (\alpha_c + \beta_c \cdot I_V^\gamma)^{-1}$$

$$\alpha_i = 0.08, \quad \beta_i = 0.01950$$

$$\alpha_c = 1.00, \quad \beta_c = 0.00191, \quad \gamma = 1.80$$

For a value of vulnerability defined for a structure (in the scale [0-100]), it is possible to calculate the accelerations y_i and y_c in correspondence of the structural first damage and its collapse. The value of vulnerability index is related to the filling out of the GNDT II Form (11P, 2.2.2.1).

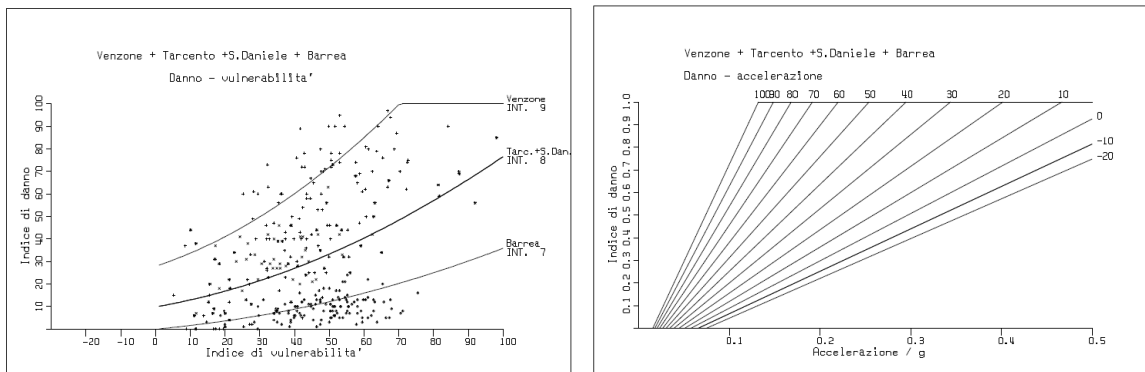


Figure 34: (a) Correlation between vulnerability and damage (b) Relation vulnerability-damage and acceleration.

In this research, different VIMs were applied to the aggregates and structural units of Castelnuovo: the GNDT 11P Forms, the “Aggregate Form” and the “Aveiro and Formisano Forms”. For the sample of data, hit by the earthquake of L’Aquila 2009, the post-earthquake surveys level of damage for aggregates was known with reference to the EMS-98 Scale. It is important to describe the correlation between the vulnerability curves associated to the VIM (mentioned in the last paragraph) and the vulnerability curves derived from the macroseismic method (§2.2.1.2), that are linked to the definition

of mean damage grade for vulnerability classes according to the EMS-98 scale.

The two vulnerability curves diverge for:

- the definition of hazard: Guagenti and Petrini refer to seismic hazard in term of peak ground acceleration (derided from the knowledge of the MCS macroseismic intensities), while macroseismic methods refers to macroseismic intensity relative to EMS-98 scale. With the definition of equation (10) and the correlations introduced in 1.1.1.2 (Margottini et al., 1992) to pass from the macrosieismic intensity to the peak ground of acceleration, this dissimilarity is overcome.
- the definition of damage: Guagenti and Petrini refer to an index of economic damage (d_e , in a [0-1] range) (GNDT, 1993), while macroseismic methods refer to the mean structural damage grade, related to the EMS-98 scale definition.

Several authors (Vicente, 2008) reported correlations between the index of economic damage (d_e) and the mean damage structural grade (μ_D): two of them are depicted in Figure 35a, that of Bramerini et al. (1995) and Dolce et al., (2000). In this thesis, the analytical correlation proposed by Bramerini et al. (1995) is used, adopted also in previous studies by the NSS (National Seismic Service):

$$\mu_D = 5 \cdot d_e^{0.52}$$

Once defined the limits of seismic acceleration, y_i , for seismic intensity I_{EMS-98} , and once transformed the index of economic damage d_e in mean damage grade, μ_D , it is possible to compare the vulnerability curves of Benedetti-Petrini with the macroseismic methodology (Giovinazzi, 2004), in the format $I-\mu_D$ (Figure 35b). The overlapping between the two vulnerability curves with respect to a central value of the average damage ($\mu_D = 2.5$) (Figure 35b) allows the determination of the correlation among the Vulnerability index (I_V) and the V parameter of the macroseismic method. The relationship is expressed in the following equation:

$$V = 0.49 + 0.0064 I_V$$

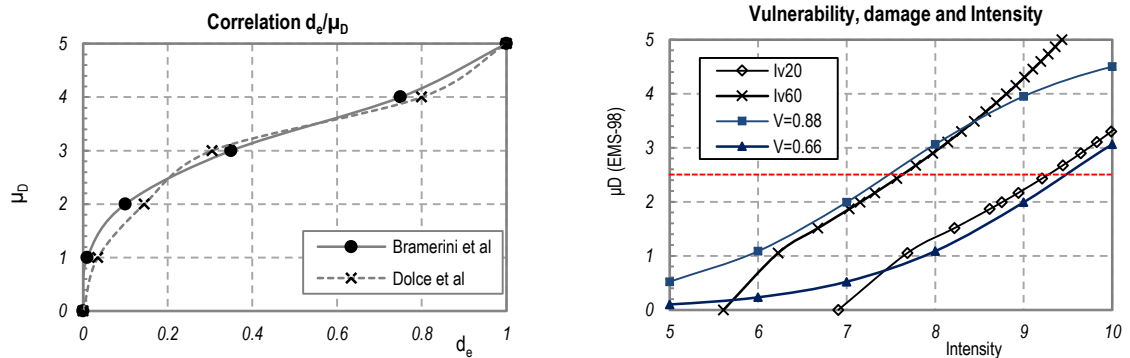


Figure 35: a) Correlations between the damage index (d_e) and the mean damage grade (μ_D); b) Macroseismic method: comparison with GNDT II level Form for A and B classes of EMS-98.

Bernardini et al., 2007a, 2007b and 2011, starting from the results of the macroseismic methods (Giovinazzi, 2005) proposed a modified analytical expression of the vulnerability curves in order to obtain the best fit correlation among the hazard (in term of macroseismic intensities), the mean damage grade (μ_D [0,5] range), and the vulnerability value (Eq.(16)). V , the vulnerability value within the analytical expression, independent from the intensity of the earthquake is associated to each vulnerability class ("A"-"F", in EMS-98) and can vary enter the [0,1] range. For the vulnerability classes of the EMS-98 for masonry structures, V are reported in the following table:

Table 15: Correlation between the I_V and the V parameters for vulnerability classes (Bernardini, et al., 2007).

V_A	V_B	V_C	V_D	V_E	V_F
0.88	0.72	0.56		0.24	0.08
$I_V = 50$	$I_V = 25$	$I_V = 0$	-	-	-

The expression of the relationship of the vulnerability curves is Eq.(16):

$$(16) \quad \mu_D = 2.5 + 3 \cdot \tanh\left(\frac{I+6.25 \cdot V-12.7}{3}\right) \cdot f(V, I) \quad 0 \leq \mu_D \leq 5$$

$$f(V, I) = \begin{cases} e^{\frac{V}{2}(I-7)} & \text{se } I \leq 7 \\ 1 & \text{se } I > 7 \end{cases}$$

$$V = 0.56 + 0.0064 I_V$$

Q represents the slope of the vulnerability function (rate of damage increases with rising intensity). In the original macroseismic method it was worth 2.3. Bernardini (2011) suggested Q=3 to have the best fit among the GNDT curves and EMS-98 functions, recommended also for masonry buildings of fairly ductile behaviour by Sandi and Floricel (1995).

The latter part of the function $f(V, I)$ in Eq.(16) is provided to take into account the perfect overlapping of the vulnerability functions for the lower-7 values of the macroseismic intensity, even if the study of vulnerability and damage expected for a low level of intensity degree is not generally taken in to account.

Ferreira et al., 2012 used the equations derived by Bernardini et al. to estimate damage scenario on aggregates using the “Aggregate Form” (5P), used in CHAPTER 5 of this thesis.

Following the same procedure of comparison of the vulnerability index methods and the macroseismic method, Formisano e et al., 2011 and Vicente et al., 2011 provide the equations to use for the calculation of the mean damage grade (μ_D) in structural units starting from the vulnerability indexes (I_{V15} and I_{V14}) of their Forms (CHAPTER 6).

2.3 ANALYTICAL METHODS

Analytical methods are VAMs that use mechanical or numerical procedures to assign seismic vulnerability on buildings. They can be divided between methods that use basic analytical methods (gained from simple calculation) or complex analytical methods, using modern refined approaches and analyses. The analytical methods require a large number of information and wide knowledge of the structures. Their adoption is linked to small sample of buildings because of the large computational effort they need for the realization of the model and the large knowledge level that is necessary to achieve in performing so refined analysis.

The analytical methods can be divided depending on the type of analysis performed, taking as reference the way of response that a masonry structure can have if excited by seismic actions. The two families are related to the out-of-plane mechanisms response of masonry structures (“mechanisms methods”) and the in-plane global response of it (see §7.1).

The analytical methods allow the calculation of the level of vulnerability, defining the safety index of the structures analysed (I_S). The safety index is defined as the ratio of the seismic capacity of the structure (i.e. in terms of peak ground acceleration, $a_{g,C}$ or reference period, T_{RC} or other seismic indicators) that produces on the structures the achievement of the chosen limit state, and the seismic demand of the site in which the structure is collocated, associated the same limit state. Since the safety index involves the seismic demand (hazard) and the structural vulnerability, it is usually considered as an index of seismic risk. In terms of peak ground acceleration, it is equal to: $I_S = a_{g,C}/a_{g,D}$.

2.3.1 MECHANISMS METHODS

The seismic response of a masonry building can have two categories of hypothetical collapse mechanisms: first way mechanisms, the out-of-plane mechanisms, and the second way mechanisms, the in-plane mechanisms (Giuffrè A., 1993). The way of seismic collapse depends on different factors related to the building characteristics. First, the age of the construction and the state of conservation of the masonry aggregate assumes great importance. A structure can have a “global box behaviour” if it has good connection among orthogonal walls, and good connection between horizontal and vertical elements, able to guarantee the horizontal distribution of shear forces.

The mechanisms methods consist on the determination of the multiplier of horizontal action that triggered a mechanisms and then compared with the seismic demand (§7.2).

2.3.1.1 FAMIVE

The FaMIVE (Failure Mechanisms Identification and Vulnerability Evaluation) (D'Ayala & Speranza, 2002) is an analytical mechanism method used for the seismic vulnerability evaluation of single buildings. With the filling of an interactive electronic Form (Figure 36), the procedure calculates load factors associated to various collapse mechanisms of vertical macro-element assemblies. The Form allows the definition of the most probable collapse mechanism of the studied masonry façade, depending on the geometrical features, the loads, the restraints and boundary condition, to which is associate the lower failure loads factor/multiplier (α_0).

This procedure could be applied in case study for which information are relative only to in situ external inspection and there are a high level of uncertainty in the value of boundary conditions and the level of loads. Since the electronic form provided the most plausible mechanisms within all possible, it could have been applied in case of post-earthquake data, as in Castelnovo aggregates, to understand the effect of the unknown level of boundary conditions and loads among orthogonal walls. The comparison would have put in light if the results of the electronic form had been equal of those actually showed by the Castelnovo aggregates.

INSPECTION FORM FOR THE SURVEY OF ORDINARY BUILDINGS

Address: Town: Date:

1 URBANISTIC DATA

1-1 Block access and escape routes: 1-4 Position of building within the block:

1-2 Shape and composition of the block: 1-5 Connection of the façade to adjacent walls:

1-3 Number of buildings in the block:

2 GEOMETRIC CHARACTERISTICS OF THE FACADE

2-1 Façade orientation: 2-5 Total height of the façade:

2-2 Number of storeys of the building: 2-6 Presence of gable:

2-3 Number of storeys of the façade: 2-7 Gable height (if present):

2-4 Length of the façade: 2-8 Additional corner in the façade:

3 GEOMETRIC CHARACTERISTICS OF OPENINGS

3-1 Number of openings per storey: 3-3 Openings layout:

3-2 Estimated opening dimensions: 3-4 Lateral pier:

3-5 Height of upper horizontal spandrel:

4 PLAN GEOMETRIC CHARACTERISTICS

4-1 Thickness at basis of façade wall: 4-4 N. int. bearing walls // to the façade:

4-2 Thickness reduction at the top (%): 4-5 Total length normal to the façade:

4-3 N. int. bearing walls perp. to façade:

5 STRUCTURAL CHARACTERISTICS

5-1 N. storeys with vaulted structures: 5-7 Level of maintenance of masonry:

5-2 Horizontal structure typology: 5-8 Connection at edges:

5-3 Direction of hor. structure: 5-9 Out of verticality:

5-4 Roof structure typology: 5-10 Ties/ing beams per storey in the façade:

5-5 Direction of roof: 5-11 Ties/ing beams:

5-6 Masonry type:

6 FURTHER VULNERABILITY ELEMENTS

6-1 Presence of vertical addition: 6-3 Specific weight reduction %:

6-2 Dimensions of vertical addition: 6-4 Chimney flue within the façade wall:

FAILURE MECHANISMS

A VERTICAL OVERTURNING	B1 OVERTURNING WITH 1 SIDE WING	B2 OVERTURNING WITH 2 SIDE WINGS	C CORNER FAILURE	D PARTIAL OVERTURNING	E VERTICAL STRIP OVERTURNING	F VERTICAL ARCH
FURTHER PARTIAL FAILURES				ASSOCIATED FAILURES		
G HORIZONTAL ARCH	H IN PLANE FAILURE	I VERTICAL ADDITION	L GABLE OVERTURNING	ROOF/FLOORS COLLAPSE	MASONRY FAILURE	

Figure 36: The electronic Form for the collection of data for FaMIVE (D'Ayala & Speranza, 2002)

2.3.2 CAPACITY SPECTRUM BASED METHODS

The capacity spectrum method provides the vulnerability of a building giving the evaluation of the capacity curve of the structure, its last displacement and performance point, under the hypothesis of global behaviour of it. The procedures then compare the seismic capacity (capacity curve) with the seismic demand, adequately reduced to take into account the inelastic behaviour. The capacity curve and the relative quantities could be estimated with different methods:

- the PO is estimated with a detailed/refined modelling of the aggregate/ss.uu., using a software, such as 3Muri® (macroelements, FME analysis) or DIANA® (finite elements, FEM analysis);
- the capacity curve is evaluated with mechanical based model. In this case, many type of mechanical simplified models can be mentioned:
 - o The capacity spectrum method introduced by Calvi (1999);
 - o Mechanical simplified method proposed by (Cattari, et al., 2004), in which capacity curves have been developed as curves bilinear elastic-perfectly plastic representative of the behaviour of a simple SDOF. These curves are characterized by the following three factors: 1. T, the period of vibration; 2. A_y, the horizontal yield acceleration characterizing the structural strength and 3. the last displacement of the structure d_u.

2.4 HYBRID METHODS

The hybrid methods represent a combination of the two categories of VAMs aforementioned: empirical and analytical methods. They generally are used for the territorial approach, in order to have a first estimation of the seismic vulnerability through the evaluation on the risk index, as a ratio among the seismic capacity and the seismic demand.

An example of hybrid method is the SAVE project (Strumenti Aggiornati per la Vulnerabilità sismica del patrimonio Edilizio e dei sistemi urbani, INGV/GNDT Research Group, Dolce and Moroni 2004), which allows to calculate the capacity of the structure under the hypothesis of the global box behaviour. The method was proposed in order to satisfy the requirement of the vulnerability assessment for public buildings, after the earthquake of the 31/10/2002 (epicentre in San Giuliano di Puglia - Molise Region) of magnitude M_w 5.8, that hit them.

The procedure was born for public heritage of Italy, such as schools, hospitals, etc., structures that are located in medium-high quality buildings, due to their social function. The mechanical characteristics of their masonry walls are generally higher than those of rural historical city centres (as those of Castelnuovo, §3.3.1), the horizontal floors are stiff and able to make the vertical structure collaborating if excited by seismic actions and the horizontal and vertical elements are well connected. For these reason, this method is no fitting for the case study of Castelnuovo and not applied in this work.

2.5 VULNERABILITY METHODS USED IN THIS THESIS

As described in the paragraphs before, there are many methods to assess the structural vulnerability of masonry buildings. The decision to carry on a certain vulnerability assessment method (VAM) is a consequence of the awareness of the type of available data, the different available tools, the level of accuracy and the “scale” of the project. The criteria to choose a certain method cover the different criteria of classification of the methods. Obviously, the greater the knowledge of the geometrical and structural characteristics of the sample of study, the greater the level of detail of the analyses that can (should) be performed.

In the scientific field, the application of different methods of vulnerability assessment to a homogeneous sample of study is particularly interesting in order to understand the similarities and the lacks of each method, taking as a reference for the aggregate behavior the results of the detailed methods, performed with analytical procedures and characterized by non-linear laws or geometrical assessments or, in the case of post-earthquake data, the damages experienced by aggregates. Moreover, once identified the structural vulnerability of the sample of data, it is possible to develop damage scenarios starting from the seismic hazard of the reference site for different intensities degrees of seismic events.

In this case, as in other cases in which post-earthquake data are available, for which the real damage grades for the buildings are known, the comparison between the estimated damage scenario and the real one can represent the judgment of goodness of one method over another one.

In this work, the chosen vulnerability methods will be applied to the case study of Castelnuovo, a small historical city centre consisting of 74 masonry aggregates, hit by the earthquake of 06/04/2009 (CHAPTER 3, CHAPTER 4). The database of the historical centre is suitable for seismic risk analysis at the territory level (at large scale).

For this reason, the Vulnerability Index Methods will be used as empirical methods, able:

- to assess urban contexts, to collect data by observation in situ and by systematic survey;
- to carry out the computation steps for the identification of the seismic vulnerability in short time consuming;
- to predict damage scenario on buildings in aggregate to be compared with the calculated estimated damage.

Moreover, thanks to the work that the DICEA's team have been performed in situ (§3.1, systematic study of the characteristics of Castelnuovo buildings), the geometric and structural characteristics of the aggregates (§3.3) and the damage mechanisms that the earthquake produced on buildings, were evaluated. Since the wide range of information acquired, the database of the aggregates is also working to perform detailed analytical analyses (CHAPTER 7).

In conclusion, both the VIMs and detailed analytical methods (mechanisms method) will be used in this work, as highlighted in red bold in Figure 11.

CHAPTER 3. CASTELNUOVO DATABASE

The chapter provides a description of Castelnuovo main characteristics, a village in the L'Aquila valley (center of Italy, Abruzzo Region), assumed as the case study to develop seismic vulnerability analyses in this thesis. The choice of this village is due to the past experience that the DICEA (Department of Civil and Environmental Engineering)'s team has been performed there after the earthquake of 06/04/2009 that hit it. That occurrence, though it must to be remembered as a catastrophic event, has allowed to better understand how the masonry aggregates of rural historical city centre behave if excited by seismic actions.

Castelnuovo is a hamlet in San Pio delle Camere Municipality, far from L'Aquila about 20 kilometres in southeast direction (Figure 37). The historical city centre is collocated on a hill about 4 km from San Pio delle Camere Municipality. The altitude of the hill is about 850 metres above the sea level. The building stock is composed of 102 aggregate buildings, divided into 324 ss.uu..

Few days after the L'Aquila earthquake, 06/04/2009, the DICEA's team, as well as all the other Universities of Italy, were engaged in the territory hit by the earthquake. Indeed, the Department of Civil Protection asked the Consortium ReLUIS (Network for Earthquake Engineering University Laboratories, <http://www.reluis.it/>) to coordinate the Italian University researchers to conduct habitability investigations of viability and buildings: at first on in public strategic and relevant buildings, afterward in productive activities and private ones.

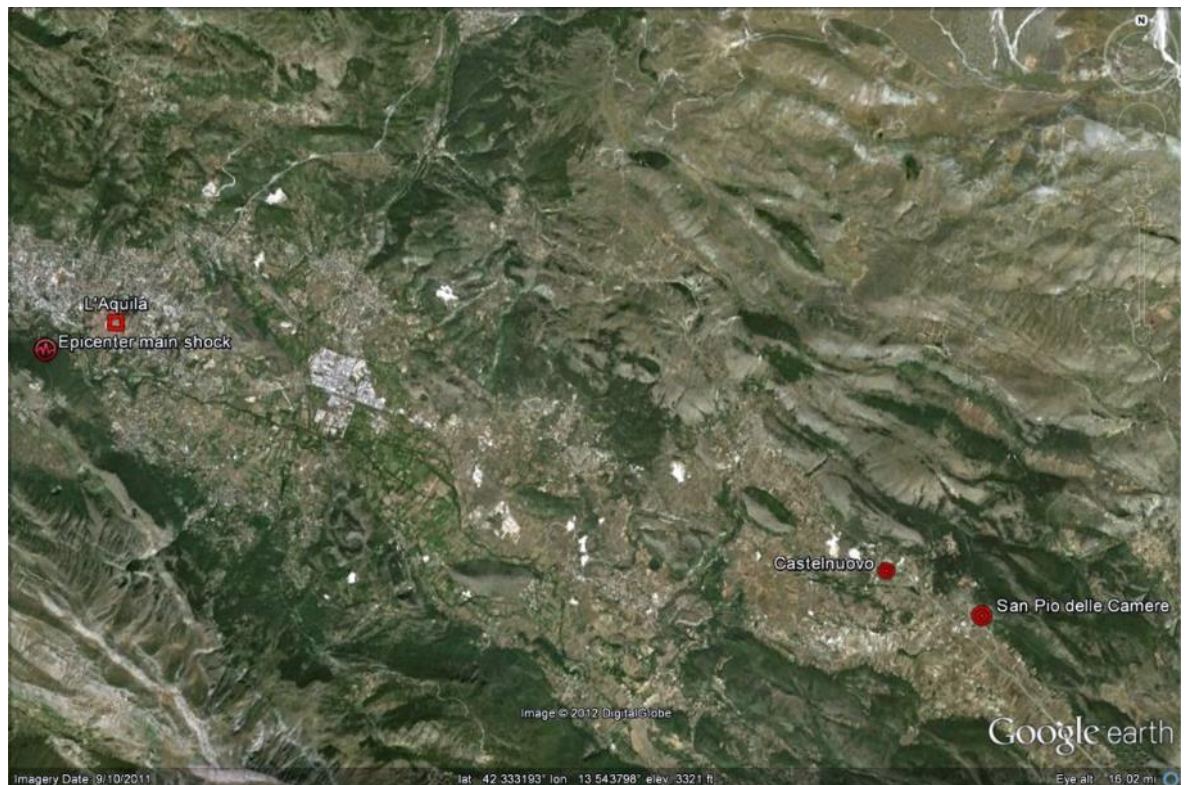


Figure 37: Territorial framework and individuation of the L'Aquila earthquake epicentre (<https://maps.google.it/>).

Prof. Ing. Andrea Vignoli coordinated about 20 people, including teachers, researchers fellows and PhD students for the Firenze University in the short period after the earthquake. From 2009, the activities continued until 2011 get involving engineering and architecture students (Pisa and Firenze Universities) for a period of training directly in situ.

These activities were aimed to evaluate the seismic vulnerability of the structures and to study the effects that the earthquake produced on aggregates. In particular, the work were made in two consequent steps (2009-2010 and 2010-2012), characterized by different level of accuracy of the in-situ surveys and the activities done (Borghini et al., 2011).

In the first step (2009-2010), a preliminary screening of the building stock were performed, collecting necessary information to correlate the seismic vulnerability (referring to the presumed conservation status of the buildings before the earthquake)

with the level of damage caused by the seismic event of 04/06/2009.

In the second step (2010-2012), a detailed survey of the building stock has been done, carefully investigating the information already collected in terms of geometry (thickness and height of the masonry walls, identification of floors and roofs system and loads, identification of level of bond, etc.), structural typologies and damage mechanisms, paying attention to the crack patterns. The analyses have been performed on a specific relevance area of Castelnuovo, limited by the perimeter of the city centre according to the “Decreto del Commissario Delegato per la Ricostruzione della Regione Abruzzo n. 3” of 03/09/2010 (Figure 38). The area inside the perimeter has an extension of about 6.25 hectares and it includes 74 aggregates, composed of 289 ss.uu. These buildings correspond to the 88% of the entire building heritage of Castelnuovo. Each aggregate has a number of identification provided by the Municipality. In addition to this number, the 74 aggregates have a progressive number starting from the NW of the village. The volumetric and geometrical characteristics of the aggregates and ss.uu. are reported in Annex 1.



Figure 38: Limit of the perimeter. Example of aggregate and division in structural units.

3.1 METHODOLOGY

For the post-earthquake survey and the study of the seismic vulnerability, the EMS-98 “European Macroseismic Scale” (Grünthal, 1998) has been adopted as a macroseismic scale. The EMS-98 (§1.1.1.2) defines six vulnerability classes (“A” ÷ “F”, defined in decreasing order of vulnerability) in which different typologies of buildings, characterized by similar seismic behaviour, are grouped. The same scale defines damage with five levels (D1 ÷ D5 defined in increasing damage order), in addition to the situation of absence of damage (D0). For all types of structures, each damage level is individuated by the damage combination in structural elements and secondary ones.

Studying the post-earthquake safety procedures for buildings and collecting data with in situ surveys, it was possible to understand which parameters are essential to the study of vulnerability and damage. Specific “Survey Forms” both for

Aggregates and ss.uu. have been developed. They summarize in a standard way all the information gained in situ by the different types of surveys. The aggregate Survey Form collects the information about the entire aggregate and the ss.uu. inside it. The first frame to identify the aggregate collocation and shape is that on Figure 39a, while a resumed layout for ss.uu. is represented in Figure 40.

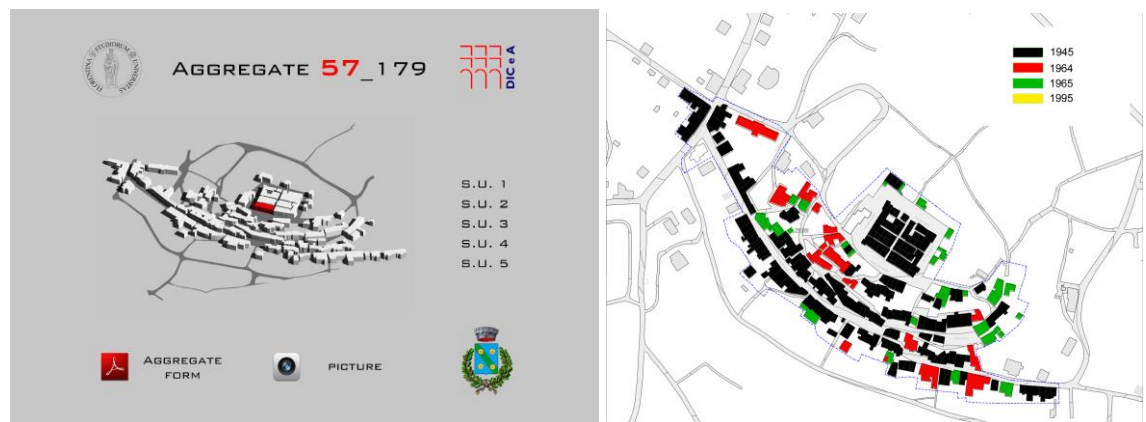


Figure 39: (a) First layout of aggregate Form. (b) Historical settlement of Castelnuovo.

3.1.1 AGGREGATE FORM

The Aggregate Form summarizes all the detailed information about each aggregate of Castelnuovo, considering it as an “unicum”. The Aggregate Form can be divided in three parts. In the first part, there is a general description of the aggregate and the identification of it within the area of Castelnuovo, through aerial photos and plans. Information about cadastral map, definitions of geometry data and damages are given for each ss.uu.. In the second part geometrical and damage surveys are reported; in particular, the damage surveys includes all the plans and the four fronts with crack patterns in evidence. A series of pictures of the ss.uu. are reported in the end, with a description of the hypothetical damages mechanisms triggered. As a conclusion, with the analysis of the collected data about evolution process and type of damages, in the third section, aggregate evolution process has been individuated, distinguish the ancient and historical ss.uu. from the modern and seismic designed recent ones.

3.1.2 S.U. FORM

The s.u. Form can be also divided into three parts. In the first part, there are general information about the s.u. and aggregate (aerial photo and aggregate shape plan). Afterwards, a description of the s.u. is reported, characterizing the main vertical and horizontal elements. Damage level and types of mechanisms activated in the s.u. are evaluated and described in this part. Figure 40 shows the pages of the ss.uu. Form for the first structural unit of the aggregate 57-179, starting on the left side.

3.2 HISTORICAL ASPECTS

Castelnuovo's first settlement presumably dates back to the medieval period; it was a fortified hamlet positioned with a quadrangular plan on the top of the hill defended by house-walls similar to a roman castrum. The “Castello”, oldest part of the city, has repeated dimensions in the blocks and buildings with mainly vaulted ground floor and basement rooms used for storage and inaccessible from upper floors, situated on the external perimeter.

The fortified hamlet of Castelnuovo is historically part of a system of settlements built in the medieval period in the L'Aquila valley, used for sighting in defence of the city of L'Aquila (Bonamico & Tamburini, 1996).

The geomorphological particularity of the place determined the settlement evolution and organization of the building stock. To the regular system of the fortified hamlet on the top of the hill, a successive expansion of building was added between the 1800 and 1900s, organized according to the terracing along the south-west of the hill, creating an urban system typical

of ridge settlements. From the mid-1900s onwards, new buildings grew up within the urban fabric in areas that had been left empty in previous urbanization both inside and outside.

S.U. FORM

SURVEY IDENTIFICATION	
TEAM NUMBER	01
DATE	08/10/2009

AGGREGATE IDENTIFICATION	
AGGREGATE NUMBER	8800179
STREET	DEL CASTELLO
HOUSE NUMBER	FROM NR UNTIL NR
TOTAL NUMBER SS.UU.	5
LONGITUDINAL DIMENSION (m)	32.10
TRANSVERSAL DIMENSION (M)	9.50

STRUCTURAL UNIT IDENTIFICATION	
STRUCTURAL UNIT NUMBER	8800179001
HOUSE NUMBERS	NR
OWNERS	DI MARCO
DESTINATION OF USE	CIVIL HOUSE
POSITION	HEADER
BUILDING STRUCTURALLY INDEPENDENT	NO

STRUCTURAL UNIT DESCRIPTION	
TOTAL NUMBER OF FLOORS	3
NUMBER OF UNDERGROUND FLOOR	0
NUMBER OF BASEMENT FLOOR	1
REGULAR IN HEIGHT	YES
SOFT STOREY	NO
PRESENZA CAVITÀ IPOGEE	NO
TOTAL HEIGHT (m)	7.50
AVERAGE HEIGHT OF STOREY (m)	2.70
LONGITUDINAL DIMENSION (m)	6.60
TRANSVERSAL DIMENSION (m)	9.50
INFORMATION QUALITY	MEDIUM

INTERVENTIONS	
TYPE	TECHNICAL SPECIFICATIONS
ENLARGEMENT	NO
RAISING	NO
REDEVELOPMENT	REPLACEMENT OF STOREYS AND ROOF STRENGTHENING OF MASONRY
MAINTENANCE	REPLACEMENT OF PLASTERING

VERTICAL ELEMENTS	
TOTAL NUMBER OF TYPES	1
TYPE	NOTES
(DISORGANISED) STONE MASONRY	REINFORCED MASONRY WITH PLASTER REINFORCED AND WELDED MESH

STAIRS	
TOTAL NUMBER OF TYPES	1
TYPE	NOTES
STONE RESTING STRUCTURE	

HORIZONTAL ELEMENTS	
TOTAL NUMBER OF TYPES	4
TYPE	NOTES
I-BEAMS AND HOLLOW TILES WITH TIES	FL-2 (WITH EXPANDED CLAY SLAB AND WELDED MESH)
WOODEN	FL-2 (REAR; EXPANDED CLAY SLAB AND WELDED MESH)
VAULT WITHOUT TIES	FL-1
VAULT WITH TIES	FL-2

ROOFS	
TOTAL NUMBER OF TYPES	1
TYPE	NOTES
WOODEN WITH ELIMINATED THRUST	

"BOX" BEHAVIOR	
DESCRIPTION	NOTE
PRESENCE OF BEAM AT ROOF	YES
PRESENCE OF BEAM AT FLOOR	NO
STIFF ROOF	YES
STIFF FLOOR	YES
SCARF BETWEEN ORTHOGONAL WALLS	YES (on the corner)

CONSERVATION STATE ANTE-EARTHQUAKE	E
OCCUPATION STATE	PARTIALLY OCCUPIED
VULNERABILITY CLASS	B
DAMAGE TYPE	MASONRY FACING EXPULSION IN PLANE MECHANISMS IN PANELS OUT-OF PLANE MECHANISMS OF FAÇADES
DAMAGE LEVEL	D4

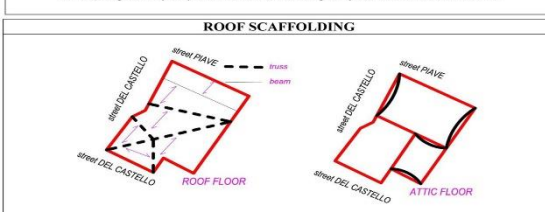
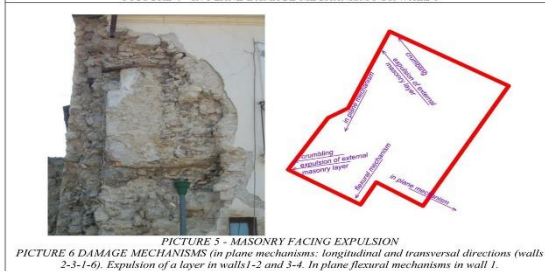
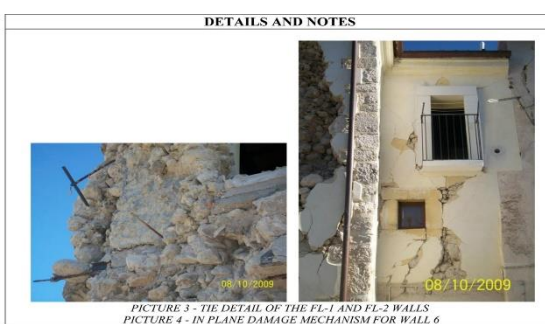
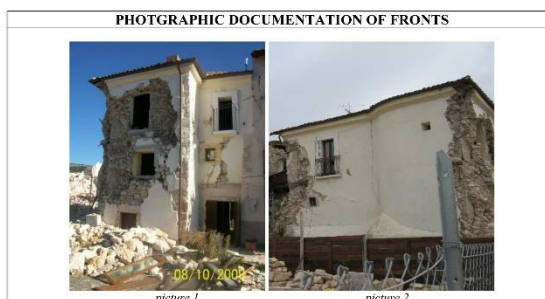
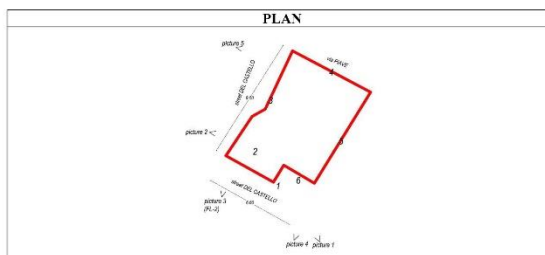


Figure 40: Pages.1, 2, 3 and 4 of the ss.uu. Form of 57-179 s.u.1.

Therefore, Castelnuovo buildings can be divided into three parts: the oldest “Castello” is the fortified section at the top of the hill, the 19th Century urban expansion follows the southern contours lines and, at the base of the hill, there is a modern expansion. Figure 39b shows the classification of the XX century, considering in detail each aggregate and, where possible, the structural units, especially enlargements, or separated constructions.



Figure 41: Castello, the oldest zone of Castelnuovo.

3.3 ANALYSIS OF THE BUILT HERITAGE

The structural analysis focused on the area within the perimeter with an extension of circa 6.25 ha (Figure 38). 74 aggregates were identified, for a total of 289 structural units within them, corresponding about to 88% of the building patrimony of Castelnuovo. There are two public aggregates, one Church and the remaining numbers are private buildings. Two distinct zones were identified due to their historical and architectural value and their construction homogeneity: the fortified area on the top of the hill, the “Castello” (Figure 41), and the area at the base of the hill.

The village of Castelnuovo is located on a elliptical hill bordered by escarpments of river erosion. From the available data and past checks carried out, it is reasonable to assume that the stratigraphic succession, from the surface to the substrate, is composed almost exclusively of white calcareous silts interspersed with sandy layers.

The surface subsoil is characterized by underground cavities dug into silt by human hands for human goals. Access to these tunnels generally corresponds to the ground floor of the buildings at street level. From a normative point of view, the soil beneath Castelnuovo falls into the “C” ground category (§Table 6) and category topographic T₂ (§Table 8).

The information collected during the surveys - relative to the urban characteristics of the village or relative to configuration, to the materials and architectural, morphological and structural elements - were elaborated and synthesised in GIS environment, to provide a qualitative and quantitative catalogue as a reference instrument of analysis and crossing data.

The 74 aggregates of Castelnuovo (Annex 1) have in total 164 513 m³ of built, for a covered surface of 55 339 m² (computed as the sum of the covered area of each floor). The aggregates are various in terms of number of structural units, shape and height. Buildings inside the perimeter are characterized for 52.3% by three floors (two floors and an underground floor, Figure 43a). Buildings consisting of four floors are 12.3%, which are mainly located in the main Streets (nineteenth century's expansion). The remaining part consists of one floor (9.1%) and two floors (26.3%) buildings.

By in situ measurements, and considering detailed analysis of out-of-plane mechanisms (§7.2) for a sample of data of 120 masonry walls (front and rear façades) the average values of geometrical characteristics were determined. Within the sample of data, there is one 1-floor building, one 4-floors and the remaining buildings have the 46% two floors (n.55 façades) and 53% three floors (n.66 façades).

- the average height of interstorey (considering the average values of ground, first and second floors) is about 2.95 meters, including half-height of structural floor, which changes floor by floor following the distribution showed in §3.3.2;
- structural thickness, the average value is 59 centimetres;
- for the ground floor (sample: 120 façades): the average height, h_{av} , is 3.05 metres and thickness, t_{av} , is 0.63 m;
- for the first floor (sample: 119 façades): the average height, h_{av} , is 2.95 metres and thickness, t_{av} , is 0.60 m;
- for the second floor (sample: 65 façades): the average height, h_{av} , is 2.90 metres and thickness, t_{av} , is 0.57 m;
- for the third floor (only one façade): the average height, h_{av} , is 1.55 metres and thickness, t_{av} , is 0.57 m.



Figure 42: Ante and post earthquake aerial photos.

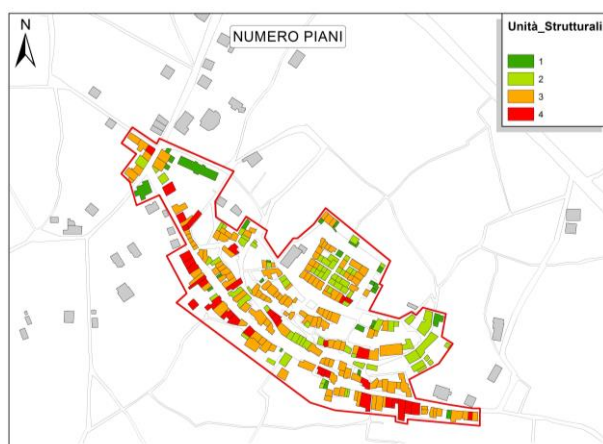


Figure 43: Number of floor for structural units.

Observing the map of Castelnuovo (Figure 44) it is possible to make a classification between the buildings inside the perimeter distinguishing by aggregation types. There are, indeed, isolated buildings (8.7% in terms of ss.uu., 10.6% in terms of volume) consisting of single structural unit, usually coinciding with an estate unit. There are row buildings (72% and 70.4%), developing in a longitudinal way and usually having the main prospect in front of the main streets and complex aggregates (19.4% and 19.1%), with irregular shapes staggered to be in accord with the soil difference in height (

Table 7).

Aggregates with two structural units could be associated to both in row or isolated aggregate type: in this work, they are

considered as row aggregates. They are 9 aggregates (6.2%), and their percentage in terms of volume is 8% (13 277 m³).

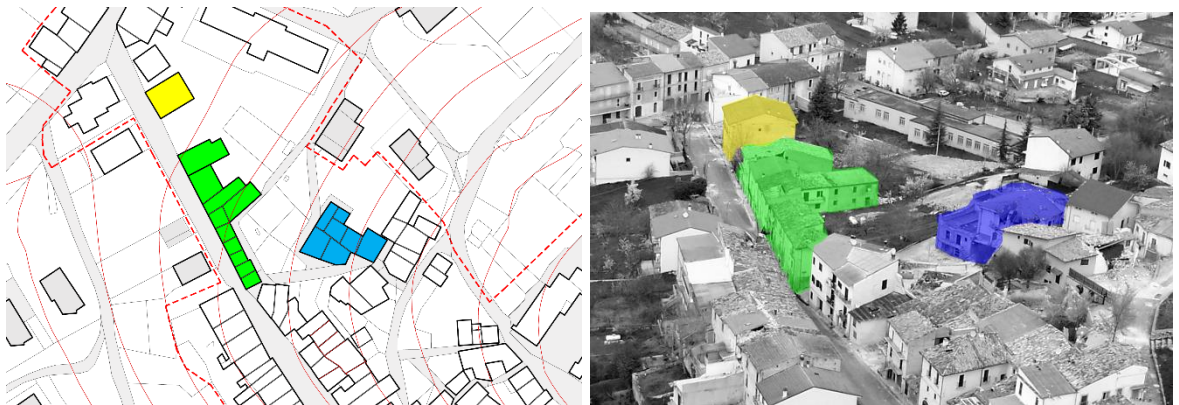


Figure 44: Different type of buildings: isolated (yellow), row buildings (green) and complex buildings (blue).

Within the stone masonry constructions (86.2%), the 8% are isolated buildings and the 92% are non-isolated buildings, respectively, 73.9% row aggregates and 18.1% complex aggregates (Table 8).

Focusing on this plan-configuration classification, the structural units in the not-isolated aggregates can have *corner* (A) position, *external* (E) or *internal* one (I) (Giovinazzi & Lagomarsino, 2004). This aspect is particularly interesting for the seismic vulnerability, since it influences the response that a structure could have if horizontal forces occur. It is worth noting that within the VIMs, the position of the s.u. inside the shape of the aggregate is taken into account both in “Formisano” and “Aveiro” Forms, in P7 and P12 respectively (§2.2.2). Those parameters are characterised by the highest impact factors. Considering only stone masonry aggregates, the isolated buildings are 8.0%, the 15.3% of ss.u. are in a corner position, 30.1% are external and 46.6% are internal ones (Table 17).

The reported percentages confirm the bigger development of row buildings, with reference to the expansion of the village in a longitudinal direction following the contour curves.

Table 16: Aggregation type: statistics and histogram.

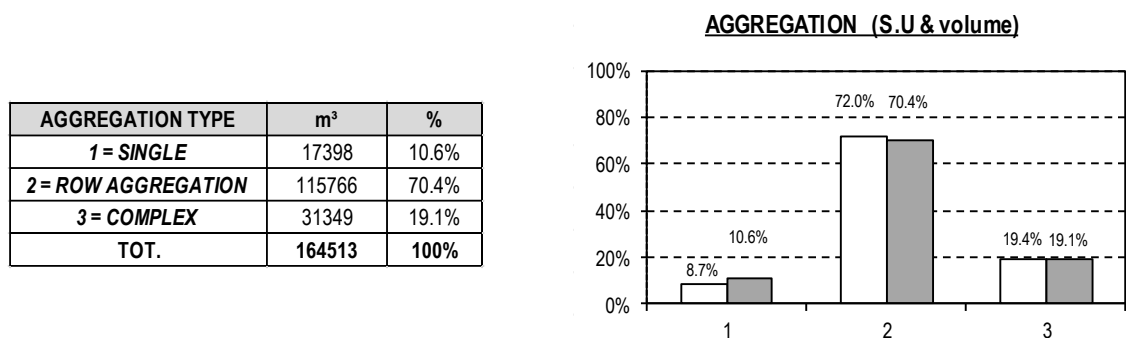
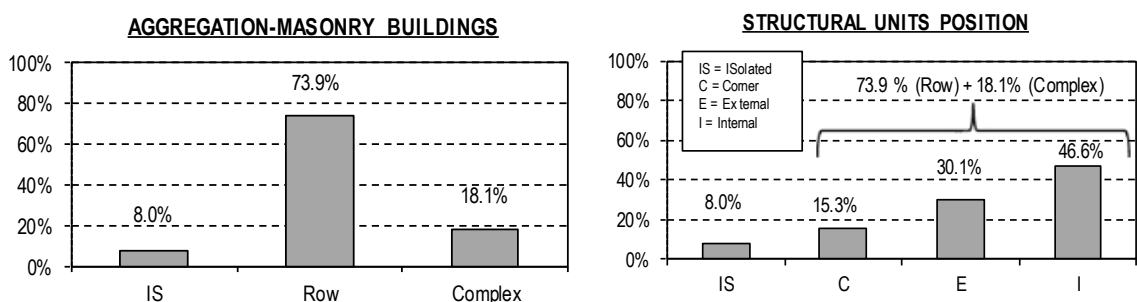


Table 17: Aggregation type and structural position for masonry aggregates: statistics and histogram.



3.3.1 VERTICAL ELEMENTS (MASONRY TYPES)

In the evaluation of the seismic vulnerability of existing masonry buildings there is the necessity to characterize the quality of load-bearing masonry walls, to know their type, construction techniques, materials and mechanical properties. The definition of the quality of the masonry is then linked to the characterization of the masonry type, to the quality of mortar and blocks and to the respect of the "rule of art", specific construction laws that, if respected, allowed the good behaviour of the panel against in-plane and out-of-plane loads. With the information gained during the in-situ inspections it was possible to fill out a "Quality Masonry Form", implemented by DICEA as part of the research project DPC/ReLUIS 2014-2018. The Form is based on the "Quality of Masonry Form" proposed by Binda et al., 2008 and allows the complete characterisation of the masonry. The Form gives as a results the "Quality of Masonry Index", a coefficient in the scale [0-10] which, following the procedure of (Borri & De Maria, 2008), allows a classification of the masonry types by their goodness to respond to seismic and in-plane actions.

In detail, the Form has three sections; in the First Part, there are general description of the masonry and information about the building location and main features. The Second Part provides the main macroscopic characteristics of the masonry front and cross-section (if present). The Third Section describes the obtained results. To the panel's masonry is assigned a numerical index, the "Index of masonry Quality" (IQM) through which estimate the mechanical characteristics enter those provided by the C.M. n.617, 2009 §Tables C8A.2.1-2 (Borri & De Maria, 2005-2008).

An extract of the Quality Masonry Form is reported in Annex 2 (graphic representations of the face and the section) for one Castelnuovo panel, one situated in Toscana very similar to those of Abruzzo Region.

From the statistical analysis of the data collected in situ for the ss.uu., the 86.2%, with a total volume of about 148 000 m³ is characterized by a vertical structure made in load-bearing stonemasonry. The predominant type of masonry is unreinforced, irregular and unorganized with two leaves, with different dimensions and irregular shape of stones/elements and low quality of the mortar (Figure 47), in specie the masonry of the oldest part of the city (called "Castello", Figure 41). Only in few cases, the masonry faces have mortar and rows, which contribute to the regularity of the position of the stones (or brick elements) too. In other cases, the stones have chaotic arrangement, especially in the central area thickness (masonry core) (Figure 47a,b). Generally, there aren't cross-section elements enter the two leaves, which appear with independent behaviour against out-of-plane loads.

From the analysis of the materials and documents coming from the historical archive, used materials come from local excavations. Only in more recently constructed buildings, in which precautions and seismic devices were followed, the used materials have greater mechanical and stiffness characteristics.

A typological classification of the stone masonry has been done, and to the types of masonry individuated, structural mechanical characteristics have been associated. Depending on the regularity of the walls weaving, stone masonry were distinguished in three sub-classes, called M1, M2 and M3, which individuate three different degrees of regularity (Figure 46). The M1 is the most frequent masonry encountered, with texture more irregular.

The masonry types are associable to the first masonry category within those provided by the (C.M. n.617, 2009) in the Table C8A.2.1. This type of masonry is called "irregular stone masonry (pebbles, stones erratic and irregular)", characterized by the mechanical characteristic shown in the Table 18. The parameters expressed are are: f_m = average compressive strength of the masonry, τ_0 = average shear strength of the masonry (due to diagonal cracking), E = average value of Young modulus and G = average value of the shear modulus.

Table 18: Mechanical characteristics of stone masonry

Masonry Category	w [kN/m ³] weight	f_m [N/cm ²] Compressive Strength		τ_0 [N/cm ²] Shear Strength	E_m [N/mm ²] Young modulus E	G_m [N/mm ²] Shear modulus G
		min	max	average		
Disorganised stone masonry (I category)	19	100	180	2	690	230
				3.2	1050	350
		140		2.6	870	290

In some cases, the buildings are built in brick masonry, in concrete blocks or in "poor concrete masonry"; the latter type means concrete with no reinforcements and with different size elements and type of aggregates.

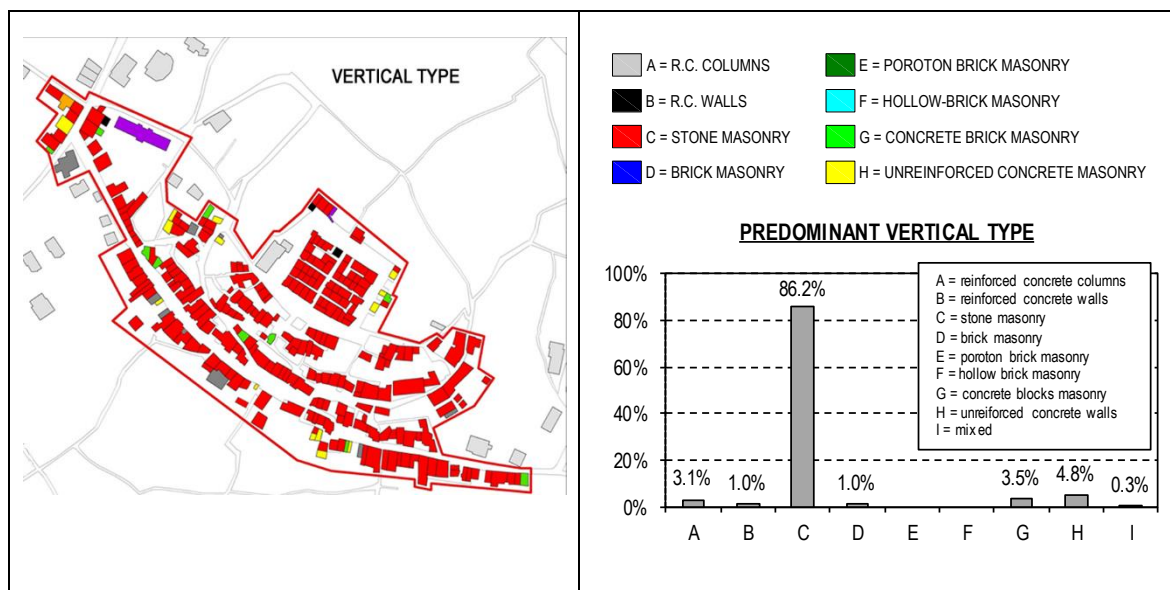


Figure 45: Masonry types and panels.

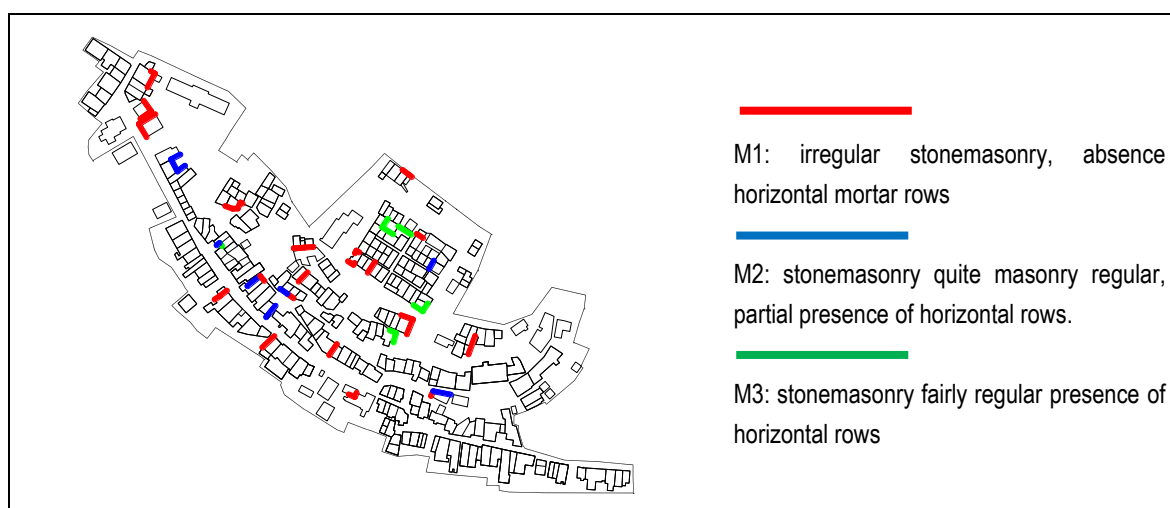


Figure 46: Masonry panels analysed.





Figure 47: Stone masonry, front and cross sections.

3.3.2 HORIZONTAL ELEMENTS (FLOOR TYPES)

In order to identify the seismic vulnerability for each structural unit, as well as for carrying out structural details on each building (local and global seismic analysis, CHAPTER 7), recurring types of horizontal elements are identified in Castelnuovo ss.uu.. Relying on the inspections in situ, a fortiori when the slabs presented substantial crack patterns (or collapses), the identification of the resistant cross-sections of the slabs was done in a direct manner. Only in few cases, the presence of plaster at the intrados did not let a full knowledge of the storey: the uniformity of the historical period of the construction site allowed to consider the same type of slabs even for those cases.

Typically, the horizontal elements of the ground floors consist of masonry barrel vaults (65.3%), in stone masonry or in brick masonry. On the first and second floors, steel slabs are present. They are defined as "PT (Putrelle e Tavelloni)" I-beams and hollow tiles, "PV (Putrelle e Voltine)" I-beams and hollow building tiles". In some cases, in the strengthened buildings in specie, "PTS" I-beams and reinforced concrete slabs are present (Figure 48a-b).

At the second floor, brick masonry vaults are present Figure 48c. These horizontal elements can be both structural, with a resistant cross section of 12-16 cm (it depends on the type of historical brick), and with a non-structural function, as the ceiling functions with resistant cross section of about 4.5-6 cm. For the ceiling vaults, called also "in folio", the bricks are arranged in horizontal way and in certain cases, for cross vaults, the section is stable also in correspondence of the main arches (Figure 52).

The data collected Figure 48 refer to the uu.ss. investigated (the percentage of them. elements is different floor to floor). From the aerial photos the type of roof covering and the slope direction were established. Roof analysed consist mainly in wooden structures (79.5%), generally with two orders of beams. Their framework is parallel to the main façades, loading orthogonal walls and not producing thrust forces on them. Only in some cases, weighted roofs are present, made with steel beams and concrete slabs or in reinforced concrete (15.2%) (Figure 48d and Table 21).

Horizontal elements are deeply described in the following. In particular, the load analysis for each type of slabs is reported, with the description of all the assumptions made for the analysis. The hypothesis concern the values assigned to permanent and live loads and the partial safety factors for the horizontal elements⁴. In particular:

- Balcony and stairs' live loads are equal to 2 kN/m²;
- Coefficient γ_i for permanent loads assumes value 1.3;
- Partition walls loads, with reference to the NTC 08 (§3.1.3.1), are calculated directly from the real case of the 10-088 aggregate (Figure 49). The Code sets that the weight of partition walls can be provided as a permanent distributed load g_{2k} . That load depends on the weight (per length unit) g_{2k} of the partitions. Two types of partition walls have been

⁴ The loads here reported are afterwards used in the study of vulnerability in CHAPTER 5 and CHAPTER 7.

individuated: holes masonry bricks and masonry bricks (respectively ciano and pink in Figure 49). For three plans, length of both types of partition walls has been calculated: once having the real distribution and load of the partition wall (kN), it has been divided by the slabs' surface (the total area of the plan of structural units, with vertical masonry elements). The found value (kN/m²) can be the real value to insert in the calculation for safety verifications. The design load is 0.8 kN/m² for the ground floor and 1.2 kN/m² for the first and second floors.

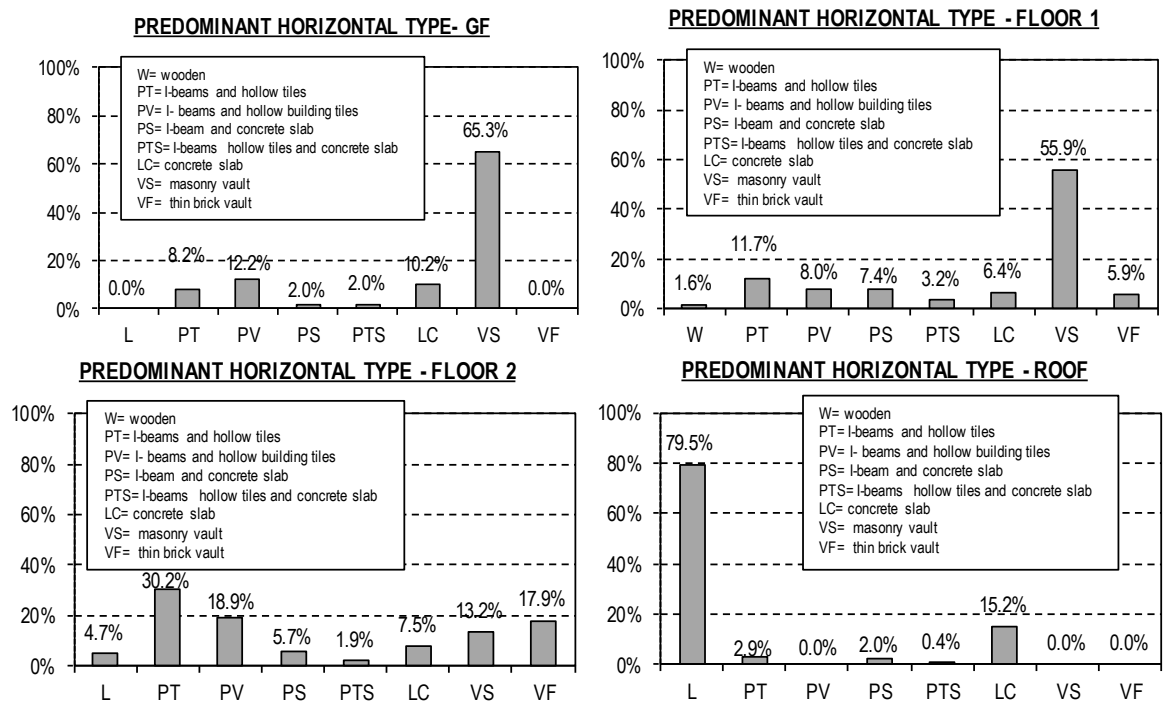


Figure 48: Predominant horizontal type for ground floor (a), first floor (b), second floor (c) and roof (d).

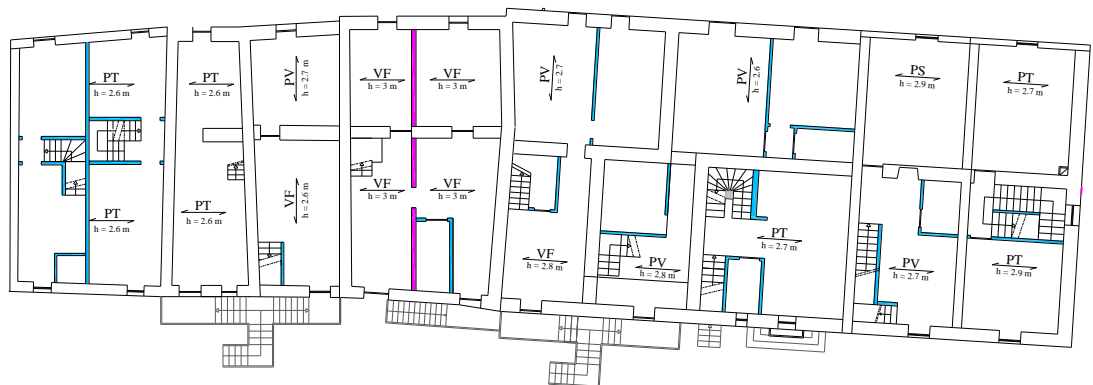


Figure 49: Partition wall's distribution at the first level of 10-088 aggregate.

The calculation of the weight of the partition walls is described in the following table:

Table 19: Partition walls' type and loads

PARTITION WALL TYPE 1: HOLES BRICK MASONRY		
DIMENSION		
Plaster's thickness (t_2)	[m]	0.03
Masonry's thickness (t)	[m]	0.12
MATERIALS		
Holes brick masonry and mortar	[kN/m ³]	15.00
Plaster	[kN/m ³]	20.00
LOADS m ²		
Self-weight structural [G_1]		
Holes brick masonry and mortar	[kN/m ²]	1.80
Carried permanent loads [G_2]		
Plaster	[kN/m ²]	0.60

[G₁]+[G₂]	[kN/m²]	2.40
PARTITION WALL TYPE 2: BRICK MASONRY		
<i>DIMENSION</i>		
Plaster's thickness (t ₂)	[m]	0.03
Masonry's thickness (t)	[m]	0.12
<i>MATERIALS</i>		
Brick masonry and mortar	[kN/m ³]	18.00
Plaster	[kN/m ³]	20.00
<i>LOADS m²</i>		
<i>Self-weight structural [G₁]</i>		
Holes brick masonry and mortar	[kN/m ²]	2.16
<i>Carried permanent loads [G₂]</i>		
Plaster	[kN/m ²]	0.60
[G₁]+[G₂]	[kN/m²]	2.76

Different types of floors and roofs are recognized in the following pictures in Castelnuovo; their weights are reported in following tables.

3.3.2.1 ROOFS

All the types of roofs' system are grouped into three categories.

1. Roof with a double order of timber beams (rafters and bending beams) (Figure 50 and Table 20);
2. Roof with only one level of timber beams (rafters that extend from the ridge to the upper wall plate or masonry);
3. Weighted roof made in steel-concrete materials.

Only for the first roof's type there is a complete description of all the components, while for the others, only the weights are schematized with the combination provided in 2.5.3 (NTC 2008). The live loads are the "use" (0.50 kN/m²) and snow load.



Figure 50: Roof type 1.



Table 20: Roof system 1: characteristics and weights

ROOF TYPE 1: HORIZONTAL BEAM(20x25), JOISTS (8x8), PLANK, CURVED TILES		
<i>DIMENSION</i>		
insulation thickness (s _i)	[m]	0.01
plank thickness (s _a)	[m]	0.03
waterproofing thickness (s _w)	[m]	0.05
h first order beam (h)	[m]	0.25
b first order beam (b)	[m]	0.20
h joist (h ₁)	[m]	0.08
b joist (b ₁)	[m]	0.08
inter-axial distance beam (i)	[m]	1.67
inter-axial joists (i)	[m]	0.64
<i>MATERIALS</i>		
Insulating	[kN/m ²]	0.10
Waterproofing	[kN/m ³]	1.00
Plank	[kN/m ³]	6.00
Timber beam	[kN/m ³]	6.00
<i>LOADS m²</i>		

<i>Self-weight structural [G₁]</i>		
Plank	[kN/m ²]	0.18
Beam	[kN/m ²]	0.18
Joists	[kN/m ²]	0.06
<i>Carried permanent loads [G₂]</i>		
Curved tiles	[kN/m ²]	0.60
Insulating waterproofing	[kN/m ²]	0.10
Waterproofing	[kN/m ²]	0.05
<i>Live Load [Q_k]</i>		
Use Load	[kN/m ²]	0.50
Snow live load	[kN/m ²]	1.55
[G₁]+[G₂]	[kN/m²]	2.76
SLE	[kN/m²]	2.75
SLU	[kN/m²]	3.85
SLV	[kN/m²]	1.20

The other two types of roof are summarised in next table:

Table 21: Roof 2 and 3: loads in kN/m²

ROOF 2: SLOPING JOISTS (10x10), PLANK, CURVED TILES, LEDGE			ROOF 3: I-BEAMS AND HOLLOW TILES, UNREINFORCED CONCRETE		
[G ₁]+[G ₂]	2.76			2.90	
SLE	2.75			4.45	
SLU	3.85			6.10	
SLV	1.20			2.90	

3.3.2.2 FLOORS

Some indications are reported for the floors' type: for the masonry stone vaults the accurate description of the elements is done (Figure 51 and Table 22); for the other floors only the loads assumed in the combinations are specified, with some explicative photos (Table 18, Table 23).



Figure 51: Stone masonry barrel vaults in the "Castello" aggregates.

FLOOR TYPE 1: STONE MASONRY VAULT, STRUCTURAL FUNCTION		
DIMENSION		
floor thickness (s_f)	[m]	0.010
average screed thickness (s_s)	[m]	0.050
average filling thickness (s_f)	[m]	0.300
masonry stone thickness (s_{sm})	[m]	0.28
plaster thickness	[m]	0.01
MATERIALS		
Filling material	[kN/m ³]	12.00
masonry stone	[kN/m ³]	19.00
Cementious plaster (screed, too)	[kN/m ²]	18.00
Granite	[kN/m ³]	27.00
LOADS m ²		
<i>Self-weight structural [G₁]</i>		
Stone Masonry	[kN/m ²]	5.32
<i>Carried permanent loads [G₂]</i>		
Floor	[kN/m ²]	0.27
Screed	[kN/m ²]	0.9
Filling material	[kN/m ²]	3.6
Cementious plaster	[kN/m ²]	0.18
partition walls	[kN/m ²]	0.80
<i>Live Load [Q_k]</i>		
Use Load	[kN/m ²]	2.00
[G₁]+[G₂]	[kN/m²]	11.10
SLE	[kN/m²]	13.10
SLU	[kN/m²]	17.40
SLV	[kN/m²]	11.70

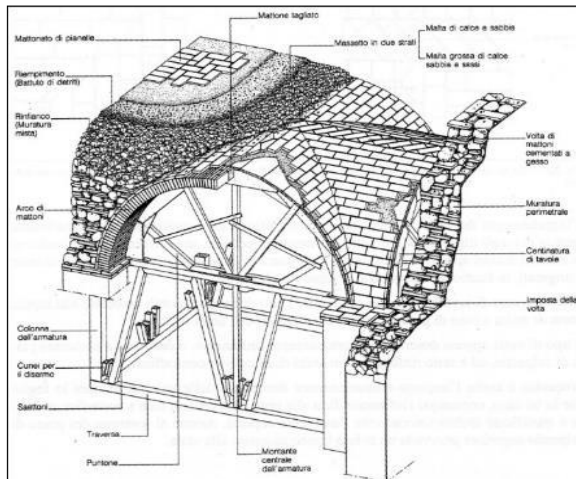


Figure 52: Brick masonry vault “in folio”: (a) representation of the construction phases (“G. Cangi – Manuale del recupero strutturale e antisismico). Some examples in Castelnuovo buildings. Last picture is a ceiling PT example.

The other types of floor are summarised in next table:

Table 23: Floor types 2 and 3: loads in kN/m²



FLOOR 2: PT (PTS) - IPE/IPN140, BRICKS, UNREINFORCED SLAB			FLOOR 3: PV - IPE/IPN140, BRICKS, UNREINFORCED SLAB		
$[G_1]+[G_2]$	5.50			3.95	
SLE	7.50			5.95	
SLU	10.15			8.10	
SLV	6.10			4.55	

Table 24: Floor types 4 and 5: loads in kN/m²

FLOOR 4: VF BRICK MASONRY VAULT, FILLING MATERIAL			FLOOR 5: VF CEILING FOLIO BRICK MASONRY VAULT, FILLING MATERIAL		
$[G_1]+[G_2]$	5.40			2.40	
SLE	7.40			2.40	
SLU	10.05			3.10	
SLV	6.00			2.40	
FLOOR 6: PT CEILING. I-BEAMS AND HOLLOW TILES			FLOOR 7: ST- STAIRS - CLAMPED TO THE MASONRY PANEL		
$[G_1]+[G_2]$	1.35			4.35	
SLE	1.35			6.35	
SLU	1.75			8.65	
SLV	1.65			4.95	

In addition to floors mentioned above, in some structure reinforced concrete slabs were individuate, in specie in more recent and seismic design structure made in brick masonry or reinforce concrete. The percentage of this type of floor covers around 10% of the first floor of Castelnuovo structural units. Their weight in seismic combination is about 6 kN/m².

3.3.3 BUILDING CELL TYPE

Resuming all the information explained above, the core housing type of Castelnuovo is generally composed by a cell with three floors, and it can include the basement floor. This cell type usually constitutes the estate unit.

The vertical elements consist in stone masonry walls, characterized by wide cross section (especially at the ground floors), of about 50-75 centimetres and characterised by unreinforced, irregular stone masonry with poor quality mortar and stone elements with different and irregular shapes.

The horizontal elements of the structural units are mixed. At basement or ground levels, stone masonry vaults are present, with 30-cm thickness cross-sections. The upper floors are generally made in mixed steel brick type, sometimes reinforced with concrete slabs. When the ceiling is present at the second floor, is made of slender brick masonry vault (*in folio*) or I-beams and hollow tiles, with cementitious plaster on the bottom face. The roofs are in most cases wooden structures, with one or double order of beams (rafters and bending beams), not thrusting on the masonry main façades.

Figure 53 shows an extract of the longitudinal section and cross section of the s.u. 8 of the aggregate 10-088, as an example of a core housing. There are three floors above ground and a basement, the inter-average levels is about three meters, while the basement level has a lower height of about 2.5 meters. The vertical elements are in irregular stone masonry. Thickness of ground floor arrives at 100 cm and it decreases with the panels' height. Vaults and steel brick type of horizontal slabs are present and the roof is mainly composed of wooden structure with double order of beams.

Figure 54 shows the longitudinal section of 57-179 aggregate, in the Castello zone. In each structural units, the ground floor consists in masonry stone vaults, and at the upper floor (coverage of the first floor) there are the structural vaults "in folio" and ceilings at the second floor, hiding the wooden roof. The vertical and horizontal structural elements are very similar of those analysed in the 10-088 aggregate.

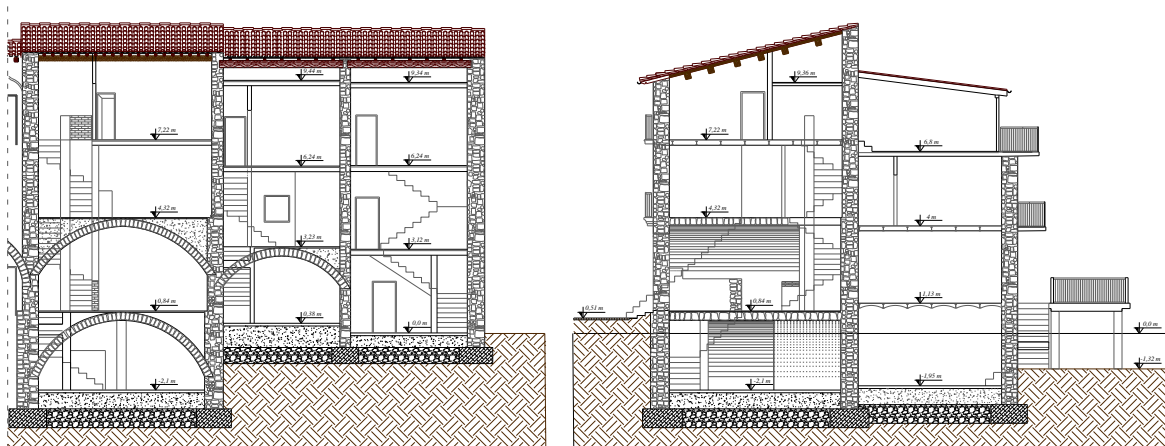


Figure 53: Extract of longitudinal section and cross-section of s.u.8 of aggregate 10-088⁵.



Figure 54: Longitudinal section for aggregate 57-179, in "Castello" buildings.

3.4 KNOWLEDGE LEVELS, CONFIDENCE FACTORS AND MECHANICAL CHARACTERISTICS

A considerable part of the Italian Seismic Code (NTC, 2008), (C.M. n.617, 2009) is completely devoted to existing buildings of different typologies: r.c., steel structures and masonry buildings. To take into account the uncertainty in the knowledge of structural properties, the Standard defines, with reference on EC8-3, an adjustment factor, called "Confidence Factor (CF)," whose value depends on the level of knowledge (KL) of properties such as geometry, reinforcement detailing and materials.

The KL and the CF depend on the completeness and reliability of available information of the structures, in terms of different aspects. The confidence factor has the purpose of grading the reliability of the structural analysis of an existing building taking into account, and synthesizing, the effect of modelling uncertainties. Its value depends on the level of knowledge acquired on the geometry, on the structural details and on the mechanical characteristics and properties of the materials (§C8A.1.A.3), as shown in Table 25. A design characteristic should be determined as:

$$(17) \quad r_{cd} = \frac{r_{cm}}{(CF \cdot \gamma_m)}$$

⁵ The foundations drawings are only indicative.

Table 25: Confidence factors (CF) and Knowledge Level.

Knowledge Level (KL)	Geometry	Constructive details	Material properties	Analysis method	Confidence Factor (CF)
KL1	Geometrical and structural surveys	Limited on-site inspections	Limited on site testing	ALL	1.35
KL2		Extended and comprehensive on-site inspections	Extended on-site testing	ALL	1.2
KL3			Comprehensive on-site testing	ALL	1

For what concern the *building geometry*, the geometry and particular elements (such as chimneys, niches, etc), crack patterns and out of plumbs, etc., should be observed by means of in situ surveys. For *construction details* connections, lintels, elements to counteract thrusts, vulnerable elements should be investigated: that can be done at two different detail level with limited in-situ inspections or extended and comprehensive ones. While, for the *material properties* the investigation should include the knowledge of *mechanical characterization of masonry type*, gained through limited in situ testing (visual inspections), extended in situ testing (Minor destructive tests - MDT and Non Destructive Tests - NDT) or comprehensive in situ testing (Destructive Tests - DT).

Depending on the gained KL, FC is determined following the provisions in Table 26.

Table 26: How getting the Knowledge Levels.

1. Geometry	2. Constructive details	3. Material properties	Knowledge Level (KL) & Confidence Factor (CF)
Geometrical & structural surveys	Limited on-site inspections	Limited on site testing	KL1 → CF=1.35
	Extended and comprehensive on-site inspections	Extended on-site testing	KL2 → CF=1.20
		Comprehensive on-site testing	KL3 → CF=1.00

If the mechanical characteristics are not determined with the in situ destructive tests, they can be derived from the actual Standard (C.M. n.617, 2009). The approach defined in the current Italian technical Code for constructions to evaluate the structural safety of existing masonry structures, against static and seismic loads, is based on the individuation of the building's masonry category and on the choice of the appropriate mechanical parameters obtained from ranges defined for each typology. Indeed, Table C8A.2.1 (Circ. 617/2009, Table C8A.2.1-2) provides average values (minimum and maximum) of the mechanical characteristics for 11 typical masonry categories of existing construction, observed in the Italian territory.

Depending on the achieved KL, the value of the design mechanical characteristic changes, since changes the average value of the characteristic to take into account in the Eq.(17):

- For KL1 the resistances are the minimum of the range proposed by the Code and the elastic moduli are the average values of the range;
- For KL2, both the resistances and elastic moduli are the average of the range;
- For KL3 there are different cases depending on the number and the type of experimental tests carried out. The provisions are defined in the Table C8A.1.1 of (C.M. n.617, 2009).

For the Castelnuovo aggregates, the knowledge level KL1 is assumed since there is the complete knowledge of building geometries and construction details but in situ test were made only in some portions of the mortar joints in a restricted numbers of aggregates. Even without non-destructive tests performed, the level of knowledge of the materials and constructive details is widespread high, due to the collapse of walls and slabs after the earthquake and the verification of link and restraint among the main vertical and horizontal elements. A KL2 could be justifiable for this case.

Moreover, in the kinematic linear and non-linear analyses for the study of local mechanisms of collapse, under the hypothesis of infinite compressive resistance for the masonry for the formation of the cylindrical hinge, CF equal to 1.35 and this is line with the achieved level of knowledge KL1.

The comparisons among the different vulnerability methods (CHAPTER 7) are made taking into account the resistance as

the minimum of the range for two levels of knowledge of the structure, KL1 and KL2.
 Table 27 shows the mechanical design characteristics for disorganised stone masonry.

Table 27: Mechanical design characteristics of stone masonry (KL2→CF=1.2).

Masonry Category	w [kN/m ³] weight	f _m [N/cm ²] Compressive Strength		τ ₀ [N/cm ²] Shear Strength	E _m [N/mm ²] Young modulus E	G _m [N/mm ²] Shear modulus G
		average	140	2.6	870	290
Disorganised stone masonry (I category)	19	design	116.7	2.17	870	290

CHAPTER 4. THE L'AQUILA EARTHQUAKE

The chapter provides in the first part the description of the L'Aquila earthquake of 06/04/2009, showing the main characteristics and making a comparison with the design acceleration response spectrum provided by the Italian Code. In the second part, the damage scenario that the L'Aquila earthquake produced on aggregates of Castelnovo is described.

Six years passed from the L'Aquila earthquake, in 06/04/2009. That earthquake was the first contemporary seismic event in Italy with an epicentre near a regional capital (Vignoli, 2012). As well as in L'Aquila, the main shock, at 3.32 a.m., affected more than 50 closed Municipalities. Most of them are complex systems of fortified villages realised in the L'Aquila valley in the medieval period. The earthquake caused substantial damage in many of these villages, included Castelnovo, in which the main shock produced high structural damages on the aggregates and even the death of five people.

4.1 EARTHQUAKE CHARACTERISTICS

The 06/04/2009 earthquake that struck L'Aquila and its province was characterized by a seismic sequence that began in December 2008. The mainshock was recorded at 03:32 hours of 06/04/2009 (epicentre coordinates N 42.3476 and 13.3800 E), with variable intensity from VIII to IX on the MCS scale, Richter magnitude (M_L) of 5.8 and moment magnitude (M_W) equal to 6.3. The earthquake was strongly felt throughout central Italy (Abruzzo, Lazio, Molise, Marche, Umbria) and in a lower way in other Regions too. The main shock was followed by a series of high replications (Figure 55). The circumscription area of origin of the earthquake extends for over 30 km along the NW – SE direction, parallel to the axis of the Apennine Mountains (Vignoli, 2012).

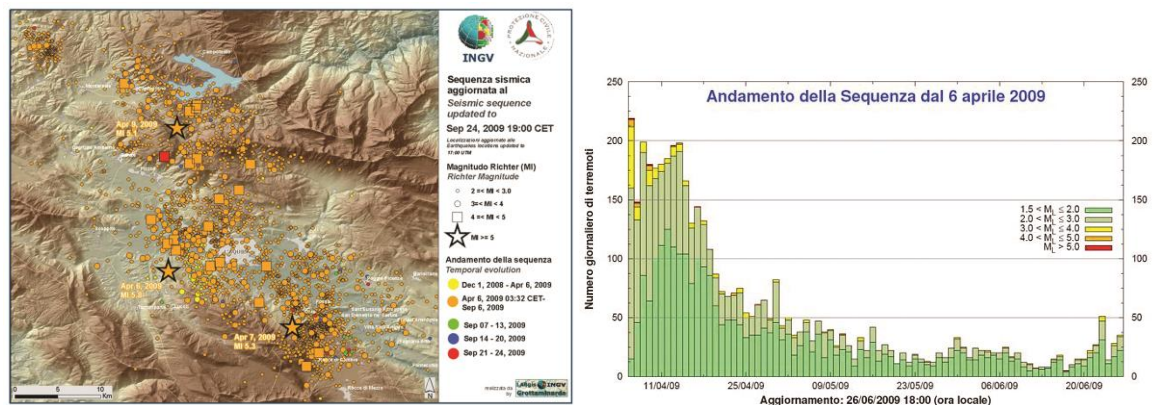


Figure 55: Seismic sequence of the earthquake of L'Aquila (source: <http://www.ingv.it>).

The Province of L'Aquila has already been affected in the past by major earthquakes (<http://www.ingv.it>). The two major earthquakes are those of 09/09/1349 (M_W 6.5) and 02/02/1703 (6.7 M_W), but the earthquake of 06/04/2009 is not comparable to these previous seismic events, characterised by a much higher release of energy.

The earthquake of L'Aquila 06/04/2009 assessed in terms of M_W is the third largest in Italy since 1972, the year of the first records of the National Strong Motion Network (RAN - <http://www.protezionecivile.gov.it>). The first two were that of Irpinia at 20:34 of 23/11/1980 with a M_W equal to 6.9 and that of Friuli Venezia Giulia at 22:00 of 06/05/1976 with a M_W equal to 6.4. The Umbria Marche earthquakes, with main shocks of 02:33 and 11:40 of 26/09/1997, had released minor value of energy characterised by a M_W the first equal to 5.7 and the second equal to 6.0.

The main shock (3:32 of 06/04/2009) in L'Aquila was recorded from 55 accelerometric stations of the RAN. In Figure 56 are located the accelerometric stations far less than 100 km from the epicentre.

In Figure 57, the accelerograms of the three components NS (North-South) WE (West-East) and UP (direction altitude) for the AQV are reported.

Furthermore, for each accelerogram was determined the respective response spectrum, calculated with a damping to 5.0%, for period variable. X refers to the NS component, y the WE component and z the UP component.

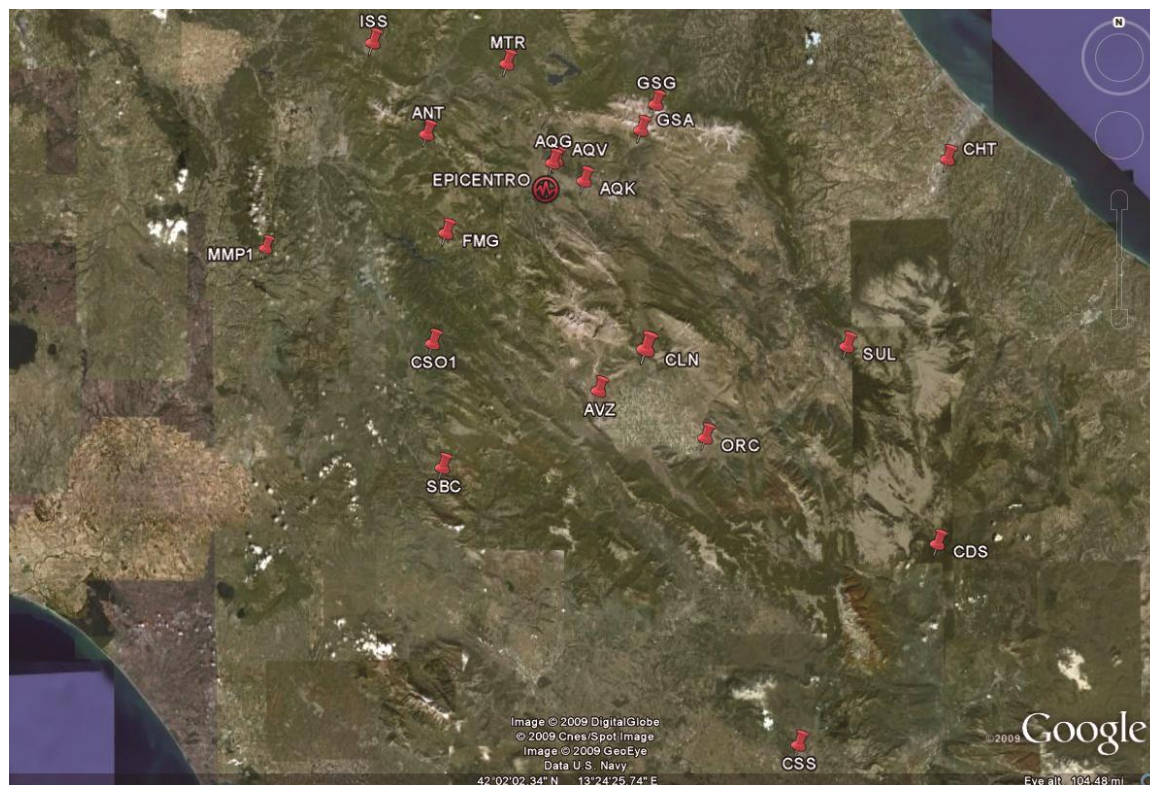


Figure 56: Location of the accelerometric stations less than 100 km far from the epicentre (L'Aquila).

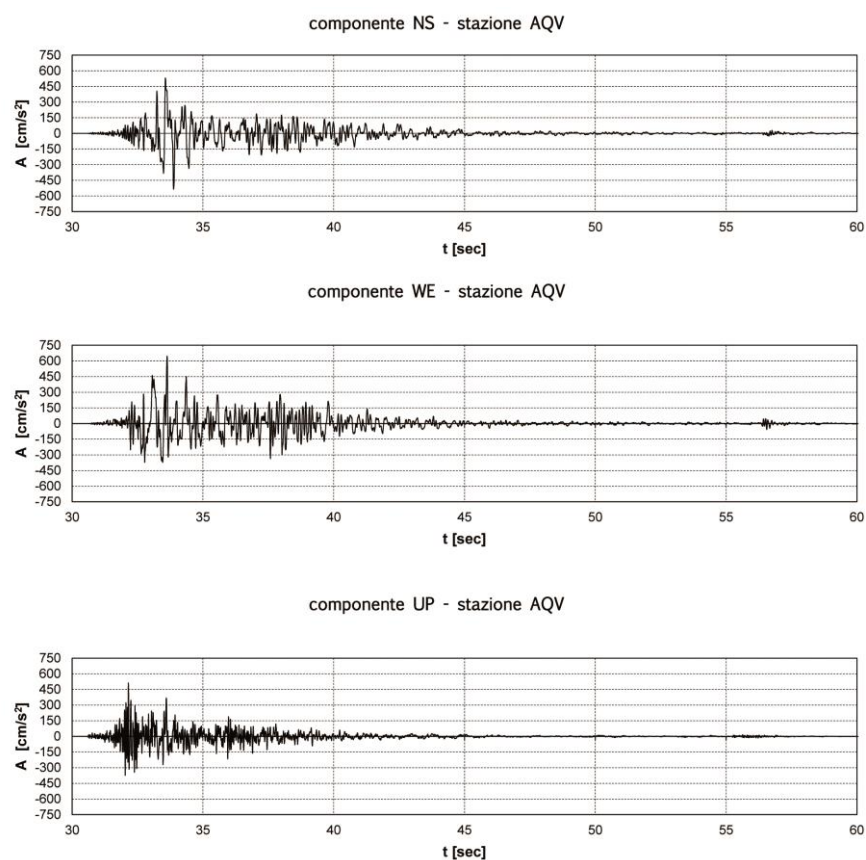


Figure 57: Accelerograms components of AQV station (L'Aquila earthquake).

The response spectrum of the recording accelerometer AQV L'Aquila has been compared with the spectra of Italian actual Code (NTC, 2008). In particular, both the maximum and minimum Code spectra have been calculated, for different types of ground, determined by an earthquake with a return period (T_R) of 475 years. The maximum spectrum has a ground "D" type and the minimum is for a ground "A" type (see also Figure 7). In detail, the code spectra have been calculated assuming the geographical coordinates of the epicentre of the earthquake of 06/04/2009, for damping 5.0% and in the absence of topographic amplification ($S_T = 1.0$). The return period of 475 years corresponds to buildings designed for limit state of preservation of life (SLV), with a V_N of 50 years of use and a class II (C_U equal to 1.0), which is a structure with V_R 50 years (civil residential house), working value for the Castelnovo aggregates also.

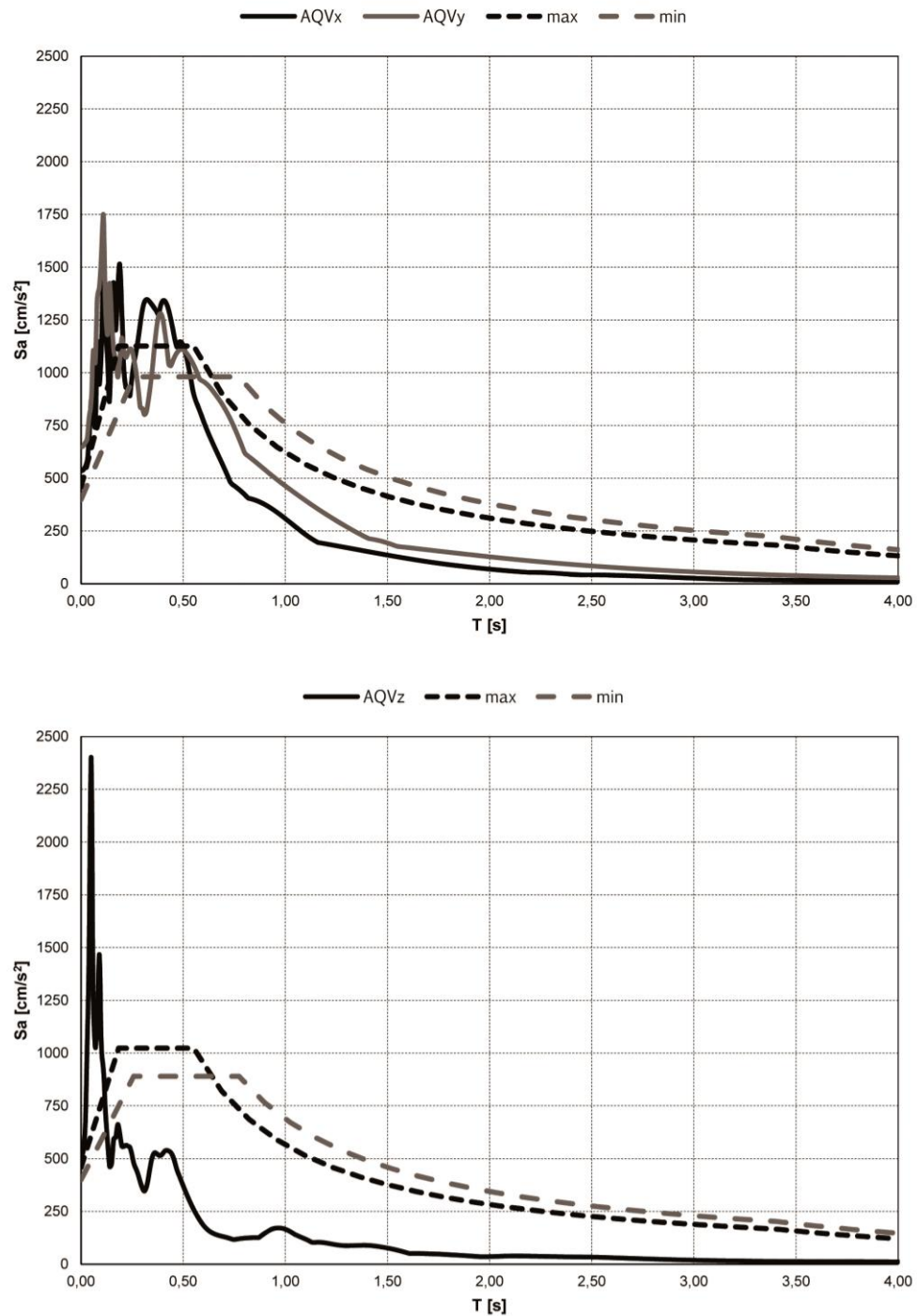


Figure 58: Comparison between AQV response spectra and the design response spectra following Italian actual code NTC, 2008. (top: horizontal components, bottom vertical components).

Particular attention should be paid on time interval recording of approximately 10.0 s (Figure 57, enter 30 and 40 sec). AQV has maximum value in the component WE (646.07 cm/s^2), with peaks concentrated in the first 5.0 sec and amplitudes around 150 cm/s^2 . The UP component reaches 512.36 cm/s^2 for AQV, i.e. of the same order of magnitude of the components NS and WE.

These observations are confirmed by the comparisons made in terms of response spectra (Figure 58), which show the importance of the vertical component of seismic event in L'Aquila.

The L'Aquila earthquake spectra had peaks higher than those required by the Code in the horizontal part (between T_B and T_C periods). For horizontal components AQV spectrum has a peak value 2.85 times higher than the maximum value of the Code spectrum. When the period exceeds T_C , the Code spectrum cover the spectra of AQV.

For the component UP the peak value of AQV is 3.90 times higher than the maximum value of Code spectrum. In this case, the peak values are concentrated on periods below T_B (lower than 0.20 s), and then the L'Aquila spectrum get below the spectra of the NTC 2008.

These differences in terms of response acceleration are not compensated by the Code spectra even putting into account the expected maximum topographic amplification, with a topographic amplification of $S_T = 1.40$ (§Table 8).

For all three components, the peaks of AQV have occurred for periods less than 0.50 s, affecting then stiff structures, i.e., masonry structures or concrete structures stiffened by the presence of panels in reinforced concrete. This to confirm the high level of damage that masonry structures suffered in specie buildings in aggregates, as it will be in deep described in next paragraph.

4.2 DAMAGE IN CASTELNUOVO BUILDING STOCK

After the 2009 seismic event, more than 80% of the aggregates in the territory suffered structural damage on horizontal and vertical elements, and the mainshock (3.32 06/04/2009) caused even the death of five people that lived in the Castello, the oldest part of the city. With the in situ surveys and with the information collected on the crack patterns of the structural elements, a class of damage was assigned to each structural units of the village following EMS-98 scale (Grünthal, 1998). Five are the degrees of the EMS-98 scale (§1.1.1.2), in addition to the absence of damage: from D0 (Figure 59) up to D5 (Figure 60) they shows increasing level of damage (D0 absence of damage; D1: Negligible to slight damage; D2: Moderate damage; D3: Substantial to heavy damage; D4: Very heavy damage; D5: Destruction or collapse).





Figure 59: (from the top). Example of Castelnuovo buildings for different level of damage (D0-D1, D2, D3 and D4).

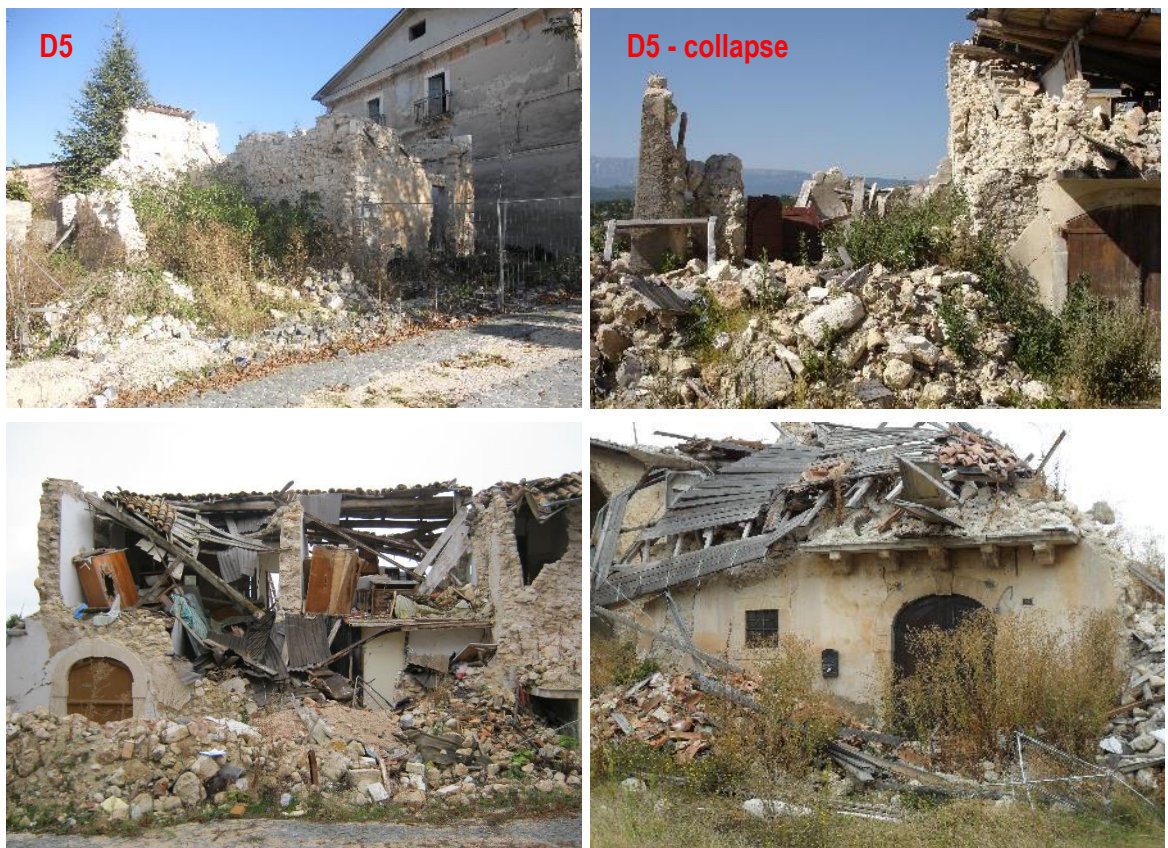


Figure 60: Example of Castelnuovo buildings with D5 damage. From the top, aggregate 05, 44 and 36.

Table 28 shows the distribution of the damage level for structural units, both in terms of % of structural units (in total 289) and volume (164 512 m³). On the right side of the table, the results of the statistical analysis are reported for the only stone masonry aggregates (§3.3.1). From the analysis of the data, more than the 61% of buildings (both in % of structural units and volume) has suffered serious damage in principal supporting structural elements (corresponding to levels of damage D4 and D5), with in some cases collapses.

The percentage grows up to more of 68% (% of ss.uu.) considering only stone masonry, which are generally characterized of a worse state of conservation and lower mechanical characteristics. In particular, only 15.2% of unit has not suffered structural damages (D0 and D1) compared with 76.8% which instead reported damages to structural elements (D3 plus D4 and D5). The D0 and D1 % in terms of volume is about 10%: small-volume aggregates have generally suffered low level of damage if compared with the wide larger ones.

In the case of masonry buildings, only the 6.8% (5.7% in terms of volume) has shown light damage. The structural units belonging to this group have been reinforced in recent years (s.u. 8 of 10-088 aggregate), have been added in further time closed to the aggregate core (ss.uu. 7a and 7b on aggregate 1-222) or are closed to units in unreinforced concrete, that made a confinement action toward them. About 8% (percentage almost stable in terms of ss.uu. and volume) have suffered moderate structural damage (D2). It is worth noting that high concentration of serious damages (D4 and D5) is placed primarily in the upper part of Castelnovo (Castello) and in the middle parts of the historical city centre.

Table 28: Distribution % of real damage level in ss.uu. (in terms of ss.uu. and volume) and for masonry aggregate only

	DISTRIBUTION OF REAL DAMAGE LEVEL				ONLY MASONRY AGGREGATES			
	ss.uu	ss.uu %	ss.uu. volume	ss.uu. % volume	ss.uu	ss.uu %	ss.uu.volume	ss.uu.% volume
D0	5	1.7%	1 575	1.0%	1	0.4%	287	0.2%
D1	39	13.5%	16 025	9.7%	16	6.4%	180	5.5%
D2	23	8.0%	11 610	7.1%	21	8.4%	11 480	7.7%
D3	46	15.9%	34 365	20.9%	41	16.5%	29 490	19.8%
D4	86	29.8%	50 481	30.7%	81	32.5%	48 878	32.8%
D5	90	31.1%	50 455	30.7%	89	35.7%	50 415	33.9%
TOT	289	100%	164 512	100%	249	100%	148 568	100%

It is possible to cross the results of the distribution of the damage grade and the position of the ss.uu. within the aggregates. The ss.uu. can have corner external or internal position or they can be isolate s.u. (§3.3). In detail, statistical analyses and histograms are reported on Table 29 and Figure 62.

For each position type, more than the 50% of ss.uu. have suffered high level of damage, with the peak of isolated buildings, in which 77% of total volumes have D4/D5 damage level. This is in agreement with the widespread distribution of high damage level on the buildings stock (Figure 60). *Isolated* building have the minimum % of volume in low level of damage (D0/D1-7%, in which usually no one structural unit belongs to class D0) and the maximum in high damage level (D4/D5-77%) (Figure 62b).

The *internal* structural units, on the opposite, have the maximum % of light damage (12%) and the 60% in high level, even if the minimum volume for D4/D5 damage level is referred to the *external* (E) ss.uu. The corner units (C) are placed in an intermediate position in all classes of damage considered.

The statistics in terms of only masonry aggregates are reported in Table 30 and Figure 63. The results confirm that irregular stonemasonry with poor quality mortar, in general, is more susceptible to suffer high level of damage in respect to other construction type.

For all the types of position within the aggregates, the percentage of D4/D5 buildings exceeds the 60% with the peak value 97% for *isolated* buildings, for which the conservation state of the masonries and the masonry type play a fundamental role. Referring to the level of damage (Figure 63b), the trend is the same: *isolated* buildings have the minimum % of volume in low level of damage (D0/D1-1%) and the maximum in high damage level (D4/D5-97%). *Internal* structural units, on the opposite, have the maximum % of low damage level (9%) and the 63% high one. The minimum volume for D4/D5 damage level is referred to the *external* ss.uu (61%).

Damage Level-structural units

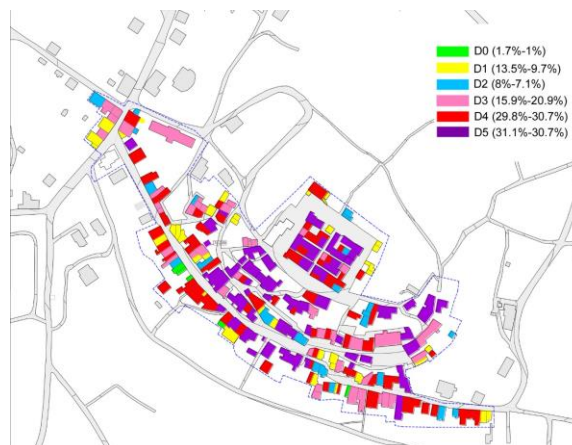
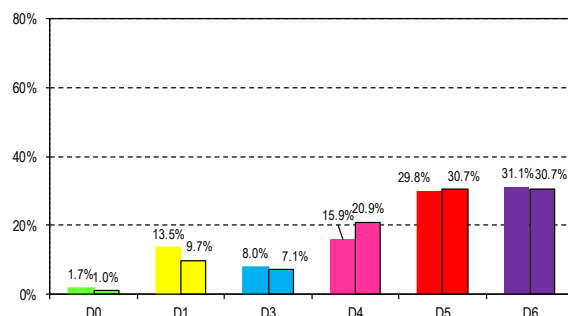


Figure 61: Histogram and maps of the damage for ss.uu.

Table 29: Distribution % of damage and position of ss.uu (in terms of volume)

POSITION / DAMAGE	D0/D1 [m³]	%	D2/D3 [m³]	%	D4/D5 [m³]	%	TOTAL [m³]	
IS = ISOLATE	1 172	6.7%	2 773	15.9%	13 453	77.3%	17 398	100%
C = CORNER	1 758	10.1%	3 107	17.8%	12 552	72.1%	17 417	100%
E = EXTERNAL	5 903	10.3%	19 997	34.8%	31 564	54.9%	57 464	100%
I = INTERNAL	8 768	12.1%	20 099	27.8%	43 367	60.0%	72 234	100%
TOT. →	17 601		45 976		100 936		164 513	

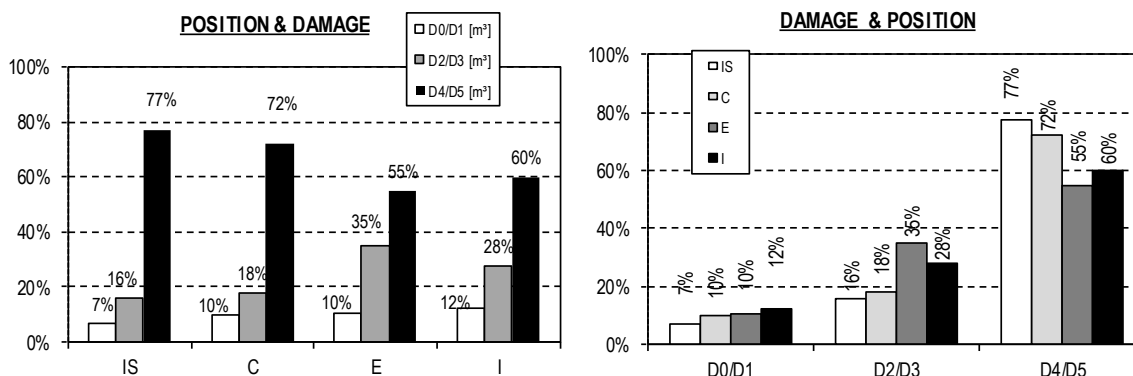


Figure 62: Histograms of damage distribution for different ss.uu. positions.

Table 30: Distribution % of damage and position of ss.uu (in terms of volume) for stone masonry aggregates

POSITION / DAMAGE	D0/D1 [m³]	%	D2/D3 [m³]	%	D4/D5 [m³]	%	TOTAL [m³]	
IS = ISOLATE	151	1.1%	280	2.1%	13069	96.8%	13500	100%
C = CORNER	1 520	9.3%	2537	15.5%	12321	75.2%	16378	100%
E = EXTERNAL	880	1.7%	18769	37.0%	31113	61.3%	50763	100%
I = INTERNAL	5 916	8.7%	19312	28.4%	42698	62.9%	67926	100%
TOT. →	8 467		40898		99202		148 568	

From the analysis of the original documents and in-situ surveys (3.1), the historical evolution of the aggregates were individuated. With this process, the temporal buildings phases were identified for the different parts of the aggregate: the original core were recognized as well as the portions added during the evolution of the construction. The core aggregate corresponds to the structural units made with the oldest construction methodology. They are characterized by irregular masonry textures, ground level with wall thicknesses that achieve 90 cm and vault structures at that level. Aggregates complete the current configuration with enlargements, creation of outbuildings and raising on rear façades.

Figure 64 shows the plans of ground level of three aggregates situated inside the perimeter. For each s.u. construction evolution and damage level are indicated.

By linking the age of construction of the aggregates and the suffered damage scenario, it is noticed that the original core of the aggregates showed high damage scenario (D4/D5), while the structural units built in succeeding times provided smaller damages to their structural elements. The outbuildings and enlargements have usually very low damage levels (D0/D1) because they are made in reinforced concrete, their conservation status is excellent and, most of time, they are separated from masonry structures.

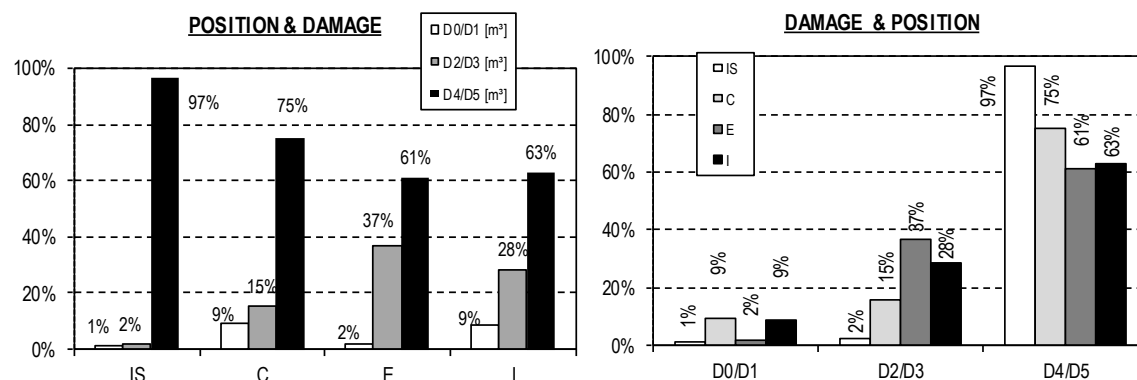
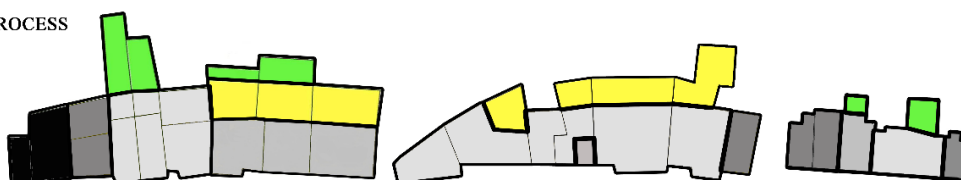


Figure 63: Histograms of damage distribution for different ss.uu. positions for masonry aggregates.

EVOLUTION PROCESS

- First phase
- Second phase
- Third phase
- Fourth phase
- Enlargement
- Outbuilding



DAMAGE LEVEL

- D0
- D1
- D2
- D3
- D4
- D5

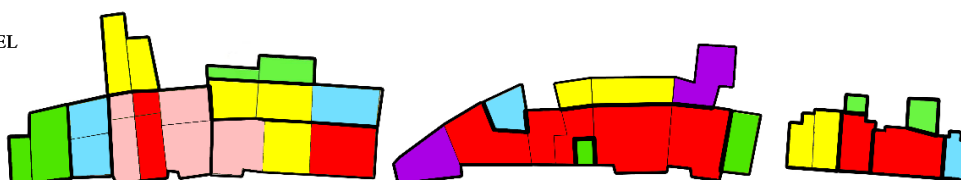


Figure 64: Three aggregates: evolution process and damage level for each structural unit.

CHAPTER 5. AGGREGATE FORM: APPLICATION OF THE 5 PARAMETERS FORM AND DEFINITION OF A NEW AGGREGATE FORM

In this chapter, the results of Vulnerability assessment method of Castelnuovo performed at territorial scale, are reported. Starting from these vulnerability results and exploiting the information achieved by the critical analysis of the real damages on aggregates after the earthquake, in the last part of the chapter a new Vulnerability Form is defined.

In this chapter, the results coming from the territorial scale vulnerability assessment of Castelnuovo through the Aggregate Form (5 parameters Forms) are reported. This Vulnerability Form (Ferreira et al., 2012) is composed by 5 qualitative parameters, and it is able to assess a vulnerability index to an aggregate, considering in its entirety. This method can be used to identify more vulnerable areas in very dense urban mesh, as in historical city centres, in order to have a preliminary screening of the buildings, to focus on them deepened analysis and administration resources. The parameters, the weights and scores of this Form are shown in Figure 65; their explanation is described in detail in par. 2.2.2.4 and in Table 13.

AGGREGATE FORM - 5 PARAMETERS					
Parameters	scores				weight
	A	B	C	D	
1 - Quality of the masonry fabric	0	5	20	50	1.50
2 - Misalignment of openings	0	5	20	50	0.50
3 - Irregularities in height	0	5	20	50	0.75
4 - Plan geometry	0	5	20	50	0.75
5 - Location and soil quality	0	5	20	50	0.75

Figure 65: 5 parameters masonry "Aggregate Form" for the evaluation of Iv.

5.1 RESULTS

5.1.1 VULNERABILITY INDEX

The filling out of the Aggregate Form was done for each masonry aggregate. Indeed, when an aggregate showed separation between structural units of different types, only for the original core of the aggregate the Form was calculated; enlargements, storages and other elements built further close to the aggregate were left apart. As examples, aggregate 10-88 and 16-515 (Figure 66). For the first aggregate, composed by 9 structural units, only the 3÷9 were considered, because the ss.uu. 1 and 2, some centimetres separated from the s.u.3., were made of reinforced concrete (Figure 66a). The aggregate 16-515, instead, has two big enlargements on the rear side (front down street), one of them made in reinforced concrete frame system (Figure 66b). The aggregates number 04 (Figure 66 c) and 73 are not considered in the vulnerability analysis since they are in r.c.. Thus, the total amount of aggregate is 72.



Figure 66: Aggregate not taken into account in the filling out of the "Aggregate Form".

The calculation of the Form for the aggregate 01-222 is reported in the following, in which there is the explanation of the calculated coefficients used for the attribution of the judgments' classes to each parameter.

In addition to the described coefficients, close to the column “scores weighted” there is the indicator for the quality of the information achieved and the correspondence value of reliability. The quality of information can assume 4 values (E, M, B and A) (Table 31), from high level of quality (E) to absent level (A), in analogy with the value already adopted in GNDT II Level Form (GNDT, 1993). High level of quality means direct information collected, that is in situ measures and surveys, presence of graphics documents, with a reliability degree next to the certainty. The global reliability is the average value of the reliability of each single parameter, as it is possible to notice the last coefficient in Figure 67.

MASONRY AGGREGATE - 5 parameters

FORM:

01-222

Parameters	CLASSES	scores	weight	scores weighted	INFORMATION QUALITY	RELIABILITY PARAMETER
1 - Quality of the masonry fabric	D	50.00	1.50	75.00	E	1.00
2 - Misalignment of openings	B	5.00	0.50	2.50	E	1.00
3 - Irregularities in height	B	5.00	0.75	3.75	E	1.00
4 - Plan geometry	D	50.00	0.75	37.50	E	1.00
5 - Location and soil quality	B	5.00	0.75	3.75	E	1.00

calculation of the parameters 2, 3 e 4

parameter 2

M = misalignment of openings

for thess.uu. - 50 cm of misalignment (Formisano et al. 2011)

N' = number of floor staggered more than 50 cm

6

N = number of floor adjacent

17

N'/N =

35.29%

M' = misalignment of openings

less or more they follow the staggered height of the floors

M = number of openings

M'/M =

35.29%

parameter 3

F = floor height difference

3

S.U. = number of buildings (structural units)

7

F/S.U. =

0.43

parameter 4

P =

195

[m]

A =

840

[m²]

16A/P² =

0.35

VULNERABILITY INDEX $I_{V,A}$

$I_{V,A} = 122.50$

VULNERABILITY INDEX (0-100) $I_{V,A}$

$I_{V,A(0-100)} = 57.65 \quad 57.65\%$

RELIABILITY

REL = 100.0%

Figure 67: Example of filling out of the 5 parameter Form.

Table 31: Information quality and reliability of the parameters.

INFORMATION QUALITY	RELIABILITY PARAMETER
E = elevata high	1
M = media medium	0.75
B = bassa low	0.50
A = assente absent	0.25

The results of the territorial scale vulnerability assessment are summarized in next tables, histograms and diagrams. Figure 68a shows the vulnerability index map. The range of $I_{V,A}$ spaces from 6.5% to 73% value, with an average value of 45.9%. For all the parameters in each aggregates, the reliability assumes maximum value.

In Figure 68b are identified three zones over the maps, in which aggregates assume similar value of $I_{V,A}$, coloured with a greyscale. Z1, the clearest, includes 3 aggregates with low values of $I_{V,A}$, under 20%. Zone 2 is the widest where $I_{V,A}$

assumes medium value. The darkest one, Z3, refers to those aggregate with high value of I_{VA} , over 60. Looking these charts, it is possible to observe that:

- there is a correspondence between the Z3 zone, in which the aggregates have major I_{VA} values, and the areas in which aggregates experienced the highest damage after the earthquake;
- this procedure is not successful to grab the high vulnerability of the “Castello” (Figure 76b), since those aggregates are includes in the medium zone Z2, but they showed high damage level in their structural parts.



Figure 68: Vulnerability indexes maps for buildings.

In Table 32 and Figure 69 the distribution of the parameters classes attributed to each parameters is illustrated. The “D” classes in the first parameter (“quality of masonry fabric”) is the most frequent class; indeed, it reaches more than 90% for the aggregates. It means that taken together, more than the 25% of ss.uu. inside each aggregate are ss.uu. belonging to class “Sc4: lose stone masonry, rubble stone masonry with low quality mortar and without dyatones in section” (Table 13). This is due to the mediocre characteristics of masonry type of Castelnuovo that are common to all the aggregates because of the similar period of construction and equality of the used materials.

For the attribution of the class, it has been referred to the percentage of ss.uu. volume in respect to the total, as in the following formula. This means that the attribution of a certain judgment to a parameter’s class is defined referring at the major percentage (in volume) of the classes of the structural units that compose the aggregates.

$$\%_i = \frac{\sum ss.uu.v_i}{aggregate_v}$$

For an historical city centre with common characteristics and situated in a circumscribed area with similar ground property, the P1 (“quality of the masonry fabric”) and P5 (“location and soil quality”) assume almost equal classes for each aggregates. Indeed, if for P1 most of aggregate shows “D” classes, for the P5 two values classes have been considered, “B” or “C”. “A” class is left out because refers to aggregates founded on rock or on a coherent soil with less than 10% (4.5°) of slope. “D” class refers to rock, coherent or heterogeneous soil with slope major of 50% (>25°) or it consider aggregate situated in ravine, cliff.

The ground under Castelnuovo is constituted of silt and there is a wide diffusion of subterranean cavities dug into it and connected with the ground floors of aggregates. To take into account the geotechnical aspect of the cavities, which could produce negative effects on the superstructure influencing the vulnerability of the structure, “D” class could have been chosen for all aggregate that grown up over a tunnel. To date, the number and the position of the cavities is unknown and specific geotechnical investigations are on going. For the reasons exposed, “B” or “C” classes of soil are chosen for aggregates. The slope’s value is the decisional criteria to choose enter those classes. Measuring in direction perpendicular to the contours lines, the average slope is the direction NE-SO is about 30% (14°) for the hill of Castelnuovo (“C” class). When the slope has a local less value “B” class has chosen. In Table 33 picture n.4 there is the map of the distribution of “B” (ciano colour) and “C” (orange colour) classes for the aggregates.

For the reasons written above, the differentiation in terms of vulnerability among aggregates in a village with circumscribed dimensions and common characteristics, such as Castelnuovo, is due principally to the parameters P2, P3 and P4 that are objective parameters.

Table 32: Distribution of the class within the 5 parameters for 72 aggregate.

DISTRIBUTION OF THE CLASS WITHIN THE P5 PARAMETRS					
	P1	P2	P3	P4	P5
A	0.0%	54.2%	56.9%	31.9%	0.0%
B	5.6%	37.5%	29.2%	25.0%	36.1%
C	4.2%	5.6%	13.9%	23.6%	63.9%
D	90.3%	2.8%	0.0%	19.4%	0.0%

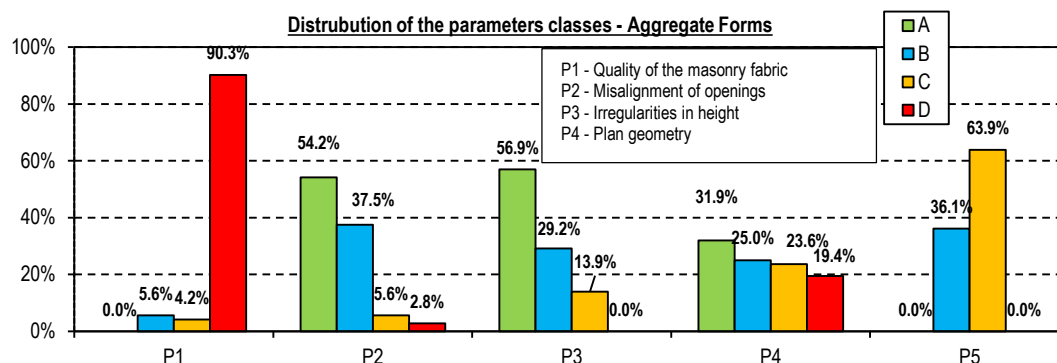


Figure 69: Distribution of the parameters' classes for 72 masonry aggregate.

The P2 refers to the relative numbers of staggered floors, dealing about the interaction of local loads of the different height of the slabs. Less than 10% (2.8% class "D" and 4.2% class "C") of aggregates have staggered floors. In the computation of this parameter, only the close floors are considered. In other words, if two adjacent ss.uu. have the same number of floors, all the floors are computed on the calculation (ad exception of the ground floor). If they have different number of floors, only in the common floors are taken into account.

P3 refers to the irregularities in height of the aggregates' structural units. The criterion of division into class is due to the deviation of the height of the ss.uu. from the average height of the aggregate. Therefore, the type of class depends on the ratio between the sum of the number of floors missing among two adjacent ss.uu. and the total number of the ss.uu. of the aggregate. About 15% are in class "C", in some cases there is more than 1 floors of different within adjacent buildings. The remaining part of buildings is divided into "A" (56.9%) and "B" classes (29.2%).

P4 gives information about the aggregate's shape and plan irregularity. It uses, as a decisional criterion, a relationship between the area, A, and the perimeter, P: $P_4 = 16A/P^2$ (Giovinazzi et al., 2004). If this ratio is near to 1, the aggregate shape is almost regular ("A" class), if it is lower than 0.5, the aggregate shape is complex and more vulnerable (class "D"). For the aggregates here analysed, there is not a favourite class, the aggregate have general different plan shape for which the ratio calculated has different values. About 32% of aggregate lies in "A" class while about 19% in "D" class.

Up to here, the results include isolated building also, as a particular type of aggregate construction. Obviously, the isolated aggregates have the best classes ("A") for the parameters regarding the interaction between ss.uu.: P2, P3 and P4.

The distribution of the I_{VA} has 45.9% as average value (Figure 70); even if the vulnerability study is done at aggregate level, it could be considered comparable to a building typology of "A" vulnerability class following EMS-98 (Grünthal, 1998) scale, referring to what express to by Bernardini et al., 2007a-b.

The minimum $I_{VA,MIN}$ is 6.5% and refers to the 66-583 aggregate (Figure 72a). It is a concrete one-floor building, located on

the top of the hill, with 3 structural units. The maximum value obtained for the building stocks is that of the 11-125 aggregate (Table 32, fig. 3), with an irregular and complex shape; it has adjacent ss.uu. having different numbers of floors and staggered slabs. In Table 34 there is the resume of the classes attributed to the aggregate 11-125 and 66-583: they are completely different each other.

Table 33: Characteristics of the building stock with reference to the Aggregate Form.

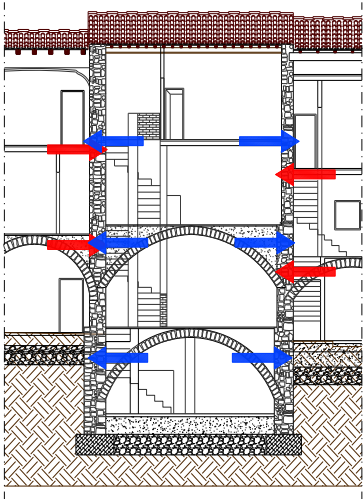


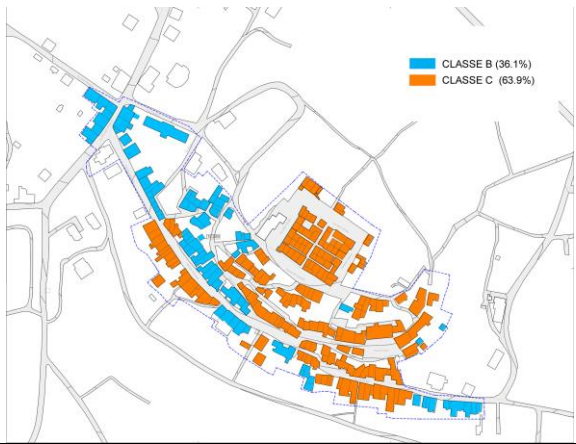
	
<p>Parameter 2: aggregate 10-088 example of A classe (only in this part of the aggregate [ss,uu 7-8-9] have discontinuity</p>	<p>Parameter 3: aggregate 50-173, 1 floor difference (1F) and 3 structural units and. 1F/3S.U. = 0.33 → class B</p>
	
<p>Parameter 4: aggregate 11-125, P = 175 m, A = 710 m²; 16A/P² = 0.37 → class D</p>	<p>Parameter 5: representation of the aggregate with the B and C classes on the soil (in ciano and in orange colour).</p>

Table 34: Aggregate Form results for aggregate 11-125 and 66-583.

Aggregate →		11-125	66-583
Parameters	Class	Scores*weighted	Scores*weighted
1 - Quality of the masonry fabric	D	75.00	7.50
2 - Misalignment of openings	D	25.00	2.50
3 - Irregularities in height	C	15.00	0.00
4 - Plan geometry	D	37.50	0.00
5 - Location and soil quality	B	3.75	15.00

The chart in Figure 70 represents the distribution of the I_{VA} found for 72 aggregate. To describe the centre of the set of data, the average value is calculated, $I_{V5,av}$, the standard deviation σ of the sample. The variation range of the vulnerability index is:

$$\Delta I_{V5} = I_{V5,av} \pm 2\sigma_{V5}$$

The choice of $k=2$ allows to consider in the range at least the 75% of the analysed values. In particular, in the case of normal distribution of the data (with the presence of one single maximum value at the average point and decreasing data

both from the two sides of the average value), about the 95% of the data will lie in the range $I_{V5,av} \pm 2\sigma_{V5}$ (Figure 69b). The sample of data is represented with histogram, too, considering the frequency of the vulnerability index. Both in 5 and 10 units of differences the index is plotted, for a total amount of 20 and 10 classes respectively (Figure 70a). The histograms are plotted both in terms of absolute frequency (number of aggregates that are present in each class) and relative frequency (expressed in % respect to the total amount). Close to the value of the number of aggregates there is the representation on terms of volume (total volume and in percentage of the total volume).

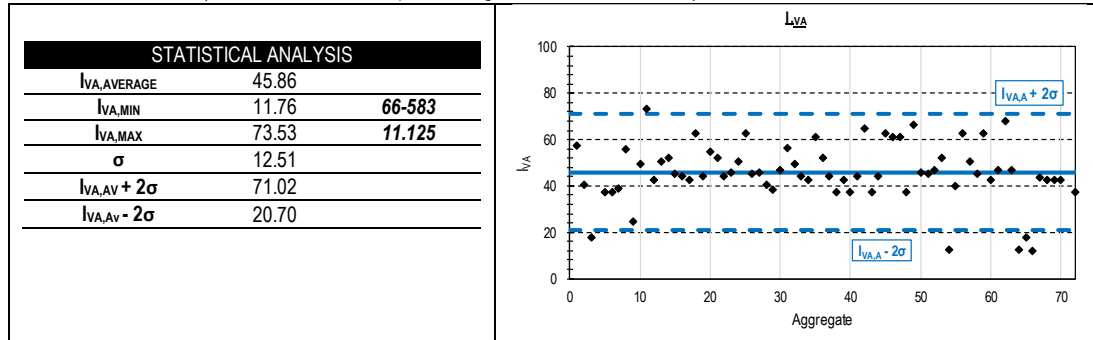


Figure 70: statistical analysis and distribution of the I_{VA} for the 72 aggregates.

Figure 71a shows the vulnerability index distribution histograms and the normal distribution of them. About 70% of the building stock have a vulnerability index value which lies from 35% to 50% value. Only 8% of buildings have an I_{VA} below 20%. If the analysis is done in volume terms, the percentage changes, because of the wide dispersion of the volume quantities within the aggregate. High vulnerability index corresponds to aggregates (not isolated buildings) having volume major than 5000 m³. Isolated building have volume less than 1000 m³. In terms of number of buildings, about 7% have vulnerability index < 20% and they correspond to only the 2.2% of the total volume in Castelnovo (of 72 aggregates).

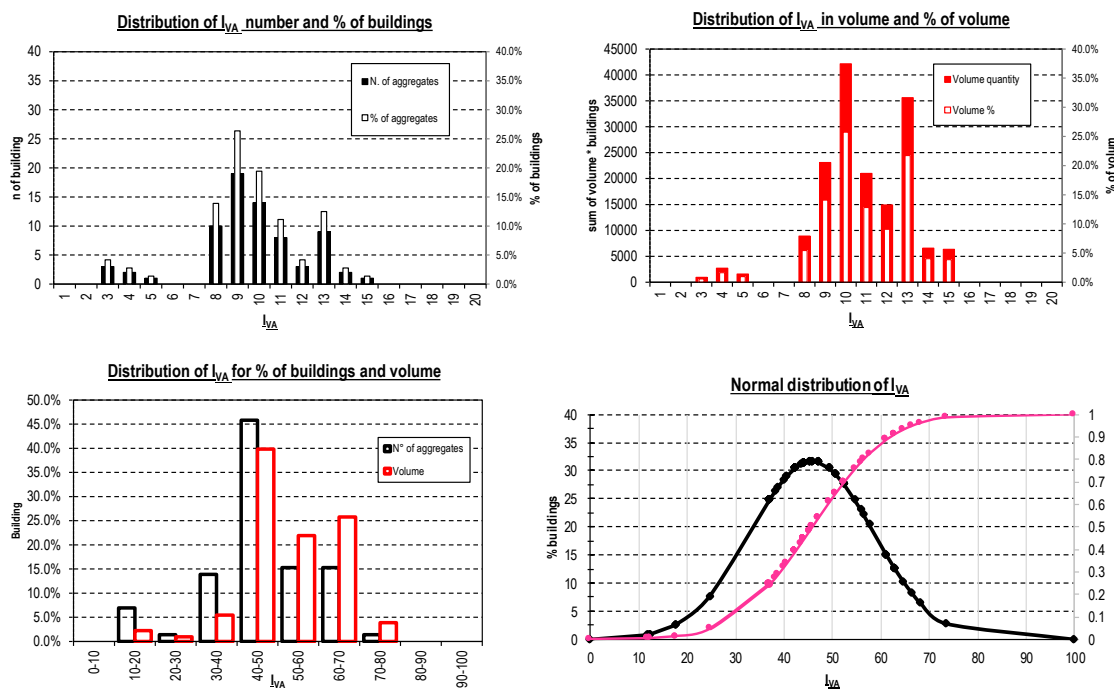


Figure 71: (a) Distribution of I_{VA} in terms of number of buildings and % of building; (b) distribution of I_{VA} in terms of volume of buildings and % of building; (c) % of buildings and volume (with less values of classes); (d) normal distribution.

§

A large number of aggregates have the same value of I_V . This is due to both the small numbers of the parameters inside the Form, to the equal value of all the parameters' classes and the identical weight for the last three parameters (Figure 72b). Only 28 different values of vulnerability index has been individuated, and 28 positions in a vulnerability classification of the aggregates. The I_{VA} attributed to major number of aggregates are 42.3% and 44.1% (Figure 73).



AGGREGATE FORM - 5 PARAMETERS					
Parameters	scores				weight
	A	B	C	D	
1 - Quality of the masonry fabric	0	5	20	50	1.50
2 - Misalignment of openings	0	5	20	50	0.50
3 - Irregularities in height	0	5	20	50	0.75
4 - Plan geometry	0	5	20	50	0.75
5 - Location and soil quality	0	5	20	50	0.75

Figure 72: a) Aggregate 66-583, one floor, three ss.uu., regular plan. b) Individuation of the same classes and weights.

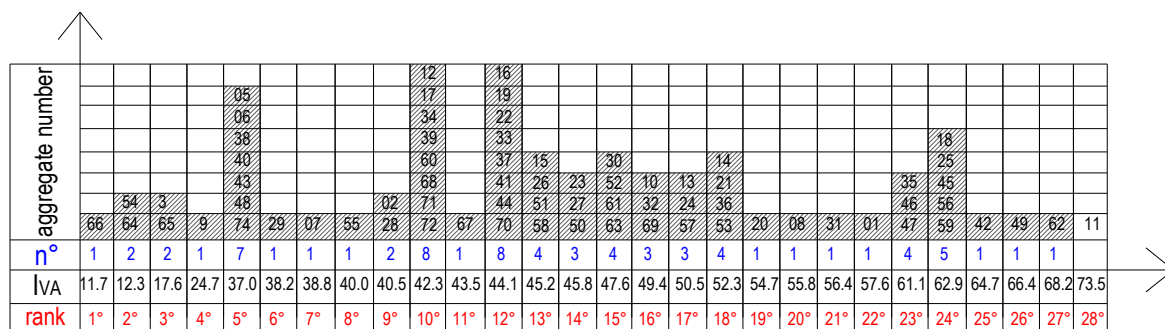


Figure 73: Aggregates ranking with increasing I_{VA}.

§

The results could be separated for aggregates and isolated buildings: the distribution of classes is exposed in Figure 74a, in which the aggregates have higher I_V rather the isolated one, due to the class assigned to the P2, P3 and P4. In Figure 74b, there is the histogram representation of the distribution of the parameters' classes for the isolated buildings. P2 and P3 assume almost exclusively "A" classes, while P4 ("Plan geometry") assumes for the 68.2% value "A", for the 22.7% class "B" and the remaining 9% is equally divided in classes "C" and "D". The amount of aggregates is 50; isolated are 22.

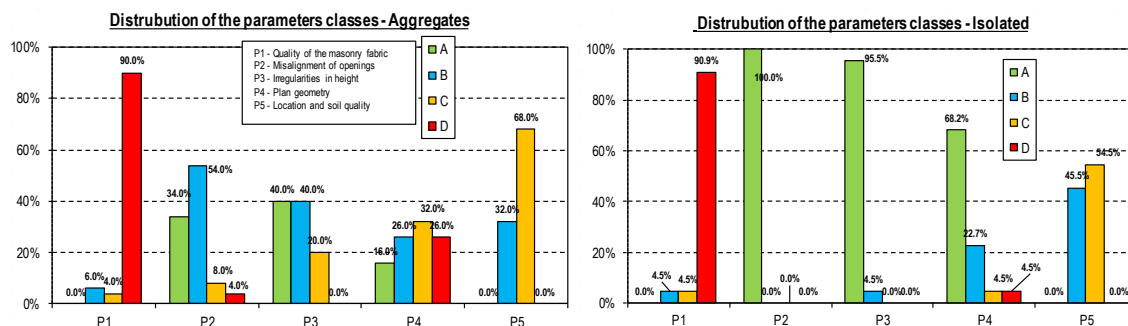


Figure 74: Distribution of the parameters classes for aggregates and isolated buildings.

Therefore, in next figure the statistical analysis and the distribution of the values of I_{VA} both for the cases of only aggregates (in dark line) and isolated buildings (in grey line) are reported. The blue line is plotted also, which represents the average value of I_{VA} found for the entire building stock of Castelnuovo (72 aggregates) already express in Figure 70b.

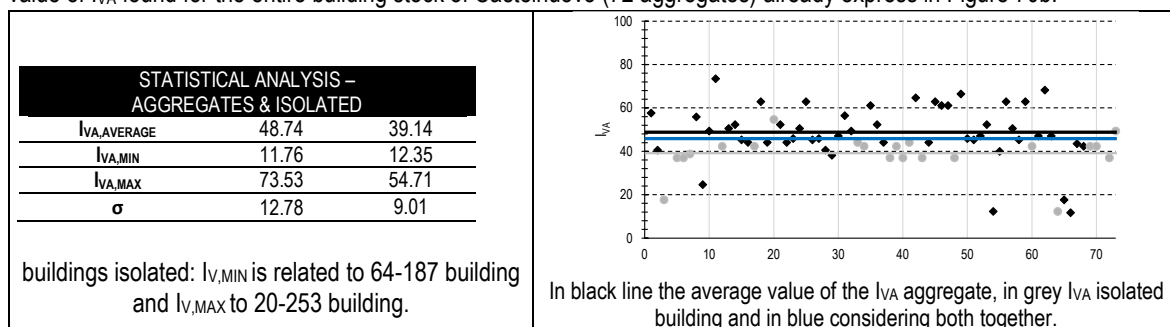


Figure 75: Results for aggregates and isolated buildings.

On the following, the analysis results without considering the “Castello” aggregates are displayed. The “Castello” is composed of 7 buildings, 6 aggregates and one isolated. As mentioned in the historical study of Castelnuovo, these aggregates constitute the oldest part of the village, collocated on the top of the hill. The state of conservation and the occupancy of these aggregate was different from the other part of the village. Figure 76 shows the ante earthquake state of the “Castello” in which it is noticed that some ss.uu. were abandoned, in dilapidated conditions in certain cases they had only the perimetral walls without slabs or roofs.



Figure 76: “Castello”, ante-post earthquake aerial photos.

The total amount of aggregates is 66. In Figure 77b there are plotted in blue line the average I_{VA} for 72 aggregates (close to the green line), in blu dotted line the $I_{VA} \pm 2\sigma$, in green line the average value of I_{VA} for 66 aggregates and in red line the average values for only the “Castello”’s aggregates. It is noticed that:

- I. the characteristics of the I_{VA} distribution are not too much influenced by the value of the 6 “Castello”’s aggregates → because of the “Castello” I_{VA} values are quite closer to the average value and they are only 6 aggregates. Indeed, the average I_{VA} of “Castello” is 53.5% (red line);
- II. The average value I_{VA} for 66 aggregates is almost the same value, but a little bit lower, removing the influence of those aggregates, which have, a higher vulnerability index than the average one. This aspect is shown in Figure 77 (b): the green line is almost overlapping the blu one (the average line I_{VA} for 72 aggregates), and the red line higher than the others.

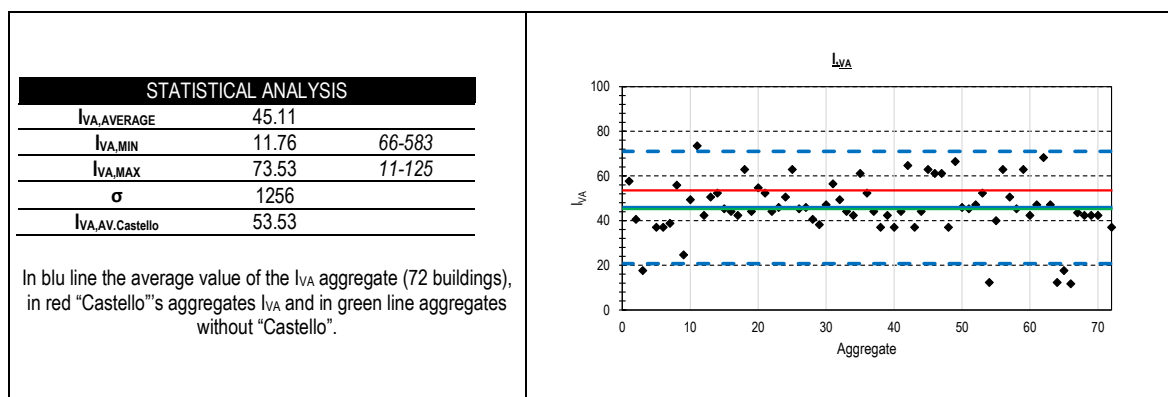


Figure 77: Results for aggregates and isolated buildings without “Castello” (66 aggregates).

5.1.2 DAMAGE

Using correlation present in literature (§2.2.3) it is possible to determine the estimated mean damage grade for aggregate (μ_D), for fixed intensity degree of earthquake, once having calculated the vulnerability index, I_{VA} . In this paragraph at first, the description of the *real* damage suffered by the aggregates in Castelnovo is recalled and afterwards the estimated mean damage grade is determined, considering the results of the vulnerability index for “Aggregate Form”.

After the 2009 seismic events, more than 80% of the aggregate suffered structural damages on horizontal and vertical elements. Figure 59, Figure 60 and Figure 61 show the *real* damage grade for each ss.uu.. Those grades have been assigned to each structural units during the post-earthquake surveys, following the grades of the EMS-98 scale (§4.2). The Figure 78b shows the real average damage grade in terms of aggregate. These ideal values were calculated considering the weighted volume of each structural units.

In order to get a more clear representation of the obtained results for damages in the map, middle classes of damage has been introduced in the classification of the EMS-98 Scale. They deal with a middle damage degrees of EMS-98: D0 (0-0.5), D1 (0.5-1), D1-D2 (1-1.5), D2 (1.5-2), D2-D3 (2-2.5), D3 (2.5-3), D3-D4 (3-3.5), D4 (3.5-4), D4-D5 (4-4.5) and D5 (4.5-5). These damage classes are used to represent for the aggregates' damage grades while for the structural units EMS-98 damage standard grades is used (D0÷D5).

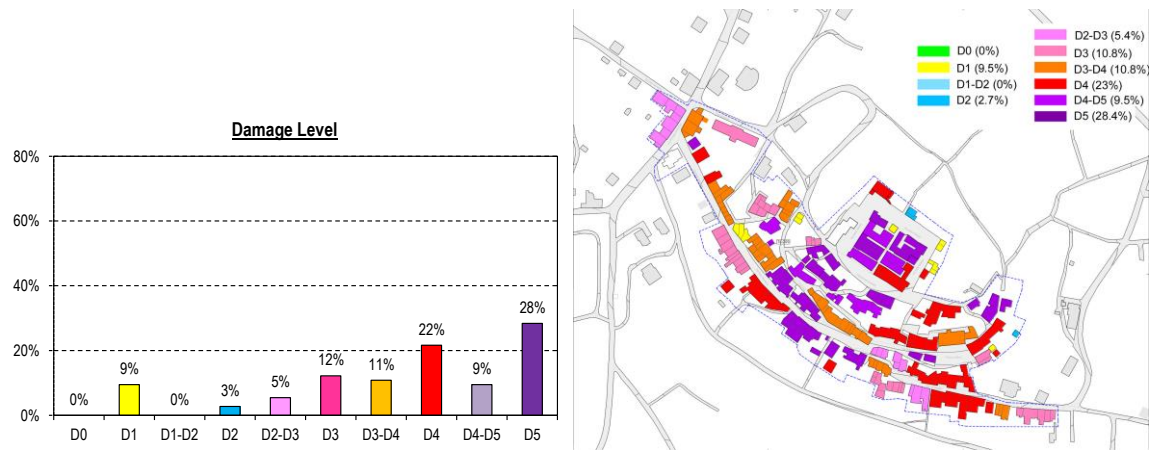


Figure 78:(a) Damage distribution for aggregates, histogram; (b) average damage grade weighted in volume.

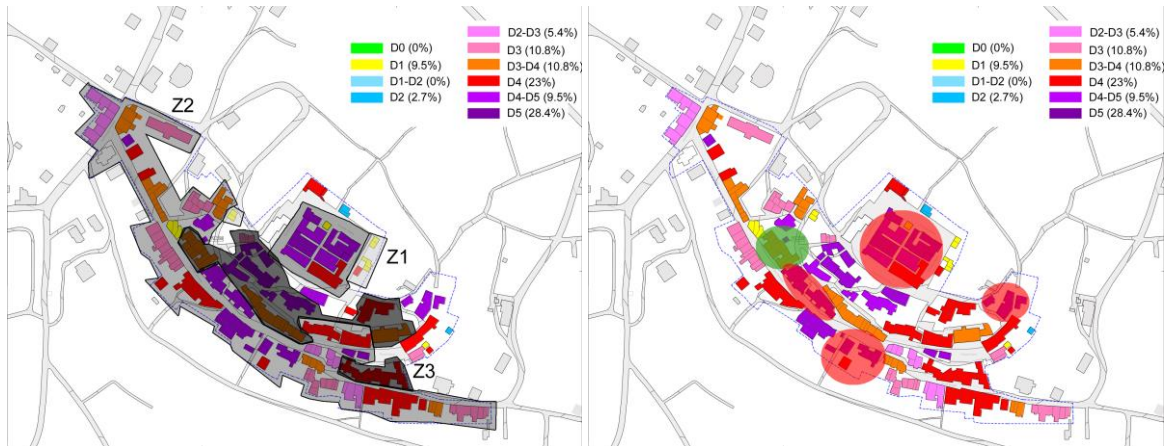


Figure 79: Real damage grade with the individuation of the major vulnerability zones.

The forecast mean damage grade is assessed using the correlation developed by Bernardini et al. (Bernardini et al., 2007a-2007b). The relationship links the forecast mean damage grade with the I_V and the macro seismic intensity of earthquake. The μ_D is related to the EMS-98 scale, taking value enter among [0;5]. The function gives a continuous value of μ_D versus I for different value of vulnerability index. V is the terms related to the aggregate's vulnerability, $V=0.56+0.0064 I_{VA}$

(Bernardini et al., 2007), in which I_{VA} is calculated with the “Aggregate Form” (5P).

$$f(V, I) = \begin{cases} e^{\frac{V}{2}(I-7)} & \text{se } I \leq 7 \\ 1 & \text{se } I > 7 \end{cases}$$

$$(18) V = 0.56 + 0.0064 I_V$$

$$\mu_D = 2.5 + 3 \cdot \tanh\left(\frac{I+6.25-V-12.7}{3}\right) \cdot f(V, I) \quad 0 \leq \mu_D \leq 5$$

In Figure 80, there is the representation of the vulnerability curves for the most and less vulnerable aggregates, the 11-125 and 66-583., for intensity degrees that produces tangible damages on the masonry structures (VI-XII).

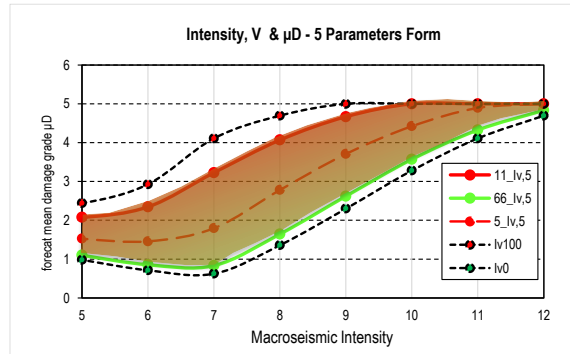


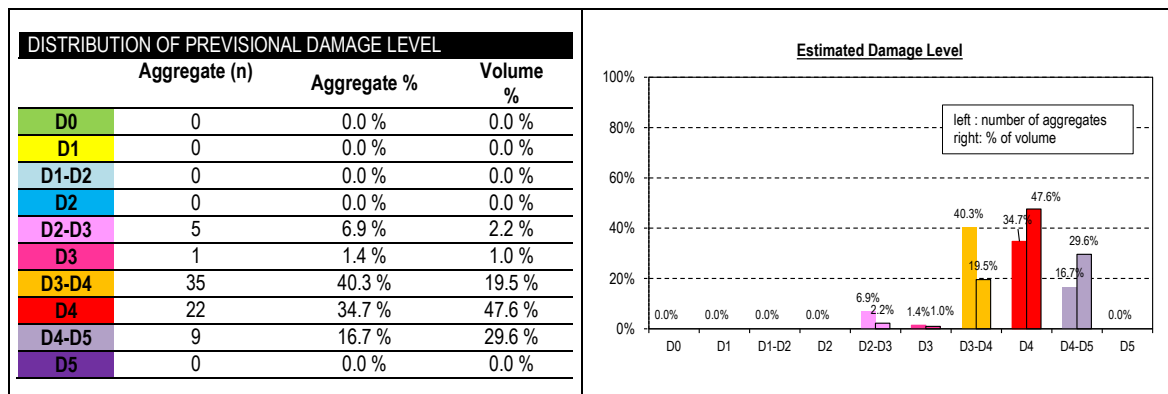
Figure 80: Vulnerability curves for the most and less vulnerable aggregates.

Next charts (Figure 81a-b) show the results in terms of the estimated mean damage grades with the vulnerability procedure. It was determined with the macroseismic intensity of 9.5 MCS (8.5 EMS-98) reached at Castelnuovo after the earthquake. In Table 35 there is the distribution of the estimated damage in terms of % respect to the total amount of aggregates (72) and for the total amount of volume (163 782 m³). For the high macroseismic intensity degree experienced, even the aggregates with a low I_V show a medium-high level damage (D2-D3).

The average damage level is 3.5 that, for the chosen scale, belongs to D3-D4 damage level (in orange colour in the map). According with the distribution of the I_{VA} , the minimum μ_D value is 2.2 (D2-D3) and refers to the 66-583, while the maximum damage level is related to the 11-125 aggregate and values 4.37 (D4-D5). Table 35 shows histogram distribution of the estimated damage. As well it happened for the distribution of vulnerability index, the lower estimated level of damage refers to small aggregates, characterized by less than 1000 m³ of volume, while high level refers to big-volume ones.

In Figure 81a, the damage zones Z1, Z2 and Z3 (introduced in Figure 68) are overlapped on the maps in which estimated damage is reported. In Figure 81b those zones are overlapped over the Castelnuovo aerial photo post-earthquake. For zones Z1, Z2 and Z3 the comparison gives good results: the zones that showed higher damage were characterised by major level of vulnerability. However, in Figure 81b there are highlighted in red circles two other zones for which there is not enough correspondence among the estimated and real damage scenario.

Table 35: Distribution % of estimated damage level



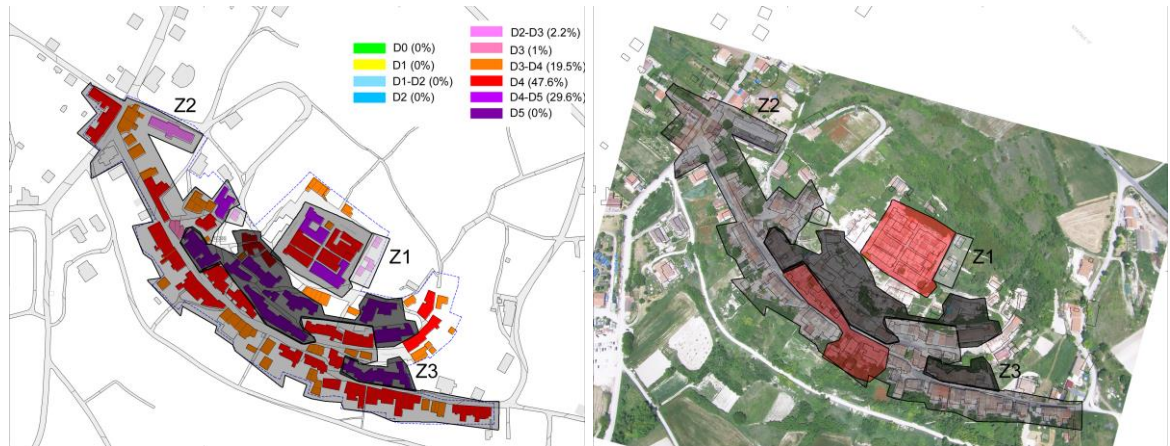


Figure 81: Estimated mean damage grade without and with zone 2 and 3; (b) Individuation of damage zones in aerial photo.

5.2 CRITICAL ANALYSIS OF THE DATA COLLECTED

The Vulnerability Index Methods are based on the evaluation of a certain number of parameters assigning to them qualitative judgments (“A”, “B”, “C” or “D” from best evaluation to the least one), each of them associated to numerical scores. Each parameter has a weight that measures its relative importance in the definition of the I_V , that is weighted sum of each scores (depending of a judgment assigned) and a relative weights.

How much does each parameter influence the I_V ?

Considering each type of Form, the percentage of influence of each parameters has already calculated (and reported in §2.2.2), by keeping all parameters in the worst conditions (as all the parameters were in “D” judgments). For the Aggregate Form, Figure 31 resumes the results of this aspect. Having the parameters equal scores for the judgments (0, 5, 20 and 50), the importance of a parameter in respect to the other is due to the parameters’ weight. P1 assumes 35% of importance, P2 the less, 12%. The others are collaborating for 18%, having them also equal values of their weights, 0.75 (Figure 31). In order to better understand the importance of each parameter in relation also with the calculated I_V , the data collected for Castelnuovo aggregates were analysed deeply. The application of the Aggregate Form has allowed the creation of a *Vulnerability ranking* for the database (28 positions).

Figure 82a shows the distribution of I_{VA} for all the aggregates of Castelnuovo. Figure 83 represents the trend of the judgment of each parameter “along” the vulnerability ranking, starting from the most vulnerable building until the least vulnerable one. On the vertical axis, there are the four possible judgments (“A”, “B”, “C” and “D”) while on the horizontal one the 72 buildings are ordered with the I_{VA} ranking. These figures allow to understand which are the judgments of parameters that show a trend in agreement with the trend of the I_{VA} and that (as we will see in next paragraph) or of the real level of damage (D_K). To have a good correlation, the judgments of each parameters contained in the Form should be “D” or “C” classes (high class of judgment) for high level of vulnerability and lower classes (“A” and “B”) for lower classes of vulnerability.

P1 and P4 show “similar” trend to the distribution I_{VA} , they assumes “negative” classes when aggregate have high vulnerability indexes. P1 refers to the “quality of the masonry fabric”: for Castelnuovo aggregates the masonry is homogeneous, with some exceptions with one-floor structures constituted in brick or hollow concrete masonries. Until the 60th aggregate position, P1 assumes “D” class. The less vulnerable aggregates show on the contrary “B” classes. P4 refers to the “plan metric configuration” and it shows a general decreasing trend of the judgments. The distribution could be well divided in three different parts: the prevalent “D” judgment section (from the beginning up the 15th element), the prevalent “C” judgment section (up the 45th building, even if with some exceptions) and the prevalence “A” structures with some reference at “B” judgments. The trend of this parameter shows a good correspondence with the one of the I_V .

P3 (“Irregularities in height”) and P5 (“Plan geometry”) show independent behaviour with the I_V classification.

Distrubution of the Aggregate index of vulnerability

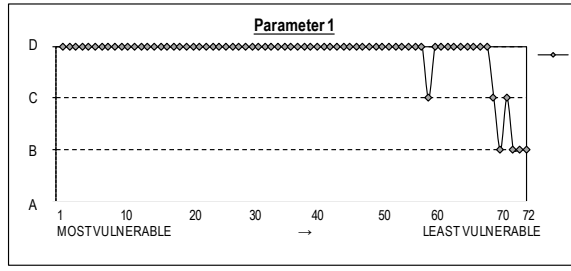
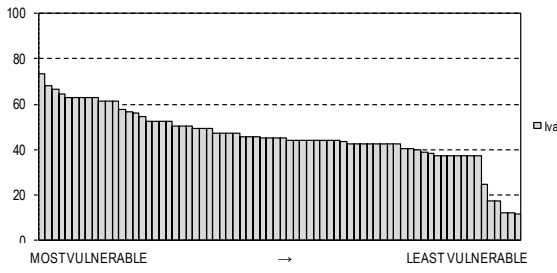


Figure 82: a) I_v distribution (5P-Form) for aggregates. b) distribution of the judgments in the P1 along the Vulnerability ranking.

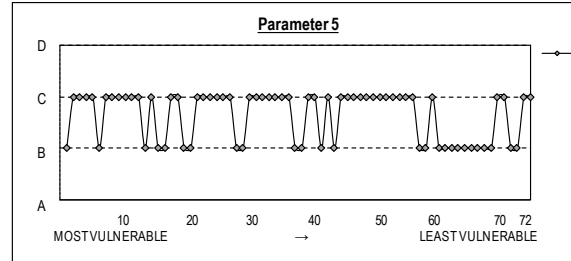
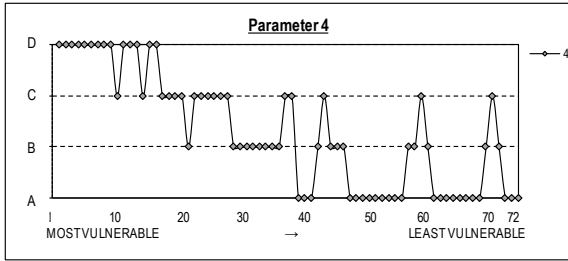
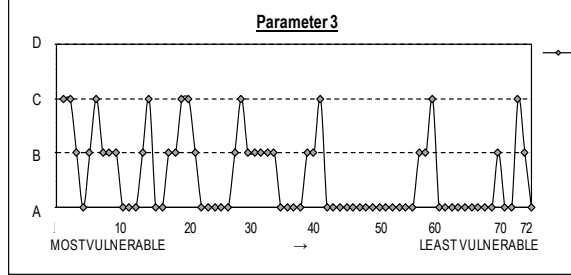
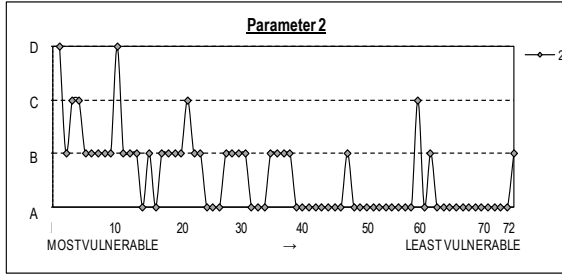


Figure 83: Distribution of the judgments in the P2, P3, P4 and P5 with the vulnerability ranking.

§

In this paragraph, a deepened study of the dependency of each parameter will be discussed.

Indeed, more objective conclusions can be obtained by means of a statistical treatment of the collected data. A correlation among the parameters can be obtained by looking at the distribution of the judgments defined for each parameters. The variable in play are seven: the five parameters of the "Aggregate Form", the I_{VA} and the distribution of the real level of damage of the aggregates (D_k).

In general, to asses statistical treatment of the data, the clouds of points enter two variables a time could be plotted. The shape of the cloud of points highlights a more or less effective correlation level among the two considered parameters. In the case of the judgments of the VIM, the variable parameters can assume discrete values for their judgments ("A"÷"D"), while the I_{VA} and D_k can assume continuous values. The classical representation of the values with the cloud of point is not fit for this case, since the points of the cloud for the parameters of "aggregate Form" can occupy only 16 fixed positions (4 possible judgments for both the parameters chosen), overlapping and hiding each other in the graph, as it is possible to see from the chart of the matrix of plot in Figure 84.

To estimate the correlation level among the parameters, considering by couple of two, the sample correlation coefficient $r_{x,y}$ is used, defined as:

$$(19) \quad r_{x,y} = \frac{\sum_{i=1}^n (x_i - \bar{x}) \cdot (y_i - \bar{y})}{\sqrt{\sum_{i=1}^n (x_i - \bar{x})^2 \cdot \sum_{i=1}^n (y_i - \bar{y})^2}}$$

In which:

- X and Y are the matrixes of the values (judgments) of the two considered variables (in this case, vectors with dimension 1x72);
- x_i and y_i values of each singular observation for the two considered variables;

- \bar{x} and \bar{y} are the average values of each variable.

The sample correlation coefficient was assessed for:

- Each distribution of the judgments for the 5 parameters (for couple of parameters);
- The distribution of the vulnerability index (I_v) and the real damage D_k .

In order to apply the formula, judgments are transformed in numerical values: to each judgment is associated both the value of the scores (defined by the Form, Table 13) and arbitrary value:

- "A"=0, "B"=5, "C"=20 and "D"=50 (real distance among the classes in the Form)
- "A"=1, "B"=2, "C"=3 and "D"=4 (fixed distance of one "step" among the classes).

The correlation index assumes values in the $[-1, +1]$ range, where +1 means an optimum direct correlation and -1 a perfect inverse correlation, while values near to 0 mean no correlation among the couple of parameters. The coefficient are inserted in the matrix of correlation, a symmetric matrix, that immediately provided an idea of the existing links among parameters. The matrix has been plotted for both the numerical solutions associated to the judgment (afore mentioned). The correlation indexes for the two solutions change, remaining stable their dimension. For the case of real judgments' scores, the correlation matrix is reported on Figure 85a. For the values assumed by the correlation coefficients, the Form's parameters can be considered as independent: the r_{xy} is always less than 0.5 for all the couple studied and, in general, very close to null value. For the second matrix, for which the values assumed for the judgments are equally-distributed the values changes a little bit (not in a significant way). Only r_{24} is major of 0.5, appearing without a clear physique explanation.

As expected from the trend of the parameters showed in the Figure 83b, the distribution of vulnerability index is more correlated with the distribution of judgments' classes of P1, P2 and P4, with correlation coefficients equal respectively to 0.71, 0.45, and 0.74 (or 0.71, 0.55 and 0.71 with the use of equidistant scores for judgments).

The last column of the correlation matrix contains the correlation indexes with the distribution of the real level of damage (D_k), calculated as in §5.1.2. P1 is the major correlated parameter with the distribution D_k with $r_{1,Dk}$ major of 0.5. The other parameters have low values of correlation or inverse one.

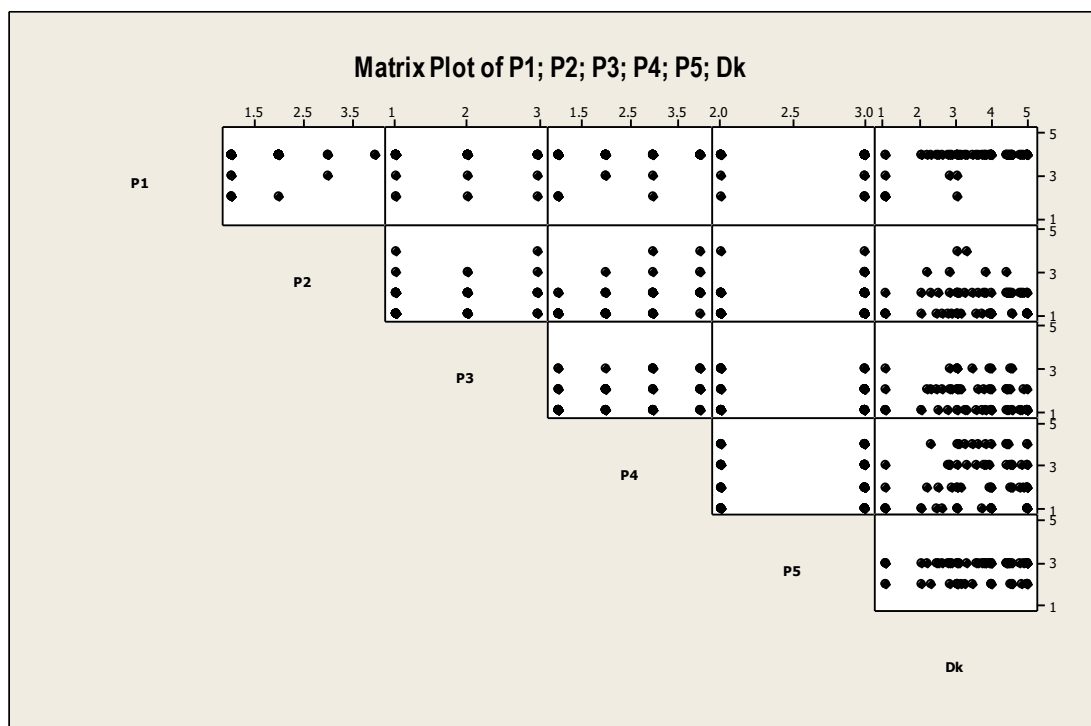


Figure 84: Matrix of plot of the Aggregate Form parameters with the level of damage.

MATRIX OF CORRELATION	1	2	3	4	5	$I_{VA,5}$	D_k
1 - Quality of the masonry		0.047	-0.130	0.157	-0.056	0.713	0.512
2 - Misalignment of openings			0.233	0.381	0.044	0.453	-0.079
3 - Irregularities in height				0.218	-0.215	0.213	-0.152
4 - Plan geometry					0.020	0.735	0.139
5 - Location and soil quality						0.144	0.037
$I_{VA,5}$ - Index of vulnerability							0.375
D_k - Real damage							

MATRIX OF CORRELATION	1	2	3	4	5	$I_{VA,5}$	D_k
1 - Quality of the masonry		0.089	-0.107	0.162	-0.057	0.711	0.508
2 - Misalignment of openings			0.283	0.560	0.072	0.553	-0.051
3 - Irregularities in height				0.267	-0.128	0.239	-0.181
4 - Plan geometry					0.050	0.714	0.172
5 - Location and soil quality						0.144	0.037
$I_{VA,5}$ - Index of vulnerability							0.375
D_k - Real damage							

Figure 85: a) (top). Matrix of correlation: indexes of correlation for each couple of parameters, I_{VA} and D_k , with the real scores of judgment. b) (bottom) matrix of correlation with equidistant scores among judgments.

As already expressed, the goal of a Vulnerability Index Method is that to assess an estimation of vulnerability on buildings which allows the determination of a forecasted damage scenario for different earthquake intensities. When a Vulnerability Index Method is applied on constructions hit by seismic events, it is possible to evaluate the goodness of the applied method evaluating the matching among the damage scenario results of the application of the method and the real one presented in the buildings after the mainshock. In particular, the good results for the method is confirmed if the vulnerability index of aggregate is higher for aggregates severely damaged. In other words, plotting vulnerability and damage results, the trend of aggregates' real damage vs vulnerability ranking decreasing, should decrease too, with negative slope.

In Figure 86a, it is possible to observe the trend of the real average damage grade (D_k) for aggregates for different values of vulnerability index defined by the application of the Aggregate Form (5P). In the x-axis there is the position of the aggregate in the vulnerability rank, from the most vulnerable up to the less vulnerable. No great correspondence is present. The linear regression used to approximate the cloud of points has a low index of determination (R^2), equal to 0.06, which proves a great dispersion of the data collected. Since some aggregates have the same vulnerability index, an average value (in volume) of the real level of damage has been calculated for the aggregates belonging to the same vulnerability class. Figure 86b shows the new graph, in which the points now refer to the 28 positions of the vulnerability index. The linear regression used to approximate the cloud of point has an index of determination equal now to 0.26 which still means a great dispersion of the data.

The last representations (Figure 87) include the plot of I_v vs D_k , in which in the x-axis there is the numerical value of the vulnerability index (instead of the position in the vulnerability ranking). The linear regression has an index of determination equal now to 0.14 for single aggregate and 0.35 for the average values of aggregates (with the same vulnerability class).

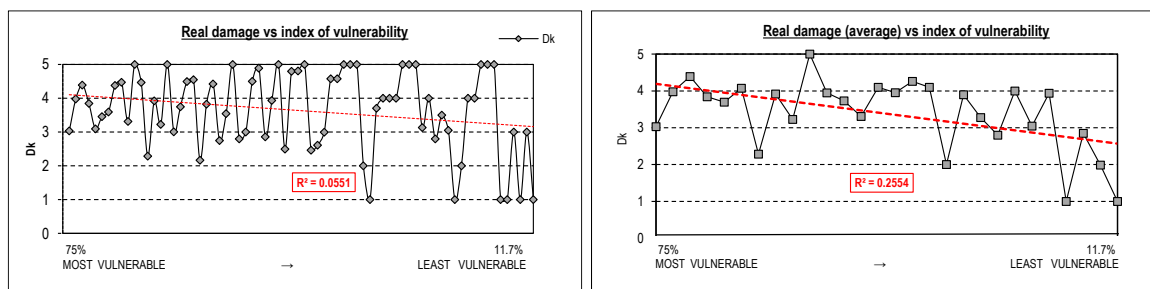


Figure 86: a) D_k vs vulnerability index ranking; b) average D_k for the 28 positions of the vulnerability ranking.

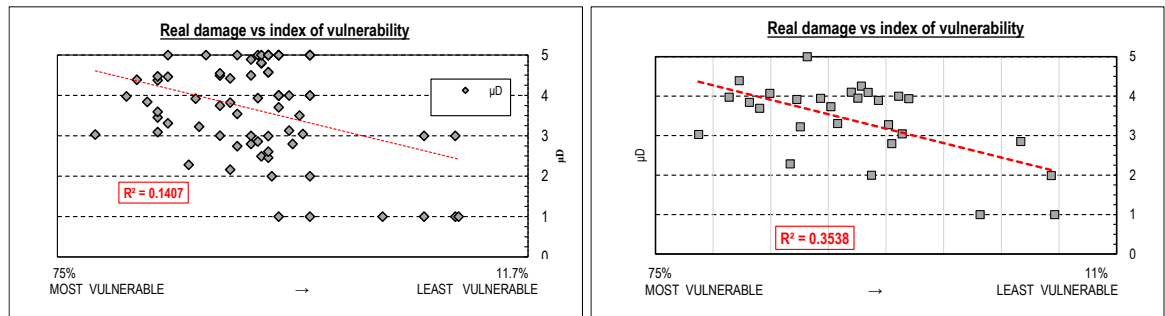


Figure 87: a) Real damage vs vulnerability index: b) average real damage for the 28 positions of the vulnerability index.

5.3 6 PARAMETERS FORM – AGGREGATE FORM

The Aggregate Form, taking into account geometric issues and qualitative information about aggregates, necessary for a territorial approach of the vulnerability study, is a tool able to individuate a preliminary screening of the buildings. From the results analysed for Castelnuovo buildings, it is noticed that the Aggregate Form is able to highlight most of the zone in which the highest damage was concentrated, even if in certain cases, some zones were missing.

In trying to upgrade that original Form, it was noticed that, for this type of qualitative analysis, the buildings' *conservation and occupation states* assume great importance. It is common that for an historical city centre, especially of limited dimensions, most of the aggregates have the same masonry type and they refers to local typology of constructions. Recent-time buildings were made in different masonry types but the original cores of the buildings, even if strengthened in time, have almost the same original characteristics. In the Form, this issue is included in the P1 ("quality of the masonry fabric"), characterised of major weight (1.5) that assumes a common class for more than 90% of aggregates, for the inferior quality of the masonries. In the Form, is missing the possibility to differentiate the aggregates' response to the seismic actions, when they belong to the same masonry type, by the criterion of good current state, that is the "results" of the occupational state, the age construction and the destination use of aggregate. For Castelnuovo an accurate study of the current state of the buildings was made: people in Castelnuovo made their houses' original documents (plans, fronts and structural sections) completely available to DICEA's team, together with the ante earthquake photos of their property.

In general, for study of vulnerability as a prevention method (in ante-earthquake conditions), it is difficult to have information on the occupancy and conservation states of the structures without having detailed surveys and wide knowledge of the history of the place. In these cases, the current state and other qualitative information of the buildings can be obtained by doing research also from public information, i.e. data collected from ISTAT census, or by analysis of aerial-historical photos and preliminary external surveys.

For Castelnuovo case study, the features linked to the "current state" are plotted in maps in Figure 89, referring at each structural units. The value used for the aggregate is the average value in volume of the structural units. For each of them, the pre-seismic occupation state was evaluated, assigning one among these enters: (1) civil homes (79.3% in terms of volume), (2) public buildings, (3) outbuildings or depots and (4) and garages (the latter 1.1% in terms of volume).

The ante-earthquake conservation status of the buildings was on average bad, inevitably tied to the occupational evaluation. Indeed, the property of the buildings was evaluated also assigning one of five levels: (1) primary home, (2) second home (55.2% in terms of volume), (3) public building, (4) habitual residence and (5) habitual rent (4.2% in volume). A considerable percentage of the buildings proved unoccupied before the earthquake, mainly due to the large migratory phenomena that make the building stock of Castelnuovo as mainly composed of second homes (most of the 60% in term of number of buildings).

In Figure 39b there is a qualitative maps of the historic evolution of the building stock; about the 70% of the whole stock existed in 1945, and all the aggregate of "Castello" are include in the first class.

Considering the features above expressed, a new parameter is implemented in the “Aggregate Form”, “P6 – Current state of the aggregate”. The judgments’ classes for the new parameter follow those already defined for the P11 of the GNDT II Level Form (11P), expressed in §2.2.2.1.

The identification of the P6’s judgments in Castelnuovo aggregates is reported in Figure 89a in terms of each ss.uu and in Figure 89b in terms of aggregates: referring both at the distribution of number of structural units and volume.

To each structural unit was assigned one of the following entries:

CURRENT STATE OF SS.UU. and AGGREGATE (% in volume)	SS.UU	AGGREGATE
A - Buildings in good condition, with no visible lesions (good conservation state).	14.8	1.6
B - Buildings with few hairline lesions, not produced by past earthquakes, or middle-high conservation state.	47.8	47.4
C - Buildings with medium-sized lesions (lesion size: 2-3 mm) or with capillary lesions of seismic origin. Building with a masonry bad state of conservation that makes mechanical characteristics mediocre	29.7	37.8
D - Building with serious crack patterns or collapse. Buildings that have a severe conservation state that determines a serious decrease of masonry resistance.	9.5	13.2

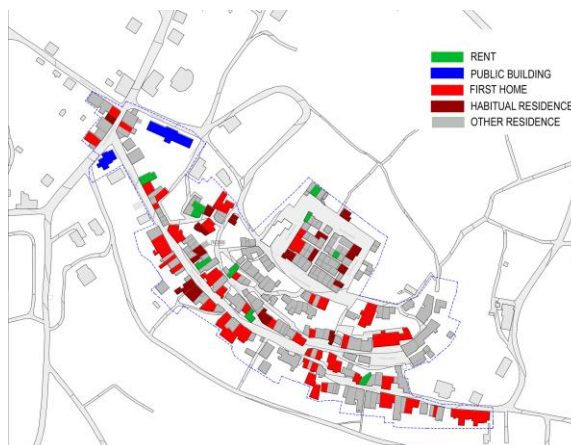
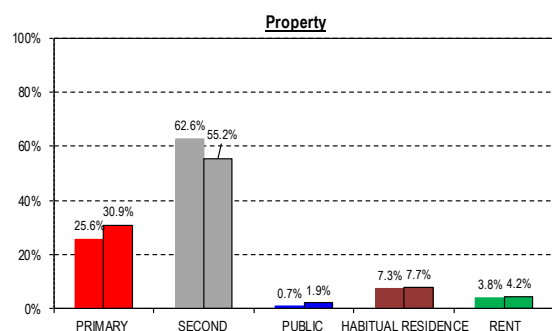
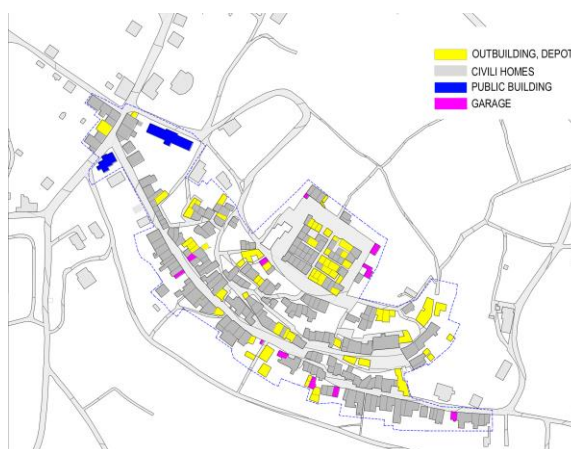
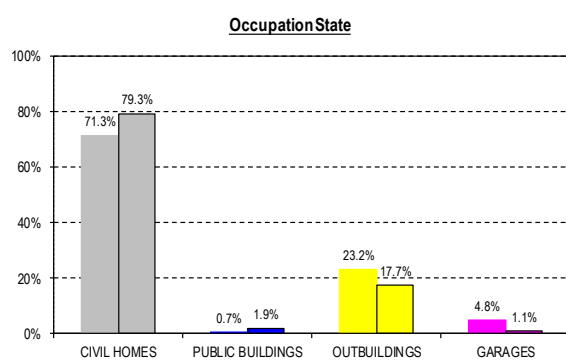


Figure 88: (a) occupation status; (b) property.

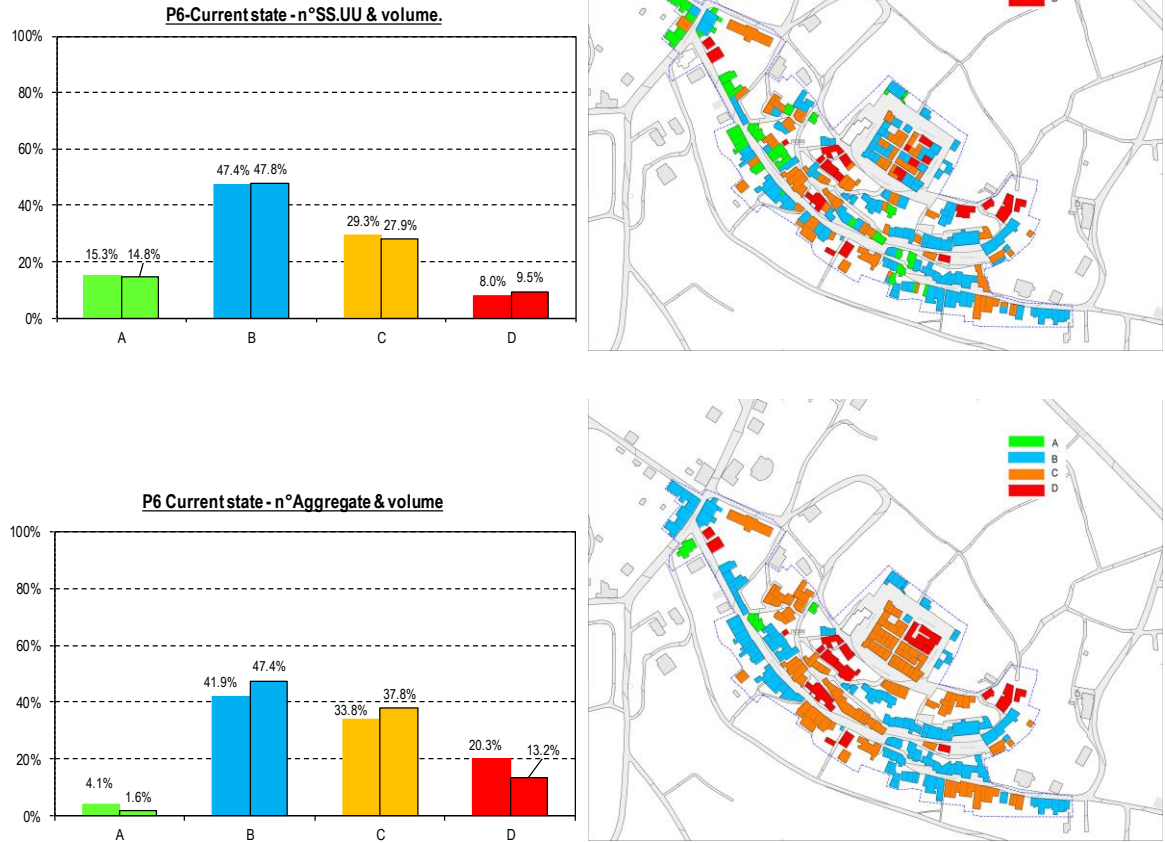


Figure 89: (a) Parameters 6 – current state for ss.uu.; (b) aggregates.

The proposed VF is composed 6 parameters: the original P1÷P5 and the “P6: current state”. The state of conservation of buildings is a predisposing factor for the identification of most vulnerable zones into historical city centres, which supposedly would suffer high damages on structural elements. Indeed, the distribution of the “D” judgments of the P6 is concentrated on aggregates that experienced high damage level.

The problem now is: how would be the best weight for the P6? And, the scores and the weights of the other parameters are well distributed in the Form, with the addition of a new parameter?

To identify the P6 weight different types of parametrical analyses have been done, with the fixed following assumptions:

- the distribution of the real damage is that one reported in §4.2 (weighted on volume of each ss.uu.);
- the relationship among Vulnerability-Damage (vulnerability curves) is expressed in paragraph 2.2.3;
- the P6’s weight and the scores related to the classes’ judgments have been individuated in order to minimize the difference between the calculated $I_{VA,6}$ and the I_{VA} that the structures should have, having showed certain level of real damage after the earthquake of 2009.

The *path* to individuate the weights and scores of the “Aggregate new Form” is described in the following.

At first the calculation of the Aggregate Form (6P) for all the aggregates considering an attempt starting weight for P6 equal to 1.5 and maintaining stable the other parameters’ scores. 1.5 is indeed the greater value of a parameter’s weight in the original definition of the Form. It has been chosen since the $r_{6,Dk}$ is the major correlation coefficient as exposed in Figure 90, that shows the correlation matrix for the parameters of the Aggregate Form with 6P. P6 is not correlate to the other P1÷P5 (correlation indexes are lower than 0.5), with a direct correlation only with the P1 (“quality of the masonry fabric”), since $r_{6,1}$ is positive.

The sample correlation coefficient between the P6 and D_k is the highest of the correlation matrix $r_{I_{VA,6},D_k}$ equal to is 0.784, that is two time higher than that $r_{I_{VA,5},D_k}$ showed in Figure 85.

MATRIX OF CORRELATION	1	2	3	4	5	6	$I_{VA,6}$	$D_{k,real}$
1 - Quality of the masonry fabric		0.047	-0.130	0.157	-0.056	0.235	0.678	0.514
2 - Misalignment of openings			0.233	0.381	0.044	-0.180	0.127	-0.082
3 - Irregularities in height				0.218	-0.215	-0.258	-0.094	-0.156
4 - Plan geometry					0.020	-0.145	0.304	0.136
5 - Location and soil quality						-0.041	0.040	0.029
6 - Conservation status							0.775	0.689
$I_{VA,6}$ - Index of vulnerability								0.784
$D_{k,real}$ - Level of damage								

Figure 90: Matrix of correlation for 6P-Form (real score for judgments).

In a second time, with the results of the 6P Form, the ideal weights of the parameters have been individuated, following the step here resumed:

1. For each aggregate a $I_{VA,6i}$ is calculated ($i=1,2,...72$). It is a function of the P6's weight, that is unknown variable, which has the attempt initial value of 1.5;
2. To each aggregate a REAL level of damage is associated (D_{ki});
3. From the level of damage, and considering the macroseismic intensity reached in Castelnuovo 8.5 EMS-98 Scale, the "real" vulnerability index has been calculated, reversing in the domain (-1;1) the formula with the hyperbolic tangent (Eq.(16)), obtaining the value V_i .
4. With the Eq.(18), it is determined the $I_{VA,Ri}$ (starting from the obtained value of V_i). The value of $I_{VA,Ri}$ is a normalised value in the range [0%,100%]. The subscript R means "real" and it refers to the vulnerability index calculated reversing the relationship enter vulnerability and *real*/ damage. In the cases in which the damage grade D5, the $I_{VA,R}$ is 100%.
5. Calculation of an absolute value of the error between the $I_{VA,Ri}$ and $I_{VA,6i}$. The error is a function of the damage grade D_{ki} of aggregates (which are known values), the scores of the classes of judgments, S_h ($h="A", "B", "C"$ and "D"), and the parameters' weights associated to each judgment, W_k (with $k=1, 2,..., 6$).

$$E_i = |I_{VA,Ri} - I_{VA,6i}| = f(D_k, S_h, W_k)$$

6. Function Z is defined as the sum of all the error E_i for the 72 aggregate analysed. It rests a function of the variables $f(D_k, S_h, W_k)$. Z is the function that should be minimize, changing the variables, in order to obtain the fitting values of vulnerability indexes estimated by the 6P Form ($I_{VA,6i}$) and those determined starting by the level of damage ($I_{VA,Ri}$).

$$Z = \sum_{i=1}^{72} |I_{VA,Ri} - I_{VA,6i}| = f(\mu_{D,R}, S_h, W_k)$$

7. The expression of Z could be better understood looking at following equation, which resume in a matrix form the expression of the vulnerability index, determined with the 6P Form.

The [S] matrix is the matrix of the parameters' coefficients (72 rows and 6 columns) and consists in the judgments (or classes) assumed by the P1÷P6 in the Form. s_{ij} can be one of the following entries: "0", "5", "20" or "50".

(W) vector (6x1 dimension) is the vector of the parameters' weights.

$$[S] \cdot (W) = (I_{VA,6}) \rightarrow (I_{VA,R})$$

$$\begin{pmatrix} s_{1-1} & \cdots & s_{1-6} \\ \vdots & \ddots & \vdots \\ s_{72-1} & \cdots & s_{72-6} \end{pmatrix} \cdot \begin{pmatrix} w_1 \\ \vdots \\ w_6 \end{pmatrix} = \begin{pmatrix} I_{VA,6-1} \\ \vdots \\ I_{VA,6-72} \end{pmatrix} \rightarrow \begin{pmatrix} I_{VA,R-1} \\ \vdots \\ I_{VA,R-72} \end{pmatrix}$$

($I_{VA,6}$) is the vector of the vulnerability index defined by the Form as the multiplication rows per columns ($[S] \cdot (W)$) and ($I_{VA,R}$) (72x1 dimension) is the vector of known terms deriving from the D_{ki} , as previous described. Both the I_{VA} vectors are normalized in a range [0, 100].

8. The generic i-equation of the system refers to one aggregate. For example, the first equation is referred to the 01-222 aggregate. It could be explicit considering the judgment really assigned to each parameter.

For the first step of evaluation, the classes' scores are stable ("0", "5", "20", "50") as well as the weight of the P1÷P5. The only unknown value is the P6's weight (w_6). Effectively, since the $I_{VA,6,1}$ is normalized, the P6's weight appears also in the calculation of $I_{VA,6}$ in the denominator, making the system composed of non-linear equations. For aggregate 01-222 $I_{VA,R}$ is equal to 13%. The 01-222 equation is:

$$s_{11}w_1 + s_{12}w_2 + s_{13}w_3 + s_{14}w_4 + s_{15}w_5 + s_{16}w_6 = I_{VA,6,1} \rightarrow I_{VA,R1} = 13\%$$

The vector (S1) (which is the first row of the matrix [S]) and the vector (W) are defined on the follow:

$$(S_1) = (s_{11}, s_{12}, s_{13}, s_{14}, s_{15}, s_{16}) = (D, B, B, D, B, B) = (50, 5, 5, 50, 5, 5)$$

$$(W) = \begin{pmatrix} w_1 \\ w_2 \\ w_3 \\ w_4 \\ w_5 \\ w_6 \end{pmatrix} = \begin{pmatrix} 1.5 \\ 0.50 \\ 0.75 \\ 0.75 \\ 0.75 \\ X \end{pmatrix}$$

The equation for 01-222 becomes:

$$50 \cdot 1.5 + 5 \cdot 0.50 + 5 \cdot 0.75 + 50 \cdot 0.75 + 5 \cdot 0.75 + 5 \cdot X = \frac{I_{VA,6,1}}{50 \cdot (1.5 + 0.50 + 0.75 + 0.75 + 0.75 + X)} \rightarrow 13\%$$

9. The equation is a non-linear function in the variable X ($=w_6$). The process of minimization of function Z have been developed with the gradient algorithm method, (available in Excel sheet) that requires a starting point of the variable to develop the process. In this case, the starting point for the unique variable is the hypothesized value of 1.5.

The process of minimization have been done considering variable gradually:

- (a) the only weight of the parameter 6 ($=w_6$);
- (b) the weight of all the parameters (vector (W)) for a total of sixth variables;
- (c) the vector (W) (six variables) and the scores judgments classes (4 variables), for a total of 10 variables.

The variables domains were fixed in certain cases, on the basis of the analysis of the state of the art of Vulnerability Forms (§2.2.2) and to better interpret the results of the Form. The parameters' weights (vector (W)) are defined positive with upper limit of 1.5. As well for the weights, the scores cannot take negative values, and constraints are set to the score to make them under 50 points, in analogy with the original Aggregate Form (5P).

The results obtained for the minimization of the function Z, for the three cases (a), (b) and (c) exposed are summarized in Figure 91. They are in line with the results, already showed, of the correlation matrix between the distribution of the classes of parameters and that one of the real damage (D_K).

AGGREGATE FORM - 6 parameters					sol. (a)		sol. (b)		sol. (c)					
Parameters	scores				weight	% of influence	weight	% of influence	scores				weight	% of influence
	A	B	C	D					A	B	C	D		
1 - Quality of the masonry	0	5	20	50	1.50	26%	0.47	32%	0	3	0	33	0.70	28%
2 - Misalignment of openings	0	5	20	50	0.50	9%	0.00	0%	0	4	19	50	0.00	0%
3 - Irregularities in height	0	5	20	50	0.75	13%	0.00	0%	0	4	19	50	0.00	0%
4 - Plan geometry	0	5	20	50	0.75	13%	0.00	0%	0	4	15	16	0.00	0%
5 - Location and soil quality	0	5	20	50	0.75	13%	0.00	0%	0	4	18	50	0.00	0%
6 - Current state	0	5	20	50	1.50	26%	1.00	68%	0	2	16	39	1.50	72%

Figure 91: Aggregate Form (6P) with different proposed solutions.

In particular, the case (a) the only one variable is the weight of the parameter 6 (w_6). The weight is estimated in 1.5 by the process algorithm, the maximum value possible.

In the solution (b), however, all the parameter's weights are variable and it is noted that the values obtained for "geometric-quantitative" parameters (P2, P3 and P4) are null. This means that, for their distribution in the Castelnuovo aggregates, they are not correlate with the distribution of damage level. The P1 ("quality of the masonry") and P6 are significative in a ratio 1:2, since the estimate P1's weight is 0.47, while P6 is about 1.

In the last analysis, (c), the variables are represented by the classes' scores and by the weights of the parameters, for a total of 10 variables. For the minimization of the function Z, the scores have a similar trend to those already present in the

Form (with increasing values from class "A" to class "D"), although less markedly. The weights of the parameters "geometric-quantitative" (P2, P3 and P4) are null and the P1-P6 weights maintain at least the same relationship of the solution expressed in the case (b).

From an analytical point of view, the function Z is minimized through the solution (c) with a decrease of 40% in respect to the (a) solution. The solution (b) is intermediate, but very similar to the (c) one. They differ only for class, maintaining the same percentage of influence on the determination of the $I_{VA,6}$ (see columns 10 and 15 in Figure 91).

From an engineering point of view, the solution that minimizes the function Z can not be provide as a result, because it deletes the influence of the three parameters "geometric-quantitative" (P2, P3 and P4) on the original Form and that of parameter P5, which assesses qualitatively the ground type. With this solution proposed, the Form would simply be composed of qualitative parameters P1 and P6 that, although they have a greater influence on a qualitative analysis of vulnerability, they cannot be considered sufficient to define vulnerability of aggregates, since they do not take into account buildings' structural and geometrical features.

The proposed solutions for the integration of the Aggregate Form, are shown in Figure 92 and are defined in order to obtain the optimal synergy between the minimization of the function Z and the definition of an Aggregate Form (6P) in which the parameters have "acceptable" weights, in line with the VIM existing in literature. Two formulations have been proposed, in which in both:

- the scores of the judgments' classes are fixed and equal to those of the Form in its original shape (0, 5, 20 and 50);
- the P1 and P6 weights are fixed to 1.5.

In the proposal 1 coherently with the minimization of the function Z, the values of the weights of the intermediate parameters (2, 3, 4 and 5) are fixed to 0.5, the minimum value assumed for hypothesis. They equally influence the definition of the vulnerability index (10%).

In the proposal 2, instead, the P4's weight is differentiated respect to the "geometric-quantitative" parameters. The correlation of the distribution of P4 and the distribution of D_K , although low, is directed, with a positive index of correlation (as showed in Figure 90).

AGGREGATE FORM - 6 parameters					PROPOSAL 1			PROPOSAL 2		
Parameters	scores				weight	Weighted scores	% of influence	weight	Weighted scores	% of influence
	A	B	C	D						
1 - Quality of the masonry	0	5	20	50	1.50	75.00	30.0%	1.50	75.00	28.6%
2 - Misalignment of open.	0	5	20	50	0.50	25.00	10.0%	0.50	25.00	9.5%
3 - Irregularities in height	0	5	20	50	0.50	25.00	10.0%	0.50	25.00	9.5%
4 - Plan geometry	0	5	20	50	0.50	25.00	10.0%	0.75	37.50	14.3%
5 - Location and soil quality	0	5	20	50	0.50	25.00	10.0%	0.50	25.00	9.5%
6 - Current state	0	5	20	50	1.50	75.00	30.0%	1.50	75.00	28.6%

Figure 92: 6 parameters Form: two proposals.

The results in the following are reported for both the proposed solutions.

The new vulnerability rankings and the distribution of the $I_{VA,6}$ are reported in Figure 93, for the 72 aggregates. The range and the distribution of are very similar in both proposals. The vulnerability index range is:

- Proposal 1: $I_{VA,6-1}$ range = [8; 75%] with 33 positions in the ranking;
- Proposal 2: $I_{VA,6-2}$ range = [7.6; 76.2%] with 39 positions in the ranking.

In analogy with the representation used for the results of Aggregate Form (5P), in Figure 94 there is the trend of the average damage real grade for aggregates for different positions of the vulnerability ranking and different values vulnerability index defined by the application of the new proposed Vulnerability Forms (6P, proposal 1 and 2).

A linear regression is used to approximate graphs containing the cloud of points of the results. For the proposal 1 the R^2

is equal to 0.67 and 0.61 for the proposal 2.

An average value (in volume) of the real damage level has been calculated for the aggregates belonging to the same vulnerability class. Indeed, since that the vulnerability index has respectively 33 (proposal 1) and 39 (proposal 2) positions for the rankings, some aggregates have the same vulnerability index value. For each proposal, the cloud of points now refers to the mentioned positions and it is shown in Figure 96. For the proposal 1, R^2 is equal to 0.79 and 0.70 for while for proposal 2. In both cases, these R^2 are three times higher then those expressed in Figure 86, which refers to the results of the Aggregate Form (5P).

From the evaluation of the obtained results:

- there are a more direct and reliable relationship between the vulnerability index of the structures and the damage real distribution;
- with both the proposal Forms, it is possible to differentiate the vulnerability of isolated buildings. Despite they usually have best condition for geometrical parameters P2, P3 and P4, they can have wide variability of judgments for the "P6-current state" because it is independent from the number of ss.uu. and for the type of aggregation.

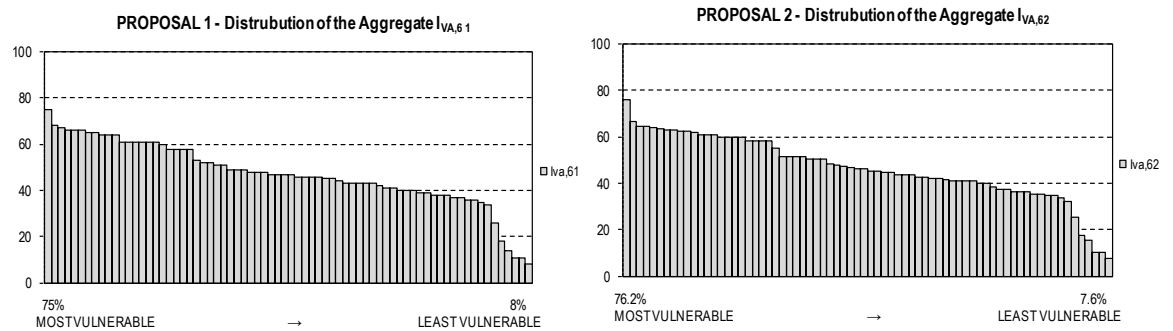


Figure 93: Distribution of the Vulnerability Index (6P Form) for aggregates. Left: proposal 1. Right: proposal 2.

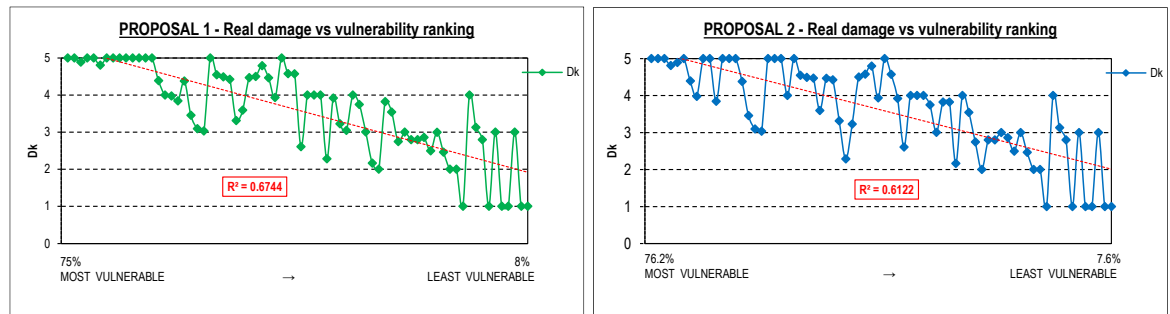


Figure 94: Real damage vs vulnerability index ranking. Left: proposal 1. Right: proposal 2.

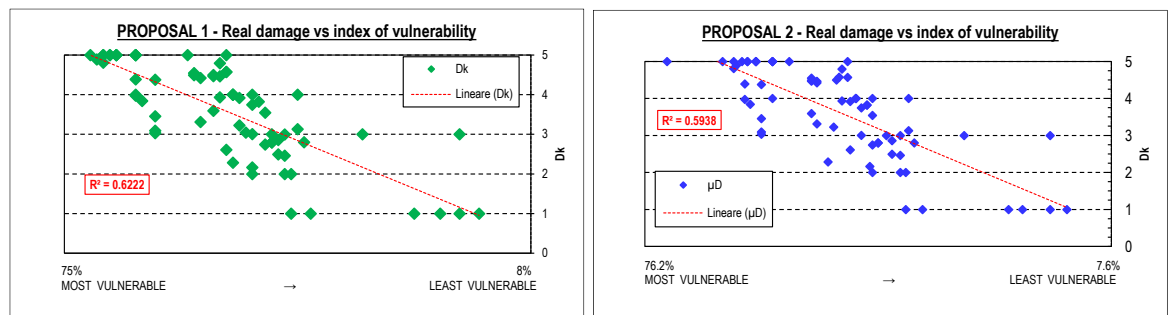


Figure 95: a) Real damage vs vulnerability index. Left: proposal 1. Right: proposal 2.

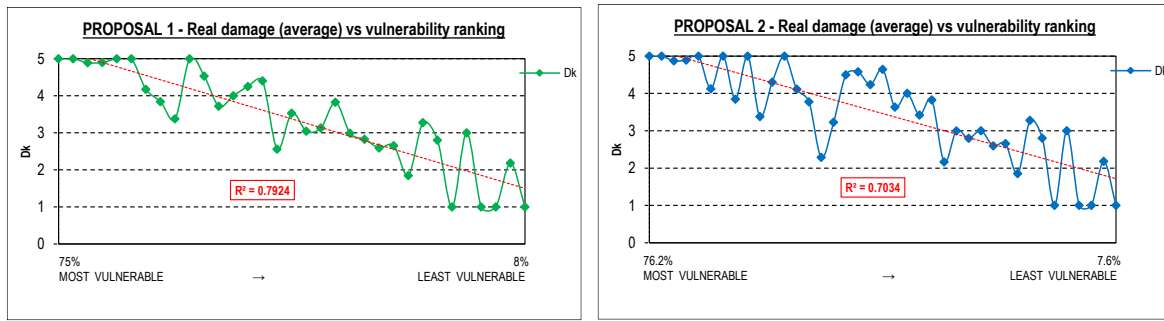


Figure 96: Average real damage for the positions of the vulnerability ranking. Left: proposal 1. Right: proposal 2.

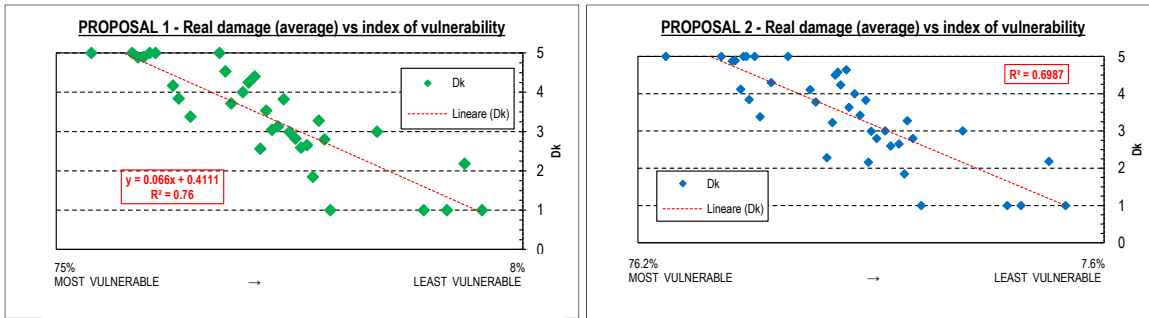


Figure 97: Average real damage for the positions of the vulnerability index. Left: proposal 1. Right: proposal 2.

Following the results of Castelnovo database aggregates, the Proposal 1 results to be the most suitable Form to evaluate the structural vulnerability. The results of the following parts refer only to that proposal.

For the solution 1, the graph of the trend of real damage vs vulnerability index in the conventional way (starting from the less value of vulnerability up to the big) is plotted in Figure 98. In the graph is individuated a range of reliability, varying the damage of 1 degree in the scale of EMS-98. The plot is working for the case of macroseismic intensity of 8.5 EMS-98, reached at Castelnovo. With a linear regression of the data, in an interval of confidence of 1 degree, the percentage of damage really capture is 65%, for which in the 33% of the cases under-estimate the damages.

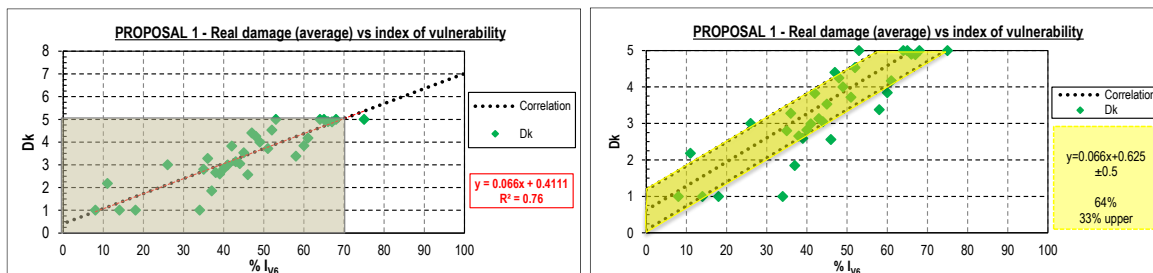


Figure 98: Vulnerability index vs real damage. Range of confidence.

The distribution of the $I_{VA,6}$ is reported in Figure 99, with the histogram representation of the $I_{VA,6}$ both in terms of % of number of aggregate (72) and in volume (163 782 m³). $I_{VA,6}$ distribution has an average value of 47.2% and a deviation of 14.1% (Cov. equal about to 30%). Considering five classes, in the distribution of the $I_{VA,6}$ is reported in the histogram of Figure 101b, from the 0-15% until the 60-75%. The high percentage (47.6%) in terms of volume lies in classes 45-60 $I_{VA,6}$. The minimum value is 8% and refers to the 54-246 aggregate, while the "old" least vulnerable aggregate (with the "Aggregate Form" 5P Form), the n. 66-583, has the new vulnerability index equal to 11%, and from the increasing vulnerability ranking, it lies in the second position. The aggregate n.54-246 (Figure 100a) is composed by two ss.uu., but it is made of unreinforced concrete with a conservation state of the ss.uu. pretty good, being habitual residence for citizens. The maximum value obtained for the building stocks is 75%, which refers to 47-051 aggregate, located in the central zone of the Village. The 11-125, the most vulnerable aggregate following the vulnerability ranking of 5P Form, comes down at the 11° position in new classification. Aggregate 47-051 (Figure 100b in red) has an irregular shape, adjacent ss.uu. with

staggered floors and, the poor state of conservation. It deserves to stay in the first position in a vulnerability ranking: after the earthquake, it collapsed almost completely in its structural parts.

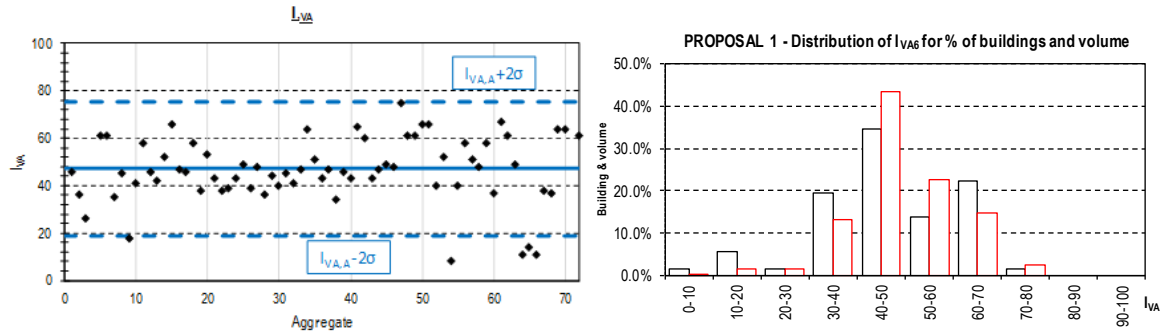


Figure 99: Proposal 1. (a) % of buildings and volume; (d) normal distribution.



Figure 100: (a) aggregate 54-246, post earthquake. (b) aggregate 47-051 photo ante earthquake.

The estimated damage grade with the 6P Form has been reported in Figure 101b. As already explained in §5.1.2, it has been determined for EMS-98 8.5 degree and for the $I_{VA,6}$ calculated. It is confirmed that for the high intensity degree, even the aggregates with a low value $I_{VA,6}$ show a medium-high level damage (D2-D3). The average damage level is 3.6 (similar to 3.5, result of the “Aggregate Form”, 5P) that, for the chosen scale, belongs to D3-D4 damage level (in orange in the map). According with the distribution of the I_{VA} , the minimum μ_D value is 2.09 (D2-D3) and refers to the 54-246, while the maximum damage level is related to the 47-051 aggregate and values 4.42 (D4-D5).

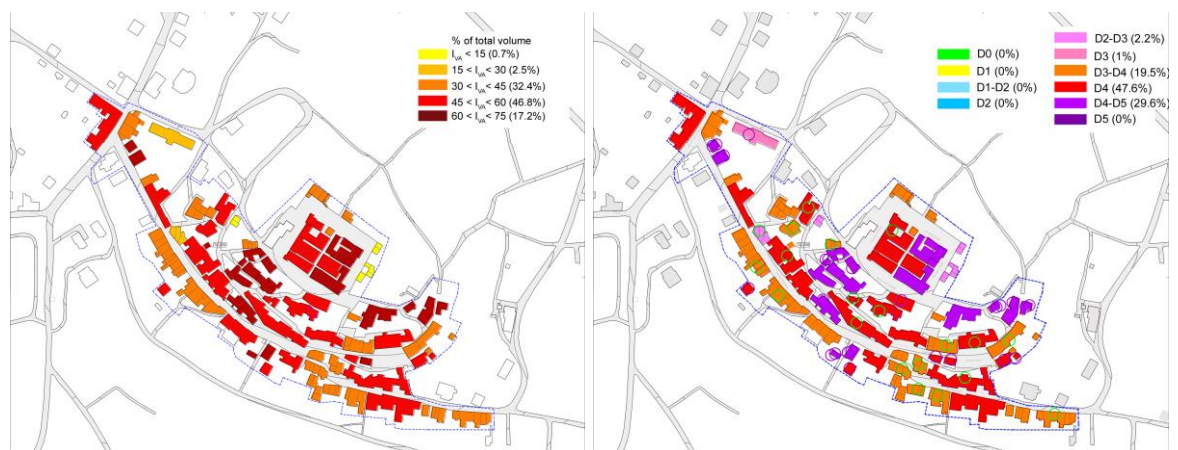


Figure 101: Distribution of $I_{VA,6}$ and $\mu_{D,E6}$.

5.4 CONCLUSION

In this chapter, the results of the application of the Aggregate Forms have been reported for the case study of Castelnuovo,

an historical city centre composed by 74 aggregates and hit by the earthquake of 2009. Starting from the vulnerability analysis performed, and exploiting the scientific literature results, an estimated average damage grade for aggregates, due the macroseismic intensity reached after the L'Aquila earthquake, was determined.

Based on the results obtained in terms of estimated damage, a comparison with the real damage showed by aggregates after the earthquake, was done.

In the presence of a large sample of buildings as to those of the historic centres, the "Aggregate Form" (5P) effectively captures the aggregates that have greater vulnerability due to their plano-altimetric conformation and their not good mechanical characteristics. However, the "Aggregate Form", not considering any parameter related to the conservation status of aggregates, has not allowed the full definition of vulnerability towards seismic actions, especially for those buildings characterized by bad conditions even before the earthquake.

The additional parameter inserted in the original "Aggregate Form" is the "P6-current state" of the building, defining its vulnerability's classes in analogy of those of GNDT II Level Form (GNDT, 1993). Furthermore, the weights of the parameters in the new Form were defined in order to ensure correspondence between the damage experienced by the aggregates and the estimated damage scenario provided by the vulnerability analysis.

The proposed Aggregate Form assume the following shape:

AGGREGATE FORM - 6 parameters					
Parameters	scores				weight
	A	B	C	D	
1 - Quality of the masonry fabric	0	5	20	50	1.50
2 - Misalignment of openings	0	5	20	50	0.50
3 - Irregularities in height	0	5	20	50	0.50
4 - Plan geometry	0	5	20	50	0.50
5 - Location and soil quality	0	5	20	50	0.50
6 - Current state of the aggregate	0	5	20	50	1.50

Figure 102: Aggregate Form proposed.

The Form is working for the historical centres characterised by buildings with load-bearing structures in stonemasonries; is then directed to aggregates of historical centres typical of central and south zones of Italy and characterized by 'poor' masonry. Examples of these city centres in central zone of Italy are those in the Arno zones (Tuscany), in the Umbrian-Marchigiano portion of the Apennines and in Abruzzo Region (see also Annex 2). These constructions are widely composed by roughly cut stones and lime-based mortars. All these materials were obtained from quarries located near the urban centres, with cross section dimension within the range of 45–60 cm (Corradi et al, 2003). The stone and brickwork are essentially effective with respect to vertical static loads but they have evidenced inadequacies against seismic loads.

CHAPTER 6. STRUCTURAL UNITS FORMS: APPLICATION AND MAIN RESULTS

For a reduced sample of Castelnuovo aggregates, the Vulnerability Forms GNDT II level (11P), “Formisano” (15P) and “Aveiro” (14P) Forms have been filled out for each structural units. The major differences for the results they provide have been individuated. Therefore, the features of the aggregates they take into account have been crossed with the results in terms of damage on structural units experienced.

The scientific literature about Vulnerability Form for structural units (ss.uu.) have been introduced in 2.2.2.1-2-3. In this chapter, the results of the filling out of the different VFs are illustrated for a reduced sample of data. As already described in CHAPTER 3, Castelnuovo consists of 74 aggregates, for a total of 289 structural units. The reduced sample of data is represented by 26 aggregates (124 ss.uu.), for which it has been possible complete the ss.uu. Forms. In the remaining cases, due to the wide high level of damage on buildings, no complete information about structural characteristics were known. The Forms were filled out only for the ss.uu. of the original system (Figure 103): in this context, outbuildings, extensions, and other elements built in more recent times, simply placed close to the original core buildings were overlooked. For example, the s.u. 6 of 55-157 aggregate: it is a reinforced frame concrete structure separated few centimetres from ss.uu. adjacent and the ss.uu.

For the structural units/aggregates analysed:

- the GNDT Form is evaluated for each structural units and for the aggregate (as it was a unique structure);
- the “Formisano Form” and “Aveiro Form” are filled out for each structural units inside the aggregate.

The Forms' frame are already explained and showed in CHAPTER 2, in Figure 67.



Figure 103: Example of ss.uu. not considered in the Forms.

6.1 GNDT II LEVEL FORM (11 PARAMETERS) FOR SS.UU. AND AGGREGATES

GNDT II Level Form is composed of 11 parameters, described in §2.2.2.1. The Form was born to study isolated buildings; in this work, it has been used at first for structural units inside the aggregates and afterward for the entire aggregates.

The results of the vulnerability assessment are plotted with histogram and charts in analogy with the representation of the results of the “Aggregate Form in CHAPTER 5. The histogram representation are plotted in terms both of relative frequency (expressed in %) of the number of structural units present in a class and in terms of % of volume.

The screening of the aggregate with the GNDT II Level Forms (11P) gave the results summarized in Figure 104, Figure 105 and Figure 106. The range of I_{v11} spaces from 19.6% (which refers to s.u 1, in aggregate 09-160) up to 70.6% (which refers to one of the bigger s.u. of the longest “in-line” aggregate 18-163), with an average value of 53.8% (Figure 104). S.u. 1 in 09-160 is represented in Figure 105 in the left: it is a three-storeys structure composed in unreinforced concrete walls, with horizontal stiff elements (r.c. type), with planimetric and in-height regularity and with holes aligned. It is an external (*header*) structural unit. In right of Figure 105, there are the aerial photos of ss.uu. 2 and 3 of aggregate 18-163, with the highest indexes of vulnerability. They have four floors, in plan and height irregularities, with the presence of terraces. They are characterised by with flexible and not-connected steel floors.

In Figure 106a there are the representation of the I_{V11} % of structural units and in term of % of the total volume for the reduced sample of data (84 117 m³). These two types of representation allow to understand that the ss.uu. with lower vulnerability indexes (less than 50%) are those with minor volume, while ss.uu. characterised by I_V within 50-60% belong to the big-volume buildings. In Figure 106b there is the map in which different colours represent the classes of I_{V11} .

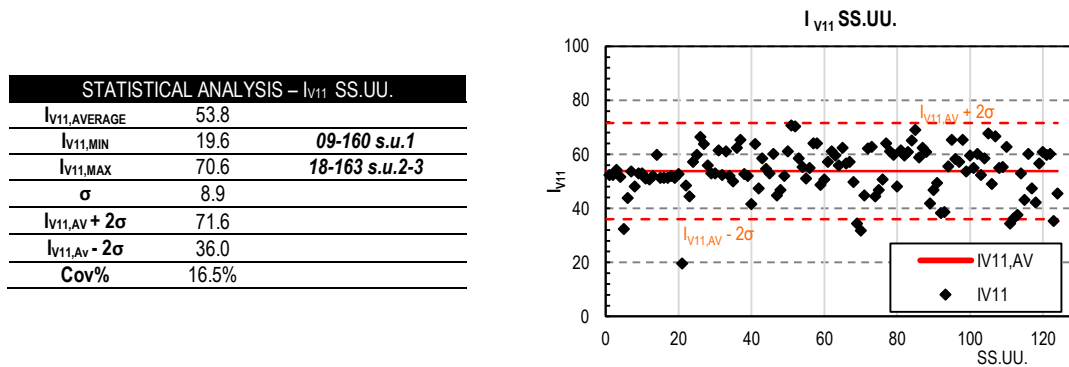


Figure 104: Statistical analysis and distribution of the I_{V11} for 124 ss.uu.

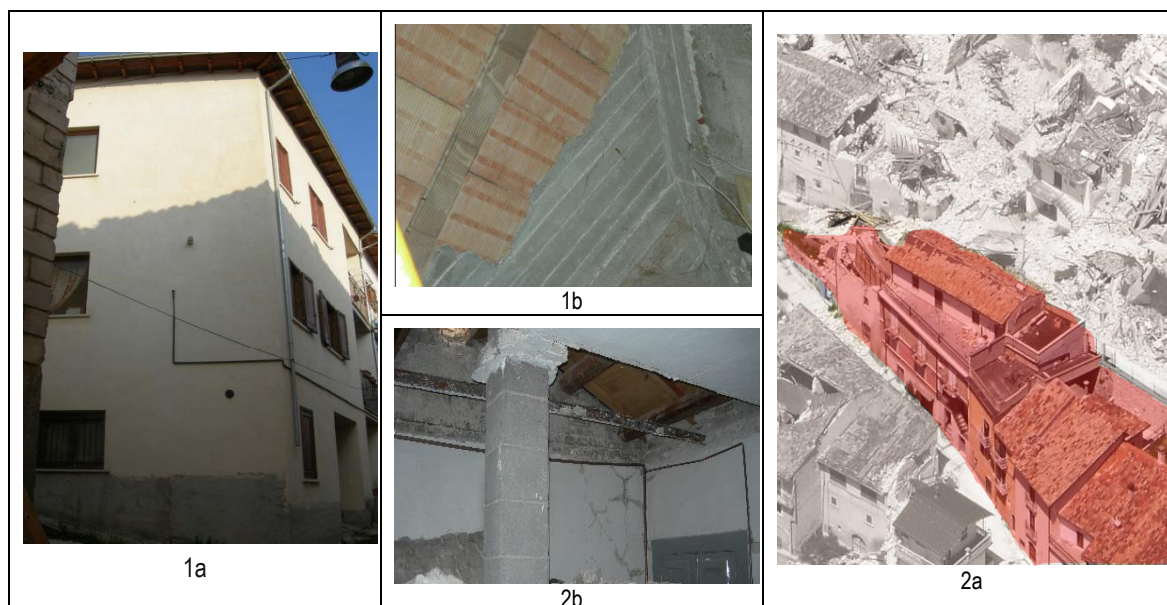


Figure 105: 09-160 s.u.1 (1a) and its reinforced concrete slab (1b). 18-163 ss.uu. 2-3 (2a) with collapsed flexible floor (2b).

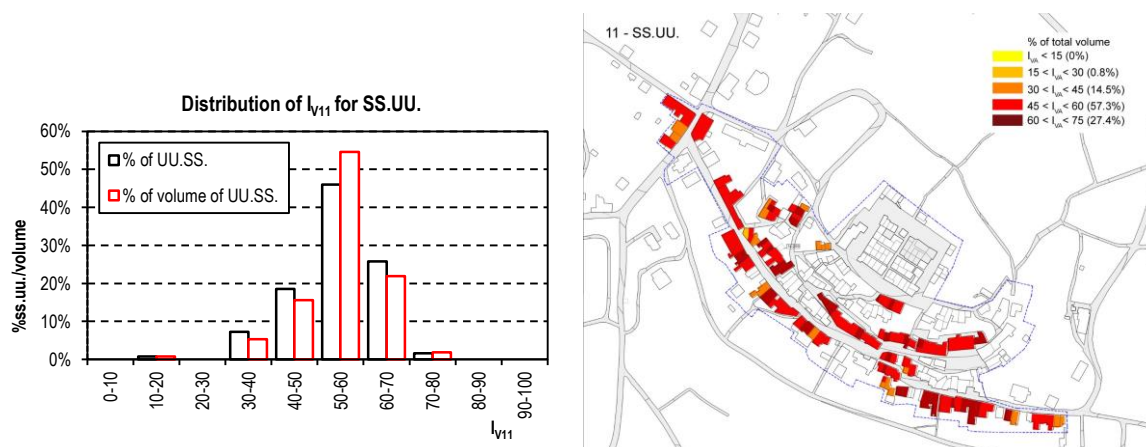


Figure 106: a) Distribution of I_{V11} in terms of % of buildings (ss.uu.) and % of volume; b) vulnerability indexes maps for ss.uu..

For what here expressed, the vulnerability index evaluated with GNDT II Level for ss.uu. is quite high, distributed close to the central value of 53%. This is due to the distribution of the judgments' classes for all the 11P, showed in Table 36 and Figure 107. High-weighted parameters lie in most of cases in "D" class.

Table 36: Distribution of the class for the 11P for 124 ss.uu..

DISTRIBUTION OF THE CLASS WITHIN THE P11 PARAMETERS											
	P1	P2	P3	P4	P5	P6	P7	P8	P9	P10	P11
A	0.0%	0.0%	3.2%	0.0%	0.0%	32.3%	70.2%	58.1%	1.6%	2.4%	20.2%
B	0.8%	7.3%	2.4%	52.4%	0.8%	30.6%	12.9%	18.5%	25.0%	12.1%	53.2%
C	9.7%	4.0%	16.9%	47.6%	12.1%	21.0%	16.9%	13.7%	67.7%	43.5%	26.6%
D	89.5%	88.7%	77.4%	0.0%	87.1%	16.1%	0.0%	9.7%	5.6%	41.9%	0.0%

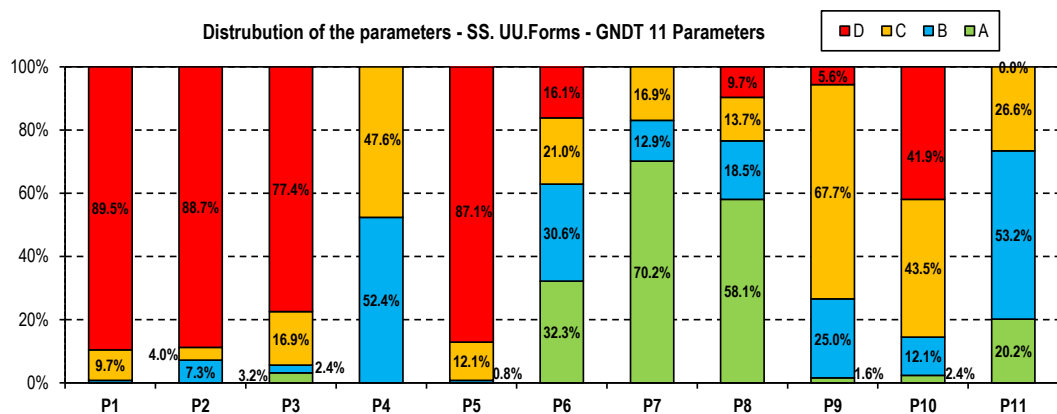


Figure 107: Distribution of the parameters' classes for 124 ss.uu..

The P3 "Conventional strength", that is the most influential parameter in the definition of the I_v ($w=1.5$, §2.2.2.2) assumes about in the 90% of ss.uu. class "D".

For the sample of data considered, the parameters P1, P2, P5, P9 and P11, with weights from 0.25 up to 1.00, have a significant influence for the I_{v11} , since they assume in most of the cases worst classes ("C" or "D"). In particular, P1 ("Type and organisation of resistant system"), P2 ("Quality of resistant system"), P3 ("Conventional strength") and P5 ("Horizontal elements – floors") fall in "D" as more frequent class (Figure 107). This is due to the age of construction of the buildings that show middling masonry characteristics, with poor quality of the mortar and chaotic irregular masonry weavings and bad restraints among main structural vertical and horizontal elements (see also §3.3).

For P4 ("Building position and type of foundation") the chosen classes are "B" (52.4%) and "C" (47.6%), referring to ss.uu. what already written in §5.1.1 for aggregates.

The roofing system (P9) is, in the most of cases, in wooden structure composed by one or two order of beams (§3.3.2.1), light and no thrusting, with a beam in reinforced concrete at the edges if it is renovated in recent time. Only in few cases, the roof is weighted and with rafters in reinforced concrete and lightening brick elements ("B" or "C" classes).

The P6 ("Plan configuration"), P7 ("Configuration in elevation"), P8 ("Maximum distance among the walls") and P11 ("Actual state") have low impact factor on the determination of the I_v and they fall in most of cases in "A" or "B" classes.

§

The GNDT Form were calculated also for 26 aggregates, even this procedure is not completely correct, since that the Form is implemented for isolated buildings. Nevertheless, it was interesting to fill out that Form, to have a numerical comparison with the "Aggregate Form" already calculated (CHAPTER 5) and to know how the results in term of I_{v11A} change, passing from ss.uu. to aggregates.

In the case of aggregates, the class assigned for each parameter is that assumed for more than the 25% (in volume) of the structural units belonging to the aggregate. Given that aggregates are generally constituted for the major part of ss.uu.

that fall in “C” or “D” vulnerability classes, this procedure is equivalent to delete the presence of more recent ss.uu. in the aggregates (characterised by a low level of vulnerability) and, precautionary, to assign the worst classes of vulnerability to the parameters (“C” or “D”).

In Figure 108a there are reported the average, the maximum and the variation of the I_{V11A} . The growth of the average I_V from 53.8% (for isolated ss.uu.) up to the about 60% is immediately evident, together with the growth of the maximum value and the extreme value.

STATISTICAL ANALYSIS – I_{V11} AGGREGATES		
$I_{V11A,AV}$	60.09	
$I_{V11A,MIN}$	34.31	22-231
$I_{V11A,MAX}$	75.82	55-157
σ	9.63	
$I_{V11A,AV} + 2\sigma$	79.35	
$I_{V11A,AV} - 2\sigma$	40.83	
Cov%	15.9%	

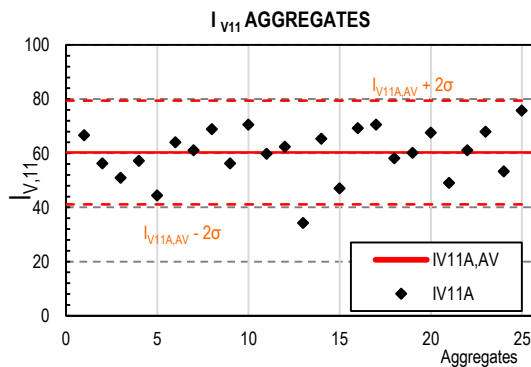


Figure 108: Statistical analysis and distribution of the $I_{V11,A}$ for 26 aggregates.

In Figure 109a there is the representation of the I_{V11A} % of aggregates and in term of % of total volume. Aggregates with lower indexes of vulnerability (less than 50-60%) are those with minor volume, while the major fraction of the volume is distributed among the higher vulnerability indexes (from 60-80% (arrows blue in the chart)).



For the reduced sample of aggregates, the one with the highest vulnerability index is 56-247 (picture in left). It is composed of 6 ss.uu. with a complex but compact shape, with articulated configuration in height, with ss.uu. built with different material and presence of non structural elements (as stairs, chimney caps and ceilings at the upper floors).

In Figure 109b there is the maps in which with different colours are represented the classes of I_{V11A} .

In Figure 110, there are the histograms of buildings and volume together for the ss.uu. and aggregates, from which it is possible to find out the growth of I_V passing from ss.uu. to aggregates, with a shifting of the bars' histogram toward higher vulnerability index on the graphs.

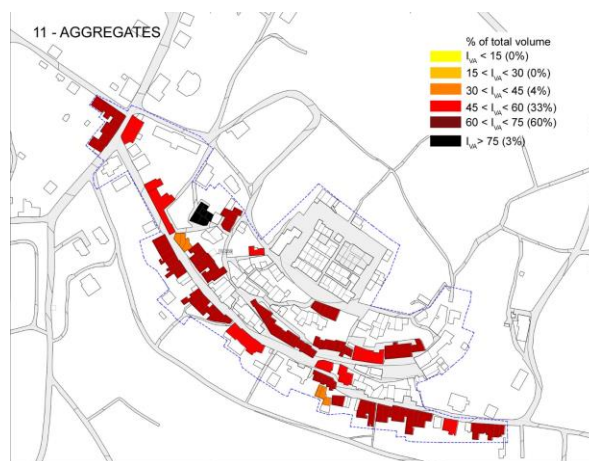
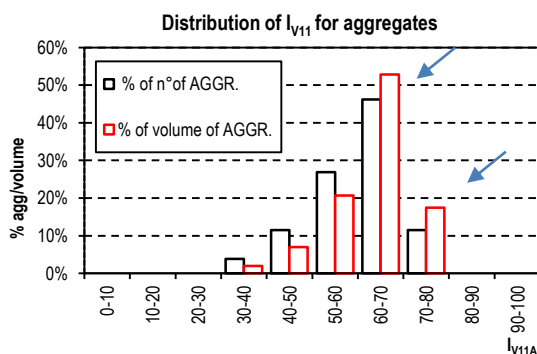


Figure 109: a) Distribution of I_{V11} in terms of % of aggregates and % of volume; b) vulnerability indexes maps for aggregates.

Most of parameters (P1, P2, P3, P4 and P5) show stable vulnerability distribution of judgment's classes both for aggregate analysis and ss.uu. one. For parameters P6 ("Plan configuration") P7 ("Configuration in elevation") there is the major redistribution of the vulnerability classes, in passing from ss.uu. to aggregates, because they take into account the assembly behaviour of ss.uu.. The ss.uu., indeed, have generally the same characteristics of shape and dimensions, being essentially squared or a little elongated, in the direction orthogonal to the main streets. The aggregates, instead, being the results of a process of assembling of the ss.uu. in time, exhibit a different and more complex shapes.

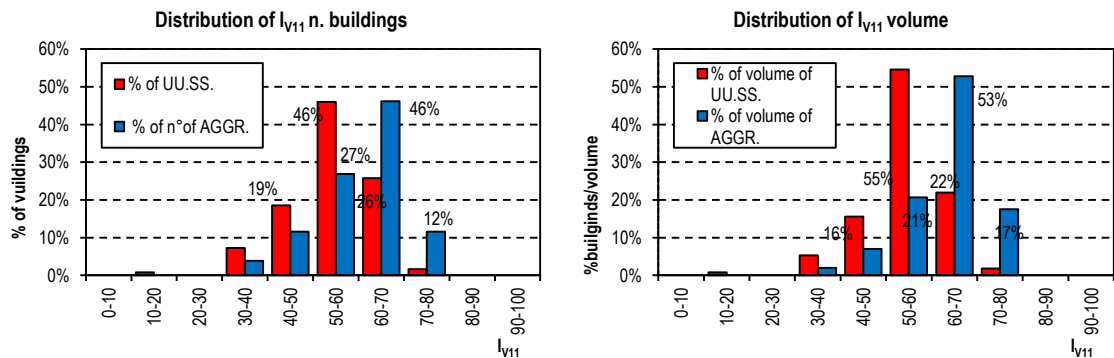


Figure 110: Distribution of I_{v11} in terms of % n° of building (ss.uu. & aggregates) and % of volume (ss.uu. & aggregates).

6.2 "FORMISANO FORM" (15P) AND "AVEIRO FORM" (14P)

With the same procedure carried out for the calculation of the vulnerability GNDT II Level Form, Vulnerability Forms for structural units were filled out ("Formisano" and "Aveiro" Forms) for 124 ss.uu.. The results are shown in the following histograms and graphs. Graphs representing the some quantities results for the two Forms are compared side by side (Figure 111, Figure 112 and Figure 113). In Figure 111 there are the distributions of the I_{v15} and I_{v14} . In both the graphs, in contonuous red line there is the average value of the vulnerability index of the structural units found with the GNDT II Level Form (11P) ($I_{v11,AV}$).

The results of the "Aveiro Form" are the closest to the ones of GNDT II Level Forms: the average vulnerability index passes from 53.8% ($I_{v11,AV}$) to 46.3% ($I_{v14,AV}$) by virtue of the degree of cooperation and containment between adjacent ss.uu.. The coefficient of variation is 18% very similar to that one of the distribution of the I_v evaluated with GNDT II Level Forms.

Wide beneficial effects, in decreasing of vulnerability indexes, are also proper of "Formisano Form" (15P): its distribution is characterised by a $I_{v15,AV}$ of 31% even if with a standard deviation much higher than in the other two cases ($\sigma=11.5$, coefficient of variation of 37%). This larger dispersion is probably linked to the high variability of the parameters inserted in the original Form (§2.2.2.3), very influential in the definition of the final global I_v .

The distribution frequencies are reported in Figure 112.

Specifically, the "Formisano Form" calculates lower vulnerability index due to two major reasons. The added parameters of P11÷P15, besides having high important factor in the calculation of the vulnerability index ($0.5\div1.5$), have negative scores for low vulnerability classes, such as "A" or "B" classes. Internal structural units, with no typological or structural differences with adjacent units, are subjected to an important reduction of their vulnerability index (in respect to the calculated I_{v11}). Furthermore, in "Formisano Form", there is not the P3 ("Conventional strength"), that, as already mentioned, is characterised by the major weight (equal to 1.5 for the GNDT II Level Form) and a frequency of structural units falling in "D" class equal to 90%.

"Aveiro Form" computes both the "conventional resistance" (P3) and the beneficial effect of the containment provided by adjacent structural buildings. While for the "Formisano Form", for the P12, the score is always negative in the range [-45,0]

for class “A” class “D”, for “Aveiro Form” the variation range is opposite [0-50] for class “A” - “D” for equal weight (1.5). This means that for an internal building belongs to class “A”: in “Formisano Form” it will have a considerable reduction of vulnerability, ($-45 \cdot 1.5 = -67.5$ points) while for “Aveiro Form” its containment is null. In “Aveiro Form”, no class has negative scores but, in parallel, it greatly penalizes buildings in corner position (class “D”, §Figure 21) with a +50 scores.

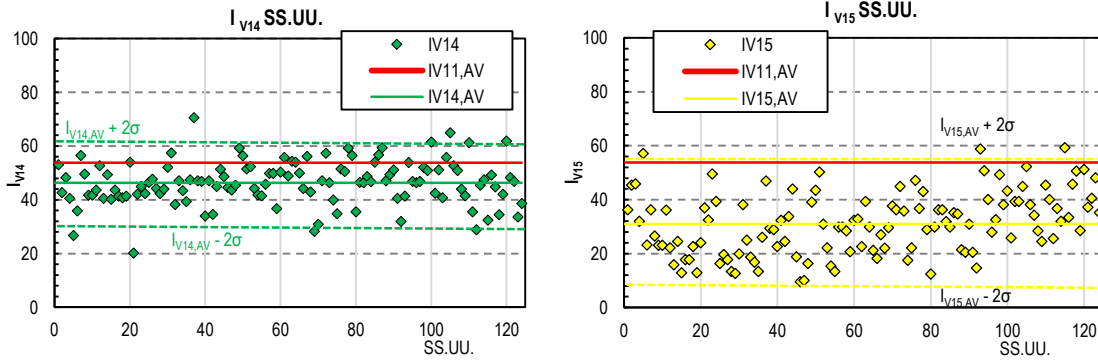


Figure 111: Distribution of the I_{V15} I_{V14} for 124 ss.uu..

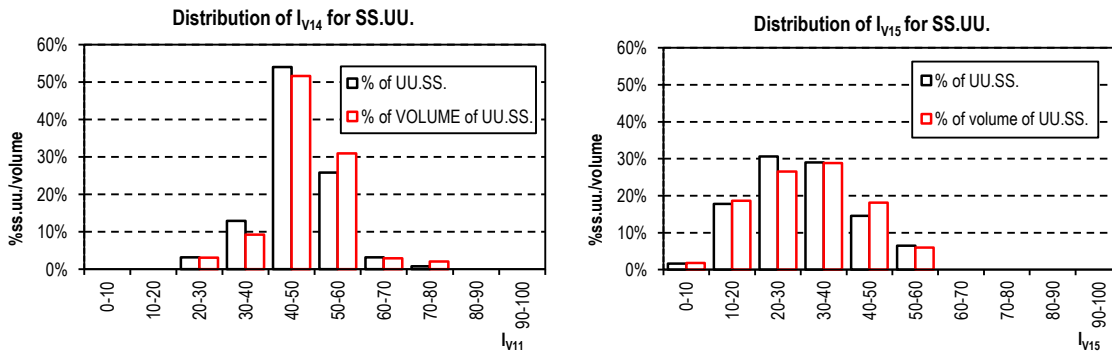


Figure 112: Distribution of I_{V15} in terms of % n° of building (ss.uu. & aggregates) and % of volume (ss.uu. & aggregates).

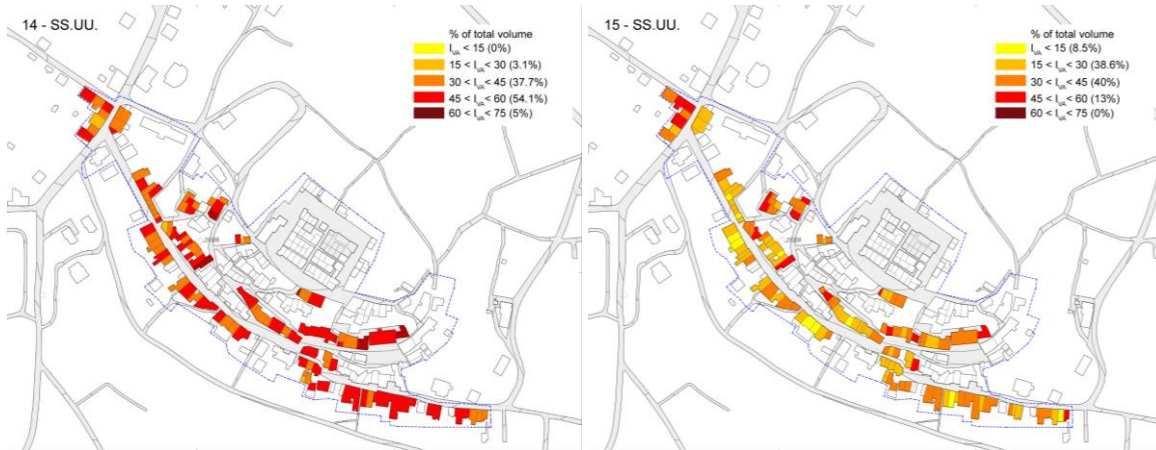


Figure 113: Vulnerability indexes maps for ss.uu..

6.3 COMPARISON AMONG THE FORMS

Figure 114 shows the distributions of the vulnerability index for the three Forms used for ss.uu., while Figure 115 shows their three normal distributions. With these representations, it is evident the marked difference in terms of obtained vulnerability indexes and the shifting of the $I_{V,AV}$ from higher values $I_{V11,AV}$ to the other ones. Moreover, considering the trend of the data, it is clearly observed that for both the GNDT and “Aveiro” Forms the results are quite centred on the mean

value (46% and 54% respectively) while for the “Formisano Form” there is not a clear maximum range of the I_{V15} and each middle class is characterised by high frequencies.

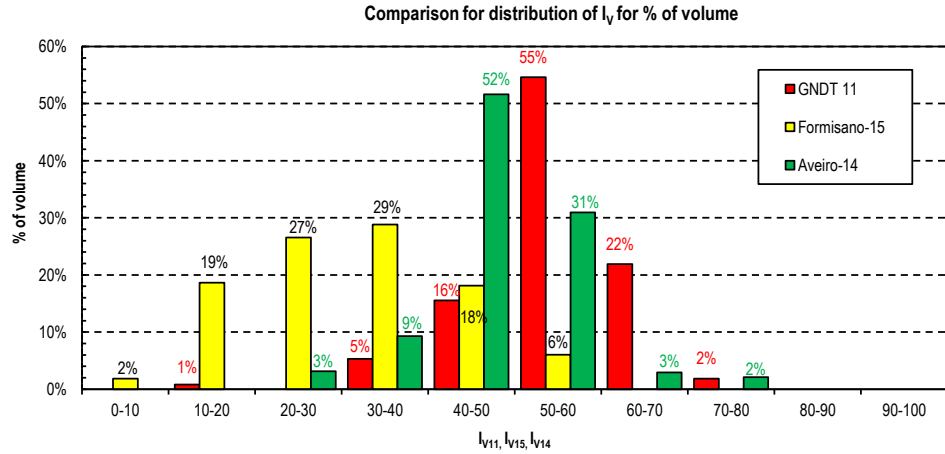


Figure 114: Comparison of the distributions of the I_V for % volume of ss.uu..

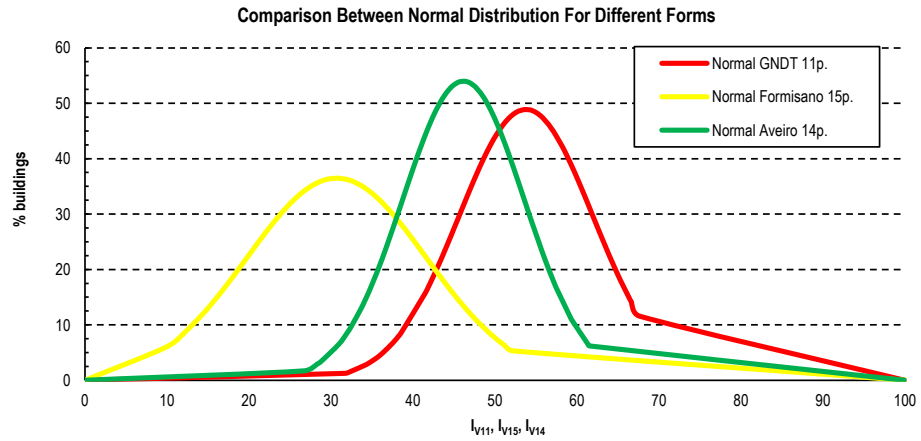


Figure 115: Comparison of the normal distributions of the I_V for ss.uu..

6.4 DAMAGE

Using the expressions defined in §2.2.3, damage scenario has been individuated starting from the vulnerability analysis results, to spatially represent the damage distribution of the building stock, referring at the scale of the structural units. In particular, for the GNDT II Level Form (both for aggregates and ss.uu.) and for “Aveiro Form” (Vicente et al., 2010), as well as for “Aggregate Form” in CHAPTER 5 the vulnerability curves used are defined by the following equations:

$$(20) \quad f(V, I) = \begin{cases} e^{\frac{V}{2}(I-7)} & \text{se } I \leq 7 \\ 1 & \text{se } I > 7 \end{cases}$$

$$(21) \quad V = 0.56 + 0.0064 I_V$$

$$(22) \quad \mu_D = 2.5 + 3 \cdot \tanh\left(\frac{I+6.25 \cdot V-12.7}{Q=3}\right) \cdot f(V, I) \quad 0 \leq \mu_D \leq 5$$

In the case of Formisano Form, both the expressions (Eq.(20-22)) and the ones that the Authors used in a previous applications of their Form (described in Formisano et. al, 2011), has been used.

The results are reported both in terms of histograms and maps. In particular, the histograms represent the distribution of the mean damage grade μ_D (EMS-98), with references to both the % in numbers of ss.uu. and % in volumes. The maps represent with different colours the different damage degrees. As well as for the results of the Aggregate Form, the μ_D , being a function of the obtained I_V , follows its distribution: the higher the I_V the higher the μ_D .

Figure 116 shows the predicted damage for vulnerability defined with GNDT II Level Form for ss.uu.. The estimated average value is $\mu_{D11,av} = 3.8$ (which correspond to D4 degree) with a max of 4.3 (D4-D5 for 18-163 s.u.2) and a minimum for 09-160 s.u.1 equal to 2.6 (D3) (Figure 117). At aggregate level, there is a growth μ_D , according with the distribution of the vulnerability index (Figure 110). The average value is $\mu_{D11A,av} = 4.0$, in the range [3.1-4.4]. For both cases, as already observed (for the analysis of I_V), the greatest damage was detected for structural units with greater volume. Indeed, in the histograms below, generally bar representing the volume percentage are bigger for higher damage levels (D4-D5). Figure 118 shows the vulnerability curves for minimum, maximum and average I_V , for different macroseismic intensities. The vulnerability curves' spindle is thinner for aggregates than that for ss.uu., but it arrives at higher damage level.

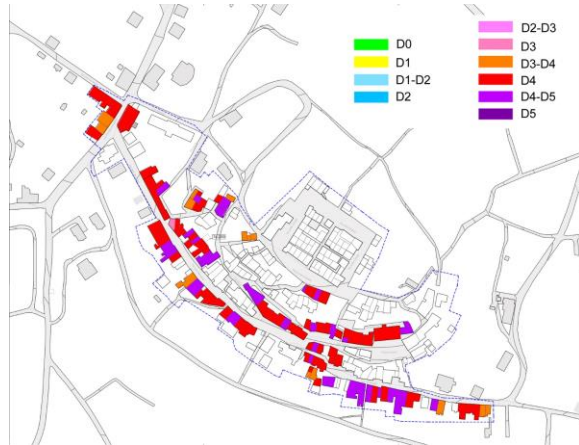
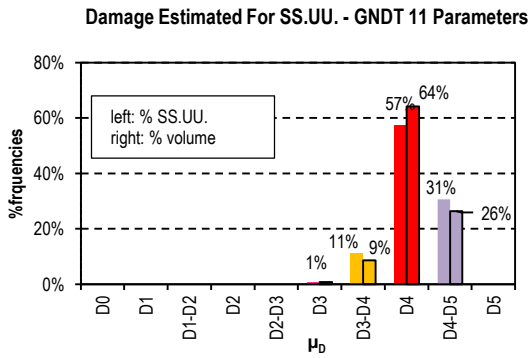


Figure 116: Histogram of the distribution of estimated μ_D (EMS-98) for ss.uu. with GNDT 11p and seismic damage maps.

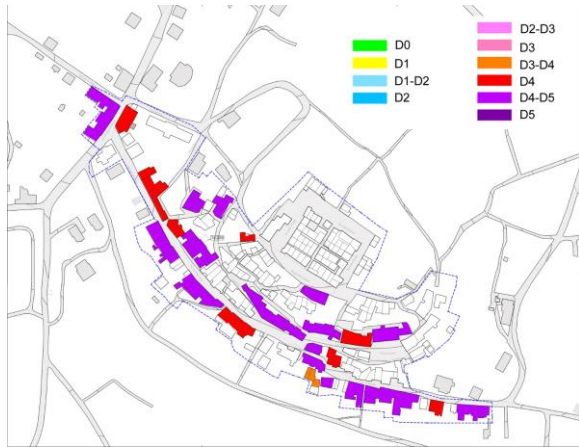
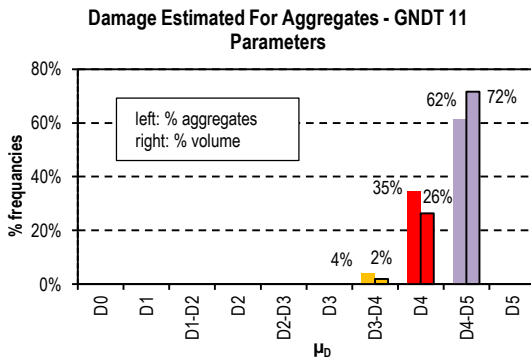


Figure 117: Histogram of the distribution of estimated μ_D (EMS-98) for aggregates with GNDT 11p and seismic damage maps.

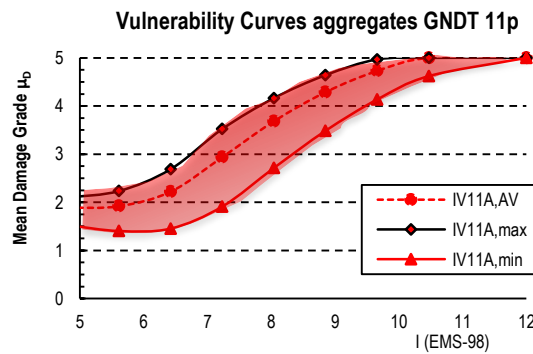
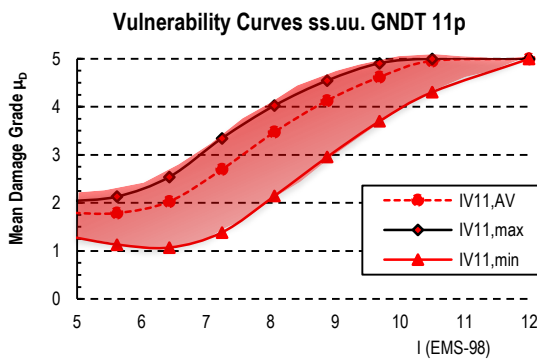


Figure 118: Vulnerability curves for the max, min and average value of the I_{V11} for: a) ss.uu.; b) aggregates.

The Figure 119 and Figure 120 refers, instead, to the calculation of the damage with the “Formisano and Aveiro Forms”, using the correlation of Bernardini *et al.* (2007), reported in Eq. (20)÷(22).

The comparison among the estimated level of damage shows that values calculated from “Formisano Forms” are generally low values, with an average value of about D3. The estimated damage index increases with the “Aveiro Form” for which the average value is $\mu_{D14,av}=3.5$ and it achieve the maximum with the GNDT II Level Form.

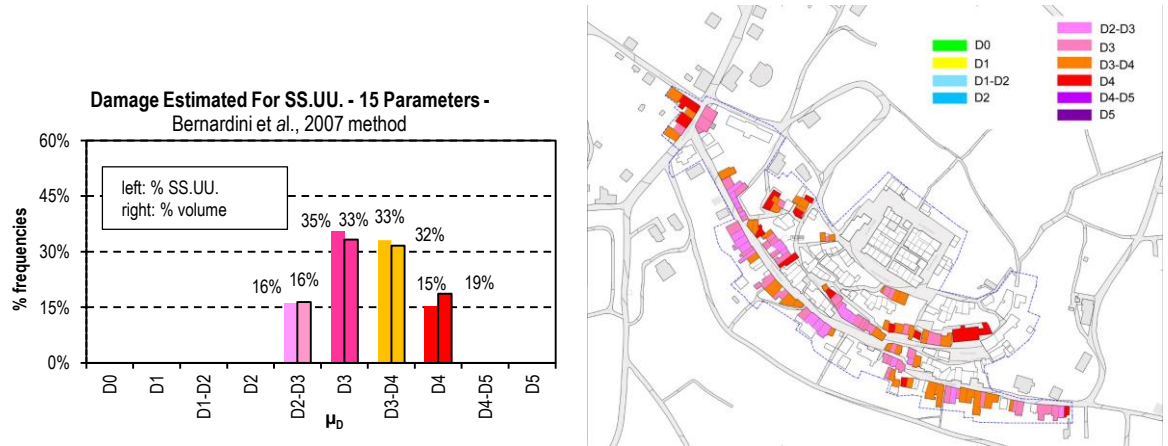


Figure 119: Distribution histogram of estimated μ_D (EMS-98) for ss.uu. with Formisano Form (15 p.) and seismic damage maps.

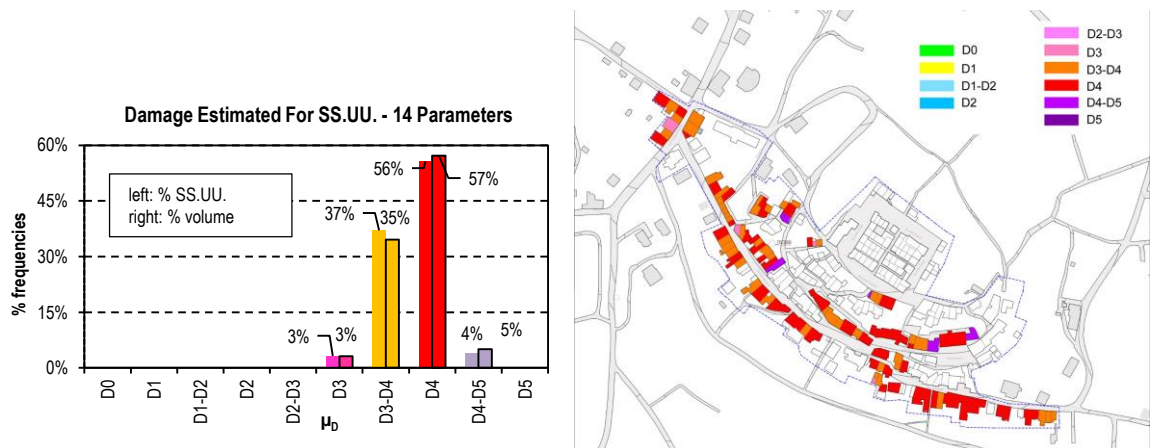


Figure 120: Distribution histogram of estimated μ_D (EMS-98) for ss.uu. with Aveiro Form (15 p.) and seismic damage maps.

§

Considering the maps of real damage scenario experienced after the 2009 earthquake (§4.2), it is possible to understand which are the Forms that were able to identify the estimated damage scenario closer to it.

The structural damage described until now refers to the entirety of the damages on structural vertical and horizontal elements of a masonry buildings (following definition of damage in EMS-8 Scale), not depending on the mechanism type triggered. In general, as it will be better showed in CHAPTER 7, the mechanisms' collapses for masonry constructions can refer to *global or local behaviours* of the masonry. Since for Castelnuovo aggregates, the more frequent damages were relative to out-of-plane mechanisms, from this point those type of collapses will deep analysed, in order to identify if there are common parameters (among those belonging to the VF) that are common for those ss.uu. that experienced major local damage.

To achieve that purpose, the vulnerability results and damage occurred on ss.uu. graphs were plotted. In particular, the real damage grade were plotted vs the positions that the ss.uu. assume in the vulnerability ranking or their vulnerability indexes.

In the cases of aggregates, it was possible to plot the trend of the real damage grade (D_k) for aggregates for the position in the vulnerability ranking (Figure 121top) and for the different values of vulnerability indexes (Figure 121bottom) defined by both the application of GNDT II Level Form (11P) and the “Aggregate Form” (6 parameters, implemented in CHAPTER 6). In red line there is the representation of the couple of data (IV_{11A} ; D_{kA}) for the GNDT II Level Form while the black points refer to the “Aggregate Form” (IV_A ; D_{kA}).

The linear regression used to approximate the cloud of points has low index of determination, equal to 0.10 for the GNDT II Level Form and 0.30 for the “Aggregate Form - 6P”. These values remain almost stable in the plot with the vulnerability index (Figure 121bottom). For both cases, the index of determination so little, means a great dispersion of the data collected in respect to the linear approximation. Despite the low value of R^2 , the provided Aggregate Form seem to be more efficient to the individuation of the estimated level of damage or better, in the determination of the best fit vulnerability ranking.

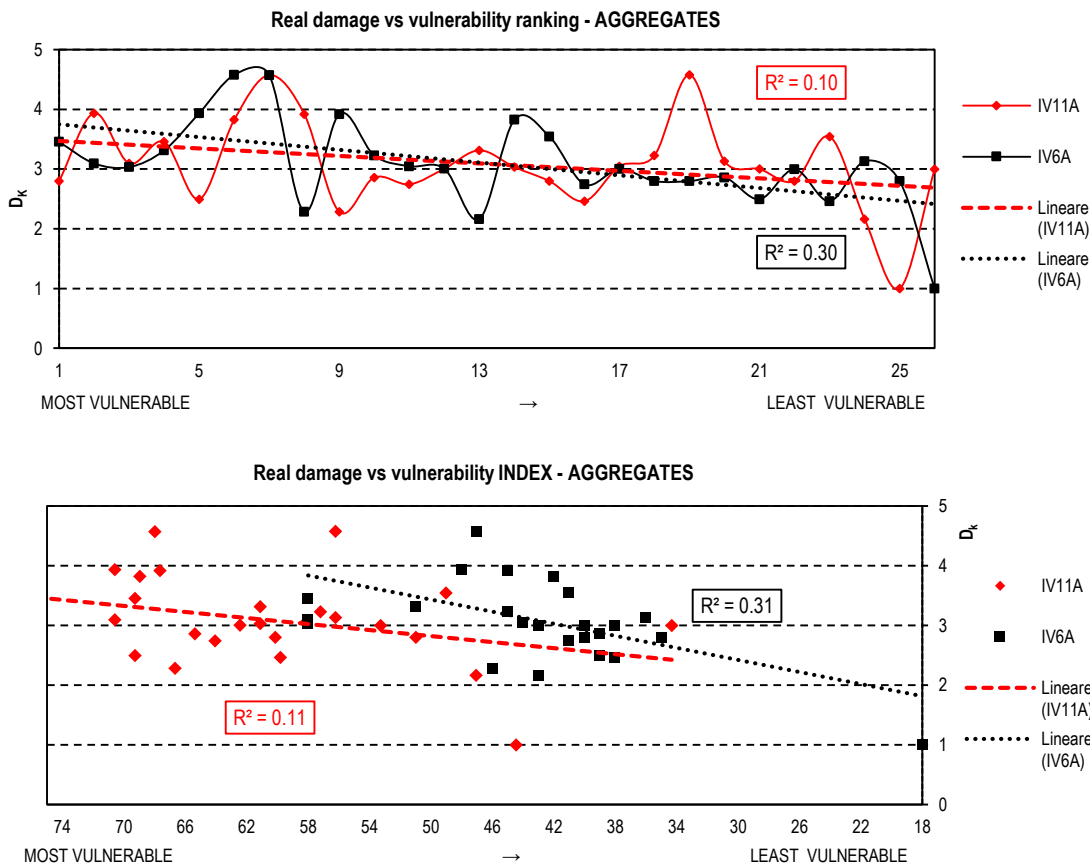


Figure 121: Real D_k vs vulnerability ranking for aggregates. In red GNDT Form and in black the Aggregate Form (6P).

In terms of structural units, the same procedure is defined for the others Forms: the plots in Figure 122 shows the trend of the D_k for the different vulnerability ranking of the different Forms. From the top, the red represents the GNDT II Level Form, the yellow the “Formisano Form” and the green the “Aveiro Form”. Despite slight, there is a defined descendent trend for the GNDT II Level and “Aveiro Forms”, while it is not recognize for the “Formisano Form” (for which the linear regression had a R^2 is almost 0).

For each ss.uu. is possible to compare the real damage D_k with the estimated one, calculated with the different Forms. The results are plotted in Figure 123, in which grey circular points represents the real damage for each ss.uu. and:

- Red squared symbols represent the estimated damage with GNDT II Level Form;
- Yellow squared represent the estimated damage with “Formisano Form”;
- Green triangular represent symbols the estimated damage with “Aveiro Form”;

The values are ordered randomly, following the progressive number. The real damage represented has scattered value, while the μ_D estimated have a distribution concentrated around their average values, since they have been calculated following specific continuous correlations (Eq. (20)÷(22)). The errors between the real damage and the estimated by all the Form is elevated.

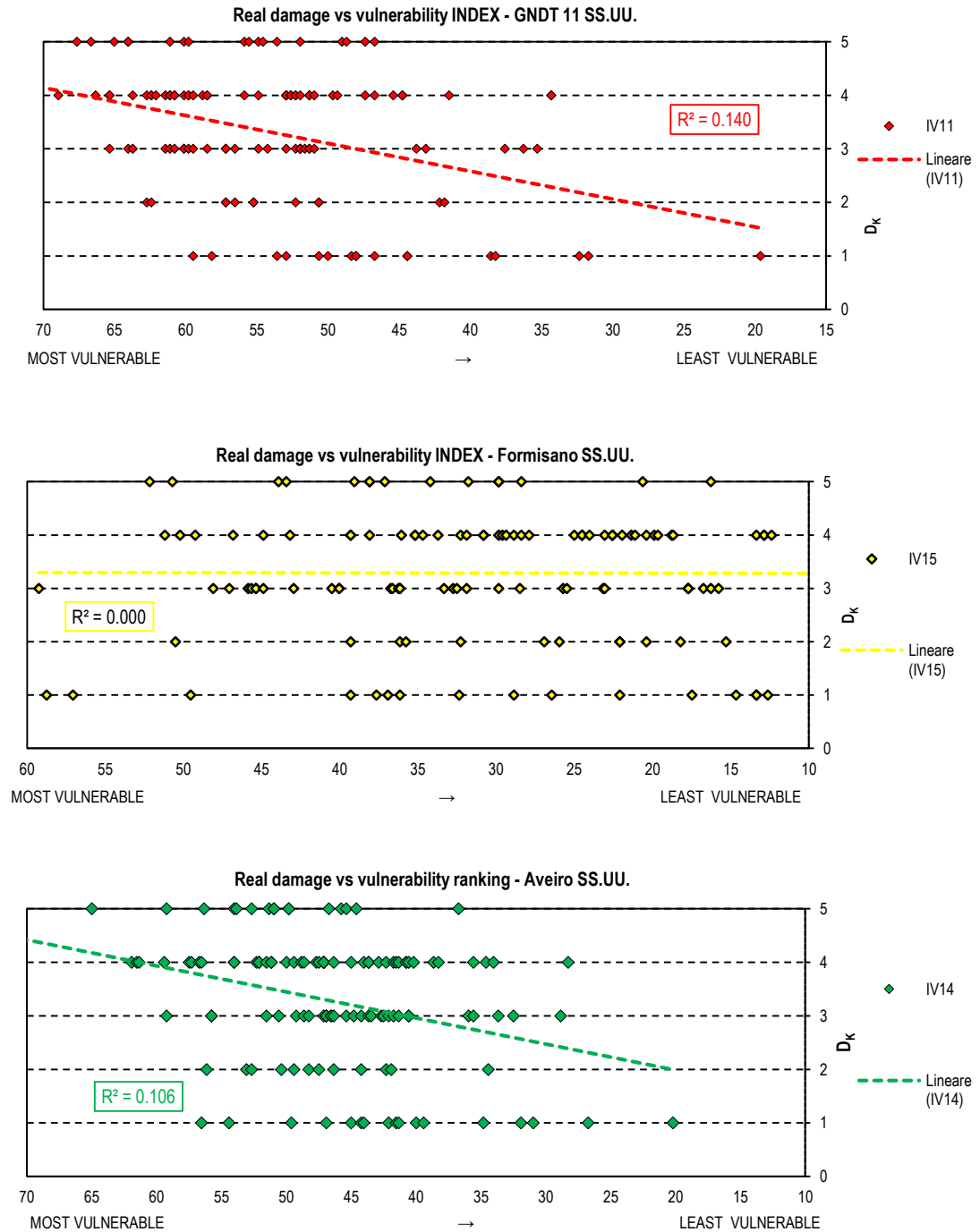


Figure 122: Form top. Real D_K vs vulnerability indexes for the ss.uu.. In red GNDT Form, yellow "Formisano" and green "Aveiro" Forms.

The greater error committed is to overestimate the damage in the case of the 01-222 s.u 7A, 09-160 s.u.4 or for structural units with good characteristics and composed by unreinforced concrete masonry walls, in corner position. Despite their low I_{vi} , the Eq.(22), for a high earthquake intensity recorded in Castelnuovo (9.5 MCS) provided a great level of estimated damage, which is in contrast with the estimate one.

In parallel, the major error in underestimate the expected damage is committed using “Formisano Form”. This situation is presented for those ss.uu. that have, despite not good state of conservation, uniform plan distribution and are collocated in internal position within the aggregates (as ss.uu. 4 in 16-515 or s.u.10 in aggregate 18-163).

Making a comparison in terms of average values (continuous lines in Figure 123), the GNDT II Level Form and “Aveiro Form” overestimate the real damage respectively of 8% and 16%, while the “Formisano Form” underestimate it of 9%.

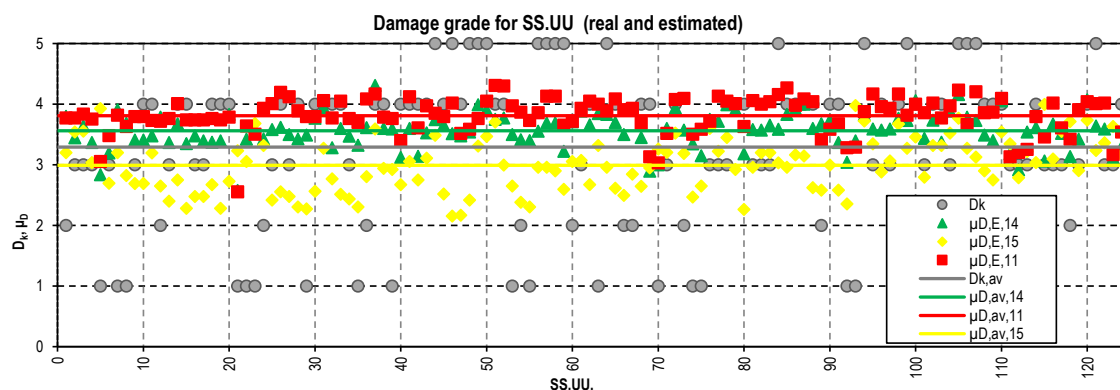


Figure 123: Distribution of the real damage for ss.uu. and estimated with different Forms.

Doing a process of approximation in terms of volume, Figure 124 provides the same results in terms of aggregates. On average, “Aveiro Form” comes close to real damage for the largest n. of aggregates (65% of the times), which, however, underestimate such damage in a larger number of cases (13 times, 50%), providing estimations strongly in defect.

The average values of the estimated damage for Formisano is 3.05, very close to the real value, 3.08 (the two lines are almost overlapped in the Figure 124). Both the other two Forms overestimate the damages: the average value for “Aveiro Form” is 3.58 (16%) and GNDT II Level Form overestimated the value of damage for 26%.

The “Formisano Form” allows detecting the damage level in a precise manner for a few aggregates, but, for others, the estimated values depart significantly from the real.

The errors among real and estimated damage scenarios are plotted in Figure 125. The bigger error for the three Forms is committed for the 09 aggregate, which has suffered low damage level.

The graph shows that the errors of estimated damage with “Aveiro Form” are in absolute smaller, but frequently in the case of underestimation (green dots represent values minor than 0).

Further consideration can be done dividing the sample of reference, despite reduced from the original, in the classes of plan configuration that the ss.uu. can have: header, internal or corner position. It is know from §4.2 that more than the 50% of structural units have suffered high level of damage, with the peak of *isolated* buildings, in which 77% of their total volumes have D4/D5 damage level. *Isolated* building have the minimum % of volume in low level of damage and the maximum in high level of damage (D4/D5-77%) (Figure 62b). The *internal* structural units, on the opposite, have the maximum % of light damage (12%), even if the minimum volume for D4/D5 damage level is referred to the *external* (E) ss.uu. The corner units (C) are placed in an intermediate position in all classes of damage considered.

In Figure 126 the comparison between the real and estimated damage scenarios is performed dividing the sample of data depending on the position occupied in the plan configuration. In particular, looking at the punctual values, there are wide large under and overestimation from all the Forms. For the *internal* position (Figure 126a), the “Aveiro Form” provides the best fitting estimation of the average damage, with an overestimation of 4%. “Formisano” results underestimates the damage for about 17% and the GNDT II Level results overestimate for about 15%.

For the case of *header* and *corner* position (Figure 126b and c), on the contrary, the “Formisano Form” is able to provide, on average, the exact value of the damage level.

It is worth noting that the sample of data is reduced in the calculation of the ss.uu. and it does not include the aggregates with worst state of conservation, of the other that were completely collapsed after the earthquake of 2009.

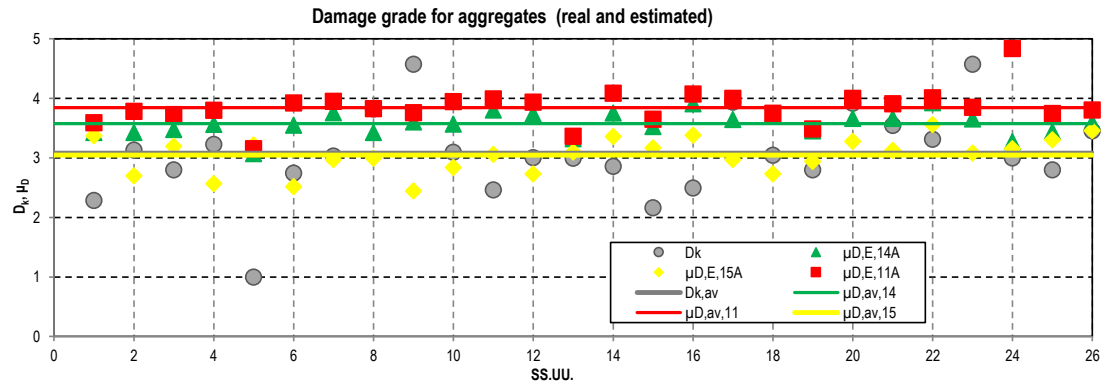


Figure 124: Distribution of the real damage for aggregates and estimated with different Forms.

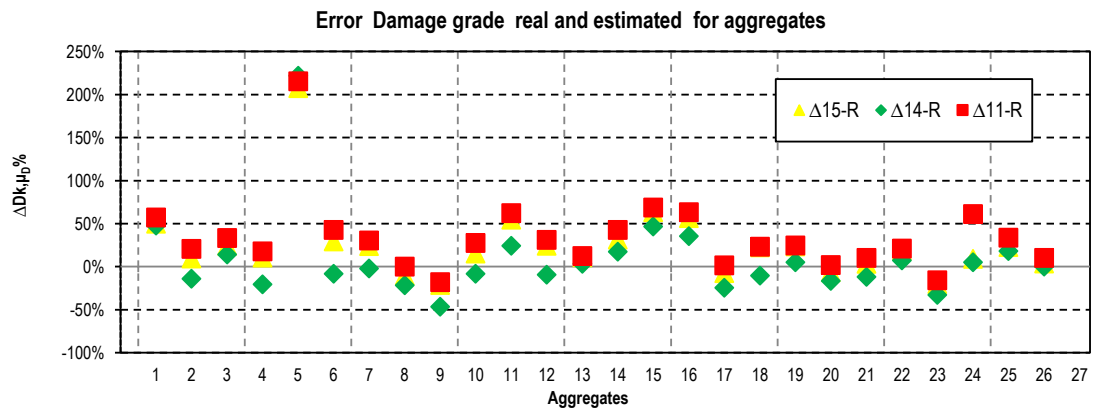
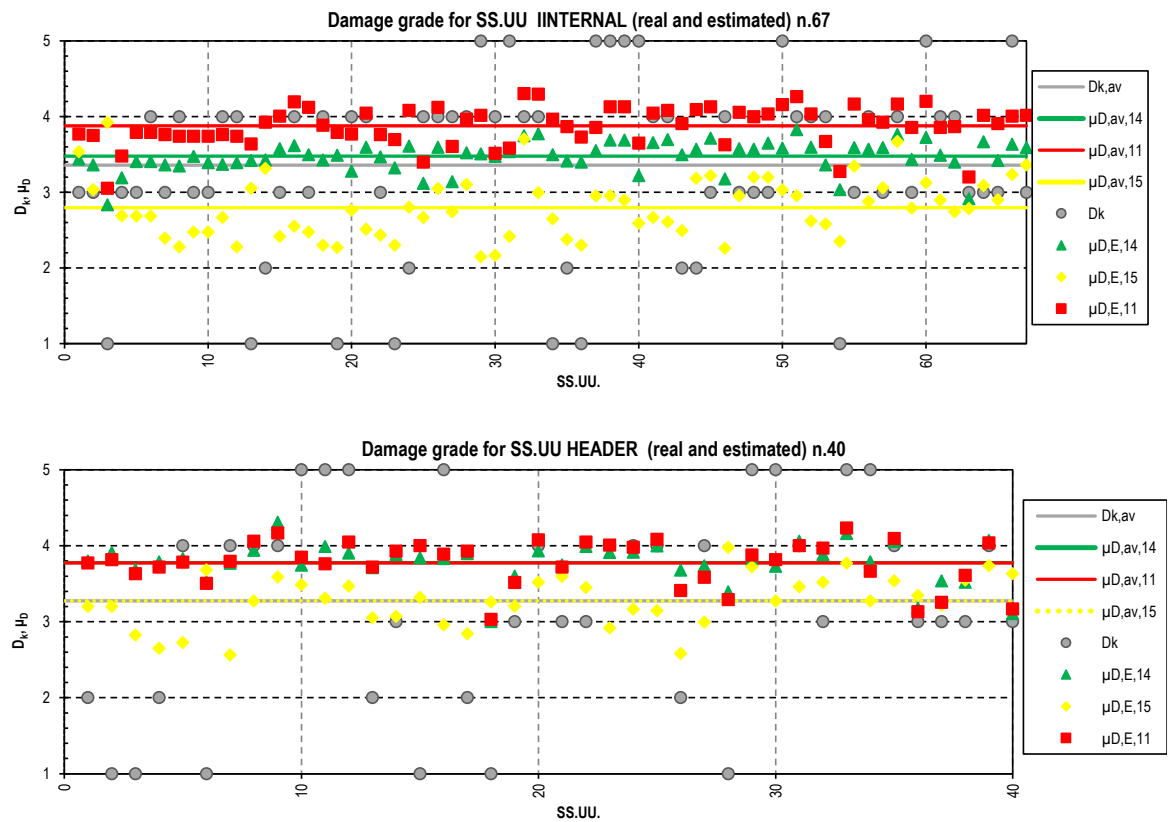


Figure 125: Errors % among the estimated and real damages.



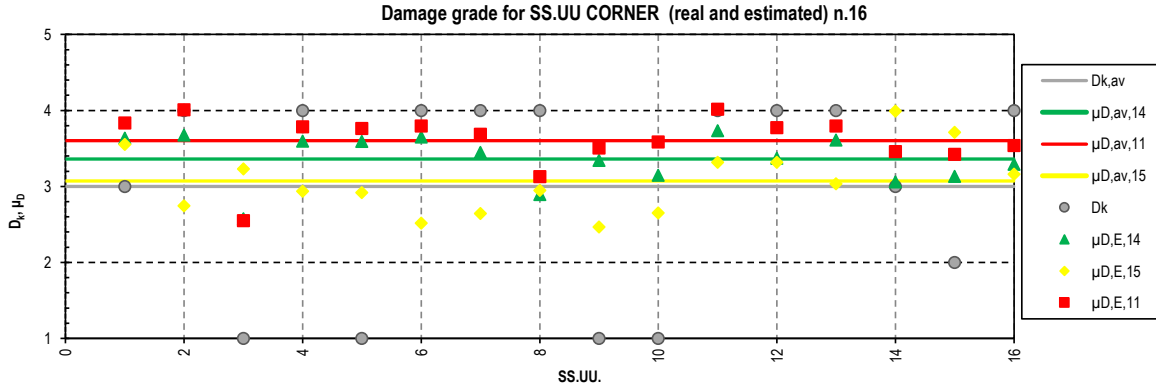


Figure 126: Distribution of the real and estimated damage for different Forms grouped for the position of the ss.uu.. (top, internal, header and corner position).

From the analysis of the obtained results in terms of vulnerability index and estimated damage, referring to the case study of Castelnuovo, one might conclude that the vulnerability GNDT II Level Form being born for isolated buildings, does not take into account the distinctive issues of the structural units belonging to aggregates and their effect of confinement. It generally tends to overestimate their vulnerability and consequently the estimated damage.

The “Formisano Form”, which in its definition includes parameters that for certain classes of judgment have negative values, manages to hold to account the distinctive features of the buildings in the aggregate, with respect to the evaluation of the GNDT II Level Form, but it significantly underestimates the expected damage for internal structural units.

The results of the “Aveiro Form” lies in an intermediate position between the results of the two previous Forms and it is the one that allows to define estimated damage scenario more in line with those in Castelnuovo, in specie for ss.uu. collocated in internal position.

6.5 CRITICAL ANALYSIS OF THE RESULTS IN RELATION WITH THE LOCAL BEHAVIOUR OF AGGREGATES

The results of the study of vulnerability and damage performed until this point have focused on the average damage on the structural unit, with reference to the macroseismic scale adopted EMS-98 (§1.1.1.2). In the following, however, the results will be limited at the damage related to *out-of-plane mechanisms collapses*, with reference to the reduced sample of aggregates defined in this chapter. This because the damage assessed on a structural unit following the definition of EMS-98 scale is referred to many factors, i.e. the damages on the main vertical and horizontal elements, and the different types of damage mechanisms.

As described in CHAPTER 7, the study of aggregates (using analytical methods) will be executed through the kinematic local analysis (overturning mechanisms), decision supported by several contributing factors in the definition of the damages of Castelnuovo database.

In the following, the main issues of each vulnerability Form parameter will be related to the capacity of the structure in terms of local mechanisms, or out-of-their plane. Thus, a new classification of damages is defined, considering the showed damages only in term of out-of-plane mechanisms of main façades. This section of the chapter would be the starting base for the definition of the new vulnerability Façade Form, defined in CHAPTER 8.

§

Within the parameters contained in the VFs those that most influence the local mechanisms (out-of-plane) and those who, in the opposite way, influence the box behaviour of the global structure, are identified.

Among the 11 parameters of GNDT II Level Form, a distinction is made considering parameters strictly related to the global capacity, others related to the activation of the out-of-plane mechanisms and still others that can affect both the two ways

of seismic response. In Figure 150a there are the identification of the influence in local or global behaviour of the parameters of the GNDT II Level Form. In particular, P3 concerns the conventional seismic resistance of the weakest plane of the structure, therefore, concerns the global capacity of the building. P8 represents the maximum distance between orthogonal walls to the principal façades. The greater the distance, the higher vulnerable to local mechanisms the structure is, because the orthogonal walls are considered as restraints against out-of-plane overturning. P4 is linked to the foundation but not directly to the calculation of out-of-plane mechanisms (Eq.(23)). The plan configuration (P6) can influence the choice of the panel analysed in overturning but not the calculation itself.

GNDT II LEVEL FORM - 11 PARAMETERS		
Parameters	Behaviour	
	Local	Global
1 - Type and organisation of resistant system	✓	✓
2 - Quality of resistant system	✓	✓
3 - Conventional strength		✓
4 - Building position and type of foundation	✓	✓
5 - Horizontal elements (floors)	✓	✓
6 - Planimetrical configuration	✓	✓
7 - Configuration in elevation	✓	✓
8 - Maximum distance among the walls	✓	
9 - Coverage/roof	✓	✓
10 - Non structural elements	✓	✓
11 - Actual state (conservation status)	✓	✓

Figure 127: GNDT Form with influence in terms of local and global behaviour of the masonry structures.

P10 and P11 can influence both the global and the local behaviour of the structure, in equal way.

In conclusion, parameter 1, 2, 5, 7, 8 and 9 influence mostly the out-of-plane mechanisms. In particular:

- P1 gives information about the connections among orthogonal walls and among walls and floors. It is related to the identification of local collapses since it measure the loss of restraints among the resistant system;
- P2 concerns the quality of resistant system. If the masonry is constituted of more than one leaf, a premature collapse for crumbling material can appear or the overturning of the only external leaf is frequent;
- P5 and P9 are linked to the horizontal elements. In particular, P5 evaluates the in-plane stiffness of the floor and the level of connections with the vertical elements. For the connection aspects: flexible floors, such as masonry in folio vaults of wooden floors, are mostly characterized by a low level of connection with the walls, while reinforced concrete floors are often more weighted, more stiff, and positioned with the reinforced concrete beams on the edges;
- P8 concerns out-of-plane local aspects since it is related to the presence of masonry alignments that have no orthogonal constraints for a considerable length. The inter-axis of the walls represent the width of the façade that overturns out-of-its plane.

In Figure 150b in grey there is the identification of the parameters really taken into account for local mechanisms.

FORMISANO FORM - 15 PARAMETERS		
Parameters	Behaviour	
	Local	Global
11 - Interaction in elevation - Pres. adjacent buildings with ≠ height	✓	✓
12 - Interaction in plan - position of the building in the aggregate	✓	✓
13 - Staggered floors	✓	✓
14 - Typological and structural differences	✓	✓
15 - Different percentage of opening areas among adjacent façades	✓	✓

AVEIRO FORM - 14 PARAMETERS		
Parameters	Behaviour	
	Local	Global
P5 Number of floors	✓	✓
P7 Aggregate position and interaction	✓	✓
P10 Wall façade openings and alignments	✓	✓

Figure 128: Additional parameter of 15 and 14 parameters Forms: influence in terms of local and global behaviour.

As already mentioned in 2.2.2.6 in the “Formisano” and “Aveiro” Forms the added parameters (in respect to GNDT II Level Form) take into account the major issues of masonry ss.uu. inside the aggregates (§2.2.2.2). Despite each parameter can be connected both at the local and global behaviours of the structure, they seems to be more incident in the local behaviour. In particular, the “interaction in plan and height” allows to understand which type and in which positions the masonry panels could collapse. “Staggered floors” and the “% of holes in façades” refers in a major way to global behaviour: the first is

linked to the capacity of transferring the seismic actions on vertical elements and the second to the definition of in plane seismic capacity (definition of the equivalent frame model of the masonry wall) (Figure 128).

6.5.1 EVALUATION OF THE DAMAGE LEVEL IN THE FAÇADES

5 classes have been individuated for the classification of the overturning mechanisms of the main façades, related to the different degrees of severity of the crack patterns found on the structures. It was necessary at first to identify the number of storeys involved in the mechanisms. Beyond the presence of external constraints that inhibit the mechanisms (§7.2.2), the mechanism could not always active throughout the available free height of the wall due to particular situations. From a theoretical point of view, the multiplier coefficient of horizontal loads is related to the kinematic chain with greater height (Figure 139). In parallel, the seismic demand is increasing with the height of the structure (§7.2.1.4) and therefore, the final verification the local mechanisms may be more restrictive considering only the last storey of the structure. In real case of Castelnuovo, most of the time there were no restraints and in about the 90% of the cases, the kinematic mechanisms have hit the total panel of the façades. In other words, the overturning invests the total height of the walls with the formation of the ideal hinge configuration at the ground floor.

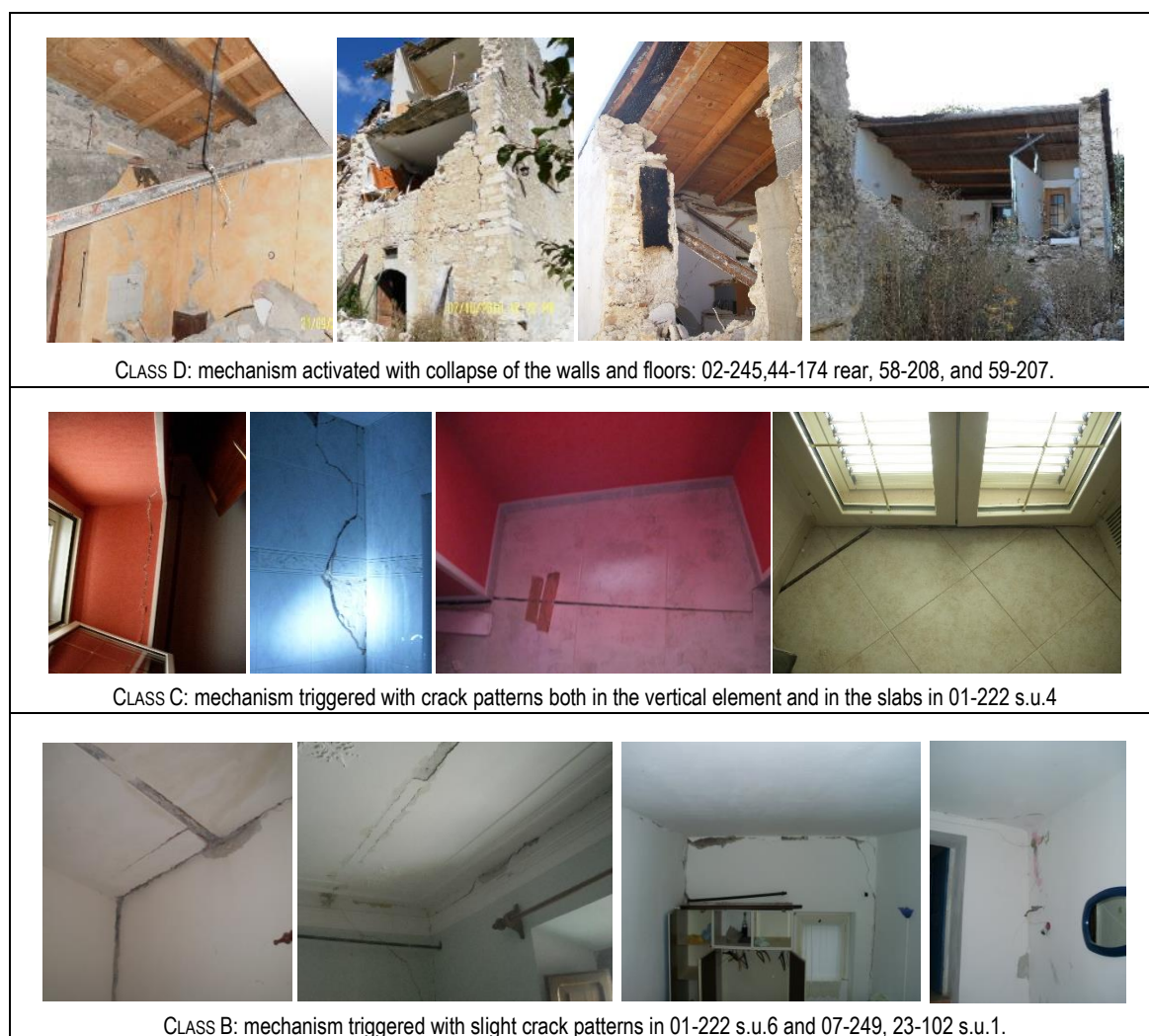


Figure 129: Classification of the damage for out-of-plane mechanisms of overturning. From the top: class D, class C, class B.

The degree of activation of the mechanism can be attributed to the different crack patterns in the façades, as reported in the following list and with reference to the Figure 129. 5 types of damage degrees have been individuated. The first refer

to the collapse, considering both the collapse of the façades (vertical elements) or horizontal floors, arriving at the absence of damage.

The classes are:

- Class "D": mechanisms activated with the collapse of the vertical elements, or the floors due to the loss of their vertical support (Figure 52);
- Class "C": mechanisms triggered with visible and important crack patterns (both for the entire high of the structure and only in some floors);
- Class "B": mechanism triggered, light crack patterns on vertical elements (Figure 124, row 3);
- Class "A": Not triggered mechanisms due to the presence of connections among orthogonal walls, among the horizontal and vertical elements or presence of effective tie-rods system.

Once defined the scale of gravity of the mechanisms, it was possible to re-perform a critical analysis of the failure mechanisms activated, setting them in one of the four classes described above ("A", "B", "C" and "D") in increasing degree of damage and gravity. The set of data refers to the façades in which analytical models (out-of-plane mechanisms) were performed, represented in Figure 130.

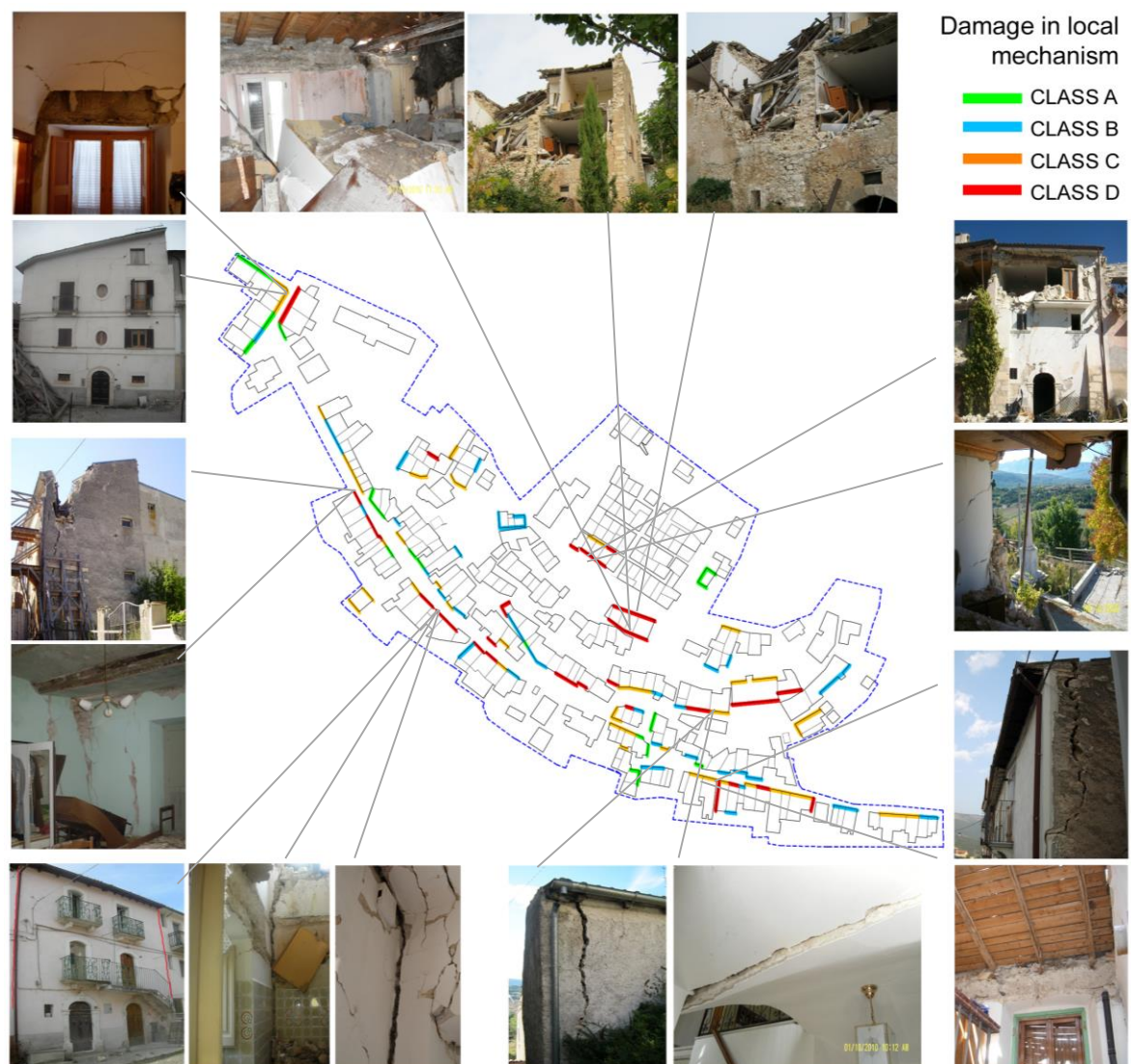


Figure 130: Damage intensity in terms of out-of-plane mechanisms for a reduced sample of buildings in Castelnuovo.

The classes of damages are distributed as reported in Figure 131. The histogram representation refers to both the number of façades in respect the total amount (188, bars in the left) and in the case of % in respect to the surface of the façade

(calculated as the multiplication of the width and the total high, as computed in the detailed analysis in CHAPTER 7). The percentages are quite stable passing from the frequencies in number and in % of surface, even if in the case of "D" classes (collapses) the % in respect to the surface is higher than in numbers. This is in accord with the classes of vulnerability of P8 ("maximum distance among walls", GNDT II Level Form). The larger the façades the higher the vulnerability index. Only in the 12% the façades the mechanisms are not triggered, while in more than the 60% there are evident crack patterns or collapses at least in one floor (classes "C" and "D").

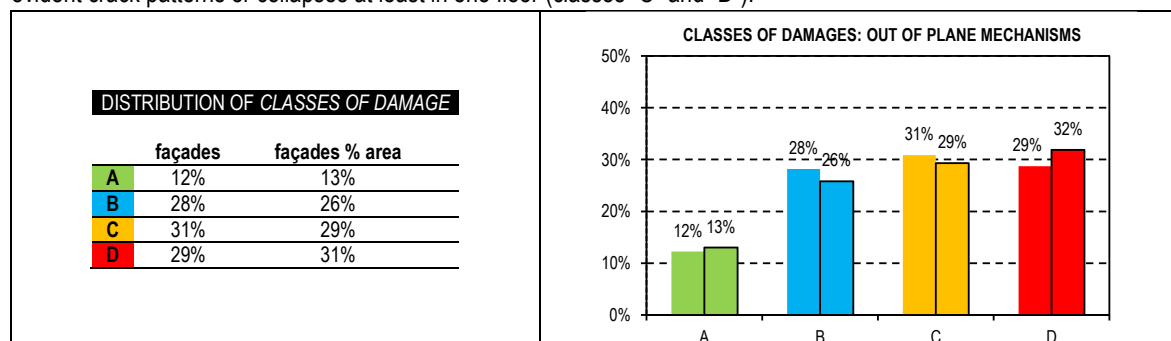


Figure 131: Distribution of classes of damages for out-of-plane mechanisms.

It is possible to cross the results of this new classification of local damage level and those of the Vulnerability assessment in terms of ss.uu., in order to identify if there is a systematic presence of some parameters in those mechanisms that are the most serious collapsed. The purpose is to understand if exist a correlation among the distributions of the parameters' classes and distribution of the damage intensity degree related to local mechanisms.

From an operative point of view, in certain case, in a header ss.uu., more than one kinematic mechanisms were individuated (considering for example the front and rear façades), while only a single value for I_v were calculated. In a conservation mode, the coupling of value is done for the I_v and the worst damage mechanisms. On the other hand, for certain ss.uu. for which the Forms were filled out, no kinematic mechanism was individuated. Among the 124 cases initially studied with the Vulnerability Forms, the comparison with the damage local level for overturning was done for 102 ss.uu..

The representations among the classes of vulnerability and damages are not easy to perform, since the values of both vulnerability parameters and the classes of damages are divided in only four classes. The variable can take only 4 discrete values ("A", "B", "C" and "D"). This aspect is already discussed in CHAPTER 5, with reference to the results of the "Aggregate Form" (5P) and the global damage level.

To estimate the level of correlation among the judgments of parameters and the classes of damage considering the local mechanisms of façades (Figure 131), the sample correlation coefficients were calculated. Numerical values were associated to the judgments, in order to apply the formula in Eq.(19). Since the scores of the parameters for the Forms (§2.2.2) are different, considering here both the three VF adopted in this work, arbitrary and with the same distance values have been associated to each parameter's judgment:

"A"=1, "B"=2, "C"=3 and "D"=4.

The index of correlation can assume values within the $[-1,+1]$ range, where +1 means an optimum direct correlation and -1 a perfect inverse correlation, while values near to 0 mean absence of correlation among the couples of parameters.

The total number of parameters for the three Forms for structural units is 19, considering the 11 parameters of GNDT II level Form (Table 38) and the addicted parameters of the Formisano and Aveiro Forms (Table 47).

The coefficient of correlation is very low for each parameters. In particular, it never passes 0.5 and the major correlation is enter P2, P3 and P11 of the GNDT II Level Form and the P11 of the "Formisano Form", highlighted in bold in next tables.

Table 37: Sample correlation coefficients for GNDT (11p.) parameters and classes of local mechanisms in façades.

P1 - 11	P2 - 11	P3 - 11	P4 - 11	P5 - 11	P6 - 11	P7 - 11	P8 - 11	P9 - 11	P10 - 11	P11 - 11
0.22	0.30	0.32	0.19	0.21	-0.02	-0.08	-0.17	0.07	0.14	0.39

Table 38: Sample correlation coefficients for Aveiro and Formisano parameters and local mechanisms classes in façades.

P5 - 14	P7 - 14	P10 - 14		P11 - 15	P12 - 15	P13 - 15	P14 - 15	P15 - 15
-0.07	-0.19	-0.10		-0.31	-0.18	-0.08	-0.13	-0.02

The sample coefficient gives information on the correlation among the parameters distribution and the distribution of the level of damage relate to out-of-plane mechanisms, but without considering the real connection among the identical classes inside each couple of parameters. The problem refers to discover if some parameter are better correlate, in considering: how many judgements are EQUAL for couples of parameters?

A possible graphical solution is presented with the “bubble graphs” (Ciavattone, 2014). The bubble graph is a graph that shows 16 possible positions of each couple of observations (“A”=“A”, “A”=“B”, “A”=“C”,...) and, for each of the 16 possibilities, a bubble that, with the measure of its area, represents the frequency of occurrence of the considered combination. These bubbles report the percentage value referred to the entire number of observations (in this case, 102 for each graph). Each parameter of the Form is put in relation with the distribution of the classes of damage for local mechanisms: there are 19 graphs.

A fit correlation among equal classes of judgments is defined with a bubble graph that has big-area-bubble only in the diagonal (or at least more than 50%): it means the equal values of judgments are indicated for both the parameters considered. The perfect graph is that one which refers to parameters that have the same distribution of judgments, or between two identical parameters (Figure 132a).

An index of goodness of the correlation among the parameters can be expressed by the sum of the percentages that lie in the tri-diagonal area of the matrix. The tri-diagonal position contains only one “position” of difference among the judgments. On the opposite side, the sum of the percentages of the bubbles in the places “A”-“D” and “D”-“A” should be relatively low (at least equal to 0). This sum represents the fraction of ss.uu. that have opposite evaluations in the considered parameters and it is a measure of the possible inverse relation among them. In Figure 132b there is the bubble graph of the P6 (GNDT) “Planimetrical configuration” that shows that there isn’t a correlation with the distribution of damage level: the sum of the diagonal trace is 20% while the sum of the “A”-“D” trace is 35% which highlight dispersion among the classes.

As expected from the results of the sample correlation coefficient, there isn’t a parameter that has a direct correlation with the façades’ damage distribution for local mechanisms. The parameters which have the higher percentages of frequency in the diagonal or tri-diagonal place are shown in Table 39. Essentially, they are the same that showed higher correlation coefficient in addition to the P9 GNDT II Level Form (“Coverage”) and the P14 of “Formisano Form” (“Typological and structural differences”).

From the value of the indexes of correlation and the shape of the graphs in the bubble, the P1, P2 and P3 are those for which we expected higher correlations; the high values of the correlation indexes for these parameters is due only to the high frequency of their judgment to fall in “D” class (Figure 107). This is in agreement with the high value of the sum of the lower triangular matrix (P2 and P3 equal to 100 and 95%). In other words, if the classes of damages vary their judgment classes, the P2 and P3 remain stable in “D” (or, in some cases “C” classes).

It is important to observe another bubble graph referring to P8 (“maximum distance among walls”)-local damage in (Figure 134). It is expected that these two parameters were strongly related since the P8 is the only parameters related with the local mechanisms behaviour in GNDT II Level Form (Figure 127). The graph shows that there are no correlation between the two parameters. This is confirmed to both the $r(P8, D_{K,LM}) = -0.17$, which highlights a light opposed trend of correlation, and the bubble graph, since a significant percentage of judgment is outside the tri-diagonal area of the matrix. This result, which can seem not reasonable, find its justification in the following reasons:

- The P8 is defined as the ratio among the maximum distance among parallel walls and the thickness of the wall for which the orthogonal walls make restraints. This parameter is evaluated considering all possible walls inside a structural units, not only those related to the main façade. For Castelnuovo aggregates, generally the longer distance among walls is that one orthogonal to the streets, which doesn’t refer to the main façade (see for example the plan in Figure 49). Re-calculating the P8 parameters applied to the main façades, no exclusively

“D” classes are found. The new values distribution for P8 has highlighted that the ranges identified by the VIM for the P8’ classes of judgment are too wide for the considered sample of façades. Further developments of this aspect will be proposed in CHAPTER 8.

- The out-of-plane mechanisms triggered are mostly influenced by pre presence of restraints (connected slabs or tie-rods), the quality and type of masonry and the geometry of the panel in terms of height and thickens. The width of the panel is a secondary element of vulnerability evaluation for overturning.

Table 39: Distribution of % in diagonal and tri-diagonal, upper sum and lower sum for the most correlated coefficients.

	P1-11	P2 - 11	P3 - 11	P9 - 11	P11 - 11	P11 - 15	P14 - 15
Diagonal	33%	32%	26%	32%	27%	24%	30%
Tri-diagonal	64%	67%	69%	80%	78%	64%	82%
Upper sum	33%	32%	31%	70%	90%	64%	64%
Lower sum	100%	100%	95%	63%	10%	60%	67%

From the analysis of the level and type of damages in main façades, it is possible to conclude that there aren’t direct and clear correlations among the distribution of the qualitative parameters relative to the Vulnerability Forms and the distribution of damages relative to local out-of-plane mechanisms.

Consequently, these parameters will not be taken directly into account in the definition of the Façade Form.

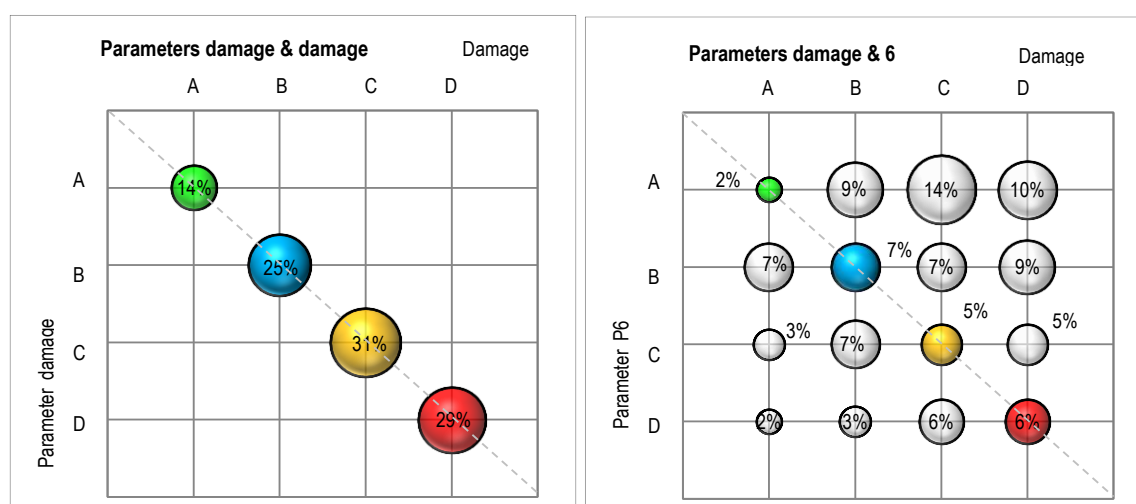
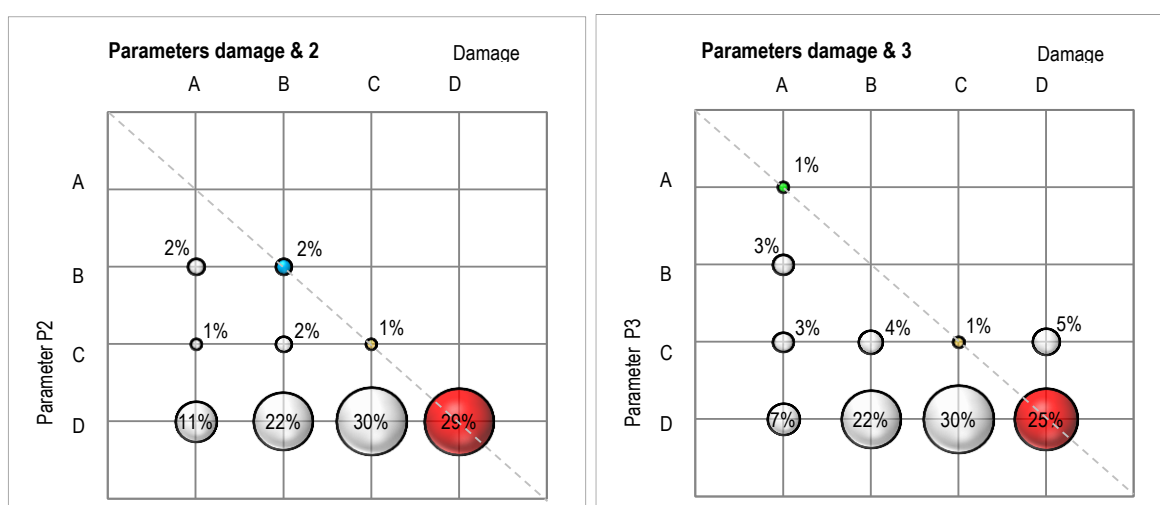


Figure 132: (a) Bubble graph for the parameter “damage level” and itself. (b) Bubble graph for “damage level” and P6 (GNDT).



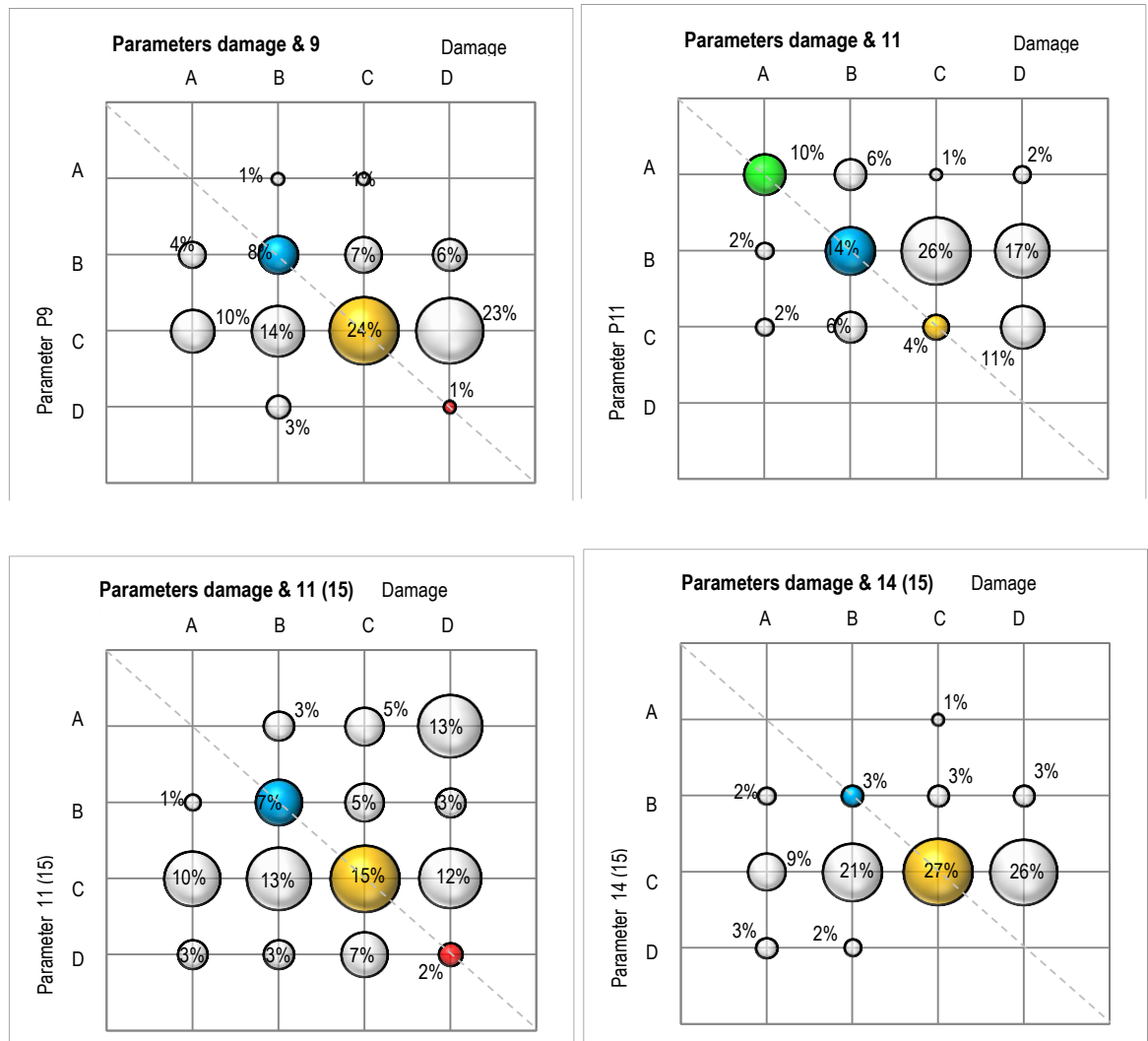


Figure 133: (from the top) Bubble graph for the parameter "damage level" and parameters 2-3-9-11 GNDT and 11-14 Formisano.

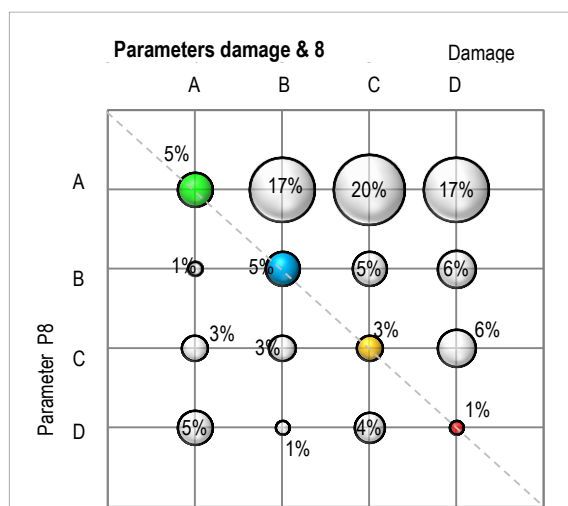


Figure 134: Bubble graph for the parameter "damage level" and parameter 8 GNDT.

CHAPTER 7. SEISMIC RESPONSE OF MASONRY BUILDINGS IN AGGREGATE

The chapter provides the general rules for the study of masonry structures in aggregate through detailed analyses, considering both the local and the global behaviour, as typical of the existing masonry structures. Kinematic linear and non-linear analysis of out-of-plane mechanisms have been chosen to evaluate the seismic capacity for a structural units. That choice is due to different aspects that as the particular constructive technologies in Castelnuovo (very similar to the central zones of Italy), the particular type of masonry (typical of rural historical city centres) and the real damages that have been critically analysed in the aggregates.

In this chapter, the evaluation of the vulnerability assessment is performed with *analytical* methods. They use mechanical or numerical procedures to assign seismic vulnerability on buildings. They can be divided between methods that use basic analytical methods or complex analytical methods, using modern approaches and analyses. The two families are related to the out-of-plane mechanisms response of masonry structures (“mechanisms methods”) and the in-plane global response of it (global “box behaviour”) (Giuffrè A. , 1993).

The analytical methods allow the calculation of the safety index of the structures analysed (I_s). The safety index is defined as the ratio of the seismic capacity of the structure (i.e. in terms of peak ground acceleration, or reference period, T_{RC}), that is the external quantity which brings the structure to the achieve of one pre-fixed limit state, to and the seismic demand referring to the site in which the structure is collocated. The safety index could be well considered a vulnerability index of the structure or, since it involves the seismic demand (hazard), an *index of seismic risk*. It allows in a more specific way respect the vulnerability indexes methods, to create vulnerability rankings on the building stock. The vulnerability ranking with empirical or hybrid methods is a relative vulnerability ranking. The rank defines which are the most vulnerable constructions among a certain group, but without provide information about the seismic verifications, not considering in their analyses the seismic demand (hazard). The risk ranking defined with detailed analysis is an absolute risk indicator e, being done with the evaluation of the vulnerability of the constructions and the hazard of the field in which they are collocated; for this, it allows to compare even structures collocated in different Regions.

7.1 INTRODUCTION

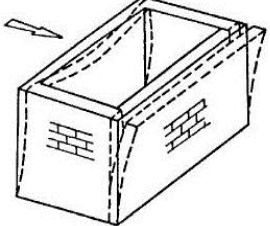
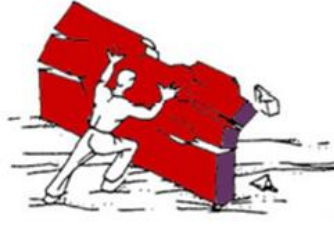
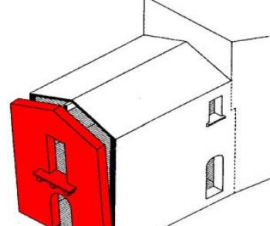
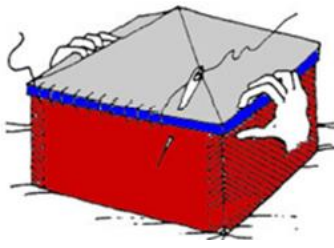
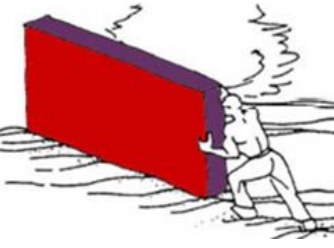
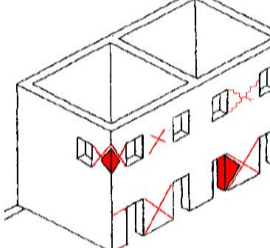
		
Absence of links connection and flexible slabs →	Each wall is subjected to out-of-plane actions (overturning, bending...) →	Out-of-plane mechanisms collapse
		
Good links and connection and stiffness of slabs →	Each wall works in its strong direction →	In plane mechanisms of collapses, global behaviour

Figure 135: Origin of out-of-plane mechanism and in-plane mechanisms (pictures from Toulitos 1996 and (STADATA, 2012).

Masonry offers good resistance to gravity loads, as self-weights, permanent loads, etc., which determine a state of compressive stress and deformation, respect to which it has high values of resistance and stiffness. The seismic action, which is schematised as horizontal load, on the contrary, determines states of stress and strain that may be incompatible with the capacity of resistance of the material (tensile strength), causing the appearance of cracks patterns that denounce the state of suffering of the structure.

Masonry structures can show two categories of collapse mechanisms against horizontal actions: “*first way mechanisms*”, the out-of-plane mechanisms (or local ones, Figure 135top), and the “*second way mechanisms*”, the in-plane mechanisms (Giuffrè A. , 1993) (Figure 135bottom). The first type of mechanisms involves local portion(s) of the structures (the reason they are called “local mechanisms”), which can collapse separately from the main core, due to loss of balance. The second way mechanisms, typical of a structures designed against seismic (or horizontal) actions, allows the seismic global response of all the parts of the structures, exploiting the in-plane stiffness and resistance of each panels.



Figure 136: a) Example of in-plane shear collapse; b) example of overturning of the main façade.

The masonry behaviour depends on different factors of the building characteristics. The age of the construction and the state of conservation of the masonry aggregate assumes great importance. In particular, the age of construction dates the possible Code used in the plan: it is possible to know if seismic actions (or, generally, horizontal actions) were included in the building's project, or, as the common way for old structures, they did not. The oldest aggregates in historical city centres are generally made in squared stone masonry and built following static rules of static science (so called “rules of art”). The floors are designed only for gravity loads and they have support only for some centimetres among the load masonry perimeter panels, almost the necessary to have only a vertical stability. The floors are made with common materials, easy traceable from the historical centre; they are not enough stiff in their plane, because the lack of a rigid slabs in reinforce concrete, which give stability to the joints or the principal beams. In this case, they do not allow the transfer of the seismic actions to the vertical elements, which shows independent out-of-plane mechanisms of collapse when a horizontal action occurs. Therefore, the lack of connections among orthogonal walls, poor connections among roofs/floors and walls make each wall not well connected with the other parts of the structures and the horizontal actions can cause simple or composed overturning of the single block walls, horizontal or vertical bending, overturning of the corner and so on (Figure 137). The single wall behaves as a monolithic rigid body (in which the different masonry leaves can work together or separately) with loss of equilibrium in out of-plane way. Indeed, the safety verifications against these types of mechanisms are based to the hypothesis of the complete monolithic body and made by the limit analysis of the equilibrium, through the kinematic approach (C8A.4, NTC, 2008 §7.2.1.8).

On the other hand, in a structure in which the slabs are enough rigid in their plane and the connections among orthogonal vertical elements and the horizontal elements are effective, all the vertical elements work together contrasting seismic actions with their in-plane stiffness, giving rise to the uniform behaviour of the structure, the “box behaviour”. The in-plane mechanisms can involve the resistant elements in the masonry walls, the piers and the spandrels (see better 7.3.2). Two

mechanisms refer to shear failure, *joints bed sliding* and *diagonal cracking* (Figure 137, right) and one refers to the flexural collapse mode, the *rocking* (CM 2009, NTC 2008, (AA.VV. Manuale delle murature storiche, 2011)). Each mechanisms provides an ultimate value of shear for the panel, $V_{R,BS}$, $V_{R,DC}$, $V_{R,R}$. The minimum of those values is the maximum shear that the panel can provide during an earthquake, called ultimate shear, V_U . This value depends on the geometrical characteristics of the panel, on the material and on the vertical loads acting in the panel.

The masonry structure behaves with its in-plane resistance and, each panel, takes some percentage of the horizontal action on the bases of its stiffness. Depending on the type of seismic analysis done, the safety verification are made in terms of resistance on piers and spandrels (static or dynamic linear analysis) or in terms of global resistance and global ductility of the structure (static non-linear analysis).

When a safety evaluation of an existing masonry building has to be performed, the first step is to consider the local mechanisms, in order to avoid local failure that are related to the complete collapse of a portion of the building. If local mechanisms occur, a global analysis has no realistic sense. Only after having checked that the out-of-plane mechanisms are avoided (in the case of effective connections among orthogonal walls, good characteristics of the masonries, scarfs in the corner among walls and horizontal elements...), the evaluation of the global capacity can be done.

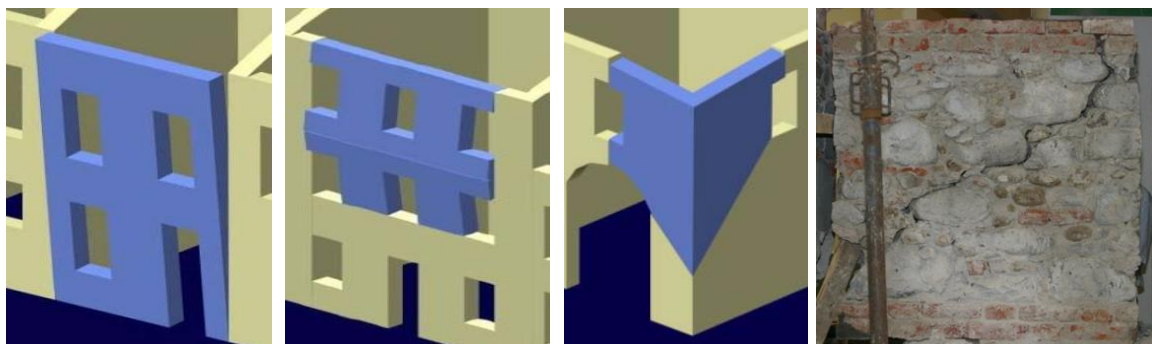


Figure 137: a) Local out-of-plane mechanisms (www.reluis.it); b) in plane mechanisms due to diagonal cracking.

General structural rules expressed up to now are generally working for masonry existing buildings. But, are there more provisions for the buildings in aggregate?

(C.M. n.617, 2009) dedicates a paragraph to aggregate buildings in which there are the explanation of the way to determine and define the structural units and the analysis type that could be performed over there. For Castelnuovo aggregates, one should refer to aggregates of rural town centres, constitute by poor mechanical properties of the masonry. Being the result of a complex historical and temporal process of evolution (Figure 4, Figure 5), aggregates are often characterized by a wide structural variety, disconnections on ss.uu. and they tend to manifest often mechanisms of first way. The walls of adjacent uu.ss. generally do not have the construction requirements of scarfs and the floors also are often poorly connected to the walls and not stiff enough to distribute horizontal actions on vertical elements.

The evaluation of the local mechanisms for ss.uu. within aggregates could relate closely the constraints offered by the various parts of the structural units, in order to consider the mechanisms of wall that really can be triggered. Thus, in addition to the usual definition of the load-bearing walls that can behave singly, for aggregates is necessary to evaluate (eventual) existing crack pattern (i.e. due to seismic past events) or make visual surveys in situ (opening essays in the walls and/or at the cantonals) in order to understand the degree of constraints between the adjacent ss.uu. and the to choose the major plausible façades to investigate (ReLUIS, 2010).

As for the global analysis, under the assumption of the "I-mechanisms inhibit", the analysis of the aggregates can be done through simplified calculations, whereas the portion of the aggregate of interest (UMI) and adjacent structural units effects should be taken into account (C8A.3, NTC 2008 and LR, 2012). It means dividing the entire aggregate in some homogeneous interacting portions that, for same origins and structural characteristics, could be studied together. The global modelling of the whole aggregate, especially if it is complex, can lead to unreliable results, primarily due to the strong assumption of being able to explicit global collaboration of all its structural parts.

7.2 OUT-OF-PLANE MECHANISMS

Out-of-plane mechanisms involve walls subjected to horizontal actions orthogonal to their plane, the plane in which they have minor stiffness. They refer to the collapse of a portion of aggregates (usually main and rear façades) for loss of equilibrium. Different types of mechanisms are individuated for masonry structures, since after main recent Italian earthquakes (Marche 1997-98, Abruzzo 2009, <http://terremotoabruzzo09.itc.cnr.it>), they showed out-of-plane mechanisms as most frequent types of collapse, in deep analysed in specific scientific works (D'Ayala and Paganoni, 2011, Lagomarsino 2012, Cattari et al., 2012).

The mechanisms can be grouped on three main sets: overturnings, vertical bendings and horizontal bendings. Within these groups, there are other subgroups in relation to the geometries and the portion of the wall involved in the mechanisms (AA.VV. Manuale delle murature storiche, 2011). The mechanisms indeed could be simple or complex, involving only the main façade or the corner portion of wall, too. In Table 40, there are some examples of mechanisms type with the ideal scheme of calculation and the explicative photos of the crack patterns, directly taken from the Castelnuevo aggregates.

In Milano et al., 2009 and “Repertorio dei meccanismi di danno, delle tecniche di intervento e dei relativi costi negli edifici in muratura nella Regione Marche” (<http://www.edilizia.regione.marche.it/>) there are available reports and abacus of out-of-plane mechanisms that, individuated in historical city centres due to the past earthquake, help the recognition of the vulnerability aspects of buildings in aggregate and allows to define how verification should be done. The documents collect images explaining the crack patterns that occur and identify, as well as an explanation of the mechanism, the aspects that most affect the activation of them: constraint conditions, symptoms and possible variants of the mechanism. In the following, the explained characteristics of the overturning mechanisms are reported, since it is the most frequently mechanism encountered in Castelnuevo aggregates.

RESTRAINS

- No connection to the plans.
- No connection between orthogonal walls.

VULNERABILITY

- Horizontal elements deformable.
- Presence of thrusts (as vaults or roof orthogonal to the façades).

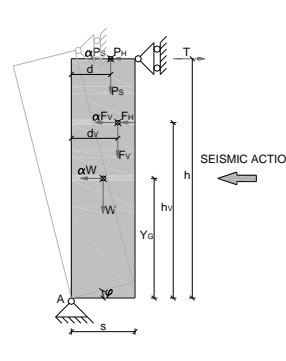

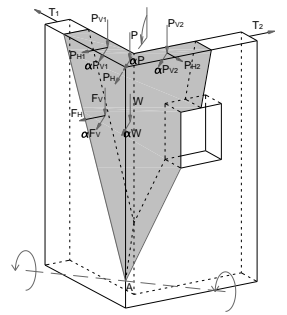

SYMPTOM

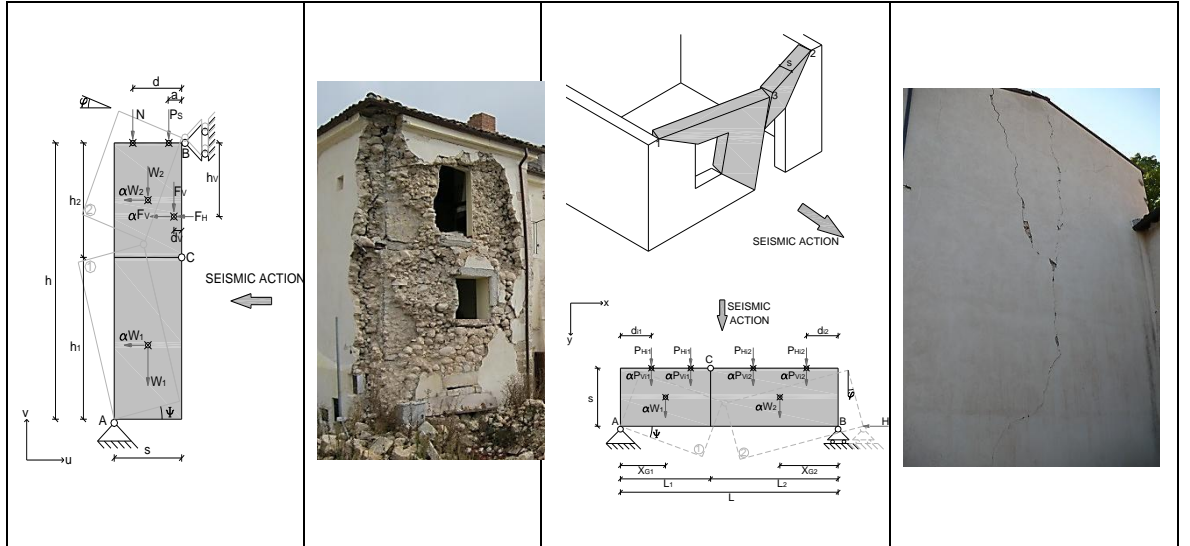
- Vertical cracks at the cantonal level.
- Deployment of the beams of the horizontal elements (crack on the floors or ceiling).

VARIANTS

- One or more leaves of the wall, in relation to the presence of connection to the plans.
- Full thickness of the wall or the out-leaf only, in relation to the characteristics of masonry cross-section.
- Different geometries of the wall, in relation to the presence of discontinuities (holes in façades, different heights).

Table 40: Type of mechanisms and examples in Castelnuevo façades (Drawings from Ciavattone Master thesis, Unifi).

Overturning: aggregate in Castello		Corner overturning, aggregate 13-158 s.u.7	
			
Vertical bending, aggregate 57-179 s.u.1		Horizontal bending, aggregate 25-217	



7.2.1 CALCULATION METHOD

The calculation method is based on the limit analysis of a rigid body, with the determination of the minimum multiplier of horizontal loads (α_0), through the application of the second theorem of the limit analysis (kinematic theorem). The method is based on equilibrium equations by writing the equation of the Principle of Virtual Work (Eq.(23)):

$$(23) \quad \alpha_0 \left(\sum_{i=1}^n P_i \delta_{x,i} + \sum_{j=n+1}^{n+m} P_j \delta_{x,j} \right) - \sum_{i=1}^n P_i \delta_{y,i} - \sum_{h=1}^o F_h \delta_h = L_{fi}$$

where:

- n is the number of blocks which characterizes the mechanisms (n° of self-weight applied in the macro-blocks);
- m is the number of the weight forces not applied to the elements of kinematic chain elements but whom masses, with the effect of seismic actions, are able to generate horizontal forces on the kinematic chains;
- o is the number of external forces, assumed independent from the seismic action, applied to the different blocks;
- P_i is the resultant of the weights-forces applied to the k -th block;
- P_j is the resultant of the weight-force not directly applied to the k -th block, but whose mass determines on it a horizontal seismic action, since it is not efficaciously transmitted to another part of the structure;
- F_h is the generic external force applied to one of the blocks;
- $\delta_{x,i}$ is the virtual horizontal displacement of the application point of the i -th weight P_i , assumed as positive if directed as the seismic force that triggered the mechanism;
- $\delta_{x,j}$ is the virtual horizontal displacement of the application point of the j -th weight P_i , assumed as positive if directed as the seismic force that triggered the mechanism;
- $\delta_{y,i}$ is the virtual vertical displacement of the application point of the P_i , assumed as positive if upwards directed;
- δ_h is the virtual displacement of the application point of the external force F_h , projected in its direction;
- L_{fi} is the total work of the possible internal forces (tie-rod extension, friction sliding in presence of good connection of the slabs; in this case, the phenomena are not contemplated in the work).

In Figure 138, there is the example of a simple overturning of a monolithic two-storey wall. There are reported all forces taken into account for two-hinge configurations. N_{Hi} are the horizontal thrusts, N_{Vi} are the vertical slabs load and W_i are the self-weights of the panels. Italian Code (NTC, 2008) provides two procedures for the evaluation of safety verification against the out-of-plane mechanisms: the use of the linear analysis and non-linear analysis. The methodology concerns the application of kinematic linear model, the calculation of the seismic capacity (acceleration or displacement depending on the type of analysis), the calculation of the seismic demand and finally compare the quantities in order to provide an safety index (I_s).

The rigid blocks are subjected to the forces:

- The blocks self-weights, applied in their barycentre, W_i ;
- The permanent weight carried by the walls (roofs, floors...), applied with a certain eccentricity e_i , N_{Vi} ;
- A system of horizontal forces proportional to the vertical mentioned above αW_i αN_{Vi} ;
- Horizontal external forces, N_{Hi} (for example those of metallic ties (+) or pushing force (vaults) (-);

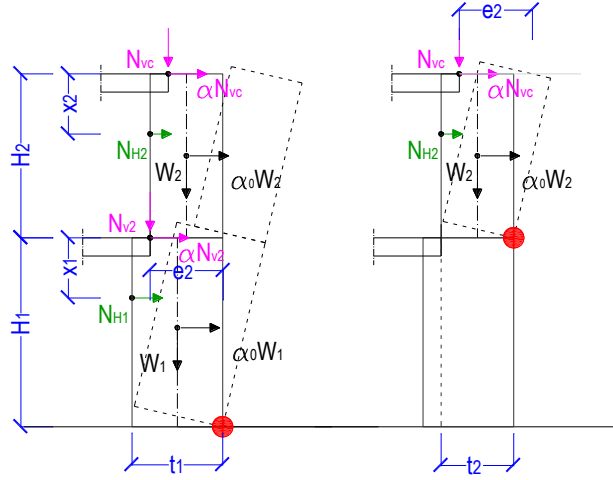


Figure 138: α_0 calculation in the case of overturning of a monolithic wall with 2 floors: forces and hinge individuations.

7.2.1.1 LINEAR KINEMATIC ANALYSES

To evaluate the capacity of structure for mechanisms method, the equation (23) is applied to each macroblock individuated. In the linear kinematic analysis, the equation of the PVW is written in the initial configuration (with infinitesimal rotation θ). The equation of the PVW is equal to the formulation of the limit equilibrium of rotation around the hinge configuration (which position can varies in different height of the structure). With this simplification, the virtual displacements associate with the application point of generic forces (δ_{xi}) are identical to the arms that the associate forces would have for the calculation of a rotation equilibrium around the hinge configuration. Thus, α_0 can be calculated as the ratio of stabilizing moment and overturning moment. An example is reported on the following: it refers to the Figure 138b, in which N_{H2} is equal to 0.

$$M_S = W_2 \frac{t_2}{2} + N_{V2} e_2$$

$$M_O = \alpha_0 W_2 \frac{h_2}{2} + \alpha_0 N_{V2} h_2$$

$$\alpha_0 = \frac{W_2 \frac{t_2}{2} + N_{V2} e_2}{W_2 \frac{h_2}{2} + N_{V2} h_2} = \alpha_{0critic}$$

Once known the α_0 , the determination of the acceleration that triggers the mechanisms comes from the knowledge of the M^* . This quantity, the participating mass to the mechanisms, is evaluated considering the virtual displacement of the application points forces associated to the kinematic movement.

$$M^* = \frac{(\sum_{i=1}^{n+m} P_i \delta_{x,i})^2}{g \sum_{i=1}^{n+m} P_i \delta_{x,i}^2}$$

where:

$n + m$ is the number of weight forces considered as horizontal seismic force;

$\delta_{x,i}$ is the horizontal virtual displacement of the application point of P_i .

The seismic acceleration of capacity is the result of the multiplying the coefficient α_0 for the g gravity and dividing this quantity for the participation mass to the kinematic movement. (C.M. n.617, 2009):

$$a_0^* = \frac{\alpha_0 \sum_{i=1}^{n+m} P_i}{M^* FC} = \frac{\alpha_0 g}{e^* FC}$$

where:

g is the gravity acceleration;

$e^* = \frac{gM^*}{\sum_{i=1}^{n+m} P_i}$ is the participation mass factor;

FC is the confident factor (C.M. n.617, 2009), equal to 1.35.

If the system of blocks is assumed as infinitively stiff, the multiplier of the horizontal forces represents directly the peak acceleration (in terms of g) of the structure motion at the level where the mechanism is connected with the rest of the structure, assuming $FC = 1$. Writing the equations for one-floor structure where only self-weight is present (Figure 138b):

$$\alpha_0 = \frac{W_2 \frac{t_2}{2}}{W_2 \frac{h_2}{2}} = \frac{t_2}{h_2} = \alpha_{0critic}$$

Figure 139 shows the trend of the α_0 versus the slenderness of the panel, calculated as the ratio between h/t , with h , panel height, varies into range 1.5-5 m and t , panel thickness, into range 25-60 cm. In particular, for a panel with a thickness of 60 cm (usual in masonry existing buildings, like in Castelnuovo), with a height of 1.5 m, the α_0 coefficient values 0.4, while when the height is 5 m, the α_0 is 0.12. The participation mass is calculated and it is the entire mass associated to the self-weight of the structure, no other force are assumed to act.

$$M^* = \frac{(\sum_{i=1}^{n+m} P_i \delta_{x,i})^2}{g \sum_{i=1}^{n+m} P_i \delta_{x,i}^2} = \frac{(W_2 \frac{h_2}{2})^2}{g W_2 \frac{h_2^2}{4}} = \frac{W_2}{g} \rightarrow e^* = \frac{gM^*}{\sum_{i=1}^{n+m} P_i} = \frac{gW_2}{gW_2} = 1 \rightarrow a_0^* = \frac{\alpha_0 g}{e^* FC} = \alpha_0 g$$

The value of the capacity acceleration is, respectively, $a_0^* = 0.4[g] = 3.92 \text{ m/s}^2$ e $0.12[g] = 1.17 \text{ m/s}^2$.

If the procedure is repeated for a panel subjected to the self-weight and the slab force on the top (N_{v2} on Figure 138c for example) e^* assumes value ~ 0.95 and the α_0 coefficient is not equal to the value of the capacity acceleration in unit of $[g]$.

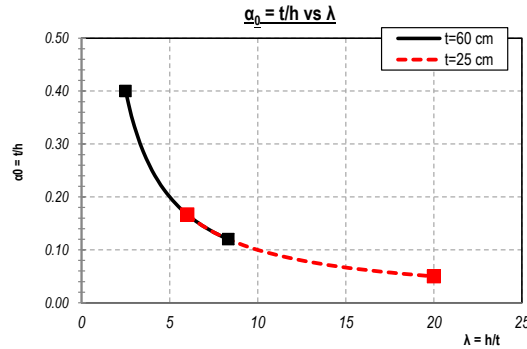


Figure 139: Single floor structure, with one single force applied (self-weight); trend of α_0 versus the panel's slenderness.

7.2.1.2 NON-LINEAR KINEMATIC ANALYSES

In order to evaluate the displacement capacity of the local mechanism until the collapse, it is possible to evaluate the horizontal multiplier in the consecutive varied configuration, which represent the development of the examined kinematic chain. The displacement associated to the development of the mechanism are indicated with d_k . An example of the shape of a capacity curve, following provision of Circ.617/09 is reported in Figure 140a. If there are no internal resistance forces which can increase with the displacement (i.e. deformation of the tie-rods), the multiplier gradually decreases up to the configuration which corresponds to capacity acceleration equal to zero that is when the block loses its equilibrium in a static condition (Figure 140b).

In the non-linear static analyses, the collapse situation of the mechanism is calculated in the deformed configuration for a finite value of θ . Indeed, in the Figure 140a there is showed the calculation of the virtual displacements associated to the self-weight (W) and floor forces (N_v) of one single floor of the structure. The displacements follow equations on the left:

$$\delta_{x\alpha_0 W} = \frac{h}{2\sin(\theta)} + \left(\frac{t}{2} - \frac{t\cos(\theta)}{2} \right) \rightarrow \delta_{x\alpha_0 W} = -\frac{h}{2}\cos(\theta)\dot{\theta} + \frac{t}{2}\sin(\theta)\dot{\theta}$$

$$\delta_{yW} = h - h\cos(\theta) - \frac{t}{2\sin(\theta)} \rightarrow \delta_{yW} = -\frac{h}{2}\sin(\theta)\dot{\theta} + \frac{t}{2}\cos(\theta)\dot{\theta}$$

$$\delta_{x\alpha_0 N_v} = h\sin(\theta) + e - e\cos(\theta) \rightarrow \delta_{x\alpha_0 N_v} = h\cos(\theta)\dot{\theta} + e\sin(\theta)\dot{\theta}$$

$$\delta_{xN_H} = \bar{h}\sin(\theta) + \bar{e} - \bar{e}\cos(\theta) \rightarrow \delta_{xN_H} = \bar{h}\cos(\theta)\dot{\theta} + \bar{e}\sin(\theta)\dot{\theta}$$

$$\delta_{yN_v} = h - h\cos(\theta) - e\sin(\theta) \rightarrow \delta_{yN_v} = -h\sin(\theta)\dot{\theta} + e\cos(\theta)\dot{\theta}$$

Deriving each quantity in order to write the displacement increment for each configuration (on the right in the equations) it is possible, writing the Equation of Principle of Virtual Work, to find the minimum value of the angle θ that makes the α_0 equal to zero. If there is only the force of the self-weight (Figure 140b), the θ minimum can also be determined in a graphic way: it is the rotation angle whit which the barycentre of the rigid body reaches the vertical position (parallel to the vertical axis crossing the hinge point). The trend of α_0 is assumed linear with the displacement. The shape of the capacity curve is than note when the displacement $d_{k,0}$ is calculated (the value with which the α_0 is 0). The α_0 vs d_k curve assumes the expression in (24):

$$(24) \quad \alpha = \alpha_0 \left(1 - \frac{d_k}{d_{k,0}} \right)$$

In which the control point displacements is calculated by the Principle of Virtual Works, assuming $\alpha_0=0$ and taking the correspondent value of $d_{k,0}$. The control point could be assumed as the point at the maximum height of the structure or the barycentre of the structures. In terms of safety verification it does no matter which one point is considered.

Once knowing the trend of α in function of the d_k , it is possible to define the capacity curve of the structure, a^* vs d^* . The participation mass M^* (equivalent oscillator SDOF) is evaluated considering the same equation for the linear kinematic analysis procedure, that is

$$M^* = \frac{(\sum_{i=1}^{n+m} P_i \delta_{x,i})^2}{g \sum_{i=1}^{n+m} P_i \delta_{x,i}^2}$$

The spectral displacement of the SDOF is obtained as average value of the P_i -displacements (weighted in the P_i force). One should define the spectral displacement, with reference to the initial virtual displacements:

$$(25) \quad d^* = d_k \frac{\sum_{i=1}^{n+m} P_i \delta_{x,i}^2}{\delta_{x,k} \sum_{i=1}^{n+m} P_i \delta_{x,i}}$$

And, assuming stable the forces P_i during the analysis, the capacity curve is defined by the Eq.(26):

$$(26) \quad a^* = a_0^* \left(1 - \frac{d^*}{d_0^*} \right)$$

d_0^* is the spectral displacement corresponding to the $d_{k,0}$ displacement;

The ultimate displacement, d_u^* , is fixed depending of the limit state considered (§7.2.1.4).

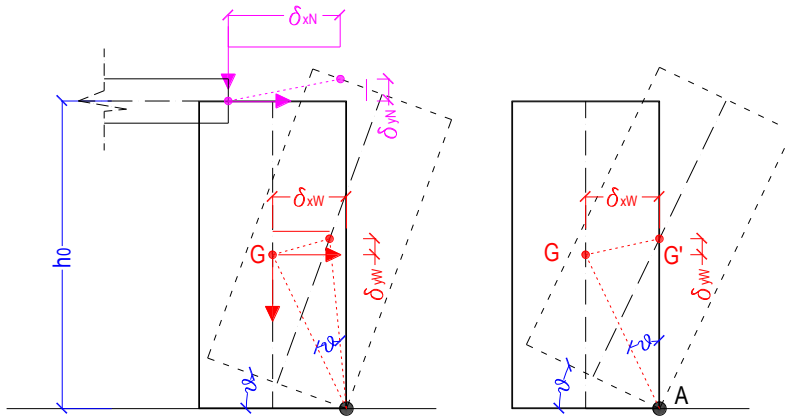


Figure 140: (a) kinematic analysis with finite rotation; (b) angle θ such as the collapse is guarantee.

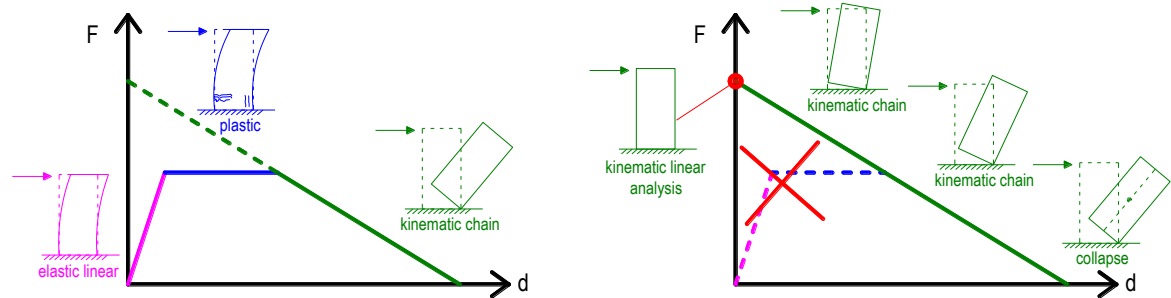


Figure 141: Evolution of the capacity curve of the mechanism.

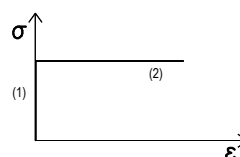
7.2.1.3 MODEL HYPOTHESIS AND ANALYSIS PROCEDURE FOR MECHANISM COLLAPSE

The procedure should be applied for all type of mechanisms that could appear on the masonry depending on the type of geometrical and restraint characteristics of the panels. All possible collapse mechanisms have to taken into account, and the most probable mechanism is that with a minimum value of α_0 . Summing, the procedure follows the following steps:

- Individuation of the mechanisms (the most probable, or all possible, depending on the geometrical dimensions, on the restraints among the walls);
- Transformation of a structure part in a labile system, with the individuation of rigid body that can rotate;
- Evaluation of the α_0 coefficient, that represents the horizontal load multiplier that triggers the mechanism;
- Evaluation of the evolution of α coefficient (horizontal load multiplier) with the growing up of a d_k , a control node displacement of the kinematic chain. The curve should be plotted up to the value $\alpha=0$, which represents the loss of resistance in terms of horizontal actions;
- Calculation of the rotation angle θ for which $\alpha=0$. It could be done both in a graphic way (when the barycentre of the structure, considering all the force in play, becomes vertically aligned with the position of the hinge) or in a analytical way, considering a succession of finite rotation and writing for each of them, the configuration of the system (Equation of Principle of Virtual Works);
- Transformation of the curve α_0-d_k in the capacity curve a^*-d^* and evaluation of the last displacement for collapse of mechanism (ultimate limit state);
- Calculation of the safety indexes, with the check of the capacity-demand in terms of acceleration and/or displacements.

In this context, at the base of that procedure there are the following hypothesis:

- Null tensile resistance of masonry, rigid perfect plastic material behaviour;



- Absence of sliding from the blocks;
- Infinite compressive resistance for the masonry (see (*) 7.2.1.9);
- Forces stable during the kinematism evolution; in this way, the resulting capacity curve ($\alpha-d_k$ or $a_0^*-d_u^*$) is almost linear (if not, the curve would be a sum of segments).

Despite of the hypothesis assumed, in the analysis, it is opportune to consider:

- The different position of the hinge configuration in the thickness due to the elimination of the infinite compressive strength of the masonry;
- Presence of steel tie-rods;
- If present, more than one layer of masonry (two layers with separated collapse mechanisms).

7.2.1.4 LIMIT STATES AND SAFETY VERIFICATIONS FOR LOCAL MECHANISMS

The resistance and the displacement capacity related to the Damage State Limit and Safety State Limit (respectively SLD e SLV, §2.1 e §2.2 (NTC, 2008)) are evaluated in the capacity curve, in correspondence of the following points:

- SLD: of the spectral acceleration a_0^* , correspondent at the activation of the damage mechanism;
- SLV: of the spectral displacement d_u^* that can be defined as the:

- a) the 40% of the displacement for which a^* is equal to 0 (d_0^*) (Figure 142);
- b) the displacement with which there is a collapse of a structural part of the building.

The latter point is not well defined in the Standard. This quantity is variable with the effective geometrical details of the panel. Usually, the limit of the displacements refers to the collapse (disconnection) of the floor. As already seen in §3.3.2, the slabs in Castelnuovo aggregates are generally flexible and the support length of the wall is around 10-20 cm. For the model calculation the eccentricity (distance from the point of application of the load up to the hinge configuration, in the cross section), a plastic distribution of stresses have been considered (that is the reaction resultant force is applied in the middle of the discharge area Figure 152b) or, for particular case, the correct distance is assumed as in the case of the vaults. 15 cm is the max displacement that the upper part wall could reach since larger displacements could induce the slab collapse. In the rigorous (standard) calculation, the displacements at the top of the structure arrives at values major of 50 cm, incompatible with the presence of slab discharging in the wall that overturns. For this reason, in the following, the calculation with non-linear analysis will be performed with both the absence and the presence of the displacement limit in the last height floor.

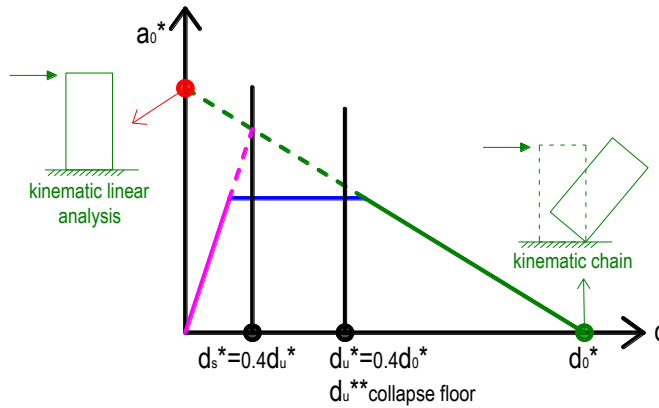


Figure 142: Scheme of the evolution of the mechanisms based on the Italian Seismic Code (C.M. n.617, 2009) (NTC, 2008).

7.2.1.5 DAMAGE LIMIT STATE (SLD)

The safety verification against the SLD is satisfied if the spectral acceleration (of activation of the mechanism) is superior of seismic demand acceleration. In the case that the verification regards an isolated element or portion of the structure clamped to the earth, the seismic acceleration is the peak ground acceleration: the acceleration response spectrum (§3.2.6, (NTC, 2008) for $T=0$.

$$a_0^* \geq a_g(P_{VR})S$$

a_g is the ground maximum acceleration;

S is the soil coefficient that keep into account the ground category and the topographic coefficient (§1.1.1.1.1).

On the contrary, if the mechanism involves a portion of the structure in a certain altitude, the verification is satisfied if:

$$(27) \quad a_0^* \geq S_e(T_1)\gamma\psi(Z)$$

$S_e(T_1)$ is the ordinate of the elastic spectrum in correspondence of T_1 , where T_1 is the first period of vibration of the whole structure in the considered direction (simplified formula, NTC 08).

$\psi(Z) = Z/H$ where H is the height of the structure (starting from the foundation) and Z is the barycentre of the restraint of the macro-blocks interested in the mechanisms;

γ is the participation coefficient modal mass; evaluated as $3N/(2N+1)$, where N is the number of floors of the structure.

In the case of local mechanisms, the SLD corresponds to the happening of first crack patterns into a local part of the structure; thus in the masonry structures this limit state is not requested (and in this work not considered).

7.2.1.6 SAFETY LIMIT STATE (SLV)

The verification of the Safety Limit State (SLV) of local mechanisms, can be carried out with one of the following two criteria.

A) Simplified Check with behaviour factor q (linear kinematic analysis)

In the case where the verification relates to an isolated element or a portion of the construction, clamped to the ground, the safety verification is satisfied if the spectral acceleration a_0^* related to the activation of the mechanism satisfies the following inequality:

$$a_0^* \geq \frac{a_g(P_{VR})S}{q}$$

In which q is the behaviour factor equal to 2 (§1.1.1.1.1).

If the local mechanism affects a portion of the construction placed at a certain altitude, the demand acceleration is typically amplified compared to those at the ground level. An approximation acceptable consists in verifying, in addition to the ground level verification (previous equation), also:

$$(28) \quad a_0^* \geq \frac{S_e(T_1)\gamma\psi(Z)}{q}$$

B) Verification with the capacity spectrum (kinematic non-linear analysis)

The safety verification consists in the comparison between the last capacity displacement d_u^* and the demand displacement d_D , obtained from the displacement spectrum in correspondence of the secant period of the structure T_s (with reference to Figure 142). It is determined using the relationship:

$$T_s = 2\pi \sqrt{\frac{d_s^*}{a_s^*}}$$

where: $d_s^* = 0.4 d_u^*$ e a_s^* is the acceleration that correspond to the displacement d_s^* .

If the seismic verification is for elements that are clamped to the earth, the equation to be considered is:

$$d_u^* \geq S_{De}(T_s)$$

Where the $S_{De}(T_s)$ is the elastic response spectrum in terms of displacement in correspondence of the T_s period.

If, on the other hand, the local out-of-plane mechanism interests a local part of construction in height, it is necessary to consider the displacement response spectrum at the altitude of the collapse mechanism, with the following relation:

$$(29) \quad d_u^* \geq S_{De}(T_1)\psi(Z)\gamma \frac{\left(\frac{T_s}{T_1}\right)^2}{\sqrt{\left(1-\frac{T_s}{T_1}\right)^2 + 0.02\frac{T_s}{T_1}}}$$

Where $\psi(Z)$ and γ are already defined, for the linear case,

$S_{De}(T_1)$ is the elastic response spectrum in terms of displacement in correspondence of the T_1 period.

7.2.1.7 RESULTS FOR THE AGGREGATE 10-088

In the figures above, different situations of clear identification of the out-of-plane mechanisms in the main façades are showed. In each case, both the photographic documentation of the out-of-plane damages and the ideal schematisation of the macroblock that collapses for overturning are provided.

As a case study to explain the procedure of the calculation of the out-of-plane mechanisms of the main façade of the structural unit 9 of the 10-088 aggregate is analysed (Figure 144 ÷ Figure 151).

7.2.1.7.1 Geometry and loads data: input

In the first part of the calculation, there is the identification of the panel geometry in terms of length, height, thickness, %

of holes, etc., and the determination of the loads that charge the panel (vertical and horizontal loads). The weights are related to the self-weights of the panel (properly individuated with the identification and measurements of all the holes in the panel) and to the type of floors that charge the panel (I-beams and hollow tiles, vaults, etc., as explained in §3.3.2). In Figure 143 there is the identification of the three storeys' plans (ground, first and second floor) of the s.u. investigated for the mechanism, with the information of the geometries and load in play.

Table 41: Aggregate 10-088 and 30-283 main façades: real photo and overturning representations


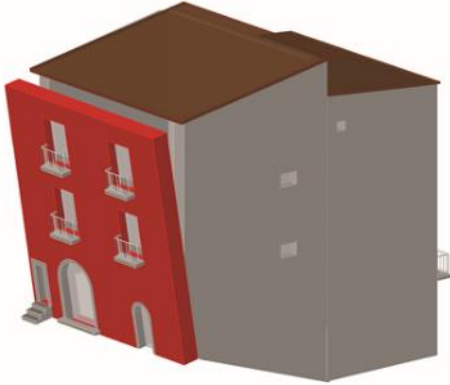

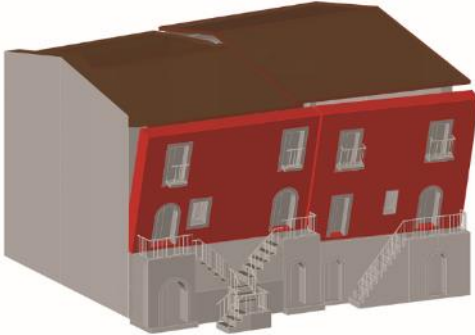
	
Aggregate 10-088 s.u.9	
	
Aggregate 10-088 s.u 4-5 and 6	



Figure 143: S.u. 9 of 10-088 aggregate.



Figure 144: Front of the s.u. 9, transverse section and identification of the 3 level of the structure.

7.2.1.7.2 Results and safety index

Three are the levels of the structures and three are the possible calculated mechanisms, with the hinge configuration respectively at ground, first and at second floor (Figure 144b, in blue are highlighted the hinges). Each mechanisms is analysed and for each of them the value of the seismic capacity (in acceleration and displacement) is provided.

To determine the safety index, the response spectra in terms of acceleration and displacements are adopted (§1.1.1.1), with the ground “A” masonry category and T_1 topographic conditions, in order to compare the capacity of the structure with the demand of the reference site, without considering the influence of the different ground type. As already written (§7.2.1.6) for the non-linear kinematic analysis the ultimate displacement of the SDOF for the structure could be defined in different way. It can be assumed as the 40% of the d_u^* or the displacement for which the upper floor collapses. In considering the latter procedure, the mechanism stops when the control point displacement expires, without considering the section of the curve corresponding at the mechanism without the load of the last floor. In this case, the framework of the last floor is at right angles to the façade and the mechanism could cause the collapse of the interest area of one I-beams (examples on Figure 52).

Table 42: Geometry and loads data: input for the kinematic linear and non-linear analysis

Aggregate		10-088		S.U.		9 - Front	
Data	Number of structure floors		3				
	H _t =		9.24		[m]		
	T ₁ =C*H ^{3/4}		0.265		[s]		
Masonry	Masonry type		Disorganised stone Masonry (Cat.I)				
	weight, w =		19		[kN/m³]		
	length, L =		9.7		[m]		
Geometry and Loads	GROUND FLOOR	1 ST FLOOR	2 ND FLOOR	-	COVERAGE		
h [m]	3.00	3.12	3.12	-	-		
t [m]	0.70	0.55	0.55	-	-		
h _w [m]	1.67	4.64	7.76	-	-		
d _w [m]	0.35	0.275	0.275	-	-		
W [kN]	273.58	276.55	276.55	-	-		
N _v [kN]	10.74	18.74	21.47	-	4.22		
e [m]	0.55	0.40	0.40	-	0.40		
h _{NV} [kN]	3.00	6.12	9.24	-	9.24		
N _H [kN]	-	-	-	-	-		
F [kN]	-	-	-	-	-		
h _{NH} [kN]	3.00	6.12	9.24	-	-		
e _{NH} [kN]	0.00	0.00	0.00	-	-		

Table 43: Results for the linear analyses.

Safety Verifications	M Stabilize	M Outrigger	Multiplicator	Capacity	Demand	IS safety index
Mechanims type	M_s [kN*m]	M_o [kN*m]	α_0	α_0^* [m/s ²]	a_D [m/s ²]	
Ground floor hinge	275.67	4269.87	0.065	0.60	1.26	0.47
1 st floor hinge	173.21	1988.96	0.087	0.78	1.26	0.62
2 nd floor hinge	88.26	533.83	0.165	1.27	2.54	0.50

In Table 42 there are the panel characteristics, with the identification of loads and geometry. In Table 43 there are the results on terms of linear analysis with the determination of both the stabilizing and destabilizing moments and the multiplier of the horizontal loads, α_0 , while in Table 44 there are the results in terms of non-linear analysis, associated to the capacity curve with all the force considered as stable during the procedure.

From a first evaluation, the less capacity for the structure is associated to the 3-floors mechanisms, with an acceleration of capacity of 0.60 m/s² in linear analysis. This is in line with the formulation of the methods just considering only the self-weight of the panel: the multiplier α_0 (and α_0^*) is inversely proportional to the structure height (see Figure 139 also). Regarding the safety index, with the linear analysis, no one of the three mechanisms studied is satisfied while the I_s is always less than one. The ground floor hinge mechanism has the minimum safety index, equal to 0.47. It is associated to the less value of the minimum multiplier horizontal loads value, 0.065. In 1st floor hinge the multiplier is 0.087 but the safety index is 0.62, while in the 2nd floor hinge mechanism the value of α_0 is 0.165 (much more high), but the safety index is 0.50. This is due to the seismic demand that grows with the height. Indeed, following the Eq. (28), the seismic demand of acceleration at the top is 2.54 m/s² while considering only one or two floors the seismic demand is 1.24 m/s².

Figure 145a shows the trend of the horizontal multiplier of the loads with the displacements of the control point, following the (24) equation (d_k - α_0 curve) and the capacity curve (d^* - α_0^*) of the three mechanisms analysed with non-linear analysis keeping displacements the collapse of the entire structure. The last displacements of the three mechanisms are reported in dotted line in the graph. In detail, each mechanism has its own capacity curve, shown in Figure 146, in which the seismic demand and the seismic capacity are reported, too.

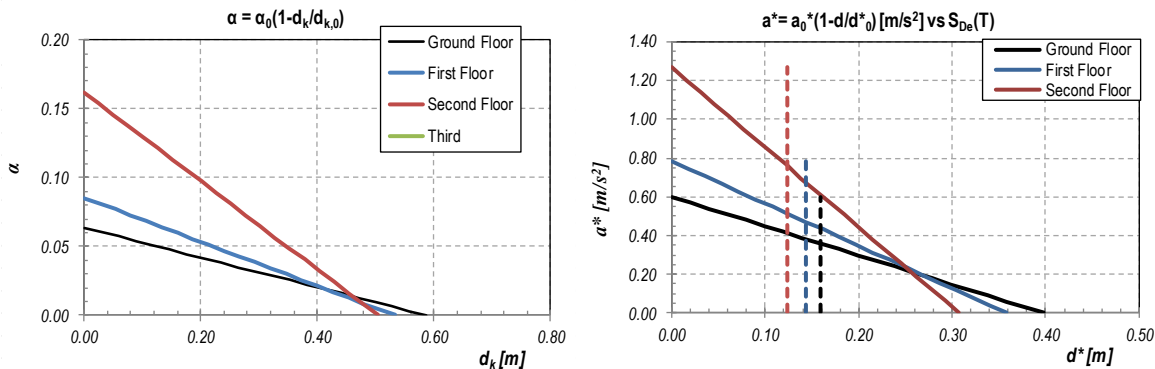
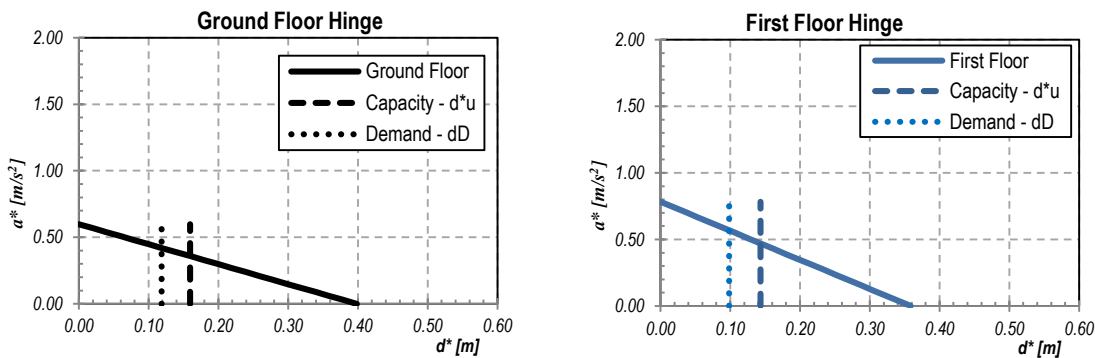


Figure 145: (a) Trend of horizontal multiplier vs displacement of the control point; (b) Capacity curves.



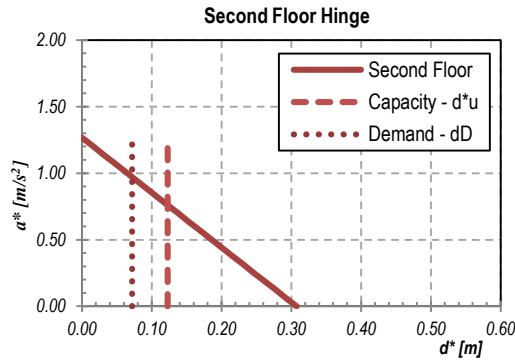


Figure 146: Capacity curve for each mechanism, individuation of the capacity last displacements and demand displacement.

The results of the non-linear analysis refreshes the first vulnerability classification of the linear analysis: the ultimate rotations for the analysed mechanisms grew up for less height mechanisms. The seismic capacity is evaluated as the 40% of the last displacement acceptable for the structure, calculated with the rigorous method. The seismic demand is evaluated with the Eq.(29) and the I_s of the mechanisms are greater than one. The most vulnerable mechanism is with the hinge configuration at the first floor, however with a safety index of 1.34.

The displacement in the curve $d_k - \alpha_0$ are extremely high, arriving at about 60 cm for the 3-floor mechanism and 32 cm for the 1-floor mechanism. These displacements are in contrast with the presence of the floor at the top of the panel, which can collapse even before the 20 cm of displacement. For this reason, in Table 45 there are the results for the non-linear analysis in the case of collapse of the top-floor associated to a max displacement of 15 cm. This length will be considered for all the mechanisms analysed, both in the case of the framework parallel to the main façade and in the orthogonal one.

Table 44: Results for the non-linear analyses.

Safety Verifications	Rotation	Capacity	Demand earth	Demand in height	Demand	I_s safety index
Mechanims type	θ_i [°]	d_u^* [cm]	$S_{de}(T_s)$ [cm]	$S_{de}(T_s)^*$ [cm]	d_D [cm]	
Ground floor hinge	3.69	15.95	11.87	-	11.87	1.34
1 st floor hinge	4.98	14.34	9.83	3.62	9.8	1.46
2 nd floor hinge	9.39	12.30	7.18	5.72	7.2	1.71

Table 45: Results for the non-linear analyses, in the case of collapse of floor for maximum displacement of 15 cm.

Safety Verifications	Rotation	Capacity	Demand earth	Demand in height	Demand	I_s safety index
Mechanims type	θ_i [°]	d_u^* [cm]	$S_{de}(T_s)$ [m]	$S_{de}(T_s)^*$ [m]	d_D [m]	
Ground floor hinge	0.93	10.02	11.14	-	11.14	0.90
1 st floor hinge	1.38	9.90	9.68	3.57	9.68	1.02
2 nd floor hinge	2.75	8.95	7.24	5.77	7.24	1.24

The difference in terms of safety indexes for the three type of analyses and for the three hinge configurations are reported in Table 46, in which it is observed that the linear analysis is precautionary given its results are in average from 2 up to 2.87 times lower that the other analyses types. The difference among the non-linear analyses are not so marked (1.38-1.5 times).

Table 46: Differences among the safety indexes.

Mechanims type	Non-Linear Linear	Non-Linear floor Linear	Non-Linear Non-Linear floor
Ground floor hinge	2.83	1.90	1.49
1 st floor hinge	2.35	1.65	1.43
2 nd floor hinge	3.44	2.49	1.38



Figure 147: Aereal photo of aggregate 18-163 after earthquake. Render of aggregate (from Fabio Ferrari, Master Thesis)

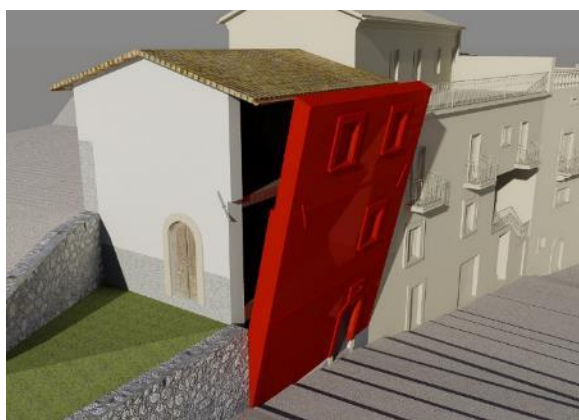


Figure 148: S.u.1. frontal and lateral overturning (from Fabio Ferrari, Master Thesis)

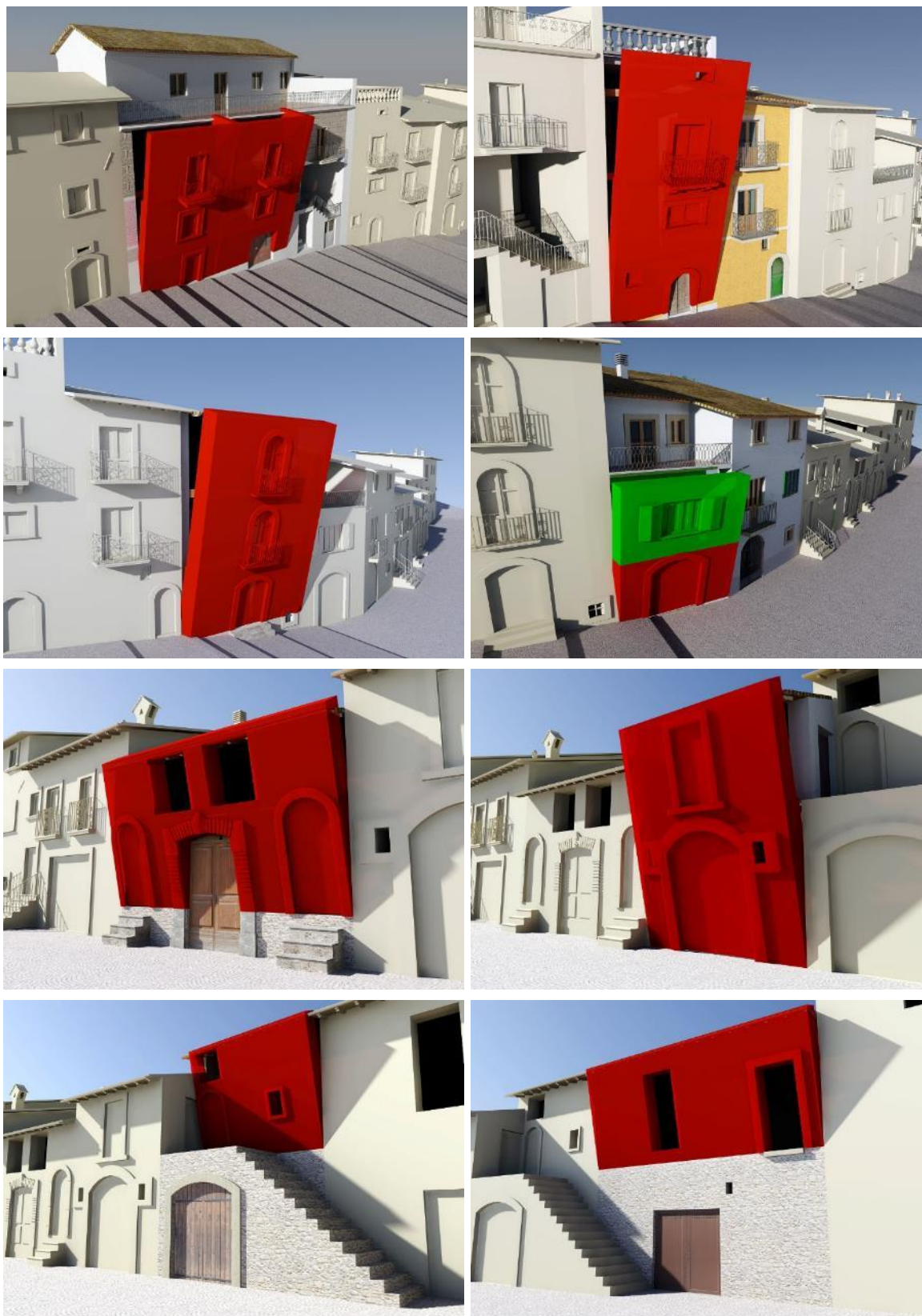


Figure 149: Overturning of ss.uu. 2 and 3, 4, 5, 7, 8, 9 and 10.

7.2.1.8 ADDITIONAL HYPOTHESIS FOR THE CALCULATION OF THE MECHANISMS HERE USED

For the case of Castelnuovo buildings, additional hypothesis were followed in the definition of the mechanisms analysis, reported in the following list:

- The horizontal forces are stable during the evolution of the mechanism;
- In-situ inspections inside the construction of Castelnuovo showed that the support length of floor inside the masonry is generally among 10÷20 cm. 15 cm has been chosen as the support length, equal for each type of horizontal floor. Only in the case of masonry vaults (generally barrel vault), the support length depends on their structural thickness and it could be different case-by-case. Figure 150 shows the actual state of s.u.1 of 16-515 aggregate. The main façade is subjected to an overturning movement around a ground floor hinge. This caused the collapse of the in folio-ceiling vaults at the ground floor (Figure 150a) and the floor breaking at the first storey (Figure 150b).
- The masonry compression resistance is infinite, and the hinge configuration is punctual one at the end of masonry cross section;
- The floor load (named N_{vi} , Figure 138) assumes values depending of the type of floor and its squared metres of interest area. If the floor has framework orthogonal to the wall, its zone of influence is half of its total coverage area, while the direction of framework is parallel to that of the wall, only a single beam's area of influence was considered.
- In certain cases, the presence of the rear annex in the buildings did not allow the calculation of the out-of-plane mechanisms in rear façades. They could be considered as restraints in the structures that impede the overturning for certain floors. Example in the ss.uu. 4, 5 and 10 -088 aggregate Table 41 bottom.



Figure 150: Effect on slabs of the overturning façade mechanisms. (a) ceiling vaults (b) floor.



Figure 151: s.u. 1 of 10-088 aggregate. (a) simple 3-floor overturning (b) overturning with corner in the third floor.

- For the header or corner façades or when an internal façade has the lateral walls well connected each other's, the corner overturning (Table 40) also has been evaluated. In the calculation of a corner mechanism a portion of masonry of orthogonal connected wall is considered. This issue makes the eccentricity (e) of the self-weight barycentre greater, making the mechanisms verification higher. A posteriori, in the Castelnuovo façades, since the scarfs at the edge of the walls are not consistent, the classical mechanisms of the single façades is assessed, not considering the corner portion of an orthogonal wall.

7.2.1.9 INFINITE RESISTANCE OF THE MASONRY

Observation for the hypothesis of the infinite resistance of the masonry

(*) The Italian Code (NTC, 2008) (C.M. n.617, 2009) allows the calculation of the kinematic (linear and non-linear) analysis, both considering the masonry compressive resistance as infinite or equal to the real values supposed. If infinite resistance is assumed the hinge configuration can be positioned at the end of the panel cross section, as the forces were absorbed by a unique point. If the infinitive compression strength is assumed, conservatively, the level con knowledge of the structure must be KL1, to whom is associated the highest safety coefficient of reduction of the resistance (CF=1.35). Otherwise, considering the real compressive design resistance (depending on the masonry type, considering the value provided by the Code in Table C8A.2.1-2, C.M. n.617, 2009), the confidence factor changes, depending on the achieved knowledge level for the buildings (§3.4) and the design mechanical characteristics are defined as:

$$R_i = \frac{R_{ck}}{\gamma_M C F i}$$

In the case of linear analysis, in §7.8.1.1 of (NTC, 2008) it is recommended to use the partial coefficient of the material γ_s for seismic calculation equal to 2 while for non-linear ones 1 (§C8.7.1.5 of C.M. n.617, 2009).

Doing the safety verification of a building façade, the designer should choose the type of analysis and the γ_s factor. In the general study of vulnerability, that is when different type of analysis are performed, it is useful to measure the gap in terms of the results that distinct analyses provide. In the definition of the seismic capacity of the façades (§7.4 and 7.5) in this project, two hypothesis are fixed: the knowledge level is the minimum (LK1) and the position of the hinge configuration is in the external side of the masonry thickness (point A, Figure 152a), in order to have the same assumption of the masonries compressive strengths.

However, an example of the translation of the hinge position is reported on the follow, in order to evaluate how change the results enter the ideal case of infinite compression resistance and the case in which the compressive resistance is finite. In the latter case, the hinge configuration is positioned in the resultant of the pressure, whose distance from the external side of the panel, z, is determined by writing the vertical translation equilibrium of the loads in play. The normal upper strength ($N_{TOT} = N_{upper}$) is the sum of the panel self-weight and the slabs loads, while the lower normal one is the restrain force of the hinge at the base. Linear elastic (A case) or plastic (B case) distribution of the stresses (Figure 152b) could be considered surrounding the hinge. In both cases, z, is determined by the equations in the follow:

$$\begin{aligned} \text{A case) } N_{TOT, upper} = N_{lower} &\rightarrow N_{lower} = \frac{f_{cd} \cdot 3z \cdot l}{2} \rightarrow z = \frac{2 N_{TOT}}{3 l f_{cd}} \\ \text{B case) } N_{lower} = k f_{cd} l &\rightarrow z = \frac{N_{TOT}}{2 l k f_{cd}} \end{aligned}$$

l is the length of the panel, f_{cd} is the design compression strength, $k = 0.85$. For each mechanism, the position z changes depending on the value of loads (N_{TOT}) and the geometrical dimension and structural characteristics of the panel.

The example refers to a case study already presented by the ReLUIS researchers (ReLUIS, 2010a). The mechanism inspects only the out-of-plane of the first and second floors of a three-floors building in aggregate located in a site characterised by this seismic hazard (SLV): $a_g = 0.251g$, $F_0 = 2.365$ and $T_c^* = 0.334$ sec.

The building is a civil building with a return period of 475 years. The soil is classified in the "A" category ($S_s=1$, $C_c=1$) and

Topographical conditions T_2 ($S_T=1.2$). The period at which begins the stable velocity is $T_C=0.334s$, that for the stable acceleration is $T_B=0.11s$ and T_D is equal to 2.60 seconds.

The panel geometry and loads are reported in Table 47. Two type of masonry have been taken into account for the definition of the influence of the materials in the result: stonework belonging to Category "I" and "III" (C.M. n.617, 2009) §Tables C8A.2.1-2. The self-weights (P_1 and P_2) are different due to the specific weights of the masonries.

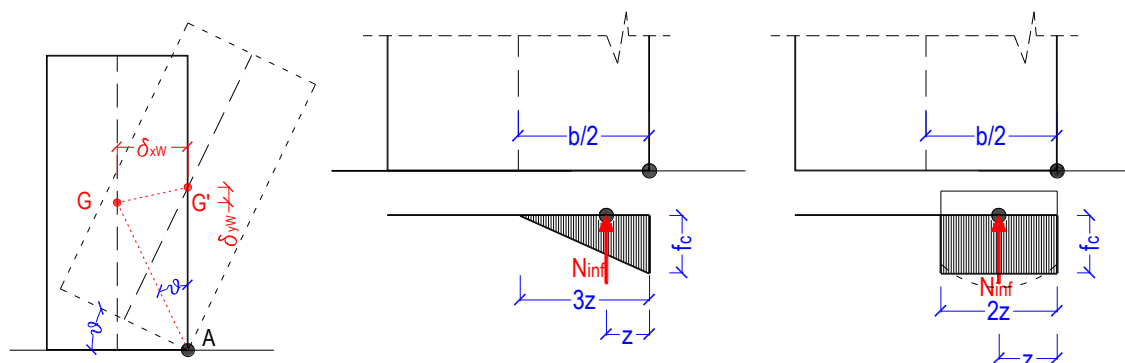


Figure 152: (a) vertically alignment of the barycentre of the panel (G') and the hinge configuration (point A). (b) Recession of the hinge configuration due the finite resistance of the masonry (elastic and plastic scheme).

Table 47: Geometry and loads for panels (Z is the height of the hinge from the foundation soil).

Geometry [m] and loads [kN] for panels				
N° floor	=	3	b_1 =	0.45
Z	=	3.3	h_1 =	2.6
h_{tot}	=	8.3	N_1 =	75.6
h_{bar}	=	3	d_1 =	0.3
l	=	6.8	P_1 =	(151.2) 167.1
			b_2 =	0.45
			h_2 =	2.4
			N_2 =	106.3
			d_2 =	0.3
			P_2 =	(139.5) 154.2

The design resistances for the masonries are different for the linear and non-linear analysis. In Table 48, the results have been compared for the first and second floor hinge height position. In particular, the z passes from the 7.95 cm in the case of linear analysis, category "I" to the 1.63 cm for the "III" category in non-linear analysis. In the case of resistance finite, the KL is KL2, the CF is 1.2 and the average resistances are averages values of those provided by the Code.

Table 48: Strengths and distance of retraction of the hinge.

CATEGORY I - Strengths f_{cd} and distance of retraction of the hinge (z) → CF=1.20				
	Elastic distribution of stresses (Figure 152b left)		Plastic distribution of stresses (Figure 152b right)	
	(A) LINEAR	(B) NON LINEAR	(C) LINEAR	(D) NON LINEAR
$y=$	2	1	2	1
$f_{cd}= N/cm^2$	58.33	116.67	58.33	116.67
z (cm)=	7.94	3.97	7.01	3.50
CATEGORY III				
$f_{cd}= N/cm^2$	133.33	266.67	133.33	266.67
z (cm)=	3.70	1.85	3.26	1.63

Case Category I

The results are compared in Table 49. The first term of comparison is the case proposed by the Code, with infinite resistance and CF=1.35. The first row refers to the infinite compressive strength (CF=1.35) and for finite compressive strength and elastic plastic distribution. Considering the linear analysis and an elastic distribution of the stress, the variation in term of capacity is about the 46%. The calculation considering the real strength cuts down the stabilizing moment in the equilibrium equation. The masonry category "I" has low mechanical compressive characteristics and, in order to assure the equivalence of external force (N_{UPPER}), the distance of retraction of the hinge arrives at about 8 cm. The demand in term of acceleration remains stable and the final result is that the I_s , safety index, in the case of "real" finite strength is lower than the "ideal" infinite compressive strength of about 29%. Despite a major identification of knowledge that the level

⁶ "I" = Disorganized irregular stone masonry and "III" = Roughly cut stone masonry with good texture.

of knowledge requires, and despite the CF passes from 1.35 to 1.20, the I_s decreases, since in the first hypothesis, the compressive strength of the masonry is considered infinite.

This result can be apparently in contrast to the basic principle of having different knowledge levels in the analysis of existing buildings. The principle is that if there is detailed information about an existing structures one should have less uncertainties in model calculations, to which correspond a fit verification of the structure for a certain limit state (increasing of safety index). However, considering an infinite resistance of the masonry under simplifying assumptions, this does not happen: the coefficients that take into account with sophisticated analysis and higher level of information (CF from 1.35 \rightarrow 1.20) are not enough small to bridge the gap between the results offered by using the different resistance values.

With the non-linear analysis, the variance reduces respectively from the 29% to the 12% for the elastic distribution and from the 23% up to the 9% for the plastic distribution. Since for the non-linear analysis the compressive strength is twice time the other (due $\gamma=1$), the distance from the “ideal” results and the “real” decreases, but the “higher I_s ” refers always to infinite compressive case (CF=1.35). It can be notice that in this case the displacement demand changes in the three conditions, it decreases being linked to the first acceleration values that triggered the mechanisms and depending from the capacity of the structure (as it will be described in §7.2.1.6).

In the case of masonry with better mechanical characteristics (“III=Roughly cut stone masonry with good texture” (C.M. n.617, 2009)), a more organised stonework with stringcourses, whose compressive strength bigger more than two time than the other, the final result in term of “ I_s linear” changes from the “ideal” case for the only 4%. In the case of non-linear analysis, the gap is equal to 0/1%, it means that the verification from the ideal compressive infinite resistance and the finite resistance is null, but this can be attributed to the masonry typology and not to the type of analysis done.

Table 49: Result for out-of-plane mechanism with and without considering the hinge retraction.

LINEAR ANALYSIS - CATEGORY I				
Infinite resistance and CF=1.35				
Mechanims type	Multiplicator α_0	Capacity α_0^* [m/s ²]	Demand a_D [m/s ²]	I_s safety index
1 st floor hinge	0.082	0.728	1.786	0.407
Finite resistance and CF=1.20 (A) elastic distribution				
1 st floor hinge	0.057	0.563	1.786	0.315
Variance	46%	29%	-	29%
Finite resistance and CF=1.20 (C) plastic distribution				
1 st floor hinge	0.060	0.593	1.796	0.332
Variance	38%	23%	-	23%

NON-LINEAR ANALYSIS - CATEGORY I				
Infinite resistance and CF=1.35				
Mechanims type	Rotation angle Θ_0	Capacity d_u^* [m]	Demand $S_{de}(T_s)$ [m]	I_s safety index
1 st floor hinge	4.714	0.123	0.106	1.166
Finite resistance and CF=1.20 (B) - elastic distribution				
1 st floor hinge	3.980	0.104	0.099	1.044
Variance	18%	18%	6%	12%
Finite resistance and CF=1.20 (D) - plastic distribution				
1 st floor hinge	4.067	0.106	0.099	1.066
Variance	16%	16%	6%	9%

7.2.1.10 METALLIC TIE-RODS

When tie-rods are present in the façades, there are two possibilities: the first is to calculate the overturning mechanisms considering the forces that these devices can explicate or considering the tie-rods as restraints for the panel that inhibit the overturning and study other mechanism such as the vertical bending. Since in Castelnuovo aggregates, despite the diffusion of tie-rods, the overturning mechanisms were the most frequent triggered, the first hypothesis was followed.

The tie-rod force represents a “positive” force, which generates only a stabilizing moment around the hinge configuration in the equation of the Virtual Works (Eq.(23)).

The results of the overturning mechanisms are assessed both with and without the influence of the metallic tie-rods forces, to evaluate their influence on the capacity in terms both of acceleration and displacement, §7.2.1.6.

The tie-rods efficacy is linked to:

1. their positions: they are collocated through the horizontal floor or in correspondence of the vertical masonry walls;
2. their dimensions
 - a. tie-rod diameter;
 - b. tie-rod section (is always intact);
 - c. plates;
3. materials, state of preservation of steel and the masonry.

In situ observations showed that in Castelnuovo aggregate the tie-rods have generally similar dimensions and geometry, with a bolted plate and an element of transversal support of the chain (Figure 153), and without a squared or circular plate. The theoretical calculation of the design tie-rod force refers to the Figure 154, for an ideal tie-rod fixed to a squared plate, on a stone masonry (disorganised stone masonry). The system metallic tie-masonry can show four types of collapse. They are:

1. the collapse of the steel:

$$T_1 = A_s f_y$$

2. the crushing collapse of the masonry, in the contact area of the metallic plate and the panel:

$$T_2 = f_{cm} a b \sqrt{\frac{A_2}{A_1}}$$

where f_{cm} is the compressive resistance of the masonry, $a = b$ are the dimensions of the metallic plate, A_1 is the area of the plate and A_2 is the distribution compressive forces area. $\sqrt{A_2/A_1}$ is major than one and should be less than 2. Precautionary, in this case, the $\sqrt{A_2/A_1}$ is assumed 1.

3. the collapse for punching of the masonry. The area involved in this mechanisms is signed in green in Figure 154 and it correspond to the horizontal lateral area calculated as the multiplication of the entire panel thickness and the perimeter of the area in correspondence of half thickness of the masonry, considering an angle of distribution of the force equal to 45° .

$$T_3 = f_{vm}(\tau_0)t \left[2 \left(a + 2 \frac{t}{2} \tan(\beta) \right) + 2 \left(b + 2 \frac{t}{2} \tan(\beta) \right) \right]$$

In this case, $\beta=45^\circ$, $a=b$.

4. the collapse for tensile stress in the lateral area

$$T_4 = f_{ctm} A_{lat}$$

Further information about the study of ancient tie-rods behaviour is available in (Vinci, 2014).

An example of calculation of a design force for a tie-rod is showed in the follow. It has been considered a stone-irregular masonry 60 cm thin (as average value of the thickness for mechanisms analysed §7.5), with this characteristics:

Table 50: Mechanical characteristics of disorganised stone masonry.

weight=	19.00	[kN/m ³]	f_{cmd} =	58.3	[N/cm ²]
f_{cm} =	140.00	[N/cm ²]	τ_{0m} =	1.08	[N/cm ²]
τ_{0m} =	2.60	[N/cm ²]	f_{tmd} =	163	[N/cm ²]
f_{tm} =	3.90	[N/cm ²]			

in which the confidence factor is equal to 1.20 (KL equal to 2), the security coefficient for the material is = 2, as the calculation would be only in linear analysis. The steel has yield strength of 240 N/mm² with γ_s is 1.05. The tie-rod has area of 3.14 cm² (Φ 20), and the plate dimension are $a=b=25$ cm. Considering an angle of distribution of 45° , the calculation of the forces associates to the four different mechanisms are:

Table 51: Tie-rod force - case of squared plated

$T_1 =$	59.8	kN
$T_2 =$	36.5	kN
$T_3 =$	22.1	kN
$T_4 =$	46.9	kN

The less values of the forces are associated to the punching and compression mechanisms collapses due to the poor mechanical characteristics of the masonry and the limited dimensions of the metallic plate.

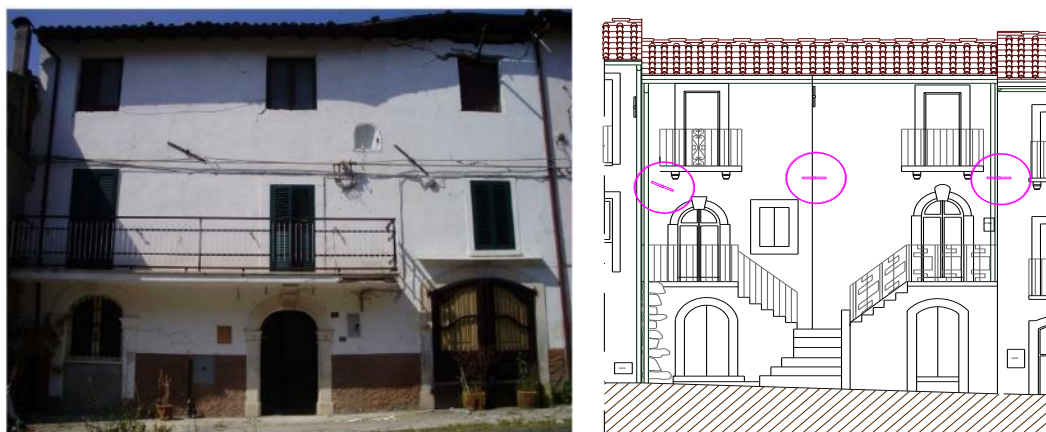


Figure 153: Example of façades with metallic tie-rods - photos (aggregate 10-088 and 13-158).

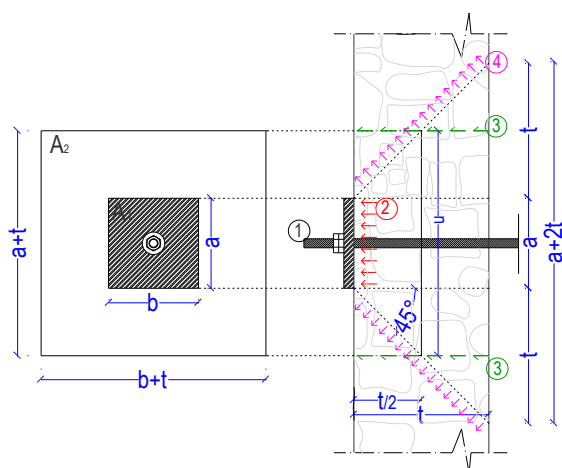


Figure 154: (a) Tie-rod. Identification of the possible collapses mechanisms. (b) Façade with squared bolt plates (01-222).

In a more realistic case in Castelnuovo, the bolted plate has an elongated shape, with a length of about 4/5 cm and an axial develop of about 40/60 cm. With these parameters, the calculation of the tie-forces collapse are:

Table 52 Tie-rod force - case of real bolted plated

$T_1 =$	59.8	kN
$T_2 =$	21.0	kN
$T_3 =$	24.2	kN
$T_4 =$	51.3	kN

The less value of the force is associated to the compression mechanisms collapse, it values 21.0 kN due to the elongated shape of the plates.

In the calculations carried out in paragraph §7.5, fixed values of 25 kN will be considered, starting with the results of the previous calculations although performed in a conservative way.

Furthermore, in the calculation it is assumed that the height of the application of the tie-rods force is at the same height of the slabs, as it is possible to see in Figure 154. Generally, in old city centres when the tie-rods are well positioned, in room covered by vaults, the height of the tie-rods corresponds to the impost of the thrusting element, in order to hold up the

horizontal pushing forces (Figure 155). In Castelnovo aggregates, the tie-rods are located in correspondence of the altitude of the storey, since the weighted vaults are mostly organised with framework parallel to the development of the aggregates. The tie-rods are positioned with the mainly goal to joint orthogonal walls and to make working together the main structural elements avoiding the activation of local mechanisms on the individual aggregate portions.



Figure 155: Masonry crossed vaults in Firenze city centres (Tiratoio Square) and Loggia dei Lanzi in Signoria Square.

7.2.1.11 OBSERVATIONS FOR THE NON-LINEAR ANALYSES

The capacity curve of the structure, in the non-linear analysis, is evaluated keeping stable the values of the forces during the analyses, and considering the capacity with the formula in Eq.(26). Two observations should be done, with reference on the non-linear analysis, for the capacity of the structure as described in 7.2.1.4, since it is not univocally defined. To understand better this point of the Code, an ideal case is reported on the follow: it is a two-floors structure panel, 1 m length. The geometry and loads of the panel are in Table 53. For this simple case, the results in term of both linear and non-linear analysis are reported. For the latter analysis, the collapse is due both to:

1. the collapse of $0.4 d_{k0}^*$;
2. the collapse of the slabs, stopping the curve $\alpha_0 - d_{k0}$; when the displacement reaches 15 cm, for the characteristics of the building stocks and the storeys of Castelnovo.

Table 53: Geometry and loads for panels.

Geometry [m] and loads [kN] for panels								
N° floor	=	2	t ₁	=	0.60	t ₂	=	0.50
L=		1	h ₁	=	3	h ₂	=	3.5
h _{tot}	=	6.5	N ₁	=	60	N ₂	=	50
h _{bar}	=	3	d ₁	=	0.45	d ₂	=	0.35

The results refers with the configuration of the rotation hinge at the ground floor, as represented in Figure 138 on the left. The forces remain stable during the mechanism, but starting from the d_{k0} of 15 cm, the force of the last floor's slab expires. The acceleration that triggers the mechanism in the initial configuration (with all the forces took into account) is 0.78 m/s^2 and considering the acceleration in Castelnovo (A ground soil an T₁ topographic category), the safety index for the linear analysis is 0.66. For the same case, without the last floor's weight, instead, the acceleration capacity is 0.98 m/s^2 and the safety index is 0.83 (Figure 156 blue dotted line). The major capacity of the second case is due to the absence of a concentrated load at the top of the structure for which the destabilizing moment is major that the stabilizing one (as confirmed in 7.2.3). The horizontal eccentricity of the load is 0.35 m and the stabilizing moment is very low in respect to the destabilizing one (for which the arm is more the 6 metres). In Figure 156 on the left there is the curve $\alpha_0 - d_k$, in which the dotted black curve refers to the case with the force, the blue dotted curve refers to the case without the last floor's load and the red curve is the real curve. The real curve is determined considering variable the forces: after the 15 cm of displacement, the slab is not more anchored to the wall and the mechanism is changed in one without the force of the last floor slab. This is traduced in a visible jump from the initial capacity until to the curve with high capacity. The results in

terms of capacity curves (following the equation (25) and (26)) are in Figure 156b in which, in addition to the capacity curves of the described cases, there is the ultimate capacity of the structure. It is individuated in correspondence of the minimum of the 0.4 of the last displacement in the curve (the red with the jump) or the displacement in correspondence of the collapse of the slab. The minimum displacement is than individuated by the collapse of the floor's load. The slope of the two sections of the capacity curve is different since the mass participating in the mechanism, to transform the curve $\alpha_0 - d_k$ into the capacity curve is different considering or not the weight of the last floor slab. The mechanism would be continue up to its real collapse, but for the case of the aggregates' façades the last displacement of the entire mechanism is that one in which collapsing floor. In this example, the displacement for the floor collapse is 0.12 m (arrow blue in the graph), and it is the value to compare with the demand in displacement. The actual Regulations in Italy are not so clear regarding the point of the determination of the capacity displacement for an out-of-plane mechanism in the case of non-linear analysis. For this reason and to evaluate the gap among the results they provide, for the non-linear analysis both the case *with and without* considering the loss of the floor load are carried out.

One should remember that the displacement demand is linked to the last displacement of the structure, as explained in 7.2.1.6. In the case of considering the displacement associated with the collapse of the floor the demand displacement is 13.3 cm. The safety verification for the non-linear analysis is not satisfied and the safety index moves to 0.86. This is a value close to the result of the linear analysis. If no forces were considered breaking during the evolution of the mechanism, the safety index would be 1.24, which means more than twice time superior of the results of linear analysis evaluated.

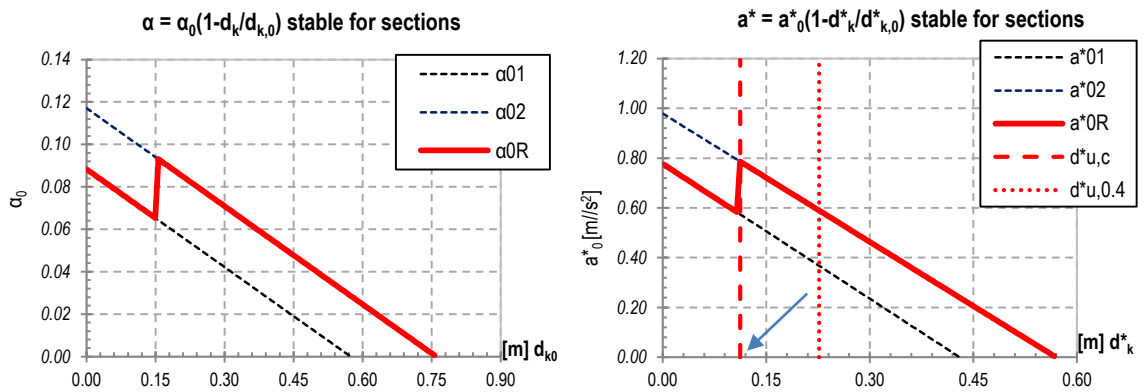


Figure 156: a) Curve $d_k-\alpha_0$; b) capacity curve for the case of collapse slab.

§

A completely different case is that one in which there is a metallic tie-rod present in the mechanism. As explained in the paragraph before, the force of the tie-rod is considered stable during the analysis and equal to 25 kN.

The collapse of the tie-rod would be reached when horizontal displacement in correspondence of the tie-rod arrives at 5 cm. After that value, its force is no more stable during the time and the capacity curves' shape are opposite of that one above presented: they start with high capacity and move toward a less one. At first, the metallic device explicates its force and after its last displacement it expires. The last displacement for the tie-rod is 5 cm (in the case analysed it is at 3 m height): this correspond at about a maximum displacement of 10.8 cm at the top floor, the position of the chosen control point (height of 6.5 m). The capacity curve with the tie-rod is higher than the capacity curve without the tie-rod: after the last displacement for the tie-rod, the $d_k-\alpha_0$ has a jump toward the capacity curve without the metallic element. In this case the slope of the two sections corresponds, since the tie-rod force is not a force that generates seismic inertia in the mechanism. The capacity curves are represented in Figure 157. The last displacement for the structure remains that defined as the $0.4d^*_{k,0}$, in which $d^*_{k,0}$ refers to the real capacity curve (in green thick line) stable for section in Figure 157b. In correspondence of the loss of the tie-rod force, the mechanical system should no stopped: the disappearance of this force does not produced a danger for preservation of human life. The seismic demand is calculated starting from the $0.4d^*_{u,0}$.

If it was present, in this case also the collapse of last floor slab should be considered, which provided the same result as estimated in the first observation of this paragraph.

This result is explained here just for completeness of the explanation of the methodology but, in the evaluation of the global seismic vulnerability the calculation of the out-of-plane mechanisms, the metallic tie-rod force is considered stable and independent from the displacements reached by the wall.

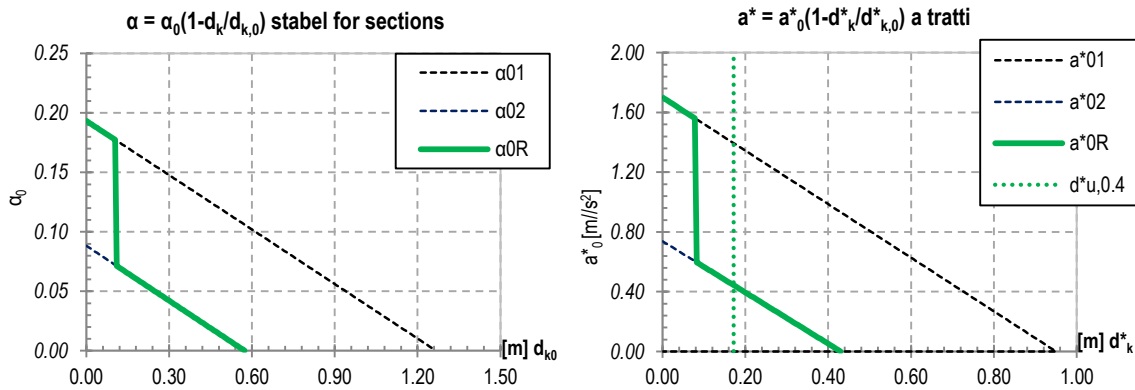


Figure 157: a) Curve $d_k-\alpha$; b) capacity curve for the case of collapse of a tie-rod.

7.2.2 DEFINITION OF THE SEISMIC CAPACITY OF OUT-OF-PLANE MECHANISM

Considering the results exposed up to now, how is it possible to define a unique value of the seismic capacity of the structure towards the out-of-plane mechanisms?

For the case study of Castelnovo, it is possible to refer both to a *theoretical* point of view based on the results of the analysis carried out using the calculation methods defined in the current Italian legislation (NTC, 2008) (C.M. n.617, 2009) and a *practical* point of view, considering the mechanisms activated on the façades or the total collapses occurred. However, the masonry type and the construction technologies, that are common in the historical city centre in L'Aquila's valley (Figure 47), lead to the necessary decision to take into account the out-of-plane mechanisms as collapse mechanisms, since they were the most frequent type of damages encountered after the seismic events. In particular, within the types of out-of-plane mechanisms, for the critical evaluation of the damage mechanisms that have been observed in the aggregates of city centres, in the first place Castelnovo, simple overturning mechanisms are the most frequent ones. The other type of local mechanisms (Table 40) are present in a marginal way and generally show mix behaviour, combining vertical bending or corner overturning (Figure 151).

Therefore, the capacity of local overturning is defined as the minimum capacity for the single of multi-storey against monolithic overturning. The position of the cylindrical hinge can "move" at each floor, depending on the number of slabs, constraints and loads in play (Figure 144). In the standard situation in Castelnovo, homes have three floors (cell type Figure 53 and Figure 54), and the cylindrical hinge could be considered at the ground, the first floor or the second floor.

There are special cases where external constraints differentiate the geometry of the mechanism to consider. This is the case of the presence of external stairs in the front of structural units. These elements are rollers for the walls and do not allow them to overturn at least for the height for which they extend. Other cases are represented by the annexes or terraces built behind the houses that, if sufficiently stiff, provide a restraint to rotation of the façades (Figure 158). Generally, external stairs are of service of one floor (the ground floor is used as a cellar with direct access from the street and the living unit starts with the first floor): the analysis is efficient for the n-1 floors of the panel, not considering the ground floor.

A further case of analysis is represent by a mechanism in which there is one or more metallic tie-rods, the treatment of which has been analysed in section 7.2.1.9. They represent constraints against overturning and their presence could cause

the transformation of the mechanism from an overturning to a vertical bending, with the generation of a horizontal and continuous hinge configuration. For some cases, the calculations carried out for both the overturning and vertical bending mechanisms showed that the seismic capacity for the vertical bending is higher than that one of overturning, that becomes the most probable mechanisms that will activate. To the vertical bending are often associated safety index major than one in even in linear analyses for the Castelnovo seismic actions. On the contrary, for overturning mechanisms, at least in "normal" conditions of the panel (without tie-rod or thrusting force), the seismic capacity enters among the 40-70% of the seismic acceleration demand (A ground and T₁ category topographic).

The critical evaluation of the damage mechanisms activated in Castelnovo reinforces the latter observation once again: critically regarding both the crack patterns and failure modes it has been possible to establish that, even in the presence of tie-rods, more frequent mechanisms were overturnings mono or multi-storeys.

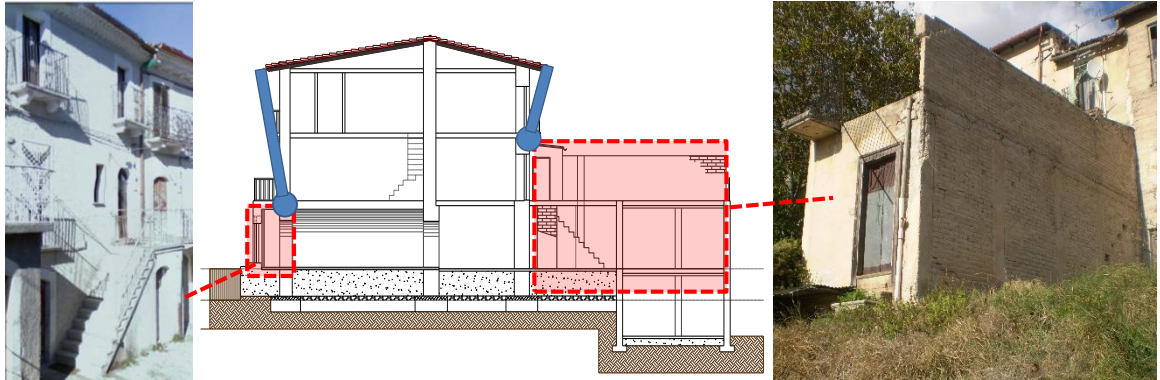


Figure 158: Restrains in the out-of-plane mechanisms: presence of external stairs or outbuilding (aggregate 10-088).

It remains to understand what should be regarded as the capacity of a simple overturning mechanism, if the hinge configuration can appear in all floors. As earlier reported (Figure 139), the capacity of the structure decreases with the growth of the wall's height, or for a fixed height, when the wall's centre of gravity moves up (7.2.3). Consequently, the smaller capacity of the system is related to the global mechanism (with formation of the cylindrical hinge at the base of the wall) which has a greater height. When the system affects only a plane (formation of the plastic hinge at the last floor (first floor in Figure 158 for example)), the capacity grows up. From a regulatory point of view, the seismic demand increases with the height of the structure, due to the height effect of the seismic motion. In light of this fact, it is not known a priori which is the system linked to the minor capacity, since the presence of the uncertainties in the evaluation of the capacity of the structure in relation to all the elements and loads in play.

For less than cases in which there is the presence of a clear constraint at a certain height (a stair, a systematic group of metallic tie-rods) the overturning for mechanisms triggered in Castelnovo's aggregates covers the entire wall. Although the prevalence of big (few centimetres) vertical cracks in the top of buildings, a high percentage of detachments of horizontal and vertical cracks are discovered even at the lower floors. Moving up to a "practical" point of view and not only regulatory one, *it is considered reasonable to assume as the panel capacity, the capacity of the mechanism related to the entire wall system (with the formation of the hinge at the base of the structure). For the limit state of preservation of life and especially for large uncertainties contained in the calculation with non-linear analysis, it is appropriate to evaluate the capacity in terms of linear analysis, as the acceleration of collapse of the mechanism, α_0^* .*

The manner to pass from the capacity acceleration α_0^* of the mechanism up to the peak ground acceleration of capacity ($a_{g,c}$) will be defined in the following.

The equations in 0 provide the value of the capacity for a mechanism. For the state limit SLV, the capacity calculated α_0^* should be compared with the demand of acceleration, using the Eq. (28). Making equal the two expressions, it is possible to evaluate the a_g of capacity for the mechanism, circumscribing the solution at the spectrum with characteristics of

Castelnuovo (Figure 7). Remember that S is the coefficient with which the ground category and topography are taken into account.

$$(30) \quad a_0^* = \frac{\alpha_0 g}{e \cdot F_C} = \frac{a_g S}{q} \rightarrow a_{gi} S = a_{0i}^* q$$

The value of a_g is defined as the peak ground acceleration of capacity of the structure and it is related to the starting point of the spectrum of acceleration (period equal to 0): for this reason, it is independent from the characteristics of the masses and stiff of the panel. With the knowledge of $a_{g,Ci}$ for each mechanism, it is possible to compared even different panels with different characteristics, in order to know which is the most vulnerable towards seismic actions evaluated with out-of-plane procedure. The PGA_C is defined as $a_g \cdot S$ and it is the starting point of the elastic spectrum in acceleration. If the latter is calculated in A category of soil and in a category topography T_1 , S assumes values 1 and the a_{gC} is equal to the PGA_C .

To evaluate the peak ground acceleration of capacity, two basic methods can be used, using a "fixed shape spectrum" or "varying the spectrum shape", defined in the following. The starting point is the knowledge of the period of the structure (T) and the value of acceleration provided by the kinematic analysis a_0^* . About the period, one should remember that the capacity acceleration refers to a global overturning of the structure, schematised as a cantilever with ground floor clamped to the earth. Consequently, the period of demand acceleration for the analysis is always equal to 0, as reported in the safety verification in 0, that means structure in-built with the ground. To calculate the capacity a_g the equation linked to the response spectra equation (1.1.1.2.1) should applied. The two different methods are linked to the possibility of referring to the spectrum acceleration profile of Castelnuovo (characterised by the seismic hazard of Castelnuovo) or to a general one, extracted by the Italian NTC 08 database, in which it is possible to recognize the $a_g \cdot S = a_0^*$ for null period, changing the base seismic hazard parameters, that are overall changing as a function of return of the structure, T_R .

Indeed, in the formula in Eq.(30), there are two elements that depends from the T_R of the structure, the a_g and the S value: the S is the multiplication of S_S and S_T and the first one depends from the a_g value. At this point, it is possible to search the a_{gCi} in two ways:

1. the spectrum with a fixed shape keeping the characteristics and shape of the demand spectrum (Castelnuovo) with the return period stable depending on the limit state considered (in this case 475 years);
2. calculation of the $a_{g,C}$ and the associated return period of the event varying the spectrum shape. With the variation of the return period, the a_g , the F_0 , T_C^* (seismic hazard) and S_S are variables, too.

In case 1, the "calculation of a_g with fixed spectrum shape" method, F_0 , T_C^* and S are fixed while the a_g is variable. It means that T_R is fixed with the value of the demand acceleration spectrum calculated initially (475 years in this case). Once the capacity of acceleration is known (a_0^*) and the behaviour factor is fixed ($q=2$) the capacity a_g is calculated just reversing the equation as:

$$(31) \quad a_{gi} S = a_{0i}^* q \rightarrow a_{gi} = \frac{a_{0i}^* q}{S}$$

This is the case in which inside the formula of the spectrum in acceleration (reported on the following), only the value of the peak ground acceleration is changing.

$$\begin{aligned} (32) \quad S_e(T) &= a_g \cdot S \cdot \eta \cdot F_0 \cdot \left[\frac{T}{T_B} + \frac{1}{\eta \cdot F_0} \left(1 - \frac{T}{T_B} \right) \right] & 0 \leq T < T_B \\ (33) \quad S_e(T) &= a_g \cdot S \cdot \eta \cdot F_0 & T_B \leq T < T_C \\ (34) \quad S_e(T) &= a_g \cdot S \cdot \eta \cdot F_0 \cdot \left(\frac{T_C}{T} \right) & T_C \leq T < T_D \\ (35) \quad S_e(T) &= a_g \cdot S \cdot \eta \cdot F_0 \cdot \left(\frac{T_C \cdot T_D}{T^2} \right) & T_D \leq T \end{aligned}$$

As reported in the definition of the seismic hazard in CHAPTER 1, the seismic characteristics of the spectrum are those of Castelnuovo, but referring to a category A of the soil and in a topographic condition of plain.

$V_R = V_N \cdot C_U = 50$ years

The seismic hazard is then defined:

$$a_g = 0.257 \text{ g} \quad F_0 = 2.37 \quad T_C^* = 0.35 \text{ sec}$$

The geotechnical conditions are assumed stable. The Figure 159a shows in red the demand elastic spectrum of acceleration of Castelnuovo, with the acceleration of 0.257 g at the starting point ($T=0$ and considering $S=1$), in green a

spectrum only with a_g higher, but with the shape stable and in blue a minor capacity spectrum, for which the a_g is 0.15 g. The dotted black vertical lines represent the three period of the spectrum (T_B , T_C and T_D), stable for every spectra there represented, since they are overall depending from the T_C^* and so from the T_R (assumed stable). With this method, it is not possible to obtain the estimation of the return period of capacity of the structure, since is the same of the demand. If the safety index is major than 1, it is possible to declare only that the $T_{R,C}$ of the structure is major than 475 years.

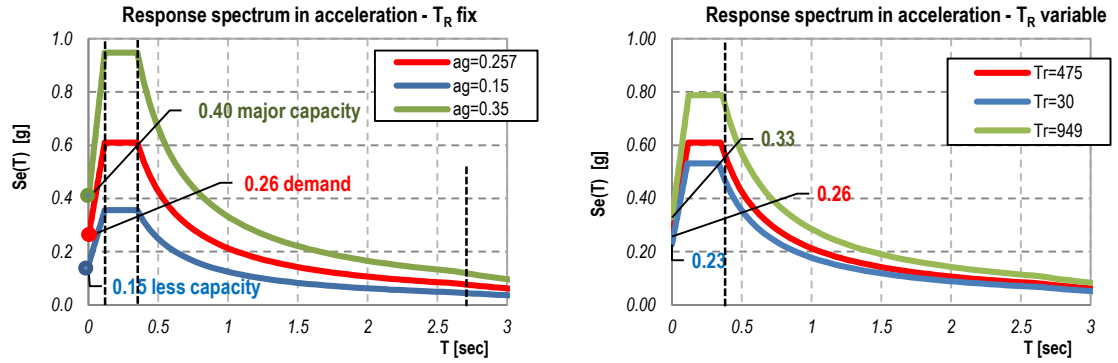


Figure 159: (a) Research of the a_{gC} with fixed T_R (475 years); (b) example of shape of the spectra with T_R variable.

§

In case 2, in the “calculation of the a_g and the return period varying the spectrum shape” the three parameters of the seismic hazard are variable with the return period. With this method, the goal is determine within the infinite spectrum of the Italian territory that one which has the acceleration capacity value (a_{gC}^*) in correspondence of $T=0$. What is it changing in this method? The S value (

Table 7) changes with the return period. This is an iterative method since it is not possible to calculate directly the value of the return period with a formulation. It is necessary to calculate the range of acceleration spectrum, interpolating the values of the $a_g F_0$ and T_C^* (and as a consequence the C_C , S_S and S values) for different values of T_R finding the spectrum that assume the researched value a_{gC}^* in the first point of the spectrum (for $T=0$). The trend of hazard parameters with the changing of T_R is reported on the figures below (Figure 160), for the seismic zone of Castelnuovo. Figure 159b shows the type of acceleration spectra for Castelnuovo, for A soil and T_1 condition for different values of T_R (respectively $T_R = 30$ and 949 years).

With this second method it is possible to obtain both (a_{gC}) PGA_C and return period acceleration of capacity, T_{RC} : nowadays, the return period is considered an indicator of the vulnerability of buildings if compared with the return period of demand, as reported in the following expression (O.P.C.M. 3728/2008).

$$I_S = \alpha_{ag} = \frac{a_{gC}}{a_{gD}} \alpha_{TR} = \frac{T_{RC}}{T_{RD}} R_{CD} = \left(\frac{T_{RC}}{T_{RD}} \right)^{0.41}$$

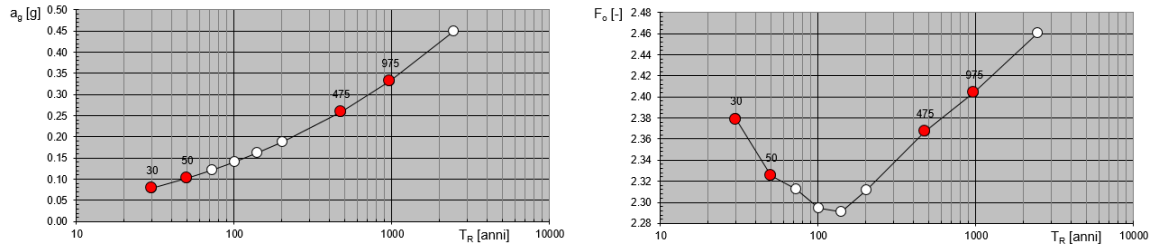


Figure 160: Variability of the parameters a_g [g] and F_0 with the return period T_R (pictures from Spettri di risposta v 1.0.3 - C.S.L.P. <http://www.cslp.it>).

§

The evaluation of the a_{gC} of the structure starting from the acceleration of the system is expressed in Eq.(31) for a case study of a mechanisms clamped to the earth, for which the seismic demand should take in to account from the acceleration spectrum in the starting point of the spectrum at $T=0$.

If the kinematic analysis is adopted for a block in height, the formulation to arrive at the $a_{g,C}$ should take into account a different section of the acceleration spectrum, linked to the point that has the coordinates $(T_1, S_e(T_1))$, that are the first period of the panel and the elastic value of response spectrum in acceleration. Even in that case the a_g can be calculated with the two methods described above, considering the shape fixed or variable of the spectrum arriving at the following formulas.

Case 1, kinematic analysis in height:

$$a_{0i}^* \geq \frac{S_e(T_{1i})\gamma\psi(Z)}{q}$$

With the T_R fixed to 475 years and the shape of the spectrum fix:

$$S_e(T_{1i}) \geq \frac{a_{0i}^* q}{\gamma\psi(Z)}$$

Depending in which section of the spectrum acceleration there is the T_1 of the structure, an $a_{g,C}$ can be calculated reversing one of the equations of the definition of the spectrum (Eq.(32)). For the cases study of Castelnovo, to each façade is assigned the own period calculated with the simplified formula (used for the static linear analysis, NTC 08),

$$T_1 = CH^{\frac{3}{4}}$$

in which H is the height of the panel from the foundation system and C is a coefficient equal 0.05 for masonry structures. For the total amount of calculations done, the period of the structure is in the range of the plateau of the acceleration spectrum, identified by the T_B and T_C period, respectively 0.117 sec and 0.350 sec. The maximum T is 0.32 sec and the min is 0.13 seconds as reported in blue dotted lines in Figure 161a. In Figure 161b, there is the identification of the acceleration for each of simplified period: in that graph also it is possible to individuate that the $S_{ei}(T_{1i})$ lie in the plateau section of the spectrum, defined by this formula $S_e(T) = a_g \cdot S \cdot \eta \cdot F_0$. The $a_{g,Ci}$ is calculated reversing the formula:

$$a_{gi} \geq \frac{S_e(T_{1i})}{F_0 \eta S}$$

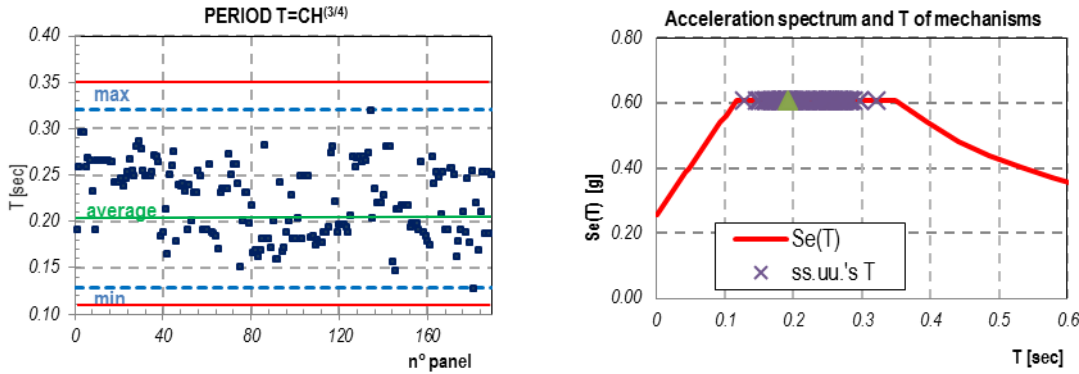


Figure 161: Period of all the out-of-plane mechanisms of the façades.

In the case 2, considering the shape spectrum variable the equation to calculate the $a_{g,C}$ is

$$(36) \quad a_{0i}^* \geq \frac{S_e(T_{1i})\gamma\psi(Z)}{q} \rightarrow S_e(T_{1i}) = \frac{a_{0i}^* q}{\gamma\psi(Z)}$$

in which the red terms are fixed, while the $S_e(T_1)$ changes with the formulas of the spectrum and the spectrum varies with the values of a_g , T_C^* and F_0 as already reported in Figure 160.

The process of identification of the $S_e(T_1)$ is iterative and analogous to the other explained for the mechanism clamped to the earth. It is necessary to calculate the range of acceleration spectrum, interpolating the values of the $a_g F_0$ and T_C^* (plus C_c , S_s values) for different values of T_R and find the spectrum that assume the researched value $S_e(T_{1i}) = (a_{0i}^* q) / (\gamma\psi(Z))$ at the period corresponding to the T_{1i} . Afterwards come back to the $a_{g,Ci}$ with the formula of the spectrum in which the structural period appears. For the mechanisms here analysed, the periods lie always in the plateau, from which the value of $a_{g,Ci}$ is calculated as:

$$a_{gi} \geq \frac{S_e(T_{1i})}{F_0 \eta S}$$

Concluding, the evaluation of the seismic safety for an aggregate can be done determining the safety index for an out-of-plane mechanism of a structural unit façade, using the kinematic linear analysis. The latter can be considered the right method in large-scale assessment for its simplicity of calculation and because it moves in a conservative way, since it underestimates the seismic capacity of the structure, in respect to more refined analysis (like the non-linear ones).

If the non-linear analysis, keeping into account the geometrical non-linear effects, can describe in a better way the real situation of the mechanisms, the safety indexes it provides are greater one-three times those coming from the linear analysis. Furthermore, the method can be applied in different way, since the last displacement of the capacity curve is not univocally indicated in the Standards recommendations (7.2.1.6). If the maximum displacement of the mechanism is calculated in the conventional way, the safety index could be significantly overestimated. The results could be not realistic, since displacement of the control point for the definition of the capacity curve can overcome even the thickness of the façade. If the maximum displacement is determined by the collapse of the floor, as done in the example reported in 7.2.1.7., the mechanism is stopped in correspondence of lower value of displacement, compatible with the panel geometry and loads in play. The safety index moves toward that of the linear analysis.

The capacity of a masonry façade is taken equal to

$$a_{g,Ci} = \frac{a_{0i}^* q}{S}$$

considering the acceleration of capacity a_0^ coming from the overturning of the total height and considering the hinge configuration at the ground floor. The behaviour factor, q , is fixed and equal to 2 and considering the A ground type and T_1 topographic category in order to have S coefficient equal to 1.*

7.2.3 PARAMETERS THAT INFLUENCE THE KINEMATIC ANALYSIS

This paragraph explains the influence of the geometrical parameters and the loads in the capacity results of out-of-plane mechanisms coming from both the linear and non-linear analyses. The goal is to identify which parameters (among those involved in the definition of the analytical model, Eq.(22)) play a crucial role in the analytical results of the kinematics analyses. To assess this comparative evaluation, an ideal façade has been exploited: it has the geometrical, structural and loads characteristics equal to the average values of the façades analysed in the case study. The panel is composed of unreinforced irregular stone masonry and the façade has these basic geometric characteristics (see also §3.3):

N = number of floors = 3;

Average interstorey of about 3 metres ($h_{av,GF}=3.05\text{m}$, $h_{av,1f}=2.95$ and $h_{av,2f}=2.90$ metres)⁷;

The width is 6.5 m;

Thickness increasing from the top to the bottom, $t_{av,GF}=0.65$ m, $t_{av,1f}=0.60$ m and $t_{av,2f}=0.57$;

The openings percentage at the ground floor is 79% of the gross areas and 87% both for the first and the second floors;

The normal stress of $\sigma_{GF}=0.28$ kN/m, $\sigma_{1f}=0.18$ kN/m and $\sigma_{2f}=0.18$ kN/m considering the normal force acting in each floors in a cross section equal to the multiplication of the thickness and the width (consider the load defined in CHAPTER 3).

The eccentricity of the slabs force, which is related to the type of storey with a triangular elastic distribution of the stresses in the resulting force, is half width of the cross section;

The confidence factor, CF, remains stable at 1.35, for the hypothesis of the infinite compressive resistance;

No vaults or metallic tie-rod are present in any floors.

The assessment method consists in the variation of one parameter at a time and evaluating the results of the analysis, with reference to the multiplier of the horizontal loads (α_0), the acceleration capacity (α_0^*) and safety index for linear analysis (I_{SL}), while for non-linear analysis the ground floor rotation (θ_i), the ultimate displacement capacity (d_u^*) and safety index (I_{SNL}). The acceleration and displacement of demand are relative to the spectra of Castelnuovo, defined in paragraph (§1.1.1.1). The results are plotted in graphs, in which in the x-axis there is always the changing quantity (parameter), while the ordinates are the results of linear and non-linear analyses, which for convenience of representation they are sometimes coupled. As regards the results of non-linear analysis, they relate to the conventional procedure, without considering the case of the collapse of the floors (§7.2.1.6). The results refer only to the activation of the ground floor hinge mechanism in accord with what already exposed in paragraph 7.2.2. The results of the analysis are provided for each of this parameter changing.

Each parameter changes initially in one single floor, Figure 162 shows the variation of the parameter “thickness” of the top floor, and then the procedure is repeated for all floors. The range of values taken by the parameters varies as a function of the average values calculated from sample analysed and reported in the characteristics of building heritage of Castelnuovo (§3.3) or enter admissible values.

For the standard case (related to the geometry and loads defined above) the results are reported in Table 54. From it were evaluated the influence of:

- Masonry type (with reference to the masonry classification in C.M. n.617, 2009, Tab. C8A.1.2.1-2);
- Confidence Factor (CF);
- Thickness (t);
- Height of the storeys (h);
- Percentage of holes in façade (% openings);
- Normal load (N);
- E eccentricity of the normal loads (distance from the point of application of the normal load and the position of the hinge configuration in the direction of the cross section);
- Tensile force of the tie-rods (T);

⁷ Subscript GF means ground floor.

i. Thrust of a masonry vault (N_H).

The results are reported in extensive way for the three initial case ("Masonry tyoe", "Confidence Factor" and "Thickness"), whereas in a synthetic way for the others. The missing graphs are showed in Annex 3.

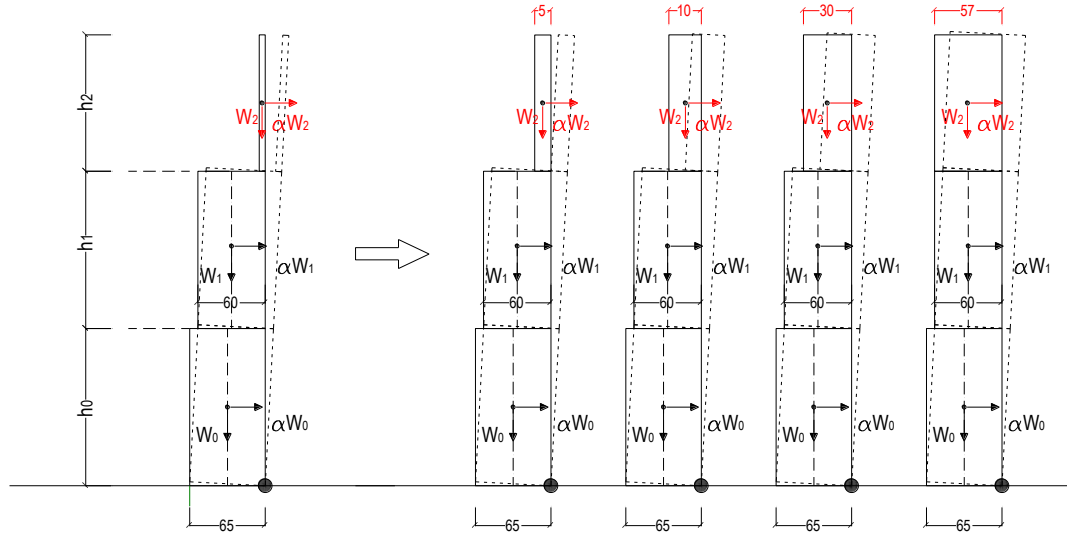
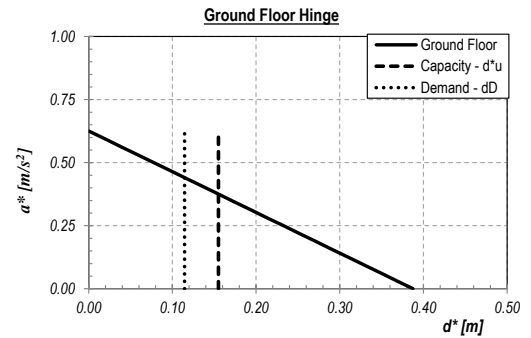


Figure 162: Example of the variation of the parameter "thickness" of the top floor.

Table 54: Results for linear and non-linear analysis for the standard case ($FC=1.35$).

Mechanims type	α_0	α_0^* [m/s ²]	a_D [m/s ²]	I_{SL}
GF hinge	0.06	0.60	1.26	0.47
	θ_i [°]	d_u^* [cm]	d_D [m]	I_{SNL}
	3.86	15.51	11.46	1.35



Influence of the masonry type

The masonry type influences the results only in defining the weight (as the multiplication of the specific weight γ_m and the volume of the panel). It is supposed the infinite compressive strength and is not considered the retraction of the hinge. The masonry type is not influential for the analysed results, since the self-weight of the structure influences equally the destabilizing moment and the stabilizing one, not changing the α_0 or the α_0^* .

Influence of the confidence factor (CF).

The CF is the confidence factor (§3.4), a safety coefficient to reduce the resistance (mechanical characteristics) of the masonry in order to take into account the uncertainty related to the knowledge process of the existing structures.

α_0^* changes with the values of the CF, proportionally to the inverse of its value (the graph is that of one hyperbola). This law is the same as for the a_{gC} . The graph of this correlation is plotted in Figure 163.

$$\alpha_0^* = \frac{\alpha_0 g}{e^* FC} \rightarrow \alpha_0^* = f\left(\frac{1}{FC}\right)$$

The θ_i does not change (Figure 164a) with CF: it is a function of only the positive/stabilizing momentum, which is stable with the CF change. d_u^* is stable since is a function of the last displacement d_{k0} at the top of the structure (Figure 164b). d_D is changing, and the I_{SNL} is changing (Figure 164c), why? The elastic displacement d_s^* is calculated as the 40% of the last displacement and for this reason it is stable.

The acceleration curve (capacity curve) is a straight line descending and the greater α_s^* the greater is α_0^* , relating to the

minor coefficient CF (as it is possible to see in next equation).

$$a_s^* = a_0^* \left(1 - \frac{d^*}{a_0^*}\right)$$

The greater the a_s^* the smaller the elastic secant period of the structure, T_s , as it is showed in the Figure 165. One should remember that the T_s is needed to calculate the demand displacement in the elastic response spectrum in term of displacement. The shape of the latter response is shown on Figure 7: to structure characterised by high period corresponds larger displacements of demand (d_D).

In conclusion, CF influences directly the capacity acceleration for the linear analysis (a_0^*), while in the non-linear analysis it influences the demand of displacement (d_D). The ratio between the indexes of security (I_{SNL}/I_{SL}) is reported in graph Figure 164d, in which the straight line grows linearly with CF: the results of the linear analysis are greater affected to the change of CF. Indeed, the percentage of variation from the extreme cases CF=1 and CF=1.35, is:

for a_{gC} and I_{SL} -26% for the linear analysis,

for the I_{SNL} -14% for the non-linear one.

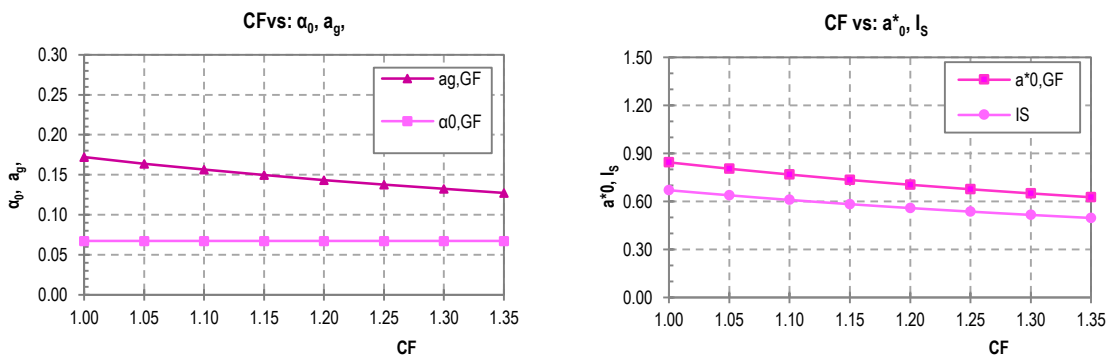


Figure 163: Results of the linear analyses a_0 , a_c^* , a_{gC} and I_{SL} for overturning mechanisms for different values of CF (1÷1.35).

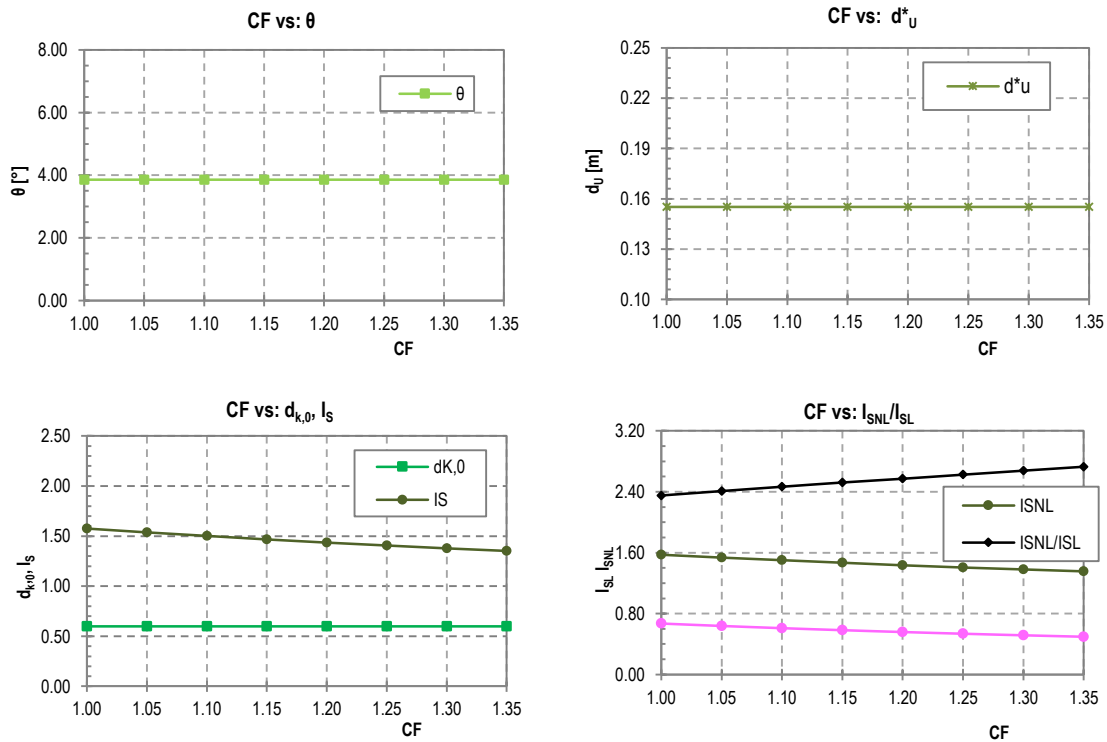


Figure 164: Results of the non-linear analyses θ , d_u^* and I_{SNL} for overturning mechanisms for different values of CF (1÷1.35). Last graph refers to the ratio between the results for the linear and non-linear analyses.

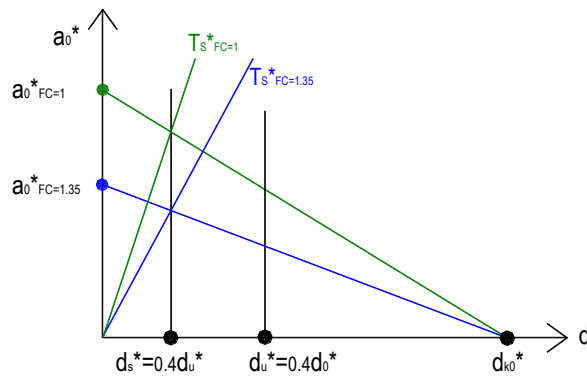


Figure 165: Capacity curves and individuation of the T_s^* for different value of CF.

Influence of the thickness (t)

In this case, the thickness changes step by step (Figure 162): at first only at the top floor, afterwards the second and first and finally the three floors together. For each step, the graphs of the results of the analyses were plotted, in order to understand, both in the linear and non-linear analyses, how much big the influence of the variation of this parameter is.

When only the last floor's thickness decreases, the capacity acceleration or displacements increase, as showed in Figure 166 and Figure 167. In the graphs there are identified in black points the results of the standard case. With black vertical continuous line, there is the individuation of the upper limit of the thickness for the last floor equal to 60 cm. After that limit there is a reversal of the trend of the results but this situation is not taken into account since it defines a unreal situation, for which the thickness of the upper wall is bigger than the lower one. With the increasing of the thickness the capacity of the structure decreases (in non-linear way). The last floor could be schematised as a seismic force localised in its barycentre: it generates a stabilizing momentum and a destabilizing one and since it is localized if height the momentum destabilizing is major than the other. The lower the force at the upper floor, the higher the structural capacity. This concept is equivalent to lower the entire structure barycentre, which means make bigger the horizontal forces that are necessary to overturn the structure.

In Figure 168 there is reported a summary of the results for the following case, in which both the first and the second floors' thickness are varying. The results trend is the same but the terms are widely amplified.

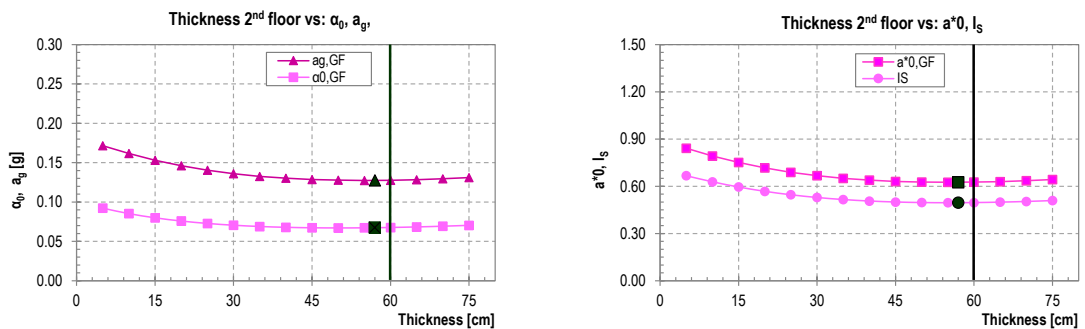


Figure 166: Results of the linear analyses for overturning mechanisms for different values of second floor's thickness.

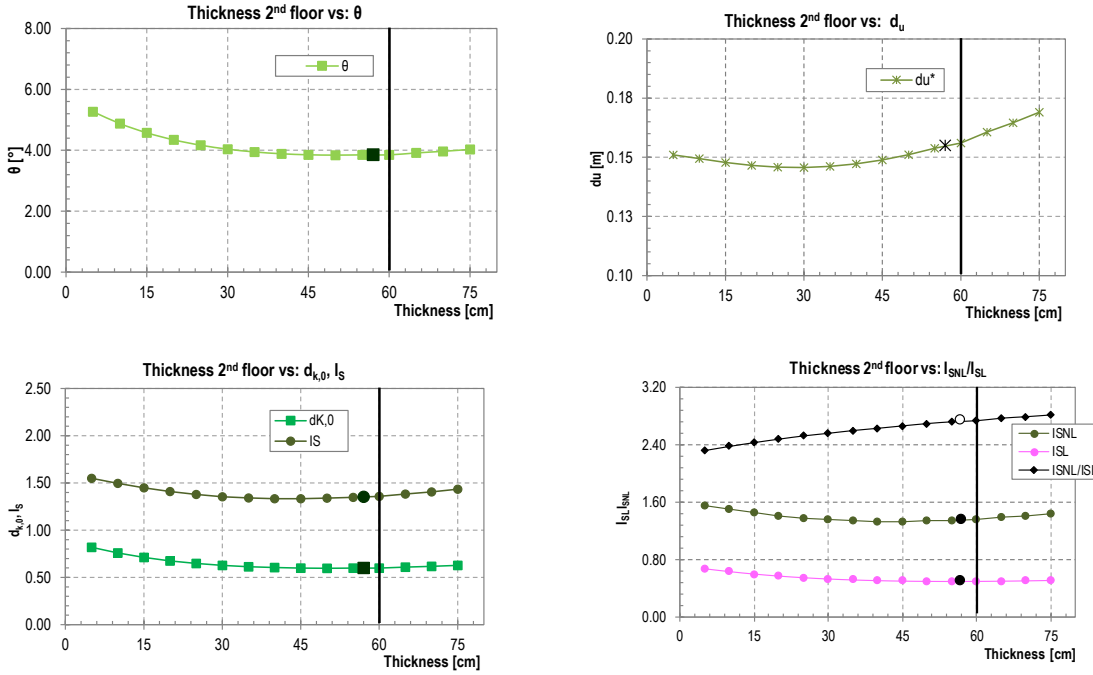


Figure 167: Results of the non-linear analyses θ_i , d_u^* and I_{SNL} for overturning mechanisms for different values of second floor's thickness. Last graph (d) refers to the ratio between the results for the linear and non-linear analyses.

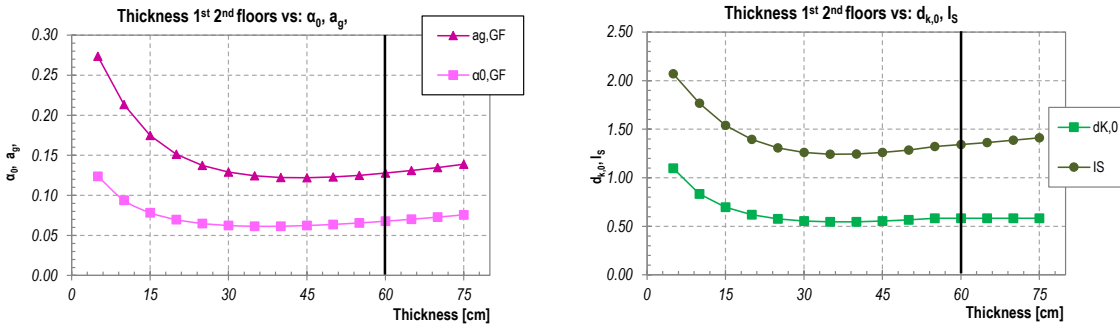


Figure 168: Results of the linear and non-linear analyses for different values of thickness of the 1st and 2nd floors (5-57 cm).

The variation of the thickness of the three storeys changes completely the situation that evolves in opposite sense. With the increase of the thickness the capacity of the structure (both in terms of α_0^* and α_{gC}) increases linearly (Figure 169 and Figure 170) and the ratio between the safety indexes is stable Figure 170d (value equal to 2.7). This results are in line with what already expressed in the definition of the kinematic method: if the thickness is changing simultaneously, the three-storeys structure behaves as a single structure for which the multiplier of horizontal loads (α_0) is proportional to the thickness of the structure and inversely proportional to the height of the structure (Figure 139 and Annex 3).

In the following, the results of variation percentages for the case analysed are showed, with reference to the variation enter the results of the maximum and the minimum parameter value changing.

When only the upper floor's thickness changes, the variation is calculated from the lower limit (5 cm) and the real case (57 cm):

- α_{gC} and I_{SL} -26% for the linear analysis,
- I_{SNL} -12% for the non-linear one.

When the thickness of first and second floor change, the variation is calculated from the lower limit (5 cm) and 57 cm:

- α_{gC} and I_{SL} -53% for the linear analysis,
- I_{SNL} -35% for the non-linear one.

For the last case, the comparison is done starting from a thickness of 15 cm, as the panel was a brick masonry, and the real thickness of about 60 cm for each floor. The results, for linear and non-linear analyses, show a variation range of about 300%. The real case has three times capacity greater than the other case which 15 cm thin.

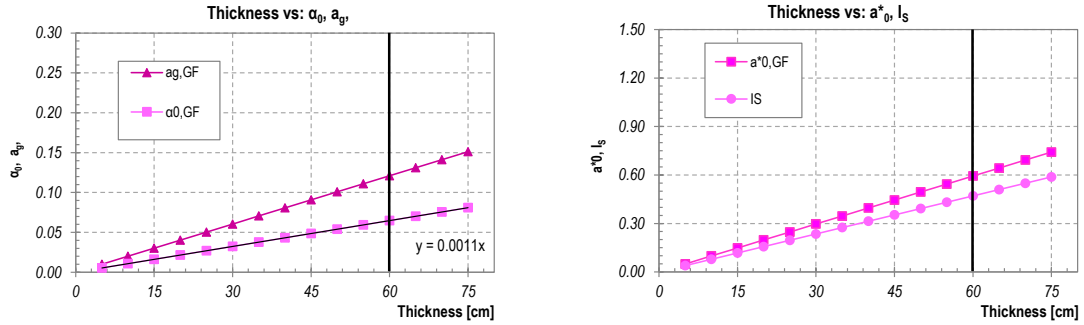


Figure 169: Results of the linear analyses for different values of ground, 1st and 2nd floors' thickness.

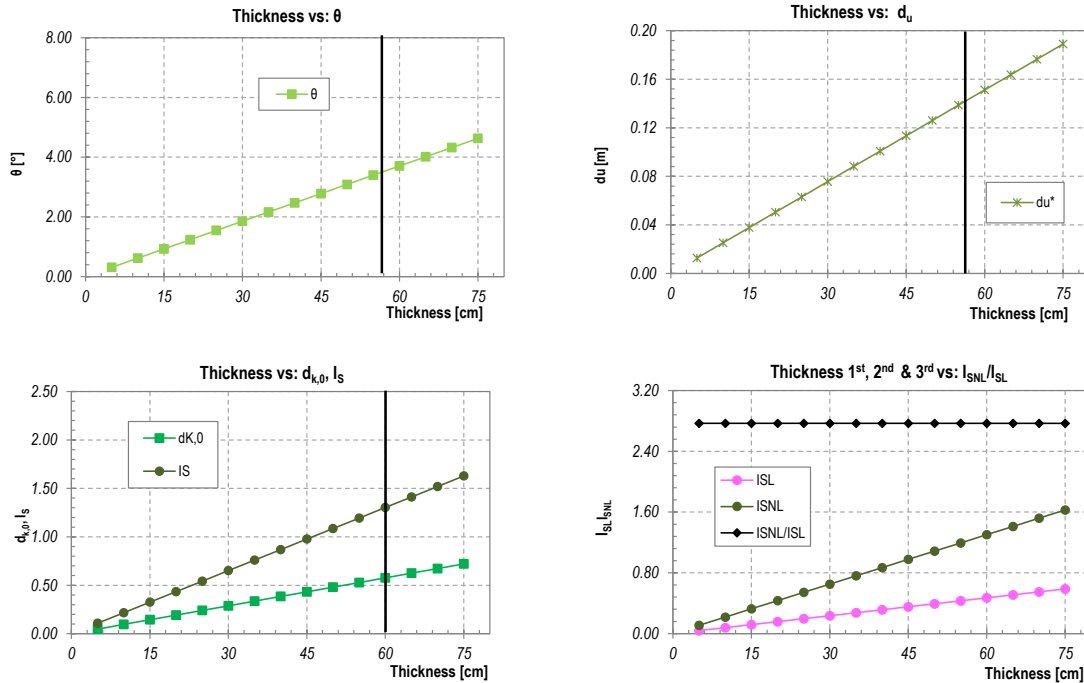


Figure 170: Results of the non-linear analyses for different values ground, 1st and 2nd floors' thickness.

Influence of the height of the interstorey (h):

The storey height significantly affects the mechanisms. Starting from the ideal case, the height's change is performed for step, starting from the top floor. The height varies enter 1 metre and 4.5 meters.

When only the height of the last floor varies, the capacity decreases with increasing height (Figure A. 3), as well as it was the case for the variation in thickness (Figure 166), due to the growth of the destabilizing momentum. The trend is not reversed even when the variation of height includes all the storeys: the multiplier of the horizontal loads (and therefore the acceleration capacity) rests inversely proportional to the height (Figure A. 7, Figure A. 8 and Figure 139).

The results in terms of the percentage of variation are showed for the three steps. For the first step, the variation is calculated from the lower limit (1 m height) up to 4.5 m:

- a_{gC} and I_{SL} -36% for the linear analysis,
- I_{SNL} -20 % for the non-linear one.

For the second step:

- a_{gC} and I_{SL} -61% for the linear analysis,
- I_{SNL} -37% for the non-linear one.

For the last case:

- a_{gC} and I_{SL} -87% for the linear analysis,
- I_{SNL} -67% for the non-linear one.

Comparing the results, the thickness affects more clearly the variation of capacity in the kinematic mechanism, when the geometric dimension are changing simultaneously at the three floors.

Influence of the percentage of holes in façade (% openings)

The average value of holes percentage is approximately 84% (for the total three floors). The results are given for step also in this case, starting to include holes in the second floor of the building, from an initial full panel.

Considering only the second floor, the capacity increases as the holes percentage increases due to the weight reduction on top of the structure. This trend is amplified with the insertion openings at first floor, while an inversion in the trend is observed of simultaneous openings in the entire structure.

The results in terms of the percentage of variation are showed for the three steps. For the first step, the calculation is done from the lower limit, that is the wall without openings, up both to 40% of openings, that represents the upper limit in Castelnovo buildings characteristics, individuated with a vertical black line in the graphs in Annex 3, and 70% .

For the first step:

- a_{gC} and I_{SL} 14% for the linear analysis (0%-40%) and 31% for (0%-70%)
- I_{SNL} 9% for the non-linear one (0%-40%) and 20% for (0%-70%);

For the second step:

- a_{gC} and I_{SL} 21% for the linear analysis (0%-40%) and 63% for (0%-70%)
- I_{SNL} 15% for the non-linear one (0%-40%) and 45% for (0%-70%);

For the last case:

- a_{gC} and I_{SL} -10% for the linear analysis (0%-40%) and -29% for (0%-70%)
- I_{SNL} -7% for the non-linear one (0%-40%) and -10% for (0%-70%);

Comparing the results to datekness, the % of opening affects minus evident the variation of capacity of the kinematic mechanisms.

Influence of the normal load (N)

The presence of normal stress does not influence significantly the mechanisms' results. In this case also, the variation of axial force of storeys is performed by step, starting from the top floor (roof's load). Initially, there is the absence of axial load (only self-weight) and subsequently the wall are charged up to a value of the normal stress present typically. In particular, the value reached at the top is 7.5 kN/m (presence of lightweight roofs in wood), while for the ground floors the considered value is 28 kN/m.

The variation of the results with the growth of the normal stress is very little, since the external load present is a small percentage of the self-load of the structure. Furthermore, only 20% of the cases analysed the roof slab rests directly on the main façade, in the remaining case, only one joist discharges in the wall considered in the overturning mechanism.

The structure's capacity decreases with increasing of the normal stress in coverage and the second floor (order variations of about 5%), while it increases when the load increases at the ground floor (order variations of 20-25% in the linear analysis). If the load increases proportionally to all floors, the results are stable as in the absence of normal stress with a decrease of the capacity of about 3.5%. In non-linear field, due to the definition of the size in play (Eq.(25)(25)), the last displacement of the SDOF, d_u^* , increase of about 15% making greater the I_{SNL} of 5%, in opposite with what happened in the linear analysis.

Influence of the eccentricity of the normal loads

The eccentricity is the distance between the point of application of the normal load and the position of the hinge configuration in the direction of the cross section, that coincides with the panel external extreme.

The eccentricity changes the stabilizing moment of the floors' weight forces. For the same reasons listed in the previous paragraph, the variation of eccentricity involves little changes in the capacity of the structure. In any case, as the distance of eccentricity increases the structural capacity increases, since it increases the arm of the stabilizing normal floors' load.

Influence of tensile force of the tie-rods (T)

The axial force of the tie-rod is a very influential parameter in the results of the analysis. It always has an effect of *increasing* the capacity, since it represents a force that exerts only a stabilizing moment. The variation of the tie-rod force is performed by step, starting from the top floor. The tie-rod is applied in correspondence of the slab's height (§7.2.1.10). The beneficial effect of the tie-rod on the results increases with the increasing of the altitude of application point. At each floor, the tie-rod's force for hypothesis can arrive up to 75 kN (n.3 tie-rods).

The results in terms of the percentage of variation are showed for the three steps. For the first step, the variation is calculated from the lower limit (no tie-rods) up to 75 kN for one floor and afterwards the tie-rods were applied to all the floors (Annex 3).

For the first step (tie-rod at the coverage floor, Figure A. 17 and Figure A. 18):

- a_{gC} , I_{SL} and I_{SNL} increase 330%.

For the second step (tie-rod at second floor):

- a_{gC} , I_{SL} and I_{SNL} increase 220%.

For the third step: (tie-rod at first floor):

- a_{gC} , I_{SL} and I_{SNL} increase 114%.

For the fourth step (tie-rod simultaneously) (Figure A. 19, Figure A. 20):

- a_{gC} , I_{SL} and I_{SNL} increase about 670%.

Influence of thrust of a masonry vault (F).

The vault's thrust is very influential parameter in the results of the analyses. It always has an effect of *decreasing* the capacity, since it represents a force that exerts only a destabilizing moment (or better, which reduces the stabilizing moment). In this case also, the variation of the thrust force is performed by step, starting from the top floor (roof's load). The thrust is applied at the altitude of the impost, about a meter below the keystone, considered fixed in this parametrical analyses.

In case the thrust reaches high values or when the vaults are at the upper floor, the mechanism is not balance and the multiplier of collapse, and accelerations of capacity are null. This means that for the forces in play, the equilibrium is not respected even in the standard situation and the structure could not support any other horizontal loads.

The results in terms of the percentage of variation are showed for the three steps. For the three steps, the variation is calculated from the lower limit (without any thrust) up to 50 kN for, in order, second, first and ground floor vault's thrust:

For the first step (Figure A. 21 Figure A. 22):

- a_{gC} and I_{SL} (linear analysis) and I_{SNL} (non-linear analysis) decrease of 166%;

For the second step (Figure A. 23 and Figure A. 24):

- a_{gC} and I_{SL} (linear analysis) and I_{SNL} (non-linear analysis) decrease of 125%;

For the third step (in which the variation is only for the ground floor) (Figure A. 25):

- a_{gC} and I_{SL} (linear analysis) and I_{SNL} (non-linear analysis) decrease of 67%. In this case the mechanism does not arrive at the loss of equilibrium, since the multiplier of the horizontal loads remains positive value for each level of thrust in that plane (from 0 up to about 50 kN).

For the last step (the thrust is present in each floor) there is a variation of (Figure A. 26 and Figure A. 27):

- a_{gC} and I_{SL} (linear analysis) and I_{SNL} (non-linear analysis) decrease of more than 500%.

A summary table is provided below, in which the results of linear and non-linear analyses are shown as a function of the variation of the investigated parameters. The results refer with the third (or in certain cases the fourth) step of the analyses, in which the parameters change in each floor from a situation of absence up to the situation of “maximum” presence of it. The percentages of variation are not equal for each parameter since they varying in a range of value not fixed, because they are relative to standard situations that occurred in the case of buildings in aggregate with particular reference to the case study of Castelnovo (§column 2, Table 55). The variation ranges of the results should be considered relative in accord to this aspect: for certain parameter the capacity results is influence by the absence/presence of other parameters in play (i.e. the presence of a vault’s thrust and tie-rod), therefore this results should be considered “ideal” and working only for a parametric analysis of one parameter at time.

Table 55: Variation of the results of the linear and non-linear analyses for geometrical and loading parameters varying.

PARAMETER	Range of variation	α_0	a_{gC}	I_S	θ	d^*_U	I_{SNL}
		%[g]	%[g]	%	%[°]	%	%
Type of masonry (Category)	I-XI	No results variation if the boundary condition are stable					
Confidence Factor (cf)	1÷1.35	0	-26	-26	0	0	-16
Thickness (t);	5÷60 cm	+300	+300	+300	+300	+300	+300
Height of the storeys (h);	1÷4.5 m	-83	-87	-87	-83	-21	-67
Percentage of holes in façade (% openings)	0÷40 %	-7	-10	-10	-7	-4	-7
Normal load (N);	0÷14 kN/m	-0.5	-3.5	-3.5	-0.5	+15	+5
E eccentricity of the normal loads	0÷60 cm	-19	-19	-19	-19	-19	-19
Tensile force of the tie-rods (T)	0÷75 kN	+669	+669	+669	+630	+636	+652
Thrust of a masonry vault (N_H).	0÷7.5xL ⁸ kN/m	-530	-530	-530	-525	-522	-527

From a theoretical/analytical point of view, the parameters *thickness*, *height*, *presence of tie-rods* and *presence of vault’s thrust* are the parameters that influence in widely way the results of local mechanisms, doing both linear and non-linear analyses. These parameters will be considered directly in the definition of the Façade Form as it will be better explained in CHAPTER 8.

⁸ L= length of the façades, considered here 6.5 m as average values.

7.3 IN PLANE MECHANISMS COLLAPSE AND GLOBAL BEHAVIOUR OF MASONRY AGGREGATES: SIGNS

In this paragraph, the explanation of the main features at the base of global seismic behaviour that a masonry existing structure could have, are reported. In previous paragraph, it has been affirmed that the seismic capacity for the aggregates of historical city centre was that referring at the out-of-plane mechanisms associated to the entire overturning of the main façade. Despite that, for completeness, a brief overview of one possibility to assess the global structural seismic analysis to masonry aggregates are defined in the follow. A more accurate assessment of the global modeling of aggregates can be found in most specific literature, i.e. (Augenti, 2004), (Galasco et al., 2004), (Magenes & Della Fontana, 2010), etc.... In a structure in which the slabs (as reinforced concrete slabs) are enough stiff in their plane and well-connected with the vertical elements, all horizontal actions (as seismic actions) pass on in the vertical elements due to their in plane stiffness. If the vertical walls are well organised each other they work together against the seismic actions, giving rise to the uniform behaviour of the structure, so called “box behaviour”. The walls respond in their plane, with the in-plane mechanisms (Figure 135b). If these mechanisms are assured, the structure can be study with a global analysis, performed in the global model of the aggregate. Within the structural analyses provided by the Code (NTC, 2008 -§7), the global analysis performed as analytical method in few examples of Castelnuovo aggregates was the static non-linear analysis, nowadays commonly used for existing masonry buildings, as suggested in current Standard (C.M. n.617, 2009). With the use of this analysis, the vulnerability estimation is done by evaluating the safety index, as well as for the out-of-plane mechanisms, defined as a ratio between the capacity peak ground acceleration and that one of demand. The capacity of the structure is calculated considering the last displacement of the structures in the capacity curves, following the procedure described at par.7.3.4.1 of (C.M. n.617, 2009).

7.3.1 TYPES OF IN-PLANE MECHANISMS IN MASONRY PANELS

The in-plane mechanisms, so called the “second way mechanisms” provide collapse failure modes of masonry panels in their plane. Two mechanisms refer to the shear failure, *joints bed sliding* and *diagonal cracking*. One mechanism refers to the flexural collapse mode, the *rocking* (Figure 171). Each mechanisms provides an ultimate value of shear for the panel, $V_{R,BS}$, $V_{R,DC}$, $V_{R,R}$. The minimum values of them is the maximum shear force that the panel can achieve during an earthquake, the ultimate shear, V_u . This value depends on the geometrical characteristics of the panel, on the material and on the vertical loads acting in the panel, due to both the masonry weight and the slabs' forces.

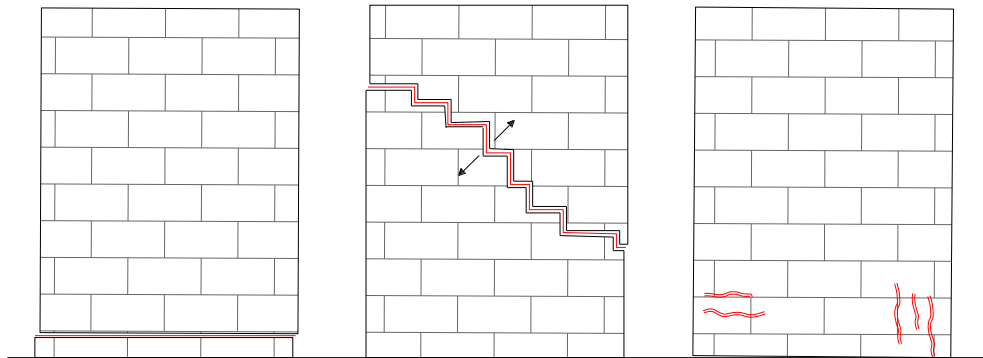


Figure 171: In plane mechanisms: (from the left) shear failure joints bed sliding, diagonal cracking and rocking.

JOINTS BED SLIDING

This collapse mechanism is due to the achievement of a limit value of the shear stress (originated by the horizontal force V) in combination with the normal (compression) stresses. This mechanism can be associated with the creation of horizontal cracks frequently in the mortar joints. In accord with the Coulomb theory, the law which explains this mechanism is represented by the formula $\tau = c + \mu\sigma$. According with the NTC 2008, the design unitary shear resistance is defined as $f_{vd} = f_{vk}/\gamma_M$ where f_{vk} could be calculated with $f_{vk} = f_{vk0} + 0.4 \sigma_m < f_{vk,lim}$, the friction ratio μ values 0.4 and

σ_m is the normal compression $\sigma_m = P/l't$. P is the axial force and $l't$ represents the compressed panel cross section: t is the thickness and b' is the length of only compressed side of the panel. The shear resistance of the panel for joints bed sliding is calculated multiplying that resistance for the compressed panel cross section $V_{R,BS} = l'tf_{vd}$.

In the Standard and in scientific literature, recommendations concern not to consider this mechanism for existing and disorganised stone masonries. Joints bed sliding is a mechanism collapse referring to new masonries or existing ones but characterised by homogeneous brick elements and aligned and ordered mortar joints with horizontal orientation.

DIAGONAL CRACKING.

The collapse is due to the achievement of a limit value of the shear stress (originated by the horizontal force V) in combination with the normal (compression) stresses. In this case, the damage mechanism originates diagonal cracks. They follow the mortar joints or both the blocks and the mortar joints, depending of the mortar mechanical characteristics and the disposition the joints. The formulation of the limit strength for Diagonal Cracking follows the Turnšek e Cačović (1971) formulation, who experimentally determined diagonal cracks in the centre of the masonry panel considering the achievement of the limit tensile stress. The cited criteria is represented by formula:

$$(37) V_{R,DC} = lt \frac{1.5\tau_{0d}}{b} \sqrt{1 + \frac{\sigma_0}{1.5\tau_{0d}}}$$

in which b is a correcting coefficient link to the distribution of the strength in the section, which is dependent to the thinness of the panel, τ_{0d} is the shear resistance linked to the diagonal cracking of the masonry, $l't$ is the cross section area, σ_0 is the compressive stress in the centre of the panel.

ROCKING.

With this collapse type, an ultimate momentum resistant is defined, $M_{R,R}$. This mechanism is due to the crushing of the compression zone in the extreme section of the panel, due to the horizontal action increasing V . If there is low value of the compression strength (N), the length of the compression zone cover partially the section, and a phenomenon of horizontal cracking in the tensile side of the panel due to the horizontal thrust (Figure 171c) arises. In this configuration, the collapse is similar of an overturning, as the panel moves ad a rigid body. The resistance moment is given by this formula:

$$(38) M_{R,R} = \frac{\sigma_0 l^2}{2} \left(1 - \frac{\sigma_0}{kf_d}\right)$$

in which k is a coefficient in the range 0.85-1.

Dependency of the degree of bond at the top of the panel the static scheme could be different. The panel can be schematised as a cantilever (free on the top) or fixed at the top, the value of the shear changes depending of the degree of restraint. In particular, for cantilever scheme: $V_{R,R}=M_{R,R}/h$, for fixed scheme on the top: $V_{R,R}=2M_{R,R}/h$.

DRIFT CAPACITY OF MASONRY PANEL

In a static non-linear analysis, the masonry panel behaviour is schematized with elastic-plastic bilinear behaviour in shear and displacement. The ultimate shear is the maximum resistant value of shear, V_U , is equal to the minimum value of shear associated to a collapse type within the ones explained above.

The shear/displacements law is divided into two parts, the first part is elastic and the line's slope is the initial stiffness of the masonry panel, which is calculated with the formula in Eq.(39).

$$(39) K_o = \frac{Glt}{1.2h} \cdot \frac{1}{1 + \frac{(4)Gh^2}{1.2El^2}}$$

The elastic part of that law stops in correspondence with the maximum shear value, which corresponds to the ultimate limit shear calculated with the collapse failure mechanisms. The second part of the law is defined as plastic law, in which the shear remains stable until the ultimate displacement of the panel. The latter is calculated depending on the associated way of collapse, and it is a percentage of the total deformable height of the panel (h_w). The NTC2008 (§C8.7.1.4) recommends: $d_u = 0.4\% h$, if the collapse is for shear mode (both diagonal cracking and joints bed sliding); $d_u = 0.6\% h$, if the collapse is for flexural mode.

7.3.2 IN-PLANE MECHANISM FOR AN IDEAL PANEL AND EXAMPLES IN CASTELNUOVO AGGREGATES

In this section, a capacity curve is constructed for an ideal panel with the geometrical data expressed in the following table.

Table 56: Panel geometry.

l=	3	[m]	t=	0.5	[m]
h=	5	[m]	h/l	1.67	
h _w =	5	[m]	b=	1.50	

The panel is composed of irregular stone masonry. The mechanical characteristics follows the C.M. 2009 in table C8A.2.1, with a LC1 level of knowledge. The mechanical characteristics are average values of characteristic of masonry.

Table 57: Panel masonry characteristics.

$\tau_{0,d}$ =	1.48	[N/cm ²]
$f_{m,d}$ =	74.07	[N/cm ²]

The panel is supposed both constrained and free on the top. The initial stiffness is $K_1 = 409$ kN/cm if constrained on the top, $K_2 = 117$ kN/cm if it is free (cantilever scheme). Assuming typical floor loads (5.6kN/m² in seismic combination) the Table 58 shows the results of the calculation of the shear values associated to each in-plane mechanisms, for both the static schemes.

Table 58. Ultimate values of the shear force.

CONSTRAINED ON THE TOP			FREE ON THE TOP		
$V_{R,DC}$ =	50.9	[kN]	$V_{R,DC}$ =	5.09	[kN]
$V_{R,BS}$ =	78.7	[kN]	$V_{R,BS}$ =	7.87	[kN]
$M_{R,R}$ =	180.2	[kN]	$M_{R,R}$ =	180.2	[kN]
$V_{R,R}$ =	72	[kN m]	$V_{R,R}$ =	36	[kN m]
Shear diagonal cracking collapse			Rocking collapse		
V_U =	50.9	[kN]	V_U =	36	[kN]

The ultimate shear resistance of the panel is due to a diagonal cracking collapse and it is $V_U = 50.9$ kN for the first scheme and for a collapse of rocking for the second scheme, $V_U = 36$ kN . The ultimate displacement of the panel is 0.4%h (2 cm) and 0.6%h (3 cm), respectively.

The shear-displacement law of the panel is showed in Figure 172 in which in black dotted line there is the shear-displacement law for the first static scheme (panel with constraints on the top) and the other red line is for the cantilever. It is evident the changement of the collapse type. The continuous lines refer to the collapse of a panel with different geometrical characteristics ($h=3$ m and $l=2$ m), with both the static scheme considered.

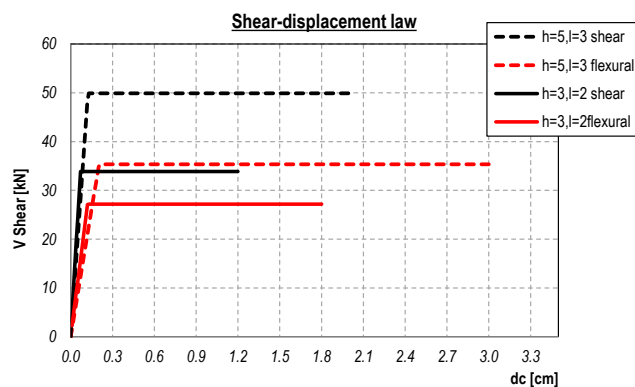


Figure 172: Shear-displacement law of the panel.

§

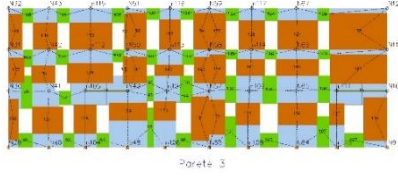
In this section, an example of the calculation of the in-plane mechanisms is described, with reference to typical masonry panels of Castelnuovo aggregates. The geometry of the panel is fixed by the geometrical limit and physic characteristic of the masonry real constructions. The studied panel is an idealistic panel that has as length the average length of the vertical elements, and for thickness, the weighted average of the panel's thicknesses present in the structural units, considering

the only ground floors. These geometrical values come from global modelling carried out in the aggregates of Castelnuevo building (3Muri© software (STADATA, 2012)), considering equivalent frame modelling scheme of the structural elements. The chosen aggregates are 10-088, 18-163, 27-415 e 57-179 (§Annex 1). In Table 59 all the geometrical characteristics of the ideal masonry panel are reported. In Table 60, there is the front of the aggregate on left and the identification of the equivalent frame panel's masonry on right.

Table 59. Geometrical characteristics of the masonry ideal panels, loads and value of the ultimate shear.

Aggregate	length (b) [m]	height (h) [m]	h/l	thickness (t) [m]	loads step.1 [t/m ²]	loads last step [t/m ²]	V _u [kN]
10-088	2.10	3.12	1.49	0.60	20.50	22.18	62.3
18-163	1.83	2.59	1.42	0.68	14.66	15.24	55.7
27-415	2.12	2.23	1.10	0.65	22.44	21.88	97.7
57-179	1.55	2.31	1.49	0.82	21.17	18.61	57.9
average	1.89	2.56	1.35	0.69	19.69	19.48	67.8

Table 60. Masonry walls investigated.

	
Aggregate 10-088	
 <p>*this wall is only a portion of the entire one studied</p>	
Aggregate 18-162	
	
Aggregate 57-179	
	
Aggregate 27-415	

In Figure 173 there are the graphs of the collapse's domains of the panels analysed. For the geometric characteristics and the average load, the results are very similar for the panel's type of the aggregates 10-088, 18-163 and 57-179, while the ideal panel of 27-415 shows higher values of shear resistant.

The yellow line represents the *joints bed sliding* failure domain, the grey represents the failure due to the *diagonal cracking* and the green one the collapse for *rocking*. In red line, there is the representation of the limit shear values in correspondence of the axial load due to the first step load of analysis and in red dotted line that one due to the last step. The black dotted line represents the shear ultimate value of the panel, for each combination of loads. The intersection between the red dotted line and the black one represents the ultimate point of the panel. Plotting the horizontal line for that point, it is possible to graphically calculate the value of the last shear of the panel, for the fixed condition of load.

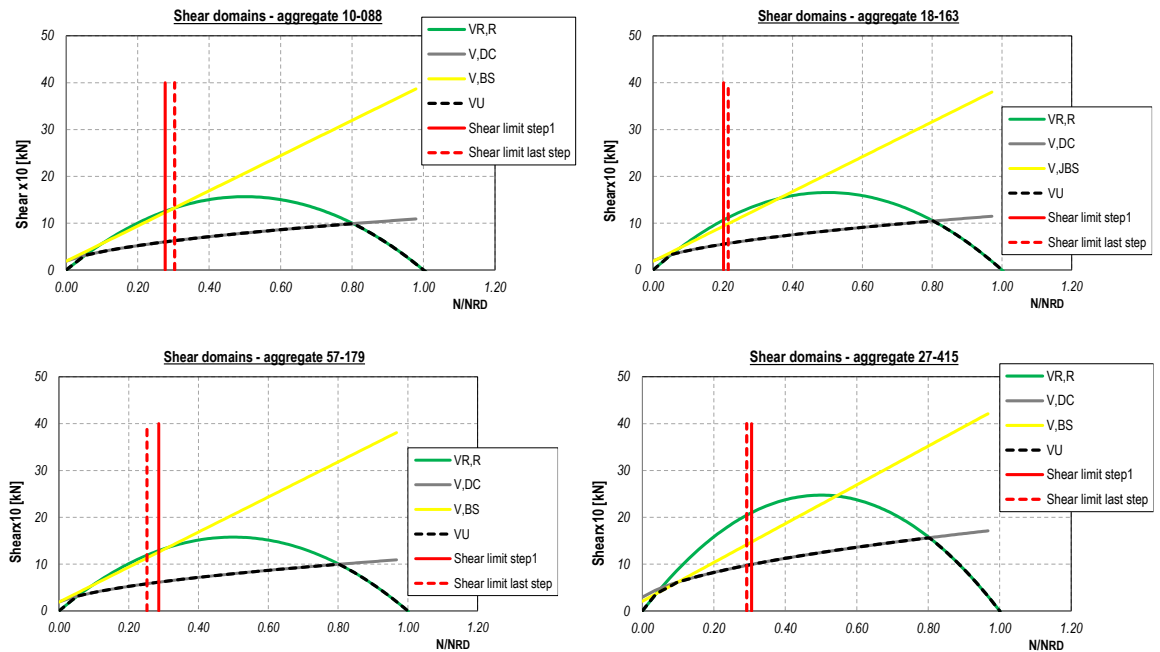


Figure 173: Collapse's domains of the panels (a) aggregate 10-088, (b) 18-163, (c) 57-179 and (d) 27-415.

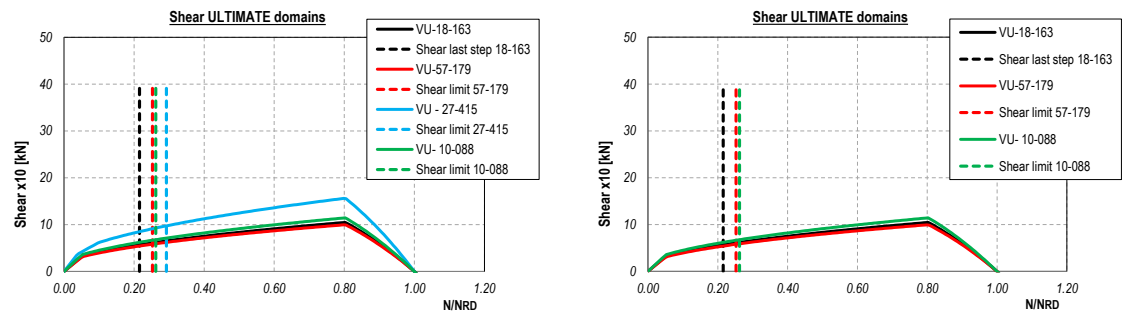


Figure 174:(a) Domains of the ideal panel. (b) Domains of the 10-088, 18-163 and 57-179 aggregate panels.

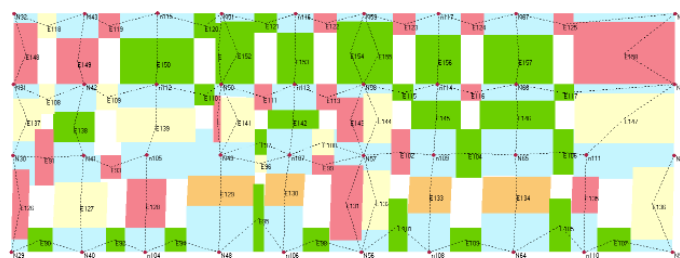


Figure 175: Panel collapse.

In Figure 174a there are all the panels' domains in which the difference in terms of shear resistance and the last step analyses loads can be observed. The minimum shear force is associated to 57-179 aggregate while the maximum is linked to the 27-415. If the latter is removed from the graph, the domains takes shape in Figure 174b. An almost complete overlap of the shape of the domains is showed. This is due to the ratio among the h and the l of the panels examined: the 27-245's slenderness is about 1, while the others have almost 1.5 h/l and equal loads in play.

From the analysis done, the plausible collapse mechanisms is due to diagonal cracking even if for panel characterised by high slenderness the collapse pass to the rocking.

Figure 175 shows the mechanisms collapse for an entire masonry wall found through a static non-linear analysis carried out in the 57-179 aggregate. The image refers to the last step of the analysis. That step corresponds to the decline of the 15% of the maximum shear of the aggregate, which is achieved with the collapse of a few panels (on the right side of the alignment). Their collapse is due to shear mechanisms for diagonal cracking and in certain cases for rocking. In particular, in yellow and orange colours are indicated the failure for shear collapse, while in pink and red colours the flexural collapses, for panel characterised by a major slenderness (or major height).

§

With the intention of studying the global behaviour of the aggregates, after having analysed the characteristics of the failure modes of the panels in their plane, the global-aggregate modelling for a reduced sample of aggregates were done. This to identify the safety level in terms of global behaviour for aggregates, once they could be studied in terms of global analysis, under the assumption of a good structural organization considering avoided the activation of the local out-of-plane mechanisms. The aggregates current state cannot ensure global seismic response ("box behaviour"), since they lacks of connections between orthogonal panels and among vertical and horizontal elements. This exercise is performed to give *information about the potential global response capacity of the aggregates if opportune structural interventions to avoid local mechanisms were done into them.*

In the global models, the hypothesis about the masonry mechanical characteristics and the achieved knowledge level are in line with those followed for the kinematic local studies. In the Figure 176, the results for the 57-179 are reported. In left there is the aggregate equivalent frame model, in which the structural deformable elements are indicated in different colours (in brown the piers, in green the spandrels and in grey the rigid nodes (Lagomarsino et al., 2013)). In right there are examples of push-over curves, results of the application of static non-linear analyses for x and y directions and for two lateral load patterns: proportional to mass (uniform) and proportional to mass and height (triangular).

From shape of the capacity curves and the last displacement, following procedure expressed in the actual Code (C.M. n.617, 2009 - chap.7), the safety indexes were evaluated, in term of global seismic capacity for the aggregates.

Without going into details of numbers, the minimum safety index for the global analysis is bigger than the safety indexes coming from the calculations of local out-of-plane mechanisms for the main façades of this aggregate.

These observations in the analytical calculations reinforce the hypothesis of having studied aggregates considering out-of-plane mechanisms in the main façades of structural units that compose it.

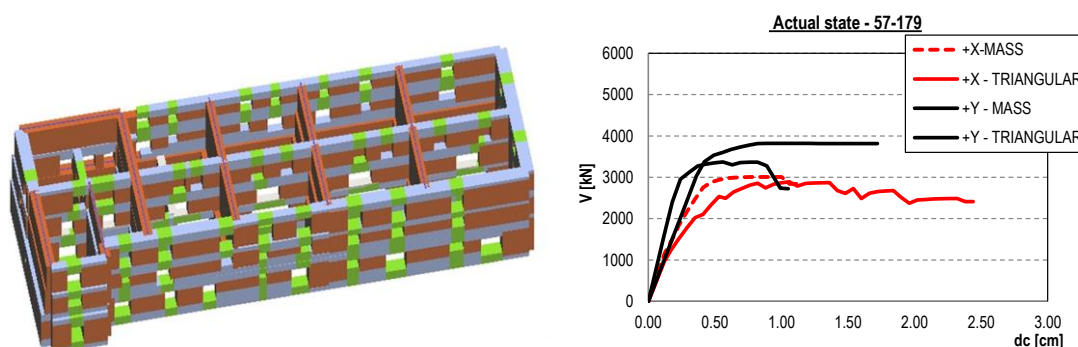


Figure 176: Global model of aggregate (equivalent frame model, 3Muri) and capacity curves.

7.4 CHOICE OF THE METHODOLOGY TO EVALUATE SEISMIC CAPACITY ON AGGREGATES

The aggregates, by definition, are composed of a set of masonry buildings (1.1). Therefore, they can be seismically analysed with the methods of analysis expressed in the previous chapters, with the seismic assessment of their local portions or the study of the global refined entire model. In particular, the local out-of-plane collapses can be calculated for each structural unit separately or in respect to the particular restraints that adjacent structural units can have. Indeed, the main façades of buildings are most affected by this type of mechanisms for the loads in play, the lack of connections and, at times, the presence of non contrast-thrusts forces of the vaults.

A different situation concerns the case of the study of masonry aggregate buildings, in their entirety. In paragraph 7.3 the in-plane failures of masonry walls, which are on the base of the calculation methods for the seismic evaluation of masonry structures were analysed. Form the analysis performed (even if reported in this work just in a qualitative way) the safety indexes are, on average, higher in respect to those coming from the local mechanisms.

Masonry aggregates of rural historical city centres should be analysed primarily through out-of-plane mechanisms. This can be explained considering different reasons:

- *The structural units that compose masonry aggregates can have different geometrical characteristics (in terms of height and thickness), different loads, different numbers of floors and staggered floors. The aggregate walls, even if the in certain case appears unique or continuous, cannot have specific restraints or do not collaborate with themselves, ensuring a “box global behaviour” of the aggregates.*
- *The lack of connections among vertical orthogonal walls and horizontal elements and vertical ones. Figure 177 shows some cases of collapses of horizontal elements due to overturning mechanisms of the main façades.*



Figure 177: Examples of lack of connections among vertical orthogonal walls and horizontal and vertical elements.

- *The damage mechanisms analysed in the post-earthquake Castelnuovo aggregates: when they did not show complete destruction or crumbling collapse, they manifested typical overturnings of main, rear and lateral façades. Even when the damage appeared concentrated on the horizontal elements – with, for instance, the collapse of vaults, ceiling vaults or steel floors (Figure 52) – it was due to the overturning, or rotation or displacements, of vertical elements that carry them.*



Figure 178: Damage mechanisms analysed in the post-earthquake Castelnuovo aggregates.

7.5 RESULTS FOR THE CASE STUDY (189 MASONRY FAÇADES)

In this paragraph, the results of the application of detailed method to out-of-plane mechanisms for the façades of Castelnuovo aggregates are reported. At first, there is the description of the sample of study, for which the main geometrical, mechanical and loads characteristics are shown. Afterwards, both the results of linear and non-linear analyses were explained, with summary histogram graphs. In particular, the histograms represent:

- the accelerations of capacity of the structures, $a_{g,c}$, (calculated as reported in §7.2.2) for the linear analyses;
- the capacity displacement of the structure, d_u^* for the non-linear analyses. The d_u^* is calculated both as reported in 7.2.1.6 paragraph, as the 40% of the capacity of the d_{k0}^* , and the capacity for collapses of slabs, for different hypothesis of the length of discharge of the slabs (described deepened in the following).

One should remember that the results here shown refers to the total amount of overturning mechanisms analysed (n.189), which correspond to the façades studied (in red in Figure 179). Therefore, for one structural units, more than one mechanism is in certain cases analysed, i.e. the front façade or the rear or lateral ones. In some other cases, principally in oldest core of the aggregates, adjacent structural units were evaluated both together in single mechanism, and separately in two different ones, in order to evaluate all the possible interaction configurations and the relative safety indexes. Furthermore, when in the façades there are tie-rods, the calculations are done with and without their influence.

The proposed Façade Form described in CHAPTER 8 is constructed starting from these results, considering a reduced subset of this sample of data, following the criteria exposed in the paragraph 8.3.



Figure 179: Individuation of the mechanisms analysed for the façades (in red).

7.5.1 GEOMETRICAL, STRUCTURAL AND LOADS CHARACTERISTICS

In this paragraph, the results of the main geometrical, mechanical and loads characteristics of the sample of study related to the calculation of the out-of-plane mechanisms are reported. They represent a portion of the whole building stock of Castelnuovo (already reported in §3.3).

Number of floors. This characteristic is the starting point of the evaluation of the aggregates since in next graphs, all the information will be grouped for floors, making homogeneous subset of the initial database. In the collected data, there are only two façades with 4-floors and 3 one-floor façades, while 94 façades (49.7%) have 2 floors and 90 have 3 floors (47.6%). The histogram of percentage of floors number distribution are reported in Figure 180a.

Length. The length is reported independently from the numbers of floors. It measures the width of the façade, or it represents the distance among orthogonal walls to the façade that overturns. The average values is about 6.5 m (Figure 180b) and the major frequencies lengths are enter 4.5 and 7.5 metres (total of 57.2%).

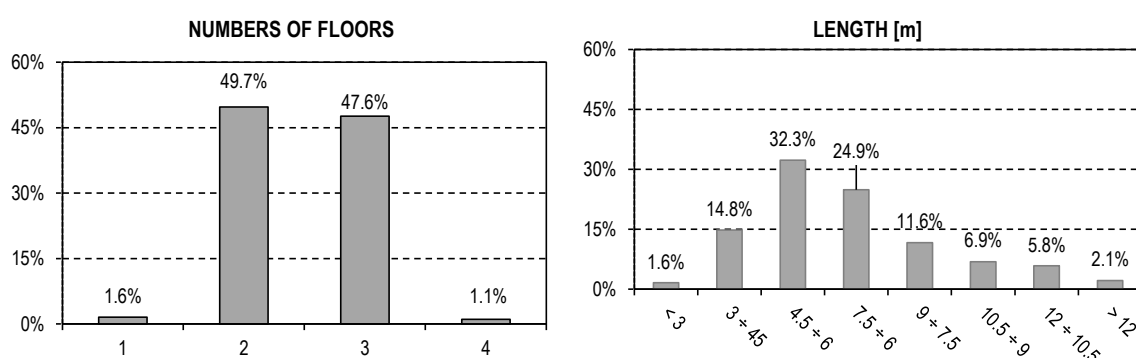


Figure 180: Distribution of number of floors and length.

Thickness, height:

In graphs in Figure 181 there are in greyscale the distributions of the thickness for each floor and in red the average value of the thickness for the all the floors. The number of the sample of data for each floor is reported on brackets in the legend: for ground floor 189 façades were analysed, 186 for the first floor, 92 for second floor and for the last floor only 2. For about the 80% of the cases, not depending on the floor, the thickness enters among 45-65 cm (Figure 181a).

The distribution of the total façades' height is represented in Figure 182a. Highest percentage of height is enter 6 and 9 metres that corresponds to two-three storeys façades, even if a significant part falls into 9-12 metres. Figure 182b contains the statistic about the height of each storey. In the major of case (more than 75%) for floors ground, 1st and 2nd the height is enter 2.3-3.2 metres, while the last floor's height is lower (in black in Figure 182b).

The *Slenderness* for each floors, that is the ratio enter the height of a plan and its thickness (h/t), and the distribution of the H/L (for total height and total length) are reported in Figure 183. Their average values correspond at about 5.2 (in red in Figure 183a) and 1.25 (Figure 183b).

The major frequencies of slenderness related to the ground and first floor fall enter 4 and 5, while it grows up for the second floor for which the thickness generally decreases for stable heights.

Net area. The distribution of the percentage of net area is shown in Figure 184; the holes cover on average the 25-35% of the total area of the panel. The minor relative percentage of holes is in the second and third floor.

Axial load. In the major part of the cases, the floors did not discharge in the main façade. In Figure 184b there is the histogram distribution of the axial load in the façade; indeed, the major percentages enters in lower loads classes. When the unit weight is in the range [0-4] kN/m means that only an influence area of a beam discharge over the façade. The load

of 10 kN/m is caused by stone vaults (3.3.2.2) typically collocated downstairs, related to the white bars in the histogram.

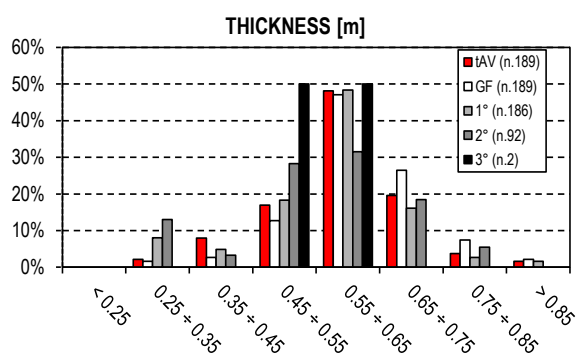


Figure 181: Distribution of thickness and height for the sample of data and different floors.

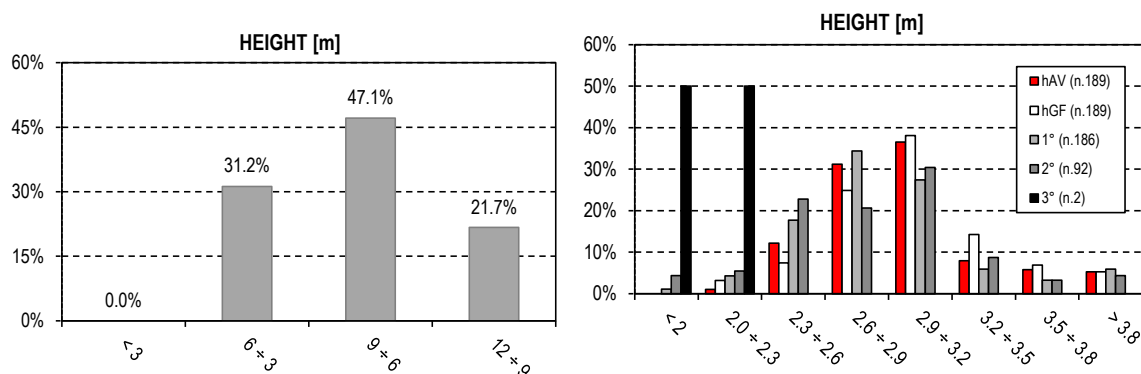


Figure 182: Distribution of the total height and height for each floors.

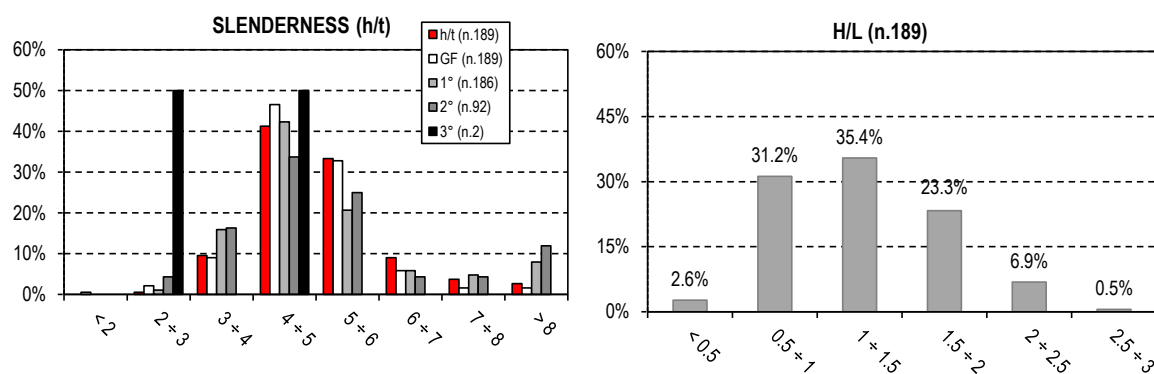


Figure 183: (a) Distribution of slenderness for different floors; (b) H/L distribution.

The distribution of the barycentre's height is reported in Figure 185a. The red bars refer to the barycentre of the total weight (considering the panel self-weight and the external loads), while the white ones refer to the barycentre of the only panel self-weight. It is worth nothing that the difference is negligible, since, as expressed in 7.2.3 the self-weight is the higher force in play in the mechanisms analysed. The distribution is composed by non-homogeneous data, since they differ for the number of floors. The barycentre distribution for each floor is showed in Figure 185b, where different colours refer to different n°-of-plane structure.

The thrusting forces of masonry vaults are present in n.62 façades, that represent the 32.8% of the total amount. The tie-rods are present in about the 30% of the cases. Among the 62 façades with the vaults presence, only the 50% have the presence of the tie-rods, too. Only in the 50% of cases, the thrusting force is contrasted by the presence of the tie-rods.

In Figure 186b, there are the distributions of the presence of qualitative parameters and specific aggregates issues related to the structural units, information found through the filling out of the Vulnerability Forms in previous chapters. The parameters are: the presence of non-structural elements, the presence of different height among the façades and the presence of staggered floors. The judgment for these parameters are differentiated for classes enter “A”, “B”, “C” e “D”, as explained in §2.2.2.

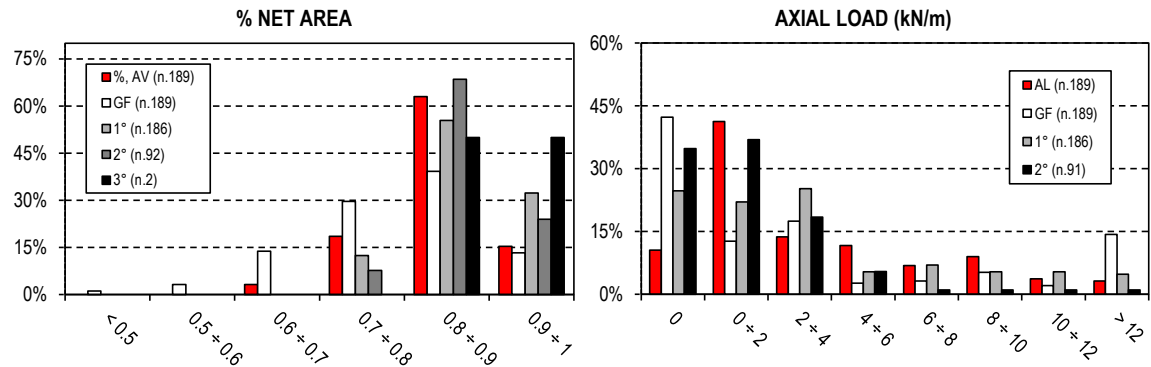


Figure 184: (a) Distribution of the net area average and for each floor; (b) Distribution of the axial load for each floor.

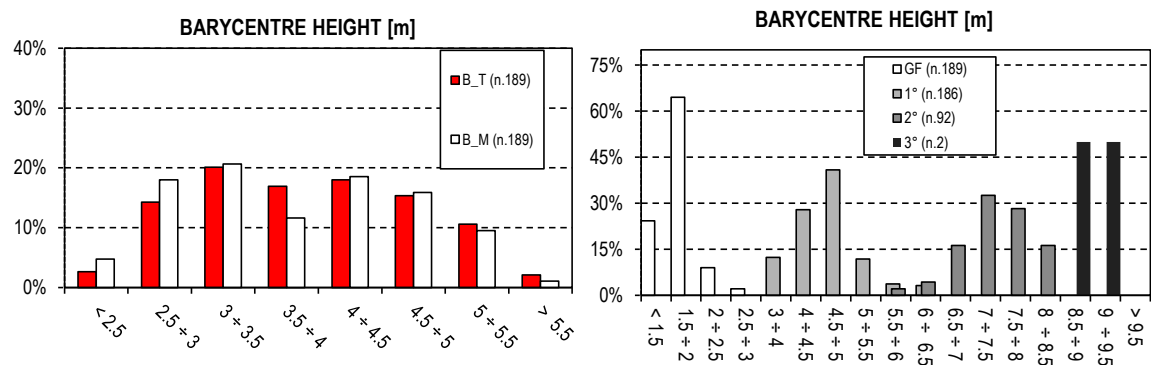


Figure 185: (a) Distribution of the barycentre in height for each floor.

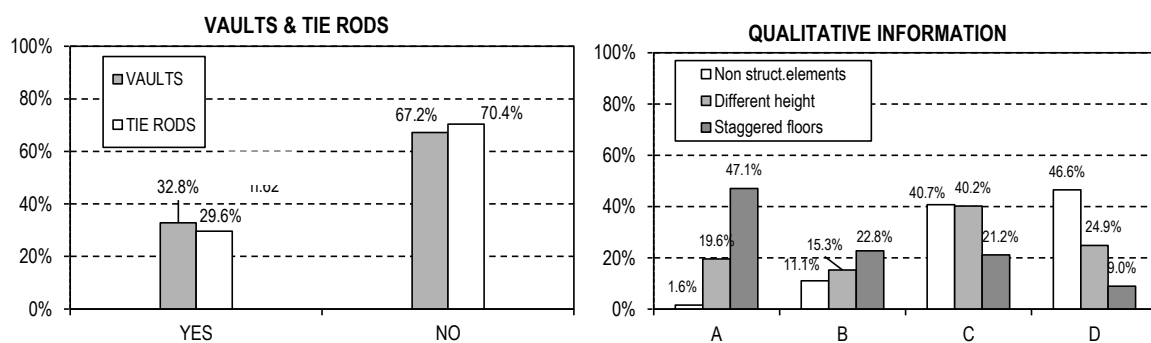


Figure 186: Vaults, tie-rods and qualitative information (parameters of the vulnerability form).

7.5.2 CAPACITY OF THE FAÇADES

The results provided in this paragraph refer to the 189 façades. The accelerations of capacity of the structures, $a_{g,c}$ is calculated for linear analysis, for the hinge configuration at the ground floor for category ground A and T_1 topographic conditions. Only for the case of external constraints, the hinge was collocated in particular position (Figure 158).

The graph in Figure 187a shows the distribution of acceleration of capacity for the presence of tie-rods for all the

mechanisms (red bars), for those with two floors (white bars) and three floors (black bars). The punctual accelerations are those in Figure 187b: the red dotted line is the demand acceleration (the peak ground acceleration of Castelnuovo $a_{gD} = 0.257g$). 42 mechanisms (22%) have capacity accelerations higher than the demand capacity and for those the safety index (a_{gC}/a_{gD}) are bigger than one.

Figure 188 shows the distribution of the capacity displacements (d_u^*) and the punctual values of them. The red rectangle indicates the range of variation of the demands displacements. In this case, since the demand displacement is a function of the ultimate (capacity) displacement of the façade, the demand displacement changes every time depending on the structure characteristics.

About the 87% of the analysis has the safety coefficient major than one. Generally, the ratio among the safety index calculated with the non-linear analysis is between two and three times more than that one calculated with linear analyses. However, the displacement of the barycentre of the last floor (assumed as the control point of the structure) arrives at very large displacement when the last displacement of the curve is more than 25 cm (since, as define in 7.2.1.2, the d_u^* is the 40% of the d_{k0}^*). The displacements so excessive can lead to situations incompatible with the presence of the top floor slabs. As described in par.7.2.1.6, in the calculations it is considered the premature collapse of the panel, stopping the results of the analysis, when the displacement of the real curve achieves the anchorage length of the slab over the wall.

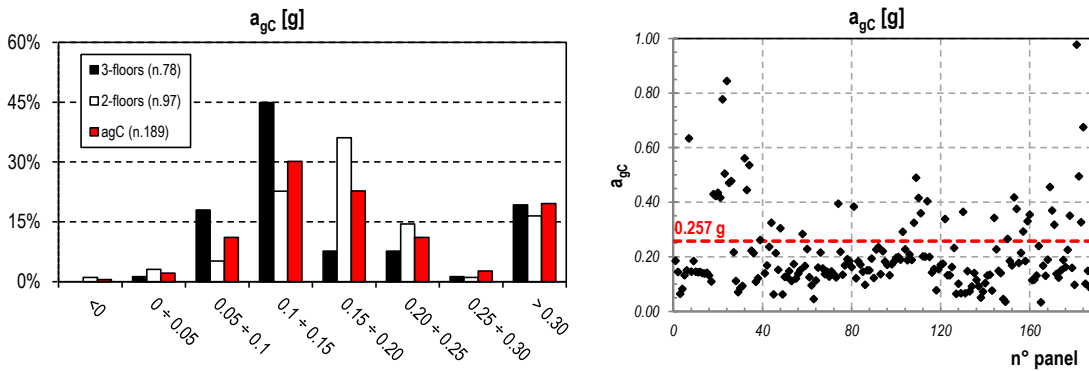


Figure 187: Capacity accelerations of the structures, a_{gC} , with the tie-rods.

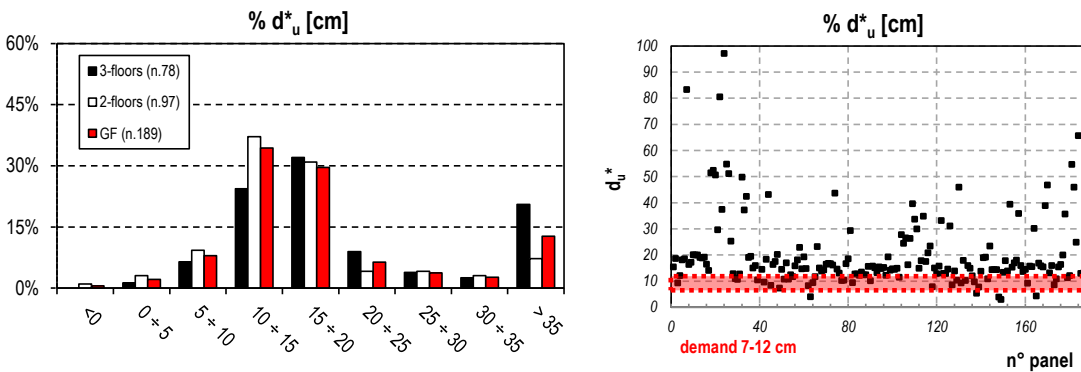


Figure 188: Last displacement (capacity displacement) of the structure with the tie-rods effective.

Results in the following refer to the absence of the tie-rods in the mechanisms, as they were ineffective. The graph in Figure 189a shows the distribution of accelerations of capacity with the tie-rods (red bars) and without (blue bars), for all the mechanisms. The mechanisms with the highest capacity (>0.3 in the red bars) divide in half their capacity and shift towards 0.1 and 0.15 unit of g. Only the 4% of cases is now verified (Figure 189b).

Figure 190 shows the distribution of the capacity displacements (d_u^*) and the punctual values of them. About the 79% of the analysis has the safety coefficient major than one.

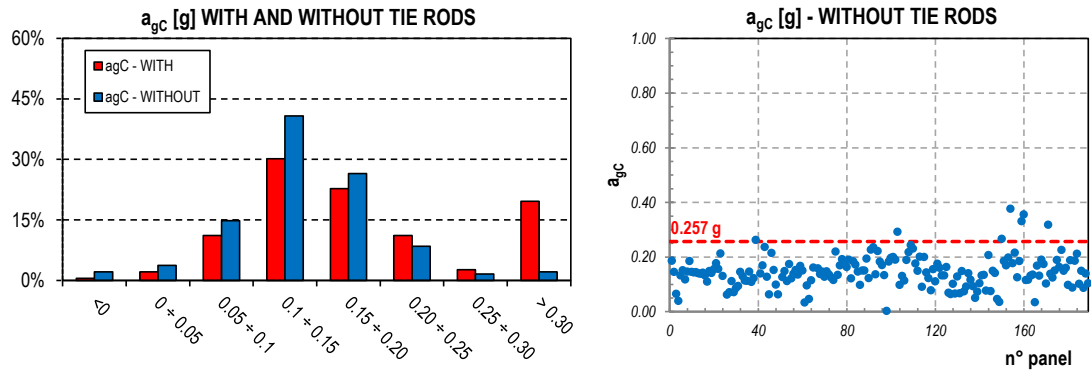


Figure 189: Capacity accelerations of the structures, a_g , with and without the influence of the tie-rods.

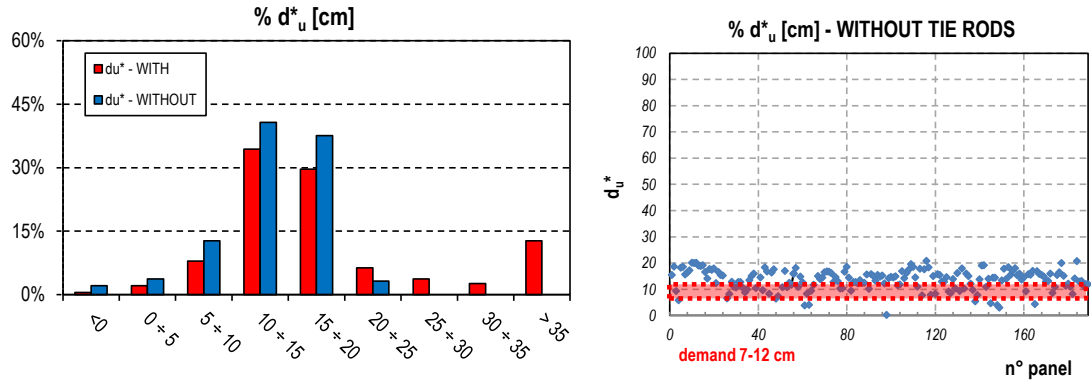


Figure 190: Last displacement (capacity displacement) of the structure with and without the tie-rods.

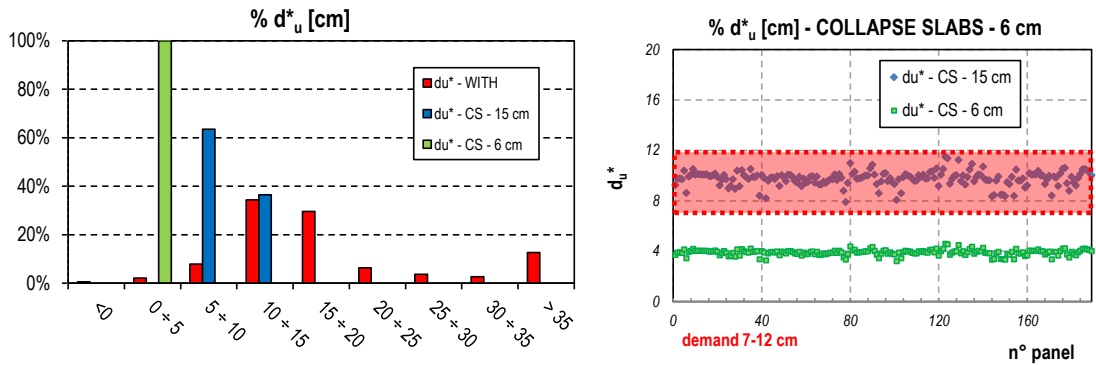


Figure 191: Last displacement (capacity displacement) of the structure for the collapse of slabs (CS).

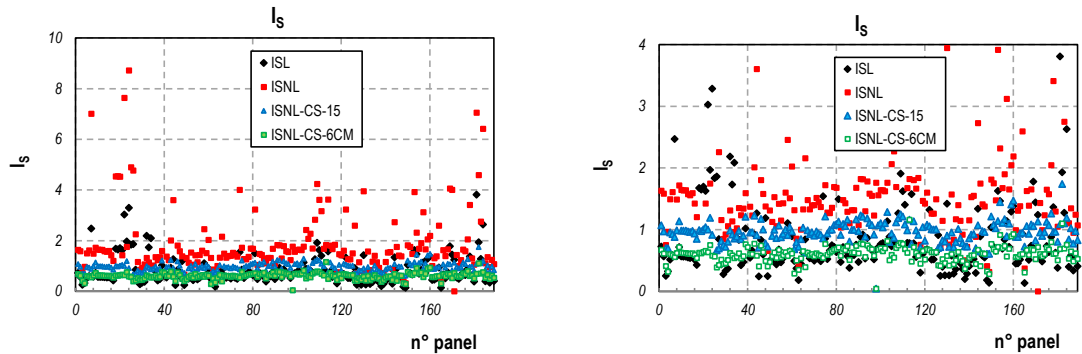


Figure 192: Safety indexes for the 189 panels for the 4 analyses (right: zoom).

In the case of stopping of the calculation for the slabs collapse, the results are reported in Figure 191 and Figure 192. The presence of the tie-rods in this case does not influence the results of the kinematic analyses, which depends otherwise from the height of the façade (number of floors) and the imposed maximum displacement of the structure. Two different cases were performed to evaluate a parametric solution: the ultimate displacements of 15 cm, corresponding to the length of anchorage of the slabs and the displacements of 6 cm, which may instead correspond to the thickness of the in folio vaults generally present at the upper floor with a ceiling function in Castelnuovo.

The results are reported in Figure 191 together with the ultimate capacity displacements of the case of presence of the tie-rods. In the case of displacement of 15 cm, the 37% of the façades has safety indexes major than one (verified) and the last displacements are concentrated close to the demand ones. The average value among the safety index for non-linear analyses and the linear ones is 1.5. The results with the collapse of the floor are closer to the results of the linear analyses. With the case of 6 cm, the total sample of study has the capacity displacements in the range 0-5 cm, and the safety verifications are satisfied only in two cases. The results of the safety index are in line with those of the linear analyses performed in rigorous way.

The safety indexes for the 189 panel for the 4 analyses done are reported in Figure 192.

CHAPTER 8. NEW VULNERABILITY FORM FOR FAÇADES IN HISTORICAL CITY CENTRES

In this chapter, a proposal for a new expeditious vulnerability assessment method for façades is defined. Based on the simple evaluation of the main issues of the aggregates façades, the method allows a first estimation of the capacity peak ground acceleration of the façade for overturning mechanism (out-of its plane).

8.1 INTRODUCTION

In CHAPTER 5 the vulnerability of the aggregates of Castelnovo through an empirical method was evaluated, by filling out the proposed Vulnerability Form ("Aggregate Form" or "6 parameters Form"). Considering the most important features for masonry aggregates, the Form was able to evaluate the vulnerability of aggregates as they were a unique structure, but characterised of a complex structural behaviour, influenced by the behaviour of the structural units that composed it. The application of the "Aggregate Form" to the case study of Castelnovo has allowed the definition of a vulnerability ranking, useful for recognizing, within a large sample of aggregates, those buildings that for irregularities plano-altimetric, loads conditions or construction technologies are the most vulnerable in front of a seismic event.

In CHAPTER 6, for a reduced sample of buildings, Vulnerability Forms for the structural units ("GNDT II Level Form", "Formisano" and "Aveiro") were assessed which have allowed the definition of the vulnerability rankings, but in this case individuating the most vulnerable structural units among the historical city centre. Being expeditious methods, the VIMs used, however, could not directly provide the capacity of the structure, neither the indicators of seismic safety (such as those defined in CHAPTER 7), results of the use of detailed methods, but only identify which aggregates may behave better than other may if invested by the seismic action.

The application of the Vulnerability Form in buildings in aggregates for which post-earthquake damage assessments was known and analysed has allowed to understand if the collapse mechanisms individuated over the structures were influenced by some particular parameters referring to the boundary conditions over the structures, loads, restraints, etc...

As defined in paragraph 6.5, the empirical vulnerability methods keeps into account structural and non-structural aspects and they consider both global and local behaviour features through different parameters. In CHAPTER 6,, analysing in detail the occurred collapse mechanisms of vertical and horizontal elements, it is worth noticed that the damage on buildings is a function of many aspects and it is not always possible to identify the degree of influence of each of them in the definition of the total damage, as defined in the EMS-98 Scale. It is worth notice also that the damage mainly present in Castelnovo can be considered typical of buildings in historical rural city centres composed of disorganized masonry characterised by lack of connections between the structural units and orthogonal main walls, which not able to manifest the global behaviour and "in-plane collapse mechanisms". The recognized type of damage in Castelnovo structural units is linked to the out-of-plane behaviours of main façades and/or the collapse for crumbling of the masonries. In particular, the manifested out-of-plane mechanisms refers mainly to the simple (or complex) overturning of the main façades, with cracks patterns visible at each storey of the structure, that can be schematised with a ground-floor hinge mechanism to whom is associated the total mass (and height) of the structure (§7.2.2).

In CHAPTER 7, consequently, the decision to study the local behaviour of the aggregates was matured assessing the degree of seismic safety in respect to overturning of the main façades. In particular, the level of safety for the façades were evaluated by the use of analytical procedures defined in Code (C.M. n.617, 2009) (NTC, 2008) for structural constructions, critically analysing their results with the damage scenario experienced in Castelnovo structural units.

With the main purpose of individuate the dependence of the showed damage from the qualitative parameters studied for each structural units defined in the VFs, the distribution of the damage in façades and that one of the judgments attributed to the "parameters' Form" were compared. Four classes representing increasing order of severity for damage in façades were individuated and catalogued, allowing the definition of a degrees of damage severity in the case only of out-of-plane mechanisms of façades (Figure 130). The analysis of correlation (§6.5) provides very low index of determination among the variable studied, that allow to understand that no evidence of interaction was delineated among the qualitative

parameters described in the vulnerability Forms and the distribution of damage level.

Considering only analytical procedures, in CHAPTER 7 the seismic safety of out-of-plane overturning mechanisms for façades were evaluated. In parallel, the influence of different façades characteristics in results of analytical model was studied. The major influence in the seismic safety definition is due to the geometrical characteristics that are, the slenderness of the panel (h/t), the presence of thrusting forces (vaults) or the presence of tie-rods, parameters that will be implemented in the definition of the Vulnerability Form for façades.

Starting with these evaluations, the idea developed in this chapter is to provide a new Vulnerability Form for façades that, containing only simple parameters that can be individuated by an in situ observation by the compiler, externally or at least with the use of Internet information (available for example from "Google Earth") allows to estimate the capacity of the façades in terms of overturning mechanisms, $a_{g,c}$. Considering the reference site and the seismic hazard of the place (§1.1.1), the Form can evaluate the Safety Index too, that represent the seismic indicators of the level of seismic security of the structure, as explained in CHAPTER 7.

In the next paragraph, the descriptions of the parameters included in the Façade Form are proposed.

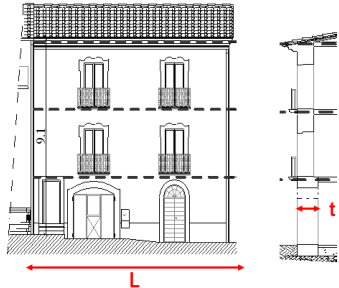
8.2 DEFINITION OF THE PARAMETERS IN THE NEW VULNERABILITY FORM FOR FAÇADES

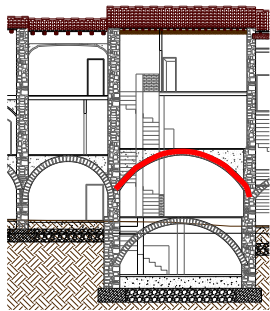

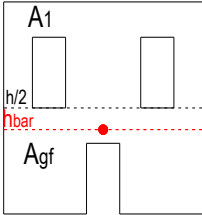
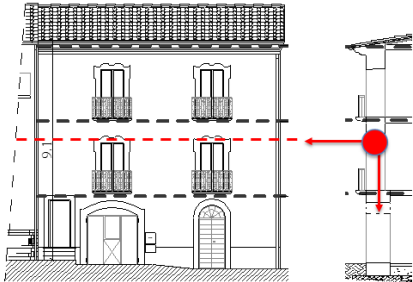
In this part of the work, the parameters that give information about the local behaviour of the masonry façade will be considered. Starting with the results expressed in previous chapters and resumed in last paragraph, these parameters are those which most influence the seismic results of the analytical procedure (C.M. n.617, 2009) for the evaluation of the kinematic analysis. These parameters will compose the proposed Façade Form. The Form is composed of 5 parameters, that are: "P1-Lateral slenderness of the façade", "P2-Presence of the thrusting force of masonry vaults or arches", "P3-Presence of the tie-rods", "P4-Barycentre position" and "P5-Horizontal multiplier of collapse".

The "P1", "P4" and "P5" are quantitative parameters, which are identified with a number that identifies a structural quantity of the mechanism. Depending on the value achieved by the parameter, a class enter "A"÷"D" is attributed to them. Finally, they are converted in qualitative parameter. The "P2" and "P3" are qualitative ones and they are defined through a judgment expressed by a class.

The parameters of the Façades Form and their classes of judgment are defined and indicated in next table.

Table 61: Façade Form: definition of the parameters and their classes.

Parameter	Description	Type of parameter	Class
P1: Lateral slenderness of the façade	<p>This parameters considers the ratio among the length (L) of the façade (interested by the kinematic analysis) and its thickness (t)</p> 	qualitative	<p>Class A. $L/t < 10$ Class B. $10 < L/t < 12$ Class C. $12 < L/t < 15$ Class D. $L/t > 15$</p>

Parameter	Description	Type of parameter	Class
P2: Presence of the thrusting force of masonry vaults or arches		qualitative	<p>Class A. no vaults or vaults that do not discharge in the main façades analysed</p> <p>Class B. ceiling vaults</p> <p>Class C. more than one structural light vault (in folio) or one last floor vault</p> <p>Class D. structural weight vault or more than one light in folio vaults.</p>
P3: Presence of the tie-rods.		qualitative	<p>Class A. more than two tie-rods or two tie-rods at the last floor</p> <p>Class B. two tie-rods</p> <p>Class C. one tie-rods</p> <p>Class D. no tie-rods</p>
P4: Barycentre position	<p>P4 is the ratio among the altitude of the barycentre of the full section façade (as no holes were in the façade) and the real altitude of the barycentre.</p> 	qualitative	<p>Class A. $P4 > 1.2$</p> <p>Class B. $1 < P4 < 1.2$</p> <p>Class C. $0.8 < P4 < 1$</p> <p>Class D. $P4 > 0.8$</p>
P5: Horizontal multiplier of collapse	<p>P5 represents the multiplier of the horizontal loads (α_0) related to the barycentre, as in the structure were present only the self-weights of the panels.</p> 	quantitative	<p>Continuous value calculated starting from the P1 and P4 parameters.</p> <p>It is calculated as the ratio of the estimated half thickness and the half height of the panel</p>

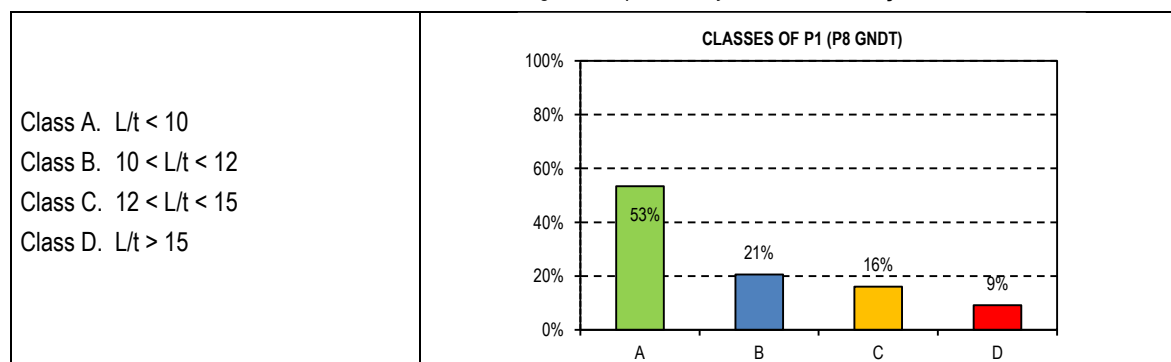
The first parameter is: *P1: Lateral slenderness of the façade (L/t)*

This parameters considers the ratio among the length (L) of the façade (interested by the kinematic analysis) and its thickness (t). If the thicknesses are available (when there is the possibility to enter in the building or to examine the plans), it represents the average value of the thicknesses' floors involved in the mechanism. In other way, it could be the thickness of the first storey, the thickness of the plan for which reliable information are present, or the average estimated thickness of the masonry considering the plausible value for the case study in which the façades are inserted. In aggregates inserted in historical city centres, the construction techniques follow the "rules of art" and the thickness could be defines as a percentage of the height of the structure. For what concern only the ground floor, the average value (§3.3.1) is enter 40/60

cm. Formally, this parameter is defined as the GDNTII Level Form P8, “maximum distance among walls”, even if it is conceptually different. GDNTII Level Form P8 (§2.2.2.1) should be calculated referring at the whole geometric of the building, not taking into account the only geometry of the façade interested by the overturning. That parameter, indeed, deals about discover among the panels of the building, the ones that are more susceptible to the out-of-plane mechanisms and for this reason, it should be taken into account all the possible ratio L/t referring at each wall.

The values obtained by the parameter could be grouped into four classes at increasing level of vulnerability, shown in the following table. The bonds values are different from those proposed by the GNDT II Level Form (Figure 19), since they are in line with the distribution of the obtained classes of judgments for the façades in Castelnuovo and reported in Table 62 right. Most of the façades lie in class “A” (53%), in accord with the fact that, at least in case of in line aggregates, the façades is lengthily limited since it usually coincide with the US division and the s.u. develops in the orthogonal direction to the main street. Only 9% of façades has length major than 15 time the thickness (that correspond to “D” class).

Table 62: Classes of P1 and distribution of the classes among the sample of study of Castelnuovo façades.

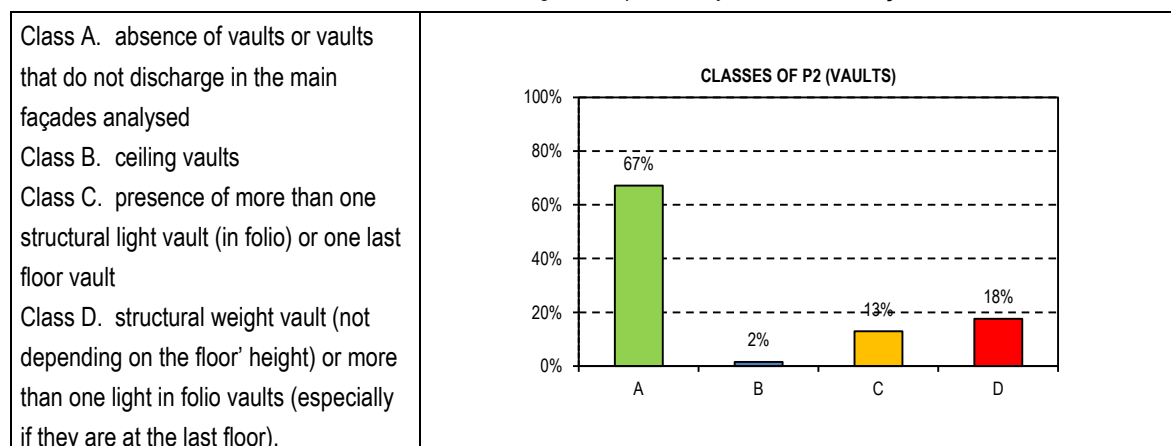


The second parameters is: *P2: Presence of the thrusting force of masonry vaults or arches.*

This parameter evaluates the vaults or arches' presence in the façade. This is a very influential parameter in the results of the analyses of local mechanisms. These thrusting forces have a *decreasing* effect of the capacity, since they could be represent as a force that exerts only a destabilizing moment. Vault or arches' forces have different influence considering the position they could have in the façades (at which storey they are present) and their type, which determines their weight and, as a consequence, their seismic mass excited by seismic acceleration. It is worth notice to distinguish among the weighted vaults and the ceiling vaults, with not structural function (as reported in paragraph 3.3.2).

From the analysis of the evaluation of the presence of the vaults in Castelnuovo aggregates, four classes were introduced for the presence of the vaults in the façades, depending on their position in height and their weight. The definition of the classes and their distribution within the sample of study of Castelnuovo are reported Table 63. More of the 30% of the façades analysed has the presence of thrusting force with about the 18% the presence of one weighted vaults or more than one thrusting forces, which represents the more vulnerability class (“D” class).

Table 63: Classes of P2 and distribution of the classes among the sample of study of Castelnuovo façades.



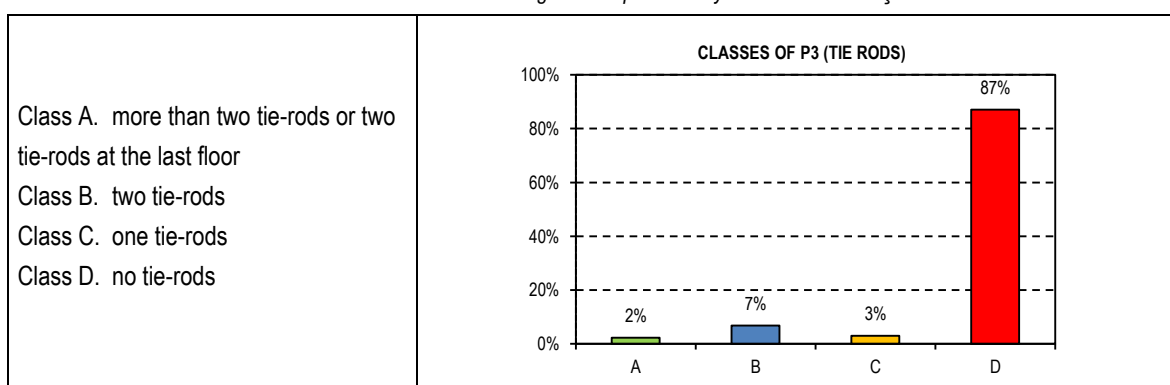
The third parameters is: *P3: Presence of the tie-rods.*

This parameter evaluated the presence of tie-rods in the façade. The axial force of the tie-rod is a very influential parameter in the results of the analysis. It always has an effect of *increasing* the capacity, since it represents a force that exerts only a stabilizing moment. The beneficial effect of the tie-rod on the results increases with the increasing of the altitude of its application point. From the analysis of the evaluation of the presence of the tie-rods in Castelnuovo aggregates, four classes were individuated. The definition of the classes and their distribution in the Castelnuovo façades are reported in the Table 64. Class “A”, i.e., is the least vulnerable and it recognises if there are in the façade or more than two tie-rods (distributed in the surface of the panel) or two tie-rods active at the last floor. It is worth noting that the type of the tie-rod and the level of its operational is not known a priori, meaning that even in the façade there are tie-rods they could be ineffective during the earthquake or, since they could be not-well designed, they could be not sufficient to impede the activation of the mechanisms. In Table 64 in addition to the definition of the classes of judgment, there are the distribution of the classes of the tie-rods for the façade in Castelnuovo keeping already into account the ineffectiveness of the functionality of the tie-rods in the façade after the earthquake shock. If the tie-rod led the mechanism activate, its influence is deleted in the analytical model. This concept will be better explained in the next paragraph.

In the analytical calculations for Castelnuovo, the maximum value considered for the tie-rod force is 25 kN, (§7.2.1.10). That value is ad hoc referred to the irregular and poor quality masonry of Castelnuovo, but it could be extended for other masonry types. If the masonry type of the façade will have higher mechanical characteristics, the value of the judgment class of the tie-rod should be taken one class upper (to take into account the major force that a tie-rod could explicate). In opposite situation: if the tie-rod is considered as not effective (because, for example, not well-connected), one should attribute a lower class to the parameter.

In the case of Castelnuovo, in only the 12% of the case, the tie-rods were present and effective, while in most of the cases, they were even not present (class “D”, Table 64).

Table 64: Classes of P3 and distribution of the classes among the sample of study of Castelnuovo façades.



The fourth and the fifth parameters deal about the geometry of the panel, in term of height, thickness and percentage of holes in the façades. The parameter are distinct in the Form, but the individuation of their classes is strictly connected and correlated each other.

The forth parameter is: *P4: Barycentre position*

It is defined as the ratio among the altitude of the barycentre of the full section façade (as no holes were in the façade and consequently calculated as the half of the height of the façade, $h/2$) and the real altitude of the barycentre (with the real disposition of the holes) and mass distribution. Here barycentre means only geometrical barycentre of the façade, without considering the influence of the external loads of the slabs or vaults that can discharge over the façade, since they are uncertain parameter in the application of this model for future vulnerability application.

Anyway, in the analytical study of the mechanisms (§7.2), the correct values of the barycentre (considering the real position of the holes) were calculated. Thus, the error in considering the approximation here adopted and the real barycentre position could be found (in the following).

The P4 is evaluated as:

$$P4 = \frac{h/2}{h_{bar}}$$

where h_{bar} can be assessed as the only geometrical barycentre (h_{bar}) or the total barycentre of the façade, considering also the weight in play ($h_{bar,Load}$).

To P4 were initially attributed 4 classes:

Class A. $P4 > 1.2$

Class B. $1 < P4 < 1.2$

Class C. $0.8 < P4 < 1$

Class D. $P4 > 0.8$

For the total sample data initially considered, the distribution of the classes of the P4 is reported in the histogram below, for the two definitions of the barycentre. The $h/2$ for about the total amount of the case is among the 0.8 and 1.2 times the height of the real barycentre. Considering the definition of the loads also, the height of the barycentre decreases (the percentage of façades with the P4 value enter the 0.8-1 value increases from 69% to 79%), according to the position of weighted loads in the ground or first floor (as masonry vaults) (see CHAPTER 3 or Figure 179). The error committed considering only the geometric barycentre is reasonably small. Thus, in the following in this study the barycentre it is geometric one.

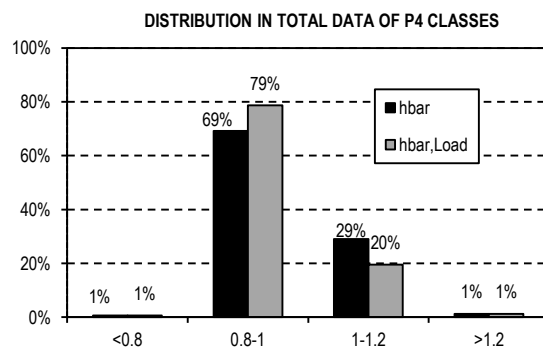
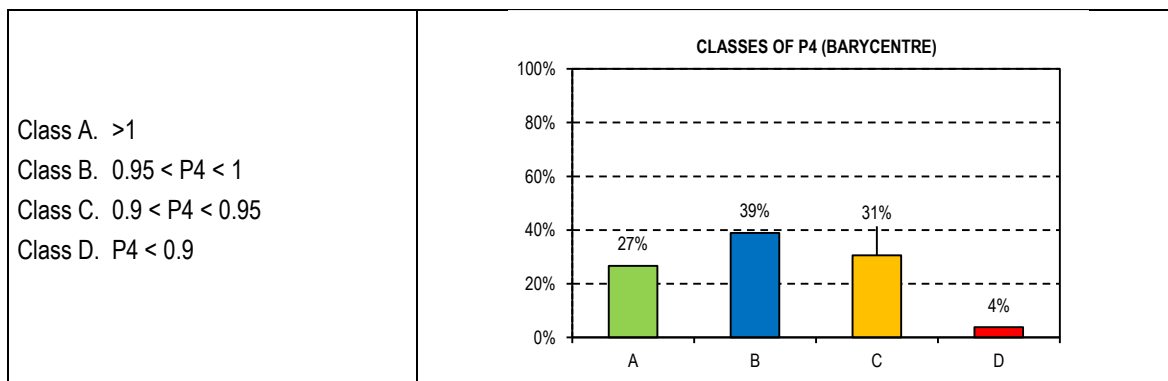


Figure 193: Distribution of the classes of the P4 parameter with the two definition of the barycentre.

Starting by the distribution P4 in Figure 193, new classes for P4 were introduced. The new definition of the classes and their distribution are reported in the histogram in Table 65. The percentages are homogeneously distributed.

Table 65: Classes of P4 and distribution of their judgments among the sample of study of Castelnuovo façades.



For the database of kinematic analysis, the attribution of the barycentre position is done with reference to the calculation of the analytical procedures, since structural dimensions in play are widely known. In the case of filling out of the Façade Form, a priori from the analytical calculations, to fill out the judgment of this parameter, the compiler should consider the distribution of the holes in façades. If the holes are distributed in the upper floors, the barycentre's height is lower than the position of the barycentre of the full section ($h/2$), while if the holes are distributed in the lower floors, the barycentre is

higher (more vulnerable situation).

This rule means that if there are uneven number of storeys, such as one of three (Figure 194), the class is attributed depending on the ratio among the *holes area* A_u in the upper floor and the lower floor A_l . With reference to the Figure 195, building n. 2 from the left, the classes can be attributed as:

Class A if $A_2 \gg A_{gf}$

Class B if $A_2 \geq A_{gf}$

Class C if $A_2 < A_{gf}$

Class D if $A_2 \ll A_{gf}$

where “ \gg ” or “ \ll ” means at least more than one hole of difference.

If the number of storeys is even, the same consideration can be fixed in reference to the sum of the holes area upper the estimated barycentre position and the lower ones. With reference to the Figure 195, building n.1 from the left, the classes are:

Class A if $(A_3+A_2) \gg (A_1+A_{gf})$

Class B if $(A_3+A_2) \geq (A_1+A_{gf})$

Class C if $(A_3+A_2) < (A_1+A_{gf})$

Class D if $(A_3+A_2) \ll (A_1+A_{gf})$.

The fifth parameter is: *P5: Horizontal multiplier of collapse (inverse of the slenderness of the panel)*

The P5 represents the multiplier of the horizontal loads (α_0). As described in 7.2.1.1, when only the self-weight is present in the wall, α_0 corresponds to the ratio among the thickness and the height of the panel Eq.(40). If there are more than one force acting, it can be calculated as the ratio among the coordinates of the barycentre t_{bar} and the h_{bar} (Eq.(41)).

$$(40) \alpha_0 = \frac{Wt/2}{Wh/2} = t/h$$

$$(41) \alpha_0 = \frac{Wt_{bar}}{Wh_{bar}}$$

From the real data analysed in the panels, the variation of the t_{bar} and the half thickness of the panel is minimum, therefore is here assumed $t_{bar}=t/2$. T dimension is determined following dispositions described for P1. From the P4 is known that the h_{bar} is a function of the half height of the panel, depending from the numbers and position of the holes in the façade. In function of the class attributed to P4, the barycentre height is determined considering the expressions in Table 66 (left). The values of the coefficients are determined with references to the façades analysed.

The distribution of the P5 parameters in the sample of data is inserted in the Table 66 on the right.

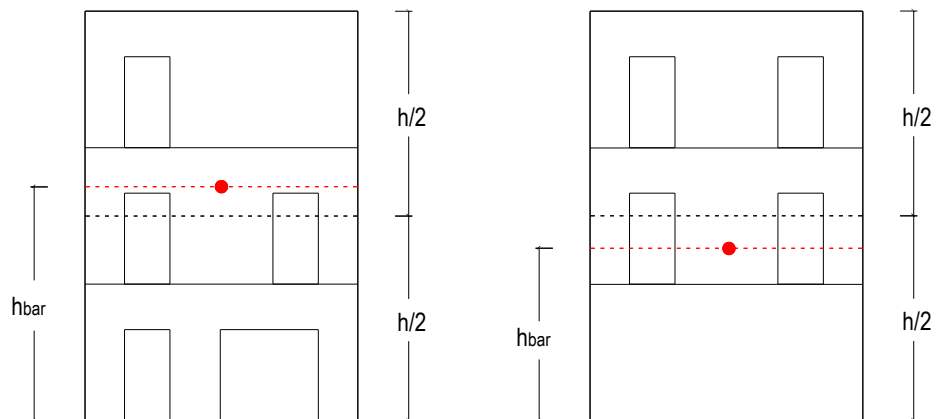


Figure 194: Example of the real barycentre position of the real barycentre and the barycentre of the full area façade.

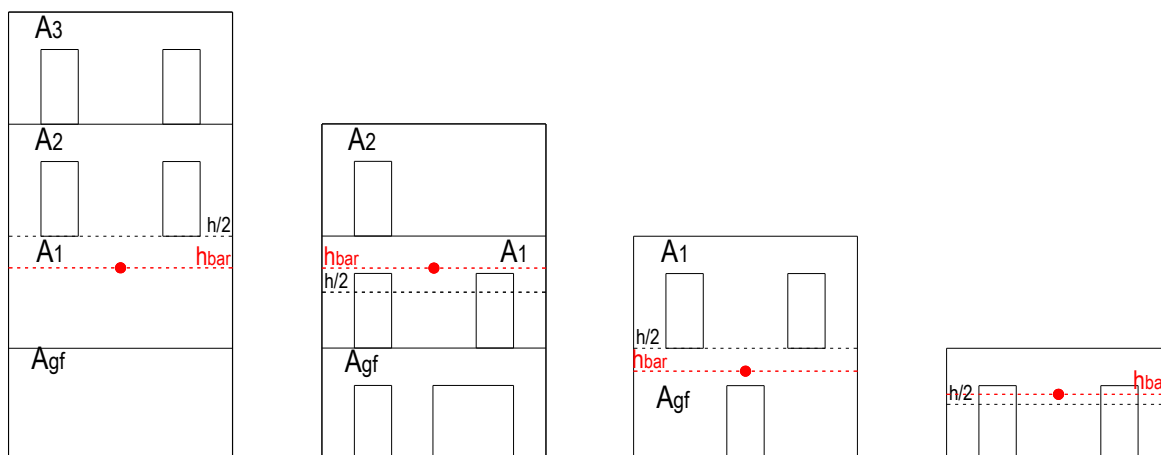
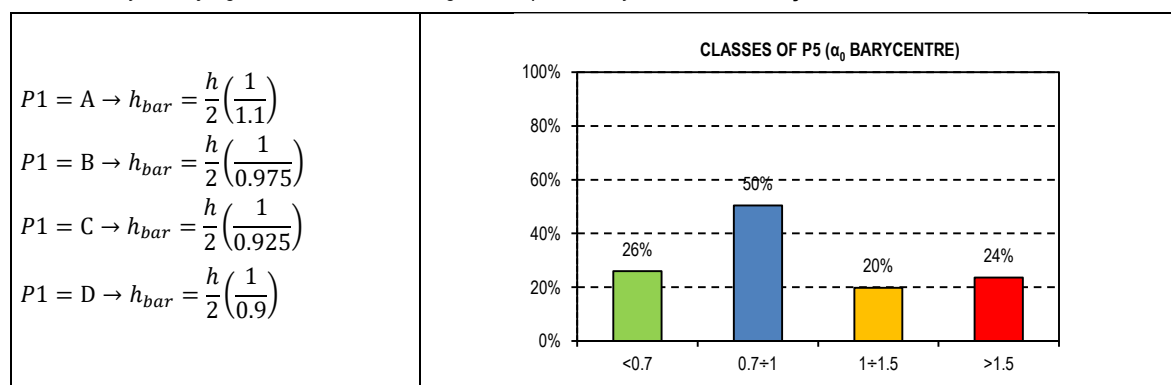


Figure 195: Example of different position of the barycentre for different numbers of floors.

Table 66: Barycentre judgments distribution among the sample of study of Castelnuovo façades.



Concluding, the five parameters contained in the Façade Form are:

- P1: Lateral slenderness of the façade*
- P2: Presence of the thrusting force of masonry vaults or arches.*
- P3: Presence of the tie-rods.*
- P4: Barycentre position*
- P5: Horizontal multiplier of collapse*

For the evaluation of these parameters it is necessary to know:

- The façade width and height, which are directly measurable from the external side of the wall.
- The panel thickness (eventually estimated, considering the type of masonry, owner information, existing plans...);
- The presence of thrusting force, only know with an in-situ inspection, after having spoken with the owner of the house, or taken from existing study of vulnerability about the historical city centres ;
- The dimension and the distribution of the holes areas in the façades (in situ external survey).

8.3 SAMPLE OF STUDY FOR THE DETERMINATION OF THE FAÇADE FORM

A screening among the 188 façades analysed with the kinematic analysis (§7.5) was carried out in order to achieve a homogenous sample of data to whom apply the proposed procedure to estimate the weights of each parameter of the Façade Form in order to estimate the capacity acceleration of the façade. In doing it, three orders of problems were individuated:

1. how to consider the tie-rod forces in the analysis results;
2. how to consider the overturning mechanisms for the façades of adjacent structural units. At the beginning, both together

and separately the mechanisms were calculated;

3. how to treat the correlations between the numerical results of the analysis (evaluated by analysing kinematic linear with the formation of the hinge to the ground floor, defined in 7.2.2) and the distribution of the real damage in the façades, considering classes of damage reported in Figure 130, associated to the out-of-plane mechanisms.

Respectively these assumptions were adopted:

1. In the mechanisms where the real out-of-plane damage was high (class “D”, Figure 129), tie-rods were not considered in the calculation, since considered as not effective. If the damage was estimated medium-severe (Class “C”), the peak ground acceleration of capacity was evaluated as the average value considering the results with and without the presence of the tie-rods in the calculation, since their contribution was not negligible.
2. Overturnings were considered single or composed by two structural units depending on the identification of the crack pattern in the adjacent ss.uu.. If two ss.uu. showed an unit behaviour, a single mechanism was evaluated with total geometric and loads. With this procedure, from the original sample of data 12 mechanisms façades were deleted.
3. To answer the third issue, another question should be posed: are the numerical analysis results in line with the real damage relative to the Castelnuovo façades?

In order to compare the analysis results and the real damages suffered by the façades, the results of analytical analysis carried out in §7.5 in standard conditions, were converted to take account of real ground category, and topographical condition of Castelnuovo site. The concept is to consider the design demand value of seismic action as that suffered by the aggregates in Castelnuovo. Although it can be regarded as a strong hypothesis, this may be partly corroborated by the fact that the seismic hazard of Castelnuovo was never updated after the 2009 earthquake and no records for real 2009 earthquake accelerogram were present in that location.

It has been considered ground C type and topographic category T₂. Since the mechanism refers to the formation of the hinge at the façade’s ground level, the passage for changing the ground conditions is accomplished by dividing the capacity by a factor S, in this case equal to 1.601. With the new results of capacity and relative the safety indexes ($I_s = a_{g,c}/a_{g,D}$), four classes were defined:

- Class D $I_s < 0.25$
- Class C $0.25 < I_s < 0.50$
- Class B $0.5 < I_s < 0.75$
- Class A $I_s > 0.75$.

The real damage classes in Castelnuovo façades and those obtained from the results of the linear analysis were compared. The sample of studies was purified from those mechanisms that differed for *more than one class of damage*. Thus, combinations of mechanisms considered in the definition of the Façade Form are marked by an X in the following table. The choice of taking into account not only the coincident classes, but even the one deviation class of damage is motivated to the arbitrariness of the definition of the real damage classes and subjectivity of the coefficients and classes as regard the analytical calculations.

Table 67: Combination of mechanisms I_s and level of damage taken into account for the sample of data.

	Safety index (in analytical procedure)				
L of E D V A E MA L GE		A	B	C	D
	A	X	X		
	B	X	X	X	
	C		X	X	X
	D			X	X

The sample data now consists of 130 total overturning mechanisms of façade. The distribution of the parameters in section 8.2 refers precisely to the sample data here analysed.

8.4 DEFINITION OF THE NEW VULNERABILITY FORM FOR FAÇADES

In the previous paragraph §8.2, the five parameters to be considered for the estimation of the capacity with the Façade Form were described. In particular, four of them through a qualitative evaluation (P1, P2, P3 and P4) and P5 through a quantitative one. The previous parameters are known easily with an in-situ inspection. Two of them can be estimated: the presence of the vaults and the panel thickness. If for the panel thickness, information about the quality masonry and characteristics could be help its definition, for the presence of vaults or arches there is the necessity to enter inside the house or to speak with the owners.

Since it is will of the authors to propose a Form that could be used in the case of low levels of information, achieved at least with external inspection of the aggregates, two are the solution provided: one considering the entire Façade Forms, with the five parameters expressed in 8.2 and the second considering only four parameters, without the P2.

Once defined the parameters, the issues to solve for the definition of the vulnerability estimation procedure are:

- the choice of the scores to assign to each judgment for the qualitative parameters. In the Façade Form they will be assessed with a letter: "A", "B", "C", "D", with increasing vulnerability;
- the choice of the parameters weights.

The following assumptions are considered:

As already done in the CHAPTER 5, to each class of parameter a number was assigned. In particular, each class of judgment has the same score in all the considered parameters: the "distance" among each class is assumed as stable, not influencing the final results. The scores associated to each judgment are A=1, B=2, C=3 and D=4. This assumption has been made considering that, once that these values are used, the importance of each parameter in the a_{gc} estimation will be consequently calculated by the numerical procedure used, the multi-linear regression (MLR).

The multi-linear regression combines the effects of five the parameters (§8.2, x_i variables) in a linear way in order to obtain a correspondent dependent parameter (y variable). In other words, if one has a table like this:

	x_1	...	x_p	y
1	$x_{1,1}$...	$x_{1,p}$	y_1
2	$x_{2,1}$...	$x_{2,p}$	y_2
...
n	$x_{n,1}$...	$x_{n,p}$	y_n

One should find the functional linear relationship among the parameters x_i , x_p in order to obtain the y variable:

$$y = m_1 \cdot x_1 + m_2 \cdot x_2 + \dots m_i \cdot x_i + b + \varepsilon_i \quad \text{with}$$

m_i represent the weights of each independent variable;

b is a constant value;

ε_i are the residuals.

In this case the Y and X variables are vector of dimension (130×1). The evaluation of the m_i and b is performed with the least squares technique, in order to minimize the errors (residuals) among the estimated variables and the real one.

For this case, the variables are the judgments/values of the five parameters P1-P5 expressed in 8.2 assumed for each façade. The capacity of the structures, expressed through the a_{gc} obtained with the detailed analyses of out-of-plane mechanisms, represents the dependent variable (y). One should remember that the a_{gc} refers to the seismic hazard of Castelnovo, with the ground condition A and the topography category T_1 ($S=1$).

In Figure 196, there is extract of the results for the multi-linear regression for both the Façade Form, with 5P ad 4P. In the first table there are the results for the 5P-Façade Form: there is the individuation of the variables (x_1, \dots, x_5), the real capacity

⁹ Number of mechanisms analysed.

value $a_{g,c}$ (y_i) and the estimation of the $a_{g,CE}$ from the MLR. There are reported the estimated errors, too, divided in over-estimation errors and under-estimation ones. The punctual value of errors is in certain cases very high: the maximum error is 44% (over-estimation) and the minimum -59% (underestimation), while the average value in errors is about 13%. In Figure 196 bottom there are the obtained results for the 4P-Façade Form. The reliability of the method decreases: the maximum error is 52% (in over-estimation) and the minimum -61%, with the average value in errors is about 27%, since in this case the MLR is applied considering only four parameters.

Starting from the estimated capacity accelerations ($a_{g,CE}$), the Safety Index were calculated as the ratio between the seismic capacity and the seismic demand: $I_{S,E} = a_{g,CE} / a_{g,D}$. The demand capacity in Castelnovo, as already described, is 0.257 g, for a ground hinge overturning mechanism. The goodness of the method could be evaluate comparing the safety index classes obtained with the real capacity accelerations ($I_S = a_{g,C} / a_{g,D}$) and those calculated with the estimated accelerations with the MLR method with both the solution proposed (5 and 4P-Forms), as reported below:

$$I_{S,E5p} = \frac{a_{g,C,E5p}}{a_{g,D}}; I_{S,E4p} = \frac{a_{g,C,E4p}}{a_{g,D}}$$

According to paragraph 8.3, five variation ranges of the I_S were individuate:

Range 1: $I_S < 0.25$

Range 2: $0.25 < I_S < 0.50$

Range 3: $0.5 < I_S < 0.75$

Range 4: $0.75 < I_S < 1.00$

Range 5: $I_S > 1.00$

For the total sample of data (130 mechanisms), with the 5P-Façade Form, about the 20% of the cases falls in different range of safety index: in particular, 10% of them falls in an upper class with the consequence to have a 10% of probability to overestimate - in not conservative way - the variation range of the I_S .

For the second solution (4P-Façade Form), the percentage changes: about the 30% of the cases falls in different range and the 15% the I_{SE} is major than that real one.

To solve this problem and make lower the percentage of the façades that have higher estimated capacity in respect to the real one, a constant value is added in the definition of the each MLR in order to maintain the same "shape" of the MLR and to reduce the estimated capacity. These values are defined in black cells in Figure 196. These values are determined in both the methods in order to achieve at least the 5% of non-conservative estimated $I_{S,E}$.

To quantify the efficacy of the analysis, in addition to the calculation of the committed errors, the determination coefficient (r^2) were calculated. It is a coefficient ranging in the [0-1] interval: it compares the estimated values $y_{i,E}$ with the real ones y_i . If the coefficient is close to 1, there is a good-perfect correlation, while low values of it (close to 0) expresses the lack of correlation among the estimated values of the capacity (with the MLR technique) and the real ones.

Numerically, the coefficient is calculated with the eq.(42)

$$(42) \quad r^2 = \frac{sq_{reg}}{sq_{tot}}$$

where

sq_{tot} is the sum of the squares of y_i

sq_{res} is the sum of the squares of $(y_i - y'_i)$ in which y'_i are the estimated capacities.

$$sq_{reg} = sq_{tot} - sq_{res}$$

For the analysed case, $r^2 = 0.87$ with the use of the 5P-Façade Forms. If the 4P-Form is used, $r^2 = 0.78$; as already expressed, this second solution shows minor reliability due to the loss of one important parameter in the determination of the real capacity against local mechanisms of overturning.

The obtained results are visualised in Figure 197, in which there is the comparison of the analytical real results ($a_{g,Ci}$) and the estimated ones obtained through the MLR, for both the solutions defined, with the 5 and 4-P Façade Forms.

In Figure 199 (and Figure 200, with a zoom) there are reported the safety indexes found for the real (I_S) case and the

estimated ones ($I_{s,E}$) with the individuation of the variation range aforementioned in different colours.

Concluding, with the presented method, knowing only 5 (4) simple and qualitative parameters of the structures, it is possible to determine the structural capacity for local out-of-plane mechanisms of façades and a definition of a safety index.

	x_1	x_2	x_3	x_4	x_5	y	y (MLR)	error	
N°	P1 - L/t	P2 - Vaults	P3 - Tie rods	P4 - Bar.	P5 = α_0	$a_{gC,R}$	$a_{gC,E-5p}$	over	under
1	4	4	4	2	0.54	0.065	0.045		-31%
2	2	4	4	3	0.59	0.061	0.052		-15%
3	2	1	4	3	0.71	0.132	0.138	4%	
4	3	1	1	2	0.62	0.635	0.532		-16%
5	3	1	4	3	0.78	0.144	0.145	0%	
6	3	1	4	3	0.73	0.140	0.139		-1%
7	2	1	4	1	0.67	0.132	0.137	4%	
8	1	4	4	3	0.69	0.110	0.064		-42%
9	1	1	2	3	0.77	0.424	0.416		-2%
10	1	1	2	2	0.82	0.436	0.422		-3%
11	2	3	1	1	1.27	0.418	0.559	34%	
12	1	1	1	1	0.79	0.778	0.556		-29%
13	2	4	2	1	0.62	0.228	0.328	44%	
...
130	2	1	4	3	1.01	0.186	0.172		-8%

max						0.778	0.559	44%	0%
min						0.061	0.045	0%	-59%
average						0.181	0.171	13%	

-0.001	-0.024	-0.135	-0.002	0.111	0.640	-0.01
m_1	m_2	m_3	m_4	m_5	b	

	x_1	x_2	x_3	x_4	y	y (MLR)	error	
N°	P1 - L/t	P3 - Tie rods	P4 - Bar.	P5 = α_0	$a_{gC,R}$	$a_{gC,E-5p}$	over	under
1	4	4	2	0.54	0.065	0.061		-6%
2	2	4	3	0.59	0.066	0.078	28%	
3	2	4	3	0.71	0.079	0.090		-32%
4	3	1	2	0.62	0.069	0.469		-26%
5	3	4	3	0.78	0.087	0.092		-37%
6	3	4	3	0.73	0.082	0.086		-39%
7	2	4	1	0.67	0.075	0.091		-31%
8	1	4	3	0.69	0.077	0.096		-13%
9	1	2	3	0.77	0.086	0.366		-14%
10	1	2	2	0.82	0.091	0.373		-14%
11	2	1	1	1.27	0.141	0.547	31%	
12	1	1	1	0.79	0.089	0.503		-35%
13	2	2	1	0.62	0.070	0.347	52%	
...
130	2	4	3	1.012	0.186	0.123		-34%

max					0.778	0.547	52%	0%
min					0.061	0.061	0%	-61%
average					0.181	0.144	20%	

-0.007	-0.131	-0.002	0.107	0.596	-0.04
m_1	m_3	m_4	m_5	b	

Figure 196: Multi-linear regression for the estimation of the a_{gC} with 5 parameter and with 4 parameters.

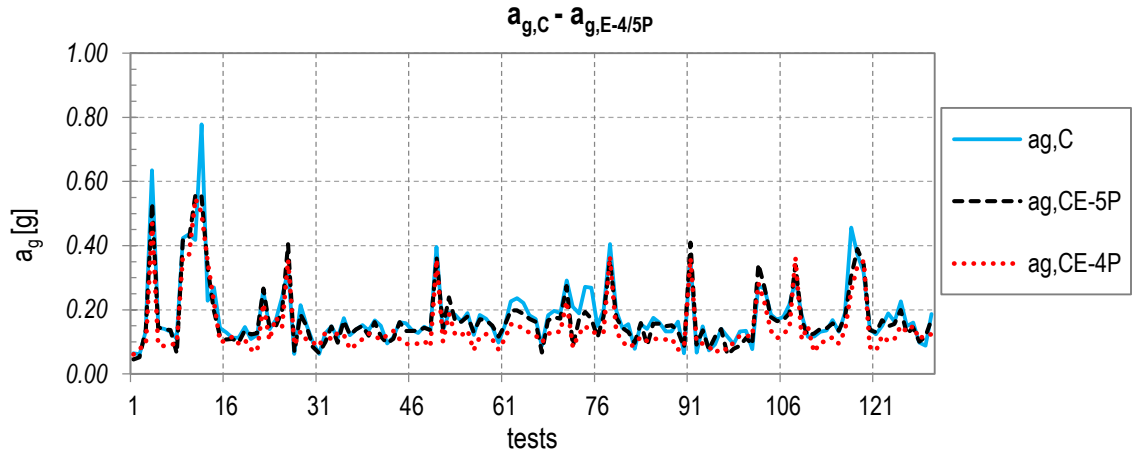


Figure 197: Trend of real and estimated capacity for the façades of Castelnuovo, for the two Façades Forms.

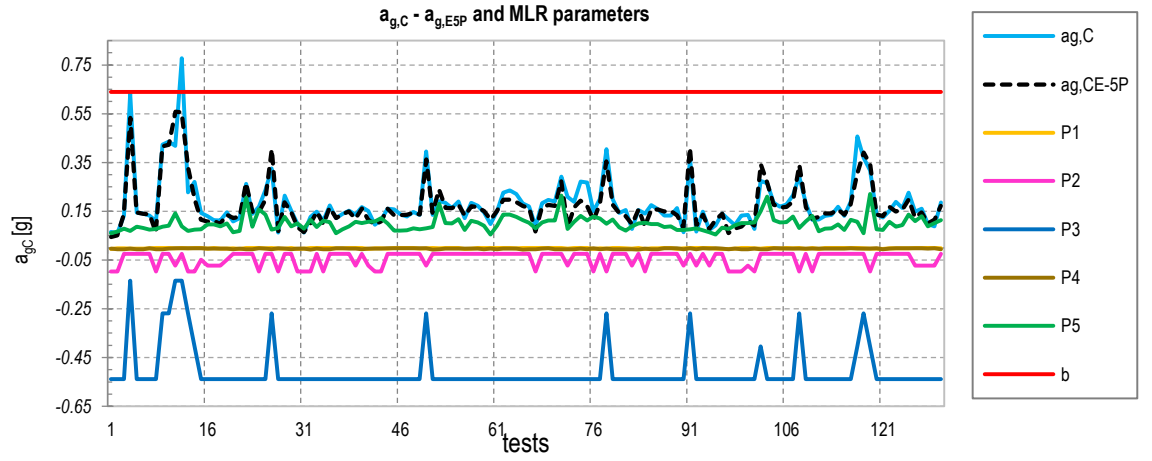


Figure 198: Trend of real and estimated capacity (5-parameters) for the façades and contribution of all parameters.

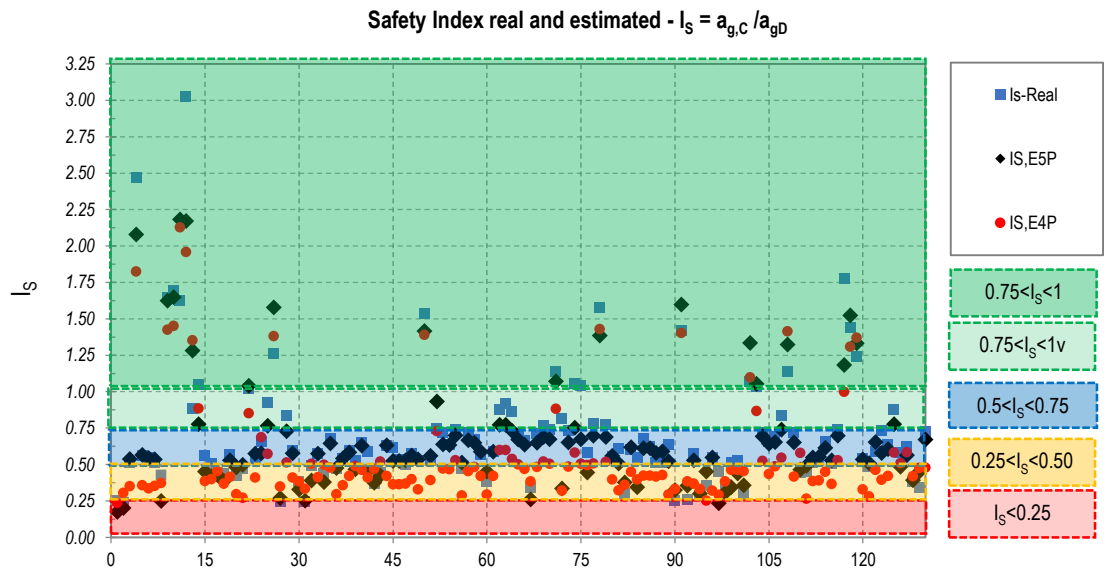


Figure 199: Real and estimated indexes of safety for the façades of Castelnuovo, for the two Façades Forms.

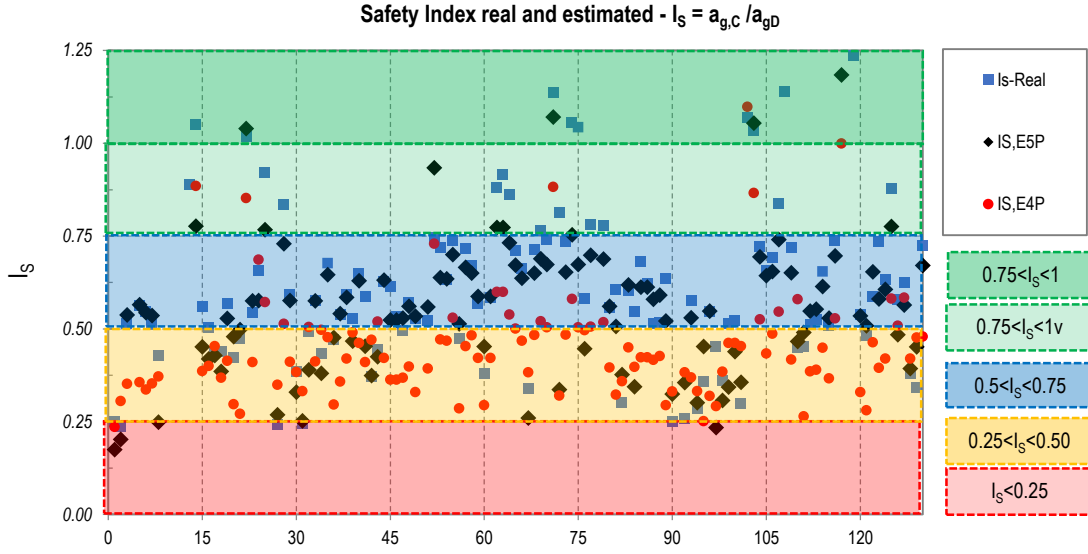


Figure 200: Real and estimated indexes of safety for the façades of Castelnuovo, for the two Façade Forms: zoom.

8.5 ESTIMATION OF THE RISK INDEX

With the method of multi-linear regression, propose in 8.4, knowing only 5 (or 4) parameters of the structures, it is possible to estimate the capacity of the façade in terms of out-of-plane mechanisms of the façades ($a_{g,CE}$).

The procedure implemented to estimate the peak acceleration of capacity is defined assuming seismic demand of the structure as it was collocated in A soil and T_1 topographic categories in order to make more general the analysis results, not depending of the ground type.

Referring to a structure clamped to the earth (cantilever static scheme) the demand acceleration is taken in correspondence of the starting point of the spectrum: the period of the structure, T , is equal to 0 and the acceleration values is equal to:

$$S_e(T) = S \cdot a_g$$

where S is the soil factor and a_g is the peak ground acceleration of the place in which the structure is collocated.

In changing the ground type the S factor changes: for Castelnuovo is determined following the §1.1.1.1.1.

If the structure was in a C ground category and with the T_2 topographic category (as really is in Castelnuovo), the S factor is equal to 1.601. This coefficient can be used to multiply the demand acceleration or alternatively divide the capacity one.

Considering the second option, the estimated capacity for example with the first solution provided by the MLR is:

$$a_{gC,E5p} = \frac{a_{gC,E5p}}{S} = \frac{a_{gC,E5p}}{1.601}$$

The safety index is, in this way, 1.601 time less, since it is always calculated as the ratio among the $a_{g,CE5p}$ and the a_g of reference for Castelnuovo (0.257 g). This procedure can be repeated for all the ground type.

The procedure still works if the structure is collocated in another place, with different seismic hazard. One should be calculated S for different ground type and different topographic characteristics and afterwards divide the estimated capacity for the S_i coefficient which is varying following the

Table 7 dispositions.

On the contrary, this procedure is not more fitting if the mechanism type changes, i.e. considering the capacity relative to mechanisms associated to partial overturns of the panel, with the hinge configuration at the first or second floor. In that case, the MLR should be done with different type of results from the numerical models and the determination of the risk index follow the rules of what already discuss in 7.2.2.

8.6 EXAMPLES OF THE METHOD TEST

The MLR methods was used to define the coefficients of a linear relationship among 5 (or 4) qualitative parameters in order to estimate the $a_{g,c}$ for the façade overturning. To achieve this procedure, 130 linear analyses were exploited, associated to 130 Castelnuovo façades, with reference to what already written in 8.3. To test the method, that is to corroborate if the coefficients of the MLR were well obtained, the proposed Façade Form was applied to other cases studies (more than 20 applications), to the façades of four other buildings in different Regions and subjected to distinct seismic actions. The buildings were studied in detail, and a very refined knowledge process was accomplished over the structural elements of the buildings. The analytical calculations of the out-of-plane mechanisms were performed allowing the calculation of the real $a_{g,c}$. Afterward, both the two examples of Façade Form (5P-4P) were applied arriving to the identification of the safety index. The comparison of the analytical and numerical (estimated) results are finally expressed, showing the reliability of the implemented method proposed. For the 22 case studies, the average errors in the capacity estimation is contained in the 15%, with peak of 20% in overestimation, but achieved only in three cases. The same percentage of errors remaining stable in the safety index, but for those, the 95% of the mechanisms lies in the same ranges of the real safety index. This errors could be considered as acceptable in the definition of the solution of the mechanisms for the detail level of the Form implemented that need only qualitative parameters.

In the follow, one case study of the test is expressed. It refers to Museum of Casa Vasari in Arezzo, in Tuscany. The evaluation of the vulnerability of the structure, a three floors building made in disorganised stone masonry, was performed at different levels by the DICEA Group in 2014. In particular, mechanisms of overturning of both the front and rear façades were performed, with the linear analysis, in a detailed way. Since no crack patterns or no restraints elements were present in the structures (i.e. external stairs), the position of the hinge configuration was not known a priori; a parametrical analyses were done, with the study of different position of the hinge configuration. The worst safety indexes for the three mechanisms were those with the hinge configuration at the ground floor and then suitable for the test the goodness of the Façade Form. The building is showed in Figure 201, in which in different colours are highlighted the overturnings analysed (green= n.1, pink= n.2 and blue=n.3); the position and type of mechanisms analysed were defined basing of the results of the knowledge process, which highlighted the degrees of connection among orthogonal walls and between the horizontal slabs and vertical elements. A refined loads analysis was carried out, arriving at the complete definition of the charges acting in the façades.



Figure 201: Casa Vasari Museum, aerial photo, plan, rear and frontal façade with the individuation of the studied mechanisms.

The demand seismic hazard of the place in which the building is collocated is characterized by a T_R of 712 year and¹⁰: $a_g=0.183$ g, $F_0= 2.419$ and $T_c^*=0.298$ sec. The ground enters in B category B (§1.1.1.1.1) with topographic category T_1 referring to Table 8, since Arezzo is situated in a hilly zone and the buildings is inserted in a flat country-slopes with average inclination $i \leq 15$. S coefficient is equal to 1.2.

The peak ground accelerations of capacity and the safety indexes performed with analytical methods are reported in Table 66.

Table 68: Peak ground accelerations of capacity and safety indexes.

	$a_{g,D}$	$a_{g,C,R}$	$I_{S,R}$
1 (green)	0.183	0.08	0.44
2 (pink)	0.183	0.120	0.65
3 (blue)	0.183	0.089	0.49

Both the Façades Form (5P-4P Forms) are afterwards applied. In next tables, there are the information asked to the compiler: the thickness, the length, the height and, on the bases of the percentage of holes in the façades, the parameters P4 (Figure 193).

OVERTURNING n.1 (green)				
Thickness	0.64	m		
Length	11.40	m		
Height	10.17	m		
P4: Barycentre position	Class A			

Once defined the input parameters, the system automatically calculates the L/t (P1), the h_{bar} and the P5 (α_0) and in the case of qualitative parameters, it defines the classes. These values are reported in the following table.

L/t	17.81		Classes 4	
$h/2$	5.09	m		
h_{bar}	4.62	m		
α_0	0.68			
P5: Horizontal multiplier of collapse α_0	0.68 m/s ²			

With the knowledge of the presence of tie-rod or vaults, the Façade Form is completed:

OVERTURNING n.1 (green)				
PARAMETERS	A	B	C	D
P1: Lateral slenderness of the façade				X
P2: Presence of the thrusting force of masonry vaults or arches.				X
P3: Presence of the tie-rods.				X
P4: Barycentre position	X			
P5: Horizontal multiplier of collapse α_0	0.68 m/s ²			

For this case L/t is major than 15 thus P1 lies in class. There is a weighted vault at ground floor and the absence of tie-rods make the P2 and P3 in classes "D". The percentage of holes in the façade is higher in upper floors: the P5 assumes "A" class. The horizontal multiplier of collapse α_0 is 0.68 m/s².

As explained in par. 8.4, the results of the estimated capacity are reported considering A ground category. To have the real capacity acceleration, that value should divided for S, equal to 1.2 in this case. The estimated safety index is the ratio among the estimated capacity and the demand (0.183 g). As it possible to see in the table below, the estimated acceleration is the 35% lower than the analytical real value. The estimated safety index is 0.28 and it enters in C classe ($0.25 < I_s < 0.50$), as well as the real one.

$a_{g,CE5P}$	0.062	[g]
$a_{g,CE-5P,groundB}$	0.052	[g]

¹⁰ Since the structure is a museum, T_R for SLV is 712 years.

$a_{g,CR}$	0.080	-35%
$a_{g,D}$	0.183	
$I_{S,Estimated}$	0.28	
$I_{S,R}$ = Index of risk REAL	0.44	-35%

The results with the 4-P Façade Form are reported in the table below. The estimated acceleration is the 19% lower than the analytical real value, since in this case the influence of the most vulnerable class for the P2 (presence of the thrusting force of masonry vaults or arches) is not take into account. The estimated safety index and the real one fall into the same range ($0.25 < I_s < 0.50$) in this case also.

$a_{g,CE4P}$	0.078	[g]
$a_{g,CE4P,groundB}$	0.065	[g]
$I_{S,Estimated4P}$	0.35	-19%

§

For the case n.2 (overturning in pink in Figure 201), the results are resumed in the following. P1 assumes "A" classes, there are one tie-rod (class "C") and one masonry weighted masonry vault. Since there are no openings in height, the P4 falls in "D" class. The estimated acceleration is greater that the real one (14%) being in not conservative approach in calculating the capacity, but in this case also, the real and estimated safety indexes fall in the same range ($0.5 < I_s < 0.75$). In the 4P Form, the presence of tie-rod without the possibility of considering the presence of the vaults (vulnerable issue) makes the estimated capacity acceleration high, much higher than the real one. The estimated safety index achieves A class even it rests minor than one. In this case, the class of the I_s is not more comparable for the real and estimated capacities, and this points out a lack of the 4P Form.

OVERTURNING n.2 (pink)				
Thickness	0.63	m		
Length	4.80	m		
Height	11.00	m		
OVERTURNING n.2 (pink)	A	B	C	D
P1: Lateral slenderness of the façade	X			
P2: Presence of thrusting forces (vaults)				X
P3: Presence of the tie-rods.			X	
P4: Barycentre position				X
P5: Horizontal multiplier of collapse α_0	0.51	m/s ²		
$a_{g,CE5P}$	0.167	[g]		
$a_{g,CE5P,groundB}$	0.138	[g]		
$a_{g,CR}$	0.119	16%		
$a_{g,D}$	0.183			
$I_{S,Estimated}$	0.75			
$I_{S,R}$	0.65	16%		

$a_{g,CE4P}$	0.205	[g]
$a_{g,CE4P,groundB}$	0.170	[g]
$I_{S,Estimated4P}$	0.93	43%

§

The last example (overturning n.3, in blue in Figure 201) there no vaults or tie-rod. It is a very large façade (about 17 m), with homogeneous distribution of holes in height (P4 lies in "C" class). The Façade Form with 5P allows the estimation of the $a_{g,c}$ with an error of 2%. With the 4P Form, despite the estimated capacity is lower 47% respect the real one, it is able

to catch the same class for the estimation of the I_s that are collocated among $0.25 < I_s < 0.5$ values.

OVERTURNING n.3 (blue)				
Thickness	0.70	m		
Length	16.89	m		
Height	12.30	m		
L/t	24.13		4	
h/2	6.15	m		
hbar	6.65	m		
α_0	0.52			
OVERTURNING n.3 (blue)	A	B	C	D
P1: Lateral slenderness of the façade				X
P2: Presence of thrusting forces (vaults)	X			X
P3: Presence of the tie-rods.				X
P4: Barycentre position			X	
P5: Horizontal multiplier of collapse α_0	0.52	m/s ²		
$a_{g,CE5P}$	0.105	[g]		
$a_{g,CE5P,groundB}$	0.088	[g]		
$a_{g,CR}$	0.089	2%		
$a_{g,D}$	0.183			
$I_{s,Estimated}$	0.48			
$I_{s,R}$	0.49	2%		

$a_{g,CE4P}$	0.057	[g]
$a_{g,CE4P,groundB}$	0.047	[g]
$I_{s,Estimated4P}$	0.26	90%

Concluding, with the in situ observations and the knowledge of some qualitative and geometrical parameters, the Façade Forms are able to estimate the capacity acceleration of the structure. In particular, the 5P Façade Form allows an accurate capacity estimation when in the façades there are no-tie-rod or vaults (error 2%), since the quantitative parameters taken into account, inserted in the Form after the study developed in §7.2.3, are sufficient to estimate the $a_{g,C}$. The Form underestimates the capacity when P2 assumes most vulnerable class (D) and there are no external tie-rods. This because in the definition of the MLR coefficients for the cases study analysed, the presence of the weighted vaults (un-activated by the presence of opportune tie-rods) made lots of time the capacity accelerations even close to zero, that means unbalance mechanisms even only for static conditions. On the contrary, the Form underestimates the real capacity when there are only tie-rods: this is in accord with the issue that the influence of the tie-rod in the evaluation of the mechanisms is high and if the tie-rods are well designed in the wall, the overturning mechanisms could not be triggered by the horizontal actions.

If the attention is paid in the safety indexes, the vulnerable classes achieved by both the estimated and the real safety indexes ($I_{s,E5P}$ and $I_{s,R}$) is the same. On the matter to the definition of the classes it should be specified that the range are defined subjectively and the range extremes defined in 8.4 could change, even if the here proposed partition is very common in the field of safety verification of existing structures.

In analogy with the 5P-Form, the 4P-Form provides the results close to the real capacity when there are vaults (class "D") whose influence is not directly computes in the Form. It highly overestimates the solution when there is one or more tie-rods, whose influence in the Form results is even higher than in the 5P Form, due the presence of one "vulnerable" parameters less (the P2). It underestimates the capacity for a façades with P1, P3 and P4 lying in high vulnerability classes without the presence of the vault (as in the n.3 overturning showed for the Museo of Casa Vasari). For what refers to the safety index, two times the estimated I_s fall in the same class of the real one, but in one case, not in a conservative way, the I_s is overestimated, in accord with the less reliability of the model of the P4 Form.

Table 69: Safety indexes classes for Casa Vasari panels.

	$a_{g,D}$	$a_{g,C,R}$	$I_{S,Real}$	$I_{S,Estimated\ 5}$	$I_{S,Estimated\ 4}$
1 (green)	0.183	0.08	0.44	0.28	0.35
2 (pink)	0.183	0.120	0.65	0.75	0.93
3 (blue)	0.183	0.089	0.49	0.48	0.26

The exposed Façade Form method is stable if applied in a façade in which the geometry and the barycentre are well defined, without the presence of the tie-rods or thrusting forces due to arches of vaults. In this case, the capacity estimation could achieve values very close to the real one, with at least error less than 5%, since the most influential parameters in the definition of the capacity are well considered in the correlation expressed by the Façade Forms. In the cases of presence of the tie-rods and vaults, the method could over-under estimated the real capacity (even in high percentage) but in most of cases in a conservative way. It is worth noting that these parameters are very difficult to determinate even in the analytical procedure, since they are linked to different and significant factors ($7.2.1.8 \div 7.2.1.11$) and this issue makes even the real capacity acceleration affected by uncertain in the definition of its value, depending on the got hypotheses in the calculations.

With the 5P Form, the estimated safety indexes are for the 95% of the case in the same range. Since the safety indexes take into account even the seismic hazard of the zone in which the façade is collocated, the evaluation of them allow to create a risk ranking among a wide large sample of study even coming from different Regions and determine the structure that should be analysed in deep and firstly and strengthened.

The last remark regards the use of the Forms with the knowledge of simple information of the structure which can achieved with the in situ external survey or knowing the major characteristics of the structural masonry typology of the building. It means that even with the estimated knowledge of the masonry thickness of the façade, it is possible to achieve a good result. In particular, for the case studies analysed in order to test the methods (for the 22 mechanisms), calculations with variated thicknesses was done. The results in term of capacity acceleration remain at least stable, with minor changes in the definition of the risk indexes, that are stable for the 90% of the case for which their class achieved is equal to those of the real one.

CONCLUSION AND OUTLOOKS

After the Italian recent seismic events (Abruzzo 2009, Emilia Romagna 2012), historical city centres have shown several structural damages with strong implications of both social and economic resources. In particular, masonry aggregates, characterized by a wide structural variety being a result of a complex historical and temporal process of evolution, most of time did not answer as a complex building but shown the activation of out-of-plane mechanisms in the major façades or local collapses.

The vulnerability assessment for existing buildings in aggregate is a key aspect for the seismic risk mitigation: as explained in CHAPTER 2 it can be performed through expeditious/empirical methods or detailed/refined ones. In particular, a seismic risk analysis addressed to earthquake emergency management requires vulnerability and damage evaluations performed at territorial scale, in order to highlight in a density mesh area the most vulnerable buildings to focus on them Administration resources. Starting with the territorial assessment results, sophisticated and numerical analysis for the definition of strengthening interventions could be performed in those aggregates that are considered the most vulnerable.

In this work, both vulnerability empirical and analytical methods have been applied to the aggregates of Castelnuovo (74 masonry aggregates) a small historical city centre in L'Aquila's valley, hit by the earthquake of 06/04/2009 (L'Aquila earthquake). The geometrical and structural characteristics of the masonry aggregates are widely described in CHAPTER 3. The complete knowledge of the main structural characteristics and the building stock has allowed the DICEA's team to make deepened studied on those masonry structures. In particular, the crack patterns observed in the aggregates, both in horizontal and in vertical structural elements, highlighted the presence of discontinuities in the resistance framework scheme. This allowed the individuation of the original core of the aggregates, the levels of connection among the different structural units that composed the aggregates and even to understand how the masonry aggregates of rural historical city centres behave if excited by seismic actions. An overall mean damage grade for each structural unit was individuated, related to the EMS-98 Scale, considering all the structural damage elements in play. The damage scenario experienced by the ss.uu. has been made in connection with the main characteristics of the L'Aquila seismic event and with the seismic hazard in Castelnuovo, widely described in CHAPTER 4.

In CHAPTER 2, an overview of the existing vulnerability assessment methods has been described, and the choice of the most appropriate VAM applied to this case study has been explained. That choice was influenced by different aspects conceiving mostly the type of available database, the different available tools to perform seismic analyses, the achieved level of accuracy of the database information and the "scale" of the project. Vulnerability Index Methods (VIMs) and analytical methods, that is linear and non-linear kinematic analysis of out-of-plane mechanisms, have been individuated as methods to assess vulnerability on masonry aggregates in this work.

In particular, the VIMs were performed to individuate (using low quality information achieved by in-situ surveys and not-complicated numerical models carried out in short time consuming), in a large urban density mesh area, the most vulnerable aggregates to whom applied primary safety verifications with refined analyses. Through the VIMs, it was possible to assess damage predicted scenario on buildings, for different earthquake macroseismic intensities. This procedure was particularly interesting for Castelnuovo aggregates, since the forecast mean damage grade was continuously compared with the observed damages on aggregates after the 2009 earthquake.

Moreover, thanks to all the structural information about aggregates achieved with in situ surveys, the Castelnuovo database of aggregates was also working as a database to perform detailed analytical analyses.

In CHAPTER 5 and 6 the results of the vulnerability analysis through VI Methods were reported. Both aggregates and structural units Forms were used, trying to define a large-scale complete vulnerability assessment of the aggregates.

In particular, CHAPTER 5 showed the results of the application of the Vulnerability Aggregate Form, composed of five qualitative parameters (5P). In the presence of a large sample of buildings as to the historic centres, the Aggregate Form

effectively captures the aggregates that have greater vulnerability due to their plano-altimetric conformations and mechanical characteristics of the masonry. For Castelnuovo aggregates, the Form identified areas in the central part in which the aggregates were characterised by a high vulnerability indexes and currently showed high structural damages. However, the 5P Form, not considering any parameter related to the conservation status of aggregates, did not allowed the full definition of seismic vulnerability, especially for those buildings characterized by bad conditions even before the earthquake. In the last part of the chapter, the definition of a new Aggregate Form was implemented. The integration of the Form involved the insertion of an additional parameter, evaluating the "P6-current state" of the aggregate.

The proposed 6P-Form assumes the following shape:

AGGREGATE FORM - 6 parameters					
Parameters	scores				weight
	A	B	C	D	
1 - Quality of the masonry fabric	0	5	20	50	1.50
2 - Misalignment of openings	0	5	20	50	0.50
3 - Irregularities in height	0	5	20	50	0.50
4 - Plan geometry	0	5	20	50	0.50
5 - Location and soil quality	0	5	20	50	0.50
6 - Current state of the aggregate	0	5	20	50	1.50

The Form is working for the historical centres characterised by aggregates with load-bearing structures in stonemasonry that is aggregates of rural historical centres typical of central and south zones of Italy (in Tuscany in Arno zones and in the Umbria or Abruzzo Region). They are characterized mostly by irregular stone masonries with poor quality mortar and irregular and not-worked shape stones, with lack of connections among orthogonal walls and among horizontal elements and vertical ones, for which the evaluation of the ordinary conservation status assumes great importance.

In CHAPTER 6, the same procedure of evaluation of vulnerability was applied to the scale of the single structural unit. The method consisted in the application of the specific VFs for structural units, GNDT II Level, "Formisano" and "Aveiro" Forms (widely describe in CHAPTER 2) to a reduce sample of study of Castelnuovo. The application of this procedure allowed the individuation of the most influential parameters for the seismic response, with particular reference to local behaviour. Through the careful evaluation of the out-of-plane mechanisms failures, a definition of damage classes for local collapses was introduced. The classification provided four distinct classes at increasing damage level from the un-triggered mechanisms up to collapse.

Afterwards, in CHAPTER 7 and 8, the attention has been paid on the mechanical models that can be used for a detailed analysis of masonry aggregates, considering both the local and the global behaviour that a masonry structure can show if excited by a seismic action. Based on the results of mechanical analyses done in a subset of the sample of original data and looking at damage mechanisms experienced in Castelnuovo aggregates, local out-of-plane mechanisms have been chosen to estimate the seismic capacity. For more than 180 façades, detailed analyses, following Standard procedures (C.M. n.617, 2009) were performed and for each of them a set of geometrical and structural parameters have been indicated, referring to the main seismic issues of the façades.

The local kinematic methodologies have been applied to each ss.uu. in main façades, considering linear and non-linear analysis, with and without the influence of the tie-rods. For less than cases in which there is the presence of constraints at a certain height (i.e. a stairs, terraces..), the overturning for mechanisms triggered by the earthquake in Castelnuovo's aggregates covers the entire wall. Although the prevalence of big vertical cracks in the top of buildings, a high percentage of detachments of floors and vertical cracks are discovered even at the lower floors. The capacity of the façade is then evaluated as the acceleration of activation of simple overturning of the entire façade, performed with linear analysis.

The analytical results of this step procedure allowed to understand that the most influential parameters in the out-of-plane overturning are: the panel height and thickness, the presence of tie-rods and thrust forces (vaults of arches).

Exploiting the analytical method results, in the last Chapter, a new Vulnerability Form for Façades has been introduced, composed by 5 parameters with the goal of determine the capacity acceleration of a façade toward the overturning of the

entire wall, knowing only simple and qualitative parameters. Among the 180 cases analysed, a reduced sample of data was used for determination of the Form, taking into account the mechanisms for which the real damage (in respect to the simple overturning) and the analytical results were not in contrast. 130 cases were then exploited, for which geometrical qualitative parameters were put in relation with and the peak ground acceleration of capacity ($a_{g,c}$) calculate in the rigorous way through standard procedures. With a process of multi-linear regression, the relationship among the parameters and the calculated seismic capacity was found giving definition of the shape and weights to the Façade Form.

The Form is composed of:

P1: Lateral slenderness of the façade

P2: Presence of the thrusting force of masonry vaults or arches.

P3: Presence of the tie-rods.

P4: Barycentre position

P5: Horizontal multiplier of collapse

The Façade Form method is stable if applied in façades for which the geometry and the barycentre are well defined, without the presence of the tie-rods or thrusting forces. In this case, the estimated capacity achieves values very close to that one calculated with standard procedures, with at least error less than 5%. In the cases of presence of the tie-rods and vaults, the method can over-under estimate the real capacity, but in most of cases in a conservative way.

The Façade Forms can be used with the knowledge of simple information of the structure which can be achieved with the in situ external survey or knowing the major characteristics of the structural masonry typology. It means that even if the masonry thickness of façade is estimated, the Form can provide suitable results, even characterised by less reliability in respect to the filling out of the complete Form.

With the in situ observations and the knowledge of some qualitative and geometrical parameters, the Form is able to estimate the acceleration of capacity of the structure ($a_{g,c}$), with reference to the out-of- plane mechanisms of overturning with the hinge configuration at the ground floor. Having information of the hazard of the site in which the structure is (demand of acceleration), the Form allows also the evaluation of the safety index, particularly useful for the definition of the vulnerability ranking in the large-scale assessment even in distinct Regions.

OUTLOOKS

The proposed Vulnerability Forms, both in the large-scale assessment (6P-Aggregate Form) and for the evaluation of the façade vulnerability (Façade Form), are based on the results achieved for the sample of data considered in the thesis, the Castelnuovo aggregates. In particular, for the Aggregates Form, the weight of the new parameter was individuated trying to overcome the differences among the structural damages scenario observed on ss.uu. after the 2009 earthquake and that estimated through the use of vulnerability indexes methods.

An improvement of the Aggregate Form could be related to the upgrading of the definition of the parameters' weights, with particular reference to the P6 one. This can be done amplifying the database, taking as reference other historical city centres, i.e. the ones in "L'Aquila's valley" as San Pio delle Camere, Onna, Poggio Picenze. They are characterised by similar construction typologies and materials and most of them were hit by the earthquake of 2009, too.

The Façades vulnerability Form, as well as the Aggregate Form was implemented considering the major features, loads and geometrical constructions of Castelnuovo structural units, the latter characterised by the lack of connections among vertical and horizontal elements and the flexibility of the slabs, with the widespread presence of tie-rods. An improvement of the method can involve the increasing of the sample of data in order to make in relation different geometrical characteristics and loads (that influence the definition of the vulnerability classes of the Form parameters).

Furthermore, other upgrading can involve the change of the calculation method for seismic capacity of the masonry façade. It could be evaluated taking under consideration different positions of the hinge configuration or with non-liner analysis defining the capacity curve considering both the conventional method and evaluating the premature collapse of slabs.

In the definition of the mechanisms could be taken into account the different degrees of connections from the orthogonal walls and the façades, allowing the estimation of the capacity for out-of-plane complex mechanisms, typical of aggregates that have good connection in the cantonal or enter orthogonal walls.

Further developments should be considered for the influence of the tie-rods force, not easily to individuate, in the kinematic analyses and the capacity results, both the linear and non-linear calculations.

REFERENCES

- AA.VV. (1988). L'ABRUZZO DEI CASTELLI. GLI INSEDIAMENTI FORTIFICATI ABRUZZESI DAGLI ITALICI ALL'UNITÀ D'ITALI. . PESCARA: CARSA EDIZIONI.
- AA.VV. (2003). MANUALE PER LA COMPILAZIONE DELLA SCHEDA GNDT/CNR DI II LIVELLO - VERSIONE MODIFICATA DALLA REGIONE TOSCANA. FIRENZE.
- AA.VV. DIRETT. SCIENTIFICO BORRI, A. (2011). MANUALE DELLE MURATURE STORICHE. ROMA: D.E.I. TIPOGRAFIA DEL GENIO CIVILE.
- AUGENTI, N. (2004). IL CALCOLO SISMICO DEGLI EDIFICI IN MURATURA. UTET UNIVERSITÀ.
- BENEDETTI, D., & PETRINI, V. (1984). SULLA VULNERABILITÀ DI EDIFICI IN MURATURA: PROPOSTA DI UN METODO DI VALUTAZIONE. L'INDUSTRIA DELLE COSTRUZIONI, VOL. 149, NO. 1, PP. 66-74.
- BERNARDINI, A. L., MANNELLA, A., MARTINELLI, A., & MILANO, L. P. (2011). FORECASTING SEISMIC DAMAGE SCENARIOS OF RESIDENTIAL BUILDINGS FROM ROUGH INVENTORIES: A CASE-STUDY IN THE ABRUZZO REGION (ITALY). PROC. OF IMECH E, PART O - J. RISK AND RELIABILITY, (P. VOL. 224: 279-296).
- BERNARDINI, A., GIOVINAZZI, S., LAGOMARSINO, S., & PARODI, S. (2007A). MATRICI DI PROBABILITÀ DI DANNO IMPLICITE NELLA SCALA EMS-98. XI CONVEGNO NAZIONALE ANIDIS L'INGEGNERIA SISMICA IN ITALIA. PISA.
- BERNARDINI, A., GIOVINAZZI, S., LAGOMARSINO, S., & PARODI, S. (2007B). VULNERABILITÀ E PREVISIONE DI DANNO A SCALA TERRITORIALE SECONDO UNA METODOLOGIA MACROSISMICA COERENTE CON LA SCALA EMS-98. XI CONVEGNO NAZIONALE ANIDIS L'INGEGNERIA SISMICA IN ITALIA. PISA.
- BINDA, L., BORRI, A., CARDANI, G., & DOGLIONI, F. (2005-2008). ALLEGATO FINALE PRODOTTI RELUIS. TASK 3B.1 - CLASSIFICAZIONE REGIONALE. "SCHEDA QUALITÀ MURARIA: RELAZIONE FINALE E LINEE GUIDA PER LA COMPILAZIONE DELLA SCHEDA DI VALUTAZIONE DELLA QUALITÀ MURARIA". RELUIS.
- BONAMICO, S., & TAMBURINI, G. (1996). CENTRI ANTICHI MINORI D'ABRUZZO: RECUPERO E VALORIZZAZIONE. ROMA: GANGEMI EDITORE.
- BORGHINI, A., DEL MONTE, E., ORTOLANI, B., & VIGNOLI, A. (2011). STUDIO DEGLI EFFETTI DEL SISMA DEL 06/04/2009 SULLA FRAZIONE DI CASTELNUOVO, COMUNE DI SAN PIO DELLE CAMERE (AQ). . XIV CONVEGNO NAZIONALE ANIDIS L'INGEGNERIA SISMICA IN ITALIA. BARI.
- BORRI, A., & DE MARIA, A. (2005-2008). ALLEGATO 3B.1-UR06-4 PRODOTTI RELUIS 2005-2008. TABELLE DI CORRELAZIONE TRA IQM E TABELLE DELLE NTC 2008. RELUIS.
- BORRI, A., & DE MARIA, A. (2008). ALLEGATO 3B.1-UR06-1 PRODOTTI RELUIS. SCHEDA DI VALUTAZIONE DELL'IQM (INDICE DI QUALITÀ MURARIA). RELUIS.
- BORRI, A., CORRADI, M., GALANO, L., & VIGNOLI, A. (2001). ANALISI SPERIMENTALI E NUMERICHE PER LA VALUTAZIONE DELLA RESISTENZA A TAGLIO DELLE MURATURE. INGEGNERIA SISMICA, 50-68.
- BOSCHI, S., BERNARDINI, C., BORGHINI, A., CIAVATONE, A., DEL MONTE, E., GIORDANO, S., . . . VIGNOLI, A. (2015). ANALISI DEI RISULTATI DI PROVE SPERIMENTALI SU MURATURE TOSCANE. ANIDIS. L'AQUILA.
- BOSCHI, S., BORGHINI, A., CIAVATONE, A., DEL MONTE, E., & VIGNOLI, A. (2014). VULNERABILITÀ SISMICA DI CENTRI STORICI: IL CASO STUDIO DI CASTELNUOVO (AQ). SAFE MONUMENTS. FIRENZE.
- BOSCHI, S., BORGHINI, A., DEL MONTE, E., ORTOLANI, B., & VIGNOLI, A. (2013). METHODOLOGY FOR ANTE AND POST-EARTHQUAKE ASSESSMENT OF EXISTING MASONRY BUILDINGS: THE CASE STUDY OF AN AGGREGATE. XV CONVEGNO NAZIONALE ANIDIS. PADOVA.
- BRAGA, F., DOLCE, M., & LIBERATORE, D. (1982). A STATISTICAL STUDY ON DAMAGED BUILDINGS AND AN ENSUING REVIEW OF THE M.S.K. 76 SCALE. PROC. OF THE 7TH EUROPEAN CONFERENCE ON EARTHQUAKE ENGINEERING. ATHENS.
- BRAMERINI, F., DI PASQUALE, G., ORSINI, A., PUGLIESE, A., ROMEO, R., & SABETTA, F. (1995). RISCHIO SISMICO DEL TERRITORIO ITALIANO. PROPOSTA PER UNA METODOLOGIA E RISULTATI PRELIMINARI. ROMA: SSN/RT/95/01.
- CALDERINI, C., CATTARI, S., DEGLI ABBATI, S., LAGOMARSINO, S., OTTONELLI, D., & ROSSI, M. (2010). DELIVERABLE D26: MODELLING STRATEGIES FOR SEISMIC GLOBAL RESPONSE AND LOCAL MECHANISMS. GENOVA: PERPETUATE PROJECT.
- CALVI, G. M. (1999). A DISPLACEMENT-BASED APPROACH FOR VULNERABILITY EVALUATION OF CLASSES OF BUILDINGS. JOURNAL OF EARTHQUAKE ENGINEERING, VOL. 3, NO. 3, PP. 411-438.
- CAROCCI, C. (2001). GUIDELINES FOR SAFETY AND PRESERVATION OF HISTORICAL CENTRES IN SEISMIC AREAS. . IN HISTORICAL CONSTRUCTIONS. . GUIMARÃES: P.B. LOURENÇO, P. ROCA (EDS.).
- CATTARI, S., & LAGOMARSINO, S. (2009). NON LINEAR SEISMIC ANALYSIS OF MASONRY BUILDINGS BY THE EQUIVALENT FRAME. ZURICH : PROC. 11° D-A-CH CONFERENCE: MASONRY AND EARTHQUAKES (INVITED PAPER).
- CATTARI, S., CURTI, E., GIOVINAZZI, S., LAGOMARSINO, S., PARODI, S., & PENNA, A. (2004). UN MODELLO MECCANICO PER L'ANALISI DI VULNERABILITÀ DEL COSTRUITO IN MURATURA A SCALA URBANA. XI CONVEGNO NAZIONALE ANIDIS L'INGEGNERIA SISMICA IN ITALIA. GENOVA.
- CATTARI, S., DEGLI ABBATI, S., FERRETTI, D., LAGOMARSINO, S., OTTONELLI, D., ROSSI, M., & TRALLI, A. (2012). THE SEISMIC BEHAVIOUR OF ANCIENT MASONRY AFTER THE EARTHQUAKE IN EMILIA. INGEGNERIA SISMICA.

-
- CHIARANDINI, A. (S.D.). LEGGI DI CORRELAZIONE TRA DANNO, INTENSITÀ E VULNERABILITÀ SISMICA SULLA BASE DEI DATI DI VENZONE, TARENTO E SAN DANIELE DEL FRIULI. UDINE: RAPPORTO. UNIVERSITÀ DI UDINE.
- CIRC. 617. (2009). MINISTERO DELLE INFRASTRUTTURE E DEI TRASPORTI. ISTRUZIONI PER L'APPLICAZIONE DELLE "NORME TECNICHE PER LE COSTRUZIONI" DI CUI AL D.M. 14/01/2008/. G.U. N. 47 DEL 26/2/09 SUPPL. ORD. N.27 (IN ITALIAN).
- COLONNA, E., MOLINA, C., & PETRINI, V. (1994). CRITERI DI VALUTAZIONE DELLA VULNERABILITÀ SISMICA DEL PATRIMONIO EDILIZIO ESISTENTE SUL TERRITORIO NAZIONALE. . INGEGNERIA SISMICA, 16-24.
- COMO, M. (2010). STATICA DELLE COSTRUZIONI STORICHE IN MURATURA. ARCHI VOLTE E CUPOLE. EDIFICI MONUMENTALI. EDIFICI SOTTO CARICHI VERTICALI E SOTTO SISMA. ARACNE EDITOR.
- CORRADI, M., BORRI, A., & VIGNOLI, A. (2003). EXPERIMENTAL STUDY ON THE DETERMINATION OF STRENGTH OF MASONRY WALL. CONSTRUCTION AND BUILDING MATERIALS, 325-337.
- D'AYALA, D., & NOVELLI, V. (2010). DELIVERABLE 8. REVIEW AND VALIDATION OF EXISTING VULNERABILITY DISPLACEMENT-BASED MODELS . PERPETUATE PROJECT: PERFORMANCE-BASED APPROACH TO EARTHQUAKE PROTECTION OF CULTURAL HERITAGE IN EUROPEAN AND MEDITERRANEAN COUNTRIES.
- D'AYALA, D., & S. PAGANONI, S. (2011). ASSESSMENT AND ANALYSIS OF DAMAGE IN L'AQUILA HISTORIC CITY CENTRE AFTER 6TH APRIL 2009. BULLETIN OF EARTHQUAKE ENGINEERING, 9:81-104.
- D'AYALA, D., & SPERANZA, E. (2002). AN INTEGRATED PROCEDURE FOR THE ASSESSMENT OF SEISMIC VULNERABILITY OF HISTORIC BUILDINGS. 12TH EUROPEAN CONFERENCE ON EARTHQUAKE ENGINEERING. LONDRA, UK.
- DAMONI, C., BELLETTI, B., & STOCCHI, A. (2013). VERIFICHE SISMICHE DI EDIFICI STORICI TRAMITE L'ANALISI CINEMATICA LINEARE E NON LINEARE. PADOVA.
- DAMONI, C., BELLETTI, B., & STOCCHI, A. (2013). VERIFICHE SISMICHE DI EDIFICI STORICI TRAMITE L'ANALISI CINEMATICA LINEARE E NON LINEARE. XV CONVEGNO NAZIONALE ANIDIS. PADOVA.
- DEL MONTE, E., & VIGNOLI, A. (2008). IN SITU MECHANICAL CHARACTERIZATION OF THE MORTAR IN MASONRY BUILDINGS WITH DRMS,. VARENNA (CO), ITALIA: 1ST INTERNATIONAL RILEM SYMPOSIUM ON SITE ASSESSMENT OF CONCRETE, MASONRY AND TIMBER STRUCTURES, 01-02 SEPTEMBER.
- DM. (1975). D. M. DEL 3 MARZO 1975 (OFFICIAL BULLETIN. N. 93 DEL 08/04/1975) .
- DM. (1987). D.M. N.141 DEL 9/1/1987.
- DOLCE, M. (1991). SCHEMATIZZAZIONE E MODELLAZIONE DEGLI EDIFICI IN MURATURA SOGGETTI AD AZIONI SISMICHE. L'INDUSTRIA NELLE COSTRUZIONI.
- DOLCE, M., & MORONI, C. (2004). LA VALUTAZIONE DELLA VULNERABILITÀ E DEL RISCHIO SISMICO DEGLI EDIFICI PUBBLICI MEDIANTE LE PROCEDURE VC (VULNERABILITÀ C.A.) E VM (VULNERABILITÀ MURATURA). INGV/GNDT- GRUPPO NAZIONALE PER LA DIFESA DEI TERREMOTI.
- DOLCE, M., ANGELO, M., MARINO, M., & MARCO, V. (2003). EARTHQUAKE DAMAGE SCENARIOS OF THE BUILDING STOCK OF POTENZA (SOUTHERN ITALY) INCLUDING SITE EFFECTS. BULLETIN OF EARTHQUAKE ENGINEERING, 115-140, 2003.
- DOLCE, M., MASI, A., MARINO, M., & VONA, M. (2004). EARTHQUAKE DAMAGE SCENARIOS OF THE BUILDING STOCK OF POTENZA (SOUTHERN ITALY) INCLUDING SITE EFFECTS. BULLETIN OF EARTHQUAKE ENGINEERING, VOL. 1, No. 1, PP. 115-140.
- DOLCE, M., ZUCCARO, G., KAPPOS, A., & A., C. (1994). REPORT OF THE EAEE WORKING GROUP3: VULNERABILITY AND RISK ANALYSIS. 10TH EUROPEAN CONFERENCE ON EARTHQUAKE ENGINEERING, (P. 309-3077). VIENNA.
- DT2. (1977). RACCOMANDAZIONI PER LA RIPARAZIONE STRUTTURALE DEGLI EDIFICI IN MURATURA. FIULI VENEZIA GIULIA.
- EC8-1. EUROCODE 8. (1998, 01). DESIGN OF STRUCTURES FOR EARTHQUAKE RESISTANCE - PART 1: GENERAL RULES, SEISMIC ACTIONS AND RULES FOR BUILDINGS, EN 1998-1. . CEN.
- FERREIRA, T., VICENTE, R., & VARUM, H. (2012). VULNERABILITY ASSESSMENT OF BUILDING AGGREGATES: A MACROSEISMIC APPROACH. 15TH WORLD CONFERENCE ON EARTHQUAKE ENGINEERING. LISBONA.
- FORMISANO, A., FLORIO, G., LANDOLFO, R., & MAZZOLANI, F. (2011). ANALISI SISMICA DI AGGREGATI EDILIZI SU LARGA SCALA: I CASI STUDIO DI TORRE DEL GRECO E POGGIO PICENZE. ATTI DEL WORKSHOP WANDER MASONRY 2011 (P. 255-266). FIRENZE: POLISTAMPA.
- GALASCO, A., LAGOMARSINO, S., PENNA, A., & RESEMINI, S. (2004). NON-LINEAR SEISMIC ANALYSIS OF MASONRY. PROC. OF 13TH WORLD CONFERENCE ON EARTHQUAKE ENGINEERING, VANCOUVER 1-6 AUGUST, PAPER N. 843.
- GIOVINAZZI, S. (2005). THE VULNERABILITY ASSESSMENT AND THE DAMAGE SCENARIO IN SEISMIC RISK. PH.D. THESIS. UNIVERSITY OF FIRENZE AND TECHNICAL UNIVERSITY CAROLO-WILHELMINA BRAUNSCHWEIG.
- GIOVINAZZI, S., & LAGOMARSINO, S. (2001). UNA METODOLOGIA PER L'ANALISI DI VULNERABILITÀ SISMICA DEL COSTRUITO . X CONVEGNO NAZIONALE L'INGEGNERIA SISMICA IN ITALIA. POTENZA-MATERA.
- GIOVINAZZI, S., & LAGOMARSINO, S. (2004). A MACROSEISMIC METHOD FOR THE VULNERABILITY ASSESSMENT OF BUILDINGS. 13TH WORLD CONFERENCE ON EARTHQUAKE ENGINEERING. VANCOUVER, B.C., CANADA.
- GIUFFRÈ, A. (1993). SICUREZZA E CONSERVAZIONE DEI CENTRI STORICI: IL CASO ORTIGIA. BARI: LATERZA.
- GIUFFRÈ, A., & CAROCCI, C. (1999). CODICE DI PRATICA PER LA SICUREZZA E LA CONSERVAZIONE DEL CENTRO STORICO DI PALERMO. ROMA: LATERZA.
- GNDT. (1993). RISCHIO SISMICO DI EDIFICI PUBBLICI - PARTE I ASPETTI METODOLOGICI. ROMA: CONSIGLIO NAZIONALE DELLE RICERCHE - GRUPPO NAZIONALE PER LA DIFESA DAI TERREMOTI.
-

-
- GÓMEZ CAPERA, A., ALBARELLO, D., & GASPERINI, P. (2007). DELIVERABLE D11. AGGIORNAMENTO RELAZIONI FRA L'INTENSITÀ MACROSISMICA E PGA. INGV-DPC.
- GRIMAZ, S., MERONI, F., PETRINI, V., TOMASONI, R., & ZONNO, G. (1996). IL RUOLO DEI DATI DI DANNEGGIAMENTO DEL TERREMOTO DEL FRIULI NELLO STUDIO DI MODELLI DI VULNERABILITÀ SISMICA DEGLI EDIFICI IN MURATURA. LA SCIENZA E I TERREMOTI - ANALISI E PROSPETTIVE DALL'ESPERIENZA DEL FRIULI - 1976/1996. UDINE.
- GRÜNTAL, G. (1998). CAHIERS DU CENTRE EUROPÉEN DE GÉODYNAMIQUE ET DE SÉISMOLOGIE: VOLUME 15 – EUROPEAN MACROSEISMIC SCALE 1998", LUXEMBOURG.
- GUAGENTI, E., & PETRINI, V. (1989). IL CASO DELLE VECCHIE COSTRUZIONI: VERSO UNA NUOVA LEGGE DANNI INTENSITÀ., (P. VOL. I PAGG. 145-153). MILANO.
- HAZUS. (1999). EARTHQUAKE LOSS ESTIMATION METHODOLOGY—TECHNICAL AND USER MANUALS. FEDERAL EMERGENCY MANAGEMENT AGENCY, WASHINGTON.
- INDELICATO, D. (2010). VALUTAZIONE E RIDUZIONE DELLA VULNERABILITÀ SISMICA DEGLI AGGREGATI EDILIZI NEI CENTRI STORICI. PHD THESIS. CATANIA.
- LAGOMARSINO, S. (2009). DAMAGE ASSESSMENT OF CHURCHES AFTER L'AQUILA EARTHQUAKE (2009). BULLETIN OF EARTHQUAKE ENGINEERING, 10:73-92.
- LAGOMARSINO, S., PENNA, A., & GALASCO, A. C. (2013). TREMURI PROGRAM: AN EQUIVALENT FRAME MODEL FOR THE NONLINEAR SEISMIC ANALYSIS OF MASONRY BUILDINGS. ENGINEERING STRUCTURES, 56: 1787-1799.
- LANG, K. (2002). SEISMIC VULNERABILITY OF EXISTING BUILDINGS. PH.D. THESIS. ZÜRICH.
- LR. (2012). REGIONE EMILIA ROMAGNA, LEGGE REGIONALE N. 16.
- MAGENES, G. M. (REPORT RS-01/08/2008). TEST RESULTS ON THE BEHAVIOUR OF MASONRY UNDER STATIC CYCLIC IN PLANE LATERAL LOADS. PAVIA: ESECMASE PROJECT, DEPARTMENT OF STRUCTURAL MECHANICS, UNIVERSITY OF PAVIA,.
- MAGENES, G., & DELLA FONTANA, A. (2010). VERIFICA DI EDIFICI IN MURATURA ORDINARIA E ARMATA CON METODI DI ANALISI STATICA LINEARE E NON LINEARE. MILANO: ANPEL.
- MARGOTTINI, C., MOLIN, D., & SERVA, L. (1992). INTENSITY VERSUS GROUND MOTION: A NEW APPROACH USING ITALIAN DATA. ENGINEERING GEOLOGY, 45-58.
- MERONI, F., PETRINI, V., & ZONNO, G. (S.D.). DISTRIBUZIONE NAZIONALE DELLA VULNERABILITÀ MEDIA.
- MILANO, L., MANNELLA, A. M., & MARTINELLI, A. (2009). SCHEDE ILLUSTRATIVE DEI PRINCIPALI MECCANISMI DI COLLASSO LOCALI NEGLI EDIFICI ESISTENTI IN MURATURA E DEI RELATIVI MODELLI CINEMATICI DI ANALISI.
- MINITAB. (S.D.). ISTRUCTION MANUAL.
- MUSSON, R., GRÜNTAL, G., & STUCCHI, M. (2010). THE COMPARISON OF MACROSEISMIC INTENSITY SCALES. BULL SEISMOL, SOC AM 14:413–428.
- NTC. (2008). D.M. 14/1/2008 (OFFICIAL BULLETIN NO. 29 OF 4/02/2008 (IN ITALIAN). ED.).
- O.P.C.M. (2008). 3728.
- PETROCELLI, E. (1999). CIVILTÀ DELLA TRANSUMANZA. IN GIORNATA DI STUDI, CASTEL DEL MONTE, 4 AGOSTO 1990, A CURA DEL MINISTERO DELL'AGRICOLTURA E DELLE FORESTE. PESCARA: ARCHEOCLUB D'ITALIA SEZIONE DI CASTEL DEL MONTE (AQ).
- RD. (1926). REGIO DECRETO N. 705 DEL 3 APRILE 1926 (OFFICIAL BULLETIN N. 102 DEL 3/05/1926). .
- RELUIS. (2010). LINEE GUIDA PER IL RILIEVO, L'ANALISI ED IL PROGETTO DI INTERVENTI DI RIPARAZIONE E RAFFORZAMENTO DI EDIFICI IN AGGREGATO.
- RELUIS. (2010A). "ESEMPIO DI CALCOLO SU RAFFORZAMENTO LOCALE DI EDIFICI IN MURATURA CON TIRANTI". UR-PD.
- RELUIS. (S.D.). LINEA DI RICERCA 1 - SUB TASK 3.B3 - UNITÀ DI RICERCA FIRENZE E GENOVA "SPECIFICHE DI PROVA E REPORT DI PROVA" PROVE DI COMPRESSIONE DIAGONALE E DRMS.
- ROSS, S. M. (2008). PROBABILITÀ E STATISTICA PER L'INGEGNERIA E LE SCIENZE, SECONDA EDIZIONE. APOGEO.
- SANDI, H., & FLORICEL. (1995). ANALYSIS OF SEISMIC RISK AFFECTING THE EXISTING IX BUILDING STOCK. PROCEEDINGS OF THE 0TH EUROPEAN CONFERENCE ON EARTHQUAKE ENGINEERING, (P. VOL. 3, PP. 1105-1110). VIENNA.
- STADATA. (2012). 3MURI MANUALE DI VALIDAZIONE. TORINO.
- TECNICHE, N. (2008). D.M. 14/1/2008. OFFICIAL BULLETIN NO. 29 OF 4/02/2008 (IN ITALIAN).
- UR-FIRENZE. (2005-2008). ALLEGATO 3.B3 - SPECIFICHE DI PROVA E REPORT DI PROVA DRMS. RELUIS.
- VICENTE, R. (2008). PH.D. THESIS. ESTRATÉGIAS E METODOLOGIAS PARA INTERVENÇÕES DE REABILITAÇÃO URBANA. . AVEIRO, PORTOGALLO.
- VICENTE, R., PARODI, S., LAGOMARSINO, S., VARUM, H., & MENDES, J. A. (2011). SEISMIC VULNERABILITY AND RISK ASSESSMENT: CASE STUDY OF THE HISTORIC CITY CENTRE OF COIMBRA, PORTUGAL. BULLETIN OF EARTHQUAKE ENGINEERING, 9:1067–1096.
- VIGNOLI, A. (2012). RICOSTRUIRE DOPO IL TERREMOTO: IL CASO CASTELNUOVO (AQ). FIRENZE: ALINEA EDITRICE.
- VIGNOLI, A., BETTI, M., & GALANO, L. (2014). I -COMPARATIVE ANALYSIS ON THE SEISMIC BEHAVIOUR OF UNREINFORCED MASONRY BUILDINGS WITH FLEXIBLE DIAPHRAGMS. ENGINEERING STRUCTURES, VOL. 61, PP. 195-208.
- VINCI, M. (2014). I TIRANTI IN ACCIAIO NEL CALCOLO DELLE COSTRUZIONI IN MURATURA. PALERMO: DARIO FLACCOVIO EDITORE.
- WHITMAN, R. (1973). DAMAGE PROBABILITY MATRICES FOR PROTOTYPE BUILDINGS . CAMBRIDGE, MASSACHUSETTS: R73-57.
-

-
- ZUCCARO, G. (2004). INVENTORY AND VULNERABILITY FOR RESIDENTIAL BUILDINGS AT NATIONAL TERRITORIAL LEVEL, RISK MAPS AND SOCIO-ECONOMIC LOSSES . NAPOLI: SAVE, INGV/GNDT PROJECT.
- ZUCCARO, G., CACACE, F., & DE GREGORIO, D. (2012). BUILDINGS INVENTORY FOR SEISMIC VULNERABILITY ASSESSMENT ON THE BASIS OF CENSUS DATA. PROC. OF 15TH WCEE. LISBONA.

ANNEX 1: CASTELNUOVO DATABASE

The table shows the 74 Castelnuovo aggregates collocated within the Perimeter, that is the area which describes the historical city centre, with their main characteristics in term of number of ss.uu., covered plan area, total area and volume.

Table A. 1: Castelnuovo aggregates 001-050

AGGREGATES INTERNAL TO THE PERIMETER						
Number progressive	Number Aggregate	Number Aggregate DPC	Covered plan area [m ²]	Total area [m ²]	Volume [m ³]	Structural Units
01	01-222	8800222	814	2 175	6 836	1-2-3-4-5-6-7A-7B
02	02-245	8800245	469	1 109	3 408	1A-1/2-2A-2B-2C-2D
03	03-216	8800216	555	555	2 493	1
04	04-098	8800098	209	209	690	1
05	005	8800	101	102	507	
06	06-087	8800087	164	164	1 893	1
07	07-249	8800249	152	390	1 202	1
08	08-519	8800519	467	1 492	4 494	1-2-3-4-5-6-7-8-9
09	09-160	8800160	181	642	1 582	1-2-3
10	10-088	8800088	852	2 513	7 034	1-2-3-4-5-6-7-8-9
11	11-125	8800125	725	1 957	6 341	1a-1b-1c-2a-2b-3-4-5-6-7
12	12-514	8800514	93	325	800	1
13	13-158	8800158	550	1 675	4 379	1-2-3-4-5-6-7
14	14-127	8800127	445	1 132	3 392	1-2-3-4
15	15-164	8800164	363	951	2 809	1-2-3
16	16-515	8800515	689	1 808	5 851	1-2-3-4-5-6-7
17	17-218	8800218	52	121	363	1
18	18-163	8800163	829	2 270	7 030	1-2-3-4-5-6-7-8-9-10-11
19	19-162	8800162	153	409	1 161	1-2-3
20	20-253	8800253	218	586	1 758	1
21	21-251	8800251	243	866	2 398	1-2-3-4
22	22-231	8800231	246	617	1 771	1-2-3-4-5
23	23-102	8800102	159	367	913	1-2a-2b-2c
24	24-217	8800217	187	576	1 565	1-2-3
25	25-217	8800217	855	2 210	6 322	4A-4B-5-6-7-8A-8B-9-10
26	26-415	8800415	372	1 287	2 433	1-2-3
27	27-415	8800415	848	2 240	5 949	4-5-6-7-8-9-10-11
28	28-280	8800280	122	257	683	1-2
29	29-370	8800370	196	532	1 540	1-2-3
30	30-283	8800283-8800483	457	1 322	3 435	283/1-283/2-283/3-283/4-483/1
31	31-159	8800159	410	1 129	3 566	1-2-4B/3-4A-5-6
32	32-241	8800241	404	1 235	3 124	1-2-3-4
33	33-521	8800521	72	171	514	1
34	34-242	8800242	50	125	275	1
35	35-239	8800239	488	1 173	5 208	1-2
36	36-161	8800161	460	919	3 031	1A-1B/2/3
37	37-092	8800092	159	298	992	1A-1B
38	38-144	8800144	27	54	151	1
39	39-084	8800084	29	57	160	1
40	40-142	8800142	40	80	280	1
41	41-255	8800255	82	163	505	1
42	42-035	8800035	514	1 016	2 775	1A-1B-1C-2-3-4-5-6
43	43-238	8800238	69	137	309	1
44	44-174	8800174	305	880	2 649	1/2-3-4-5A-5B
45	45-049	8800049	403	1 128	3 338	1-2-3-4-5-6
46	46-237	8800237-8800244	55	224	686	237-1, 244-1
47	47-051	8800051-8800236	451	1 331	3 992	236-1,236-2,051-1A,051-1B,051-2,051-3,051-4
48	48-235	8800235	18	37	82	1
49	49-233	8800233	268	754	2 284	1-2-3-4-5
50	50-173	8800173	157	348	1 042	1-2-3

Table A. 2: Castelnuovo aggregates 051-074

AGGREGATES INTERNAL TO THE PERIMETER						
Number progressive	Number Aggregate	Number Aggregate DPC	Covered plan area [m ²]	Total area [m ²]	Volume [m ³]	Structural Units
51	51-050	8800050	186	467	1 400	1
52	52-171	8800171	131	344	938	1-2
53	53-234	8800234	188	603	1 503	1-2
54	54-246	8800246	72	133	352	1-2
55	55-157	8800157	413	1 071	2 723	1-2-3A-3B-3C-4/5-6
56	56-247	8800247	341	730	2 218	1-2-3A-3B-3C-4
57	57-179	8800179	330	990	2 981	1-2-3-4-5
58	58-208	8800208	438	1 056	3 184	1-2-3-4-5-6-7-8-9
59	59-207	8800207-8800204	569	1 441	4 040	204-1,204-2,204-3,204-4,207-1,207-2,207-3,207-4,207-5,207-6
60	60-203	8800203	55	55	331	1
61	61-176	8800176	769	2 076	5 941	1-2-3-4-5-6-7-8-9
62	62-178	8800178-8800166	512	1 433	4 304	178-1,178-2,178-3,178-4,166-1,166-2,166-3,166-4,166-5,166-6
63	63-167	8800166	340	680	2 036	7-8-9-10-11-12
64	64-187	8800187	47	142	344	1
65	65-584	8800584	83	83	203	1-2-3
66	66-583	8800583	71	72	238	1-2
67	67-177	8800177	134	221	584	1A-1B
68	68-200	8800200-8800198-8800574	253	642	1 856	198-1, 200-1A, 200-1B, 200-2, 574-1A, 574-1B
69	69	8800	316	632	1 896	1
70	70	8800	134	134	402	1
71	71	8800	85	85	508	1
72	72	8800	47	47	279	1
73	73	8800	13	13	40	1
74	74-209	8800209	36	74	216	1
T totale			21 787	55 339	164 512	

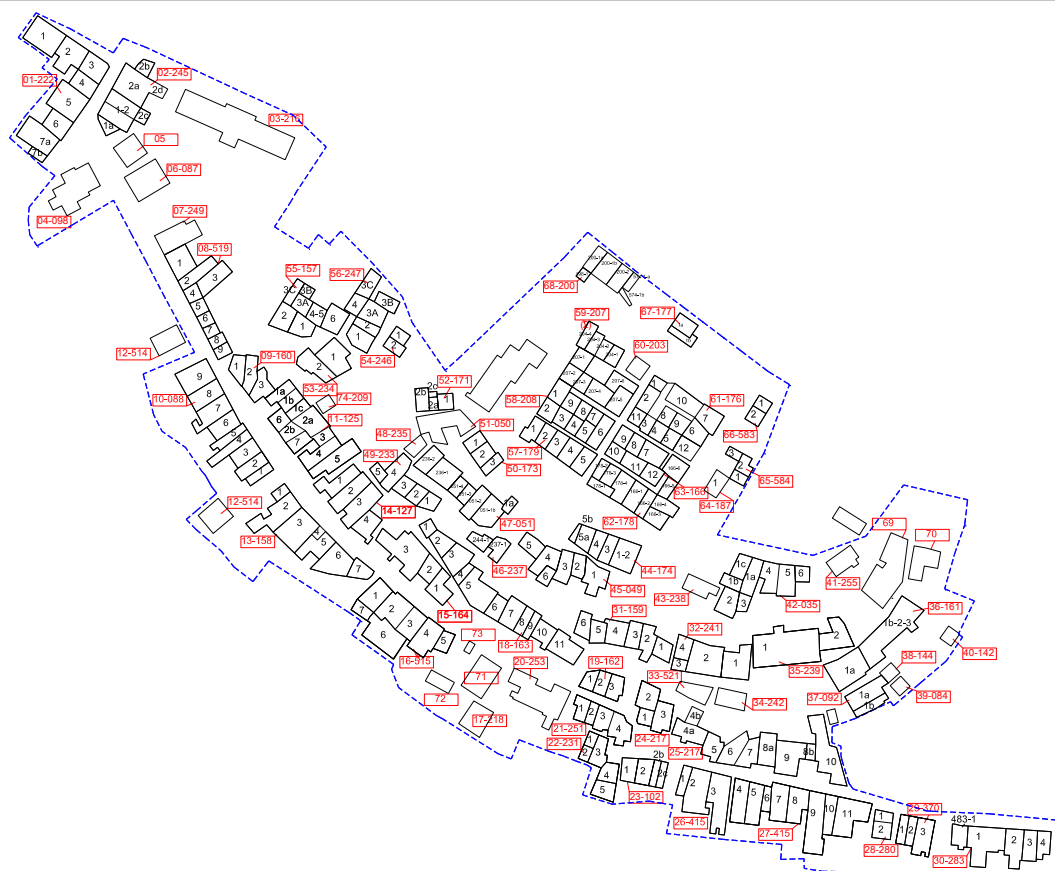

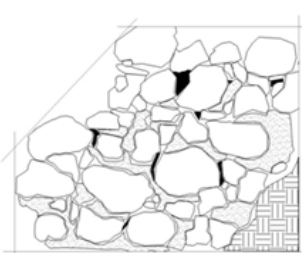



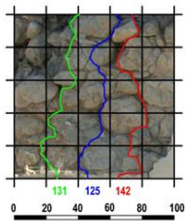



Figure A. 1: Aggregates identification.

ANNEX 2

Extract of the “Masonry Quality Form” for one masonry panel of Castelnuovo aggregate (n.57-179) and some examples of panels belonging to masonry collocated in Tuscany and Umbria Regions.

PARTE SECONDA RILIEVO DELLA TIPOLOGIA MURARIA	
2. TESSITURA DEL PARAMENTO	
FOTOGRAFIA DEL PARAMENTO	RESTITUZIONE GRAFICA DEL PARAMENTO
	  <div style="font-size: small;"> Legenda: Pietra Malta Vuoto Intonaco Vegetazione </div>

PARTE SECONDA RILIEVO DELLA TIPOLOGIA MURARIA		
2. TESSITURA DEL PARAMENTO		
ORIZZONTALITÀ DEI FILARI Schema grafico	SFALSAMENTO DEI GIUNTI Schema grafico	INGRANAMENTO SUL PIANO ESTERNO Schema grafico
		  VALORE DI LTM: 133 INGRANAMENTO: MEDIO VULNERABILITÀ: LV3 – VUL. MEDIA


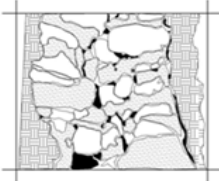

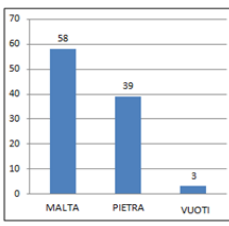
PARTE SECONDA RILIEVO DELLA TIPOLOGIA MURARIA										
4. SEZIONE MURARIA										
FOTOGRAFIA DELLA SEZIONE MURARIA	RESTITUZIONE GRAFICA DELLA SEZIONE	GRAFICO Con indicazione della percentuale di pietre di malta e di vuoti								
	  <div style="font-size: small;"> Legenda: Pietra Malta Vuoto Intonaco Vegetazione </div>	 <table border="1" style="font-size: small; margin-top: 10px;"> <thead> <tr> <th>Categoria</th> <th>Percentuale (%)</th> </tr> </thead> <tbody> <tr> <td>PIETRA</td> <td>39%</td> </tr> <tr> <td>MALTA</td> <td>58%</td> </tr> <tr> <td>VUOTI</td> <td>3%</td> </tr> </tbody> </table>	Categoria	Percentuale (%)	PIETRA	39%	MALTA	58%	VUOTI	3%
Categoria	Percentuale (%)									
PIETRA	39%									
MALTA	58%									
VUOTI	3%									



Figure A. 2 Type of masonry in Toscana and Umbria (central Regions of Italy). Masonry panels tested with destructive test diagonal test in order to determine the shear resistance τ_0 (Borri et al., 2001)

ANNEX 3: INFLUENCE OF THE GEOMETRICAL AND STRUCTURAL PARAMETERS IN THE ANALYSIS RESULTS

1. Influence of the height of the interstorey (h)

1.1 Variation of the second floor's height

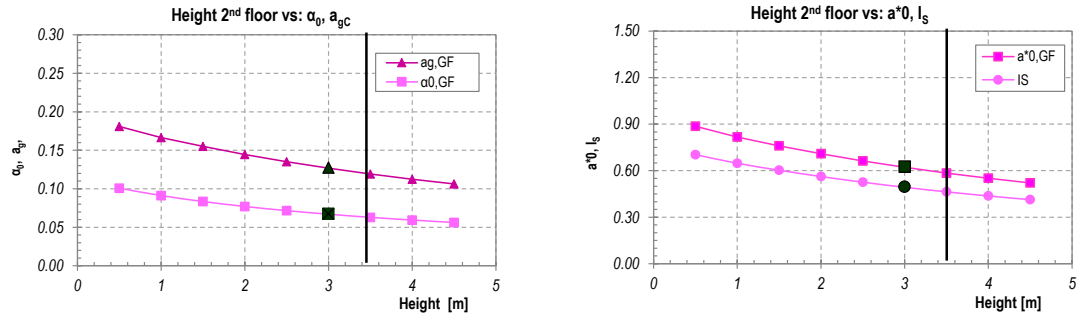


Figure A. 3: Results of linear analyses for different values of 2nd floor's height.

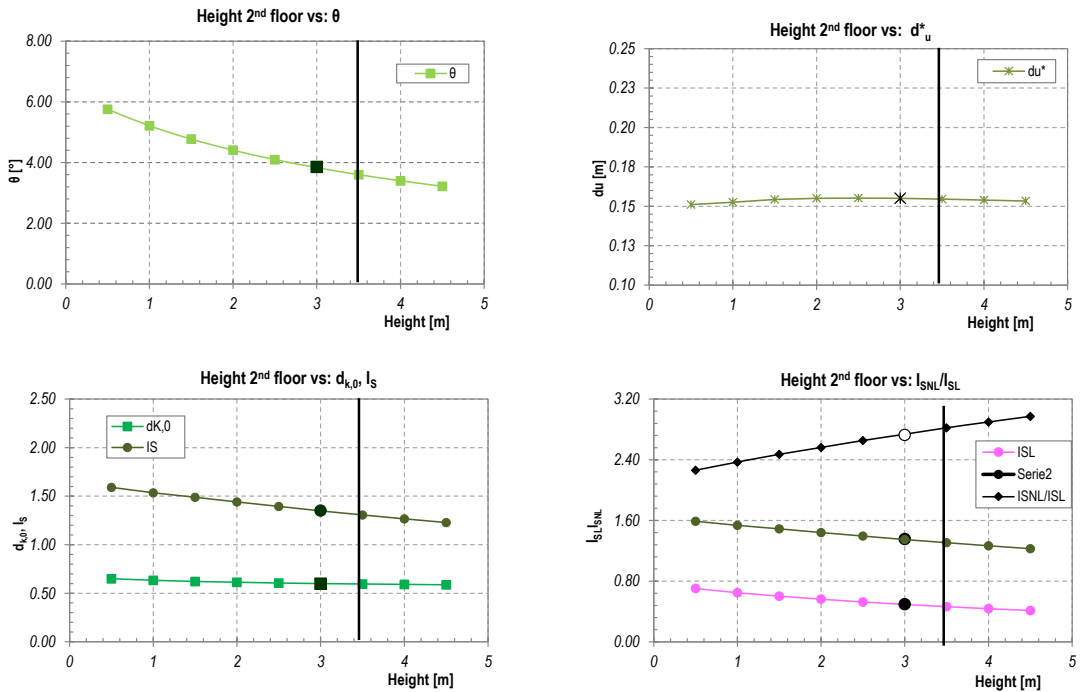


Figure A. 4: Results of non-linear analyses for different values of 2nd floor's height.

1.2 Variation of the first and second floor's height:

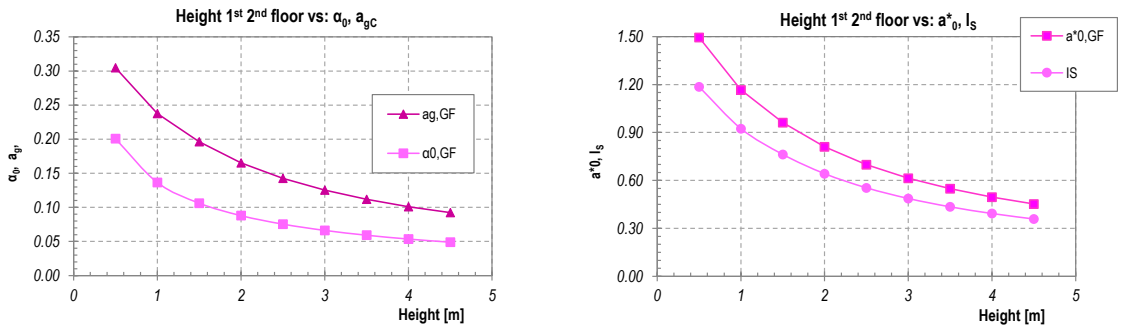


Figure A. 5: Results of linear analyses for different values of 1st and 2nd floor's height.

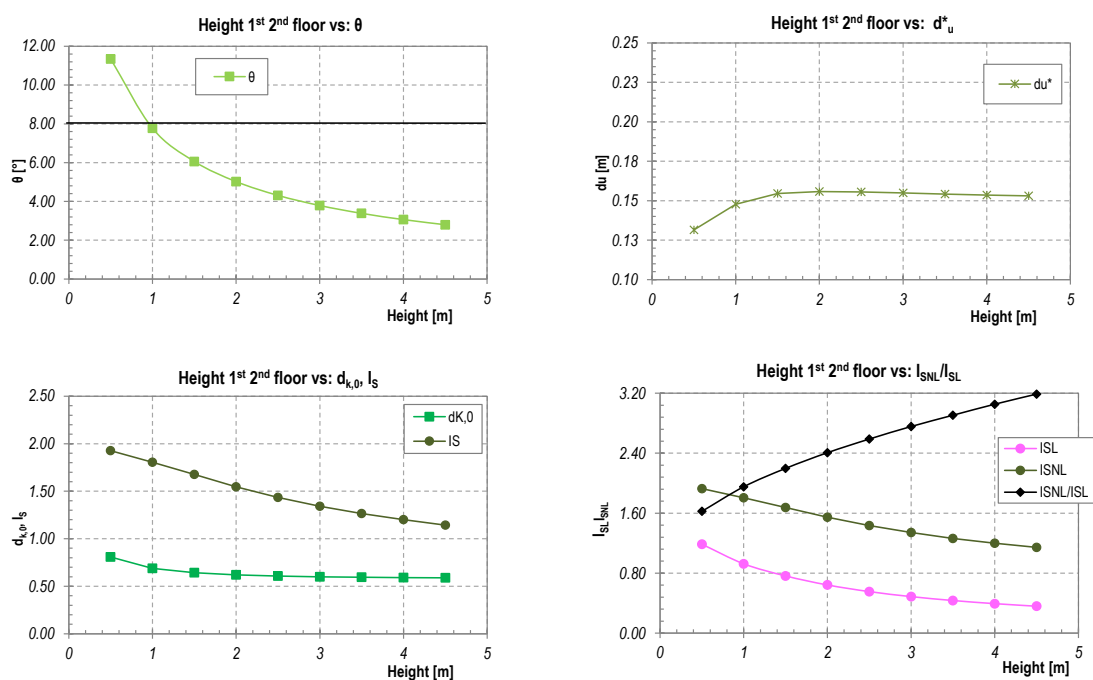


Figure A. 6: Results of non-linear analyses for different values of 1st and 2nd floor's height.

1.3 Variation of all the floors' height:

(in horizontal black line there is the limit of the described parameters in the standard graphs, to simplify to compare at first glance the different of % of variation with the other cases analysed).

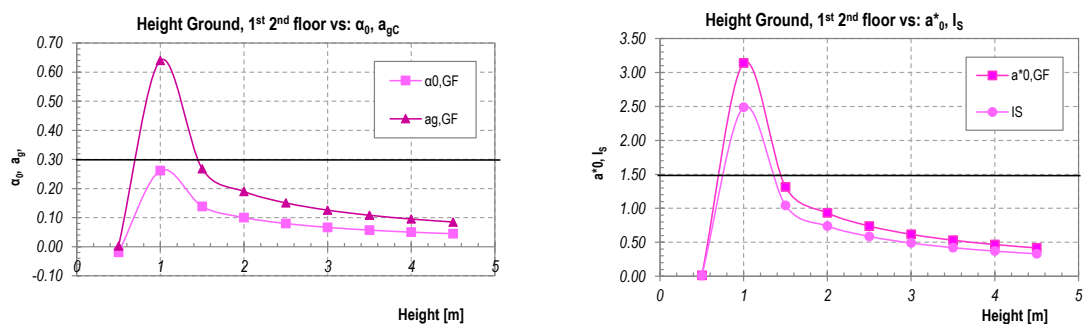
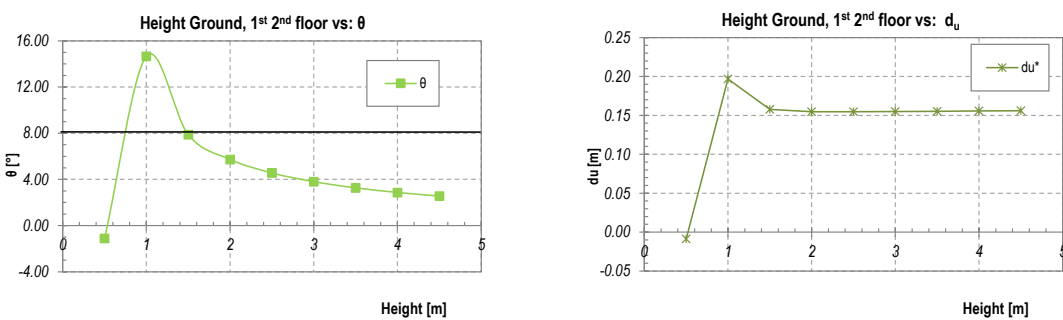


Figure A. 7: Results of linear analyses for different values of ground, 1st and 2nd floor's height.



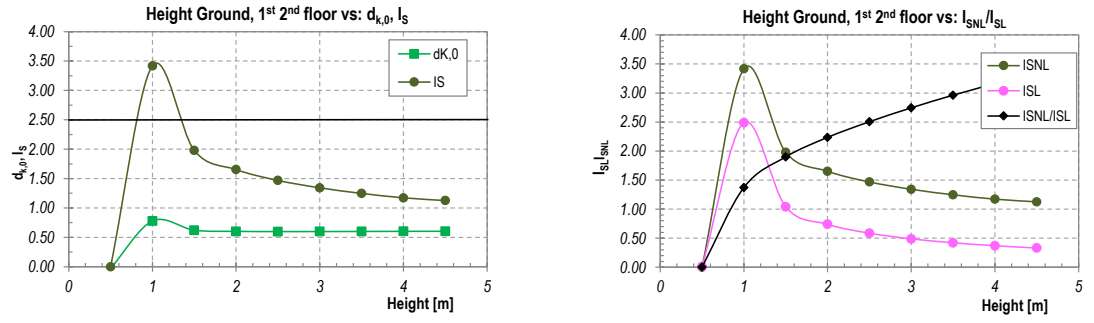


Figure A. 8: Results of non-linear analyses for different values of ground, 1st and 2nd floor's height.

2. Influence of the holes percentage in façade (% openings):

2.1 Variation of the second floor's % of openings

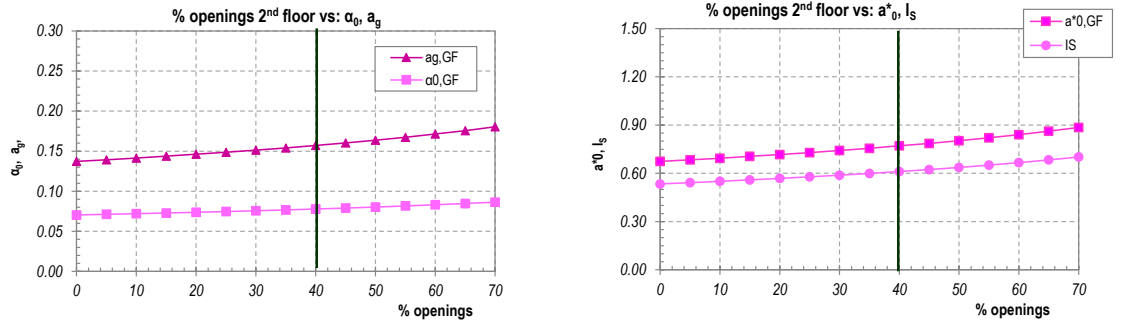


Figure A. 9: Results of linear analyses for different values of 2nd floor's % of openings.

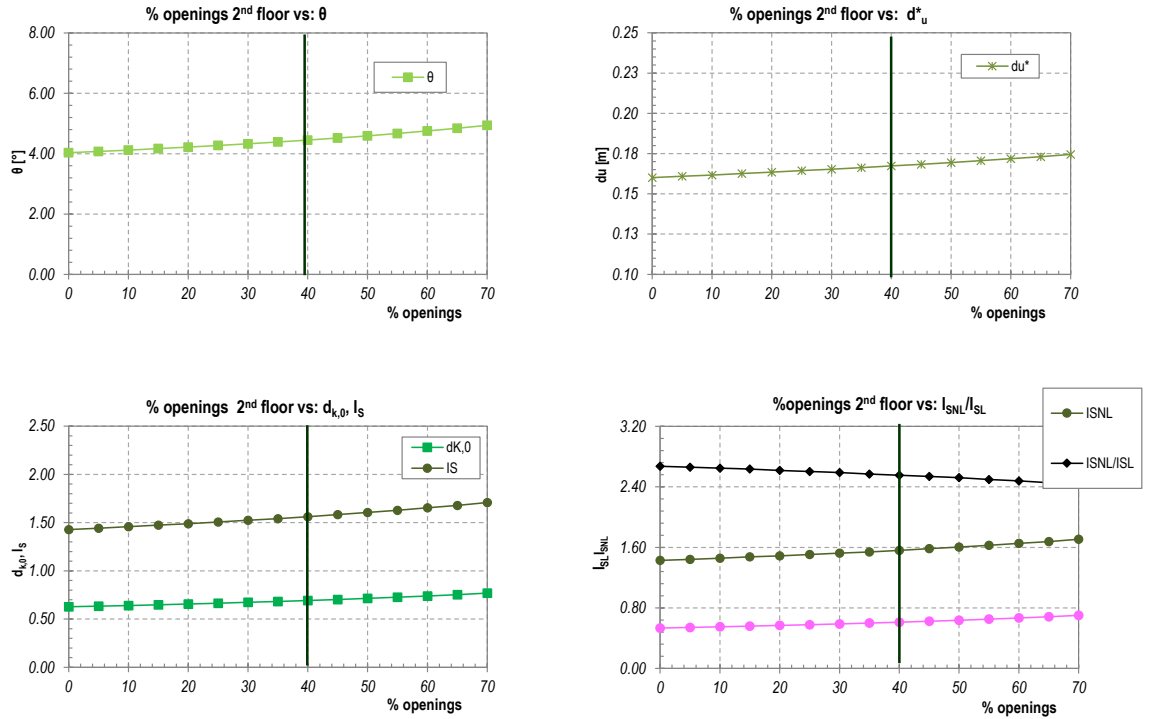


Figure A. 10: Results of non-linear analyses for different values of 2nd floor's % of openings.

2.2 Variation of the first and second floors' % of openings

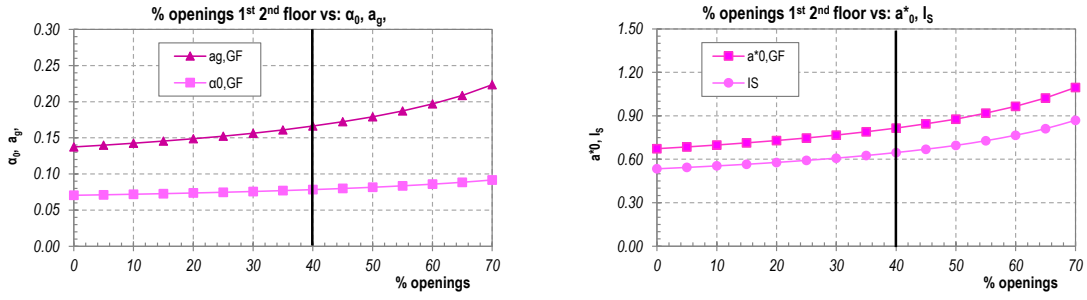


Figure A. 11: Results of linear analyses for different values of 1st and 2nd floor's % of openings.

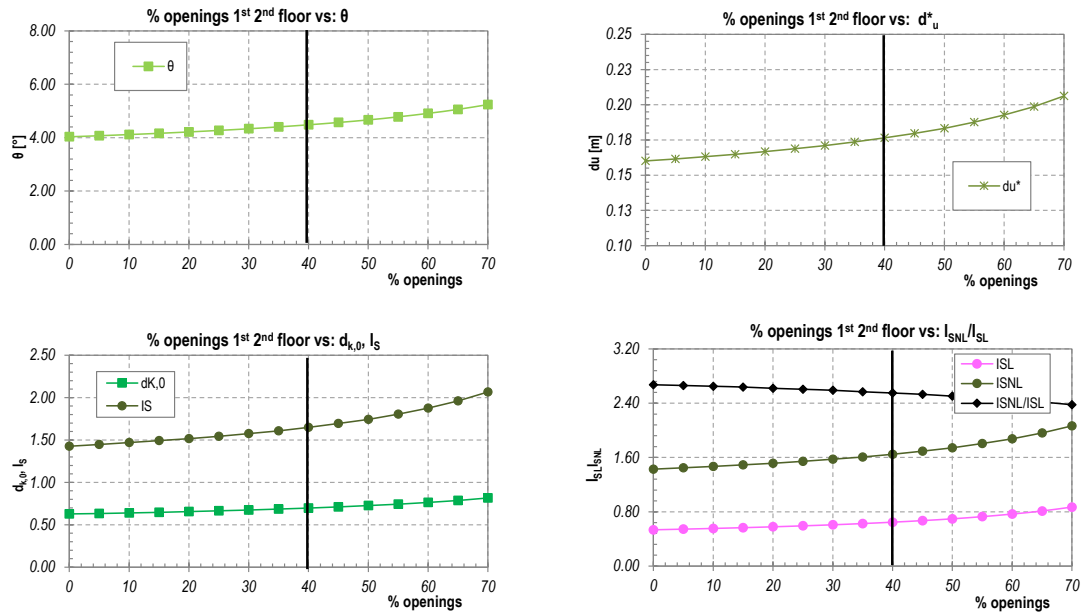


Figure A. 12: Results of non-linear analyses for different values of 1st and 2nd floor's % of openings.

2.3 Variation of all the floors' % of openings:

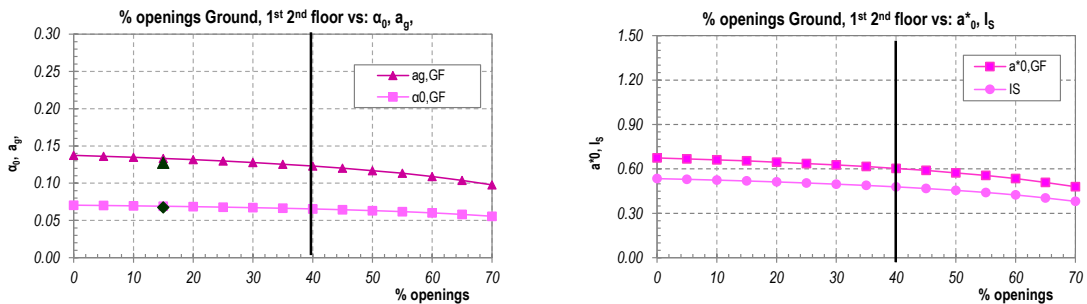


Figure A. 13: Results of linear analyses for different of holes % for all the floors.

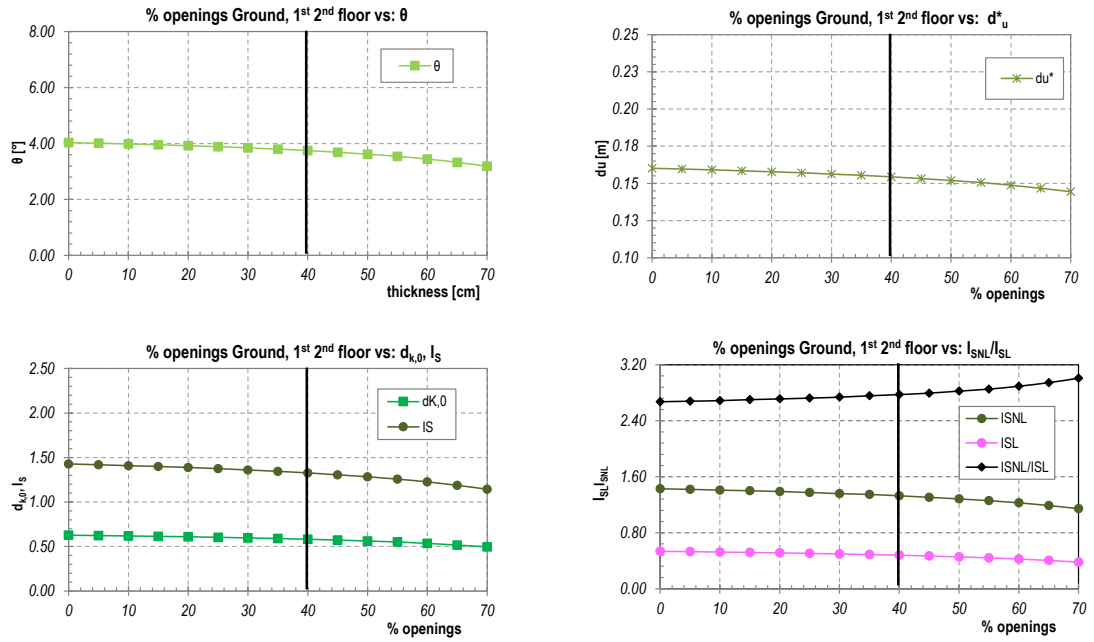


Figure A. 14: Results of non-linear analyses for different values of ground, 1st and 2nd floor's % of openings.

3. Influence of tensile force of the tie-rods (T)

3.1 Tie-rods at the second floor. In black horizontal lines there is the upper limit standard for the sizes represented in the others graphs, to have a direct comparison with the other graphs looking at first glance the shape and level of the size in the plots.

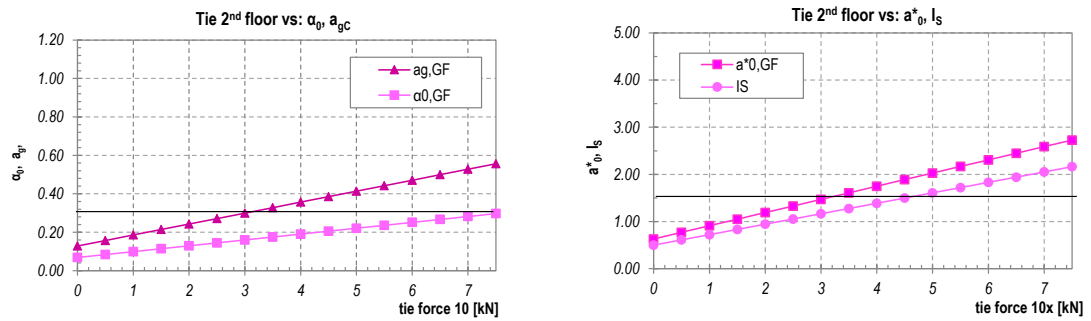
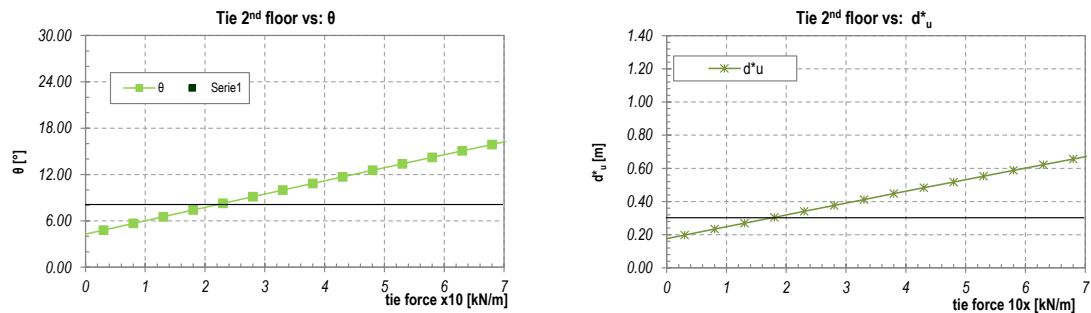


Figure A. 15: Results of linear analyses for different values of 2nd floor's tie-rod force.



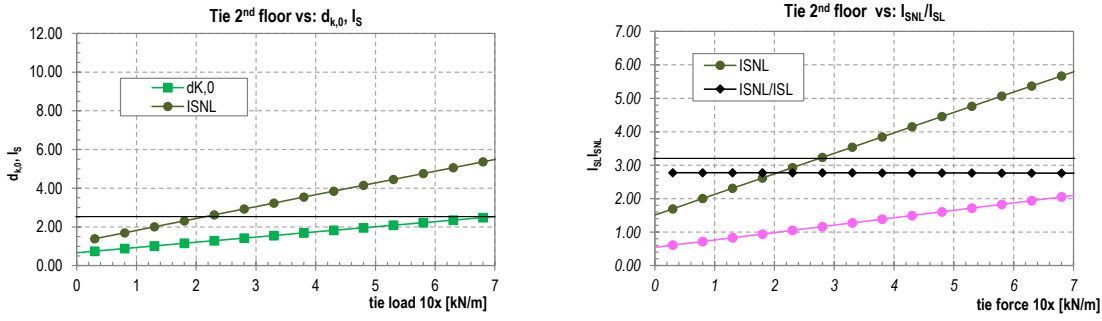


Figure A. 16: Results of non-linear analyses for different values of 2nd floor's tie-rod force.

3.2 Tie-rods at the second and first floors

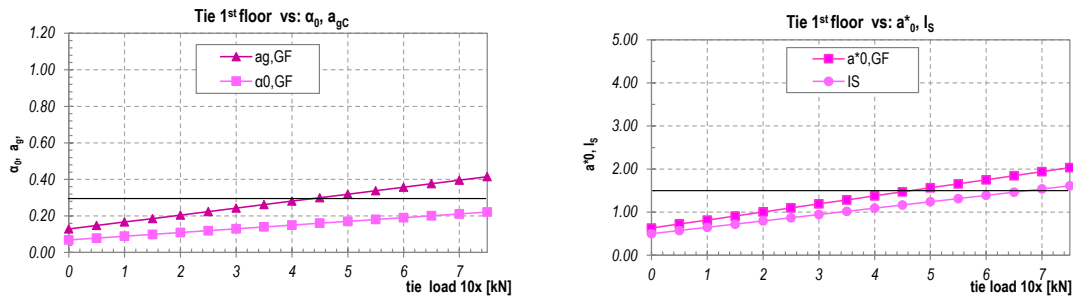


Figure A. 17: Results of linear analyses for different values of first and 2nd floor's tie-rod force.

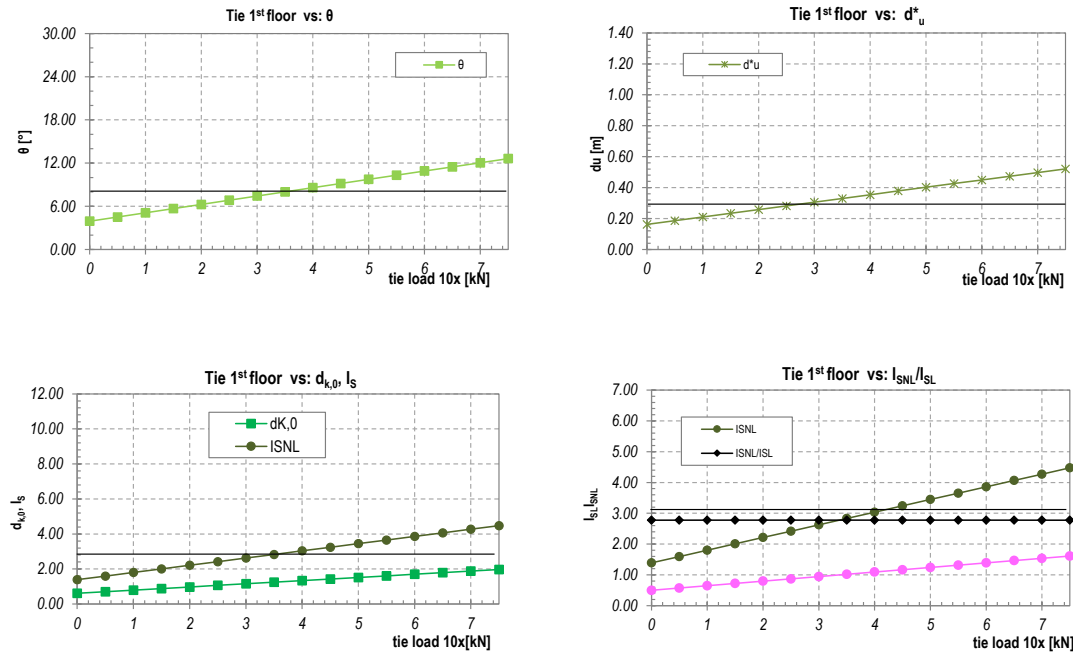


Figure A. 18: Results of non-linear analyses for different values of first and 2nd floor's tie-rod forces.

3.3 Tie-rods forces in each floor.

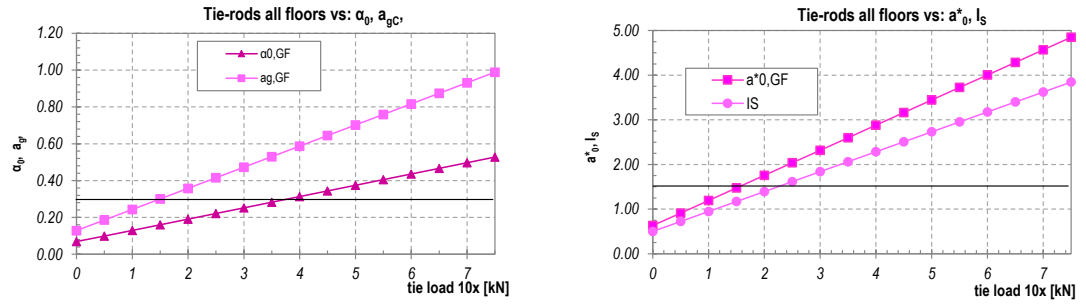


Figure A. 19: Results of linear analyses for different values of ground, 1st and 2nd floor's tie-rod forces.

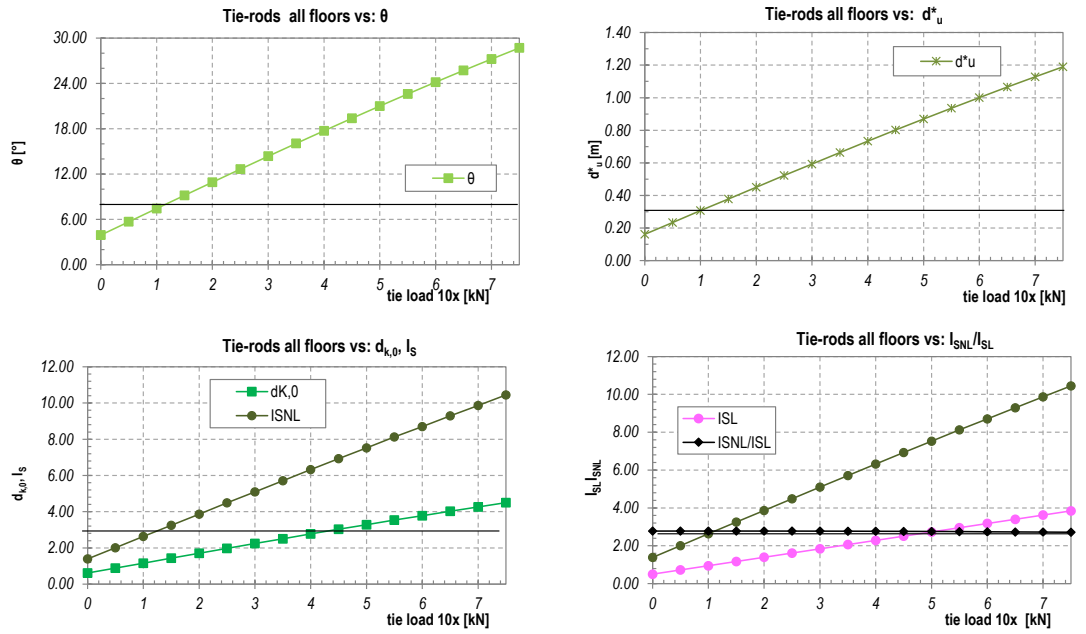


Figure A. 20: Results of non-linear analyses for different values of ground, 1st and 2nd floor's % tie-rod forces.

4. Influence of the thrust of vaults (N_H)

4.1 Thrust only at the second floor.

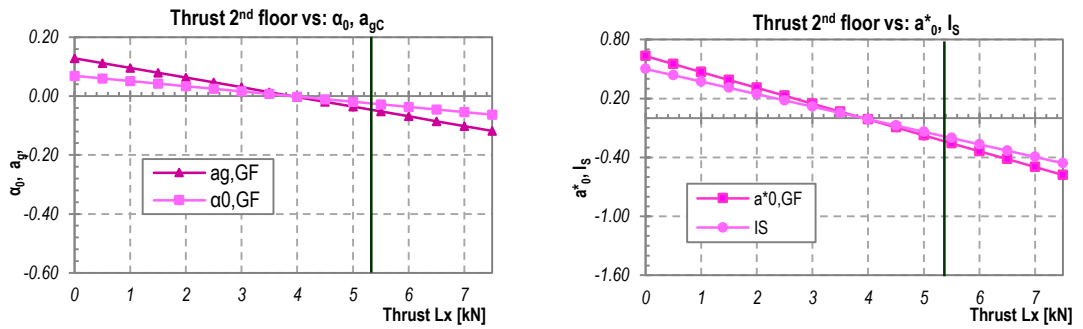


Figure A. 21: Results of linear analyses for different values of 2nd floor's vaults thrust.

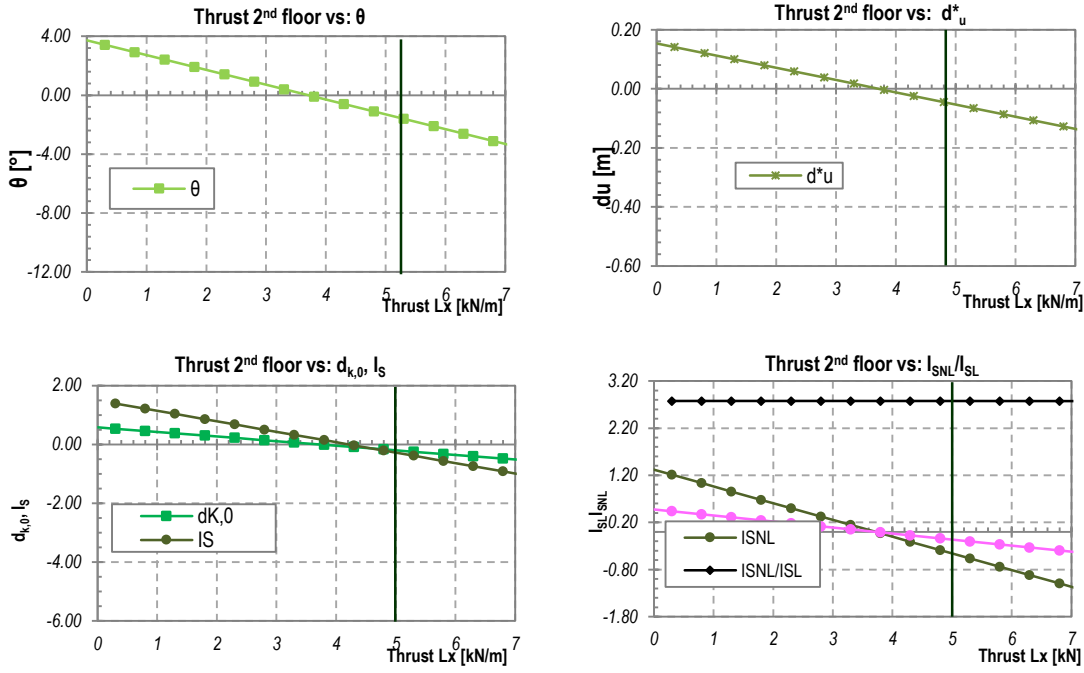


Figure A.22: Results of non-linear analyses for different values of 2nd floor's vaults thrust.

4.2 Thrust only at the first floor.

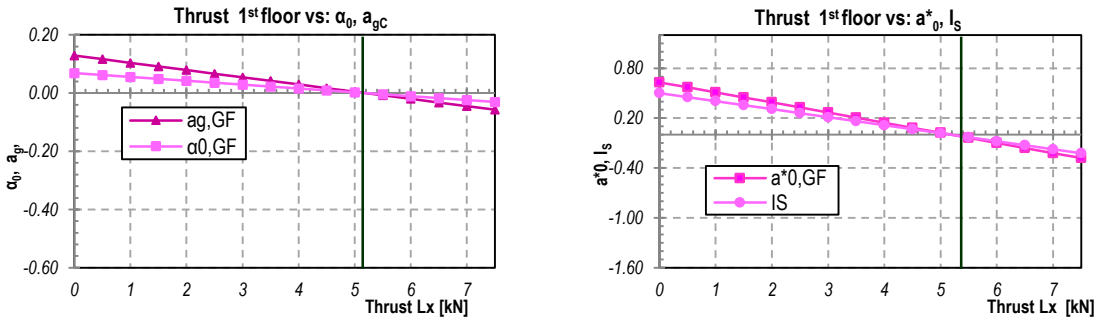
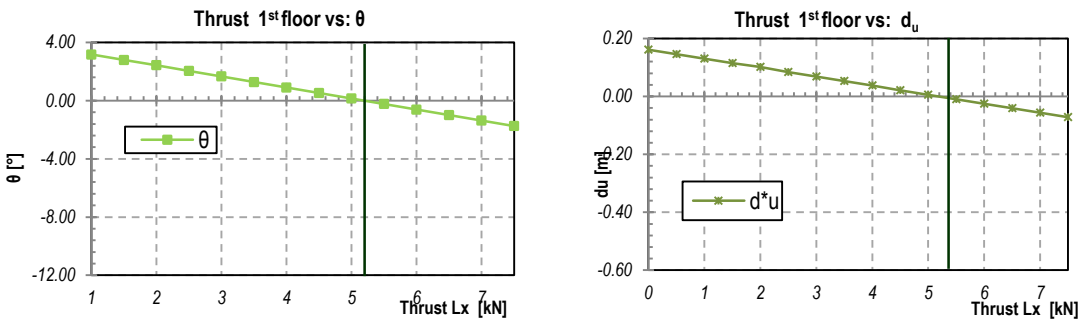


Figure A.23: Results of linear analyses for different values of 1st floor's vaults thrust.



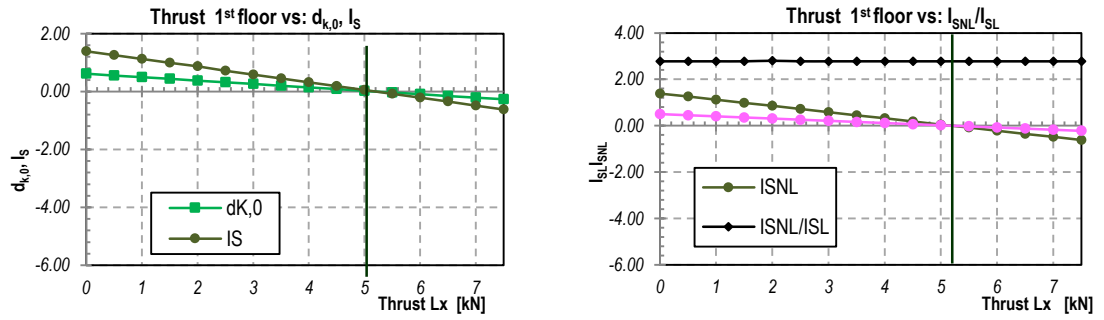


Figure A. 24: Results of non-linear analyses for different values of 1st floor's vaults thrust.

4.3 Thrust only at the ground floor (only linear analysis)

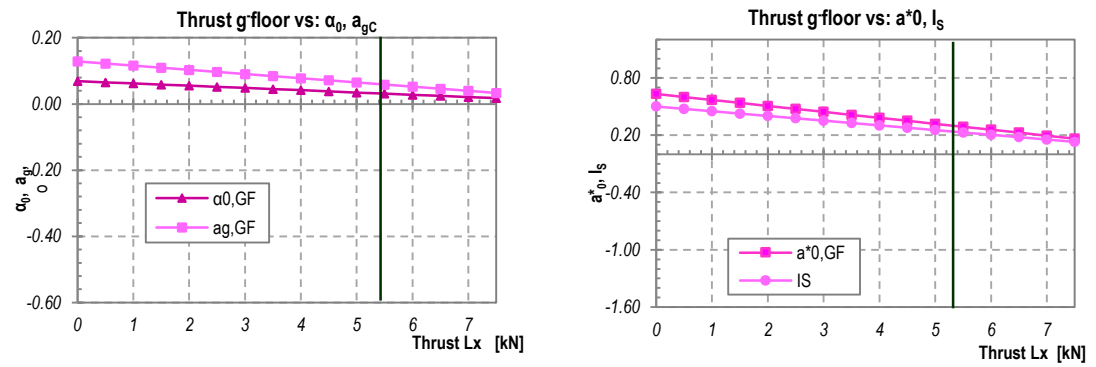


Figure A. 25: Results of linear analyses for different values of ground floor's vaults thrust.

4.4 Tie-rods forces in each floor.

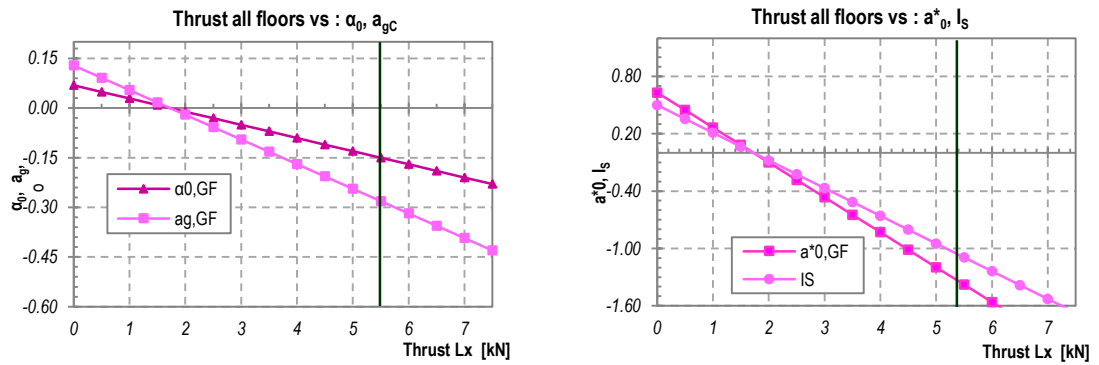


Figure A. 26: Results of linear analyses for different values of ground, 1st and 2nd floor's vaults thrusts.

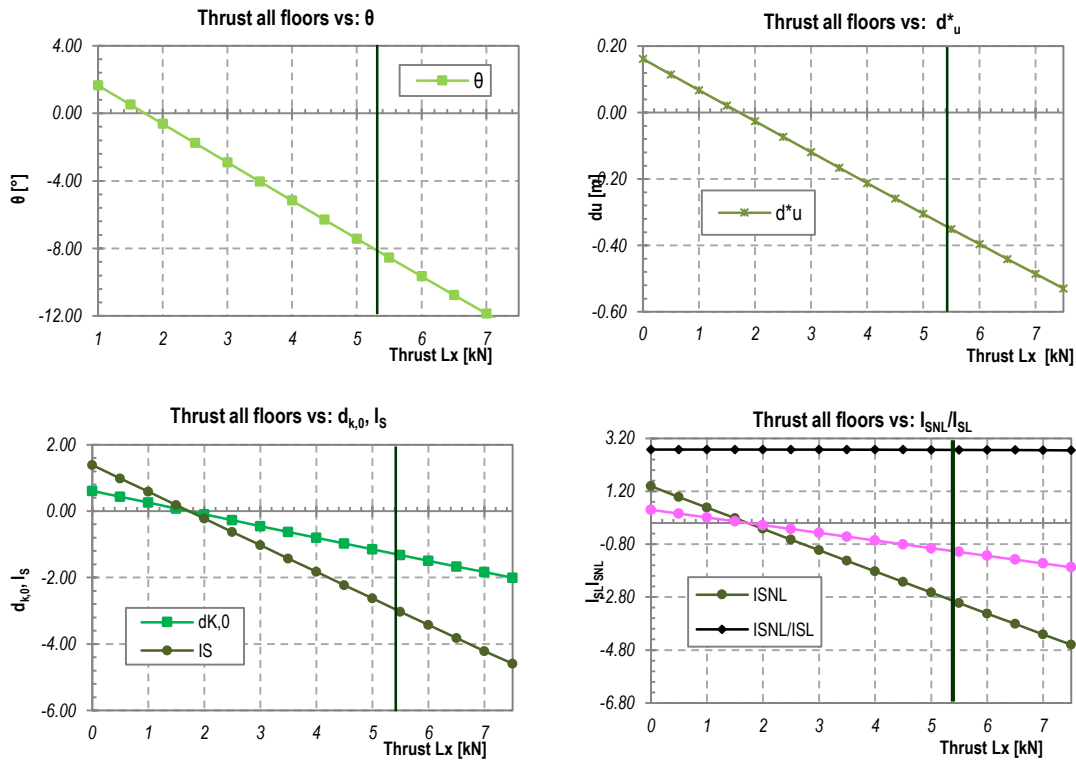


Figure A. 27: Results of non-linear analyses for different values of ground, 1st and 2nd floor's vaults thrusts.

